

PROTEOMIC RESPONSES OF HUMAN CELLS TO LOW DOSE IONIZING RADIATION

By

NISHAD S

LIFE01201304006

Bhabha Atomic Research Centre, Mumbai, India

A thesis submitted to the

Board of Studies in Life Sciences

In partial fulfillment of requirements

for the Degree of

DOCTOR OF PHILOSOPHY

of

HOMI BHABHA NATIONAL INSTITUTE



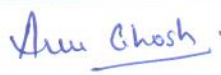
July 2019

Homi Bhabha National Institute¹

Recommendations of the Viva Voce Committee

As members of the Viva Voce Committee, we certify that we have read the dissertation prepared by Mr. Nishad S entitled "Proteomic responses of human cells to low dose ionizing radiation" and recommend that it may be accepted as fulfilling the thesis requirement for the award of Degree of Doctor of Philosophy.

Chairman - Dr. Vinay Kumar  Date: 24/12/2019

Guide / Convener - Dr. Anu Ghosh  Date: 16/12/19

Examiner - Prof. P. Venkatachalam  Date: 16/12/2019

Member 1- Dr. B. L. Das  Date: 16/12/2019

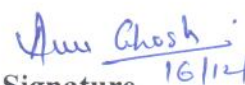
Member 2- Dr. Bhakti Basu  Date: 16/12/2019

Final approval and acceptance of this thesis is contingent upon the candidate's submission of the final copies of the thesis to HBNI.

I/We hereby certify that I/we have read this thesis prepared under my/our direction and recommend that it may be accepted as fulfilling the thesis requirement.

Date: 16-12-2019

Place: Mumbai


Signature 16/12/19
Guide

¹ This page is to be included only for final submission after successful completion of viva voce.

STATEMENT BY AUTHOR

This dissertation has been submitted in partial fulfillment of requirements for an advanced degree at Homi Bhabha National Institute (HBNI) and is deposited in the Library to be made available to borrowers under rules of the HBNI.

Brief quotations from this dissertation are allowable without special permission, provided that accurate acknowledgement of source is made. Requests for permission for extended quotation from or reproduction of this manuscript in whole or in part may be granted by the Competent Authority of HBNI when in his or her judgment the proposed use of the material is in the interests of scholarship. In all other instances, however, permission must be obtained from the author.

Nishad S

DECLARATION

I, hereby declare that the investigation presented in the thesis has been carried out by me.
The work is original and has not been submitted earlier as a whole or in part for a degree
/ diploma at this or any other Institution / University.

Nishad S

List of publications arising from the thesis

Journals

1. “Comparative proteomic analysis of human peripheral blood mononuclear cells indicates adaptive response to low-dose radiation in individuals from high background radiation areas of Kerala”, **Nishad S** and Anu Ghosh, *Mutagenesis*, **2018**, 33, 359-370.
2. “Dynamic changes in the proteome of human peripheral blood mononuclear cells with low dose ionizing radiation”, **Nishad S** and Anu Ghosh, *Mutation Research/Genetic Toxicology and Environmental Mutagenesis*, **2016**, 797, 9-20.
3. “Gene expression of immediate early genes of AP-1 transcription factor in human peripheral blood mononuclear cells in response to ionizing radiation”, **Nishad S** and Anu Ghosh, *Radiation and Environmental Biophysics*, **2016**, 55, 431-440.

Conferences

1. iTRAQ-based proteomic analysis of human cells exposed to low dose chronic natural background radiation. **Nishad S** and Anu Ghosh. 11th Annual meeting of Proteomic Society of India, Dec 2-4, 2019. ICAR-NDRI, Karnal.
2. Proteomic responses of human peripheral blood mononuclear cells from individuals residing in HLNRA of Kerala. **Nishad S** and Anu Ghosh. International Conference on Radiation Research: Impact on Human Health and Environment (ICRR-HHE 2016). Feb 11-13, 2016. Anushakti Nagar, Mumbai.
3. Time and dose dependent expression in the proteome of human peripheral blood mononuclear cells with gamma irradiation. **Nishad S** and Anu Ghosh. International Conference on Radiation Biology (ICRB 2014). Nov 11-13, 2014, INMAS, New Delhi.
4. Proteomic responses of human peripheral blood mononuclear cells to acute gamma ray irradiation. **Nishad S** and Anu Ghosh. 5th Annual meeting of Proteomic Society of India, Nov 28-30, 2013. IISc, Bangalore.

Nishad S

Dedicated
to
My Beloved Parents

ACKNOWLEDGEMENTS

My first words of gratitude are reserved for my supervisor Dr. Anu Ghosh, Group leader, Radiation Signaling Group, Radiation Biology & Health Sciences Division (RB&HSD), BARC, for her guidance, motivation, suggestions and sustained support during my Ph. D programme.

I would like to express my sincere thanks to my doctoral committee: Chairperson, Dr. Vinay Kumar, Head, RB&HSD, BARC, and members Dr. B. L. Das, RB&HSD, BARC and Dr. Bhakti Basu, Molecular Biology Division, BARC for their valuable suggestions, constructive criticisms and timely revisions during the study.

I accord my sincere thanks to Dr. Hema Rajaram, Dean, Life Sciences, Homi Bhabha National Institute for coordinating all official works related to Ph. D.

I am very thankful to Dr. G Jaikrishan, OIC, Low Level Radiation Research Laboratory (LLRRL), Kollam and lab members of LLRRL for coordinating the blood sample collection from the high level natural radiation areas of Kerala. Thanks are also due to Ms. J.A. Prabhu, Mr. Sangram Kamble, Trombay dispensary, BARC for their assistance during blood sample collection. I am grateful to all the volunteers who donated blood samples for this study.

I am deeply obliged to Mr. P.K.M. Koya, LLRRL, for his suggestions during statistical analysis of the data.

I express my heartfelt thanks to my lab members Dr. Himanshi N M, Dr. Somnath Ghosh, Ms. Neha Paraswani, Mr. Paresh P. Khadilkar, Ms. Pritam N. Bhoir, Ms. Meenakumari B for their moral support, motivation and help during my research.

I thankfully acknowledge the mass spectrometry facilities of ACTREC, Navi Mumbai and IIT Bombay, Mumbai for MALDI-TOF MS. I also thank Dr. H.N. Bhilwade, RB&HSD and Mr. Prayag Amin, RB&HSD for their technical help.

Any word of thankfulness will be too small for my companion Shyama Dharan, for her help and good will for me. I humbly thank her for the pains she took, her prayers and her words of motivation which kept me going at the times of despair. Very special thanks to my beloved Kannan and Achooty for sacrificing their weekends for my thesis.

This list is obviously incomplete, but allow me to submit that the omissions are inadvertent and I once again record my heartfelt gratitude to all those who cooperated with me in this endeavour.

Nishad S

ABBREVIATIONS

API	Activator protein-1
APS	Ammonium per sulfate
ATM	Ataxia Telangiectasia Mutated
ATR	Ataxia Telangiectasia and Rad3-related protein
BCA	Bicinchoninic acid assay
BEIR	Biological Effects of Ionizing Radiation
BER	Base excision repair
bp	Base pair
BRIT	Board of Radiation and Isotope Technology
BSA	Bovine serum albumin
cDNA	Complementary DNA
cGy	Centigray
CO ₂	Carbon dioxide
C _T	Threshold cycle
CV	Coefficient of variation
Da	Dalton
DAVID	Database for Annotation, Visualization and Integrated Discovery
DDR	DNA damage response
DIGE	Difference in-gel electrophoresis
DMSO	Dimethyl sulfoxide
DNA	Deoxyribonucleic acid
DNA-PK	DNA-dependent protein kinase
dpi	Dots per inch
DSBs	Double strand breaks
DTT	Dithiothreitol
EDTA	Ethylenediaminetetraacetic acid
ERR	Excess relative risk
FA pathway	Fanconi anemia pathway
FAS	French Academy of Sciences
FC	Fold change
FDR	False discovery rate

g	Gram
GAPDH	Glyceraldehyde-3-phosphate dehydrogenase
GOTERM	Gene Ontology Term Enrichment
Gy	Gray
Gy/min	Gray per minute
h	hour
H2AX	H2A histone family, member X
HLNRA	High-level natural background radiation area
HPLC	High performance liquid chromatography
HR	Homologous recombination
HR-LC	High resolution-liquid chromatography
IARC	International Agency for Research on Cancer
ICLs	DNA interstrand crosslinks
ICRP	International Commission on Radiological Protection
IEF	Isoelectric focusing
IPG strips	Immobilized pH gradient strips
IR	Ionizing radiation
iTRAQ	Isobaric Tags for Relative and Absolute Quantification
kDa	Kilo dalton
KEGG	Kyoto Encyclopedia of Genes and Genomes
keV/ μ m	kiloelectronvolts per micrometre
LC-MS	Liquid chromatography- mass spectrometry
LET	Linear energy transfer
LNT	Linear no-threshold
LSS	Life Span Study
M	Molar
m/z	Mass-to-charge ratio
MALDI-TOF	Matrix-assisted laser desorption ionization-time of flight mass spectrometry
mGy	milligray
mGy/y	milligray per year
min	minutes
ml	Millilitre

MMR	Mismatch repair
MOWSE score	Molecular Weight SEArch score
MS	Mass spectrometry
mSv	millisievert
mSv/y	millisievert per year
NER	Nucleotide excision repair
NF-kB	Nuclear factor of kappa light B-cells
ng/ μ l	Nanogram per microliter
NHEJ	Nonhomologous DNA end joining
NLNRA	Normal-level natural background radiation areas
nm	Nanometre
OD	Optical density
PBMCs	Peripheral blood mononuclear cells
PBS	Phosphate Buffered Saline
PCA	Principal component analysis
PI	Propidium iodide
PMF	Peptide mass fingerprinting
ppm	Parts per million
PVDF	Polyvinylidene fluoride
Q-TOF	Quadrupole time-of-flight mass spectrometry
RNA	Ribonucleic acid
ROS	Reactive Oxygen Species
rpm	Rotation per minutes
RPMI-1640	Roswell Park Memorial Institute-1640
RR	Relative risk
RT-PCR	Real time polymerase chain reaction
SCX	Strong cation exchange
SD	Standard deviation
SDS	Sodium dodecyl sulphate
SDS-PAGE	Sodium dodecyl sulphate-Polyacrylamide gel electrophoresis
sec	Second
SEM	Standard error of mean
SILAC	Stable Isotopic Labeling of Amino Acids in Cell Culture

SMRs	standard mortality ratios
SPSS	Statistics Program for Social Sciences
SSBs	Single strand breaks
Sv	Sievert
$t_{1/2}$	half-life
TEAB	Triethylammonium bicarbonate
TEMED	Tetramethylethylenediamine
TF	Transcription factor
TLS	Translesion synthesis
TMT	Tandem mass tag
TOF	Time-of-flight
UNSCEAR	United Nations Scientific Committee on the Effects of Atomic Radiation
UPLC	Ultra-performance liquid chromatography
UV	Ultra violet
WHO	World Health Organization
α - particle	Alpha particle
β -actin	Beta actin
γ -rays	Gamma-rays
μg	Microgram
$\mu\text{g/ml}$	Microgram per millilitre
μL	Microlitre
$\mu\text{R/ h}$	Microroentgen per hour
^{206}Pb	Lead-206
^{208}Pb	Lead-208
^{220}Rn	Radon-220
^{222}Rn	Radon-222
^{226}Ra	Radium-226
^{232}Th	Thorium-232
^{238}U	Uranium-238
2DE	Two-dimensional polyacrylamide gel electrophoresis

CONTENTS

SUMMARY I
LIST OF FIGURES III
LIST OF TABLES IX
CHAPTER 1: INTRODUCTION	
1.1. Sources of ionizing radiation exposures on humans 2
1.2. Definition of low dose and/or low dose-rate ionizing radiation 4
1.3. Health risks from exposure to low doses of ionizing radiation 4
1.4. Risk assessment models of radiation exposures 5
1.5. High-level natural background radiation areas of the world. 8
1.5.1. High-level natural background radiation areas of Kerala, India 9
1.5.2. Epidemiological studies in HLNRA, Kerala 11
1.6. Cellular and molecular responses of low dose radiation 14
1.6.1. Cellular defence mechanisms against radiation induced DNA damage 15
1.6.2. Cellular defense mechanisms against radiation-induced ROS 18
1.7. Non-targeted effects of ionizing radiation 19
1.7.1. Radiation-induced genomic instability 20
1.7.2. Radiation-induced bystander effects 21
1.7.3. Radiation-induced adaptive response 21
1.8. Radiation proteomics using advanced quantitative proteomics techniques 23
1.8.1. Gel-based quantitative proteomics methods 24
1.8.2. Gel-free quantitative proteomics methods 28
1.8.2.1. Label based methods 29
1.8.2.2. Label free based methods 35
1.9. Evidences of radiation-induced alterations in the cellular proteome 36
1.10. Objectives of the thesis 37

CHAPTER 2: MATERIALS AND METHODS

2.1. Ethics statement	39
2.2. Blood sample collection	39
2.2.1. Acute radiation exposure studies	39
2.2.2. Chronic radiation exposure studies	40
2.3. Isolation of peripheral blood mononuclear cells	40
2.4. Irradiation of human PBMCs	41
2.5. Cell viability analysis by flow cytometry	41
2.6. DNA damage analysis by alkaline comet assay	42
2.7. Preparation of protein extracts from PBMCs for proteomics	43
2.8. Protein estimation by BCA protein assay	43
2.9. Two-dimensional polyacrylamide gel electrophoresis	44
2.9.1. Isoelectric focusing of extracted proteins	44
2.9.2. Second dimension electrophoresis	45
2.9.3. Gel staining	45
2.9.4. Gel image processing and analysis	46
2.10. Protein identification by MALDI-TOF mass spectrometry	46
2.11. Proteomic analysis by HR-LC based iTRAQ method	47
2.11.1. In-solution tryptic digestion	48
2.11.2. iTRAQ labeling of tryptic peptides	48
2.11.3. Strong cation exchange fractionation	49
2.11.4. Reverse phase LC-MS/MS analysis	51
2.11.5. Protein identification and quantification	52
2.12. Western blot analysis	53
2.13. RNA extraction and gene expression studies	54
2.14. Statistical analysis	58
2.14.1. Statistical analysis for protein expression with acute <i>in vitro</i> radiation	58
2.14.2. Statistical analysis for protein expression with chronic low dose radiation: Gel-based 2DE method	59

2.14.3. Statistical analysis for protein expression with chronic low dose radiation: Gel-free iTRAQ based method 60
2.14.4. Functional pathway analysis for gel-based (2DE) and gel-free (iTRAQ) methods 60
2.14.5. Statistical analysis for gene expression data 61

CHAPTER 3: RESULTS

3.1. Responses of human PBMCs to acute <i>in vitro</i> IR 63
3.1.1. Proteome analysis with 2DE-MS 63
3.1.1.1. Assessment of intra-individual variability in the PBMC proteome 63
3.1.1.2. Proteome changes in PBMCs 68
3.1.1.3. Dose dependent changes in proteome of PBMCs 69
3.1.1.4. Time dependent changes in proteome of PBMCs 74
3.1.1.5. Effect of IR on the viability of PBMCs 76
3.1.1.6. Analysis of DNA damage in PBMCs 77
3.1.1.7. Functional classification of differentially expressed proteins 80
3.1.1.8. Individual variability of protein expression 82
3.1.1.9. Assessment of technical variation 84
3.1.1.10. Western blot validation of selected radiation responsive proteins 87
3.1.1.11. RT-PCR of selected radiation responsive proteins 88
3.1.1.12. Principal component analysis for predicting radiation dose groups 92
3.1.1.13. Gender specific differences in IR induced differential protein expression 94
3.1.2. Gene expression of AP1 family genes 99
3.1.2.1. Evaluation of expression values for β -actin reference gene 100

with radiation	
3.1.2.2. Time kinetics of AP1 genes in PBMCs with acute dose of 300 mGy 101
3.1.2.3. Time kinetics of AP1 genes in PBMCs with acute dose of 1Gy 108
3.1.2.4. Inter-individual variations in expression of AP1 genes 113
3.1.2.5. Principal component analysis of the gene expression data set 114
3.2. Responses of human PBMCs to chronic low dose IR 116
3.2.1. Basal and induced proteome analysis with 2DE-MS in HLNRA and NLNRA individuals 116
3.2.1.1. Effect of chronic radiation on the proteome of HLNRA subjects 121
3.2.1.2. Dose-response analysis of the differentially modulated proteins 127
3.2.1.3. Functional pathway analysis 129
3.2.1.4. Estimation of variability in protein expression 132
3.2.1.5. Statistical power analysis of the study 135
3.2.1.6. Western blot validation of selected radiation responsive proteins 136
3.2.1.7. Principal component analysis for identification of radiation dose group 138
3.2.2. Basal proteome analysis with iTRAQ in HLNRA and NLNRA individuals 139
3.2.2.1. Effect of chronic radiation on the proteome of HLNRA subjects 139
3.2.2.2. Assessment of technical variation 140
3.2.2.3. Relative abundance of identified proteins in HLNRA subjects 143
3.2.2.4. Functional annotation of differentially expressed proteins 147

3.2.2.5. Classification of differentially expressed proteins by gene ontology (GO) based on biological processes 147
3.2.2.6. Key radiation related biological processes enriched in HLNRA groups 148
3.2.2.6.1. Proteins involved in DNA damage repair and DNA damage response signaling 152
3.2.2.6.2. Proteins involved in signaling pathways 154
3.2.2.6.3. Proteins involved in stress activated protein kinase pathways 158
3.2.2.6.4. Proteins involved in post-translational modifications 160
3.2.2.6.5. Proteins involved in chromatin modifications 163
3.2.2.6.6. Proteins involved in RNA processing and splicing 165
3.2.2.7. Classification of differentially expressed proteins by gene ontology (GO) based on molecular function 168
3.2.2.8. Classification of differentially expressed proteins by gene ontology (GO) based on cellular component 170
3.2.2.9. KEGG pathways affected by chronic low dose radiation exposure 171
3.2.2.10. Key radiation related KEGG pathways enriched in HLNRA groups 172
3.2.2.11. Real time PCR analysis of selected radiation responsive proteins 181
3.2.2.12. Transcription factors differentially expressed in HLNRA individuals 185
3.2.2.13. Cell redox homeostasis proteins differentially expressed in HLNRA individuals 189
3.2.3. Comparison of 2DE-MS and iTRAQ protein profiles in HLNRA individuals 191
3.2.4. Comparison of protein expression profiles with acute and chronic radiation in human PBMCs 193

CHAPTER 4: DISCUSSION 196
CHAPTER 5: KEY CONCLUSIONS AND FUTURE DIRECTIONS 236
REFERENCES 241
APPENDIX A 283
APPENDIX B 307
APPENDIX C 308
APPENDIX D (Journal publications) 314

SUMMARY

Much progress has been made in understanding basic principles of radiation-induced effects on mammalian systems. Still there remains huge uncertainty over the molecular mechanisms that drive cellular responses of cells at low doses of radiation (below 100 mSv). Ever since the completion of human genome project, it has been repeatedly stressed that much of the biological response of cells is dictated not at the mRNA level, but by fine tuning the expression of proteins. The broad objective of the present work was therefore, to use a proteomics approach to understand molecular processes altered with acute and low dose chronic radiation in primary human PBMCs. Our data established the human PBMC proteome as a dynamic system that responded to IR with subtle, but specific changes in abundance to maintain cellular homeostasis. In the initial experiments, irradiation of human PBMCs with 300 mGy and 1 Gy of Co⁶⁰ gamma rays delivered acutely resulted in significant dose and time dependent proteomic responses. IR induced differential expression of 23 proteins (fold change ± 1.5 -fold, $P \leq 0.05$) involved in many self-defense mechanisms was observed. Among them were key proteins involved in cellular processes like redox homeostasis (CLIC-1, PRDX6), or proteins that served as molecular chaperones (GRP78) and considered pro-survival. There were minimal inter-individual variations (CV of 33.7% at 300 mGy and 48.3% at 1 Gy), and male and female samples showed similar responses. Transcript profiling of various members of fos (*FosB*, *FosL1*, and *FosL2*) and jun (*c-jun*) family genes that constitute important redox sensitive transcription factor activator protein 1 (AP-1) was carried out with the same acute radiation doses of 300 mGy and 1 Gy. The results suggested that discrete dimer of AP1 may be formed in a cell-type manner in response to specific doses of IR.

For understanding effects of chronic radiation, comparative proteomic analysis was performed for individuals residing in the high level natural radiation areas (HLNRA) of Kerala, India (with annual background radiation levels between ≤ 1 mGy to >45 mGy) and individuals residing in the adjoining normal level natural radiation areas (NLNRA) with annual background radiation levels (≤ 1.5 mGy). An integrated gel-based (2DE-MS) and gel-free (isobaric Tags for Relative and Absolute Quantification; iTRAQ) method was used for an expansive snapshot of baseline proteome. In addition, induced responses were studied by observing proteomic responses of PBMCs from HLNRA and NLNRA challenged with a high dose of 2 Gy. The data show for the first time that in human cells, low doses of chronic radiation can induce several proteins *in vivo*, which can detect the damage, initiate a DNA damage response signaling and repair, and mediate chromatin remodeling. It also provided mechanistic evidence of a pro-survival radiation induced adaptive response in human PBMCs. The findings reiterated the growing opinion that shape of the dose–response curve for low dose/dose rate exposures may not be linear. A further validation of candidate proteins with targeted proteomics will help to identify persistent signatures of low dose radiation exposure in humans.

LIST OF FIGURES

S. No.	Figures	Page No.
1.	Fig.1.1. Average annual effective dose from natural radiation sources.	2
2.	Fig.1.2. Average annual effective dose from man-made sources.	3
3.	Fig.1.3. Dose-response models for the assessment of health risks from exposure to low dose radiation.	6
4.	Fig.1.4. Schematic diagram of IR induced targeted (direct and indirect) and non-targeted effects observed in biological systems.	20
5.	Fig.1.5. Schematic diagram showing general workflow of protein separation, identification and quantification with 2DE and DIGE.	27
6.	Fig.1.6. Schematic workflow used for LC-MS/MS based global quantitative proteome analysis.	29
7.	Fig.1.7. Label based gel free quantitative proteomics methods using mass spectrometry.	31
8.	Fig.1.8. Chemical structure of an iTRAQ reagent.	33
9.	Fig.1.9. Chemical structure of a generic TMT reagent.	34
10.	Fig.1.10. General workflow for LC/MS-based label-free protein quantification.	35
11.	Fig.2.1. Representative standard curve of BSA used for protein estimation.	44
12.	Fig. 2.2. Representative SCX chromatogram.	50
13.	Fig.2.3. Representative melting curves for the RT-PCR products of <i>PRDX6</i> and <i>GAPDH</i> genes.	58
14.	Fig.3.1. Optimization of 2D gel electrophoresis for human PBMCs.	65
15.	Fig.3.2. Intra-individual variability in the human PBMC proteome.	67
16.	Fig.3.3. Representative 2D images of human PBMC proteome from a healthy individual irradiated with 300 mGy and 1 Gy.	70
17.	Fig.3.4. Dose dependent changes in expression of proteins in irradiated PBMCs (300 mGy and 1 Gy) as compared to sham irradiated cells.	73
18.	Fig.3.5. Temporal changes in expression of proteins in irradiated	75

	human PBMCs (300 mGy and 1 Gy) as compared to sham irradiated cells.	
19.	Fig.3.6. Flow cytometric profile of human PBMCs from an individual with and without irradiation with PI staining.	77
20.	Fig.3.7. Induction of DNA damage in gamma irradiated PBMCs.	79
21.	Fig.3.8. Cellular functions of radiation modulated proteins in human PBMCs.	80
22.	Fig.3.9. Heat map showing radiation-associated changes in the relative level of differentially expressed proteins in the sham irradiated and irradiated (300 mGy and 1 Gy) human PBMCs.	81
23.	Fig.3.10. The distribution of CV data calculated for differentially modulated proteins at the studied dose (300 mGy and 1 Gy) and time points (1 h and 4 h).	83
24.	Fig.3.11. The scatter plot illustrates the contribution of variance among the technical replicates for a healthy individual to the total variance at 1 h time point at indicated dose (300 mGy and 1 Gy) points.	86
25.	Fig.3.12. The scatter plot illustrates the contribution of variance among the technical replicates for a healthy individual to the total variance at 4 h point at indicated dose (300 mGy and 1 Gy) points.	86
26.	Fig.3.13. Western blot validation for differentially expressed proteins.	88
27.	Fig.3.14. Comparison of gene expression data with 2DE proteomics data.	90
28.	Fig.3.15. Individual variations in gene expression in response to IR.	91
29.	Fig.3.16. Principal component analysis for the protein expression data set after irradiation with 300 mGy and 1 Gy at 1 h and 4 h post-irradiation.	93
30.	Fig.3.17. Representative images of human PBMCs for a male and female individual.	96
31.	Fig.3.18. Principal component analysis of the protein expression data set for gender specific differences	98
32.	Fig.3.19. Threshold cycle (C_T) values for β -actin reference gene	100

	following radiation exposure in human PBMCs.	
33.	Fig.3.20. Time kinetics of AP1 genes for individuals after irradiation with 300 mGy at the respective time points (0 h, 1 h, 4 h).	102
34.	Fig.3.21. Heat map showing alterations in gene expression in human PBMCs for seven AP1 genes.	103
35.	Fig.3.22. Relative fold changes of <i>fosB</i> , <i>fosL1</i> , <i>fosL2</i> and <i>c-jun</i> genes for the 10 individuals after irradiation with 300 mGy at the respective time points (0 h, 1 h, 4 h).	106
36.	Fig.3.23. Relative fold changes of <i>cfos</i> , <i>junB</i> and <i>junD</i> genes for the 10 individuals after irradiation with 300 mGy at the respective time points (0 h, 1 h, 4 h).	107
37.	Fig.3.24. Time kinetics of AP1 genes for individuals after irradiation with 1 Gy at the respective time points (0 h, 1 h, 4 h).	109
38.	Fig.3.25. Relative fold changes of <i>fosB</i> , <i>fosL1</i> , <i>fosL2</i> and <i>c-jun</i> genes for the 10 individuals after irradiation with 1 Gy at the respective time points (0 h, 1 h, 4 h).	111
39.	Fig.3.26. Relative fold changes of <i>c-fos</i> , <i>junB</i> and <i>junD</i> genes for the 10 individuals after irradiation with 1 Gy at the respective time points (0 h, 1 h, 4 h).	112
40.	Fig.3.27. Individual variations in AP1 gene expression in response to IR.	113
41.	Fig.3.28. Principal component analysis of the AP1 gene expression data set.	115
42.	Fig.3.29. Representative 2D-image showing ‘baseline expression’ of human PBMC proteome for an individual from NLNRA and HLNRA.	119
43.	Fig.3.30. Representative 2D-image showing ‘induced expression’ of human PBMC proteome for an individual from NLNRA and HLNRA.	120
44.	Fig.3.31. Scatter plot showing inter-group variations in protein expression between baseline and 2-Gy challenged human PBMCs from HLNRA and NLNRA.	121
45.	Fig.3.32. Box-plot distribution of expression for differentially	124

	expressed proteins of PBMCs, in individuals from NLNRA and HLNRA.	
46.	Fig.3.33. Scatter plot showing intra-group variations in protein expression between baseline and 2-Gy challenged human PBMCs from HLNRA and NLNRA.	126
47.	Fig.3.34. Scatter plot showing the Pearson correlation analysis of protein expression to annual dose (range: 10.74–20.25 mGy/y) received by HLNRA individuals.	128
48.	Fig.3.35. The distribution pattern of CV data for the altered proteins in the baseline (NLNRA and HLNRA) and 2-Gy challenged [NLNRA (2 Gy) and HLNRA (2 Gy)] human PBMCs.	133
49.	Fig.3.36. Coefficient of variation data for the differentially modulated proteins in the baseline (NLNRA and HLNRA) and 2-Gy challenged [NLNRA (2 Gy) and HLNRA (2 Gy)] human PBMCs.	134
50.	Fig.3.37. Relationship between statistical power and sample size.	135
51.	Fig.3.38. Immunoblot validation of selected proteins (GRP78, PDIA1 and PRDX6).	137
52.	Fig.3.39. Principal component analysis for the protein expression data set with chronic radiation.	138
53.	Fig.3.40. The distribution of the number of peptides and peptide sequence coverage of the identified proteins in HLNRA groups by iTRAQ method.	141
54.	Fig.3.41. Experimental variation analysis based on Coefficient of Variation (%).	142
55.	Fig.3.42. Adjusted <i>P</i> -value distribution of differentially expressed proteins in HLNRA dose groups	144
56.	Fig.3.43. Distribution of differentially expressed proteins identified in HLNRA groups at different fold change filters (2 fold, 1.5 fold, 1.2 fold).	145
57.	Fig.3.44. Distribution pattern of significantly (± 1.2 fold; adjusted <i>P</i> -value of ≤ 0.1) altered proteins in three HLNRA groups.	146

58.	Fig.3.45. Distribution pattern of biological processes enriched in HLNRA dose groups.	148
59.	Fig.3.46. Important radiation related biological processes enriched in HLNRA groups	149- 151
60.	Fig.3.47. Relative fold changes of proteins enriched in HLNRA groups compared to NLNRA for DNA damage repair and DDR signaling process.	153
61.	Fig.3.48. Relative fold changes of proteins enriched in HLNRA groups compared to NLNRA for intracellular signal transduction, canonical Wnt signaling, PI mediated signaling and calcium-mediated signaling biological processes.	155- 157
62.	Fig.3.49. Relative fold changes of proteins enriched in HLNRA groups compared to NLNRA for MAP Kinase cascade, JNK cascade and p38-MAP Kinase cascade biological processes.	159
63.	Fig.3.50. Relative fold changes of proteins enriched in HLNRA groups compared to NLNRA for Protein phosphorylation and Protein ubiquitination biological processes.	161- 162
64.	Fig.3.51. Relative fold changes of proteins enriched in HLNRA groups compared to NLNRA for chromatin modification biological process.	164
65.	Fig.3.52. Relative fold changes of proteins enriched in HLNRA groups compared to NLNRA for mRNA processing, mRNA splicing, via spliceosome, RNA splicing and RNA processing.	166- 167
66.	Fig.3.53. Distribution pattern of molecular function ontology enriched in HLNRA dose groups.	168
67.	Fig.3.54. Key molecular function categories enriched in Group II, Group III and Group IV individuals of HLNRA dose groups.	169
68.	Fig.3.55. Key cellular component categories enriched in Group II, Group III and Group IV individuals of HLNRA dose groups.	170
69.	Fig.3.56. Distribution pattern of KEGG pathways enriched in HLNRA dose groups.	171
70.	Fig.3.57. Key radiation altered KEGG pathways enriched in Group II,	173

	Group III and Group IV individuals of HLNRA dose groups.	
71.	Fig.3.58. Relative fold changes of proteins enriched in HLNRA groups compared to NLNRA for Focal adhesion, ECM-receptor interaction and regulation of actin cytoskeleton KEGG pathway.	174-175
72.	Fig.3.59. Relative fold changes of proteins enriched in HLNRA groups compared to NLNRA for Fanconi anemia DNA repair KEGG pathway.	176
73.	Fig.3.60. Relative fold changes of proteins enriched in HLNRA groups compared to NLNRA for calcium signaling KEGG pathway.	178
74.	Fig.3.61. Relative fold changes of proteins enriched in HLNRA groups compared to NLNRA for PI3K-Akt signaling KEGG pathway and HIF-1 signaling KEGG pathway.	179
75.	Fig.3.62. Relative fold changes of proteins enriched in HLNRA groups compared to NLNRA for Rap1 signaling KEGG pathway.	180
76.	Fig.3.63. Threshold cycle (C_T) values for endogenous control genes in human PBMCs of NLNRA and HLNRA dose groups.	182
77.	Fig.3.64. Gene expression data of 18 candidate genes belonging to different biological processes in HLNRA dose groups, as compared to NLNRA individuals.	184
78.	Fig.3.65. Scatter plot showing comparison of differential expression of proteins as measured by 2DE-MS and iTRAQ in HLNRA individuals, as compared to NLNRA individuals.	192
79.	Fig.3.66. Scatter plot showing comparison of acute [(300 mGy and 1 Gy) and chronic IR induced proteome expression profiles measured by 2DE-MS in human PBMCS.	194-195

LIST OF TABLES

S. No.	Tables	Page No.
1.	Table 2.1. Details of the number of SCX fractions collected and pooled according to retention time values.	50
2.	Table 2.2. List of primers used for the RT-PCR analysis	56-57
3.	Table 3.1. Differentially expressed proteins due to physiological responses in human PBMCs.	66
4.	Table 3.2. Identification of proteins differentially expressed after acute IR in human PBMCs derived from healthy individuals.	71
5.	Table 3.3. Dose (300 mGy and 1 Gy) and time dependent (1 h and 4 h) changes in expression of proteins differentially modulated after acute IR in human PBMCs.	72
6.	Table 3.4. Fold change in expression of proteins calculated from the technical replicates of a healthy individual.	85
7.	Table 3.5. Fold changes in expression of proteins uniquely modulated in male or female individuals.	97
8.	Table 3.6. Mean fold change of gene expression in PBMCs with acute 300 mGy at the respective time points (0 h, 1 h and 4 h post irradiation).	105
9.	Table 3.7. Mean fold change of gene expression in PBMCs with acute 1 Gy at the respective time points (0 h, 1 h and 4 h post-irradiation).	110
10.	Table 3.8. List of differentially expressed proteins identified by MALDI-TOF/TOF tandem mass spectrometry.	118
11.	Table 3.9. Differentially expressed proteins in human PBMCs with chronic exposure to high background natural radiation.	123
12.	Table 3.10. Intra-group variations in protein expression between baseline and 2-Gy challenged human PBMCs from HLNRA (HLNRA vs HLNRA + 2 Gy) and NLNRA (NLNRA vs NLNRA + 2 Gy).	125
13.	Table 3.11. Gene ontology analysis of radiation responsive proteins using DAVID bioinformatics analysis.	131
14.	Table 3.12. Transcription factors differentially expressed in HLNRA dose groups.	186-188
15.	Table 3.13. Cell redox homeostasis proteins differentially expressed in HLNRA dose groups.	190

CHAPTER 1

INTRODUCTION

1.1. Sources of ionizing radiation exposures on humans

Humans are continually exposed to ionizing radiation (IR) from natural and anthropogenic sources. The global average annual effective dose from these sources for the human population is about 2.8 millisievert (mSv), of which nearly 80% (~2.4 mSv) comes from natural background radiation. The main contributors of natural radiation exposures are cosmic rays coming from outer space, terrestrial radionuclides, and intakes of radionuclides through inhalation and ingestion (Fig.1.1). A significant contribution (~50%) to natural background radiation exposure is from inhalation dose imparted by the radon gas and its decay products. The sources of radionuclides and their decay products in the soil determine the level of terrestrial radiation and the internal exposure through inhalation and ingestion [1].

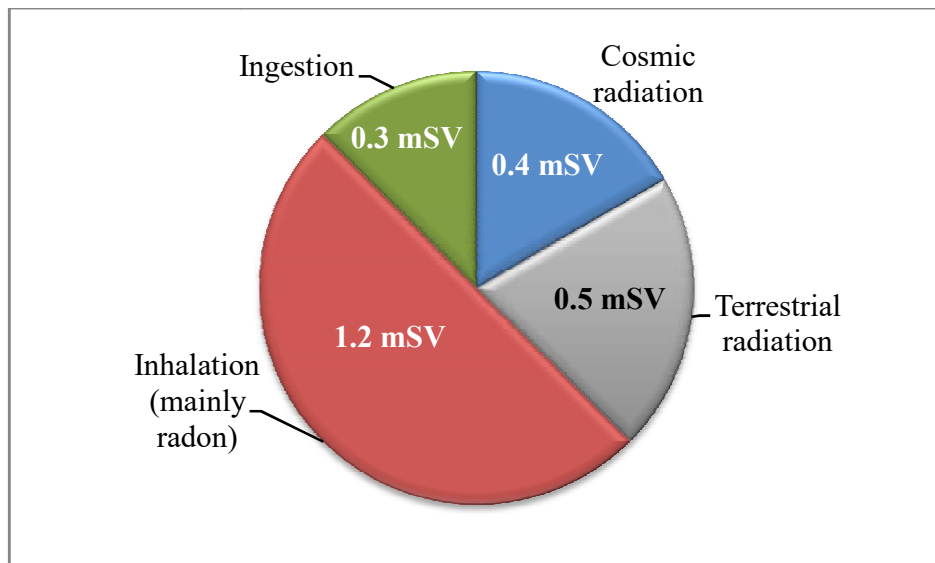


Fig.1.1. Average annual effective dose from natural radiation sources. Data source: United Nations Scientific Committee on the Effects of Atomic Radiation (UNSCEAR) report [1].

The major sources of manmade radiation exposure to the public are medical procedures (diagnostic and radio-therapeutic), occupational, radioactive fallout from nuclear weapons test and nuclear accidents (**Fig.1.2**). Among them, medical use of radiation is by far, the most significant source. Due to technological advances, medical use of radiation is fast expanding and includes exposures from diagnostic radiology, radiotherapy, nuclear medicine and interventional radiology. In recent years, widespread applications of nuclear and radiation technologies have led to a steady increase in the number of workers who might be exposed to radiation in the course of their occupations. This includes medical technicians and physicians, nuclear industry workers, airline crews and astronauts. The release of radionuclides into the environment from nuclear weapons test and nuclear power plant accidents act as minor sources of radiation exposure to humans [1].

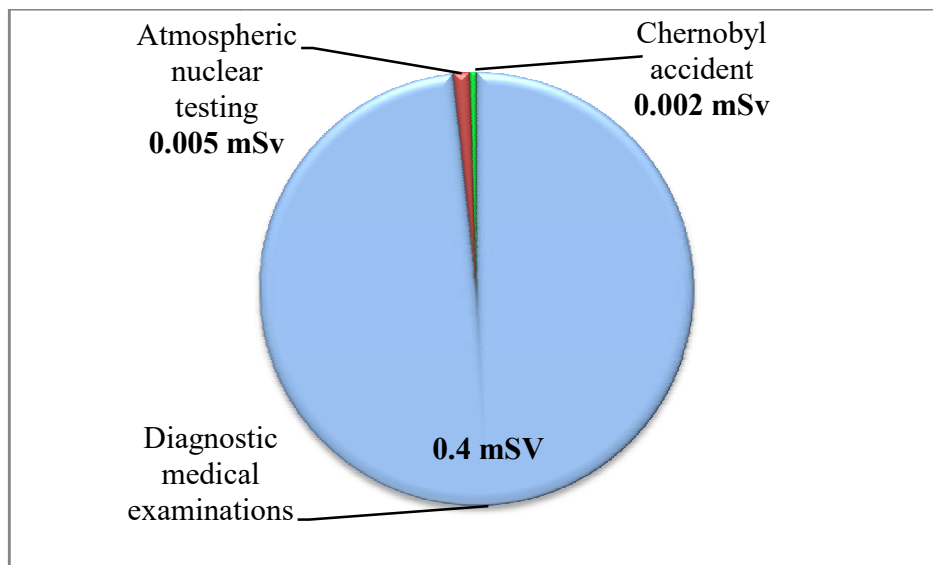


Fig.1.2. Average annual effective dose from man-made sources. Data source: United Nations Scientific Committee on the Effects of Atomic Radiation (UNSCEAR) report [1].

1.2. Definition of low dose and/or low dose-rate ionizing radiation

The national and international authorities involved in radiation protection and regulation: [United Nations Scientific Committee on the Effects of Atomic Radiation (UNSCEAR), International Commission on Radiological Protection (ICRP), National Academy of Sciences (NAS) - Biological Effects of Ionizing Radiation (BEIR) VII report and French Academy of Sciences (FAS)] define “low dose low-linear-energy-transfer (LET) radiation” as “*doses in the range of near zero up to about 100 mSv and low dose rates of 0.1 mGy per min averaged over an hour*” [2-5].

1.3. Health risks from exposure to low doses of ionizing radiation

The effects of low dose radiation on human cells and the associated risks from such exposures are of significant interest to the medical and scientific community. The biological effects of radiation vary depending on the physical nature (high LET or low LET), duration (acute or chronic), doses (high or low) and dose-rates (high or low) of exposure. IR deposits energy as tracks of ionizations within cells and the average energy deposited per track length (keV/ μm) is termed as linear energy transfer (LET). Based on the LET, IR is classified as low LET (sparsely ionizing: γ -rays, x-rays) and high LET (densely ionizing: α -particles, heavier ions, protons). The high dose radiation exposures over short period of time are termed as acute high dose radiation effects and the low dose radiation exposures over long period of time are termed as chronic low dose radiation effects. The biological effects of radiation are broadly categorized by the radiation protection science into non-stochastic and stochastic effects. The non-stochastic effects or the harmful tissue reactions (earlier called deterministic effects) occur above a

threshold radiation dose and severity of the effects is directly proportional to radiation dose received. The stochastic effects are probabilistic in nature and the probability of occurrence is proportional to radiation dose without a threshold value (e.g. carcinogenesis, genetic effects).

The biological effects at high doses of IR, which are well above the low dose range for environmental or therapeutic radiation exposures (>1 Gy) have been clearly documented [1, 6-11]. However, health risks associated with low doses (below 100 mSv) and low dose-rates (0.1 mSv/min) remain controversial due to the lack of direct human evidences. For low-LET radiation, the shape of the dose-response curve in the region of low dose or dose rate exposures is also debated [12]. As early as 1950's the technical report series of the World Health Organization (1959) emphasized the significance of direct studies on humans for assessment of radiation risk from low dose/dose rates exposures [13]. Most available estimates of radiation risk in humans exposed to low-dose radiation are currently generated from the epidemiological studies conducted on the atomic bomb survivors (Life Span Study, LSS) cohorts of Japan [14]. Limited data is also available from occupational workers (medical workers and nuclear industry workers) and from populations exposed to high level natural background radiation. The radiation risk estimation for low dose exposures have important implications in formulating guidelines for radiation protection and medical practice, compensation programs and radiation contamination issues [12, 15].

1.4. Risk assessment models of radiation exposures

Dose and dose rate present a contentious issue for risk estimation for low dose radiation exposures. The data from LSS cohort and other epidemiological studies

performed on populations exposed to low doses of radiation do not show any statistically significant cancer effects for individuals in the dose group less than 100 mSv [16-22] making it difficult to determine the shape of dose response curve at these dose. Hence, for assessment of risks in the lower dose ranges, we depend on experimental studies on animals or cultured cells or suitably exposed groups of human models or hypothetical models. Various hypothetical models of dose response curves have been postulated. These alternative schools of thoughts of dose-response relationship for risk assessment at low dose exposures, as shown in **Fig.1.3**, are linear threshold, hormesis, supralinear and linear no-threshold models [23-26].

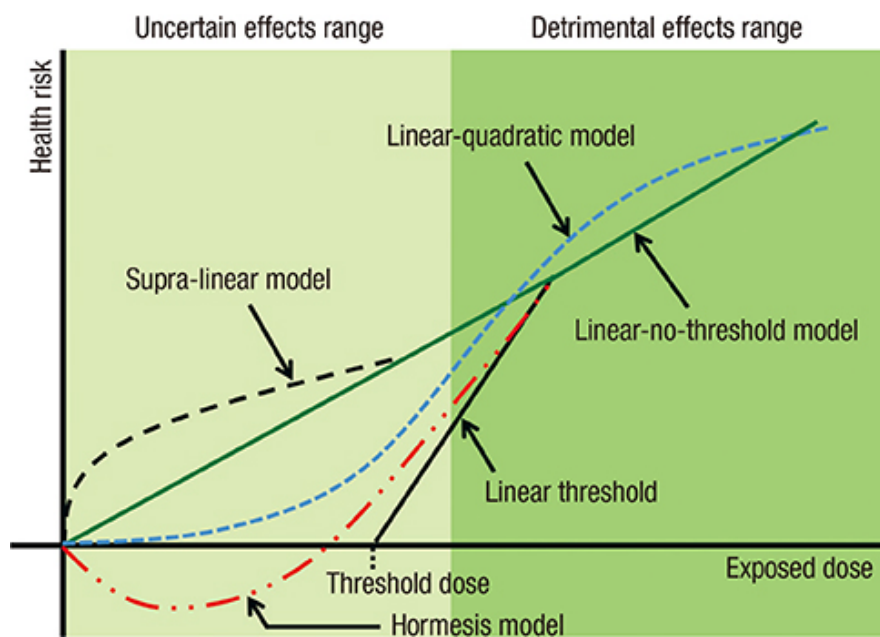


Fig.1.3. Dose-response models for the assessment of health risks from exposure to low dose radiation. Adapted from Seong KM, et al. 2016 [25].

During the early years of 20th century, the linear threshold dose response model was used for risk estimation to establish radiation exposure limits for occupational workers and for medical procedures for humans. This model states that there are no harmful effects of radiation below a certain “defined threshold” dose [27]. In spite of many experimental evidences for the linear threshold dose response, its failure to explain the effects at low dose/dose rate limits its applicability [28].

The radiation hormesis model explains the beneficial effects of low dose radiation exposures on humans through stimulation of immune system and up-regulation of cellular defense mechanisms [29]. The dose-response relationship is non-linear with a characteristic U-shaped curve at low doses. Many experimental data are available for radiation hormesis concept at the epidemiological and radiobiological level [26, 28, 30, 31]. A non-significant decrease in the cancer incidence and mortality was reported from the epidemiological studies performed in high level natural radiation areas (HLNRA) of Kerala [Excess relative risk (ERR) = - 0.13 per Gy (95% confidence interval, CI: - 0.58, 0.46)] and China [Relative risk (RR) = 0.99 (95% CI, 0.87 to 1.14)] [16, 17]. The radiation hormesis model uses the concepts of adaptive response, activation of cellular oxidative stress defence mechanisms and DNA repair pathways to explain the radiobiological effects observed at low dose/dose rate radiation [25, 28, 29, 32]. The hormesis model is further supported by statistical re-analysis conducted on the International Agency for Research on Cancer (IARC) cohort data on the exposed nuclear workers from 15 different countries which showed lower standard mortality ratios (SMRs) in nuclear workers than in the non-exposed group [33].

The supralinear dose response model postulates radiation associated risk increases more than linear curve (supralinear) at low doses. The radiobiological mechanisms of radiation induced bystander effect and low-dose hypersensitivity are used to scientifically explain the supralinear concept of dose-response relationship. Various studies have demonstrated an increase in cell death and induction of DNA damage and repair in non-irradiated cells bordering the irradiated cells (bystander cells) [34-38]. The low dose hypersensitivity predominates at radiation doses up to 0.5 Gy [25, 26, 39]. As the dose increases, the supralinear model becomes comparable to the linear models.

The linear no-threshold (LNT) model describes the proportionality between radiation dose and associated risk without a threshold dose. This model was introduced by the ICRP in 1966 [40]. The LNT model postulates several hypotheses: (i) there is no safe dose of IR and every dose is associated with a predictable risk (ii) risk increases linearly with dose, regardless of the dose rate (iii) compared to the radiation dose, the biological modifiers are small enough to be safely ignored [40]. Presently, LNT model is considered as the most practical model for administrative purposes [41]. It has been used in radiation protection since the past five decades and is currently recommended by most radiation advisory bodies such as ICRP [2], BEIR VII report [4] and UNSCEAR [1] for radiation protection across the world.

1.5. High-level natural background radiation areas of the world

The global average annual effective dose from natural radiation has been assessed by UNSCEAR to be ~2.4 mSv. However, there are some high-level natural background radiation areas (HLNRAs) in the world where the background radiation is high due to local geology and geochemistry [1]. In these HLNRAs, the sum of cosmic and terrestrial

radiation leads to chronic low dose (external and internal) exposure situations where the annual effective dose to the public is well above the defined level.

Some of the important HLNRA in the world with high levels of terrestrial radiation are located at Kerala, India; Guarapari, Brazil; Yangjiang, China and Ramsar, Iran [1]. The sources of naturally occurring radionuclides and their decay products vary across these HLNRA [42]. The elevated level of terrestrial radioactivity in the HLNRA of Kerala (India), Guarapari (Brazil) and Yangjiang (China) is caused by Thorium-232 (^{232}Th) and its decay products in the monazite sand. The average annual background radiation doses in these areas range from < 1 mGy to ~ 260 mGy. The radioactive source of background radiation in Ramsar (Iran) is due to Radium-226 (^{226}Ra) content in waters flowing from the sulfurous hot springs. The average annual absorbed dose from external exposures received by the population in the HLNRA of Kerala (India) is 4.5 mGy, while the average annual effective dose from external exposures received by other HLNRA is 4 mSv in Guarapari (Brazil), 2.1 mSv in Yangjiang (China) and 6 mSv in Ramsar (Iran) [43, 44].

1.5.1. High-level natural background radiation areas of Kerala, India

In India, the 55-km long and 0.5-km wide coastal belt in the southwest state of Kerala, is one of the widely studied HLNRA in the world. It extends from Neendakara panchayat (Kollam district) in the south to Purakkadu panchayat (Alapuzha district) in the north. The elevated levels of background radiation are due to monazite sands with a high content of ^{232}Th (8-10%), ^{238}U (0.3%) and its decay products. The radioactive ^{232}Th parent [half-life ($t_{1/2}$) = 14×10^9 y] decays to stable Lead-208 (^{208}Pb) through nine

radioactive daughters. The decay chain of ^{238}U [$(t_{1/2}) = 4.5 \times 10^9$ y] comprises 13 radioactive daughter nuclides which decays to stable Lead-206 (^{206}Pb). The radionuclide decay of both ^{232}Th and ^{238}U occurs through emission of alpha particles, beta particles and gamma photons with characteristic energies to stable Lead [45, 46].

The annual background radiation levels in this area vary from ≤ 1 to ≥ 45 mGy. This wide variation in the background radiation dose levels is due to non-uniform distribution of monazite in the beach sand [47]. The monazite content in the beach sand varies from 0.1-5% and is a rich source for other rare earth metals like ilmenite, rutile, zircon, and silmanite. The areas with a background dose rate of ≥ 1.5 mGy/y are classified as HLNRA and those with ≤ 1.5 mGy/y as normal level natural radiation areas (NLNRA). The dose rate value (1.5 mGy/y) used approximately corresponds to the equivalent dose rate of 1 mSv/y and is in accordance with the external dose component (cosmic and terrestrial) of the world average dose of 0.9 mSv/y [1]. The major contributors of radiation exposure to the inhabitants of the HLNRA include (1) external exposure due to gamma rays from cosmic rays and terrestrial radionuclides (^{232}Th , ^{238}U and their decay products), (2) internal exposure due to inhalation of radon (^{222}Rn), thoron (^{220}Rn), and their progenies (3) internal exposure due to ingestion of radionuclides through consumption of food. The median outdoor radiation dose received by the human population residing in these areas is ~ 4 mGy/y [48, 49]. A highly heterogeneous distribution of indoor radon and thoron gases has been reported for this area [50-52]. The average internal effective dose due to radon and thoron exposure is 0.61 ± 0.39 mSv/y (radon = 0.12 ± 0.09 mSv/y and thoron = 0.52 ± 0.38) to individuals in HLNRA and 0.74 ± 0.52 mSv/y (radon = 0.19 ± 0.18 mSv/y and thoron = 0.60 ± 0.44) to NLNRA subjects [52].

As compared to the other HLNRA regions of the world, the high background radiation area of Kerala is densely populated and inhabited for generations with low migration rates. There are historical accounts since 1st century AD of human settlement on the south-west coast of India, which was known as Malabar Coast. Kollam (erstwhile Quilon), the city close to the high background area, was an important port before the Christian era and was frequented by Arab and Chinese merchant ships [49].

1.5.2. Epidemiological studies in HLNRA, Kerala

Over the decades, several epidemiological studies have been conducted in the HLNRA of Kerala. One of the earliest studies on the morphological measurements of skeletal and dental variants in wild rats did not show any genetic effects attributable to high background radiation [53]. A one-time population survey covering ~70,000 individuals was conducted to find out any significant association of infertility, sex-ratio, multiple births, gross abnormalities, abortion and infant mortality rate with background radiation [54]. In early 90's the Regional Cancer Center (RCC), Trivandrum established a cohort of 3, 85,103 inhabitants in HLNRA of Kerala to assess the carcinogenic effects. The incidence of cancer was examined using a sub-cohort of nearly 70,000 residents from the cancer registry followed for 15 years (10.5 years average). The estimated ERR of cancer, excluding leukemia was -0.13 Gy^{-1} (95% CI: -0.58, 0.46), and showed non-significant relationship between external gamma radiation exposure and cancer risk [16].

A highly contentious study published in 1972 reported an elevated frequency of Down syndrome cases among the populations from HLNRA (12/12,918) with no cases of Down syndrome (0/5,938) in the control population [55]. The study was heavily

criticized for shortcomings in the study design and analysis [56]. Later, more extensive studies were carried out to screen 1,41,540 newborns (140,558 deliveries) from HLNRA and NLNRA for all major congenital anomalies observable at birth (Down's syndrome, clubfoot, hypospadias, congenital heart disease, cleft lip/palate, neural tube defects) and still birth. A case-control study of mental retardation and cleft lip/palate [57] and analysis of sex ratio at birth was conducted to understand reproductive health status of the population [58]. These prevalence studies found no significant association between incidence of major congenital anomalies, including Down's syndrome, and background radiation dose.

Other studies conducted over the years include cytogenetic studies for monitoring of newborns and adults for spontaneous frequency of chromosomal aberrations. The incidence of both structural (dicentric, translocations, inversions, centric fragments, acentric fragments, minutes, multiple aberrations, chromosome breaks, chromosome gaps, chromatid breaks, chromatid gaps) and numerical (aneuploidy and polyploidy) chromosomal aberrations have been studied. The study screened 1,267,788 metaphases from 27,295 newborns (NLNRA: 9,997 and HLNRA: 17,298) during the period 1986-2007 [59, 60]. In addition, baseline frequency of micronuclei and telomere length attrition in newborns and adults was assessed in the population [61-64]. None of these studied end-points have shown any significant correlation with high level background radiation level of the area.

In contrast, a report published in 2002 showed higher prevalence of radiation-associated heritable mtDNA point mutations (22/595 in HLNRA vs. 1/200 in NLNRA; $P \leq 0.01$) in the population using saliva samples and estimated mutation risk in HLNRA

relative to NLNRA as 7.39 (95% CI: 1.003-54.5) [65]. The study was criticized for relatively wide confidence intervals with lack of precision in risk estimates, historic dosimetry methods and selection of buccal cells, which are highly susceptible to many confounding factors like tobacco chewing, tobacco smoking and alcohol consumption. Moreover, the regions of mitochondrial DNA used for the study were prone to higher mutation rate and heteroplasmy in mitochondrial DNA was not considered [66, 67].

Another study to investigate heritable DNA mutations was conducted using microsatellite and minisatellite marker loci. This work identified higher, but statistically non-significant, microsatellite mutation frequency in HLNRA compared to NLNRA (7.25×10^{-3} vs 3.64×10^{-3} ; $P = 0.547$) [67]. Vivek et al. 2012 studied basal level DNA damage (spontaneous DNA strand breaks and alkali-labile sites) in lymphocytes of adult individuals by alkaline comet assay. The authors reported the effect of age and residential area status on the rate of spontaneous DNA damage. The basal level DNA damage increased with age in NLNRA residents ($P = 0.02$), while a significant negative correlation ($P = 0.002$) was observed in subjects from HLNRA [68]. However, quantification of spontaneous level of DNA double strand breaks (DSBs) in the population using γ H2AX marker did not find any significant correlation with background radiation exposure [69]. On the other hand, PBMCs from individuals residing in HLNRA, when challenged with a high dose (2Gy or 4Gy), showed lower DNA strand breaks and better repair (as measured using comet assay and γ H2AX) compared to individuals from NLNRA [70, 71]. In a report by Ramachandran et al., peripheral blood samples taken from individuals from HLNRA, when challenged with a high dose, showed lower frequency of micronuclei but only in individuals older than 40 y

of age [72]. The authors concluded that the protective effect of low dose priming exposure observed in HLNRA individuals may be due to efficient DNA repair or higher induction of DNA repair proteins, and emphasized the need for detailed studies on the transcription/protein profile of various DNA repair genes.

More recently, a whole transcriptome analysis on human peripheral blood mononuclear cells (PBMCs) using microarray identified an enrichment of DNA damage response (DDR), DNA repair, cell cycle arrest, apoptosis and chromatin modification genes in HLNRA individuals. The study compared individuals from normal [Group I, ≤ 1.50 mGy/y] and high level natural radiation areas belonging to three different background dose groups [Group II: 1.51-5.0 mGy/y; Group III: 5.01-15mGy/y and Group IV: >15.0 mGy/y]. Differential modulation of many genes involved in major DNA repair pathways were represented in the HLNRA subjects from the high dose (≥ 5 mGy/y) groups [73].

1.6. Cellular and molecular responses of low dose radiation.

IR elicits a complex network of cellular events in different cell types. Radiation interacts randomly with biological macromolecules (DNA, proteins, and lipids) along charged particle tracks either through direct events in the molecule (ionization or excitation) or, more frequently, through indirect mechanisms mediated by reactive oxygen species (ROS) produced by radiolysis of water. DNA is considered to be the primary target of radiation damage and various types of damages like the base damages, DNA single strand breaks (SSBs), DSBs, DNA interstrand crosslinks (ICLs), DNA-protein cross links are induced with IR [1]. The oxidative stress created by IR mainly

leads to DNA sugar backbone oxidation, DNA base (purines and pyrimidine) oxidations, depurination and depyrimidation damages [74]. The presence of histone proteins and double helix structure makes the DNA less susceptible to oxidative modifications compared to lipids and proteins [75]. The failure to repair the oxidized DNA bases increases the genome mutation risk during DNA replication. The oxidative stress created by IR also, reversibly or irreversibly, damages the amino acid side chains of proteins by oxidation. This oxidation produces carbonyl derivatives and can be used as a biomarker of protein oxidation and oxidative stress [76]. Proteins with amino acids lysine, arginine, histidine, proline, threonine, cysteine and methionine are more susceptible to carbonyl derivative formation through oxidation. These carbonyl products inactivate the active site of enzymes, disrupt the native conformations of proteins, causes aggregation of damaged proteins and programmed cell death [77]. Among the biomolecules, lipids are most susceptible to oxidative modifications through lipid peroxidation and produces peroxy radical products. The byproducts of lipid peroxidation produce many aldehydes [malondialdehyde (MDA) and 4-hydroxy-2-nonenal (HNE)] which react with DNA to produce cytotoxic DNA interstrand cross links [75, 78].

1.6.1. Cellular defense mechanisms against radiation induced DNA damage

IR induced DNA damage evokes a multifaceted cellular DNA damage response called the DDR signaling, which coordinates the interaction of sensors, signal transducers, and effector proteins to ensure foolproof DNA repair aided through cell-cycle arrest, and changes in transcription and protein profiles [79]. In multi-cellular organisms, cells with heavily damaged DNA are eliminated from the system by the

process of apoptosis, which thus prevents the transmission of cancer-causing mutated cells. The signal transduction cascade of DDR is activated primarily through post-translational modifications (mainly phosphorylation) of DNA damage sensor proteins like the phosphatidylinositol 3-kinase-like protein kinase (PIKKs) family members-ataxia telangiectasia mutated (ATM), ataxia telangiectasia and Rad3-related protein (ATR) and DNA-dependent protein kinase (DNA-PK).

Human cells have evolved many DNA repair systems specific for different types of DNA lesions modulated through activities of various enzyme systems. The mismatch repair (MMR) detects and repairs mispaired DNA bases created by DNA replication errors and thereby improves the fidelity of DNA replication [80]. The base excision repair (BER) is responsible for replacing the damaged bases produced by oxidation, deamination and alkylation. The DNA glycosylase enzyme of BER recognizes and removes the damaged base without significantly disturbing the DNA double helix structure. The damaged base removal creates an abasic (apurinic/apryimidinic) site, which is further filled by synthesis of new DNA by either short-patch repair or long-patch repair pathways of BER [81, 82]. The nucleotide excision repair (NER) eliminates damages that distort DNA double helix such as pyrimidine dimers and intrastrand crosslinks. Two NER sub-pathways are active in human cells: Transcription-coupled NER (TC-NER) and global genome NER (GG-NER). The TC-NER removes the adducts or structures that block the progression of the RNA polymerase enzyme along the actively transcribed DNA strand. GG-NER pathway eliminates bulky DNA lesions formed anywhere in the genome and is independent of transcription. These two sub-

pathways of NER differ only in the initiation process of DNA damage recognition step and share the same enzyme machinery for subsequent repair steps [82, 83].

The DSBs are the most deleterious type of DNA damage and mis-repaired or unrepaired DSBs can lead to genomic instability, carcinogenesis and cell death. The repair of DSBs may proceed through either nonhomologous DNA end joining (NHEJ) or homologous recombination (HR) pathways. The NHEJ pathway is highly error prone as it mediates direct re-ligation of two broken ends of a DNA using Ku proteins (Ku70-Ku80) and DNA ligase IV complex. NHEJ pathway is active throughout the cell cycle because it does not require homologous DNA template for DSB repair [84, 85]. The HR pathway mediates the high-fidelity repair of DSBs using a homologous DNA sequence of the sister chromatids and is only active in S and G2 phases of the cell cycle. The eukaryotic RecA homolog Rad51 protein, mediates the homology search and DNA strand invasion.

The covalently linked interstrand cross links of DNA double helix are most cytotoxic and mutagenic DNA lesions that obstruct essential processes such as DNA replication and transcription. Although the major source of ICLs induction is by DNA cross linking chemicals (mustard gas, mitomycin C, psoralens, cis-platinum), the induction of ICLs by non-ionizing (ultra violet radiation A) and ionizing radiations are also reported [86]. Malondialdehyde, the IR induced byproduct of lipid peroxidation and prostaglandin biosynthesis, acts as a DNA cross-linking agent. The genotoxic ICLs are removed from the eukaryotic cells using the Fanconi anemia DNA repair pathway (FA pathway). The FA pathway repairs the cross-links by utilizing an enzyme system of 19 proteins (FANCA to FANCT) in addition to the components of classic DNA repair

pathways of homologous recombination and nucleotide excision repair [87]. The Fanconi anaemia proteins also play an important role in maintaining genomic integrity through stabilization of replication forks and the regulation of cytokinesis [78, 88].

1.6.2. Cellular defense mechanisms against radiation-induced ROS

The indirect effects of ionization, through radiolysis of cellular water, produce ROS. The ROS consist of free radicals (superoxide, hydroxyl radical) and non-radical oxygen species (singlet oxygen, H₂O₂) formed within a time scale of pico seconds (10⁻¹² s). The highly active ROS damages DNA, proteins and lipids by oxidation, and play an important role in regulation of cell survival. The oxidative stress caused by the radiation disrupts the redox balance of the cells and this disruption activates the cellular antioxidant defense system and redox sensitive transcription factors. The antioxidant defence system consists of non-enzymatic and enzymatic components. The non-enzymatic antioxidants consist of low molecular weight substances such as glutathione (GSH), ubiquinone (coenzyme Q10), ascorbate (vitamin C), α -tocopherol (vitamin E), vitamin A, melatonin, ferritin and lipoic acid, that prevent the oxidation of biomolecules by ROS scavenging. The antioxidant enzymes include superoxide dismutase (which converts O₂⁻ anions to H₂O₂ and O₂), catalase (which converts H₂O₂ to H₂O), thioredoxins (which reduce oxidized proteins), peroxiredoxins and glutathione peroxidase (which reduce peroxides and H₂O₂ to alcohol or H₂O). These enzymes play significant roles in redox homeostasis [89, 90]. The redox homeostasis also modulates the expression of many redox sensitive transcription factors such as activator protein 1 (AP-1), nuclear factor erythroid 2-related factor 2 (Nrf2), nuclear factor κ B (NF- κ B),

hypoxia-inducible transcription factor 1a (HIF-1a), and p53. These transcription factors regulate the increased expression of antioxidant enzymes and modulate other cellular functions such as immunity, inflammation, development, cell proliferation, survival and apoptosis. Most transcription factors modulate a common set of genes that share the characteristics of rapid, but transient induction [91-93]. This set of genes, collectively referred to as ‘immediate early genes’ (IEGs) or ‘primary response genes’ (PRGs), are expressed at low or undetectable levels in many cell types, but are rapidly and transiently activated without the need for ‘*de novo*’ protein synthesis in response to various stimulations, including IR [94]. The biological responses to redox-based signaling rely on the cellular ROS levels: low to medium ROS levels activate stress-responsive survival pathways for survival whereas high levels of ROS promote apoptosis [75, 89, 95].

1.7. Non-targeted effects of ionizing radiation

The non-targeted effects (NTEs) of IR are cellular responses that do not require a direct exposure to cell nucleus [96]. These responses are typically non-linear and are particularly significant at low doses (**Fig.1.4**). The cellular responses induced by NTE depend on radiation dose, quality of radiation (high LET or low LET), duration of exposure, and dose rate [97, 98]. The NTEs include various phenomena such as radiation-induced genomic instability (RI-GI), radiation-induced bystander effects (RIBE) and radiation-induced adaptive response (RI-AR) [12, 34, 37, 99-101]. Both beneficial (protective) as well as deleterious effects of NTEs have been demonstrated in many biological model systems under *in vitro* and *in vivo* conditions [36, 96, 101-103]. A thorough understanding NTE would help to develop proper radiation protection guidelines for the public and occupational workers.

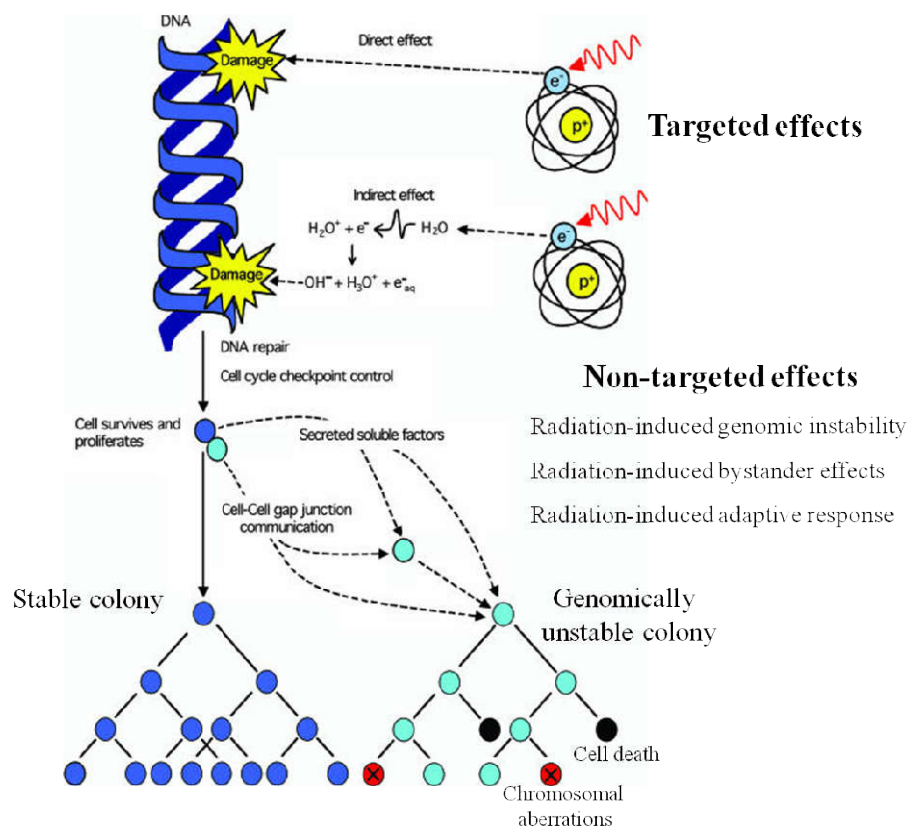


Fig.1.4. Schematic diagram of IR induced targeted (direct and indirect) and non-targeted effects observed in biological systems. Adapted from Morgan and Sowa, 2005 [104].

1.7.1. Radiation-induced genomic instability

Radiation-induced genomic instability (RI-GI) is a non-targeted biological effect of radiation characterized by persistent accumulation of genetic changes within a clonal population of cells. The major genetic aberrations induced by RI-GI include chromosome breaks or aberrations, DNA mutations, micronuclei formation, gene mutations or amplifications, changes in ploidy levels and mini- and microsatellite instabilities. The cellular abnormalities include increased transformation, enhanced rates of apoptosis or cell death. The genetic changes accumulated are transmitted to the clonal progenies of

irradiated cells for many generations after initial exposure [36, 37, 101, 102, 105]. The reports on observations of RI-GI on human populations exposed to radiation and radiation induced human carcinogenesis are highly controversial [96, 106-111].

1.7.2. Radiation-induced bystander effects

Radiation-induced bystander effects (RIBE) is defined as the ability of irradiated (target) cells to elicit the biological responses in neighboring non-irradiated (non-targeted) cells or in cells that receive secreted factors from irradiated (target) cells. The biological responses induced by RIBE in non-irradiated cells were found to be comparable to direct response of irradiated cells. The RIBE has been demonstrated in several *in vitro* and *in vivo* model systems for many biological end points at mGy ranges of low LET radiation and single ion exposure of high LET radiation [34, 35, 96, 99, 101, 105, 112, 113]. The UNSCEAR (2006) classified the bystander effects observed by the cell types into four subcategories: (1) Bystander effects after cytoplasmic irradiation (2) Bystander effects after low fluences of alpha particle irradiation (3) Bystander effects after irradiation with a charged-particle microbeam (4) Bystander effects after transfer of medium from irradiated cells [96].

1.7.3. Radiation-induced adaptive response

Radiation-induced adaptive response (RI-AR) is the phenomena where a sublethal conditioning dose (priming dose) of IR reduces the detrimental effects of subsequent higher IR dose (challenging dose). The biological responses induced by RI-AR is generally reliant on the priming dose, challenging dose, adaptive window time,

radiation type, dose rate, cell systems, cell culture conditions and stage of the cell cycle [96]. The RI-AR phenomena was first reported by Olivieri, et al (1984) in human lymphocytes as reduction in frequency of radiation induced chromosomal aberrations [114]. The RI-AR has since been observed in a variety of endpoints, including decreased frequency of chromosome aberrations, micronucleus formation, DNA damage induction, mutation rate, sister-chromatid exchanges, cell transformations, altered gene or protein expressions, and apoptosis or cell death. There is some evidence to suggest RI-AR in human populations exposed to environmental or occupational sources. Human PBMCs taken from individuals residing in HLNRA of Kerala, India, when challenged with a high dose radiation showed adaptive response for induction of micronuclei and DNA strand breaks as compared to individuals from NLNRA [70-72]. The peripheral blood samples from individuals residing in HLNRA of Ramsar, Iran also showed lower induction of micronuclei frequency and chromosome aberrations after a challenge with a high dose, as compared to subjects from control areas [103, 115, 116]. Similar results with micronuclei frequency after a high challenge dose were also observed in human lymphocytes from medical radiation workers and nuclear workers [117, 118]. On the other hand, lymphocytes collected from children chronically exposed to radiation doses from Chernobyl accident fallout showed no evidence of radio-adaptive response after challenge dose exposure for the endpoints (chromosome and chromatid aberrations) studied [119]. The precise mechanism of action of RI-AR is not fully elucidated, leading to ambiguities. There are several probable mechanisms of the RI-AR that have been suggested. These include activation of cellular defence mechanisms, apoptosis, gene expression and alteration in expression of existing proteins or expression of new proteins

etc. [34, 96, 103, 120, 121]. A study conducted by our group on human PBMCs showed critical role of antioxidant responses mediated through concerted activation of NF- κ B and Nrf2 during RI-AR of human cells [120]. Other studies have indicated role of NHEJ and BER genes in RI-AR of human PBMCs [122, 123].

1.8. Radiation proteomics using advanced quantitative proteomics techniques

Proteins are considered building blocks of life and key functional molecules of the cell. The term proteome can be defined as the entire protein complement expressed by a genome and proteomics as the analysis of proteins in a cell, tissue, or organism under defined conditions [124]. Generally, the number of genes cannot be directly correlated with actual protein levels or protein function due to the regulation of gene expression at multiple levels during transcription, translation and post-translational modification. Protein expression pattern of an organism is also regulated by several other factors like cell types, tissue types, development stage and environmental stresses including radiation [125, 126]. Thus, the whole proteomic analysis may provide more mechanistic information in a single experiment than gene expression profiling and more accurate information than could be obtained from measurements of a small set of proteins. Radiation proteomics involves systematic analysis of radiation modulated proteins in a cell, tissue or organism at a given time and state. It is an advanced and powerful tool to detect protein biomarkers of IR exposures [7, 8]. The radiation proteomics study covers not only changes in IR induced protein expression but also its function, modifications, structure and interactions.

Quantitative proteomics refers to the ability of a method to detect small changes in protein or peptide abundance (absolute or relative) in response to a changed state under defined conditions. The absolute quantification is used to determine actual amount or copy number of target protein in a sample, where as relative quantification is used to calculate the relative change in expression of target proteins between two different conditions. Many proteomic platforms such as gel-based (two-dimensional electrophoresis) or gel-free (label-based or label-free) techniques in combination with mass spectrometric (MS) techniques are used for quantitative proteomic (protein expression changes) analysis. Each technique has its own advantages and limitations, and combinations of these methods may provide better coverage of proteome [127].

1.8.1. Gel-based quantitative proteomics methods

The standard gel-based technique combines protein separation by sodium dodecyl sulfate polyacrylamide gel electrophoresis (SDS-PAGE) and identification of the separated proteins by mass spectrometry techniques. The most widely used gel-based quantitative proteomics platforms are two-dimensional gel electrophoresis (2DE) and two-dimensional difference in-gel electrophoresis (2D-DIGE) that resolves proteins on the basis of their physicochemical properties [125, 128, 129].

Two-dimensional gel electrophoresis combined with matrix-assisted laser desorption ionization-time of flight mass spectrometry (MALDI-TOF MS) techniques is considered to be the preferred method to resolve and array proteins since it provides quantitative maps of intact proteins. It is simple, robust, low cost technology and relatively easy to implement in molecular biology experiments using whole cell protein

extracts from different cell or tissue types. Proteins are resolved in first dimension with isoelectric focusing (IEF) based on the isoelectric point (pI) and in second dimension with SDS electrophoresis based on molecular weight (**Fig.1.5A**). The post run visualizations of protein spots is achieved using visible stains (silver and coomassie blue staining) or fluorescent stains (sypro ruby and deep purple). The sensitivity of the technique is ~1 ng protein per spot. The high resolving power of the technique enables us to visualize hundreds of proteins, including isoforms and post-translational modifications in a single run. After staining and image acquisition, further software based image analysis is required to detect differentially modulated proteins. The software programs commonly used for image analysis are PDQuest (Bio-Rad), Melanie (Gene Bio), Image Master 2D Platinum (GE Healthcare), Dymension-3 (Syngene) and Progenesis (Shimadzu Biotech). The total snap shot of cellular proteins provided by the 2D gels may be used to assess the sample quality and reproducibility of the sample preparation process [130-136]. However, it is highly labor intensive technique and requires experienced technicians to obtain reproducible results. The inherent gel to gel variation created due to differences in run parameters necessitates technical replicate gels for each biological sample. It is very difficult to focus and detect highly acidic, basic, hydrophobic, membrane proteins and low abundant proteins on 2D gels. Moreover, proteome coverage by 2DE is experimentally limited to 10-120 kD molecular mass with display of abundant proteins from total cell lysates [129, 134, 137]. However, despite the advent of newer technologies, 2DE still remains a mature, widely accepted and successfully implemented top-down method for providing simultaneous information on abundance, charge and various isoforms of thousands of proteins in a single run [138].

An advanced version of conventional 2DE, the 2D-DIGE technique differentially labels protein mixtures from different experimental groups with fluorescent tags. The reproducibility and sensitivity is higher compared to conventional 2D gels, and it also shows greater ability to detect protein isoforms and post-translational modifications. This technique resolves pre-stained protein samples with cyanine-based fluorescent dyes (Cy2, Cy3, and Cy5) of distinct excitation and emission wavelengths on the same gel (**Fig.1.5B**). The similar mass and charge of cyanine dyes enables co-separation of identical proteins under similar electrophoretic conditions, and thereby minimizes the gel-to-gel variation. As a gel based technique it still faces same technical limitations associated with conventional methods. Moreover, labelling of lysine and cysteine amino acids limits the protein coverage on the gels. The manual excision of protein spot for identification with mass spectrometry is also problematic [129, 135, 139-143].

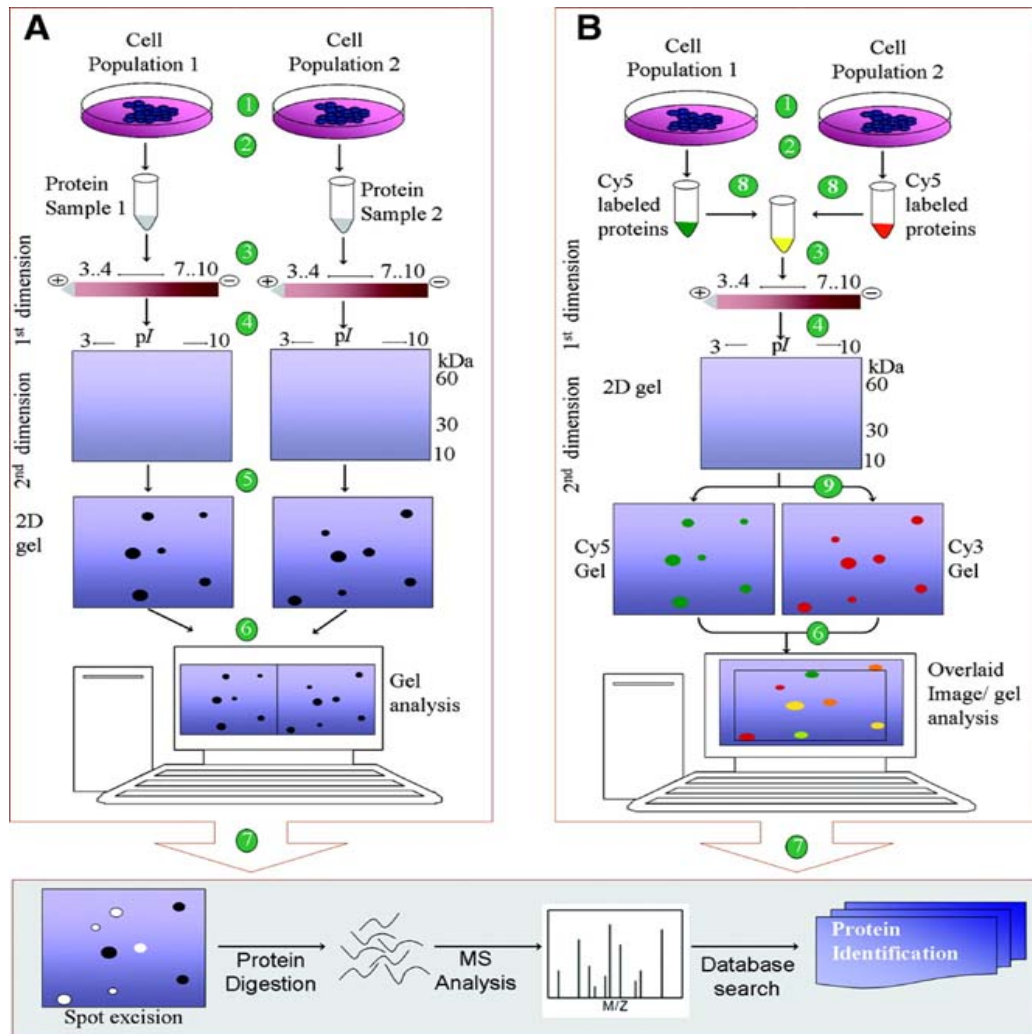


Fig.1.5. Schematic diagram showing general workflow of protein separation, identification and quantification with (A) two-dimensional gel electrophoresis (2DE) (B) difference in-gel electrophoresis (DIGE) technique. Adapted from Baharvand, H., A. Fathi, et al., 2007 [144].

1.8.2. Gel-free quantitative proteomics methods

The gel-free proteomic quantification methods are mainly dependent on liquid chromatography (LC)-based separation and mass spectrometry (MS)-based identification or quantification of proteins. It generally uses micro- or nano-capillary reverse phase HPLC column (μ -LC or n-LC) for chromatographic separation of peptides based on relative hydrophobicity (hydrophobic C18 columns as stationary phase and polar solvents as mobile phase). Electro spray ionization (ESI) based tandem mass spectrometry (MS/MS) instruments such as quadrupole-time of flight (QTOF), linear ion trap quadrupole (LTQ), LTQ-Orbitrap and Tribrid mass spectrometer (MS3) ion trap-Orbitrap (Orbitrap Fusion™) platform are generally used for protein identification and quantification [128, 145-148]. The gel-free are mainly classified into two categories: label-based (metabolic labeling and chemical labeling) approaches and label free (spectrum counting and ion intensity-based) approaches. A typical proteomic workflow includes (1) Proteomic sample preparation with trypsin digestion (2) Separation of tryptic peptides by LC (3) Analysis with tandem MS (4) Data analysis for protein identification and quantification (**Fig.1.6**). These methods allow multiplex experiments which compare more than one treatment conditions in a single LC-MS. The gel free methods can be used for absolute or relative quantification and has the ability to detect post-translational modifications [148-153]. It offers improved dynamic range, accuracy and high-throughput compared to conventional gel based methods.

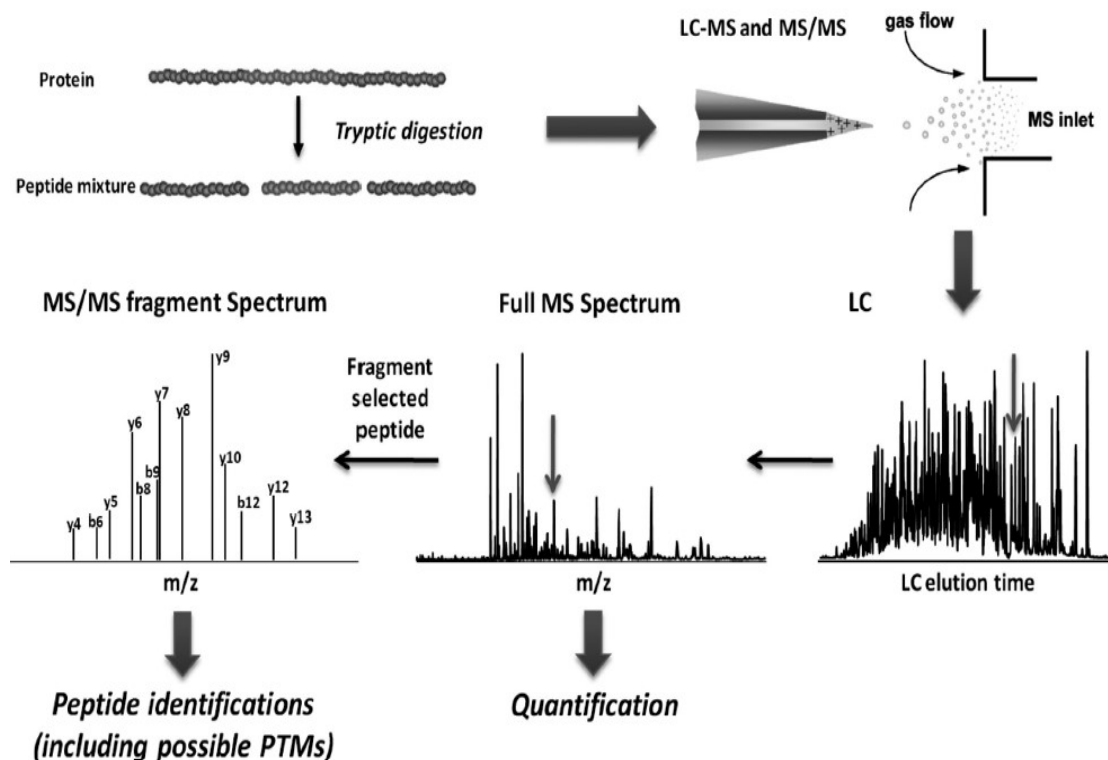


Fig.1.6. Schematic workflow used for LC-MS/MS based global quantitative proteome analysis. Adapted from Xie et al., 2011[153]

1.8.2.1. Label based methods

The label-based methods use stable-isotope or isobar tags to label proteins or tryptic peptides and the quantification is achieved by calculating the MS/MS intensity of the specific peptide tags from the target proteins by a mass spectrometer. The labels are introduced into proteins or peptides by metabolic or chemical methods. In metabolic labeling, labeled isotopic or heavy amino acids (^{13}C -arginine, ^{15}N -lysine) are incorporated into the cellular proteins through the growth medium (**Fig. 1.7**). The most popular metabolic proteomic quantitative technique is SILAC (Stable Isotopic Labeling of Amino Acids in Cell Culture) method. In SILAC experiments, cells are cultured in growth media containing normal or heavy labeled (^{13}C -arginine, ^{15}N -lysine) amino acids

for 6–8 passages and the MS¹ spectral intensities are compared between normal and heavy labeled peptides for relative quantification. However, protein identification is available from MS/MS scan. The use of SILAC methodology is limited to only few biological samples because of the metabolically active incorporation of isotopic amino acids and is not suitable for primary cells or non-culturable cells. Moreover, the methodology is highly laborious, expensive and multiplexing is limited to maximum three experimental conditions [127, 152-156].

In chemical labeling, isotopic or isobaric tags are introduced into the cellular proteins by chemical reaction and not through biological metabolism. This method incorporates the chemical tags by forming covalent links with the proteins rather than using the cellular metabolism and thereby can be introduced into all type of protein (cellular, tissue and biofluids) samples. The multiplexing ability of chemical labeling methods is higher compared to metabolic labeling methods (**Fig.1.7**). The major chemical labeling methods used for quantification are isotopic (ICAT: Isotope-Coded Affinity Tags) and isobaric (iTRAQ: Isobaric Tags for Relative and Absolute Quantification; TMT: Tandem mass tag). The ICAT methodology is suitable mainly for cysteine containing proteins which greatly reduces its applicability in quantitative proteomics field. The ICAT labeling may change the chromatographic retention time of labeled peptides and the presence of biotin group in the mass spectrum may interfere with protein database search [147, 157].

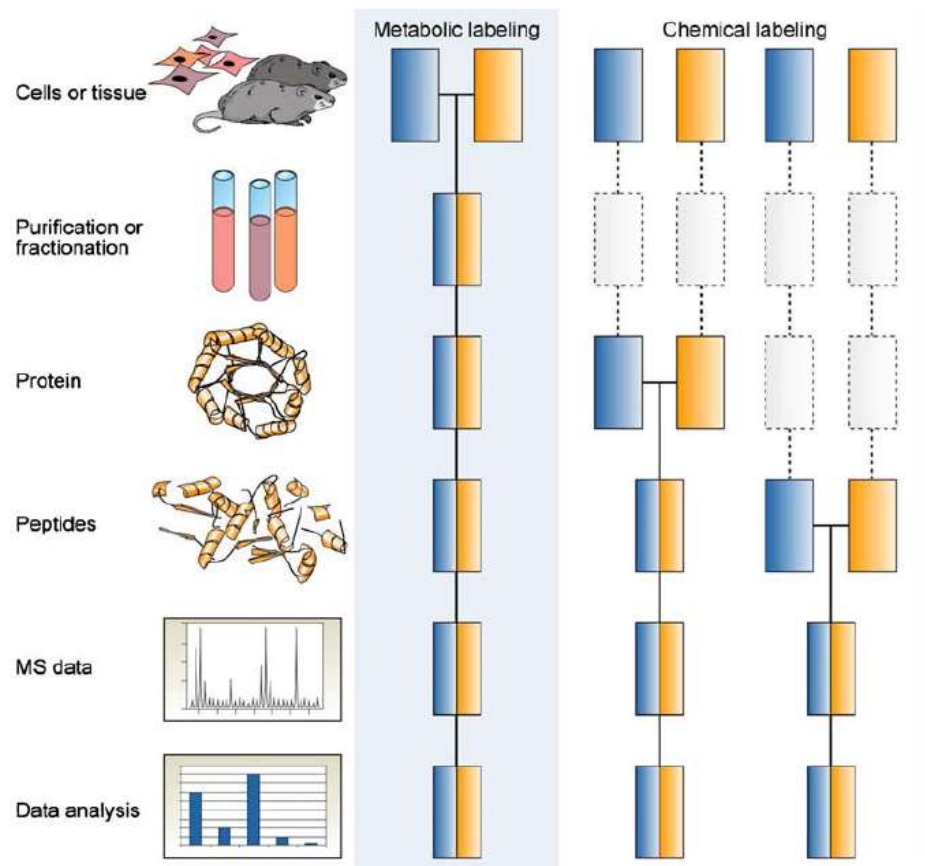


Fig.1.7. Label based gel free quantitative proteomics methods using mass spectrometry. The blue and yellow boxes represent two different experimental conditions. Horizontal thick lines indicate the stage at which experimental samples are combined prior to further analyses and the dashed lines indicate possible stages for introduction of experimental variation. Adapted from Bantscheff et al., 2007 [154].

The most common and widely used isobaric label based approach for relative protein quantification is iTRAQ and TMT. The isobaric tags comprises of a charged reporter group (which release unique reporter ions during MS/MS cleavage), neutral balance group (which maintain overall mass of isobaric tags) and peptide reactive group (amine specific reactive group). These peptide reactive groups of isobaric tags react with

primary amines (N-terminus amines and ϵ -amino group of lysine) to form a covalent linkage with target proteins. The availability of multiplex tags enable simultaneous analysis of multiple samples in a single LC-MS/MS (iTRAQ: up to 8 samples; TMT: up to 16 samples) analysis. The isobaric peptides generated from multiple experimental conditions generally co-elute from the LC column and appears as a single peak at MS level, and the MS/MS fragmentation releases the signature reporter group with neutral loss of balance group. The intensity of unique reporter ions released during the fragmentation of the isobaric tags at MS/MS level are used to quantify target proteins since the reporter ion intensity is directly proportional to the labeled peptide from the target proteins. Moreover, the strong signature b-ions and y-ions produced at MS/MS levels allow simultaneous protein identification along with protein quantification. The commercially available iTRAQ reagents developed by AB Sciex (Framingham, MA, USA) can be used to compare 4 to 8 different biological samples in a single experiment. The iTRAQ reagent comprises of dimethyl piperazine as reporter group, carbonyl group as balance group and N-hydroxy-succinamide (NHS) esters as peptide reactive group (**Fig.1.8**). The mass range of reporter group varies from 114-117 Da (with balance mass 31-28 Da) with a total mass tag of 145 Da in 4-plex reagents, where as the mass range is from 113-121 Da (with balance mass 192-184 Da) with a total mass tag of 305 Da in 8-plex reagents. The reporter mass of 120 Da (with balance mass 185 Da) is omitted from 8-plex reagents to avoid contamination of spectra with phenylalanine immonium (m/z 120.08) ion. The MS/MS fragmentation of the iTRAQ reagents will release unique reporter groups at m/z 114, 115, 116 and 117 in a 4-plex reaction, and reporter ions at m/z 113, 114, 115, 116, 117, 118, 119 and 121 in an 8-plex analysis [145, 147, 158-160].

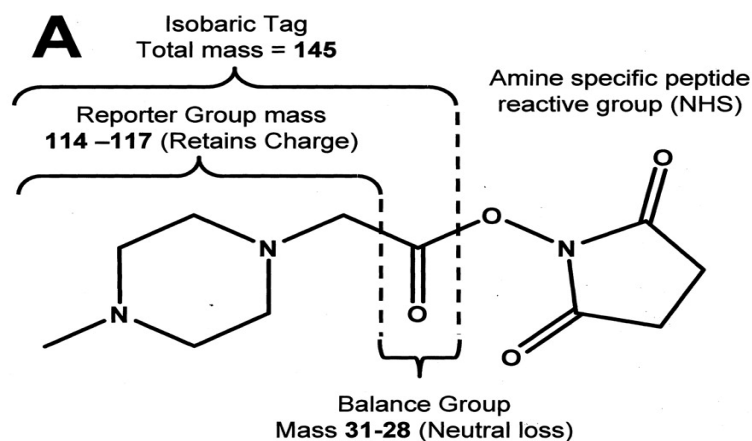


Fig.1.8. Chemical structure of an iTRAQ reagent. The charged reporter group, neutral balance group and primary amine reactive peptide groups are labeled. Adapted from Philip L. Ross et al., 2004 [158].

The TMT reagents manufactured by Thermo Scientific (Rockford, IL, USA) has similar amine labeling chemistry (N-terminus and ϵ -amine group of lysine in peptides) as iTRAQ reagents with slight variation in the reporter group structure. The basic structure of TMT reagents comprises a charged reporter group, neutral balance group and amine reactive peptide reactive group (**Fig.1.9**). TMT reagents enable relative quantification of proteins up to 10 different biological samples [146, 147].

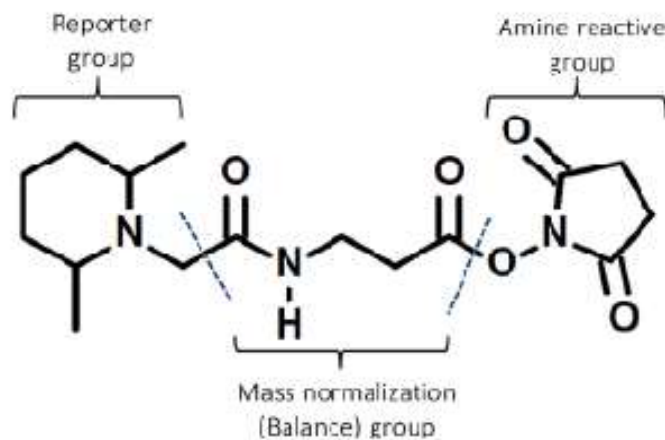


Fig.1.9. Chemical structure of a generic TMT reagent. The charged reporter group, neutral balance group and primary amine reactive peptide groups are labeled. Adapted from Rauniyar et al., 2014 [146].

The advantage of chemical labeling methods over metabolic labeling is its high labeling efficiency due to covalent linkage with target proteins. This methodology can be used to label any protein sample derived from multiple sources such as cells, tissue samples or biological fluids and have high relevance for clinical applications. The higher multiplexing potential of the technology can be employed for time course and dose responses studies in different model systems. However, variations in sample processing may introduce experimental errors. To overcome these variations sufficient technical replicates should be used during analysis. The use of primary amine-containing buffers (Tris buffers and ammonium bicarbonate buffers) should be avoided for efficient labeling of proteins. The analysis with isobaric or isotopic tags are also more costly compared to gel based methods.

1.8.2.2. Label free based methods

The label free quantitative proteomic methods perform quantitation of peptides or proteins without using any stable chemical tags with LC based tandem mass spectrometry instruments. The label free strategies are simple, cost-effective and can be used with all type of biological (cells, tissues and biological fluids) samples (

Fig.1.10). The methodology is less prone to variations caused by chemical labelling methods and can be used for the analysis of unlimited number of samples. The label free based relative quantification methods are broadly classified into spectrum counting approach and peptide peak intensity-based approach [153, 159]. However, the method relies heavily on the MS/MS fragment data of peptides both in number and abundance for protein quantification. Moreover, multiplexed comparative proteomic analysis of the samples in a single MS run is not possible [151].

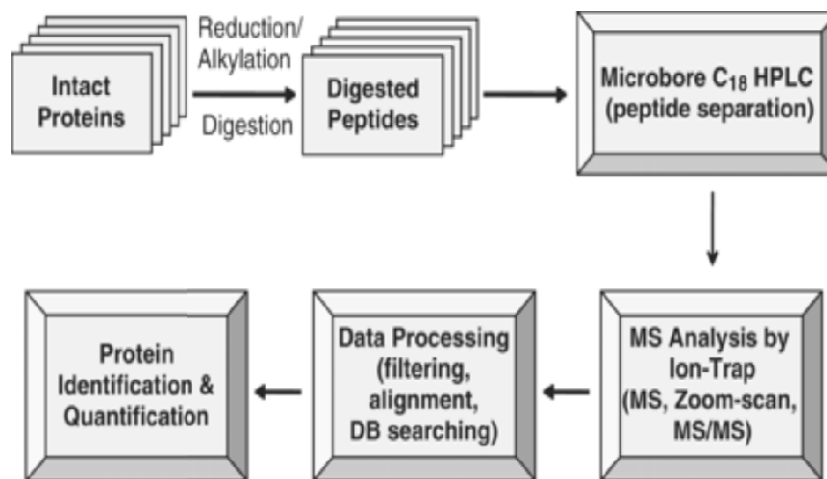


Fig.1.10. General workflow chart for LC/MS-based label-free protein quantification. Adapted from Brown et al., 2008 [161]

1.9. Evidences of radiation-induced alterations in the cellular proteome

Many models have been used to study the effects of IR on cellular proteome. Majority of the studies are based on mammalian tumour cell lines and high dose single exposures. There is limited information available on the time and dose response of proteins after irradiation with non-transformed primary cell systems [6, 126, 162]. The extrapolation of available data generated with cell culture or animal model systems to humans is considered inappropriate [163]. To investigate the effect of radiation directly on humans, human PBMCs are considered ideal because of ease of collection from individuals through minimally-invasive means. They also show low inter-individual variation as compared to other biofluids. Also, since these cells are in the G₀ resting stage of the cell cycle, they may effectively mimic the *in vivo* conditions. The PBMCs are considered to be highly radiosensitive and therefore, can be used as sensitive indicators to capture early molecular events following IR [164]. Very few studies are available which discuss whole proteome changes in human PBMCs with radiation under *in vitro* conditions [165-167]. A major drawback of most of these studies has been that only one or two biological replicates were used. Due to large variation of responses observed between the individual donors, firm confirmation of results could not be achieved [167]. This necessitates the need to study the radiation induced changes in whole proteome of human PBMCs by using more number of biological replicates. Moreover, there is no information about the effects of chronic low dose exposures on human proteome.

1.10. Objectives of the thesis

Radiation proteomics offers great promise to understand not only ‘real-time’ dynamic changes in the cell due to radiation but also to study the adaptive response (AR) that may be mounted to maintain homeostasis in the cellular system. There are only a few studies that present whole proteome changes in response to acute low dose radiation and none with continuous low dose radiation. The human population residing in the HLNRA of Kerala, India offers a unique prospect of providing mechanistic understanding of cellular effects of low dose radiation directly on humans. This being the first ever such study on HLNRA, a combination of gel-based (2DE-MS) and mass spectrometry based gel-free (iTRAQ) quantitative proteomic method was proposed to provide an exhaustive list of processes altered with low dose.

The specific objectives of the thesis are:

- 1) Proteomic profiling of human PBMCs with acute *in vitro* ionizing radiation
- 2) Proteomic profiling of human PBMCs from High Level Natural Radiation Areas of Kerala to understand effects of chronic low dose radiation
- 3) Proteomic approach to understand radio-adaptive response in human PBMCs exposed to chronic low dose radiation

CHAPTER 2

MATERIALS and METHODS

2.1. Ethics statement

Ethics permission for the project was obtained from the Medical Ethics Committee, Bhabha Atomic Research Centre (BARC), Mumbai, India. Blood samples were collected from healthy volunteers with written informed consent. Personal information was collected using a standard questionnaire as per the guidelines of the ethics committee.

2.2. Blood sample collection

Human peripheral blood samples were collected from random healthy adults in sterile EDTA lined vacutainers (BDTM Vacutainers, NJ, USA). Approximately 10-12 ml of venous blood was collected from each individual using standard venipuncture technique with a hypodermic needle by a trained pathologist. The details of the samples collected (number of samples, age and gender) used for the each study are given in the respective results section (Chapter 3) of the thesis.

2.2.1. Acute radiation exposure studies

The blood samples for acute *in vitro* irradiation studies were collected from Mumbai region of Maharashtra state at the Trombay Dispensary, Medical Division, BARC, Mumbai. Samples were collected from each individual during the same time of the day to minimize variations. The samples were processed within 30 min of blood withdrawal to maintain consistency of processing.

2.2.2. Chronic radiation exposure studies

The samples for chronic irradiation studies were collected from HLNRA of Kerala, India. The control samples were collected from individuals living in adjoining NLNRA of Kerala, India. Volunteers were brought to the Government Community Health Centre, Kollam district, Kerala for blood collection and samples transported to the Low-Level Radiation Research Laboratory (LLRRL), Kollam at 0° C for further processing.

A halogen quenched Geiger Muller (GM) tube-based survey meter (Type ER-709, Nucleonix Systems, India) was used to measure the external gamma radiation levels in each subject's house. The survey meter was placed at a height of 1 m above the ground level to measure the indoor and outdoor radiation in $\mu\text{R/h}$. The indoor radiation measurements were taken from the room with a maximum occupancy and outdoor measurements were taken at a distance of 3 m from the main entrance of the subject's dwelling. A mean of three readings was taken for each measurement. A conversion factor of 0.0767 ($= 0.8763 \times 24 \text{ h} \times 365 \text{ days} \times 10^{-5}$) was used to convert the measured absorbed doses in air ($\mu\text{R/h}$) into annual absorbed dose (mGy/y). The age and sex specific occupancy factor used for the calculation were according to an earlier study [16].

2.3. Isolation of peripheral blood mononuclear cells

The PBMCs were isolated from whole blood using density gradient centrifugation with Histopaque-1077 (Sigma Aldrich, St Louis, USA) at room temperature. The blood samples were carefully overlaid on the histopaque media in a ratio of 1:1 (v/v) in a 15 ml sterile polypropylene tube and centrifuged at 400 g at room temperature for 30 min.

The buffy layer containing PBMCs was collected and the supernatant containing plasma or platelets was discarded. The isolated PBMCs were washed twice with ice-cold 1x Phosphate Buffered Saline (PBS) pH 7.4 at 250 g for 10 min. The collected pellets were re-suspended in ice cold RPMI-1640 (Sigma Aldrich, St Louis, USA) supplemented with 100 U/ml penicillin and 100 mg/ml streptomycin. For each isolation, cells were counted and their viability assessed by trypan blue (0.4 %) exclusion method.

2.4. Irradiation of human PBMCs

The isolated PBMCs were irradiated in 500 μ l of RPMI-1640 media at room temperature using a ^{60}Co gamma ray source (Blood irradiator, 2000, BRIT, India). The radiation doses (Gy) and dose rates (Gy/min) used for irradiation of samples for each study is mentioned in the respective results sections. The irradiated cells were incubated in RPMI-1640 media at 37°C in a humidified, 5% CO₂ atmosphere for the required time before analysis. Unirradiated cells incubated under similar conditions for the same duration served as sham- irradiated control.

2.5. Cell viability analysis by flow cytometry

The cells (1×10^6 cells/ml) were prepared for the propidium iodide based flow cytometry analysis as described by Riccardi and Nicoletti (2006) with slight modifications [168]. In brief, cells were irradiated with 300 mGy and 1 Gy dose and incubated for 1 h and 4 h post-irradiation at 37 °C in a humidified, 5% CO₂ atmosphere. At the respective time points, the cells were harvested and washed twice with ice-cold PBS buffer (pH 7.5). The cell pellets were re-suspended in PBS containing 50 μ g/ml propidium iodide, 0.1% sodium citrate (w/v) and 0.1% Triton X-100 (v/v), and incubated

in dark for 1 h. After incubation, the cells were harvested and analyzed for sub-diploid (sub G1) peak. A total of 10,000 cells were acquired with a flow cytometer (Cyflow, Partec) and analyzed using FloMax[®] software. Sham-irradiated control cells were processed in a similar manner. All chemicals were procured from Sigma-Aldrich Corp MO, USA.

2.6. DNA damage analysis by alkaline comet assay

The DNA strand breaks induced by radiation in human PBMCs was measured with alkaline comet assay. The PBMCs (1×10^6 cells/ml) were irradiated (300 mGy and 1 Gy) and incubated at 37 °C in a humidified, 5% CO₂ atmosphere for the required time (5 min, 1 h and 4 h post-irradiation) under minimal light to prevent introduction of additional DNA damage in the cells. Sham irradiated cells incubated under similar conditions for the same duration served as control. The fully frosted slides were evenly layered with cell suspension containing low-melting agarose (0.8% in 0.9% saline) and incubated for solidification. Two slides were prepared per experimental point for each individual. The slides were immersed in lysis buffer (2.5 M NaCl, 100 mM EDTA, 1% Triton X-100, 10 mM Tris-Cl, pH 10.0 and 10% DMSO) for 1 h at 4 °C. After the incubation time, the lysis buffer was replaced with alkaline buffer (300 mM NaOH, 1 mM EDTA pH \geq 13.0) and incubated at room temperature for 20 min. Electrophoresis was performed at 25V constant voltage for 30 min. After electrophoresis, the slides were washed with neutralizing buffer (0.4 M Tris-HCl, pH 7.5) and stained with SYBR Green II. The images (50 images per slide) were captured with a fluorescence microscope (Carl Zeiss Axio-vision) at 40 \times magnification. The SCGE-PRO image analysis software was used to analyze the acquired images for % DNA in comet tail [169].

2.7. Preparation of protein extracts from PBMCs for proteomics

Protein extracts were prepared from PBMCs by sonication in cell lysis buffer (10 mM Tris buffer, pH 7.0) containing 1x protease inhibitor cocktail (Roche Diagnostics, Mannheim, Germany). A pulse 'On' of 10 seconds and pulse 'Off' of 30 seconds at an amplitude of 40 was used to sonicate the cells with an ultrasonicator (Misonix, USA). The cells were maintained on ice during the process of sonication. The cell extract was centrifuged at $20,000 \times g$ for 40 min at 4 °C and the clear supernatant containing proteins was collected.

2.8. Protein estimation by BCA protein assay

The protein concentration was determined by bicinchoninic acid (BCA) method using bovine serum albumin (BSA) as the standard as recommended by the manufacturer (Bangalore Genei, India). In brief, the working BCA reagent (WR) was prepared by mixing reagent A (BCA, sodium carbonate, sodium tartrate and sodium bicarbonate in 0.1 M NaOH) with reagent B (4% cupric sulfate) in a ratio of 50:1(v/v). A series of dilutions of BSA standard were prepared ranging from 0.5 mg/ml to 1 mg/ml from 5 mg/ml of stock solution. The BSA standards and the unknown protein samples were mixed with WR in a microplate and incubated at 37°C for 30 min. After the incubation, OD was measured at 562 nm on a plate reader and the concentration of the unknown sample was prepared from the BSA standard curve. A representative standard curve of BSA is shown in the **Fig.2. 1**.

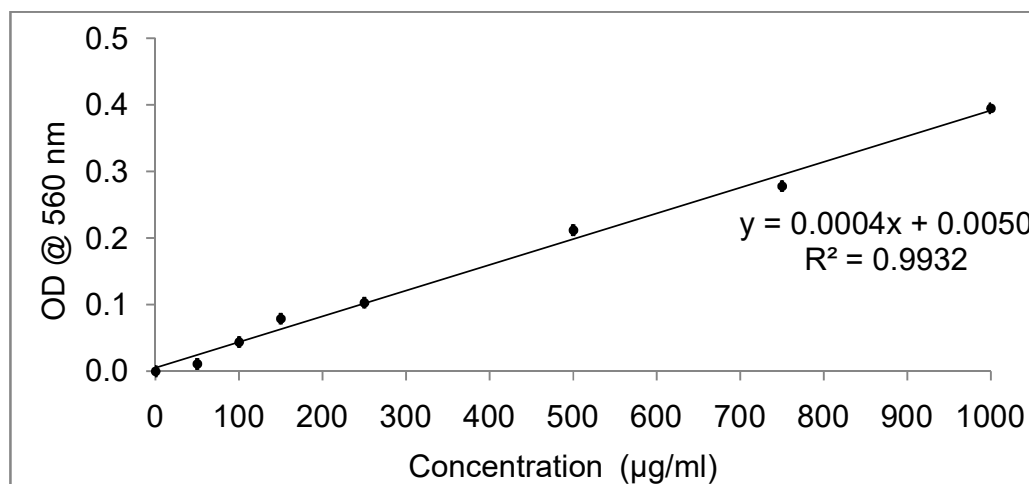


Fig.2. 1. Representative standard curve of BSA used for protein estimation

2.9. Two-dimensional polyacrylamide gel electrophoresis

The prepared protein extracts were treated with benzonase endonuclease (Sigma-Aldrich MO, USA) at a final concentration of 0.5 U/µl of protein extract for 30 min at 37°C to remove nucleic acid contaminations. The cell extracts were further purified with Ready Prep 2D clean up kit (Bio-Rad, CA, USA) before loading on immobilized pH gradient (IPG) strips (Bio-Rad, CA, USA).

2.9.1. Isoelectric focusing of extracted proteins

The IPG strips (17 cm) were rehydrated with pre-estimated protein samples dissolved in rehydration buffer (7 M urea, 20 mM Dithiothreitol (DTT), 4% 3-[(3-cholamidopropyl)-dimethylammonio]-1-propanesulfonate (CHAPS), 0.2% carrier ampholytes, 0.0002% bromophenol blue). IPG strips of two pH ranges: pH 4-7 and pH 3-10 were used in the study. The protein samples (1000µg) were introduced into the IPG strips by passive method of rehydration using disposable rehydration trays. Isoelectric

focussing (IEF) was performed at 20 °C in a Protean IEF cell (Bio-Rad) using a three step programme: 250 V for 20 min, 10,000 V for 4 h, and finally 60,000 Volt-h. After IEF, the strips were equilibrated first in an equilibration buffer I [6 M urea, 2% SDS, 0.05 M Tris-Cl (pH 6.8), 20% Glycerol and 2% DTT], and then in equilibration buffer II containing 2.5% iodoacetamide instead of DTT.

2.9.2. Second Dimension electrophoresis

The second dimension electrophoresis was conducted using a Protean II XL cell (Bio-Rad, CA, USA) vertical gel electrophoresis system on 10% polyacrylamide SDS-PAGE gels [30% acrylamide/ N,N'-methylbisacrylamide solution, 1.5 M Tris (pH 8.8), 10% SDS, 10% APS, TEMED]. The gels were run at a constant voltage of 85 V at 4 °C until the bromophenol blue dye migrated out of the gel. For molecular weight range determination, molecular weight markers (Bangalore Genei, India) were applied during SDS-PAGE. All the chemicals used for 2DE were procured from Bio-Rad CA, USA.

2.9.3. Gel Staining

After electrophoresis, 2DE gels were rinsed with milliQ water to remove excess SDS detergents and incubated with a fixative solution (50% methanol and 10% acetic acid in deionized water) for 30 min on a rotary shaker with gentle mixing. After fixation, the gels were stained with coomassie blue R-250 for 5-6 h on a rotary shaker. The de-staining was performed with a de-staining solution (10% methanol and 10% acetic acid in deionized water) on a rotary shaker. The images were digitally acquired with a resolution of 300 dpi using a gel documentation system (Syngene, UK) or Image Scanner III (GE Healthcare, IL, USA) and saved as TIFF (Tag Image File Format) format.

2.9.4. Gel image processing and analysis

The 2D gel images were processed using PDQuest software (ver 8, Bio-Rad, CA, USA). The 2D gel images were loaded into the PDQuest and clustered into control and treatment groups for comparative proteomic analysis. Each protein spot on the gel was marked by a standard spot number (SSP#), automatically assigned by the software. Manual editing was done to correct ambiguous protein spots. Spot height (also known as peak value) of the Gaussian spot was employed to quantitate the level of each protein spot. The 2DE gels from all the samples of each treatment group were normalized together and a master gel (reference gel) was prepared using extensive matching and land-marking. The normalization factor was computed based on the raw quantity of each spot in a member gel, divided by the total quantity of valid spots in the gel. The normalization procedure allowed compensation for subtle differences in sample loading and inconsistencies in gel staining. Only the proteins which were present in all biological and technical replicates were considered for data analysis. The normalized spot intensity values of all the quantified protein spots were exported into Microsoft Excel (Microsoft Corporation, USA) for further statistical analysis.

2.10. Protein identification by matrix-assisted laser desorption ionisation-time of flight mass spectrometry

The protein spots of interest were excised manually from the gels for identification. The gel plugs were destained by repeated washings with 50 mM NH_4HCO_3 /acetonitrile (ACN) (v/v). An enzymatic in-gel digestion was performed with trypsin (25 ng/ μl) overnight at 37°C. The tryptic peptides were eluted with serial

extractions with 0.1% trifluoroacetic acid (TFA), 0.1% TFA in 50% ACN and 100% ACN. The reconstituted peptide fragments (0.1% TFA in 50% ACN) were then mixed (v/v) with matrix-assisted laser desorption ionisation-time (MALDI) matrix (α -cyano-4-hydroxycinnamic acid or alpha-matrix) and analysed with MALDI-TOF mass spectrometry (TOF-MS) (UltraFlexII or Autoflex, Bruker Daltonics, Germany) in positive ion reflector mode. The mass range (m/z 800–4500) was externally calibrated using the peptide calibration standard (Bruker Daltonics) with nine standard peptides. The peak list was processed using Flexanalysis 3.0 software (Bruker Daltonics) and searched against SWISS-PROT database, specified for *Homo sapiens* taxonomy using Mascot search engine (<http://www.matrixscience.com>). The search parameters were set as one missed cleavage, fixed modifications as ‘carbamidomethyl on cysteine’, and variable modification of ‘oxidation on methionine’, error tolerance of ± 100 ppm for Peptide mass fingerprinting (PMF) and ± 0.5 Da for MS/MS ion search. Protein matches were computed using a probability based Molecular Weight SEarch (MOWSE) score, and MOWSE scores greater than 56 were considered as significant ($P \leq 0.05$).

2.11. Proteomic analysis by HR-LC based iTRAQ method

Equal quantities (w/w) of proteins extracts from each of the 10 samples per experimental group (NLNRA and HLNRA groups) were pooled for iTRAQ analysis. The proteins in the pooled samples were precipitated using 10% trichloroacetic acid (TCA) by centrifugation at 18,000 g for 10 min at 4°C. The protein pellet was washed thrice with ice-cold acetone at 18,000 g for 10 min at 4°C to remove traces of TCA. The washed protein pellet was dissolved in dissolution buffer (pH 8.5) containing 0.5M triethylammonium bicarbonate (TEAB) provided with the iTRAQ Reagent Multiplex kit

(Sigma-Aldrich Corp. MO, USA) and centrifuged at 20,000 g for 10 min to collect the supernatant. The protein concentration of the supernatant was re-estimated with BCA assay with bovine serum albumin as a standard.

2.11.1. In-solution tryptic digestion

In-solution digestion of the pooled proteins (100 µg) from each experimental group was performed with sequencing grade modified trypsin (Promega, Madison, WI, USA). Each sample aliquot was treated with denaturant (2% SDS) for 1 h at room temperature. Disulfide bonds of proteins were reduced with 50 mM tris-(2-carboxyethyl) phosphine (TCEP) at 60°C for 1 h on a thermomixer (Eppendorf, Hamburg, Germany). Alkylation was performed by replacing the TCEP solution with cysteine-blocking reagent (200 mM iodoacetamide). After 30 min of incubation in the dark, the proteins were digested with trypsin with a substrate-to-enzyme ratio of 20:1 overnight at 37° C. The digested peptides were concentrated using a vacuum centrifuge (Eppendorf, Hamburg, Germany).

2.11.2. iTRAQ labeling of tryptic peptides

The extracted tryptic peptides concentrated by vacuum centrifugation were reconstituted with 0.5 M TEAB (pH 8.5). Tryptic peptides of each treatment group were labelled with iTRAQ reagents [114 for Group I (NLNRA), and 115 for Group II, 116 for Group III and 117 for Group IV of HLNRA) using the iTRAQ reagent multiplex kit according to manufacturer's recommendations (AB SCIEX, MA, USA). Three technical replicates were labelled for each control and treatment group. The required vials of isobaric tags were thawed and reconstituted with HPLC grade absolute ethanol. Labeling

was performed for 1 h at room temperature, and after incubation, the reaction was quenched with 50 μ l of MS grade water. The iTRAQ labeling and LC-MS analysis was done at a commercial facility of M/s. Sandor Life Sciences Pvt. Ltd., Hyderabad, India

2.11.3. Strong cation exchange fractionation

The iTRAQ-labelled peptides were vacuum dried and the pellets were reconstituted in 50 μ l of strong cation exchange (SCX) buffer A (5 mM KH_2PO_4 + 25% ACN, pH 3). Equal volumes (25 μ l) of labelled peptides from each treatment groups were pooled into one tube and diluted (1:3) with buffer A (200 μ l) to a final volume of 300 μ l and filtered using 0.45 μ m syringe filters. The labelled peptides were cleaned using a Bio-Basic SCX (Dimensions: 150 mm x 4.6 mm, 5 μ Particle Size, 300 \AA pore size) column (Thermo Scientific, Waltham, MA, USA). The peptides were sequentially eluted from the column using a 75 min gradient at a flow rate of 1 ml/min. The gradient used for elution as follows: 30 min with 100% Buffer A, followed by a linear increase to 25% Buffer B (5 mM KH_2PO_4 + 25% ACN + 350mM KCl, pH 3), a second linear increase to 100% B for 10 min, and a final equilibration with 100% Buffer A for 15 min. A total of ten fractions were collected based on the retention time values (**Table 2. 1**) and desalted on Zip-Tip C18 cartridges (Millipore Corp., MA, USA). Every SCX fraction was concentrated by vacuum centrifugation and stored at -80 $^{\circ}$ C until LC-MS/MS analysis. Representative SCX chromatogram of the results is shown in **Fig. 2. 2**.

2.11.4. Reverse phase LC-MS/MS analysis

The separation and quantification of labelled peptides were performed using nano-Acquity UPLC system (Waters Corp., MA, USA) coupled with Q-TOF Synapt G2 mass spectrometer (Waters Corp., MA, USA). Each SCX purified peptide fraction was re-dissolved in 0.1% formic acid (10 μ l) and 1 μ l of solution was injected into liquid chromatography system with nano-Acquity UPLC BEH C18 column (Internal diameter-75 μ m, Length-150 mm, Particle size-1.7 μ m, Column pore size-130A°, pH Range-2 to 10, Mode-reversed phase). The eluted peptides were directed into Q-TOF instrument for mass spectrometric analysis for 200 min gradient run (flow rate-0.3 μ L/min) using different combinations of buffer A (0.1% Formic Acid in MS Grade water) and B (0.1% formic Acid in ACN).

S.No	Time (min)	Flow (μ L/min)	%A	%B	Curve
1	Initial	0.3	98	2	Initial
2	2	0.3	98	2	6
3	120	0.3	5	50	6
4	140	0.3	20	80	6
5	150	0.3	20	80	6
6	160	0.3	98	2	6
7	180	0.3	98	2	6

The instrumental parameters of Q-TOF Synapt G2 mass spectrometer used for the study were as follows:

Polarity	ES+
Analyser	Resolution Mode
Capillary (kV)	3.5000
Source Temperature (°C)	80
Sampling Cone	40.0000
Extraction Cone	4.9000
Source Gas Flow (mL/min)	0.00
Desolvation Temperature (°C)	350
Cone Gas Flow (L/Hr)	28.0
Nanoflow Gas Pressure (Bar)	0.2
Purge Gas Flow (mL/h)	1000.0
Desolvation Gas Flow (L/Hr)	1000.0

2.11.5. Protein identification and quantification

The raw data acquired from the Q-TOF Synapt G2 mass spectrometer was processed with MassLynx 4.1 (Waters Corp., MA, USA). The raw data files were converted to mzML format using the MSconvert proteowizard tool. Spectra acquired from each of the technical replicates were submitted individually to MassLynx 4.1 for peak list generation. Protein identification and quantification were simultaneously performed using the Mascot 2.3.02 software (Matrix Science, London, UK) by searching the individual peptide peak lists based on their m/z values against the UNIPROT database, specified for *Homo sapiens* taxonomy. The search parameters of maximum missed cleavage of one were allowed in the trypsin digests with a peptide mass tolerance of 2.85 Da and a fragment tolerance 1.5 ppm. Carbamidomethyl (C), iTRAQ4plex (N-term), iTRAQ4plex (K) were chosen as fixed modifications and Oxidation (M) was set as

variable modifications. The false discovery rate (FDR) was estimated by using the automatic decoy database search algorithm of Mascot software. Minimum of one unique peptide was included for identification of each confident protein and protein sequence coverage (%) was recorded. The quantification of proteins/peptides was based on the ion abundance ratios calculated using inbuilt algorithm of Mascot with protein ratio type as 'median' and 'median ratio' as normalization methodology. The results were then exported into Microsoft Excel (Microsoft Corporation, USA) for manual data interpretation.

2.12. Western blot analysis

Pre-estimated (40-50 µg) protein lysates were separated by electrophoresis on 4–12% Bis-Tris NuPage gels (Invitrogen, NJ, USA). The resolved proteins were electroblotted onto a PVDF membrane (Millipore Corp., MA, USA) using wet blotting system (XCell II™ Blot Module, Invitrogen) at 25 V, overnight at 4°C. The membrane was blocked in 5% BSA (Sigma–Aldrich) in TBS-T (Tris buffered saline containing 0.1% Tween 20) and probed with the respective primary antibodies overnight at 4°C. After washing, the blots were incubated with horse radish peroxidase-conjugated secondary antibody (Santa Cruz Biotechnology, INC) for 1 h at room temperature and protein bands were visualized using Super Signal West Dura Extended Duration Substrate (ThermoScientific, IL, USA). The chemiluminescence signals were captured using gel documentation system (Syngene) and band intensity was calculated using Image J software. The relative intensity of the proteins was calculated after normalizing with GAPDH as the loading control. The GAPDH antibody (rabbit monoclonal, 14C10) was procured from Cell Signaling Technology (MA, USA) whereas all other antibodies

[GRP78: rabbit polyclonal, sc-13968; HSP90 α/β : rabbit polyclonal, sc-7947; PDIA1: goat polyclonal, sc-2005 and PRDX6: mouse monoclonal, sc-101522] were obtained from Santa Cruz Biotechnology, Inc. (TX, USA).

2.13. RNA extraction and gene expression studies

RNA was extracted from PBMCs using HiPurATM Total RNA Miniprep Purification Kit (HiMedia Laboratory Pvt. Ltd., Mumbai, India) using manufacturer's instructions. Briefly, the cells were homogenized with lysis buffer containing β mercaptoethanol (10 μ l/1ml lysis buffer) and filtered through red colored hi-shredder column at 14,000 rpm for 2 min. The filtrate was collected, mixed with equal volume of 70% ethanol and passed through blue colored hi-shredder column at 14,000 rpm for sec. The RNA trapped column was retained and washed subsequently with a series of pre-wash or wash solutions at 14000 rpm. After the washing steps, the purified RNA was eluted from the column using elution buffers at 14000 rpm. The concentration and the purity of RNA were determined by measuring the ratio of UV absorbance at 260 and 280 nm using Picodrop microliter spectrophotometer (Pico 100, Picodrop Ltd, UK). An aliquot of each RNA preparation was run on 1 % agarose gel and visualized with ethidium bromide to check the integrity. RNA (500 ng) was then reverse transcribed to cDNA using Transcriptor High Fidelity cDNA kit (Roche Diagnostics, GmbH, Germany).

Real-Time quantitative Polymerase Chain Reaction (RT-qPCR) was performed on LC480 Real-time PCR machine (Roche Diagnostics, GmbH, Germany). The SYBR GREEN chemistry (Roche Diagnostics Pvt. Ltd., GmbH, Germany) based analysis with

12.5µl reaction volume was used to study mRNA expression. The primer sets used are given in **Table 2. 2**. The cycling conditions consisted of a pre-incubation step at 95 °C for 5 min, followed by 40 cycles of denaturation at 95 °C (10 s), annealing at 60 °C (30 s) and extension at 72 °C (30 s). The C_T (cycle threshold) of the target gene was compared to that of two reference genes (β-actin and GAPDH) for normalization. The stable expression of reference genes was validated in three studied samples at the study conditions. Melting curve analysis was performed for each primer set to confirm product-specific amplification. A representative melting curve image for the amplified products is given in **Fig.2.3**. The relative change in gene expression from real-time PCR experiments was analyzed with the 2^{-ΔΔC_t} method by Livak and Schmittgen (2001) [170]. The formula used for relative expression changes is given below:

$$R = \frac{(E_{\text{target}})^{\Delta C_t \text{ target (Mean control-Mean sample)}}}{(E_{\text{target}})^{\Delta C_t \text{ target (Mean control-Mean sample)}}}$$

R= Relative expression, E= PCR efficiency and C_T (cycle threshold)

Gene	Nucleotide sequence 5'→3'
<i>C-FOS</i>	F-CCCTCAGTGGAACCTGTCAAG
	R-CATCAAAGGGCTCGGTCTTC
<i>FOSB</i>	F-CCAAAACCCACTCCCTTCCT
	R-CAGGCATACAGCAGGGAATC
<i>FOSL1</i>	F-CTGGGAGAGAACAGGAACAAGAG
	R-ATGAGACAGGGAACTGAGACTGA
<i>FOSL2</i>	F-AGGCGTGCCTCATAAATCTG
	R-TTCTCTCCCTCCCTCTCAAAA
<i>C-JUN</i>	F-GGCCGGGAGCGAACTT
	R-GTCTCGGTGGCAGCCTTAAG
<i>JUND</i>	F-TCAAGACCCTCAAAGCCAGAA
	R-TTGACGTGGCTGAGGACTTTC
<i>JUNB</i>	F-GCCTGTGTCCCCATCAA
	R-GTTCCGCAGCCGCTTTC
<i>CLIC</i>	F-TCAGCGGCTCTCTGATCC
	R-AACTAGGCCTCCCCACCA
<i>GRP78</i>	F-TAAGTGGGGTTGCGGATG
	R-TCAGCACCGCACTTCTCA
<i>HSP 90</i>	F-AACCGCATCTATCGCATGA
	R-CATCAGGAACTGCAGCATTG
<i>PNP</i>	F-GGGACAGTGGAGAGGAGTATATG
	R-AGCATGGGAATTTATGAAGAGC
<i>PRDX6</i>	F-TCAATAGACAGTGTGAGGACCA
	R-TTTCTGTGGGCTCTTCACAA
<i>PDI</i>	F-GGAATGGAGACACGGCTTC
	R-TTCAGCCAGTTCACGATGTC
<i>ATR</i>	F-ACGACTCGCTGAACTGTACG
	R-TGGTGAACATCACCCCTTGG
<i>BLM</i>	F-AGTGTTGTGGCCGTTGTTTC
	R-TGCTCAGAAGCTCTTGCACT
<i>ERCC4</i>	F-CCACTGACACTCGGAAAGC
	R-CACGCATATCCACAACCTATGC
<i>FANCA</i>	F-GGGGACGACGATGACAAT
	R-ATGGTGAACCATGTGCAGAA
<i>FANCI</i>	F-CAGAATCAAGCAGTGAAAGGAA
	R-AGGGGGAACCTTTGAAGATG
<i>FANCM</i>	F-TCTGCAGTTCTCTTGCCACTG
	R-AGGCCTCGGGAACCTTACAAT
<i>MLH1</i>	F-AGGAAGAACGTGAGCACGAG
	R-CGTCTAGATGCTCAACGGAAG

<i>ATRX</i>	F-GAGCCCTGTCAGCAATGAGT
	R-GCTGTCACACTGTTTGTGCT
<i>CHD8</i>	F-TGAAGACGTAGCCATCTTGC
	R-ACATGCCGATGTCCTTGG
<i>EMSY</i>	F-TCAGAGAAACAGACGGCAAG
	R-GCGCCCCTCAAAGTTATC
<i>COPS5</i>	F-ATGCTCAGGCTGCTGCATA
	R-GATACCACCCGATTGCATTT
<i>MAPK1</i>	F-AGATTCCAGCCAGGATACAGAT
	R-AGACAGGACCAGGGGTCAA
<i>MINK1</i>	F-CTGGACGACATCGACCTGT
	R-CCACCTCCACAAGCTCAAAG
<i>SMG1</i>	F-TTCTGGAAGACATGGAAGCA
	R-CACTGATGGAGGAGGGACAT
<i>BIRC6</i>	F-GATCACAGAACATGCCCAGA
	R-GGTTCTCATTTCCTTCCTTTGA
<i>DAPK1</i>	F-CTGGCTTCTAAGCCCACAGT
	R-GGCTCCTCACACTCACGTTC
<i>DVL2</i>	F-CCATGAGCTTTCATCTTACACCT
	R-ACTCCGTGTCGACCCACT
<i>ZNRF3</i>	F-GCTCGAGCAAGGATCCAG
	R-CAAGGAGACCACGACGAAG
<i>β-ACTIN</i>	F-ATA CCC CTC GTA GAT GGG CAC
	R-GAG AAA ATC TGG CACCAC ACC
<i>GAPDH</i>	F-GGCATCCTGGGCTACACT
	R-GAGTGGGTGTCGCTGTTG

Table 2. 2. List of primers used for the RT-PCR analysis

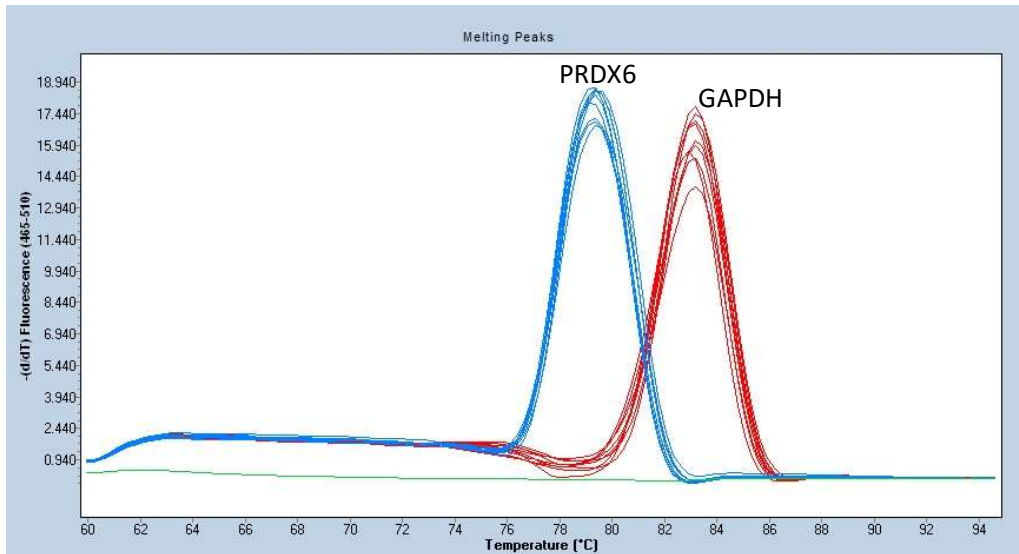


Fig.2.3. Representative melting curves for the RT-PCR products of *PRDX6* and *GAPDH* genes.

2.14. Statistical analysis

2.14.1. Statistical analysis for protein expression with acute *in vitro* radiation

Normalised spot intensity values of at least 1.5-fold difference as the mean value of the biological replicates compared with the control mean values at any of the studied dose/time points was considered as significant alteration. Statistical significance between the groups was analysed by Student's t-test ($P \leq 0.05$). Spot wise standard deviation (SD), arithmetic mean and coefficient of variation (ratio of the standard deviations of normalised spot volumes to the means, expressed in percentage; CV%) values were calculated for each spot that showed differential expression. Heat map visualization was performed using Matlab software. The principal component analysis (PCA) was performed with normalized spot densities of all quantified expressed proteins to visually

assess patterns of radiation induced or gender specific differences in protein expression. The functional pathway analysis was performed using the UniProt/SwissProt protein database.

2.14.2. Statistical analysis for protein expression with chronic low dose radiation: Gel-based 2DE method

Normalized spot intensities were compared between NLNRA and HLNRA (at background and after 2 Gy irradiation *ex vivo* irradiation) using independent sample t-test. A significance level of 0.05 was used and no adjustments for multiple tests were carried out. Coefficient of variation of normalized spot intensity, the ratio of standard deviation to mean expressed as %, was used to assess the variation in differential expression. The box plot visualizations of the protein expression data were prepared by using Statistics Program for Social Sciences (SPSS 11.5; IBM, NY, USA). Correlation analysis for all the differentially modulated proteins to evaluate the relationship between protein expression and annual dose received by HLNRA individuals (range: 10.74–20.25 mGy/y) was also performed using SPSS 11.5 as above. Factor analysis on raw spot densities of all quantified proteins was employed to identify underlying factors using principal component as the method of extraction (PCA analysis). Analysis was carried out to assess the power of detecting different fold changes from 1.25 to 3 and sample sizes from 1 to 20, assuming an overall CV of 34% (as observed in this work study), using the formula $n = \frac{2(Z_{\alpha/2} + Z_{\beta})^2 \times \log(CV^2 + 1)}{[(\log_e R)]^2}$, where n is a sample size, $Z_{\alpha/2}$ is value from the standard normal distribution (two sided) corresponding to significance level (α), Z_{β} is

value from the standard normal distribution corresponding to power $(1 - \beta)$, R is the fold change and CV is the coefficient of variation

2.14.3. Statistical analysis for protein expression with chronic low dose radiation: Gel-free iTRAQ based method

The relative fold change was calculated as the average ratio of each HLNRA dose group (Label 115 for Group II, 116 for Group III and 117 for Group IV) with respect to NLNRA samples (Label 114 for Group I). These modulated proteins were further analyzed using advanced statistical and pathway analysis tools. For all statistical analyses, data from three technical replicates for each treatment and control were used. CV was used as the method of tool to assess the experimental variation among the technical replicates. Normality of protein expression data set was checked using the Kolmogorov-Smirnov normality test. The statistical significance of the protein expression among the technical replicates was calculated by Student's t-test ($P \leq 0.05$) using the SciPy package of Python. The calculated P -values were subsequently corrected for FDR in multiple testing experiments by Benjamini-Hochberg (BH) method [171]. Proteins with fold change 'cut off' of ± 1.2 fold with a BH adjusted $P \leq 0.1$ were considered significantly modulated.

2.14.4. Functional pathway analysis for gel-based (2DE) and gel-free (iTRAQ) methods

The open source software DAVID (Database for Annotation, Visualization and Integrated Discovery) version 6.8 (<http://david.abcc.ncifcrf.gov/>) was used to identify enriched biological processes in HLNRA subjects compared to NLNRA individuals. The biological pathways modulated in HLNRA dose groups were predicted using Kyoto

Encyclopedia of Genes and Genomes (KEGG) module. The UniProt identification numbers of the altered proteins were used for the Gene Ontology Term Enrichment (GOTERM) enrichment analysis by searching against the human proteome database as previously described [172, 173]. This analysis identified over-representation of certain group of proteins common to biological process, molecular function, cellular component and biological pathways. The GOTERM biological process and pathways was considered significantly enriched when the enrichment P -value calculated by Fisher's exact test was $P \leq 0.05$.

2.14.5. Statistical analysis for gene expression data

Genes which showed P -values ≤ 0.05 using Student's t-test were considered to be differentially regulated. Statistical significance levels were further assessed with Bonferroni corrected P value ($P \leq 0.005$) for the subjects. A multivariate analysis on the gene expression data set, PCA was performed to visually assess similarities and differences between samples and to check dominant patterns of gene expression. All the statistical analysis was performed with SPSS version 11.5 (IBM, NY, USA).

CHAPTER 3

RESULTS

3.1. Responses of human PBMCs to acute *in vitro* IR

3.1.1. Proteome analysis with 2DE-MS

Initially, a wide range pH 3-10 linear gradient IPG strips were used as the first dimension in order to detect maximum number of proteins. The protein spot pattern analysis revealed clustering of protein spots in the central pH region of 4-7. Hence subsequently, narrow range IPG strips of pH 4-7 linear gradients were used for all further analysis, which led to an improved separation and visualization (**Fig.3.1**). The 2D proteome spot pattern analysis on IPG strips of pH 4-7 showed an average of 260 ± 26 (SE) protein spots per gel. This was comparable to 246 spots identified in an early work on 2DE gels from PBMCs isolated from healthy individuals [174].

3.1.1.1. Assessment of intra-individual variability in the PBMC proteome

We first measured individual variability in human PBMC proteome over time due to changes in physiology. This assessment of intra-individual variability is important for better interpretation of comparative proteomic experiments of biomarkers discovery for stress indicators like radiation. The study was performed using blood samples from three healthy male volunteers (age group 25–30 years) with no clinical signs of inflammation. The collection of blood samples was done at three time points (termed as T1, T2 and T3) with an interval of 15 days between each collection. Protein maps were created with pH 4-7 IPG strips with two technical replicates at each time point. Then, all 18 gels for the three biological replicates (6 gels per time point) were normalised together. Pairwise comparisons were performed by taking protein expression at T1 as the baseline (control)

and comparisons were made between T1 vs T2 and T1 vs T3 time points. Proteins which were present in all biological replicates (in both technical replicates) with a relative expression change of ± 1.5 fold in spot intensity at any time point of analysis, and P -value of ≤ 0.05 was considered as significant. The protein fold change between the groups (T1 vs T2 and T1 vs T3) was calculated by taking mean of spot intensity of all the gels in each group.

The study revealed stability of PBMC proteome over time. There were only a small set of proteins that showed significant (± 1.5 fold, $P \leq 0.05$) alterations with time (**Table 3.1**). A comparison between T1 vs T2 time point identified differential expression of 7 proteins. Four proteins were over-expressed (three ACT isoforms and LDHB) whereas three proteins were under-expressed [CALR, F13A, ALBU (2)]. When comparison was made between T1 vs T3 time point, 5 proteins were found to be differentially modulated. Of these, three proteins were over-expressed (two ACT isoforms and FIBG) and two proteins were under-expressed (CALR and F13A). The differentially modulated protein spots were analysed by MALDI-MS. The SWISS PROT accession number, MASCOT score, sequence coverage and peptide match for the identified proteins are given in **Table 3.1** and marked on **Fig.3.2**.

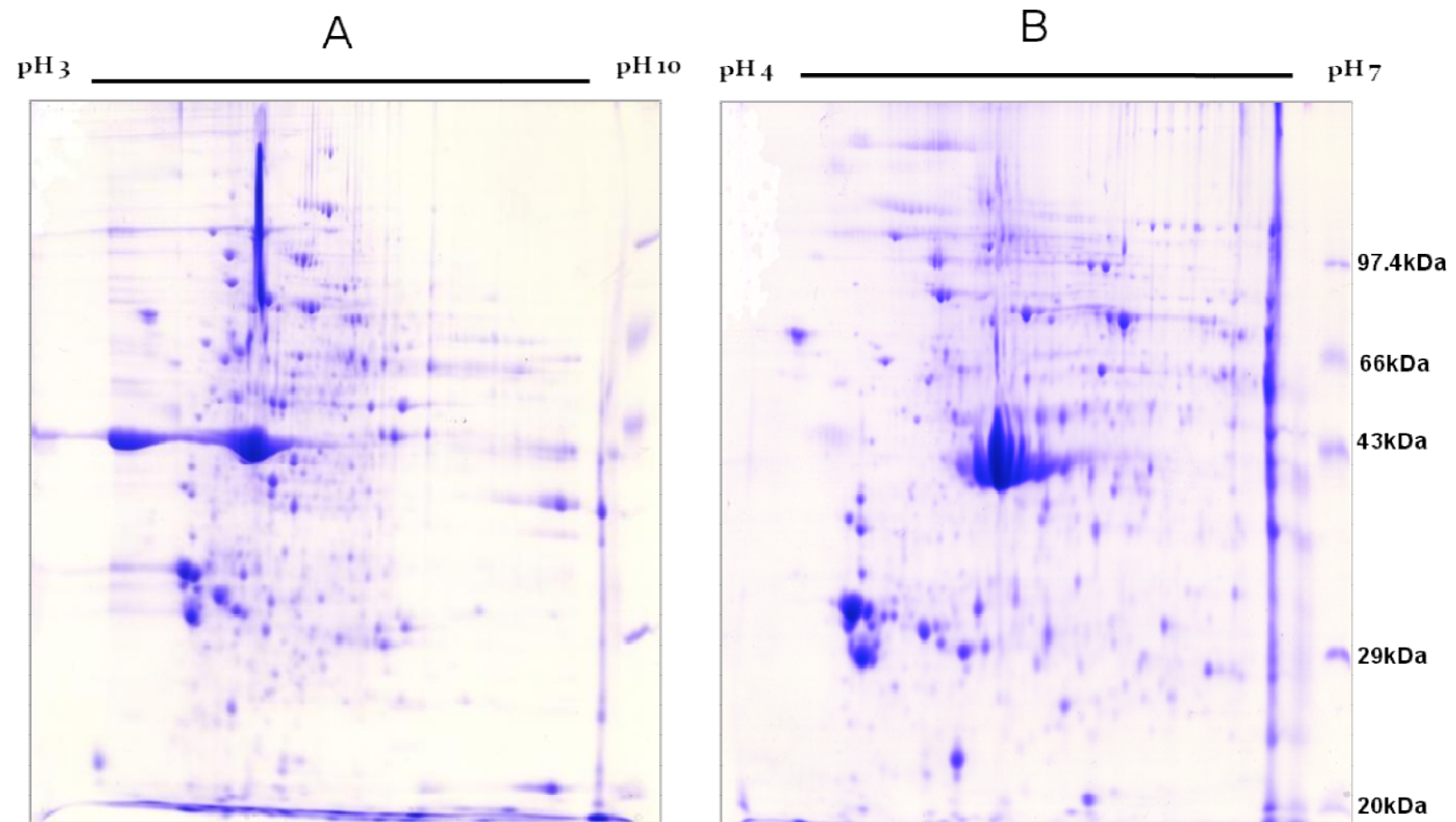


Fig.3.1. Optimization of 2D gel electrophoresis for human PBMCs. Proteins were separated in the first dimension by IEF on IPG strips with (A) pH 3-10 (B) pH 4–7 gradient. The second dimensional separation was on 10% SDS-PAGE gels. Proteins were visualized by staining with coomassie blue.

Sl.No	Protein_Name	SWISS PROT Accession No.	T1 vs T2		T1 vs T3		Mascot Score Sequence	Sequence coverage (%)	Peptide matches
			Fold change	<i>P</i> value	Fold change	<i>P</i> value			
1.	Actin gamma/Actin beta (1) [ACT (1)]	P63261/ P60709	1.99	<i>P</i> =0.01	1.89	<i>P</i> =0.01	65	36.3	9
2.	Actin gamma/Actin beta (2) [ACT (2)]	P63261/ P60709	1.94	<i>P</i> =0.04	2.15	<i>P</i> =0.22	85	41.3	11
3.	Actin gamma/Actin beta (5) [ACT (5)]	P63261/ P60709	2.33	<i>P</i> =0.05	2.23	<i>P</i> =0.05	114	40	12
4.	Albumin Serum [ALBU (2)]	Q56G89 75	0.47	<i>P</i> =0.05	1.46	<i>P</i> =0.20	75	27.0	10
5.	Calreticulin (CALR)	P27797	0.61	<i>P</i> =0.04	0.66	<i>P</i> =0.01	71	25.9	8
6.	Coagulation factor XIII A chain (F13A)	P00488	0.52	<i>P</i> =0.04	0.65	<i>P</i> =0.04	142	32.0	15
7.	Fibrinogen gamma chain (FIBG)	P02679	1.58	<i>P</i> =0.06	1.52	<i>P</i> =0.02	105	38.2	12
8.	l-lactate dehydrogenase B chain (LDHB)	P07195	2.21	<i>P</i> =0.05	1.20	<i>P</i> =0.78	105	38.3	12

Table 3.1. Differentially expressed proteins due to physiological responses in human PBMCs. *P*-values represent the significance of the change in the expression levels of proteins calculated with Student's t-test ($P \leq 0.05$). The proteins are listed 1–8 as labeled on **Fig.3.2**.

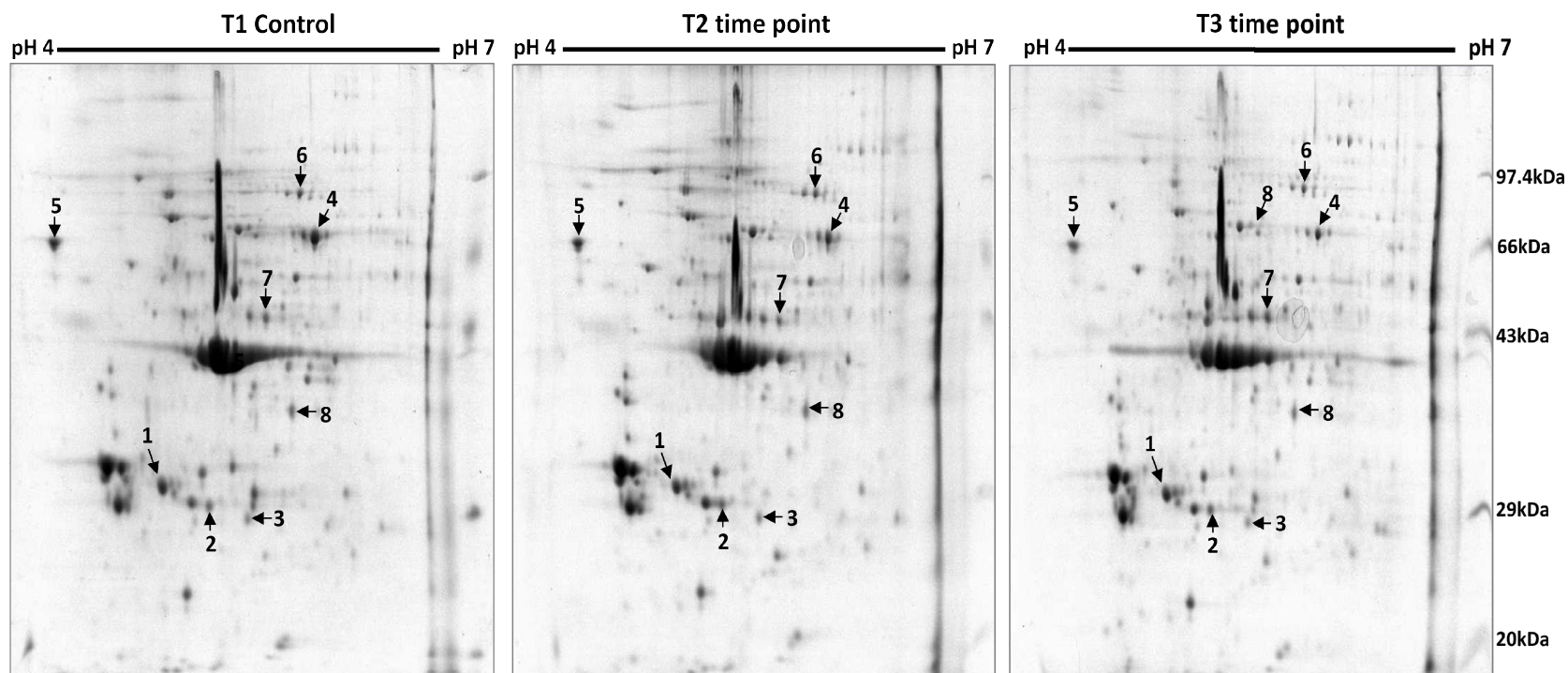


Fig.3.2. Intra-individual variability in the human PBMC proteome. Representative 2D image of human PBMCs for an individual separated at respective time points (T1, T2 and T3). The positions of highly variable proteins due to physiological responses are marked with arrows and are numbered as listed in **Table 3.1**.

3.1.1.2. Proteome changes in PBMCs

Using a gel-based 2DE-MS methodology, proteome of G₀ PBMCs was analyzed following two different radiation doses (300 mGy and 1 Gy) to understand effect of low and moderately high acute doses of IR. Sham irradiated cells were used as control. Blood samples were collected from eight donors (four male and four females). All individuals (age group: 25–45 years) were healthy non-smokers. The number of samples used in the present study was broadly in accordance with the optimal sample size defined by Maes et al., for 1.5-fold differential expression at $P \leq 0.05$ statistical significance [175]. Irradiation of PBMCs was performed at room temperature using Co⁶⁰ γ -rays (Blood irradiator, 2000, BRIT, India) at a dose rate of 0.4 Gy/min. After irradiation, cells were incubated in RPMI-1640 media at 37 °C in a humidified, 5% CO₂ atmosphere for the required time (1 h or 4 h) before extraction of proteins.

At each harvest time (1 h and 4 h), 2DE gels from eight samples were normalized together and a master gel (reference gel) was prepared using extensive matching and land-marking across multiple gels. The profiles of the radiation exposed replicate group (300 mGy or 1 Gy) were then compared with sham irradiated control replicate group to identify the differentially expressed proteins. The highly reproducible protein maps for the two dose points are shown in **Fig.3.3**. An analysis was also performed to investigate the potential gender differences in responses to radiation.

3.1.1.3. Dose dependent changes in proteome of PBMCs

When proteins were classified according to radiation dose, 23 PBMC proteins showed differential modulation (fold change ± 1.5 fold; $P \leq 0.05$) either with 300 mGy or with 1 Gy, compared to the sham irradiated cells. The differentially altered protein spots were identified by MALDI-TOF mass spectrometry. The SWISS PROT accession number, MASCOT score, sequence coverage and peptide match for the identified proteins are given in **Table 3.2** and marked on **Fig.3.3**. As expected, most protein expression changes were subtle, with only three proteins showing ≥ 2.5 -fold change. Six proteins were found to be significantly modulated with only low dose (300 mGy) (**Fig.3.4A**, **Table 3.3**) and five proteins with only high dose (1 Gy) (**Fig.3.4B**, **Table 3.3**), when compared with sham irradiated cells. Proteins such as thiol specific antioxidant, peroxiredoxin-6 and cytoskeletal proteins (vinculin, tubulin alpha and beta) showed significant alterations with 300 mGy. On the other hand, proteins like Ras-related Rap-1b protein, enzymes involved in purine metabolism (purine nucleoside phosphorylase) and A1 isoform of protein disulfide-isomerase displayed significant change with 1 Gy. There were 12 proteins that were significantly up or down regulated with both the doses as compared to basal expression in sham irradiated control cells (**Fig.3.4C**, **Table 3.3**).

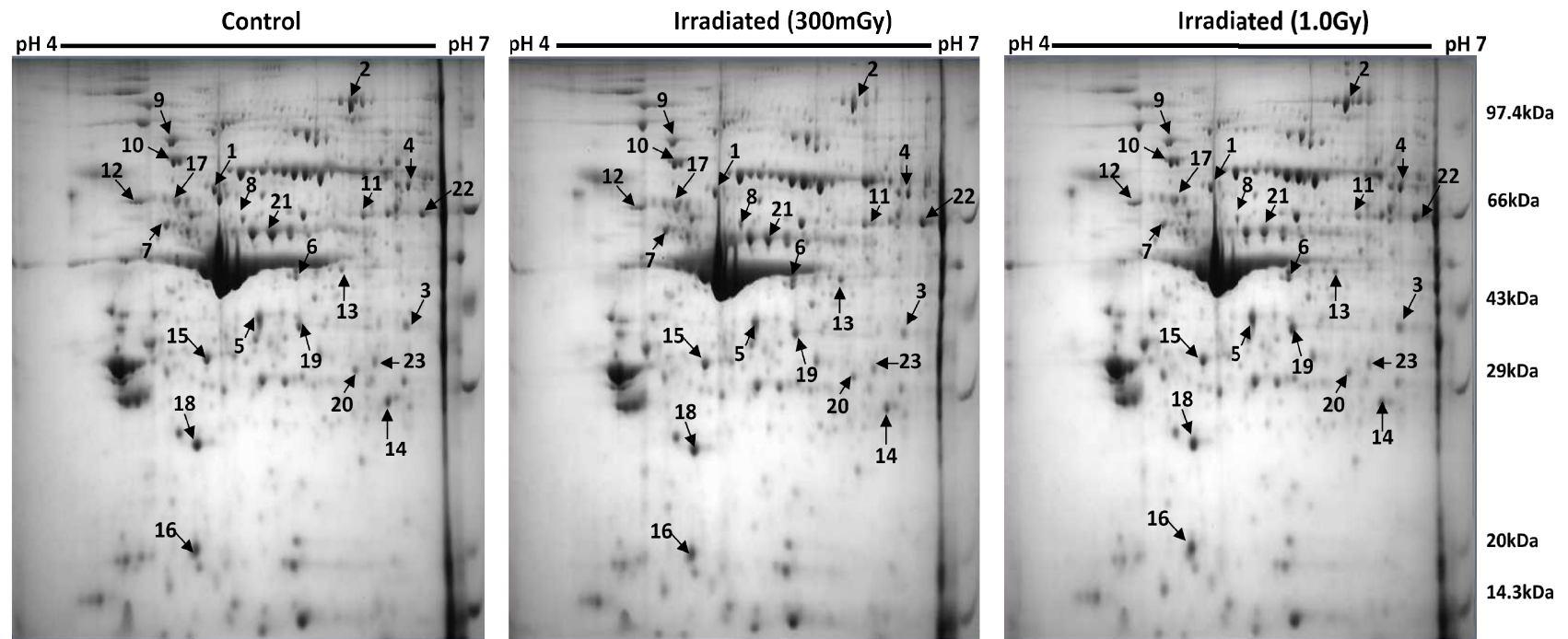


Fig.3.3. Representative 2D images of human PBMC proteome from a healthy individual irradiated with 300 mGy and 1 Gy. Proteins were separated in the first dimension by IEF on IPG strips with pH 4–7 gradient, then in the second dimension on 10% SDS-PAGE gels. Proteins were visualized by staining with coomassie blue. The proteins were identified by mass spectrometry and are numbered as listed in **Table 3.2**.

Spot No.	Protein Name	SWISS PROT Accession Number	Mascot Score	Sequence coverage	Peptide matches	Molecular weight (KDa)/pI	
						Theoretical	Measured
1.	Plastin-2 (PLS-2)	P13796	130	31.3%	18	70.8/5.2	96.3/5.0
2.	Vinculin (MV)	P18206	116	24.3%	22	124.3/5.4	109.5/6.1
3.	PDZ and LIM domain protein 1(PDLIM1)	O00151	96	54.1%	10	36.6 /6.6	36.4/6.5
4.	WD repeat-containing protein 1(WDR1)	O75083	57	24.6%	6	67.0/6.2	73.0/6.7
5.	Actin gamma/Actin beta (ACT)	P63261/ P60709	70	28.8%	8	42.0 /5.2	38.1/5.3
6.	Actin gamma/Actin beta (ACT)	P63261/ P60709	88	33.9%	10	42.0 /5.2	46.0/5.6
7.	Tubulin beta chain/beta2A/beta2B chain/beta4B chain (TUBB)	P07437/Q13885/Q9BVA1/ P68371	69	29.5%	9	50.0/4.6	60.8/4.7
8.	Tubulin alpha-1B chain/1A chain/1C chain/ 4A chain/8Chain/3C/D Chain/3E chain (TUBA)	P68363/Q71U36/Q9BQE3/P68366//Q9NY65/Q13748/Q6PEY	134	47.9%	17	50.8 /4.8	62.5/5.2
9.	Heat shock protein HSP 90-alpha/beta (HSP90)	P07900/ P08238	84	22.1%	17	85.0/4.8	91.6/4.8
10.	78 kDa glucose-regulated protein (GRP78)	P11021	60	20.6%	10	72.4/4.9	83.0/4.8
11.	T-complex protein 1 subunit beta (TCP1)	P78371	127	37.0%	14	57.8 /6.0	63.5/6.2
12.	Protein disulfide-isomerase A1(PDIA1)	P07237	197	40.2%	19	57.5/4.6	67.7/4.5
13.	Leukocyte elastase inhibitor (LEI)	P30740	97	32.2%	11	42.9/5.9	48.3/6.0
14.	Peroxiredoxin-6 (PRDX6)	P30041	56	38.8%	6	25.14/6.0	27.0/6.4
15.	Chloride intracellular channel protein 1(CLIC)	O00299	149	67.6%	15	27.25/4.9	31.2/5.0
16.	Ras-related protein Rap-1b (RAP1B)	P61224	186	67.4%	14	21.0/5.5	22.0/4.9
17.	Rab GDP dissociation inhibitor alpha (RabGDI α)	P31150	88	29.3%	14	51.18/4.9	68.7/4.8
18.	Rho GDP-dissociation inhibitor 2 (RhoGDI β)	P52566	52	40.8%	7	23.0/4.9	25.5/4.9
19.	L-lactate dehydrogenase B chain (LDHB)	P07195	96	41.6%	12	37.0/5.7	36.4/5.6
20.	Purine nucleoside phosphorylase (PNP)	P00491	93	49.8%	12	32.4/6.5	27.5/6.1
21.	Fibrinogen gamma chain (FGG)	P02679	73	26.5%	8	52.10/5.3	58.6/5.4
22.	Fibrinogen beta chain (FGB)	P02675	139	42.0%	23	56.6/9.3	63.0/6.9
23.	Thrombospondin-1(THBS1)	P07996	67	12.8%	12	133.3/4.6	29.0/6.2

Table 3.2. Identification of proteins differentially expressed after acute IR in human PBMCs derived from healthy individuals. The proteins are listed 1-23 as labeled on **Fig.3.3**.

Sl. No.	Protein Name	300 mGy 1 h			1.0 Gy 1 h			300 mGy 4 h			1.0 Gy 4 h		
		Mean \pm SD	<i>P</i> value	CV	Mean \pm SD	<i>P</i> value	CV	Mean \pm SD	<i>P</i> value	CV	Mean \pm SD	<i>P</i> value	CV
1.	PLS-2	-1.30 \pm 0.46	<i>P</i> = 0.19	59.4	-1.10 \pm 0.47	<i>P</i> = 0.82	48.8	1.82 \pm 0.31	<i>P</i> < 0.001	16.8	1.84 \pm 0.96	<i>P</i> = 0.042	52.3
2.	MV	-1.50\pm0.20	<i>P</i> = 0.002	31.3	1.13 \pm 0.4	<i>P</i> = 0.40	36.2	-1.10 \pm 0.48	<i>P</i> = 0.74	50.9	1.12 \pm 1.23	<i>P</i> = 0.80	110
3.	PDLIM1	-1.90 \pm 0.06	<i>P</i> < 0.001	12.1	-1.20 \pm 0.21	<i>P</i> = 0.056	25.0	-1.50 \pm 0.19	<i>P</i> < 0.001	28.2	-1.60 \pm 0.31	<i>P</i> = 0.01	47.6
4.	WDR1	-1.10 \pm 0.03	<i>P</i> < 0.001	3.5	2.12 \pm 0.48	<i>P</i> < 0.001	43.1	-1.90 \pm 0.23	<i>P</i> < 0.001	22.8	-1.50 \pm 0.49	<i>P</i> = 0.08	74.7
5.	ACT	2.02\pm0.77	<i>P</i>=0.007	38.2	1.53\pm0.49	<i>P</i> = 0.019	31.9	1.69\pm0.4	<i>P</i>=0.002	23.4	1.68\pm0.41	<i>P</i>=0.002	24.6
6.	ACT	1.45 \pm 0.42	<i>P</i> = 0.019	28.9	1.77 \pm 0.35	<i>P</i> < 0.001	20.0	No change					
7.	TUBB	-1.40 \pm 0.39	<i>P</i> = 0.07	54.4	1.28 \pm 0.39	<i>P</i> = 0.081	30.5	-2.30\pm0.27	<i>P</i> < 0.001	61.9	1.01 \pm 1.3	<i>P</i> = 0.98	129.5
8.	TUBA	1.52\pm0.14	<i>P</i> < 0.001	9.5	1.18 \pm 0.53	<i>P</i> = 0.376	44.8	No change					
9.	HSP90	-1.10 \pm 0.38	<i>P</i> = 0.79	39.9	-1.20 \pm 0.31	<i>P</i> =0.26	35.4	-2.20\pm0.29	<i>P</i> < 0.001	63.1	-2.10\pm0.21	<i>P</i> < 0.001	43.2
10.	GRP78	1.83\pm0.43	<i>P</i> < 0.001	23.8	1.33 \pm 0.42	<i>P</i> = 0.06	31.3	-2.60\pm0.13	<i>P</i> < 0.001	36.0	-1.30 \pm 0.28	<i>P</i> = 0.04	37.2
11.	TCP1	-2.0 \pm 0.14	<i>P</i> < 0.001	27.4	-2.20 \pm 0.25	<i>P</i> < 0.001	56.3	No change					
12.	PDIA1	-1.20 \pm 0.32	<i>P</i> = 0.221	37.9	-1.50\pm0.37	<i>P</i> = 0.047	53.9	No change					
13.	LEI	No change						-1.6\pm0.26	<i>P</i> = 0.005	42.3	-1.2 \pm 0.02	<i>P</i> < 0.001	2.7
14.	PRDX6	1.54 \pm 0.23	<i>P</i> < 0.001	14.8	1.27 \pm 0.42	<i>P</i> = 0.108	32.9	No change					
15.	CLIC	1.40 \pm 0.22	<i>P</i> < 0.001	15.8	1.88\pm0.67	<i>P</i>=0.007	35.6	1.84\pm0.44	<i>P</i> < 0.001	23.7	-1.40 \pm 0.14	<i>P</i> < 0.001	19.4
16.	RAP1B	-1.10 \pm 0.58	<i>P</i> = 0.58	66.3	1.52\pm0.65	<i>P</i> = 0.05	42.6	1.77 \pm 1.04	<i>P</i> =0.07	59.1	1.80 \pm 1.27	<i>P</i> =0.12	70.3
17.	RabGDI α	-1.40 \pm 0.12	<i>P</i> < 0.001	16.7	-1.70\pm0.11	<i>P</i> < 0.001	19.3	No change					
18.	RhoGDI β	1.92 \pm 0.63	<i>P</i> = 0.004	32.7	2.25 \pm 0.28	<i>P</i> < 0.001	12.6	No change					
19.	LDHB	-2.0 \pm 0.49	<i>P</i> = 0.036	97.9	-1.20 \pm 0.19	<i>P</i> = 0.042	23.4	-1.70 \pm 0.33	<i>P</i> = 0.011	54.3	-1.80\pm0.42	<i>P</i> = 0.02	74.6
20.	PNP	-1.10 \pm 0.22	<i>P</i> = 0.478	23.4	-1.50\pm0.12	<i>P</i> < 0.001	18.3	No change					
21.	FGG	1.24 \pm 0.63	<i>P</i> =0.31	50.9	1.50 \pm 0.21	<i>P</i> < 0.001	14.4	-1.8 \pm 0.14	<i>P</i> < 0.001	24.8	1.21 \pm 0.3	<i>P</i> = 0.08	24.6
22.	FGB	2.09 \pm 0.94	<i>P</i> = 0.013	44.9	2.94 \pm 1.36	<i>P</i> = 0.005	46.2	-1.10 \pm 0.66	<i>P</i> = 0.741	71.7	1.10 \pm 0.97	<i>P</i> = 0.786	88.2
23.	THBS1	1.16 \pm 0.29	<i>P</i> = 0.15	25.1	-1.30 \pm 0.19	<i>P</i> = 0.01	25.0	-1.50\pm0.33	<i>P</i> = 0.02	51.4	-3.10 \pm 0.06	<i>P</i> < 0.001	19.9

Table 3.3. Dose (300 mGy and 1 Gy) and time dependent (1 h and 4 h) changes in expression of proteins differentially modulated after acute IR in human PBMCs. The represented fold change is mean change (\pm SD) in spot intensity in irradiated PBMCs derived from eight individuals relative to sham irradiated PBMCs. All changes in expression which passed the selection criteria (fold change \pm 1.5-fold, *P* \leq 0.05) are represented in ‘**bold**’. The symbol (–) depicts down regulation. The proteins are listed 1–23 as labeled on **Fig.3.3**.

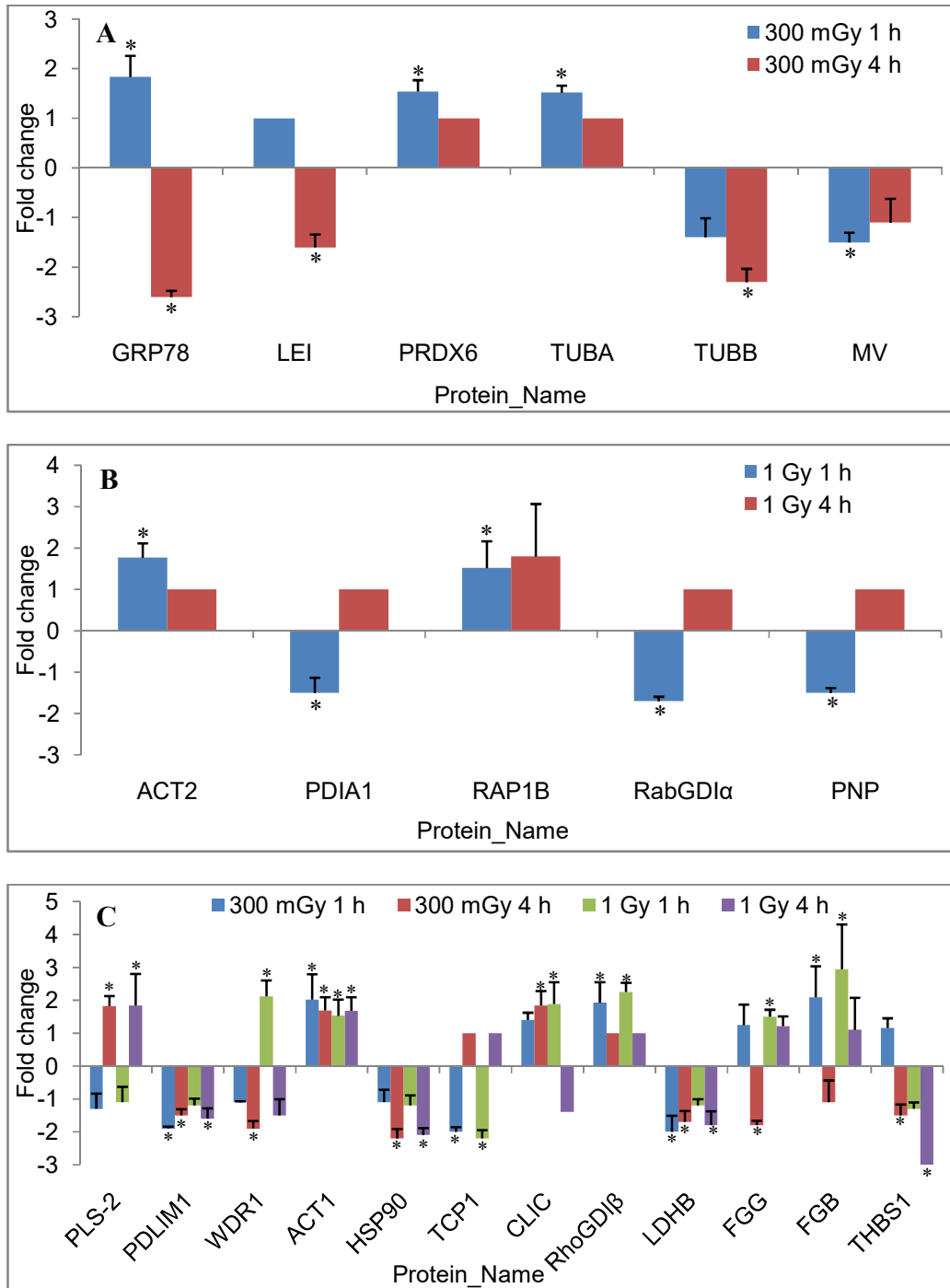


Fig.3.4. Dose dependent changes in expression of proteins in irradiated human PBMCs (300 mGy and 1 Gy) as compared to sham irradiated cells. The fold change of abundance is shown for proteins that changed in expression with (A) 300 mGy, (B) 1 Gy, (C) both doses. Symbol (*) represents significance (fold change ± 1.5 ; $P \leq 0.05$) and the abbreviations used are as listed in **Table 3.2**.

3.1.1.4. Time dependent changes in proteome of PBMCs

Proteins were then classified according to time of analysis post-irradiation independent of the dose used. There were 11 proteins that showed significant changes in expression when the proteome was analyzed 1 h after irradiation (**Fig.3.5A, Table 3.3**), but not at late time point (4 h). In contrast, only 5 proteins showed such changes 4 h post-irradiation, but not when analyzed at an early time point (1 h), irrespective of the dose used (**Fig.3.5B, Table 3.3**). There were 7 proteins that showed protracted expression with the change in expression seen at 1 h and 4 h (**Fig.3.5C, Table 3.3**). This showed that most changes in the proteome were early and brief. Protein fibrinogen beta showed highest up-regulation (2.94 fold) while protein thrombospondin 1 showed highest down regulation (-3.1 fold).

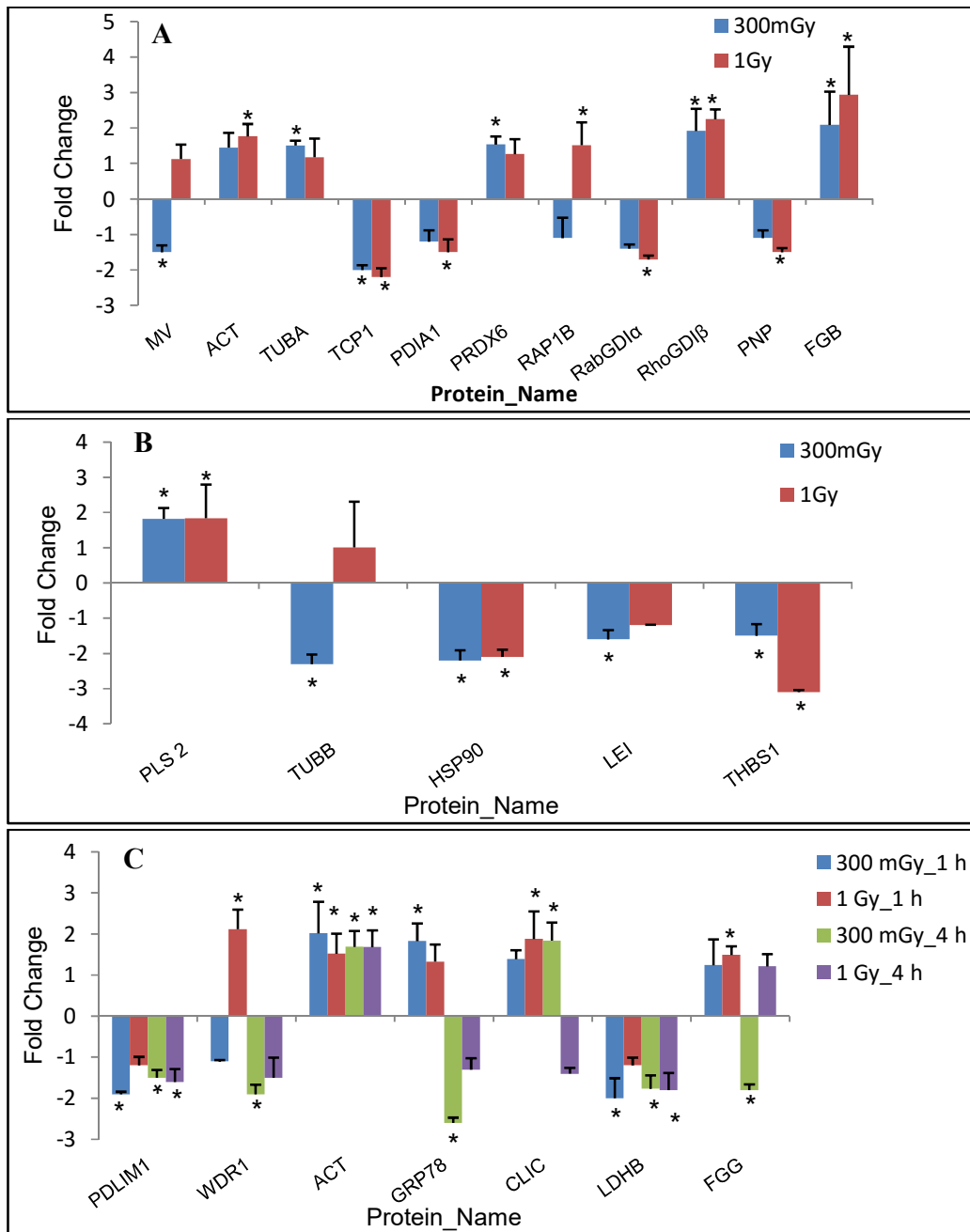
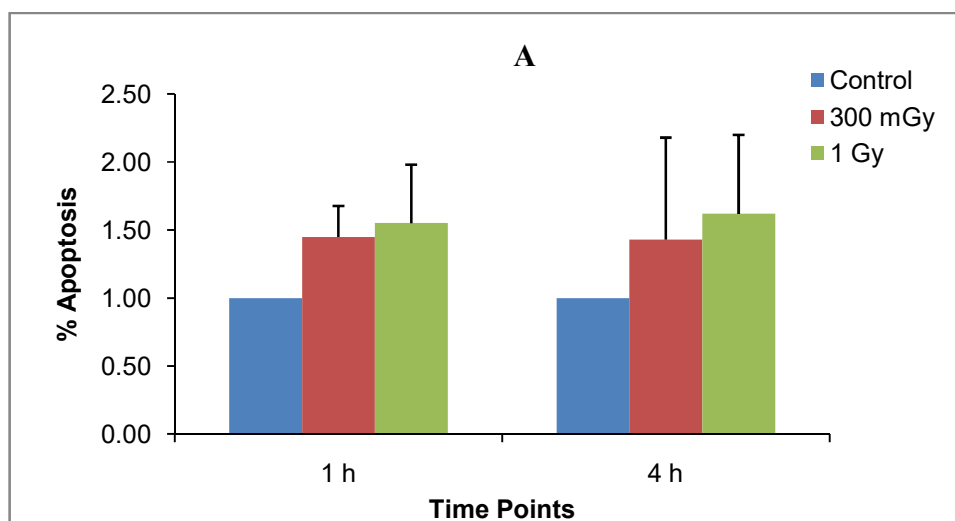


Fig.3.5. Temporal changes in expression of proteins in irradiated human PBMCs (300 mGy and 1 Gy) as compared to sham irradiated cells. The fold change of abundance at each dose is shown for proteins that changed in expression (A) 1 h post-irradiation, (B) 4 h post-irradiation, (C) both 1 h and 4 h post-irradiation. Data are expressed as the mean \pm SD of 8 studied samples as given in **Table 3.3**. Symbol (*) represents significance (fold change ± 1.5 ; $P \leq 0.05$). The abbreviations used are as listed in **Table 3.2**.

3.1.1.5. Effect of IR on the viability of PBMCs

Human peripheral blood lymphocytes are known to be more sensitive to undergo spontaneous apoptosis as compared to other cell types. Preliminary analysis of PBMC viability was assessed using trypan blue exclusion assay and >90 % of PBMCs were seen to be viable. To further assess the cytotoxic effects of radiation on human PBMCs, viability was assayed at the irradiation doses and time points used for 2DE. PI staining followed by measurement of DNA (sub-G1 peak) content using flow cytometry was performed and percentage of cells undergoing apoptosis was measured. There was no significant difference in the sub-G1 peak in the DNA histogram for cells irradiated either with 300 mGy or 1 Gy as compared to sham irradiated cells. For PBMCs irradiated with 300 mGy, apoptosis was $1.45 \pm 0.23\%$, $P=0.73$ and $1.43 \pm 0.75\%$, $P=0.95$ at 1 h and 4 h, respectively. After 1 Gy irradiation, PBMCs showed a mean apoptosis of $1.55 \pm 0.43\%$, $P=0.58$ and $1.62 \pm 0.58\%$, $P=0.69$ at 1 h and 4 h, respectively (**Fig.3.6 A-B**).



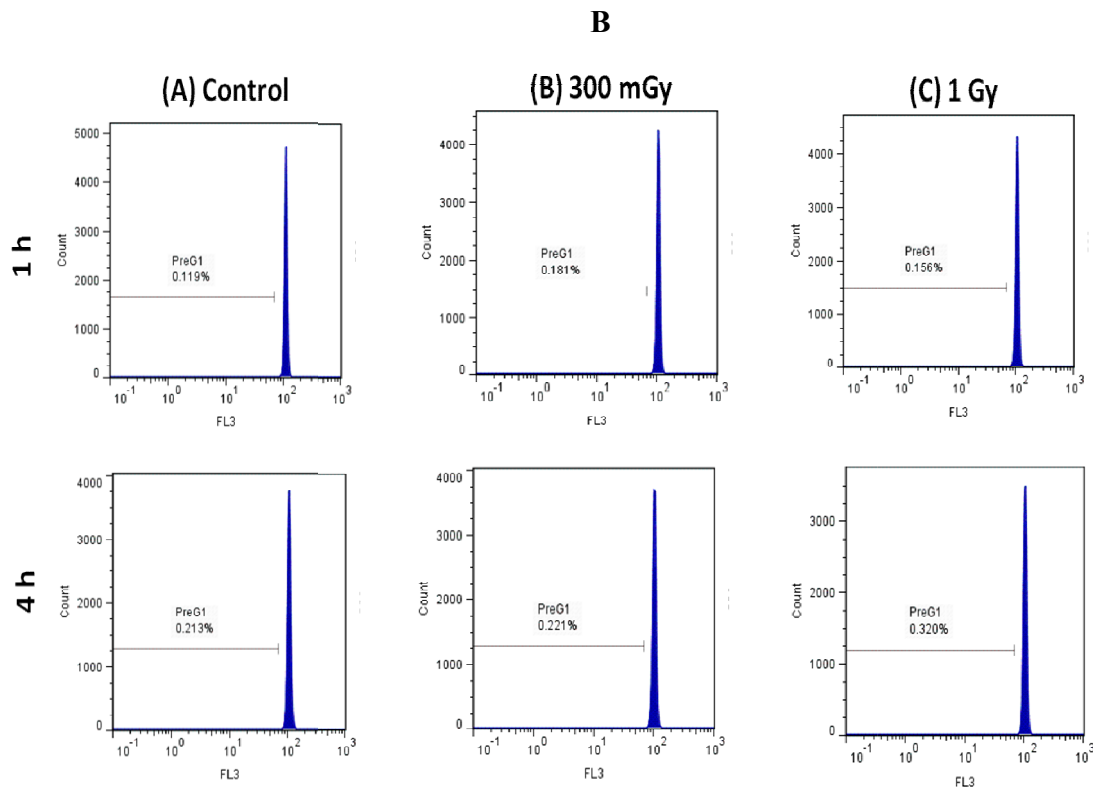
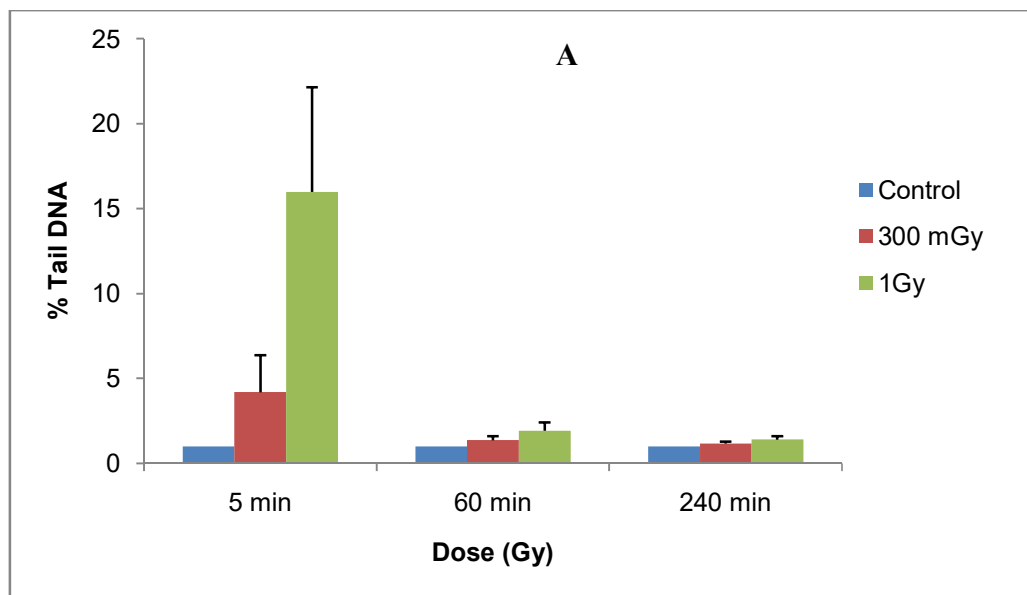


Fig.3.6. Flow cytometric profile of human PBMCs from an individual with and without irradiation with PI staining. (A) Mean percentage of apoptosis (\pm SD) in PBMCs of control and irradiated (300 mGy and 1 Gy) cells. (B) Representative flow cytometric profile for an individual showing dose and time dependent change in % apoptotic cells after 1 h (A, B, C upper panel) and 4 h (A, B, C lower panel), respectively. The peak analysis of the gated cells was from 10,000 events.

3.1.1.6. Analysis of DNA damage in PBMCs

In order to correlate association between initial DNA damage and cell viability, DNA strand breaks induced by radiation was estimated at the dose points chosen for 2DE. PBMCs were collected from the same eight individuals analyzed for 2DE and irradiated with 300 mGy or 1 Gy. Alkaline comet assay was performed at three time points (5 min, 1 h and 4 h post-irradiation). A significant increase in DNA damage was observed early after irradiation (5 min) with 300 mGy and 1 Gy, as compared to sham

irradiated cells. The mean % DNA in tail was 4.19 ± 2.19 for 300 mGy and 15.98 ± 6.17 for 1 Gy, showing clear dose dependent increase. When individual responses of samples were compared, % tail DNA varied from 1.2% to 6.4% at 300 mGy and 7.3% to 21.9% at 1 Gy among the studied samples (**Fig.3.7A-B**). For both 300 mGy and 1 Gy irradiated cells, the % DNA in tail decreased sharply and returned to the level of background damage within 1 h after irradiation, which is the earliest time point considered for proteomic analysis. Similarly, at 4 h post-irradiation, point at which late proteome changes were assessed, there was no difference in % DNA in tail in cells irradiated with 300 mGy or 1 Gy as compared to basal damage.



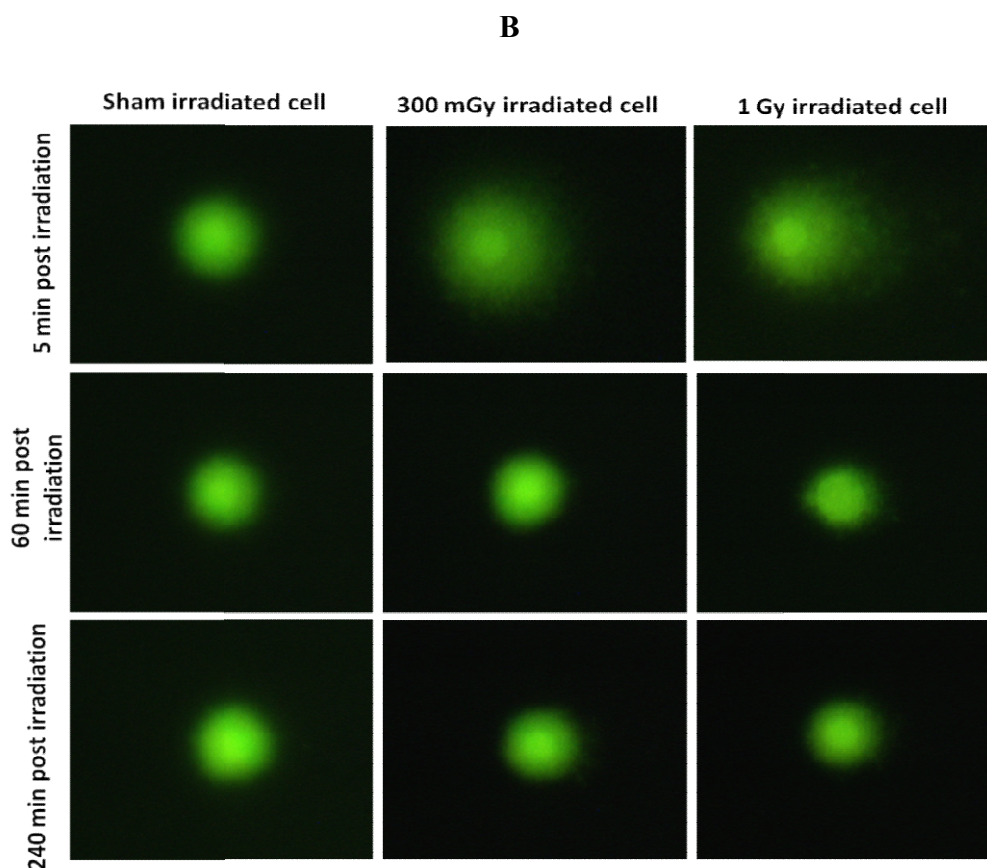


Fig.3.7. Induction of DNA damage in gamma irradiated human PBMCs. DNA damage as measured by alkaline comet assay 5 min, 60 min (1 h) and 240 min (4 h) after irradiation with either 300 mGy or 1 Gy and compared with sham irradiated control. (A) Mean percentage of DNA (\pm SD) in comet tails in the 8 studied samples. The significance was determined using t test ($P < 0.05$). (B) Representative of SYBR green stained comets prepared from a healthy individual.

3.1.1.7. Functional classification of differentially expressed proteins

Using the UniProt/SwissProt protein database the 23 identified proteins were broadly classified into seven groups according to their general biological function (**Fig.3.8**): cytoskeleton associated proteins (PLS-2, MV, PDLIM1, WDR1, two ACT isoforms, TUBB, TUBA), molecular chaperones (HSP90, GRP78, TCP1), protein and peptide processing (PDIA1, LEI), cellular redox homeostasis (PRDX6, CLIC), signaling (RAP1B, RabGDI α , RhoGDI β), cellular metabolic process (LDHB, PNP) and extracellular proteins (FGG, FGB, THBS1) (**Fig.3.9**). Of these, the cytoskeleton and associated proteins formed the largest group with eight proteins.

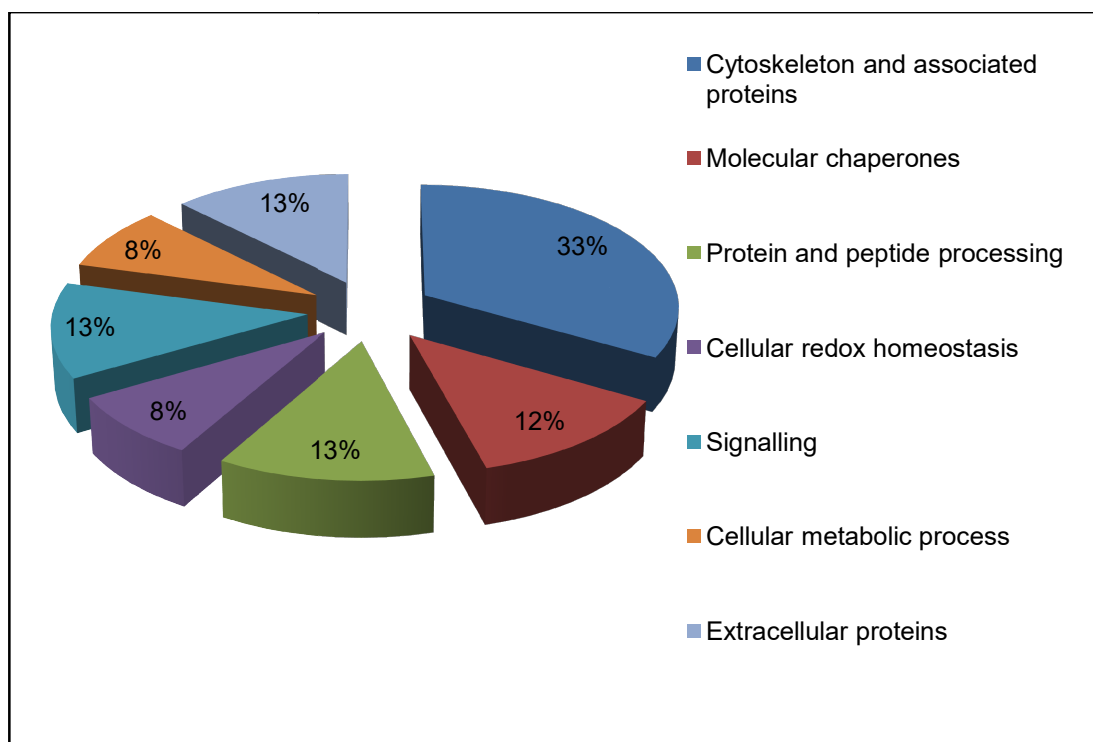


Fig.3.8. Cellular functions of radiation modulated proteins in human PBMCs.

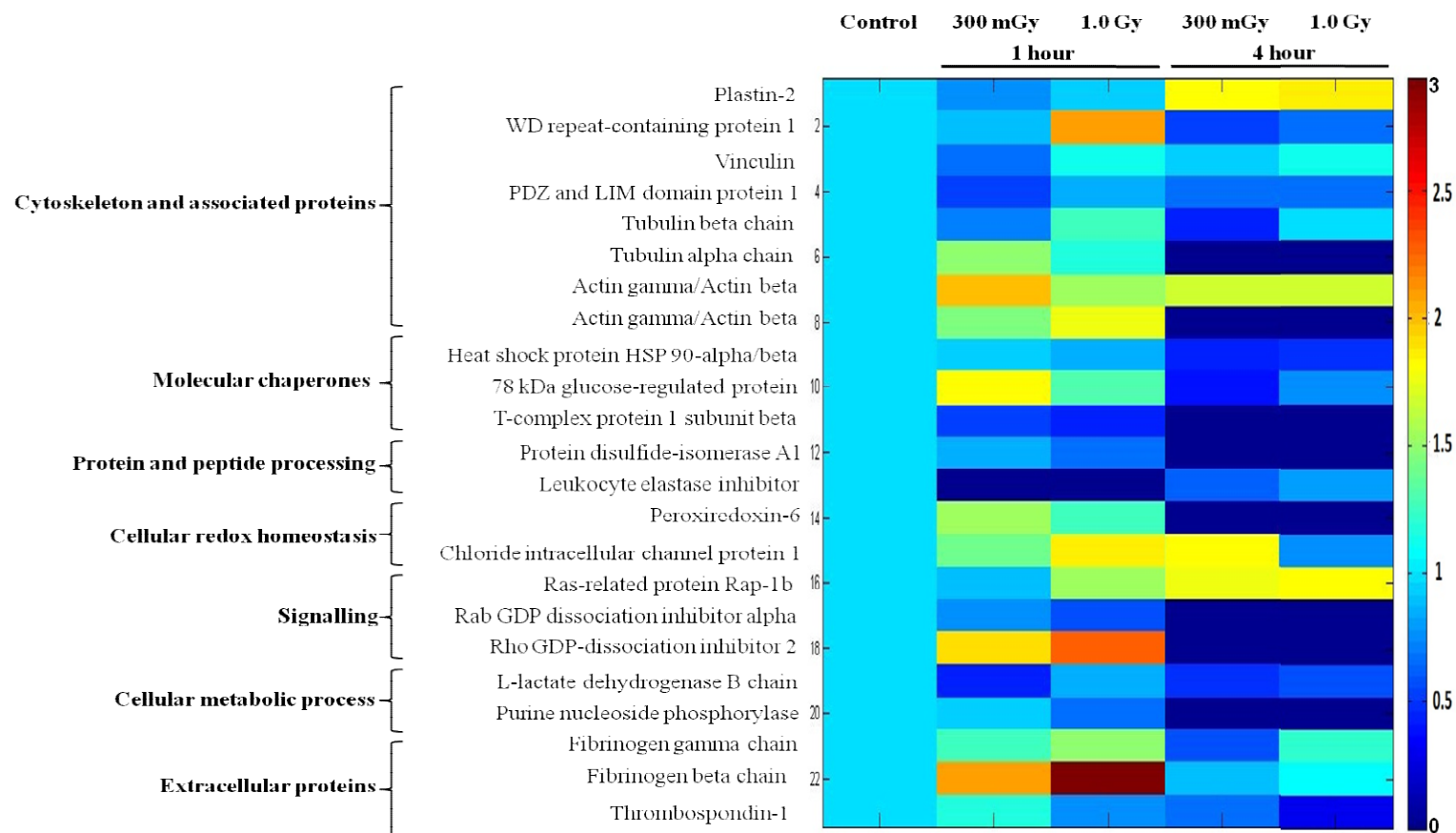


Fig.3.9. Heat map showing radiation-associated changes in the relative level of differentially expressed proteins (fold change ± 1.5 fold and $P \leq 0.05$) in the sham irradiated and irradiated (300 mGy and 1 Gy) human PBMCs. Relative spot intensity of differentially regulated proteins in irradiated samples, at indicated time points (1 h and 4 h), averaged for 8 studied individuals, is shown in each column. Rows represent individual proteins grouped according to their biological function.

3.1.1.8. Individual variability of protein expression

In the field of comparative proteomic experiments with human samples, it is necessary to know and quantify variance among individuals under the stress conditions. This level of variability is usually measured in terms of coefficient of variation, expressed in percentage; CV%. In the present study, CV% of the 23 protein spots that showed differential expression either with time and/or dose were found to vary from 3.5% to 97.9%, with a mean of ~33.7% when assessed 1 h post-irradiation. At 4 h post-irradiation, the CV of the protein spots were found to vary from 2.7% to 129.5%, with a mean of 48.3% (**Table 3.3**). Typically lower the CV, more precise the estimate. A CV threshold of 50% is usually employed to filter out the highly variable and uninformative proteins. Using this filter, at the early time point of 1 h, almost 78% of the proteins that showed differential expression with 300 mGy and a high 91% of the proteins which showed differential expression with 1 Gy showed CV values $\leq 50\%$ (**Fig.3.10**). At 4 h, almost 70% proteins at 300 mGy and 47% at 1 Gy that showed differential expression presented CV values less than 50%. This indicated good stability of expression of radiation induced proteins (**Fig.3.10**).

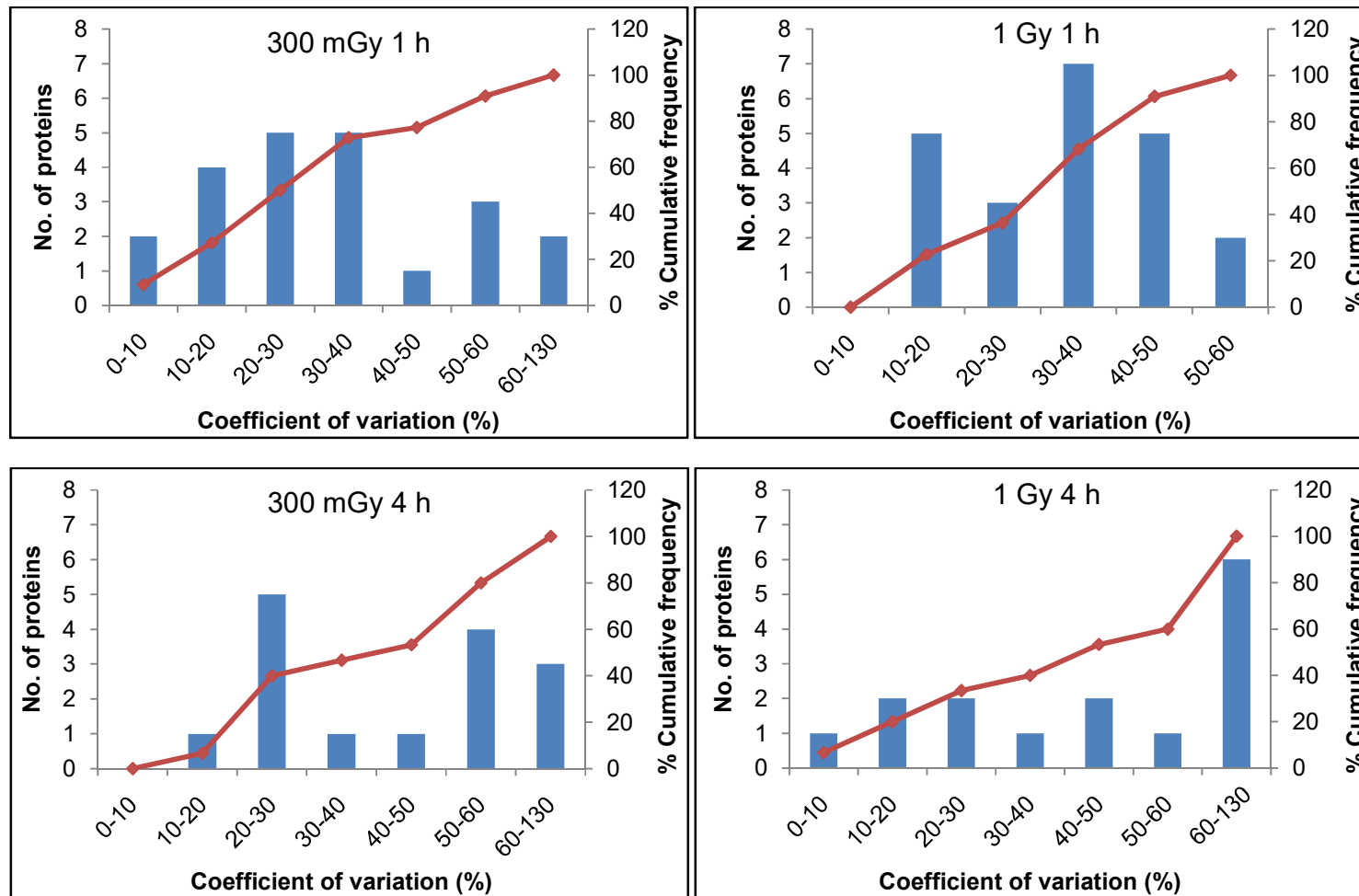


Fig.3.10. The distribution of CV data calculated for differentially modulated proteins at the studied dose (300 mGy and 1 Gy) and time points (1 h and 4 h).

3.1.1.9. Assessment of technical variation

The CV was used as a tool to evaluate the contribution of variation due to sample preparation and run parameters to the total variation. Protein expression was compared between two duplicate gels of a representative individual sample for all the 23 identified radiation responsive proteins (**Table 3.4**). The CV values for the 23 proteins derived from the representative individual were plotted against the combined variation (derived from 8 individuals) for the same proteins (**Fig.3.11, Fig.3.12**). The average technical variation was calculated to be 9.7% for proteins expressed at 1 h (10.6% at 300 mGy vs 8.9% at 1 Gy) and 15.6% for proteins that showed change in expression at 4 h (15% at 300 mGy vs 16% at 1 Gy) (**Table 3.4**). The average contribution of the technical variation (%CV) to the total variation was thus, 12.7%. The scatter was found to be more at late time point of 4 h than at early time point of 1 h (**Fig.3.12**).

Sl. No.	Protein Name	300 mGy 1 h		1.0 Gy 1 h		300 mGy 4 h		1.0 Gy 4 h	
		Mean \pm SD	CV						
1.	Plastin-2	- 1.20 \pm 0.23	26.9	- 1.20 \pm 0.07	8.76	1.98 \pm 0.24	12.27	2.09 \pm 0.31	14.91
2.	WD repeat-containing protein 1	- 1.10 \pm 0.02	2.68	2.19 \pm 0.11	5.09	- 1.40 \pm 0.11	14.42	- 1.30 \pm 0.24	30.3
3.	Vinculin	-1.60 \pm 0.06	9.20	1.03 \pm 0.10	9.97	-1.30 \pm 0.13	17.55	-1.40 \pm 0.14	19.55
4.	PDZ and LIM domain protein 1	- 1.80 \pm 0.03	6.23	- 1.30 \pm 0.09	11.87	- 1.40 \pm 0.07	10.41	- 1.70 \pm 0.11	18.82
5.	Tubulin beta chain	- 1.10 \pm 0.14	15.45	- 1.10 \pm 0.07	6.94	- 1.80 \pm 0.14	25.42	- 2.0 \pm 0.15	28.85
6.	Tubulin alpha chain	1.57 \pm 0.03	1.84	1.44 \pm 0.08	5.5	No change			
7.	Actin gamma/Actin beta	1.82 \pm 0.14	7.77	1.25 \pm 0.07	5.89	1.76 \pm 0.16	9.32	1.19 \pm 0.10	8.06
8.	Actin gamma/Actin beta	1.75 \pm 0.10	5.57	1.99 \pm 0.09	4.62	No change			
9.	Heat shock protein HSP 90-alpha/beta	- 1.20 \pm 0.09	10.73	- 1.10 \pm 0.19	20.45	-1.80 \pm 0.07	11.97	- 1.40 \pm 0.11	15.74
10.	78 kDa glucose-regulated protein	2.00 \pm 0.17	9.15	1.59 \pm 0.10	6.26	- 1.60 \pm 0.08	12.77	- 1.40 \pm 0.12	15.81
11.	T-complex protein 1 subunit beta	- 1.80 \pm 0.06	10.49	- 2.10 \pm 0.08	16.61	No change			
12.	Protein disulfide-isomerase A1	- 1.30 \pm 0.12	15.49	- 1.4 \pm 0.10	13.90	No change			
13.	Leukocyte elastase inhibitor	No change				- 1.4 \pm 0.11	15.20	- 1.2 \pm 0.01	0.93
14.	Peroxiredoxin-6	1.61 \pm 0.10	6.4	1.36 \pm 0.07	5.4	No change			
15.	Chloride intracellular channel protein 1	1.47 \pm 0.08	5.69	1.95 \pm 0.16	8.22	1.84 \pm 0.11	5.84	- 1.20 \pm 0.15	17.62
16.	Ras-related protein Rap-1b	- 1.40 \pm 0.09	12.97	1.74 \pm 0.13	7.19	1.56 \pm 0.10	6.25	1.64 \pm 0.12	7.46
17.	Rab GDP dissociation inhibitor alpha	- 1.30 \pm 0.03	4.27	- 1.50 \pm 0.04	5.52	No change			
18.	Rho GDP-dissociation inhibitor 2	1.85 \pm 0.12	6.4	2.14 \pm 0.11	5.29	No change			
19.	L-lactate dehydrogenase B chain	- 1.60 \pm 0.19	29.58	- 1.20 \pm 0.09	11.04	- 2.0 \pm 0.05	9.87	- 1.40 \pm 0.12	15.76
20.	Purine nucleoside phosphorylase	- 1.20 \pm 0.06	7.68	- 1.40 \pm 0.05	6.63	No change			
21.	Fibrinogen gamma chain	1.62 \pm 0.23	13.88	1.60 \pm 0.10	6.03	- 1.71 \pm 0.11	19.02	- 1.10 \pm 0.13	13.88
22.	Fibrinogen beta chain	2.30 \pm 0.31	13.48	2.60 \pm 0.37	14.13	- 1.30 \pm 0.20	26.54	- 1.20 \pm 0.13	15.47
23.	Thrombospondin-1	1.22 \pm 0.15	12.22	- 1.10 \pm 0.10	10.49	- 1.40 \pm 0.19	27.41	- 2.40 \pm 0.05	19.87

Table 3.4. Fold change in expression of proteins calculated from the technical replicates of a healthy individual. The represented fold change is mean change (\pm SD) in spot intensity in irradiated PBMCs derived from the replicate gels of an individual relative to sham irradiated PBMCs. The symbol (-) depicts down-regulation.

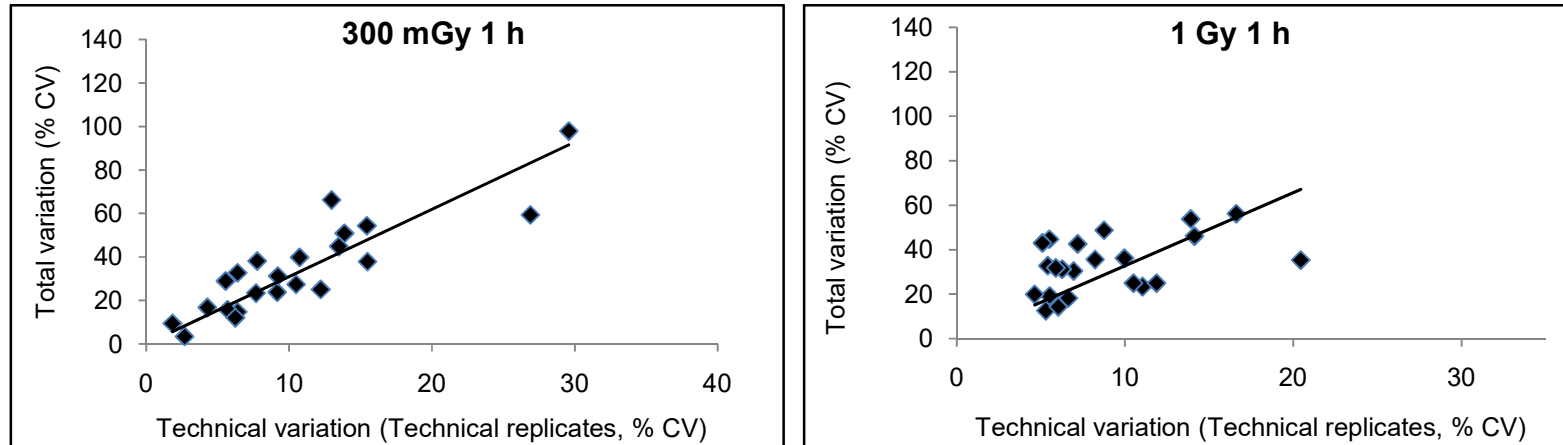


Fig.3.11. The scatter plot illustrates the contribution of variance among the technical replicates for a healthy individual to the total variance at 1 h time point at indicated dose (300 mGy and 1 Gy) points.

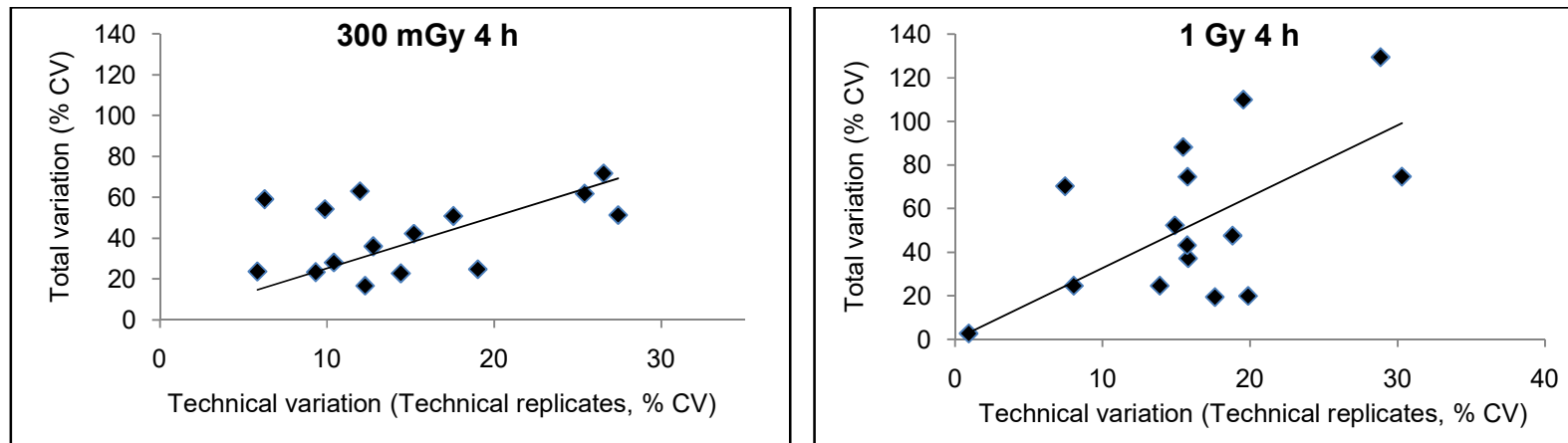
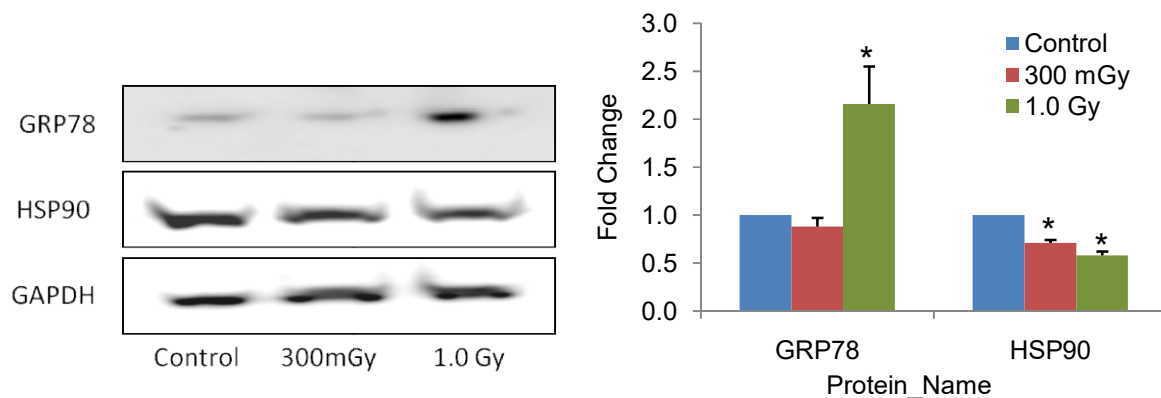


Fig.3.12. The scatter plot illustrates the contribution of variance among the technical replicates for a healthy individual to the total variance at 4 h point at indicated dose (300 mGy and 1 Gy) points. Mean fold change (\pm SD) of differentially expressed protein spots calculated was used to determine coefficient of variation (CV%).

3.1.1.10. Western blot validation of selected radiation responsive proteins

Four key radiation responsive proteins, namely GRP78, HSP90 α/β , PDIA1 and PRDX6 were validated by immunoblotting. The pooled protein lysate from the same eight subjects used for 2DE were analyzed at 1 h post-irradiation by western blot. The protein bands were quantified using Image-J software normalised to expression of housekeeping gene GAPDH expression. The observed expression levels at 300 mGy when compared with sham irradiated controls were: GRP78 (-1.13 fold, $P = 0.13$), HSP90 (-1.42 fold, $P = 0.004$), PDIA1 (-1.62 fold, $P = 0.01$) and PRDX6 (1.14 fold, $P = 0.04$). With 1 Gy, the expression values obtained were GRP78 (2.16 fold, $P = 0.05$), HSP90 (-1.71, $P = 0.02$) PDIA1 (-1.88 fold, $P = 0.0001$) and PRDX6 (1.42 fold, $P = 0.05$) (**Fig.3.13**). The expression levels obtained with western blot analysis were broadly consistent with the 2DE proteomic data.



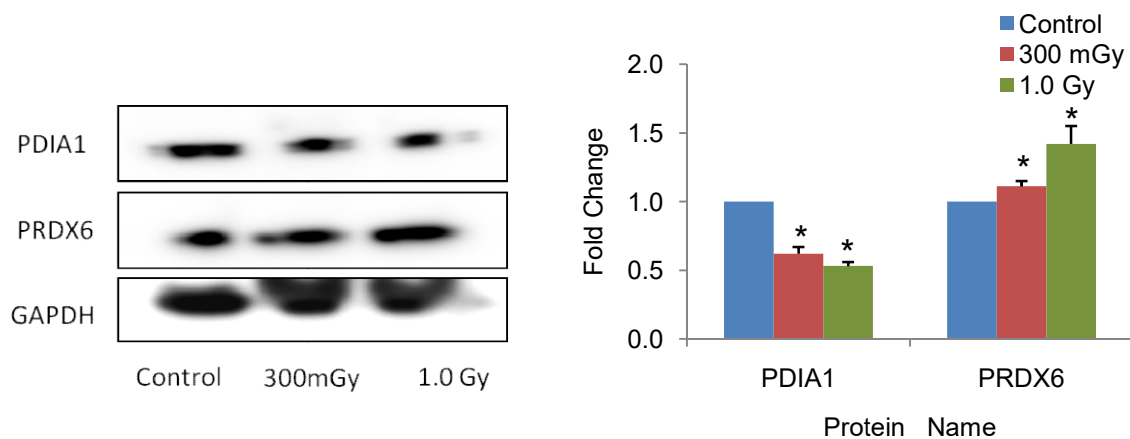


Fig.3.13. Western Blot validation for differentially expressed proteins. Lysates of irradiated samples (300 mGy and 1 Gy) and sham irradiated control were separated on 4–12 % Bis–Tris gels. Proteins were transferred onto PVDF membranes and probed with specific antibodies. The bars correspond to the mean values of three technical replicates of eight pooled biological samples \pm SD. The significance was determined using t test (* $P \leq 0.05$).

3.1.1.11. RT- PCR of selected radiation responsive proteins

To evaluate the transcriptional activity of some of the radiation response proteins, six representative candidate genes (PNP, Prdx6, Hsp90, CLIC, PDI and Grp78) were selected and analysed at same dose and time points as 2DE. Peripheral blood was collected from the same eight individuals and RNA was extracted at three time points: 5 min (termed 0 h), 1 h and 4 h post-irradiation. Since RNA expression generally precedes protein expression, analysis was also performed at an additional early time point of 5 min post irradiation (termed 0 h). Gene expression analysis was performed with RT-PCR using SYBR green based method. The fold changes in expression observed with low

doses of 300 mGy at 5 min post- irradiation for PNP, Prdx6, Hsp90, CLIC, PDI and Grp78 were 1.67 ± 0.32 ($P=0.05$), 1.22 ± 0.24 ($P=0.38$), -1.06 ± 0.10 ($P=0.61$), 1.18 ± 0.23 ($P=0.46$), -1.02 ± 0.12 ($P=0.90$) and 1.26 ± 0.21 ($P=0.24$), respectively. Thus, all but PNP showed insignificant change. By 1 hour, the expression level of all, but PNP came back to the baseline level (at $P \geq 0.05$): PNP (1.28 fold), Prdx6 (-1.09 fold), Hsp90 (-1.03 fold), CLIC (1.09 fold), PDI (1.02) and Grp78 (1.06 fold). There was no significant change in expression 4 h post-irradiation, except for a small increase for Hsp90, with most transcripts at the baseline level (**Fig.3.14A**). Even at high dose of 1Gy, 4 genes showed statistically insignificant up-regulation at 0 h as compared to sham-irradiated controls: PNP (1.19 fold, $P=0.48$), Prdx6 (1.16 fold, $P=0.58$), CLIC (1.36, $P=0.34$) and Grp78 (1.14 fold, $P=0.39$). Two genes: Hsp90 (-1.34, $P=0.02$) and PDI (-1.02, $P=0.77$) showed down-regulation in comparison to sham-irradiated controls. The expression levels of most genes remained unchanged at 1 h and reduced to baseline 4 h post-irradiation (**Fig.3.14B**). Thus, though small alterations in gene expression at mRNA level were observed for the genes analyzed, most changes were not statistically significant. Thus, the correlation between mRNA expression and protein expression was poor. Most genes showed a high inter-individual variation among the samples (**Fig.3.15 A, B**), with higher scatter at the early time point of 5 min post irradiation.

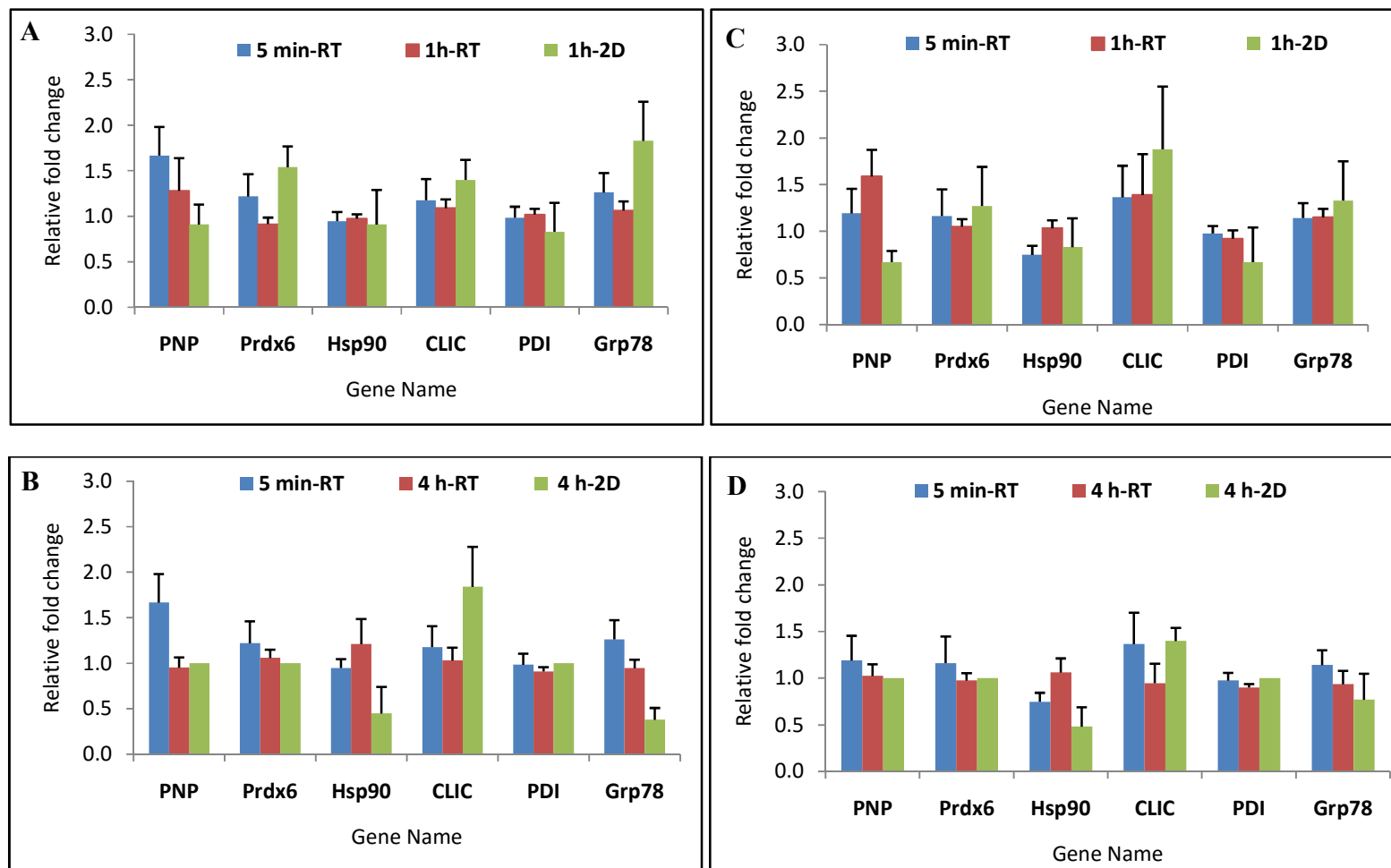


Fig.3.14. Comparison of gene expression data with 2DE proteomics data at radiation dose 300 mGy (A-B) and 1 Gy (C-D). The bars correspond to the mean FC values of eight biological replicates \pm SEM.

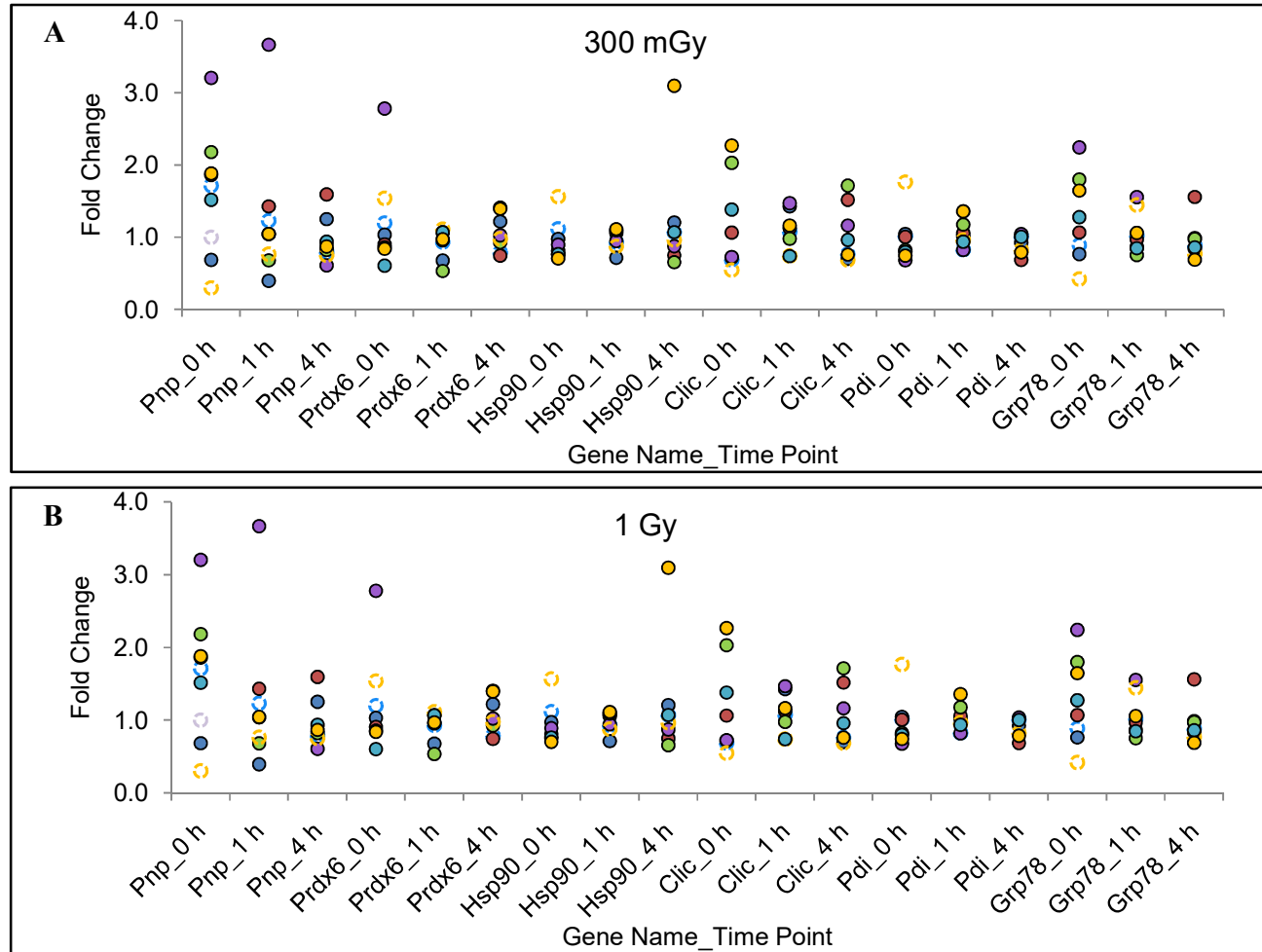


Fig.3.15. Individual variations in gene expression in response to IR, expressed as relative fold change in six radiation response genes with time (0, 1, 4 h) (A) after 300 mGy irradiation (B) after 1 Gy irradiation. Data for each individual is shown as a circle.

3.1.1.12. Principal component analysis for predicting radiation dose groups

To visualize the temporal and radiation dose effects in the PBMC samples, principal component analysis was performed using the raw spot intensity data of all the quantified proteins. PCA was able to interpret relationships between experimental groups and allowed clustering of low dose irradiated (300 mGy) and high dose irradiated (1 Gy) samples compared to sham irradiated controls, at both time points (1 h and 4 h). The first two principal components explained ~36.43% of the data variance at 1 h (**Fig.3.16A**) and ~41.49% variance at 4 h (**Fig.3.16B**). Interestingly, though the variance was high as seen in **Fig.3.12**, the clustering was tighter at 4 h than at 1 h. This indicated the utility of PCA in predicting groups based on radiation dose.

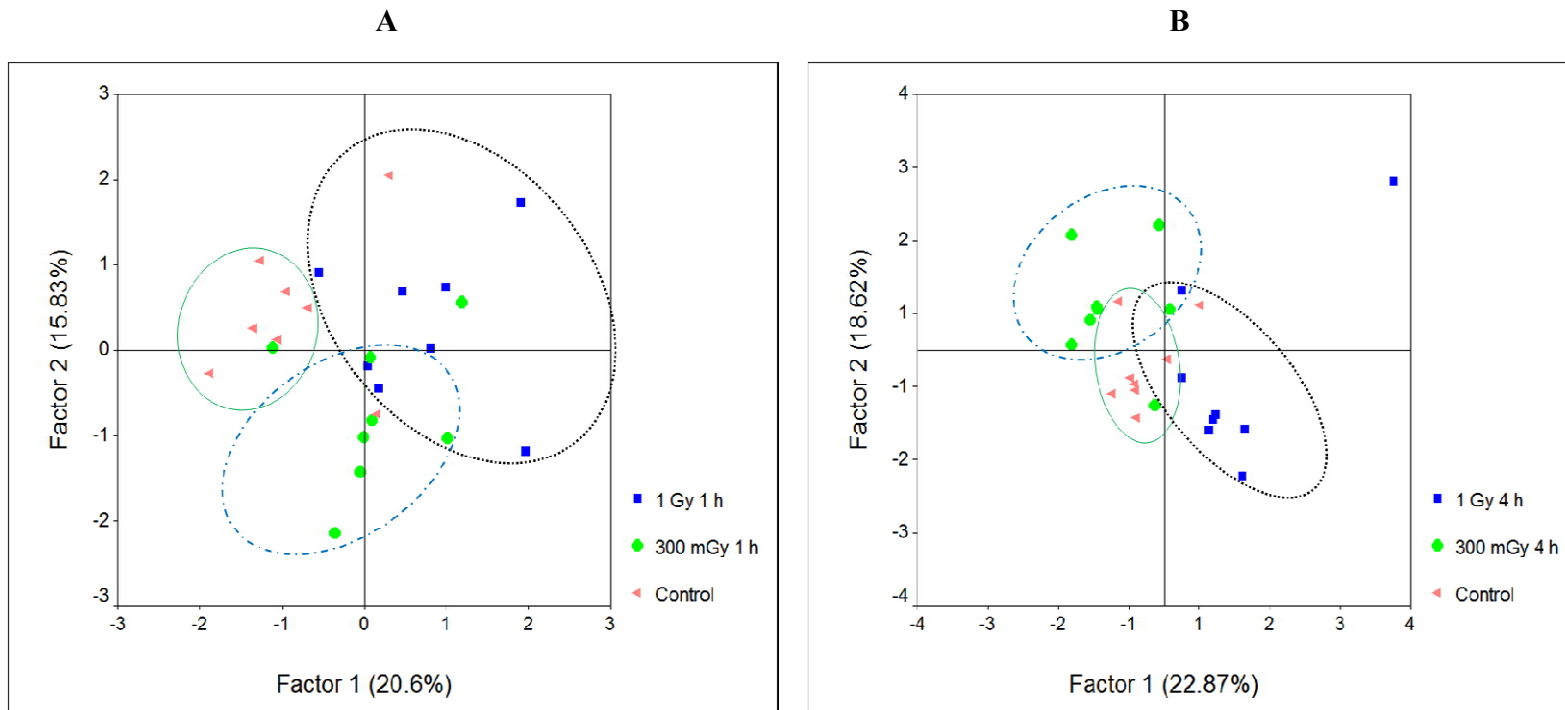


Fig.3.16. Principal component analysis for the protein expression data set after irradiation with 300 mGy and 1 Gy at (A) 1 h and (B) 4 h post-irradiation. PCA identified three clusters using the raw spot intensity data of all the quantified proteins. Biological replicates belonging to each group (8 subjects/group) were colour coded.

3.1.1.13. Gender specific differences in IR induced differential protein expression

As discussed in section 3.1.1.2, the combined analysis with 8 samples (4 male/4 female) identified 23 proteins significantly altered in irradiated human PBMCs (300 mGy and 1 Gy) when compared to sham irradiated cells with fold change ± 1.5 fold ($P \leq 0.05$). To understand the potential gender specific differences in IR induced protein responses, the above data was apportioned to analyze male and female samples separately. For this, two analysis set were created. In the first set, the proteomic maps of irradiated samples (300 mGy and 1 Gy) from male subjects were compared with sham irradiated male controls at both time points (1 h and 4 h post irradiation). In second analysis set, the proteomic maps of irradiated samples (300 mGy & 1 Gy) from female subjects were compared with sham irradiated female controls at both time points (1 h and 4 h post irradiation). Proteins which were present in all biological replicates with $P \leq 0.05$ were considered as differentially modulated. Statistical significance was assessed using two-tailed Student's t-test ($P \leq 0.05$). Bioinformatics analysis of the total protein profile showed that there was no difference in the average number of observed proteins observed between both genders. The dose and time dependent analysis of IR modulated proteins showed that there were three proteins uniquely modulated by IR in males while there were four such proteins found uniquely in females (**Fig.3.17**). Six of these seven potential gender specific proteins were identified with MALDI TOF mass spectrometry (**Table 3.5**). One protein (spot no. F) could not be identified due to insufficient amount of peptide signals in the mass spectra. The average inter-individual % CV for the modulated proteins was found to be higher for female than for male samples. A multivariate analysis of the protein expression data using PCA was performed to visually assess similarities

and differences between the two groups. PCA clearly defined three clusters according to the radiation dose both at 1 h (**Fig.3.18A**) and 4 h (**Fig.3.18B**), but was unable to distinguish between male and female individuals.

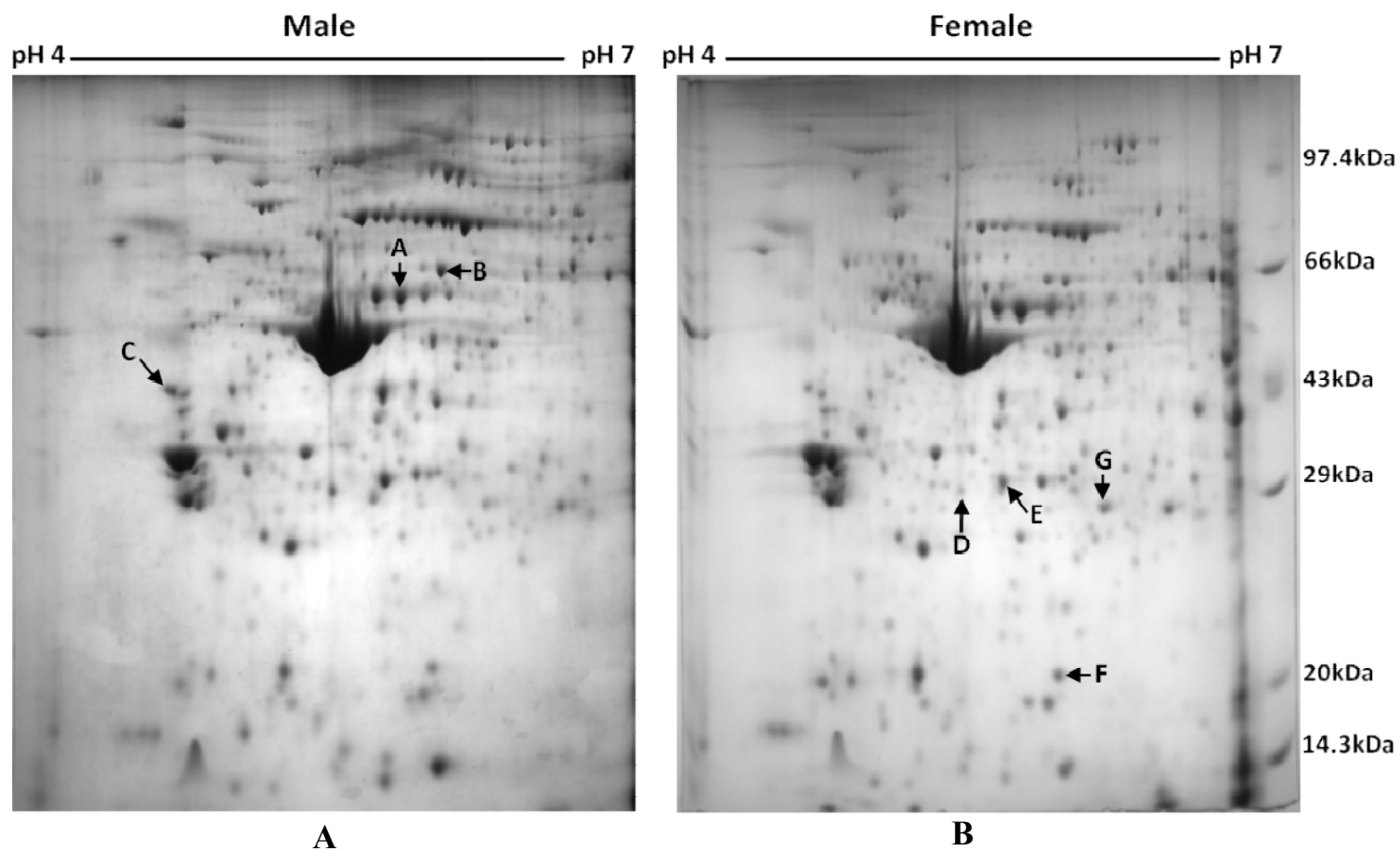


Fig.3.17. Representative images of human PBMCs for a (A) male, and (B) a female individual. The positions of gender specific radiation responsive proteins are marked with arrows on the respective gels, and are numbered as listed in **Table 3.5**.

Spot label	Protein Name	300 mGy 1 h		1 Gy 1 h		300 mGy 4 h		1 Gy 4 h	
		Mean \pm SD	CV (%)	Mean \pm SD	CV (%)	Mean \pm SD	CV (%)	Mean \pm SD	CV (%)
Proteins modulated uniquely in male samples									
A	Fibrinogen gamma chain (FIBG)	1.6 \pm 0.3 <i>P</i> = 0.006	18	1.7 \pm 0.3 <i>P</i> = 0.002	10.3	No change		No change	
B	Protein disulfide-isomerase A3 (PDIA3)	1.6 \pm 0.5 <i>P</i> = 0.05	30.2	1.5 \pm 0.4 <i>P</i> = 0.034	24.4	No change		No change	
C	Tropomyosin beta chain (2) [TPM2 (2)]	No change		No change		1.1 \pm 0.4 <i>P</i> = 0.5	31.72	1.5 \pm 0.4 <i>P</i> = 0.03	23.5
Proteins modulated uniquely in female samples									
D	Actin gamma /Actin beta ACT	-1.6 \pm 0.3 <i>P</i> = 0.03	41.8	-1.5 \pm 0.3 <i>P</i> = 0.11	49.3	No change		No change	
E	Actin gamma /Actin beta [ACT (5)]	-1.5 \pm 0.3 <i>P</i> = 0.042	38.9	-1.1 \pm 0.2 <i>P</i> = 0.7	20.1	No change		No change	
F	NI	-1.8 \pm 0.2 <i>P</i> = 0.004	36.8	-1.6 \pm 0.3 <i>P</i> = 0.046	49.2	No change		No change	
G	Proteasome activator complex (PSME1)	No change		No change		1.6 \pm 0.4 <i>P</i> = 0.03	24.92	1.9 \pm 0.7 <i>P</i> = 0.04	36.4

Table 3.5. Fold changes in expression of proteins uniquely modulated in male or female individuals. The represented fold change is mean change (\pm SD) in spot intensity in irradiated PBMCs derived from 4 male or female individuals relative to sham irradiated PBMCs. The symbol (–) depicts down regulation. The proteins are listed A–G as labeled on **Fig.3.17**.

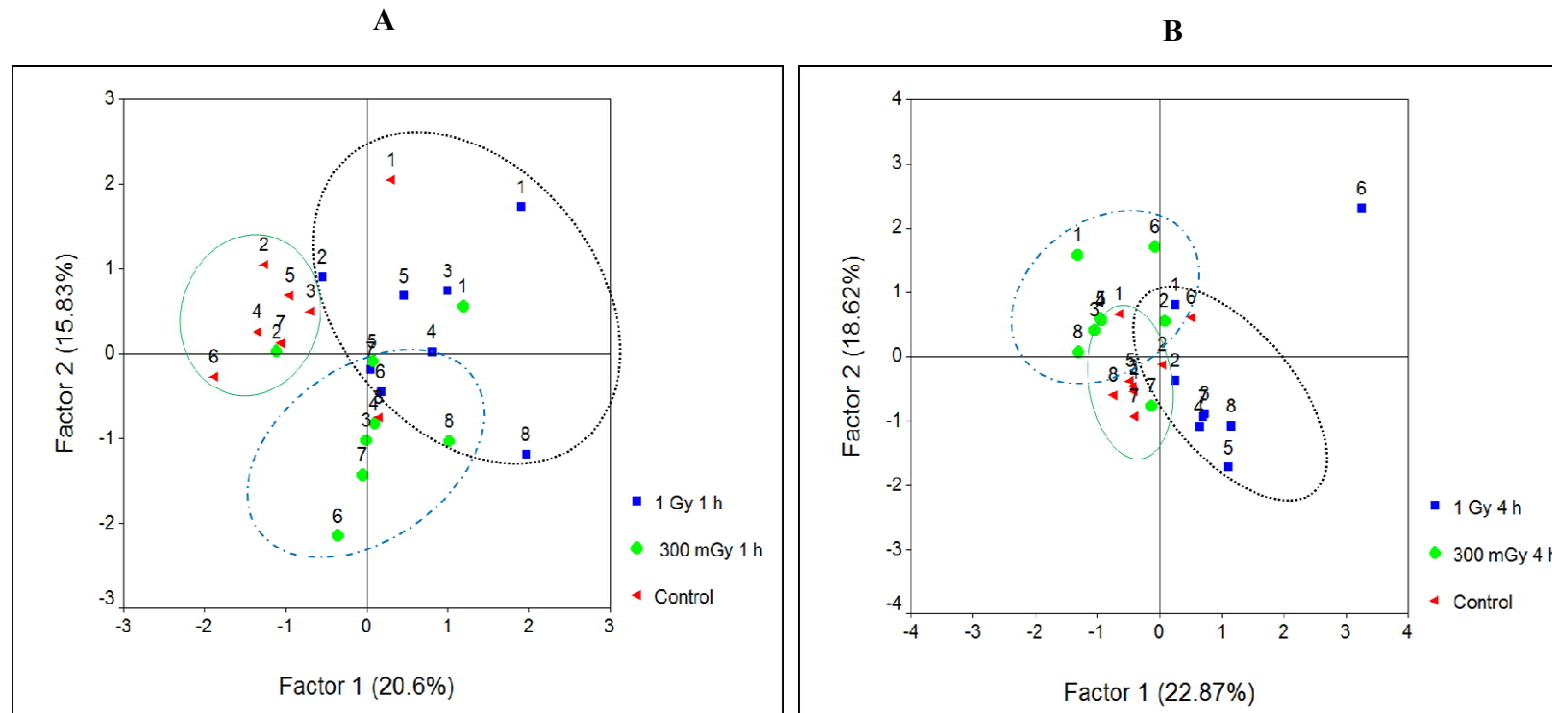


Fig.3.18. Principal component analysis of the protein expression data set for gender specific differences (A) 1 h post-irradiation and (B) 4 h post-irradiation. Each dot represents an individual. Individuals marked 1-4 were female samples, while individuals marked 5-8 were male samples.

3.1.2. Gene expression of AP1 family genes

Transcription factors (TF) are diverse family of proteins that translate extracellular signals into consequent cellular effects by regulating specific gene targets. Many TFs like activator protein-1 (AP-1) have been implicated in the inducible expression of genes in response to genotoxic agents like IR [75]. Several studies have reported changes in expression of single (or few) members of AP-1 family genes in response to external stress, though none have analyzed coordinated expression of genes that constitute AP-1 dimer. We therefore, studied mRNA profiles of fos family (*cfos*, *fosB*, *fosL1* and *fosL2*) and jun family (*c-jun*, *junB* and *junD*) genes for ten individuals (age group: 25–30 years). The isolated PBMCs were irradiated *ex vivo* with two doses (300 mGy and 1Gy) at a dose rate of 0.417 Gy/min using a Co⁶⁰ γ -ray source (Blood irradiator, 2000, BRIT) at room temperature. The irradiated PBMCs were divided into three sets for RNA extraction: one set was processed immediately within 5 min post-irradiation (termed as 0 h time point), and the other two sets was processed 1 h and 4 h post-irradiation. The cells were incubated in RPMI-1640 media at 37 °C in a humidified 5% CO₂ atmosphere for the required time before RNA extraction. Each set consisted of a sham-irradiated control incubated for the same duration under similar conditions. Genes which showed a statistical difference at the 95% confidence level using Student's t-test ($P \leq 0.05$) were considered to be differentially regulated. The dose and time points used were similar to that used earlier with 2DE-MS (section 3.1.1). As discussed earlier, there was only a negligible decrease in cell viability under these conditions (**Fig.3.6**). *β -actin* was used as an endogenous control gene to normalize the expression of target genes.

3.1.2.1. Evaluation of expression values for β -actin reference gene with radiation

We first analysed the threshold cycle values (C_T) of β -actin in human PBMCs collected from three individuals at the dose/time points used in this study. The C_T values of the β -actin found to vary between 17 and 19 cycles with the irradiation doses or time points, indicating stable expression in human PBMCs (Fig.3.19). Thus, there was minimum inter-individual variation in the β -actin gene indicating its suitability for quantitative gene expression studies on G_0 human PBMCs with γ -irradiation. The validation of reference genes for an experiment under a specific set of conditions and tissue type is important for the proper interpretation of the results.

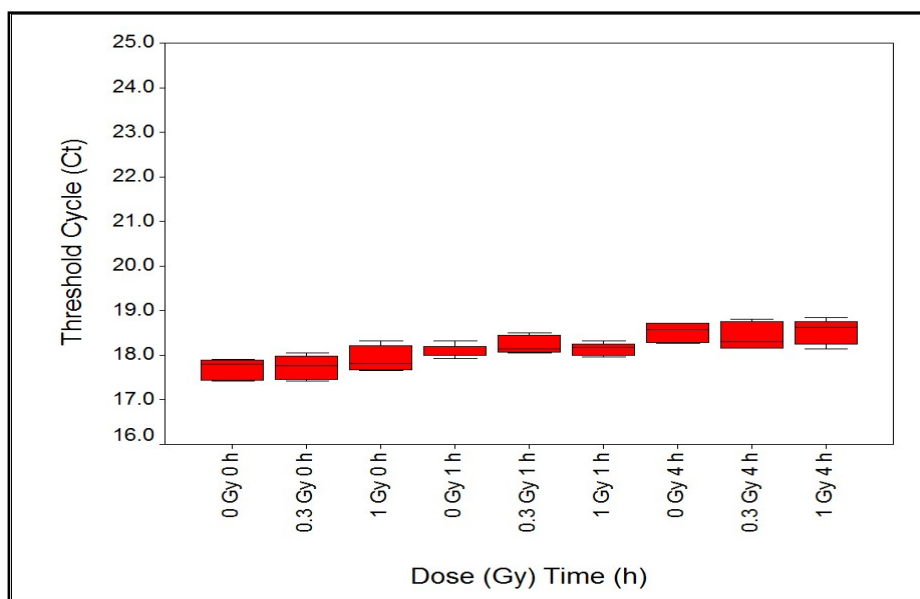


Fig.3.19. Threshold cycle (C_T) values for β -actin reference gene following radiation exposure in human PBMCs. Each box represents C_T values for three individuals, at the respective dose (0, 0.3 and 1 Gy) and time points (0, 1 and 4 h), analyzed in duplicate. For each individual icon, the middle horizontal line is the median, the top and bottom of the boxes are the 25th and 75th percentiles, and the upper and lower horizontal lines (whiskers) indicate the ranges.

3.1.2.2. Time kinetics of AP1 genes in PBMCs with acute dose of 300 mGy

When analyzed immediately following irradiation (termed 0 h), human PBMCs showed significant alterations in gene expression for three out of four fos family genes (*fosB*, *fosL1* and *fosL2*) and one out of three jun family genes (*c-jun*) with 300 mGy. The studied samples showed two distinct trends in gene expression. Six out of ten individuals showed transient, but significant (≥ 1.5 fold, $P \leq 0.001$) up-regulation for *fosB*, *fosL1*, *fosL2* and *c-jun* as compared to sham-irradiated controls. The remaining four individuals showed down-regulation for these same four genes (**Fig.3.20A**). Based on this opposing expression pattern, the samples were grouped into: ‘Group I responders’ (samples coded 1–6) which showed up-regulation for *fosB*, *fosL1*, *fosL2* and *c-jun* genes and ‘Group II responders’ (samples coded 7–10) which showed down-regulation for the same four genes (**Fig. 3.21**). The Group I responders showed an average fold change (FC) of 1.90 ± 0.32 , 2.14 ± 0.45 , 1.92 ± 0.51 and 2.09 ± 0.51 for *fosB*, *fosL1*, *fosL2* and *c-jun*, respectively, as compared to sham-irradiated controls. The Students’s t-test *P*-value for all four genes was ≤ 0.001 , indicating strong up-regulation (**Table 3.6**). The average FC for Group II responders for *fosB*, *fosL1*, *fosL2* and *c-jun* were 0.53 ± 0.22 ($P = 0.006$), 0.60 ± 0.14 ($P = 0.001$), 0.52 ± 0.16 ($P = 0.001$) and 0.59 ± 0.28 ($P = 0.03$), respectively (**Table 3.6**).

For *c-fos*, *junB* and *junD* genes, no significant change in gene expression was observed ($FC \leq 1.1$) in both Group I and Group II responders at the studied dose/time points, as compared to sham-irradiated controls (**Fig.3.20B**). The observed FC in Group I responders for *c-fos*, *junB* and *junD* was 1.01 ± 0.12 ($P = 0.79$), 1.12 ± 0.19 ($P = 0.16$) and 1.06 ± 0.13 ($P = 0.32$), respectively. The FC in Group II responders for *c-fos*, *junB*

and *junD* genes was 0.98 ± 0.19 ($P = 0.82$), 0.91 ± 0.09 ($P = 0.08$) and 1.01 ± 0.04 ($P = 0.58$), respectively (Table 3.6).

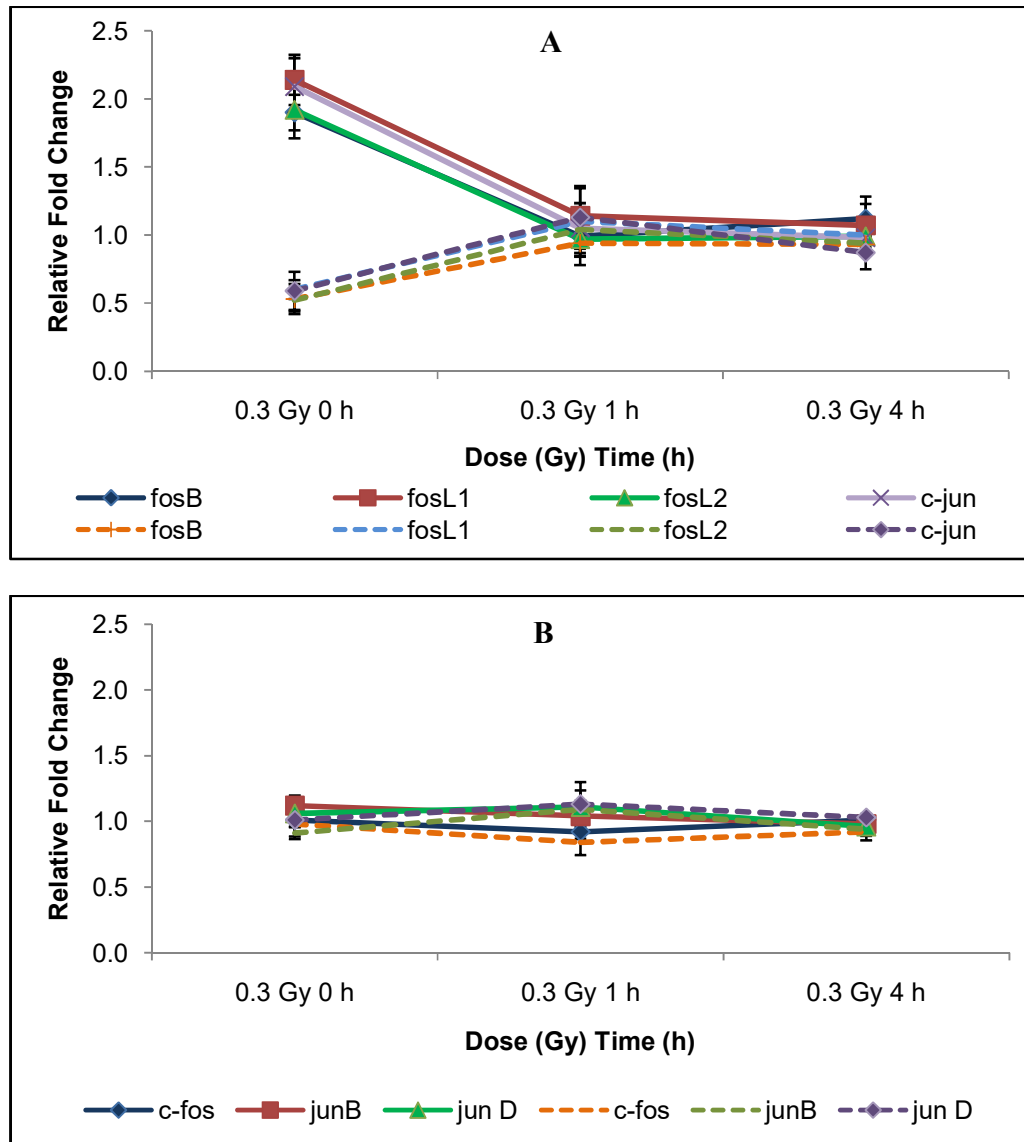


Fig.3.20. Time kinetics of AP1 genes for individuals after irradiation with 300 mGy at the respective time points (0, 1, 4 h). (A) Profile of genes which showed significant change in expression (*fosB*, *fosL1*, *fosL2* and *c-jun*) and (B) profile of genes which did not show significant change in expression (*c-fos*, *junB* and *junD*), when compared with sham-irradiated controls. The *thick lines* represents average gene expression for six individuals grouped as ‘Group I Responders’ and on the *dash lines* represents average gene expression for four individuals grouped as ‘Group II Responders’. Error bars represent SEM calculated from the respective individuals in each group.

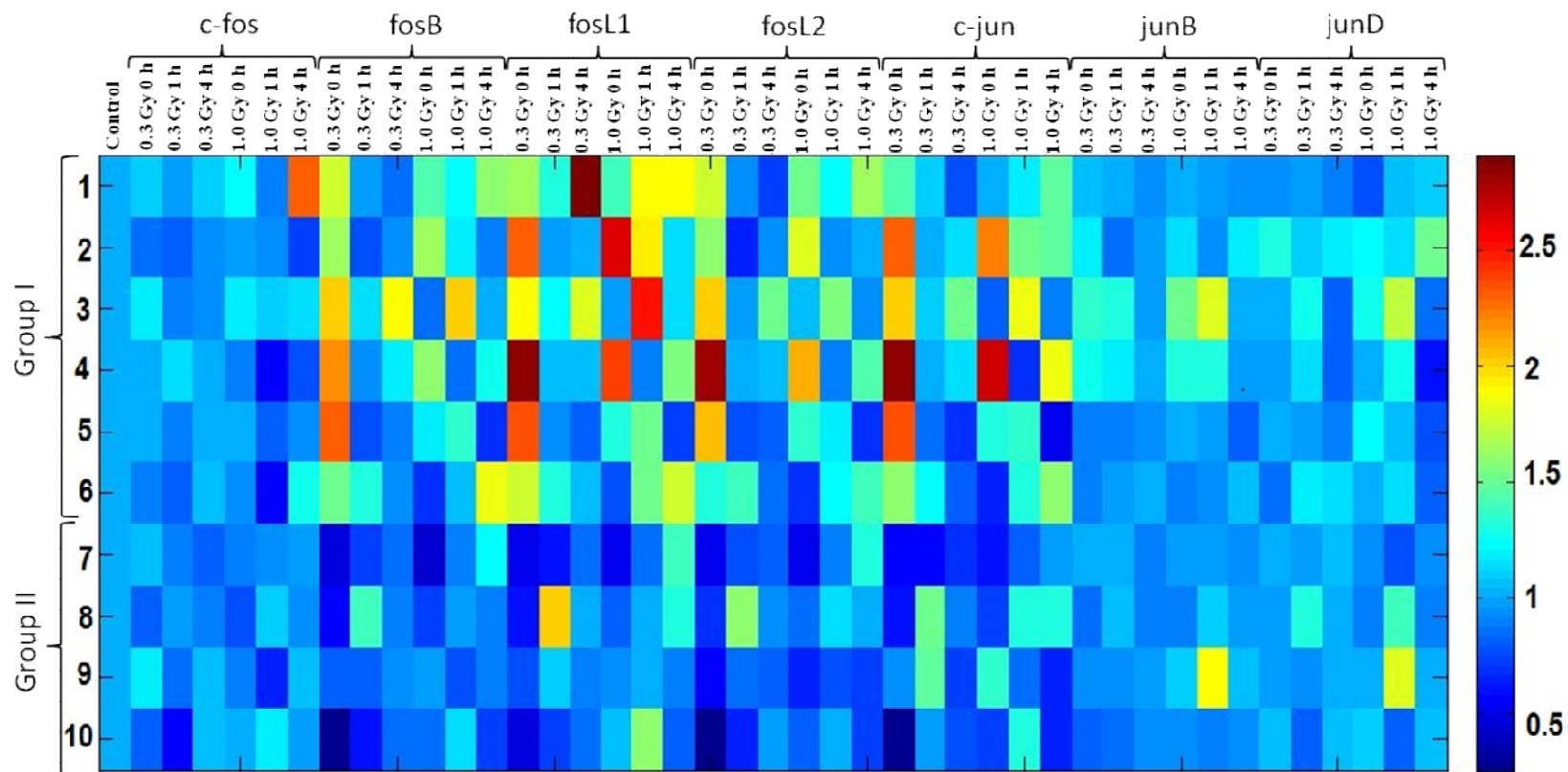


Fig.3.21. Heat map showing alterations in gene expression in human PBMCs for seven AP1 genes, expressed as fold change in irradiated (0.3 and 1 Gy) cells *vis-a-vis* sham-irradiated cells at the indicated time points (0, 1 and 4 h). Each row represents an individual. Numbers on the left represent sample codes. Samples 1–6 grouped as ‘Group I responders’; Samples 7–10 grouped as ‘Group II responders’.

By one hour, the expression levels of most genes for both Group I as well as Group II responders were back to the baseline level of sham-irradiated controls and remained at that level after 4 h (**Fig.3.20A-B**). This indicates that there was no differential expression as compared to sham-irradiated controls at 1 h and 4 h post-irradiation with 300 mGy (**Table 3.6**). Few individuals among Group I and Group II responders showed an exception to the rule with a biphasic up-regulation either at 1 h or 4 h post-irradiation. Individual 1 (sample code 1) and individual 3 (sample code 3) among Group I responders showed a deviation with an up-regulation for *fosL1* gene at 4 h post-irradiation (**Fig.3.22**). The individual 3 also exhibited an up-regulation pattern for *fosB* gene at 4 h time point (**Fig.3.22**). The individual 8 (sample code 8) among Group II responders showed an up-regulation for *fosL1* and *fosL2* at 1 h post-irradiation with 300 mGy, and returned to the baseline at 4 h (**Fig.3.22**).

Gene Name	Group I responders					
	0 h		1 h		4 h	
	FC	<i>P</i> -value	FC	<i>P</i> -value	FC	<i>P</i> -value
<i>cfos</i>	1.01 ± 0.12	0.79	0.92 ± 0.13	0.18	1.01 ± 0.07	0.64
<i>fosB</i>	1.90 ± 0.32	4.84 E-05	0.99 ± 0.22	0.91	1.12 ± 0.40	0.49
<i>fosL1</i>	2.14 ± 0.45	0.0001	1.14 ± 0.16	0.07	1.07 ± 0.39	0.66
<i>fosL2</i>	1.92 ± 0.51	0.001	0.97 ± 0.25	0.76	0.99 ± 0.29	0.93
<i>cjun</i>	2.09 ± 0.51	0.0004	1.05 ± 0.13	0.34	0.98 ± 0.25	0.83
<i>junB</i>	1.12 ± 0.19	0.16	1.04 ± 0.17	0.59	0.98 ± 0.03	0.12
<i>jun D</i>	1.06 ± 0.13	0.32	1.11 ± 0.12	0.06	0.96 ± 0.17	0.58
Group II responders						
<i>cfos</i>	0.98 ± 0.19	0.82	0.84 ± 0.19	0.14	0.92 ± 0.13	0.26
<i>fosB</i>	0.53 ± 0.22	0.006	0.94 ± 0.32	0.71	0.93 ± 0.11	0.21
<i>fosL1</i>	0.60 ± 0.14	0.001	1.10 ± 0.52	0.72	1.00 ± 0.25	1.00
<i>fosL2</i>	0.52 ± 0.16	0.001	1.04 ± 0.39	0.83	0.94 ± 0.12	0.34
<i>cjun</i>	0.59 ± 0.28	0.03	1.13 ± 0.43	0.57	0.87 ± 0.24	0.32
<i>junB</i>	0.91 ± 0.09	0.08	1.09 ± 0.29	0.57	0.94 ± 0.03	0.01
<i>jun D</i>	1.01 ± 0.04	0.58	1.13 ± 0.34	0.48	1.03 ± 0.05	0.32

Table 3.6. Mean fold change of gene expression in PBMCs with acute 300 mGy at the respective time points (0 h, 1 h and 4 h post irradiation). The FC ± SD represents mean fold change ± standard deviation for six individuals (termed as ‘Group I responders’) and four individuals (termed as ‘Group II responders’) relative to respective sham irradiated control. *P*-values were calculated using Student’s t-test. The significant *P*-values (*P* ≤0.05) are represented in bold.

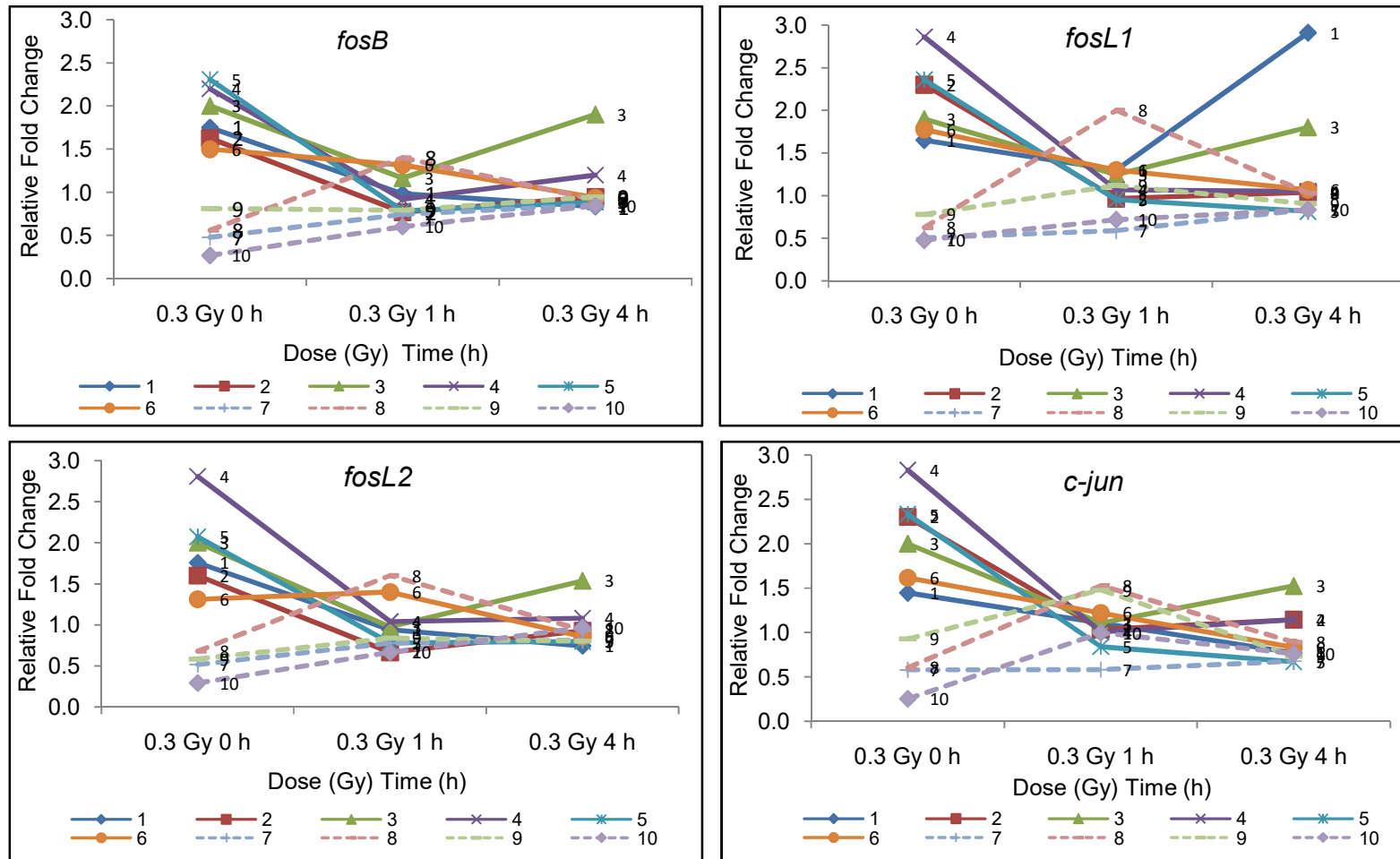


Fig.3.22. Relative fold changes of *fosB*, *fosL1*, *fosL2* and *c-jun* genes for the 10 individuals after irradiation with 300 mGy at the respective time points (0 h, 1 h, 4 h), which showed significant change in expression. Individuals (1 - 6) marked with thick lines (—) were grouped as ‘Group I responders’ and individuals (7-10) marked with dash lines (-----) were grouped as ‘Group II responders’.

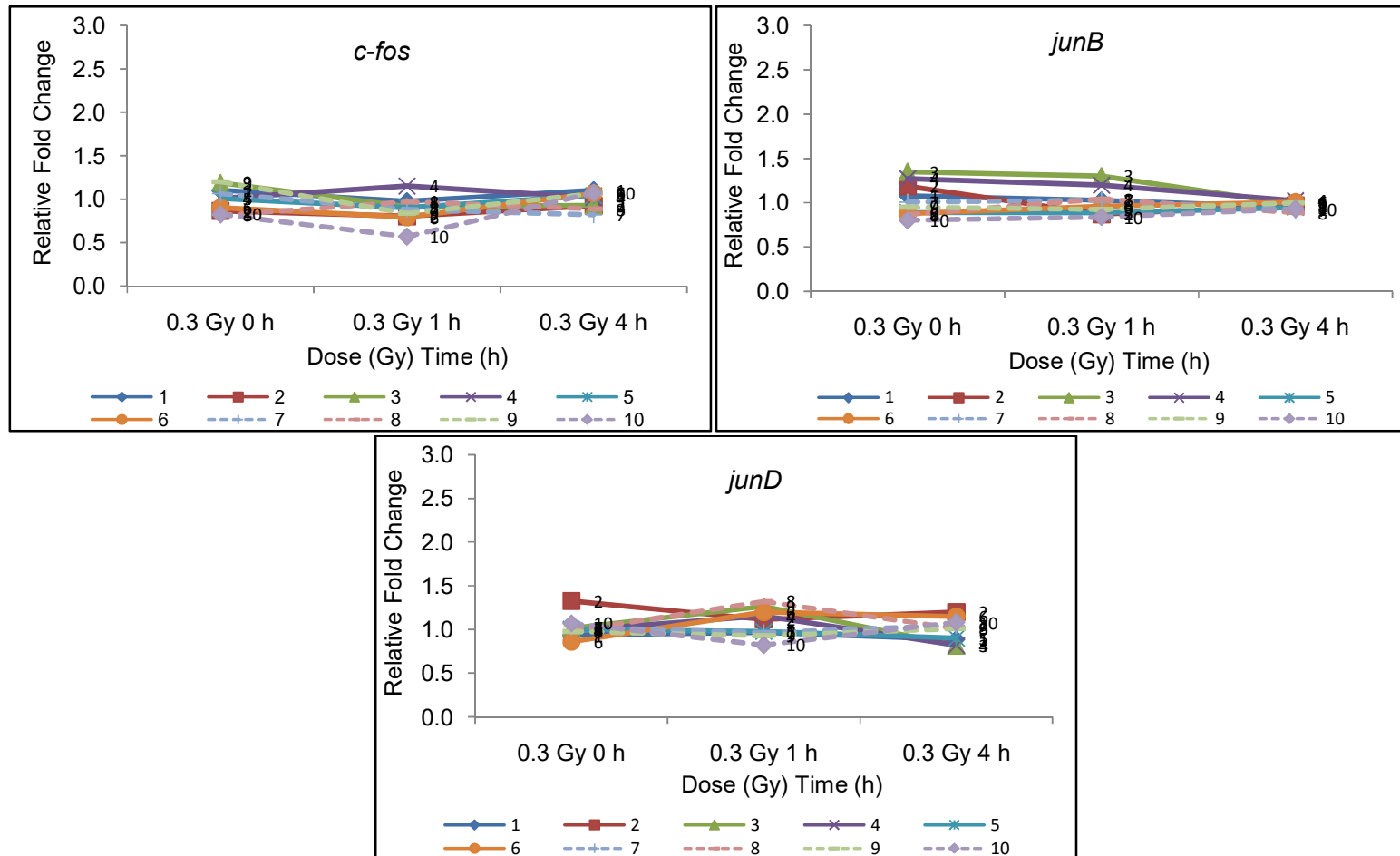


Fig.3.23. Relative fold changes of *c-fos*, *junB* and *junD* genes for the 10 individuals after irradiation with 300 mGy at the respective time points (0 h, 1 h, 4 h), which did not show change in expression, when compared with sham irradiated controls. Individuals (1 - 6) marked with thick lines (—) were grouped as ‘Group I responders’ and individuals (7-10) marked with dash lines (.....) were grouped as ‘Group II responders’.

3.1.2.3. Time kinetics of AP1 genes in PBMCs with acute dose of 1 Gy

With relatively high dose of 1Gy, the studied individuals showed a similar trend in gene expression seen with low dose of 300 mGy at 0 h post-irradiation. The Group I individuals showed an up-regulation and Group II individuals showed a down-regulation at *fosB*, *fosL1*, *fosL2* and *c-jun*, respectively (**Fig.3.24A**). However, the expression changes were not statistically significant (at $P \leq 0.05$) with an exception of *fosL2* (mean FC = 0.70 ± 0.15 , $P = 0.008$) for Group II individuals (**Table 3.7**). No significant change in gene expression was observed for *c-fos*, *junB* and *junD* genes as compared to sham-irradiated controls (FC ≤ 1.1) at the studied dose/time points (**Fig.3.24B**). The observed fold changes at 1 Gy post-irradiation were lower than that observed with 300 mGy (**Table 3.7**). By one hour again, the gene expression levels were back to baseline of sham-irradiated controls (average FC ~ 1.0) and remained at that level even after 4 h (**Fig.3.25** and **Fig.3.26**). The group I responders showed an exemption with an up-regulation for *fosL1* (mean FC = 1.71 ± 0.53 , $P = 0.01$) and *junD* (mean FC 1.23 ± 0.24 , $P = 0.04$) at 1 h (**Table 3.7**). This again indicates no differential expression for both Group I as well as Group II responders as compared to sham-irradiated controls.

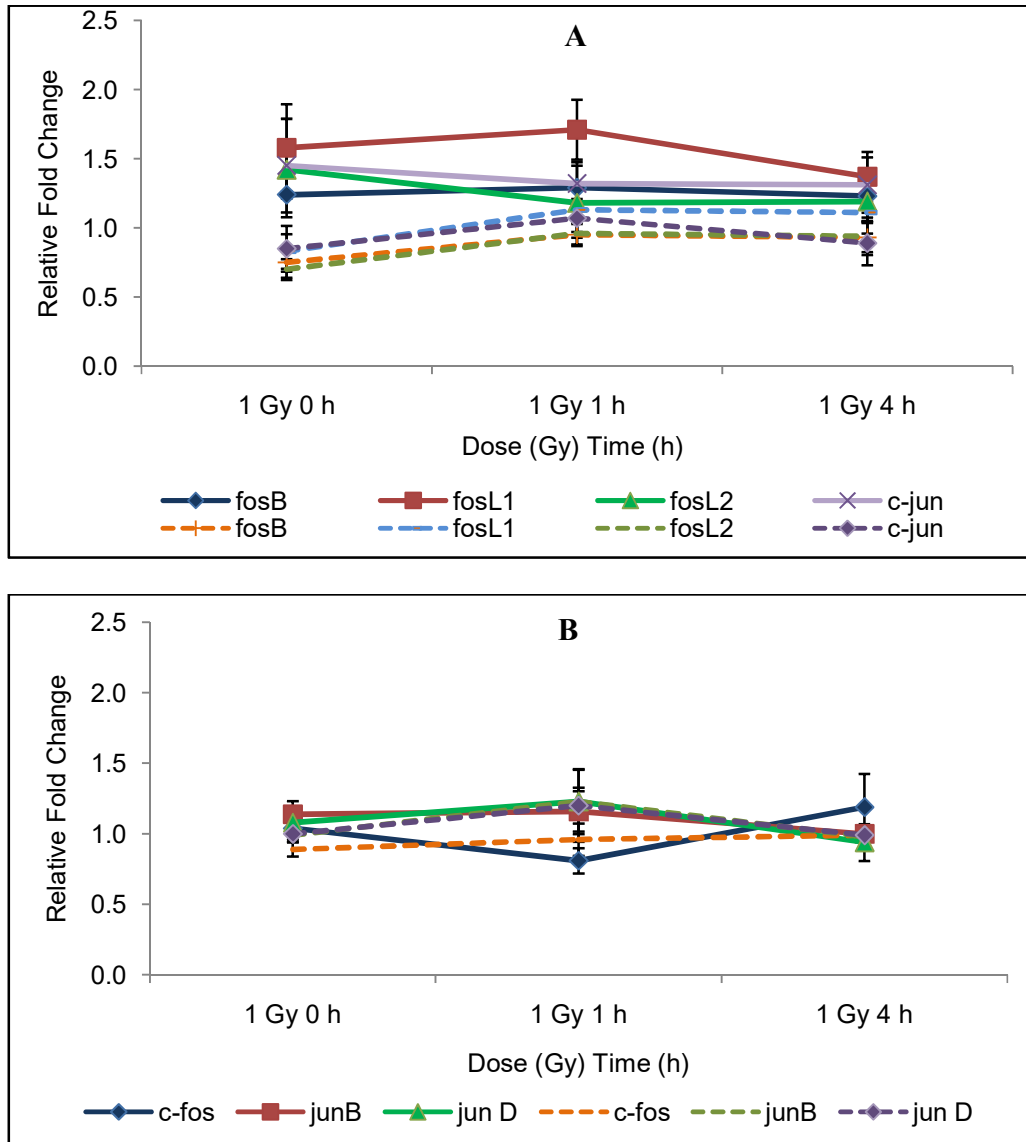


Fig.3.24. Time kinetics of AP1 genes for individuals after irradiation with 1 Gy at the respective time points (0 h, 1 h, 4 h). (A) Profile of genes which showed significant change in expression (*fosB*, *fosL1*, *fosL2* and *c-jun*) and (B) Profile of genes which did not significant change in expression (*c-fos*, *junB* and *junD*), when compared with sham irradiated controls. For each gene at the respective dose/time point, each point on the *thick lines* represent average gene expression for 6 individuals grouped as ‘Group I responders’ and the *dash lines* represent average gene expression for 4 individuals grouped as ‘Group II responders’. Error bars represent standard error of the mean calculated from the mean values obtained from the individuals in respective groups.

Gene Name	Group I responders					
	0 h		1 h		4 h	
	FC	<i>P</i> value	FC	<i>P</i> value	FC	<i>P</i> value
<i>cfos</i>	1.04 ± 0.14	0.48	0.81 ± 0.22	0.06	1.19 ± 0.58	0.43
<i>fosB</i>	1.24 ± 0.40	0.17	1.29 ± 0.39	0.10	1.23 ± 0.44	0.24
<i>fosL1</i>	1.58 ± 0.77	0.10	1.71 ± 0.53	0.01	1.37 ± 0.44	0.07
<i>fosL2</i>	1.42 ± 0.51	0.07	1.18 ± 0.23	0.09	1.19 ± 0.36	0.22
<i>cjun</i>	1.45 ± 0.83	0.21	1.32 ± 0.38	0.07	1.31 ± 0.49	0.16
<i>junB</i>	1.14 ± 0.23	0.18	1.16 ± 0.35	0.30	1.00 ± 0.13	0.99
<i>jun D</i>	1.08 ± 0.19	0.33	1.23 ± 0.24	0.04	0.94 ± 0.32	0.64
Group II responders						
<i>cfos</i>	0.89 ± 0.10	0.07	0.96 ± 0.23	0.76	0.99 ± 0.05	0.60
<i>fosB</i>	0.75 ± 0.22	0.07	0.95 ± 0.16	0.53	0.93 ± 0.21	0.56
<i>fosL1</i>	0.83 ± 0.25	0.22	1.13 ± 0.32	0.45	1.11 ± 0.30	0.50
<i>fosL2</i>	0.70 ± 0.15	0.008	0.96 ± 0.16	0.63	0.94 ± 0.27	0.70
<i>cjun</i>	0.85 ± 0.33	0.41	1.07 ± 0.28	0.65	0.89 ± 0.32	0.53
<i>junB</i>	0.99 ± 0.09	0.77	1.23 ± 0.46	0.36	0.98 ± 0.06	0.47
<i>jun D</i>	1.00 ± 0.08	0.98	1.20 ± 0.51	0.46	0.99 ± 0.07	0.75

Table 3.7. Mean fold change of gene expression in PBMCs with acute 1 Gy at the respective time points (0 h, 1 h and 4 h post-irradiation). The FC ± SD represents mean fold change ± standard deviation for six individuals (termed as ‘Group I responders’) and four individuals (termed as ‘Group II responders’) relative to respective sham irradiated control. *P*-values were calculated using Student’s t-test. The significant *P*-values ($P \leq 0.05$) are represented in bold.

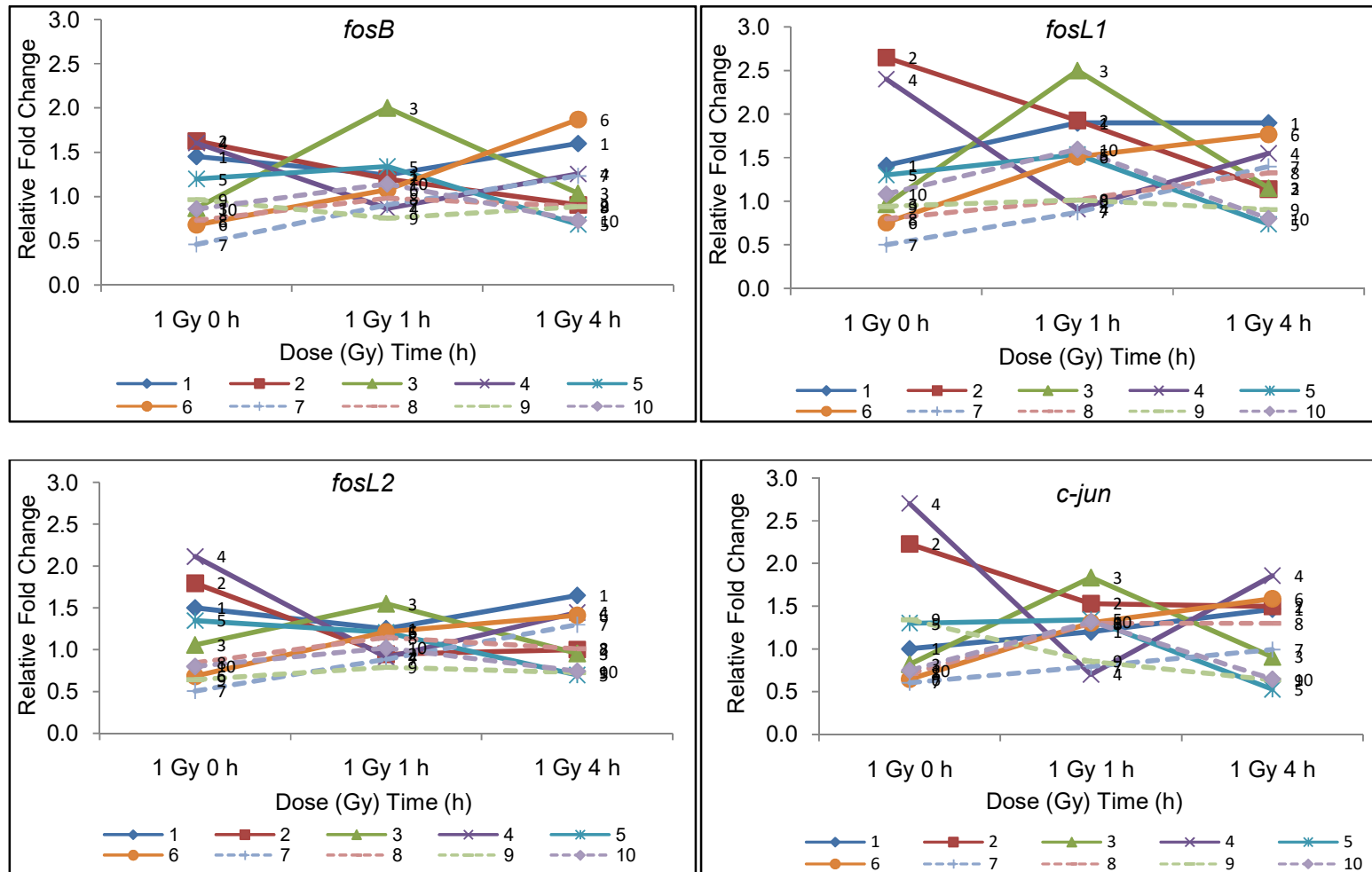


Fig.3.25. Relative fold changes of *fosB*, *fosL1*, *fosL2* and *c-jun* genes for the 10 individuals after irradiation with 1 Gy at the respective time points (0 h, 1 h, 4 h), which showed significant change in expression. Individuals (1 - 6) marked with thick lines (—) were grouped as ‘Group I responders’ and individuals (7-10) marked with dash lines (·····) were grouped as ‘Group II responders’.

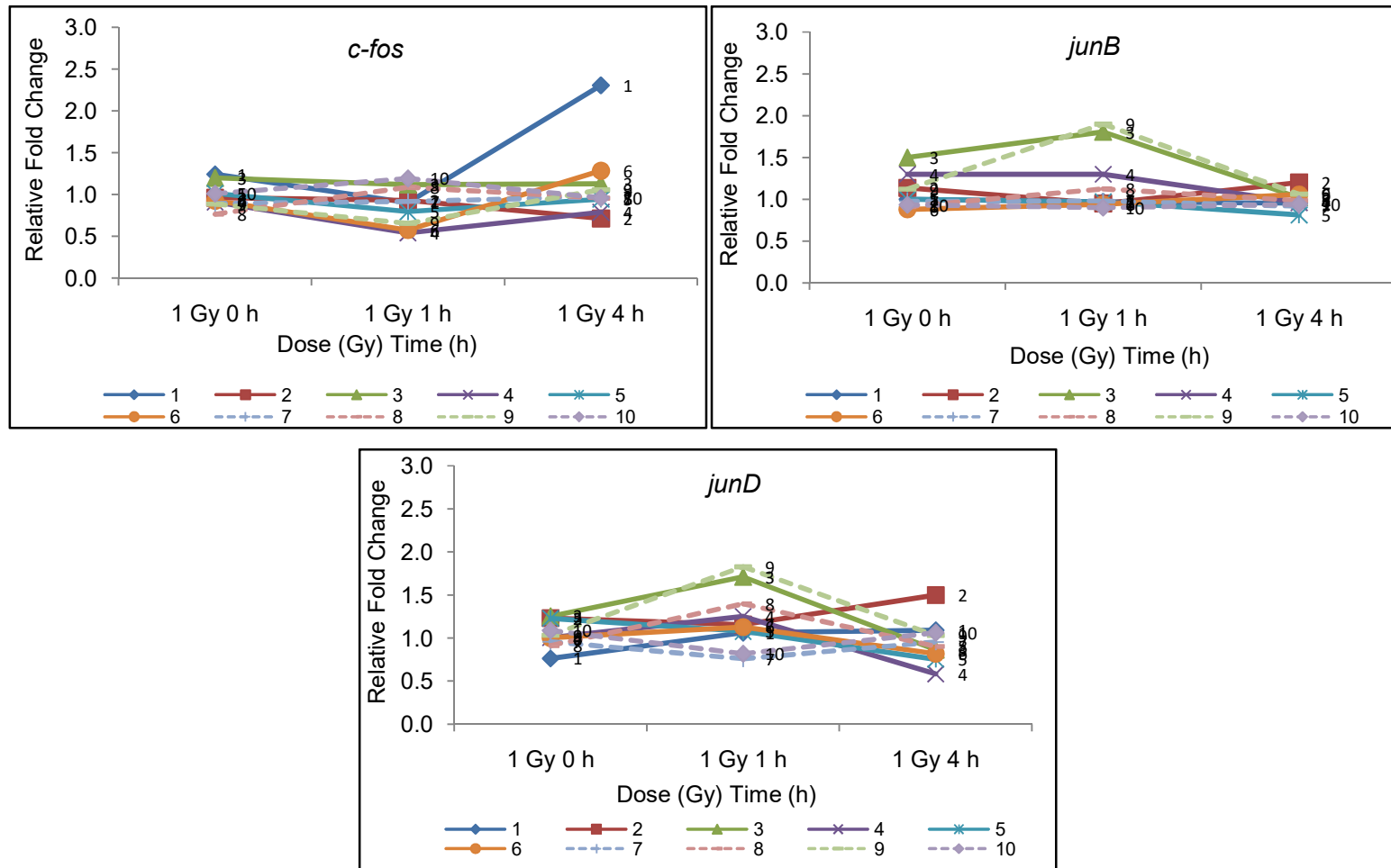


Fig.3.26. Relative fold changes of *c-fos*, *junB* and *junD* genes for the 10 individuals after irradiation with 1 Gy at the respective time points (0 h, 1 h, 4 h), which did not show significant change in expression. Individuals (1 - 6) marked with thick lines (—) were grouped as ‘Group I responders’ and individuals (7-10) marked with dash lines (.....) were grouped as ‘Group II responders’.

3.1.2.4. Inter-individual variations in expression of AP1 genes

Distinct individual-level differences in gene expression were seen after irradiation with 300 mGy (**Fig.3.27A**) and 1 Gy (**Fig.3.27B**) for both Group I responders and Group II responders.

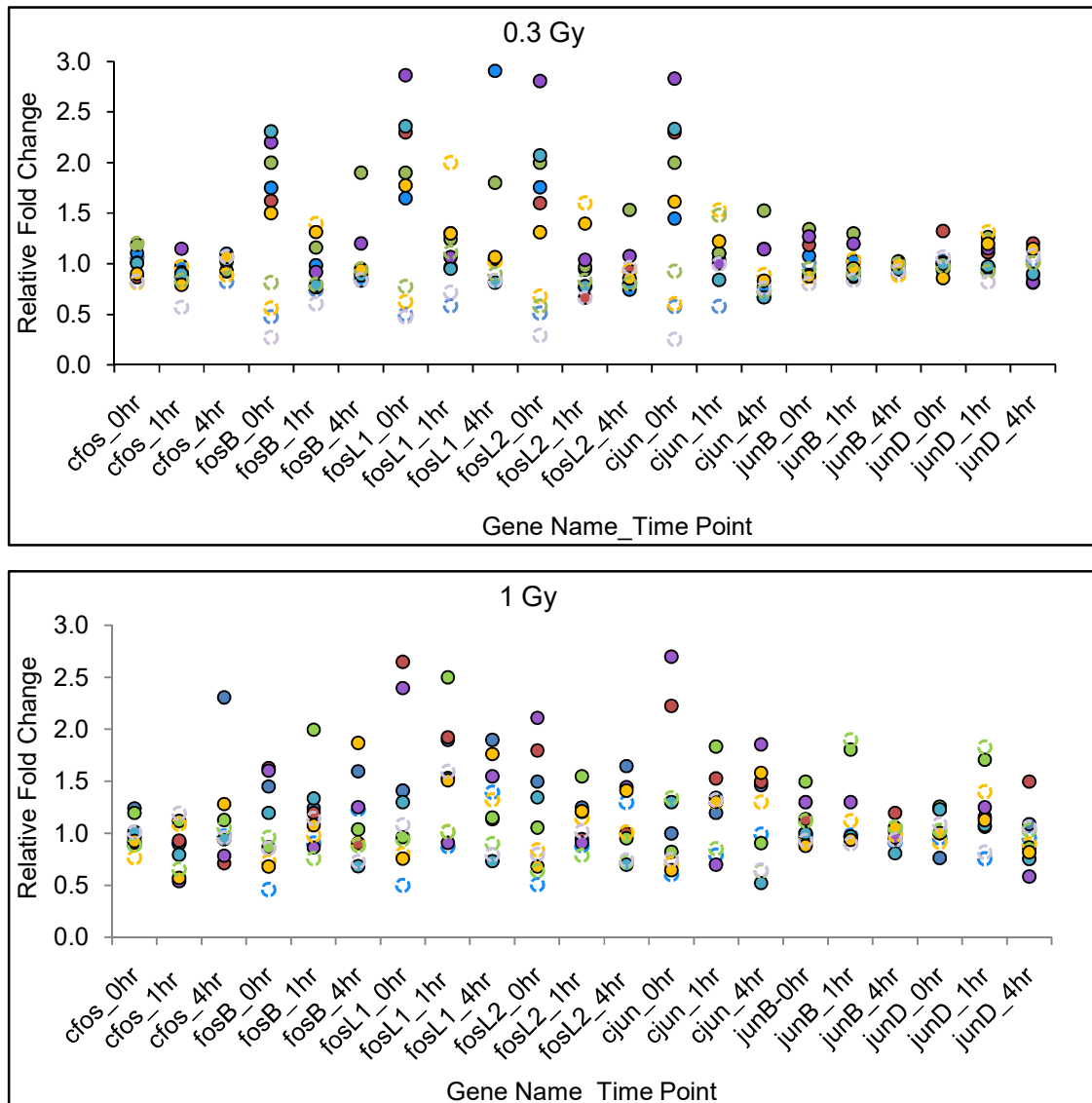


Fig.3.27. Individual variations in AP1 gene expression in response to IR, expressed as relative fold change in seven early response genes with time (0, 1, 4 h), (A) after 300 mGy irradiation (B) after 1 Gy irradiation. Data for each individual are shown as a circle; *filled circle* for ‘Group I responders’ and *open circle* for ‘Group II responders’.

3.1.2.5. Principal component analysis of the gene expression data set

When multivariate principal component analysis was performed on the gene expression data set to assess the similarities and differences between samples. The first two components of the PCA explained 98.75 % of the variance at 300 mGy (**Fig.3.28A**) and 97.59 % of the variance at 1 Gy (**Fig.3.28B**). The analysis clearly identified the two groups (Group I and Group II individuals) after 300 mGy. However, the division between the two groups was not very distinct at 1 Gy.

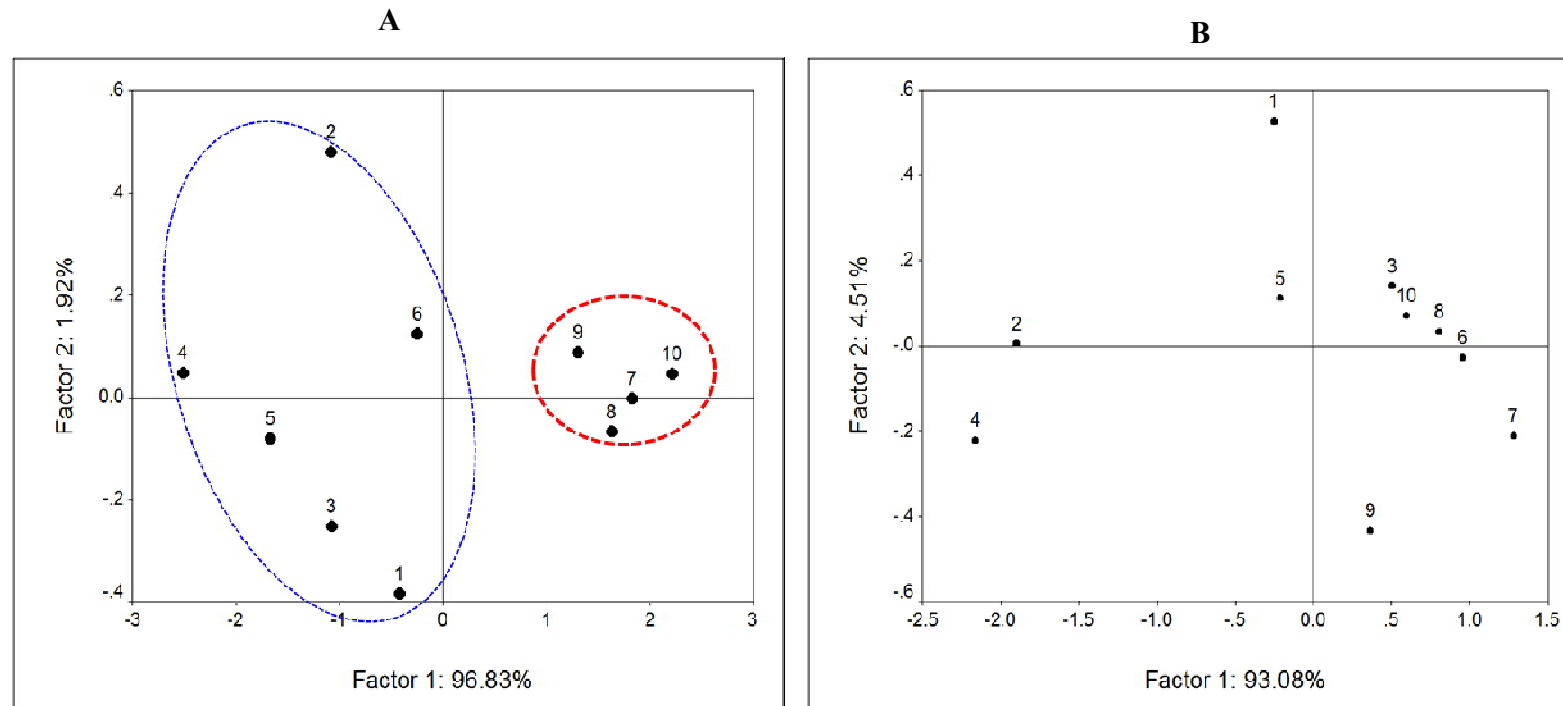


Fig.3.28. Principal component analysis of the AP1 gene expression data set. Principal components (PC) 1 and 2, explaining variance at 0 h post-irradiation with (A) 300 mGy, score 98.75 % and (B) 1 Gy, score 97.59 %, are plotted. *Each dot* represents an individual. Samples 1-6 were Group I responders; samples 7-10 were Group II responders.

3.2. Responses of human PBMCs to chronic low dose IR

To investigate the chronic low-dose radiation-induced molecular effects on humans, whole proteome analysis was performed on PBMC samples collected from HLNRA individuals of Kerala. Two quantitative proteomic methodologies 2DE gel based and iTRAQ based gel free approach was employed.

3.2.1. Basal and induced proteome analysis with 2DE-MS in HLNRA and NLNRA individuals

For the study, blood samples were collected from 20 random healthy males from the region. Of these, 10 individuals were from HLNRA (average age: 41.8 ± 6.07 y) and 10 subjects from NLNRA (average age: 32.2 ± 2.2 y). The optimum sample number required for the analysis was calculated from the protein expression data obtained with acute radiation 2DE-MS experiments performed on PBMCs. Using the formula $n = \frac{2(Z_{\alpha/2} + Z_{\beta})^2 \times \log(CV^2 + 1)}{[(\log_e R)]^2}$, a sample size of 10 individuals per group was arrived to detect a fold-change of 1.5 with 80% power at 5% level of significance, where n is a sample size, $Z_{\alpha/2}$ is the value from the standard normal distribution (two-sided) corresponding to significance level (α), Z_{β} is value from the standard normal distribution corresponding to power ($1 - \beta$), R is the fold change and CV is the coefficient of variation [176]. The mean CV of 34%, as observed with acute irradiation experiments was used for the calculation.

The 2D maps were prepared to compare subjects from HLNRA and NLNRA (NLNRA vs HLNRA). In addition, PBMCs from same individuals were challenged with an *ex vivo* dose of 2 Gy to understand radioadaptive response, if any [NLNRA (2 Gy) vs

HLNRA (2 Gy)]. The mean annual dose received by NLNRA (N = 10) and HLNRA (N = 10) individuals used for 2DE-MS was 1.35 ± 0.08 mGy (range: 1.27–1.50 mGy/y) and 15.60 ± 3.04 mGy (range: 10.74–20.25 mGy/y), respectively. A ^{60}Co gamma ray source (Blood irradiator, 2000, BRIT, India) was used for the *ex vivo* radiation at a dose rate of 0.466 Gy/min. The 2D proteomic maps were prepared at an individual level [10 biological replicates per group for all the four groups, *viz* NLNRA (baseline), HLNRA (baseline), NLNRA (2 Gy) and HLNRA (2 Gy)] because the sample pooling strategies nullifies the calculation of biological variations. The normalization of all 40 gels was performed together using PDQuest image analysis software to minimise the variability due to slight variations in protein load per gel, staining efficiency or image acquisition. Both inter-group comparisons for NLNRA *vs* HLNRA and NLNRA (2 Gy) *vs* HLNRA (2 Gy) as well as intra-group comparisons for NLNRA *vs* NLNRA + 2 Gy and HLNRA *vs* HLNRA + 2 Gy were performed to identify differential protein abundance. MALDI-TOF/TOF mass spectrometry was employed to identify the differentially altered proteins and the particulars for the identified proteins (SWISS PROT accession number, MASCOT score, sequence coverage and peptide match) are given in **Table 3.8**. A representative basal and induced 2D proteome profile for an individual residing at NLNRA and HLNRA is shown in **Fig.3.29** and **Fig.3.30**, respectively.

SI.No	Protein name	SWISS PROT Accession No.	Mascot Score	Sequence coverage	Peptide matches
1.	Fibrinogen beta chain (FIBB)	P02675	139	42.0%	23
2.	Fibrinogen gamma chain (FIBG)	P02679	105	38.2%	12
3.	Ras-related protein Rap-1b (RAP1B)	P61224	186	67.4%	14
4.	Rho GDP-dissociation inhibitor 2 (RhoGDI β)	P52566	52	40.8%	7
5.	Tropomyosin beta chain (1) [TPM2 (1)]	P07951	62	24.3%	9
6.	Tropomyosin beta chain (2) [TPM2 (2)]	P07951	62	23.9%	9
7.	Vimentin (VIME)	P08670	266	62.2%	38
8.	Actin gamma/Actin beta (3) [ACT (3)]	P63261/P60709	85	40.3%	10
9.	ATP synthase subunit beta (ATPB)	P06576	273	71.8%	30
10.	Glucose-regulated protein 78 kDa (GRP78)	P11021	197	44.2%	28
11.	Heat shock protein 90-alpha/beta (HSP90)	P07900/P08238	93	26.1%	17
12.	L-lactate dehydrogenase B chain (LDHB)	P07195	105	38.3%	12
13.	Protein disulfide-isomerase A1 (PDIA1)	P07237	161	38.0%	20
14.	Peroxiredoxin 6 (PRDX6)	P30041	200	65.2%	14
15.	Tropomyosin alpha-4 chain (TMP4)	P67936	80	34.7%	11
16.	Actin gamma/Actin beta (1) [ACT (1)]	P63261/P60709	65	36.3%	9
17.	Actin gamma/Actin beta (2) [ACT (2)]	P63261/P60709	85	41.3%	11
18.	Actin gamma/Actin beta (4) [ACT (4)]	P63261/P60709	100	34.9%	9
19.	Albumin Serum [ALBU (1)]	Q56G89	98	17.0%	11
20.	Albumin Serum [ALBU (2)]	Q56G89	75	27.0%	10
21.	Calreticulin (CALR)	P27797	71	25.9%	8
22.	Chloride intracellular channel protein1 (CLIC)	O00299	193	78.4%	15
23.	Coagulation factor XIII A chain (F13A)	P00488	142	32.0%	15
24.	Heat shock cognate 71 kDa protein (HSP70)	P11142	70	21.7%	13
25.	Leukocyte elastase inhibitor (LEI)	P30740	102	33.0%	10
26.	Plastin-2 [PLS2]	P13796	201	44.2%	27
27.	Protein disulfide-isomerase A3 (PDIA3)	P30101	162	40.4%	17
28.	Proteasome activator complex subunit1 (PSME1)	Q06323	137	66.3%	17
29.	Tubulin beta chain (TUBB)	P07437	69	29.5%	9
30.	Vinculin (MV)	P18206	116	24.3%	22
31.	Ssp2801 (Not identified)	----	----	----	----
32.	Tubulin alpha-8/4A/1C/1B chain (TUBA)	Q9NY65/ P68366/ Q9BQE3/ P68363	68	25%	8
33.	Actin gamma/Actin beta (5) [ACT (5)]	P63261/P60709	114	40%	12

Table 3.8. List of differentially expressed proteins identified by MALDI-TOF/TOF tandem mass spectrometry. The proteins are listed 1–33 as labeled on **Fig.3.29** and **Fig.3.30**. The abbreviations of names of proteins are given in bracket.

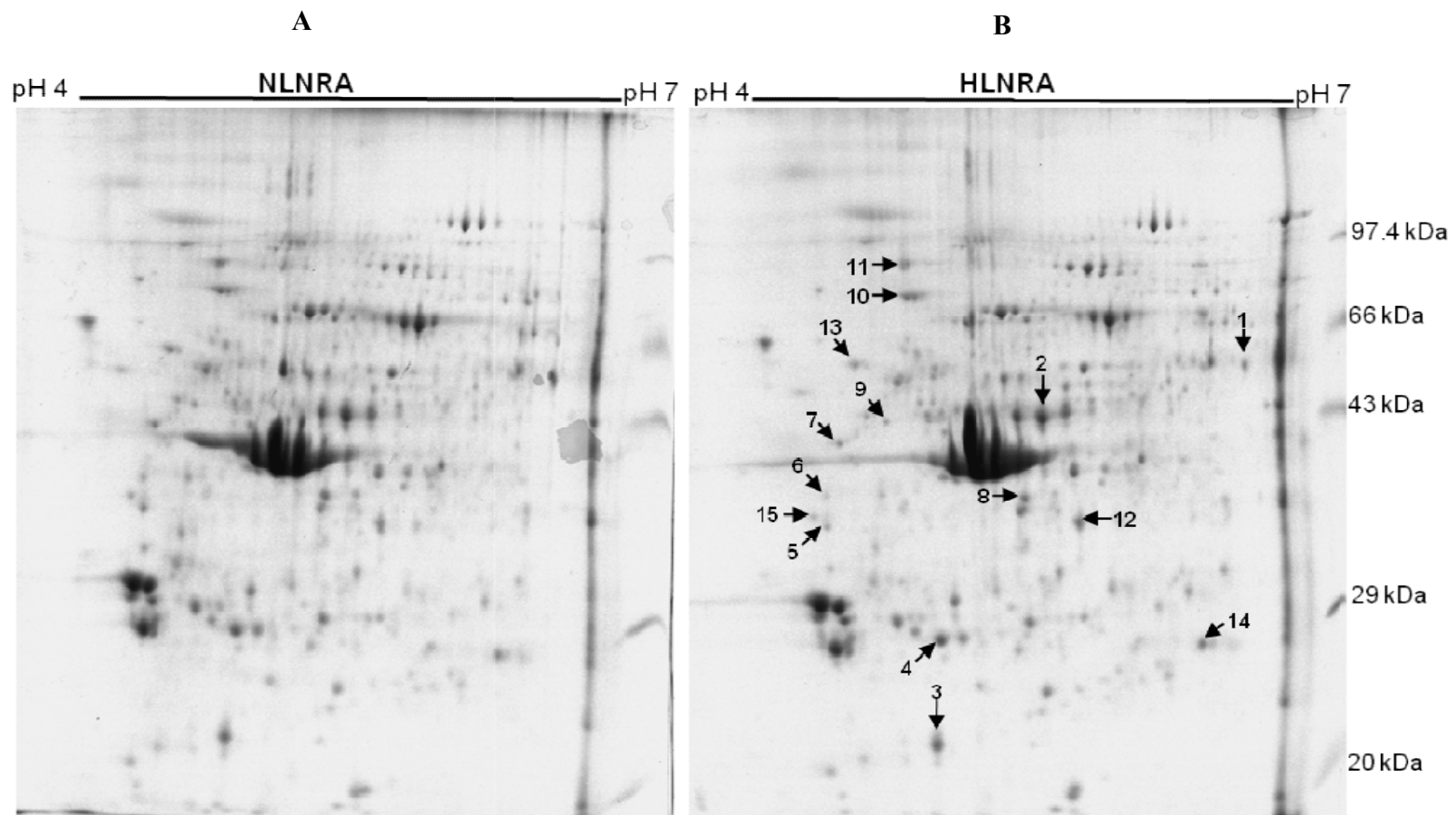


Fig.3.29. Representative 2D-image showing ‘baseline expression’ of human PBMC proteome for (A) an individual from NLNRA, and (B) an individual from HLNRA. The radiation responsive proteins, marked with arrows, were identified by MALDI-TOF mass spectrometry and are numbered as listed in **Table 3.8**.

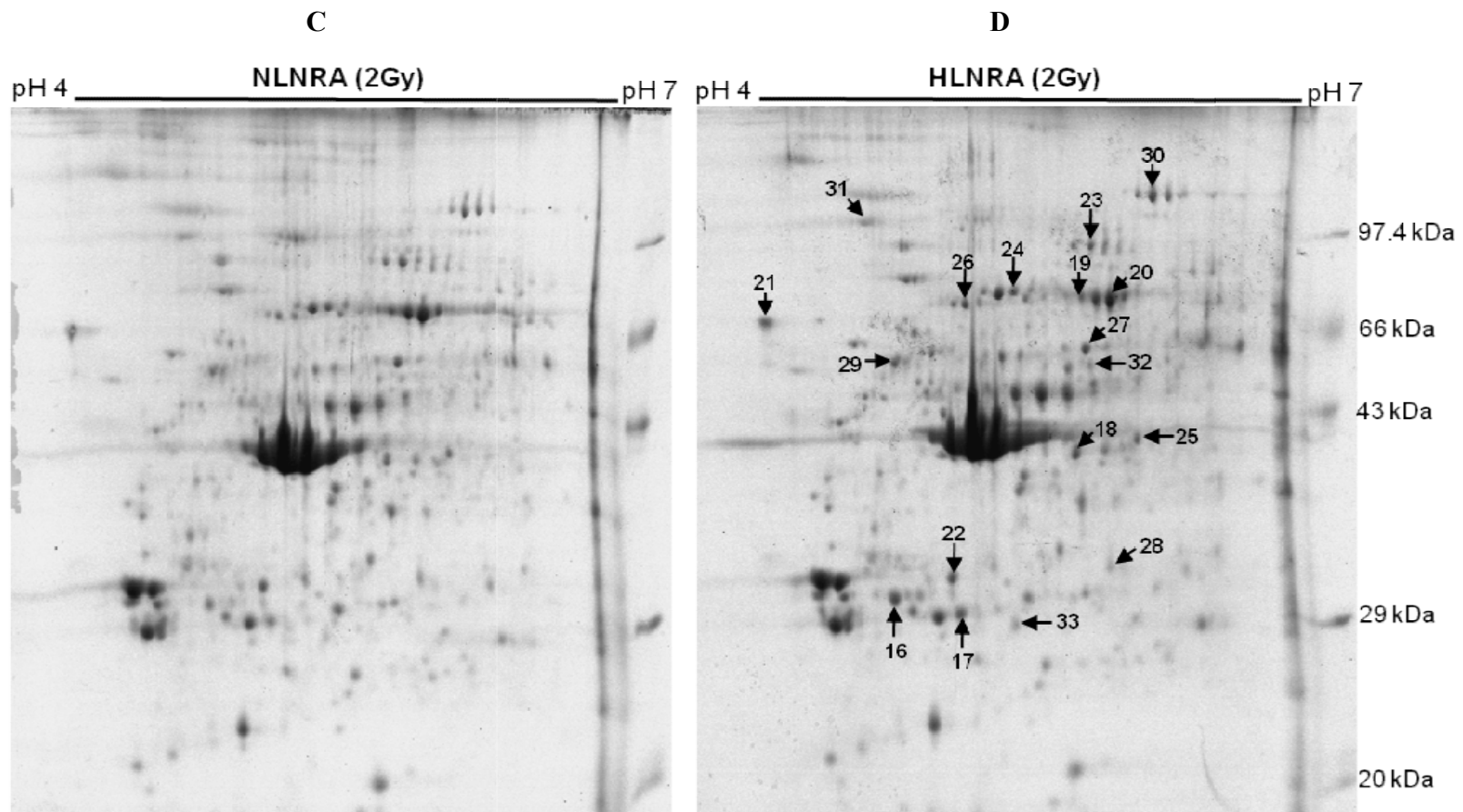


Fig.3.30. Representative 2D-image showing ‘*induced expression*’ of human PBMC proteome challenged with 2 Gy for (C) an individual from NLNRA (D) an individual from HLNRA. The radiation responsive proteins, marked with arrows, were identified by MALDI-TOF mass spectrometry and are numbered as listed in **Table 3.8**.

3.2.1.1. Effect of chronic radiation on the proteome of HLNRA subjects

Differential protein abundance alterations of fifteen proteins were found in individuals from HLNRA, as compared to individuals from NLNRA ($P \leq 0.05$) (Table 3.9, Fig.3.31). Six proteins were over-expressed (FIBB, FIBG, ACT-isoform 3, GRP78, LDHB and PDIA1) whereas nine proteins were under-expressed (RAP1B, RhoGD1 β , two isoforms of TPM2, VIME, ATPB, HSP90, PRDX6, TPM4) (Table 3.9, Fig.3.32A).

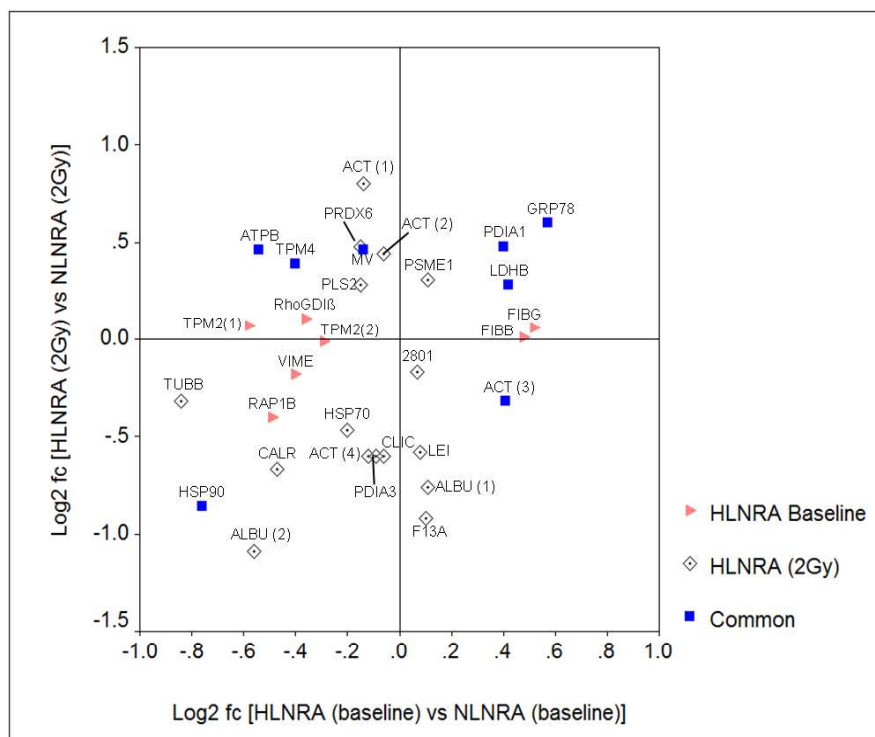


Fig.3.31. Scatter plot showing inter-group variations in protein expression between baseline and 2-Gy challenged human PBMCs from HLNRA and NLNRA. Each point corresponds to the log₂ transformed fold change of a single protein. The orange polygons represent significant variation in HLNRA as compared to NLNRA. The clear polygons represent significant variation in HLNRA (2 Gy) as compared to NLNRA (2 Gy). The blue polygons represent proteins common between HLNRA and HLNRA (2 Gy). The proteins were identified by MS and are abbreviated as listed in Table 3.8.

The *ex vivo* dose of 2 Gy significantly altered 24 proteins in HLNRA (2 Gy) as compared to NLNRA (2 Gy) samples ($P \leq 0.05$) (**Table 3.1, Fig.3.31**). Eleven proteins were over-expressed (two isoforms of ACT, MV, PLS2, PSME1, ATPB, GRP78, LDHB, PDI1A, PRDX6 and TPM4), whereas 13 proteins were under-expressed (two isoforms of ACT, two isoforms of ALBU, CALR, CLIC, F13A, HSP70, LE1, PD1A3, TUBB, 2801, HSP90) (**Table 3.9, Fig.3.32B**). Due to insufficient amount of peptide signals in the mass spectra one protein (spot no. 31) could not be identified.

The 2D proteomic maps prepared from NLNRA or HLNRA individuals were also compared with their respective 2-Gy *ex vivo* irradiated cells (NLNRA vs NLNRA + 2 Gy and HLNRA vs HLNRA + 2 Gy). Protein abundance alterations of 18 proteins (11 over-expressed and 7 under-expressed) were observed when the comparison was made among the two groups from the control areas, i.e. for NLNRA vs NLNRA + 2 Gy (**Table 3.10, Fig.3.33**). The comparisons made among the two groups of HLNRA subjects *viz.*, HLNRA vs HLNRA + 2 Gy showed differential modulation of 17 (13 over-expressed and 4 under-expressed) proteins (**Table 3.10, Fig.3.33**). Nine of these altered proteins were common between the two sets of individuals (**Fig.3.33**).

Sl.No	Protein name	Mean fold change in HLNRA vs NLNRA	P value	Mean fold change in HLNRA (2Gy) vs NLNRA (2Gy)	P value
1.	Fibrinogen beta chain (FIBB)	1.39	P=0.03	1.01	P=0.97
2.	Fibrinogen gamma chain (FIBG)	1.43	P=0.04	1.04	P=0.82
3.	Ras-related protein Rap-1b (RAP1B)	0.71	P=0.04	0.76	P=0.12
4.	Rho GDP-dissociation inhibitor 2 (RhoGDIβ)	0.78	P=0.04	1.08	P=0.59
5.	Tropomyosin beta chain (1) [TPM2 (1)]	0.67	P=0.05	1.05	P=0.86
6.	Tropomyosin beta chain (2) [TPM2 (2)]	0.82	P=0.05	0.99	P=0.97
7.	Vimentin (VIME)	0.76	P=0.02	0.88	P=0.43
8.	Actin gamma/Actin beta (3) [ACT (3)]	1.33	P=0.05	0.80	P=0.05
9.	ATP synthase subunit beta (ATPB)	0.69	P=0.05	1.38	P=0.04
10.	Glucose-regulated protein 78 kDa (GRP78)	1.48	P=0.01	1.52	P=0.01
11.	Heat shock protein 90-alpha/beta (HSP90)	0.59	P=0.05	0.55	P=0.04
12.	L-lactate dehydrogenase B chain (LDHB)	1.34	P=0.05	1.21	P=0.05
13.	Protein disulfide-isomerase A1 (PDIA1)	1.32	P < 0.001	1.39	P < 0.001
14.	Peroxiredoxin 6 (PRDX6)	0.91	P=0.05	1.38	P=0.05
15.	Tropomyosin alpha-4 chain (TMP4)	0.76	P<0.001	1.31	P=0.05
16.	Actin gamma/Actin beta (1) [ACT (1)]	0.91	P=0.36	1.74	P=0.02
17.	Actin gamma/Actin beta (2) [ACT (2)]	0.96	P=0.82	1.36	P=0.05
18.	Actin gamma/Actin beta (4) [ACT (4)]	0.92	P=0.76	0.66	P=0.05
19.	Serum Albumin [ALBU (1)]	1.08	P=0.72	0.59	P=0.04
20.	Serum Albumin (ALBU (2))	0.68	P=0.06	0.47	P=0.01
21.	Calreticulin (CALR)	0.72	P=0.23	0.63	P < 0.001
22.	Chloride intracellular channel protein 1 (CLIC)	0.96	P=0.77	0.66	P=0.04
23.	Coagulation factor XIII A chain (F13A)	1.07	P=0.70	0.53	P=0.01
24.	Heat shock cognate 71 kDa protein (HSP70)	0.87	P=0.54	0.72	P=0.05
25.	Leukocyte elastase inhibitor (LEI)	1.06	P=0.69	0.67	P=0.05
26.	Plastin-2 [PLS2 (1)]	0.90	P=0.63	1.21	P=0.05
27.	Protein disulfide-isomerase A3 (PDIA3)	0.94	P=0.57	0.66	P=0.03
28.	Proteasome activator complex subunit1 (PSME1)	1.08	P=0.62	1.24	P=0.05
29.	Tubulin beta chain (TUBB)	0.56	P=0.10	0.80	P=0.04
30.	Vinculin (MV)	0.90	P=0.47	1.39	P=0.05
31.	Ssp2801 (Not identified)	1.05	P=0.81	0.89	P=0.05
32.	Tubulin alpha-1B chain (TUBA)	1.30	P=0.24	0.80	P=0.16
33.	Actin gamma/Actin beta (5) [ACT (5)]	0.86	P=0.36	1.24	P=0.23

Table 3.9. Differentially expressed proteins in human PBMCs with chronic exposure to high background natural radiation. The mean change in spot intensity in HLNRA subjects (baseline or 2-Gy challenged) relative to NLNRA subjects are represented as fold change. The P values in ‘**bold**’ represent significant ($P \leq 0.05$) changes in the expression determined using Student’s t-test. The proteins are listed 1–33 as labeled on **Fig.3.29** and **Fig.3.30**. The abbreviations of names of proteins are given in brackets.

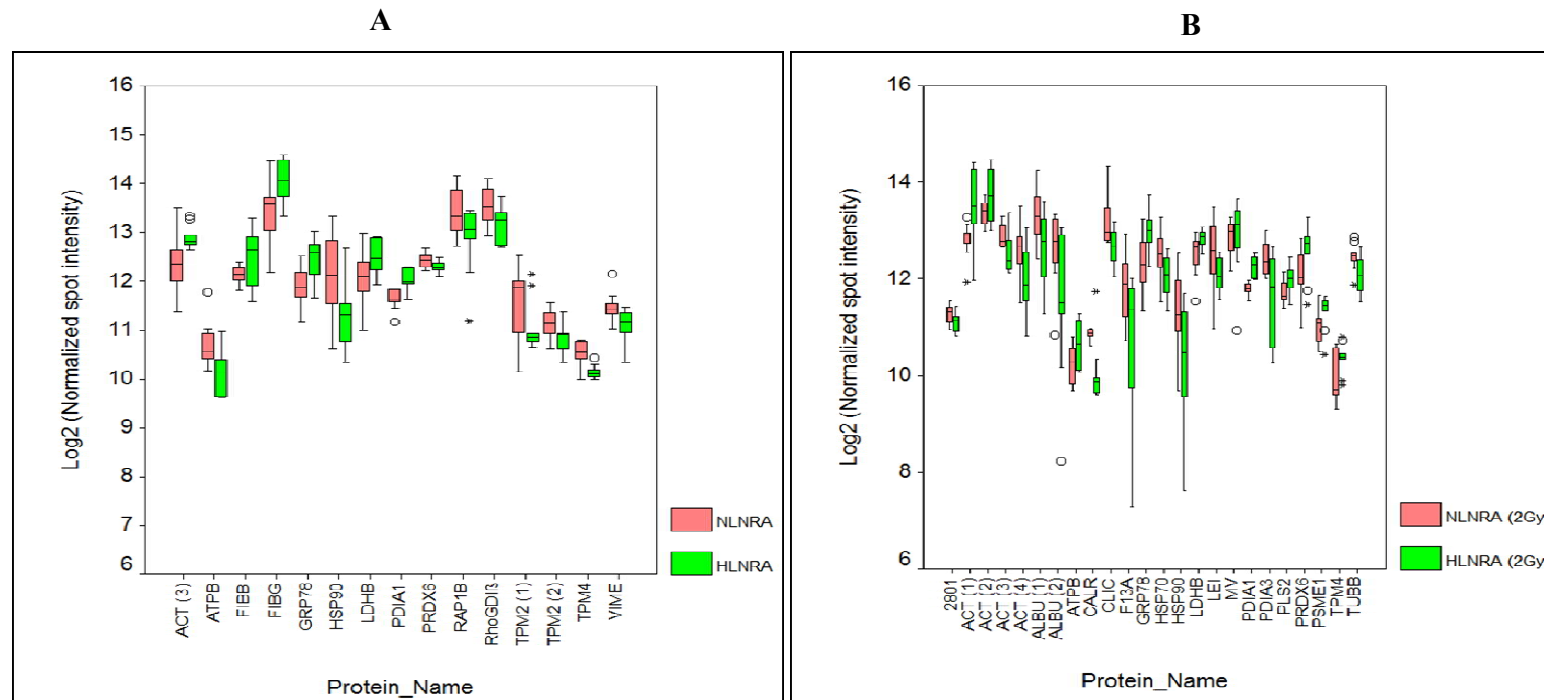


Fig.3.32. Box-plot distribution of expression for differentially expressed proteins of PBMCs, in individuals from NLNRA and HLNRA. (A) Variations in baseline expression. (B) Variations after a challenge dose of 2 Gy. Each distribution contains log₂ transformed normalised spot intensity values from 10 individuals. The top and bottom of the box represents the 25th and 75th percentiles and the whiskers shows the maximum and minimum values. The black 'bold line' is the median value. The open 'circles' indicates outliers and 'stars' indicates extreme values.

Sl.No	Protein name	Mean fold change (\pm SEM) in NLNRA vs NLNRA (2Gy)	<i>P</i> value	Mean fold change (\pm SEM) in HLNRA vs HLNRA (2Gy)	<i>P</i> value
1.	Fibrinogen beta chain (FIBB)	1.35 \pm 0.16	<i>P</i>=0.05	1.10 \pm 0.23	<i>P</i> =0.97
2.	Fibrinogen gamma chain (FIBG)	1.29 \pm 0.18	<i>P</i> =0.44	0.88 \pm 0.11	<i>P</i> =0.20
3.	Ras-related protein Rap-1b (RAP1B)	1.50 \pm 0.15	<i>P</i>=0.04	1.61 \pm 0.16	<i>P</i>=0.03
4.	Rho GDP-dissociation inhibitor 2 (RhoGDI β)	0.97 \pm 0.12	<i>P</i> =0.67	1.40 \pm 0.15	<i>P</i>=0.03
5.	Tropomyosin beta chain (1) [TPM2 (1)]	0.74 \pm 0.14	<i>P</i>=0.05	1.01 \pm 0.21	<i>P</i> =0.98
6.	Tropomyosin beta chain (2) [TPM2 (2)]	0.88 \pm 0.12	<i>P</i> =0.26	1.09 \pm 0.14	<i>P</i> =0.79
7.	Vimentin (VIME)	0.87 \pm 0.13	<i>P</i> =0.11	0.92 \pm 0.09	<i>P</i> =0.56
8.	Actin gamma/Actin beta (3) [ACT (3)]	1.48 \pm 0.14	<i>P</i>=0.05	0.81 \pm 0.09	<i>P</i>=0.05
9.	ATP synthase subunit beta (ATPB)	0.79 \pm 0.10	<i>P</i>=0.05	1.50 \pm 0.18	<i>P</i>=0.05
10.	Glucose-regulated protein 78 kDa (GRP78)	1.40 \pm 0.12	<i>P</i>=0.05	1.45 \pm 0.09	<i>P</i>=0.01
11.	Heat shock protein 90-alpha/beta (HSP90)	0.66 \pm 0.11	<i>P</i>=0.04	0.70 \pm 0.18	<i>P</i> =0.06
12.	L-lactate dehydrogenase B chain (LDHB)	1.41 \pm 0.07	<i>P</i>=0.05	1.28 \pm 0.09	<i>P</i>=0.03
13.	Protein disulfide-isomerase A1 (PDIA1)	1.14 \pm 0.06	<i>P</i>=0.04	1.21 \pm 0.10	<i>P</i>=0.02
14.	Peroxiredoxin 6 (PRDX6)	0.86 \pm 0.10	<i>P</i> =0.15	1.29 \pm 0.13	<i>P</i>=0.05
15.	Tropomyosin alpha-4 chain (TMP4)	0.73 \pm 0.11	<i>P</i>=0.01	1.19 \pm 0.08	<i>P</i>=0.04
16.	Actin gamma/Actin beta (1) [ACT (1)]	0.81 \pm 0.05	<i>P</i>=0.03	1.46 \pm 0.18	<i>P</i>=0.05
17.	Actin gamma/Actin beta (2) [ACT (2)]	1.25 \pm 0.17	<i>P</i> =0.88	1.49 \pm 0.11	<i>P</i>=0.04
18.	Actin gamma/Actin beta (4) [ACT (4)]	1.79 \pm 0.32	<i>P</i>=0.04	1.98 \pm 0.74	<i>P</i> =0.74
19.	Serum Albumin [ALBU (1)]	1.58 \pm 0.22	<i>P</i>=0.05	0.84 \pm 0.16	<i>P</i> =0.48
20.	Serum Albumin (ALBU (2))	1.14 \pm 0.25	<i>P</i> =0.81	0.74 \pm 0.14	<i>P</i> =0.06
21.	Calreticulin (CALR)	0.86 \pm 0.27	<i>P</i>=0.05	0.67 \pm 0.16	<i>P</i>=0.04
22.	Chloride intracellular channel protein 1 (CLIC)	1.48 \pm 0.17	<i>P</i>=0.05	1.20 \pm 0.21	<i>P</i> =0.98
23.	Coagulation factor XIII A chain (F13A)	1.17 \pm 0.12	<i>P</i> =0.35	0.62 \pm 0.14	<i>P</i>=0.04
24.	Heat shock cognate 71 kDa protein (HSP70)	1.08 \pm 0.09	<i>P</i> =0.69	1.02 \pm 0.09	<i>P</i> =0.61
25.	Leukocyte elastase inhibitor (LEI)	1.49 \pm 0.21	<i>P</i>=0.05	1.09 \pm 0.17	<i>P</i> =0.70
26.	Plastin-2 [PLS2 (1)]	1.26 \pm 0.19	<i>P</i> =0.80	1.31 \pm 0.10	<i>P</i>=0.02
27.	Protein disulfide-isomerase A3 (PDIA3)	1.04 \pm 0.11	<i>P</i> =0.92	0.70 \pm 0.12	<i>P</i>=0.04
28.	Proteasome activator complex subunit1 (PSME1)	0.91 \pm 0.43	<i>P</i> =0.10	1.00 \pm 0.08	<i>P</i> =0.61
29.	Tubulin beta chain (TUBB)	1.23 \pm 0.17	<i>P</i> =0.69	1.29 \pm 0.11	<i>P</i>=0.05
30.	Vinculin (MV)	0.79 \pm 0.07	<i>P</i>=0.05	1.19 \pm 0.15	<i>P</i> =0.43
31.	Ssp2801 (Not identified)	1.15 \pm 0.16	<i>P</i> =0.75	0.91 \pm 0.11	<i>P</i> =0.11
32.	Tubulin alpha-1B chain (TUBA)	1.25 \pm 0.12	<i>P</i>=0.04	1.37 \pm 0.54	<i>P</i> =0.25
33.	Actin gamma/Actin beta (5) [ACT (5)]	1.07 \pm 0.09	<i>P</i> =0.84	1.55 \pm 0.12	<i>P</i>=0.04

Table 3.10. Intra-group variations in protein expression between baseline and 2-Gy challenged human PBMCs from HLNRA (HLNRA vs HLNRA + 2 Gy) and NLNRA NLNRA (NLNRA vs NLNRA + 2 Gy). The mean changes in spot intensity in HLNRA or NLNRA individuals relative to respective controls are represented as fold change. The *P*-values in ‘**bold**’ represent significant ($P \leq 0.05$) changes in the expression determined using Student’s t-test. The proteins are listed 1–33 as labeled on **Fig.3.29** and **Fig.3.30**. The abbreviations of names of proteins are given in brackets.

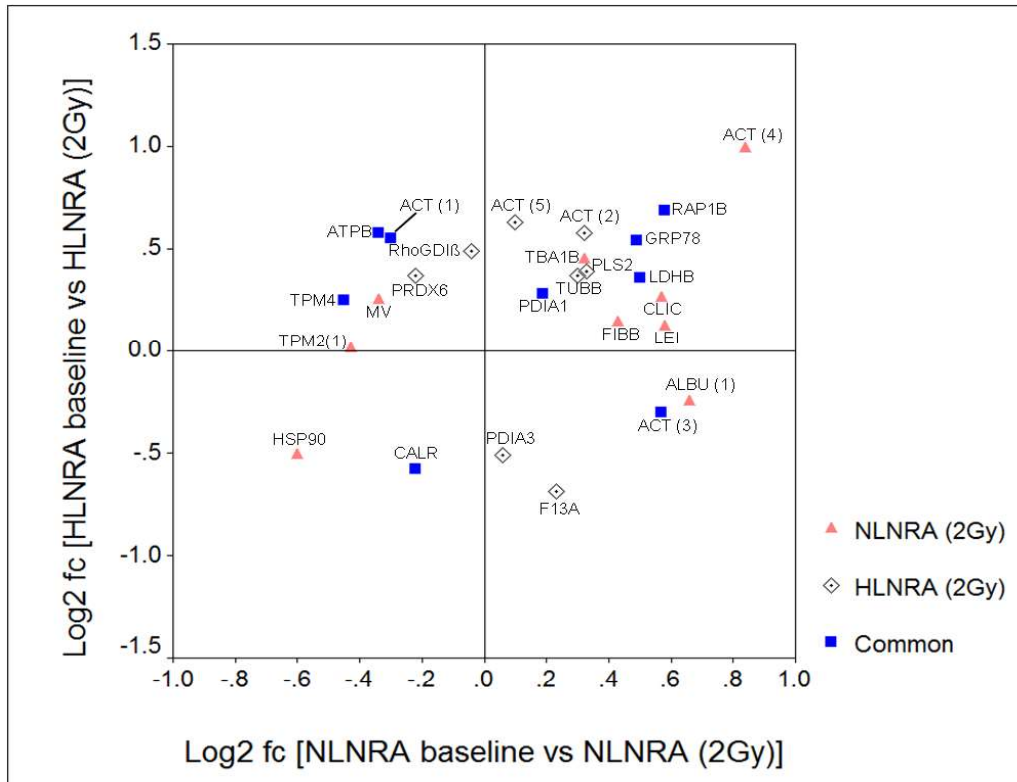


Fig.3.33. Scatter plot showing intra-group variations in protein expression between baseline and 2-Gy challenged human PBMCs from HLNRA and NLNRA. Each point corresponds to the log₂ transformed fold change of a single protein. The orange polygonals represent significant variation in NLNRA (2 Gy) as compared to NLNRA. The clear polygonals represent significant variation in HLNRA (2 Gy) as compared to HLNRA. The blue polygonals represent proteins common between NLNRA (2 Gy) and HLNRA (2 Gy). The proteins were identified by mass spectrometry and are abbreviated as listed in **Table 3.10**.

3.2.1.2. Dose-response analysis of the differentially modulated proteins

When the annual dose (range: 10.74 - 20.25 mGy/y) received by HLNRA individuals (N=10) were plotted against the corresponding log₂ normalized spot intensity values of a specific protein individually for all the 31 differentially expressed proteins, four proteins (TMP4, ACT3, PSME1 and ALBU1) showed significant correlation ($P \leq 0.05$) with radiation dose (**Fig.3.34A**). The Pearson correlation coefficients (r) was positive with radiation dose for ACT3 ($r = 0.78$, $P = 0.01$) and ALBU1 ($r = 0.84$, $P = 0.002$), whereas TMP4 ($r = -0.74$, $P = 0.01$) and PSME1 ($r = -0.82$, $P = 0.003$) showed negative correlation. No significant correlation with the annual dose received by an individual was seen for proteins involved in cell redox or stress homeostasis such as PDIA1 ($r = 0.17$, $P = 0.64$), PDIA3 ($r = 0.02$, $P = 0.95$), GRP78 ($r = 0.08$, $P = 0.82$), PRDX6 ($r = -0.30$, $P = 0.40$), LDHB ($r = -0.28$, $P = 0.44$) and ATPB ($r = -0.23$, $P = 0.52$) (**Fig.3.34B**).

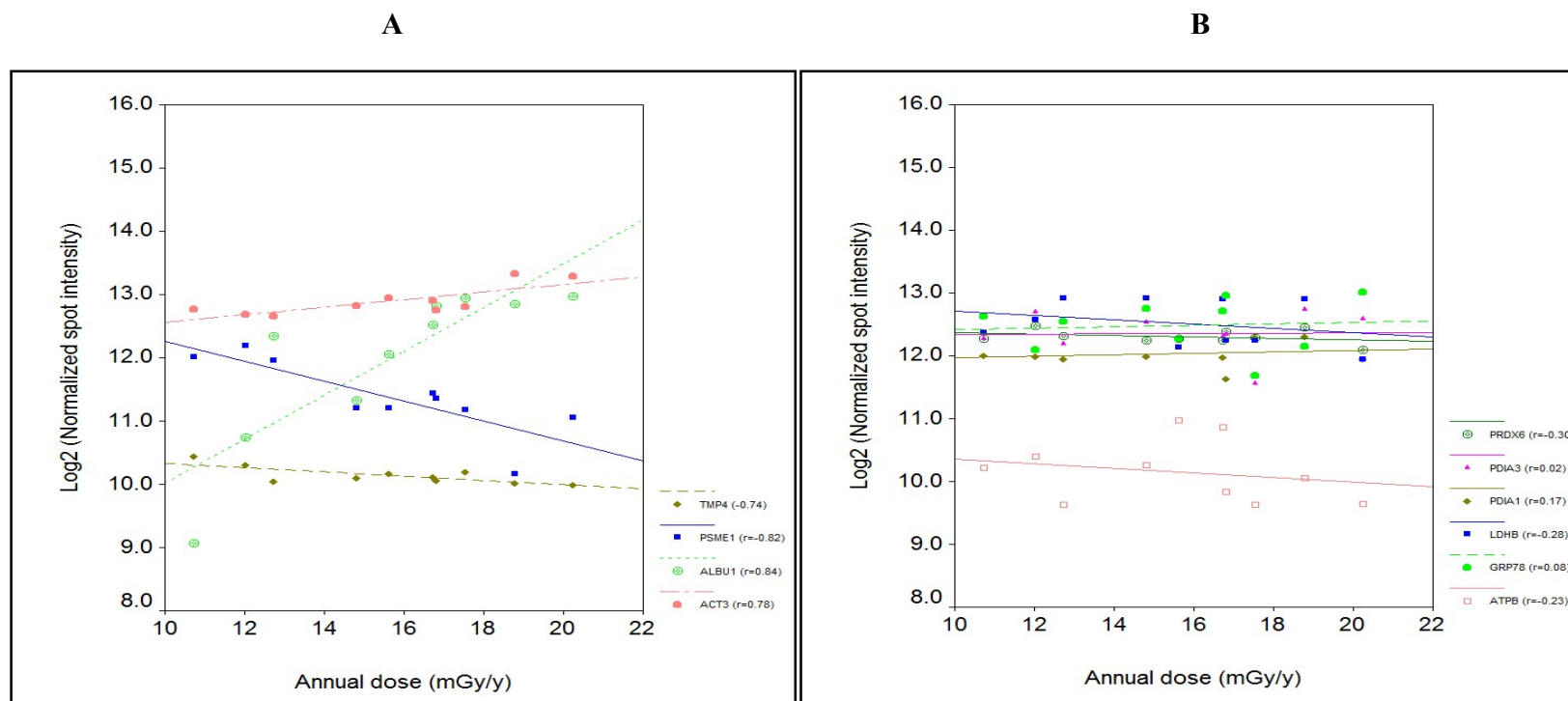


Fig.3.34. Scatter plot showing the Pearson correlation analysis of protein expression to annual dose (range: 10.74–20.25 mGy/y) received by HLNRA individuals ($N = 10$). (A) Four proteins showed statistically significant correlation. (B) Proteins involved in cell redox/stress homeostasis. Each point corresponds to the log₂ transformed normalised spot intensity data of a single protein for an individual. The best-fit line for each protein is shown with the Pearson correlation coefficient (r) values in legend.

3.2.1.3. Functional pathway analysis

The DAVID pathway analysis distinguished 44 biological processes significantly ($P \leq 0.05$) activated in HLNRA samples. This included enrichment of important processes such as protein folding (HSP70, HSP90, PDIA3, CALR), cell redox homeostasis (PRDX6, PDIA1, PDIA3), cell-matrix adhesion (VINC, FIBB, FIBG), protein refolding (HSP70, HSP90), regulation of protein ubiquitination (HSP90A/B), regulation of ERK cascade (RAP1B, FIBB, FIBG), negative regulation of extrinsic apoptotic signalling pathway (FIBB, FIBG) and response to reactive oxygen species (PRDX6, PDIA1) (**Table 3.11**).

Sl. No	Term	Count	P Value	Genes
1.	GO:0006928~movement of cell or subcellular component	7	2.476E-09	GDIR2, VIME, TBB5, ACTB, VINC, TPM4, ACTG
2.	GO:0070527~platelet aggregation	6	3.455E-09	CLIC1, ACTB, VINC, FIBB, FIBG, ACTG
3.	GO:0006457~protein folding	5	0.0001354	HSP7C, HS90A, PDIA3, HS90B, CALR
4.	GO:0034975~protein folding in endoplasmic reticulum	3	0.0001643	PDIA3, GRP78, CALR
5.	GO:0002576~platelet degranulation	4	0.0004673	F13A, VINC, FIBB, FIBG
6.	GO:0038096~Fc-gamma receptor signaling pathway involved in phagocytosis	4	0.0008604	HS90A, ACTB, HS90B, ACTG
7.	GO:1900026~positive regulation of substrate adhesion-dependent cell spreading	3	0.001027	CALR, FIBB, FIBG
8.	GO:0030049~muscle filament sliding	3	0.0014476	VIME, TPM2, TPM4
9.	GO:0006986~response to unfolded protein	3	0.0017665	HSP7C, HS90A, HS90B
10.	GO:0061684~chaperone-mediated autophagy	2	0.00446	HSP7C, HS90A
11.	GO:0048010~vascular endothelial growth factor receptor signaling pathway	3	0.005103	HS90A, ACTB, ACTG
12.	GO:1900034~regulation of cellular response to heat	3	0.0055251	HSP7C, HS90A, HS90B
13.	GO:0045454~cell redox homeostasis	3	0.0058152	PRDX6, PDIA1, PDIA3
14.	GO:0072378~blood coagulation, fibrin clot formation	2	0.0059425	FIBB, FIBG
15.	GO:0098609~cell-cell adhesion	4	0.0073527	HSP7C, PRDX6, GRP78, HS90B
16.	GO:0007160~cell-matrix adhesion	3	0.0078662	VINC, FIBB, FIBG
17.	GO:0006936~muscle contraction	3	0.0109679	TPM2, VINC, TPM4
18.	GO:0090277~positive regulation of peptide hormone secretion	2	0.011851	FIBB, FIBG
19.	GO:0036500~ATF6-mediated unfolded protein response	2	0.0133229	GRP78, CALR
20.	GO:0009651~response to salt stress	2	0.0133229	HS90A, HS90B
21.	GO:0031639~plasminogen activation	2	0.0133229	FIBB, FIBG
22.	GO:0033160~positive regulation of protein import into nucleus, translocation	2	0.0147926	HS90A, HS90B
23.	GO:0045793~positive regulation of cell size	2	0.0147926	HS90A, HS90B

24.	GO:0034116~positive regulation of heterotypic cell-cell adhesion	2	0.0162603	FIBB, FIBG
25.	GO:0050821~protein stabilization	3	0.0172941	HS90A, HS90B, CALR
26.	GO:0034329~cell junction assembly	2	0.0177258	ACTB, ACTG
27.	GO:0051258~protein polymerization	2	0.0191893	FIBB, FIBG
28.	GO:0043254~regulation of protein complex assembly	2	0.0206507	HSP7C, HS90A
29.	GO:0042026~protein refolding	2	0.0221099	HSP7C, HS90A
30.	GO:0031396~regulation of protein ubiquitination	2	0.0235671	HS90A, HS90B
31.	GO:0043623~cellular protein complex assembly	2	0.0264753	FIBB, FIBG
32.	GO:0070374~positive regulation of ERK1 and ERK2 cascade	3	0.0276891	RAP1B, FIBB, FIBG
33.	GO:0007596~blood coagulation	3	0.0303714	F13A, FIBB, FIBG
34.	GO:0045921~positive regulation of exocytosis	2	0.0308219	FIBB, FIBG
35.	GO:0042730~fibrinolysis	2	0.0308219	FIBB, FIBG
36.	GO:0071353~cellular response to interleukin-4	2	0.0351498	GRP78, HS90B
37.	GO:2000352~negative regulation of endothelial cell apoptotic process	2	0.0408916	FIBB, FIBG
38.	GO:0002474~antigen processing and presentation of peptide antigen via MHC class I	2	0.0437502	PDIA3, CALR
39.	GO:0046034~ATP metabolic process	2	0.0466006	HSP7C, ATPB
40.	GO:0045907~positive regulation of vasoconstriction	2	0.0466006	FIBB, FIBG
41.	GO:0042220~response to cocaine	2	0.0466006	HS90A, HS90B
42.	GO:1902042~negative regulation of extrinsic apoptotic signaling pathway via death domain receptors	2	0.0480227	FIBB, FIBG
43.	GO:0050714~positive regulation of protein secretion	2	0.0522769	FIBB, FIBG
44.	GO:0000302~response to reactive oxygen species	2	0.0545128	PRDX6, PDIA1

Table 3.11. Gene ontology analysis of radiation responsive proteins using DAVID bioinformatics analysis.

3.2.1.4. Estimation of variability in protein expression

The inter-individual variation in proteomic expression with chronic radiation stress was calculated using CV as a tool. The CV (%) was calculated for each protein spot that showed differential expression among all individuals of NLNRA and HLNRA. The CV of the protein spots which showed differential expression ranged from 6.7 to 80.4%, with an overall mean CV of ~34%. At the basal level, a mean CV of 35.6% (range: 11.5–80.4%) was seen in NLNRA samples, whereas a mean CV of 33.3% (range: 7.7–67.2%) was observed in HLNRA samples. Even when the samples were challenged with the 2 Gy dose, the CV values remain comparable to the basal level with mean values of 32.3% (range: 6.7–62.5%) for NLNRA (2 Gy) and 38.8% (range: 12.7–77.6%) for HLNRA (2 Gy) (**Fig.3.35**). The proteins grouped under cytoskeletal [CALR, TUBB, ACT (2), ACT (4), ACT (1), TPM2 (1), PLS2] and extracellular [ALBU (2), F13A, FGB] protein families showed more dilatant CV values (>50%) (**Fig.3.36**). The combined CV for all the samples from all four groups was ~34%.

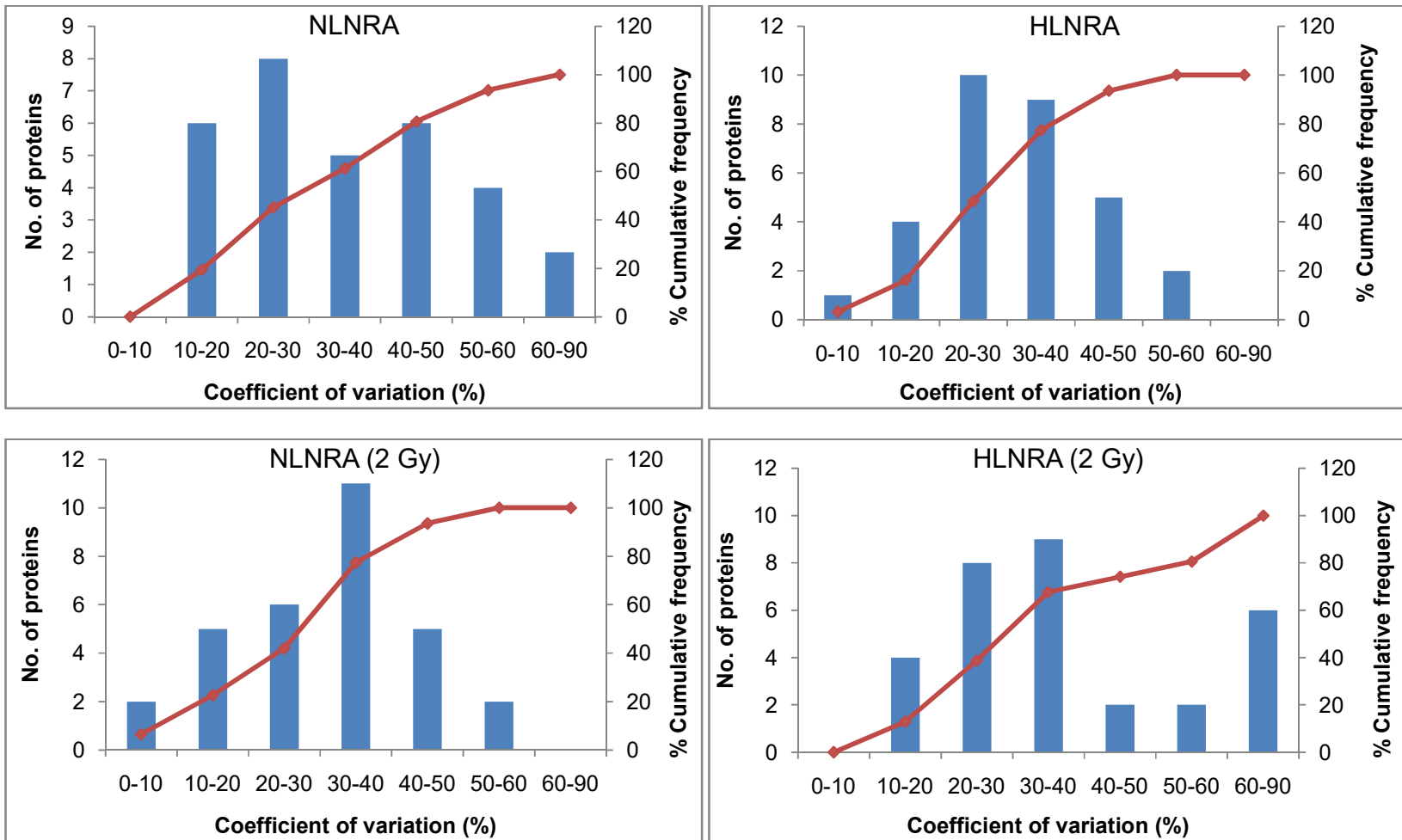


Fig.3.35. The distribution pattern of CV data for the altered proteins in the baseline (NLNRA and HLNRA) and 2-Gy challenged [NLNRA (2 Gy) and HLNRA (2 Gy)] human PBMCs.

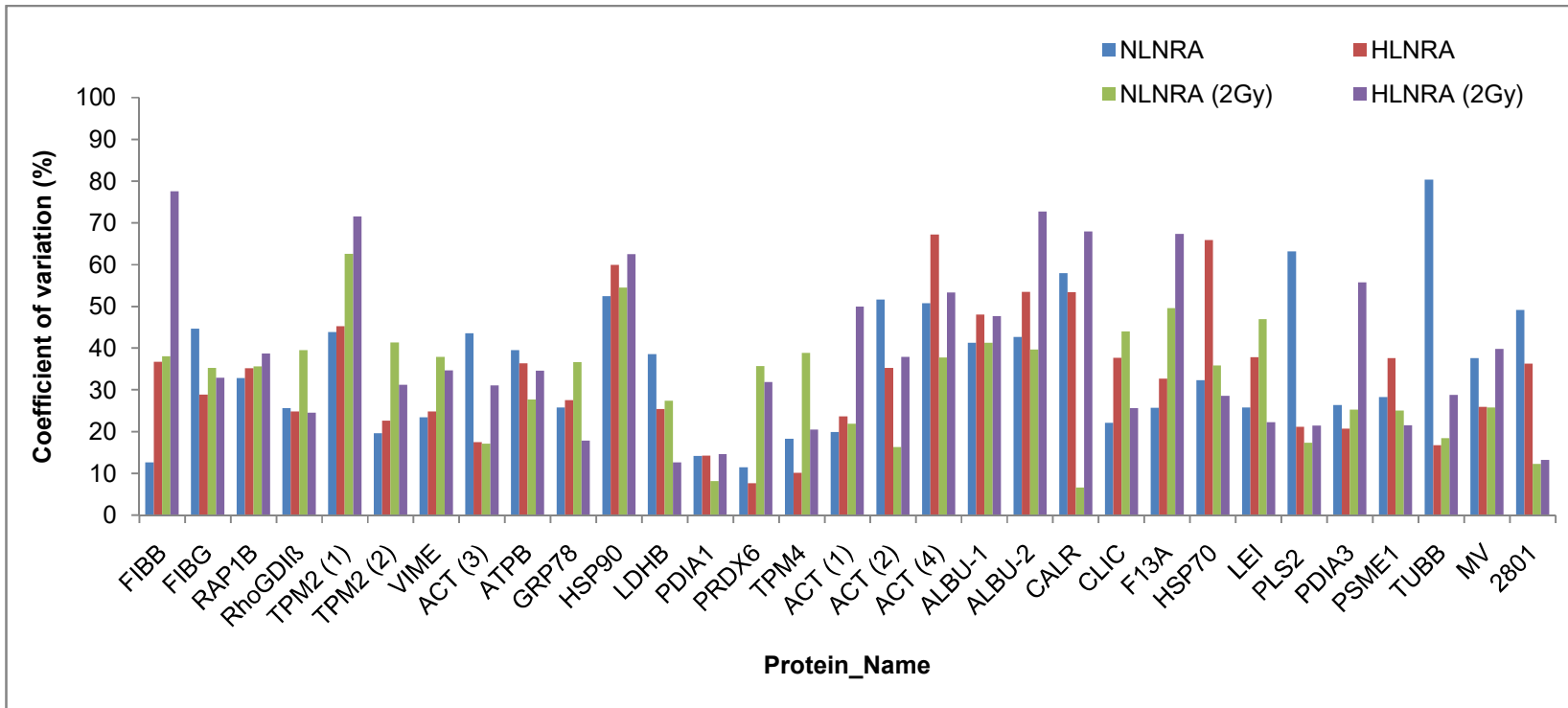


Fig.3.36. Coefficient of variation (CV%) data for the differentially modulated proteins in the baseline (NLNRA and HLNRA) and 2-Gy challenged [NLNRA (2 Gy) and HLNRA (2 Gy)] human PBMCs.

3.2.1.5. Statistical power analysis of the study

Analysis was carried out to assess the statistical power (with 5% significance level) of the study at different fold changes from 1.25 to 3, assuming an overall CV of 34%, using the formula used for estimating sample size (Fig.3.37). The sample size used in the present study (10 individuals per group) was sufficient to detect a 1.5-fold change in protein abundance with 80% statistical power. However, the present study was able to detect even small changes in protein expression, albeit with low statistical power.

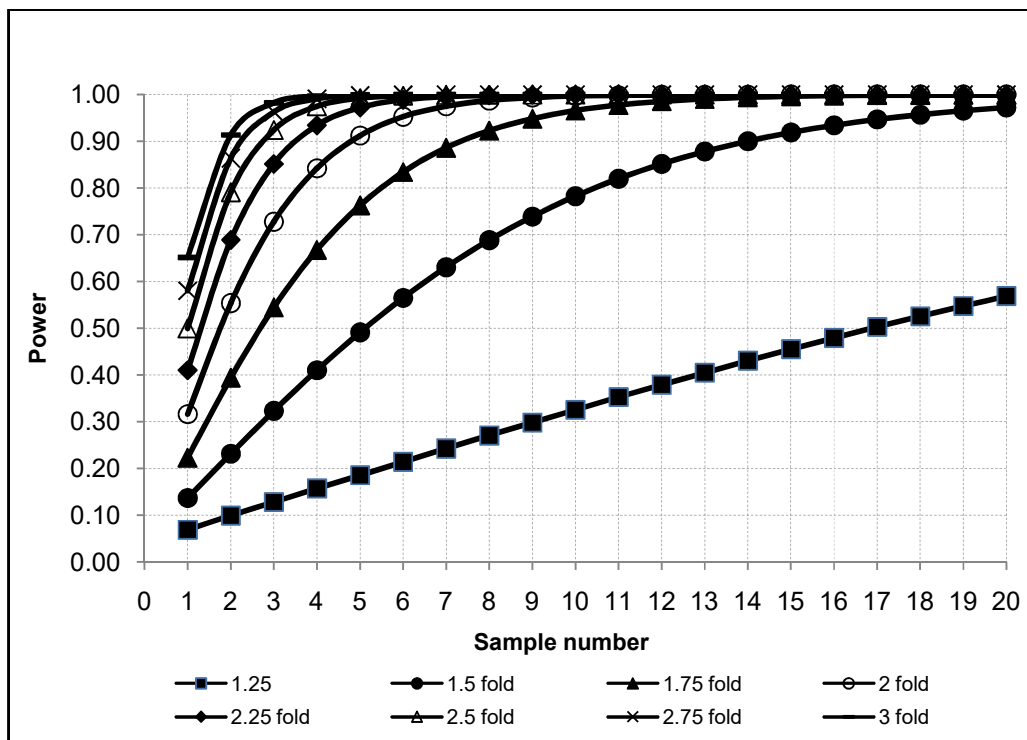


Fig.3.37. Relationship between statistical power and sample size. Results are plotted for various fold changes at 5% significance level and assuming CV of 34% observed in this study. Results show that a sample size of N = 10 in an experimental design detects a 1.5-fold change close to 80% power.

3.2.1.6. Western blot validation of selected radiation responsive proteins

To validate some of the major proteins affected by low dose chronic radiation, western blot analysis was performed with additional set of 10 samples each from HLNRA and NLNRA (**Fig.3.38A**). The average background dose of collected samples was 13.30 ± 3.15 mGy/y (range: 7.29–17.79 mGy/y) in HLNRA and 1.33 ± 0.09 mGy/y (range: 1.23–1.46 mGy/y) in NLNRA. Protein lysates (50 μ g) from each experimental group [NLNRA, HLNRA, NLNRA (2 Gy) and HLNRA (2 Gy)] was pooled and immunoblotted using primary antibodies against GRP78, PRDX6 and PDI. The protein bands were quantified using Image-J software normalised to GAPDH expression. The baseline expression observed in HLNRA samples as compared to NLNRA samples for GRP78 (3.21 fold), PDIA1 (1.28 fold) and PRDX6 (1.34 fold) was consistent with the 2DE proteomic data (**Fig.3.38B**). Similar trend in protein expression pattern was observed with 2Gy-challenged HLNRA samples: GRP78 (1.65 fold), PDIA1 (1.3 fold) and PRDX6 (1.21 fold), in comparison with respective controls (**Fig.3.38C**).

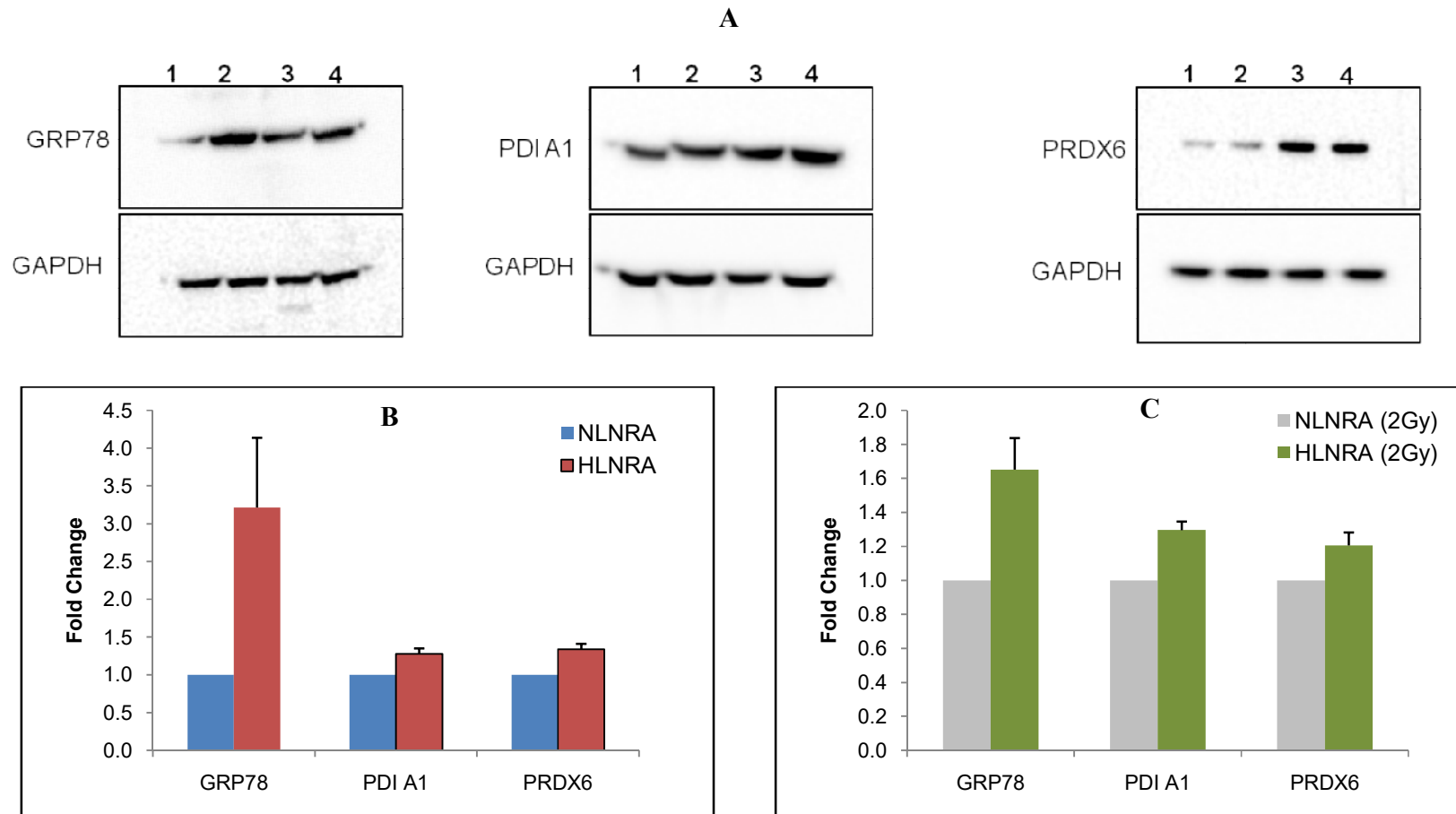


Fig.3.38. (A) Immunoblot validation of selected proteins (GRP78, PDIA1 and PRDX6). Pooled protein lysates from 10 subjects each for four experimental groups NLNRA (lane 1), HLNRA (lane 2), NLNRA (2 Gy) (lane 3) and HLNRA (2 Gy) (lane 4) were separated on 4–12% Bis-Tris gels, transferred to a PVDF membrane, probed with specific antibodies. Histograms presenting mean \pm SD of fold change in relative protein expression for (B) NLNRA vs HLNRA, and (C) NLNRA (2 Gy) vs HLNRA (2 Gy).

3.2.1.7. Principal component analysis for identification of radiation dose groups

Factor analysis on raw spot densities of all quantified proteins was performed using principal component as the method of extraction. The first two components of the PCA (Factor 1: 14.4% and Factor 2: 12.38%) explained ~26.8% of the data variance and could distinctly differentiate four groups based on radiation dose. The clustering was tighter for the *ex vivo* 2 Gy irradiated samples (Fig.3.39).

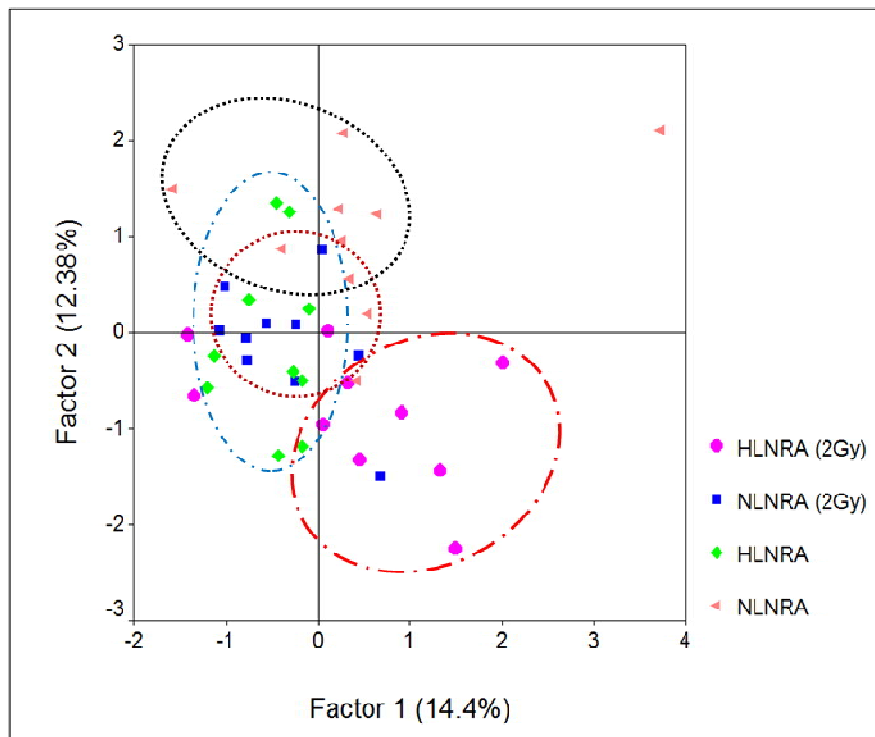


Fig.3.39. Principal component analysis for the protein expression data set with chronic radiation. PCA identified four clusters using the raw spot intensity data of all the quantified proteins. Biological replicates belonging to each group (10 subjects/group) were colour coded.

3.2.2. Basal proteome analysis with iTRAQ in HLNRA and NLNRA individuals

The chronic low dose radiation induced proteomic responses were characterized in human PBMCs isolated from individuals residing in HLNRA and compared with human PBMCs collected from individuals residing in adjoining NLNRA. The analysis was performed using High Resolution Liquid Chromatography (HR-LC) based iTRAQ quantitative proteomic method. For the analysis, samples from NLNRA were classified as (Group I: ≤ 1.5 mGy/y), while subjects collected from HLNRA were classified into three dose groups: Group II: 1.5-5.0 mGy/y; Group III: 5.01-14.0 mGy/y; Group IV: ≥ 14.01 mGy/y. The mean annual dose received by NLNRA subjects was 1.38 ± 0.08 mGy (range: 1.27-1.50 mGy/y; N=10). The mean annual dose received by HLNRA groups was 3.07 ± 0.86 mGy in Group II (range: 1.84-4.49 mGy/y; N=10), 10.50 ± 1.86 mGy (range: 7.98-13.61 mGy/y; N=10) in Group III and 17.08 ± 1.75 mGy (range: 14.69-20.25 mGy/y) in Group IV, respectively. The average age of the collected subjects from NLNRA (Group I) was 32.6 ± 2.55 y (range 29-36 y) and HLNRA groups was 38.2 ± 7.77 y in Group II (range 26-46 y), 37.5 ± 6.88 y in Group III (range 28-48 y) and 42.6 ± 5.83 y in Group IV (range 34-49 y), respectively.

3.2.2.1. Effect of chronic radiation on the proteome of HLNRA subjects

The iTRAQ analysis identified a total of 4166 proteins from 15073 peptides in human PBMCs of experimental subjects. Of these, 1699 proteins contained sufficient iTRAQ signal for relative quantitation. The partial list of proteins showing UNIPROT accession number, peptide matches, protein sequence coverage (%), average protein ratios and adjusted *P*-values are given in **Appendix A**. The distribution of the number of

unique peptides and peptide sequence coverage (%) of the identified proteins are shown in **Fig. 3.40A-B**, respectively. Over 72% of the identified proteins were represented by ≥ 2 peptide matches and ~61% of the identified proteins showed more than 5% peptide sequence coverage.

3.2.2.2. Assessment of technical variation

The experimental variation among the iTRAQ technical replicates was assessed with % CV as the method of tool using the relative protein ratios calculated for the 1699 identified proteins in HLNRA subjects in comparison with NLNRA subjects (Group I). Almost 89.1% of identified in Group II (**Fig. 41A**), 81.8% in Group III (**Fig. 41B**) and 78.2% in Group IV (**Fig. 41C**) showed %CV $\leq 20\%$, while 95% of proteins had a CV value $\leq 50\%$ among technical replicates, indicating good stability of expression.

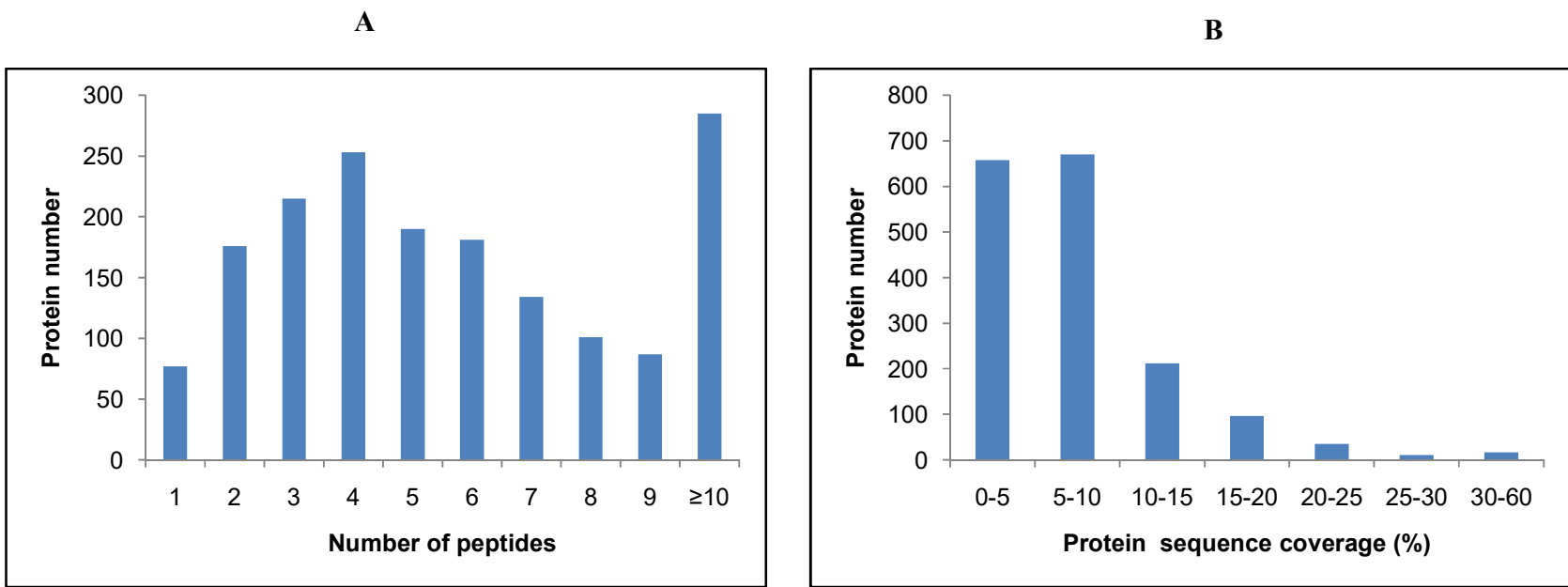


Fig.3.40. The distribution of the (A) number of peptides (B) peptide sequence coverage of the identified proteins in HLNRA groups by iTRAQ method.

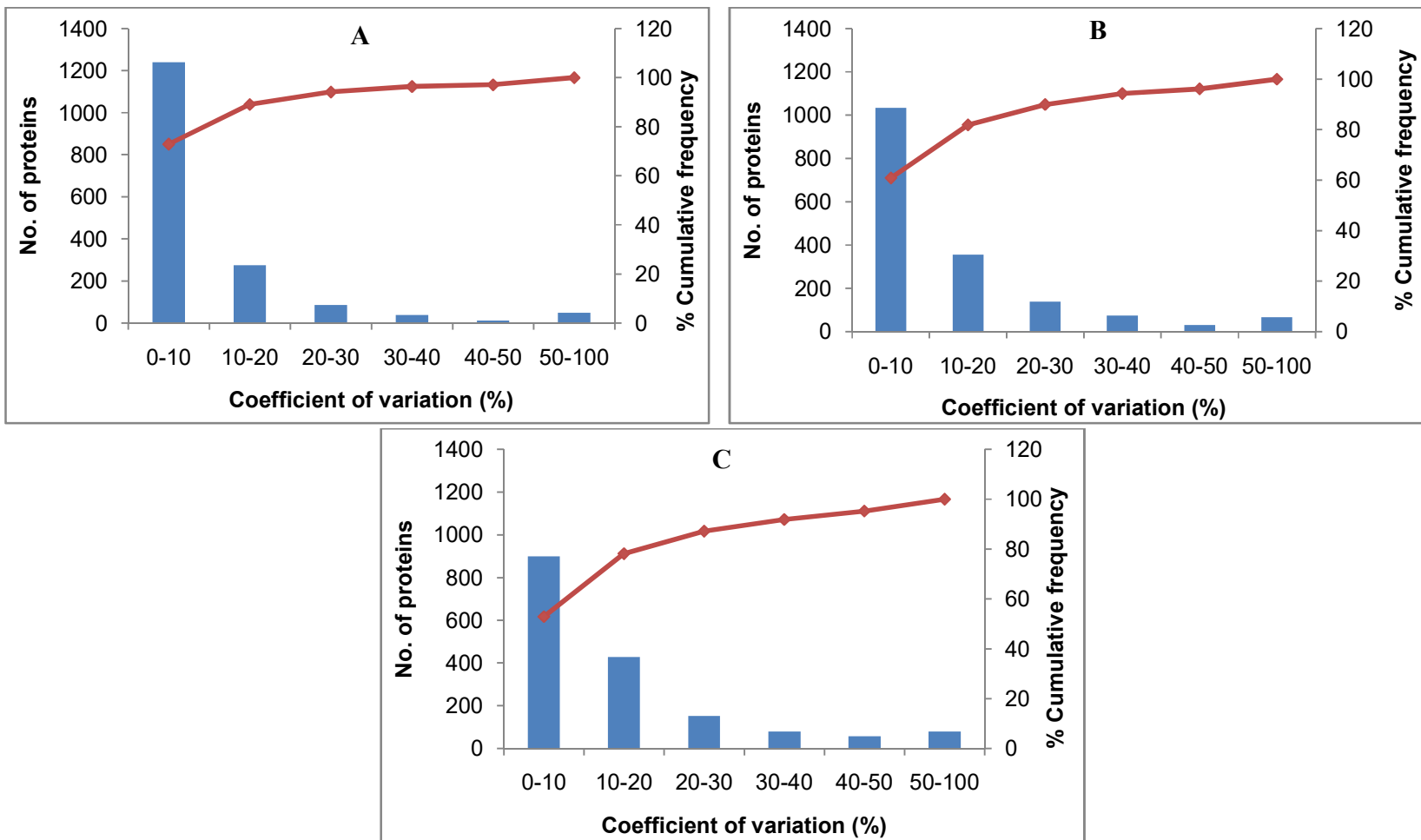


Fig.3.41. Experimental variation analysis based on Coefficient of Variation (%). The CV values calculated between (A) Group II vs NLNRA (B) Group III vs NLNRA (C) Group IV vs NLNRA, respectively were represented.

3.2.2.3. Relative abundance of identified proteins in HLNRA subjects

The Student's t-test *P*-values calculated between the technical replicates of treatment and control samples were adjusted with Benjamini-Hochberg method to reduce FDR. The distribution pattern of the calculated adjusted *P*-values in various dose groups is shown in **Fig.3.42**. Overall, the adjusted *P*-values of the majority of the proteins included in the analysis were ≤ 0.05 with values of 96.10% in Group II, 94.97% in Group III and 85.12% in Group IV dose groups of HLNRA.

For the initial filtering of the data, differential protein expression between NLNRA and HLNRA [Group I vs Group II; Group I vs Group III and Group I vs Group IV] subjects was performed by applying three different fold change threshold (2-fold, 1.5-fold, 1.2-fold) filters. The 2-fold filter threshold identified modulation of 9 proteins in Group II vs Group I (8 up-regulated and 1 down-regulated), 102 proteins in Group III vs Group I (100 up-regulated and 2 down-regulated) and 14 proteins in Group IV vs Group I (7 up-regulated and 7 down-regulated) (**Fig.3.43A-C**). Similarly, the 1.5-fold change threshold identified modulation of 361 proteins in Group II vs Group I (359 up-regulated and 2 down-regulated), 1198 proteins in Group III vs Group I (1194 up-regulated and 4 down-regulated) and 113 proteins in Group IV vs Group I (100 up-regulated and 3 down-regulated) (**Fig.3.43A-C**). The threshold filter of 1.2-fold identified significant modulation of 1460 proteins in Group II vs Group I (1454 up-regulated and 6 down-regulated), 1471 proteins in Group III vs Group I (1466 up-regulated and 5 down-regulated) and 692 proteins in Group IV vs Group I (663 up-regulated and 29 down-regulated) (**Fig.3.43A-C**).

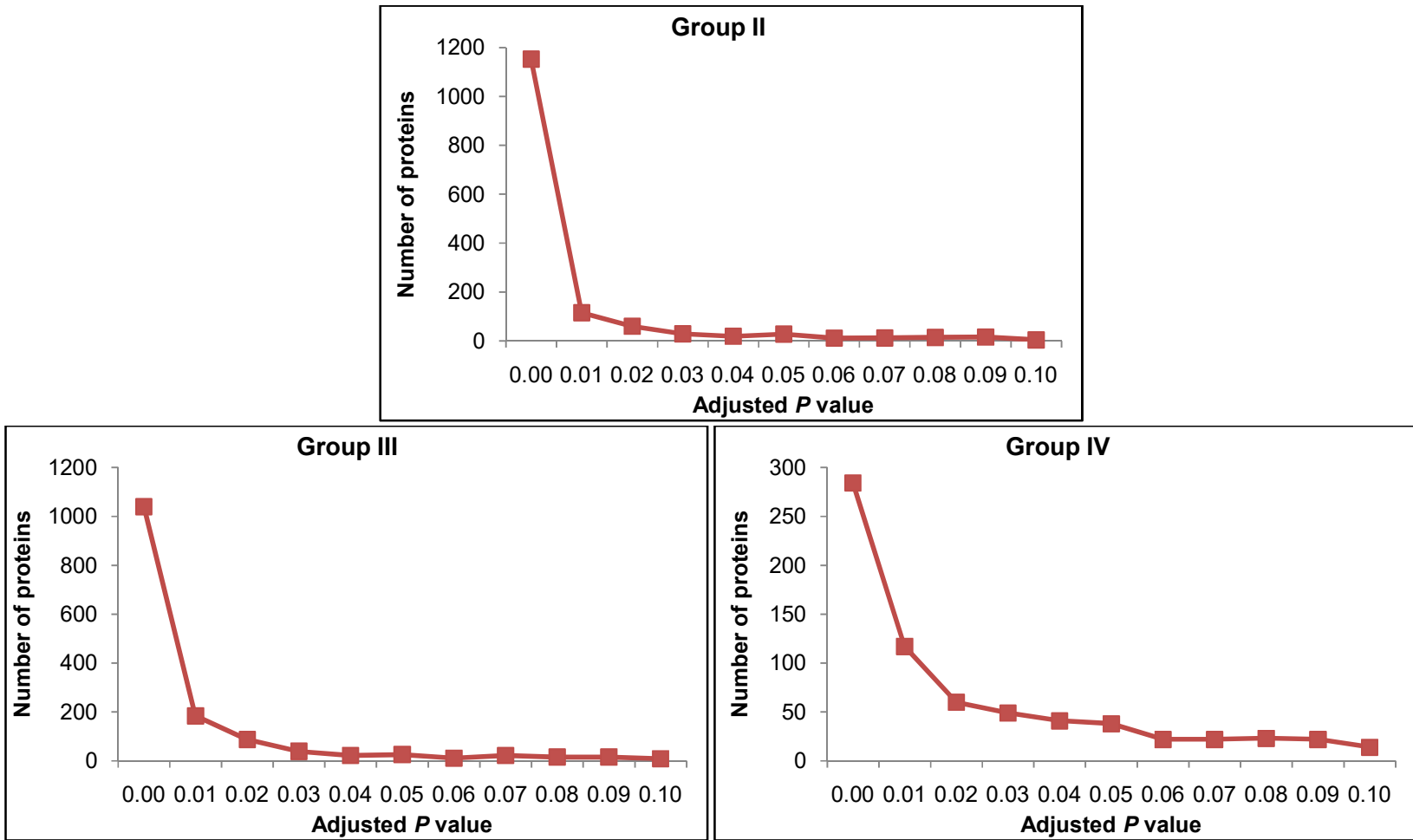


Fig.3.42. Adjusted *P*-value distribution of differentially expressed proteins in HLNRA dose groups

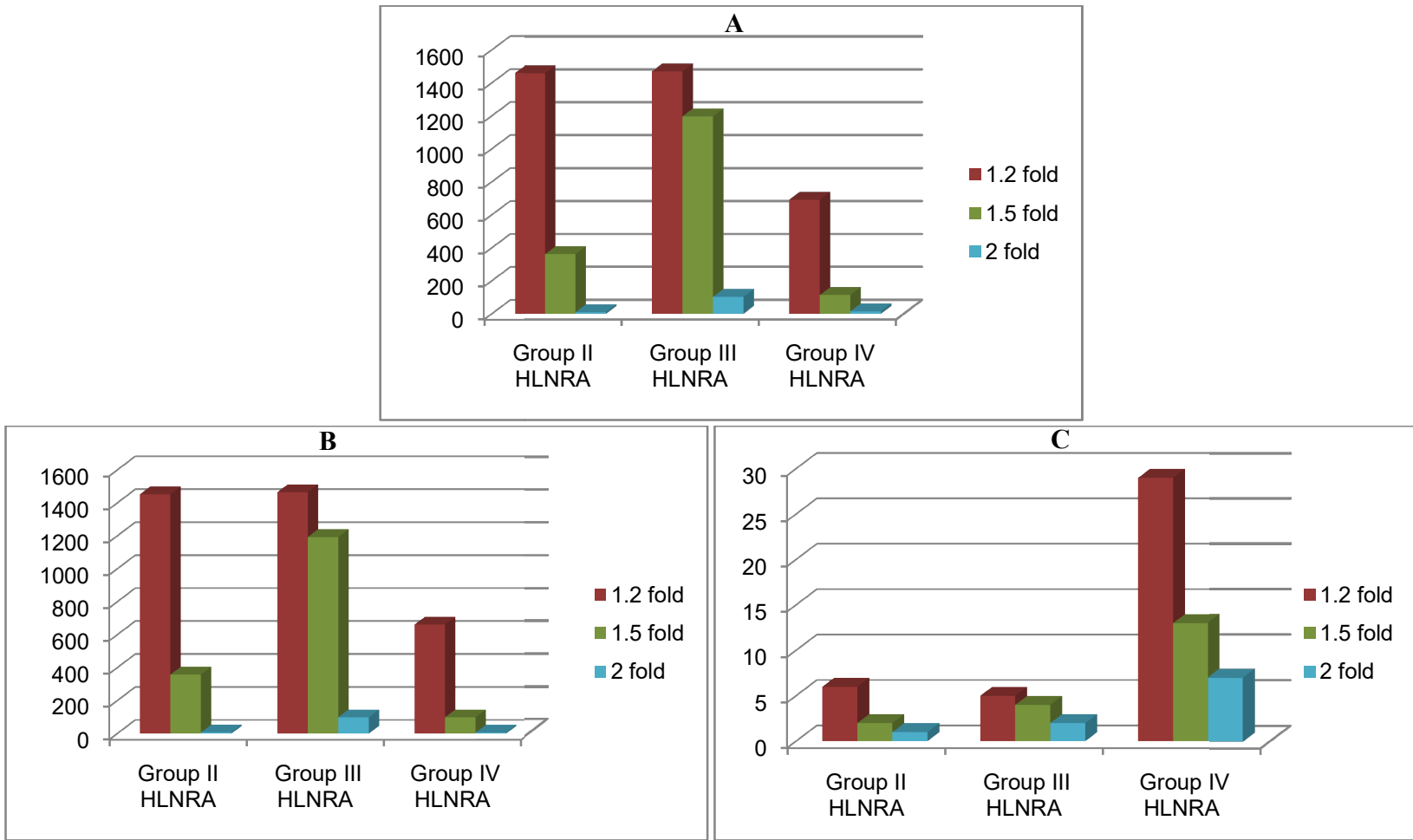


Fig.3.43. Distribution of differentially expressed proteins identified in HLNRA dose groups at different fold change filters (2 fold, 1.5 fold, 1.2 fold). (A) Total number of altered proteins (B) Up-regulated proteins (C) Down-regulated proteins.

In biological systems, even small changes in expression levels of proteins can regulate many cellular functions at the molecular level [177]. In order to avoid exclusion of proteins with subtle, yet functionally relevant, changes in expression, differentially expressed proteins chosen by a ratio ≥ 1.2 or ≤ 0.83 with an adjusted P -value of ≤ 0.1 in at least one dose group, were selected for further analysis. Overall, a total of 1565 proteins were found to be significantly altered in HLNRA individuals as compared to NLNRA. The top 10 up-regulated and down-regulated list of differentially modulated proteins is given in **Appendix B**. Out of these 635 proteins were common among all three HLNRA dose groups with 66, 57 and 19 proteins unique for Group II, Group III and Group IV, respectively. Almost 750 proteins were shared among Group II and Group III HLNRA dose groups, 9 proteins among Group III and Group IV, and 29 proteins among Group II and Group IV (**Fig.3.44**).

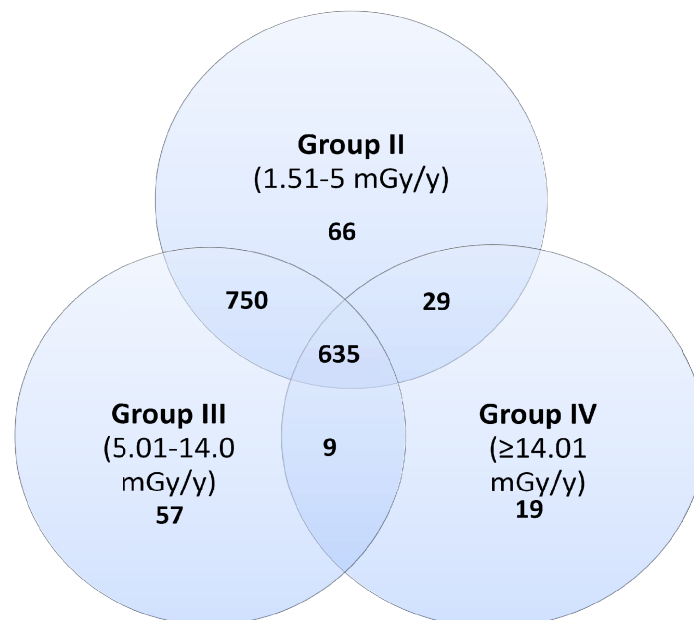


Fig.3.44. Distribution pattern of significantly (± 1.2 fold; adjusted P -value of ≤ 0.1) altered proteins in three HLNRA dose groups.

3.2.2.4. Functional annotation of differentially expressed proteins

A total of 1565 proteins were functionally annotated using DAVID according to the biological processes, molecular function, cellular component and KEGG pathways.

3.2.2.5. Classification of differentially expressed proteins by gene ontology (GO) based on biological processes

The DAVID analysis identified 204 biological processes significantly ($P \leq 0.05$) enriched in three HLNRA dose groups compared to NLNRA subjects (**Fig.3.45**). Number of proteins involved in each biological processes and their relative protein expression differed among the three HLNRA groups. Interestingly, enriched biological processes decreased as the annual background dose received by the subjects increased with 167 processes in Group II, 157 processes in Group III and 88 processes in Group IV. Of the 204 biological processes ($P \leq 0.05$) enriched, 57 processes were common among all three dose groups of HLNRA samples, though the number of proteins involved in each pathways and their relative protein expression differed among the three HLNRA groups. Many biological processes were radiation dose dependent with 20, 11 and 22 biological processes observed exclusively in Group II, Group III and Group IV, respectively when compared with Group I. (**Fig.3.45**).

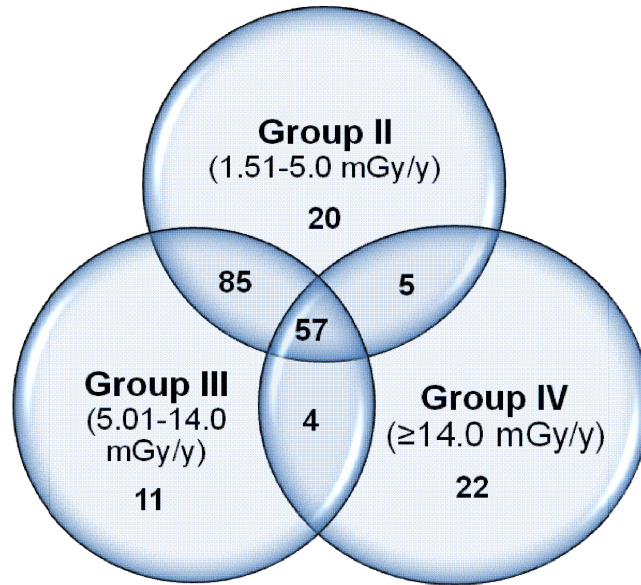
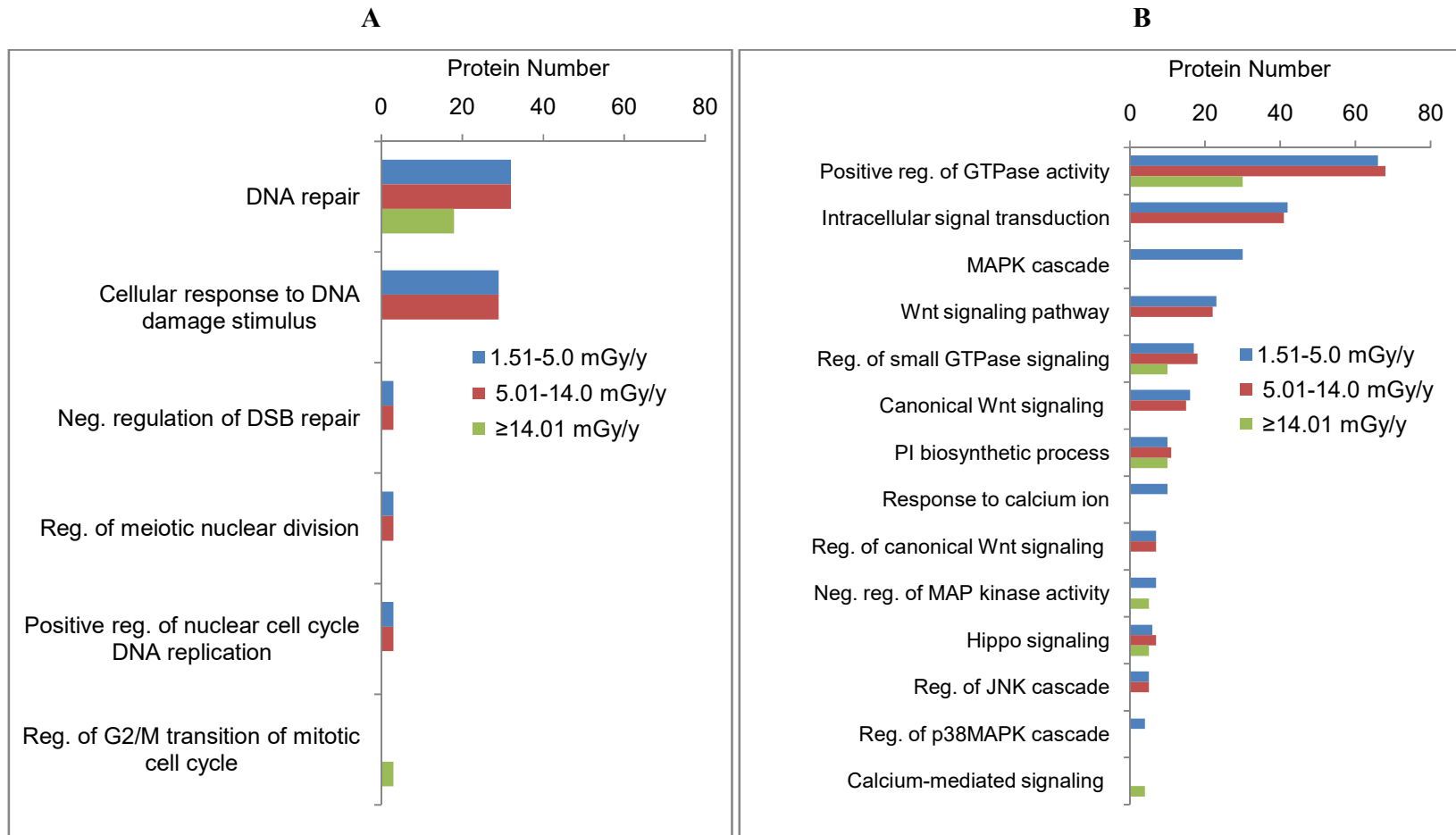
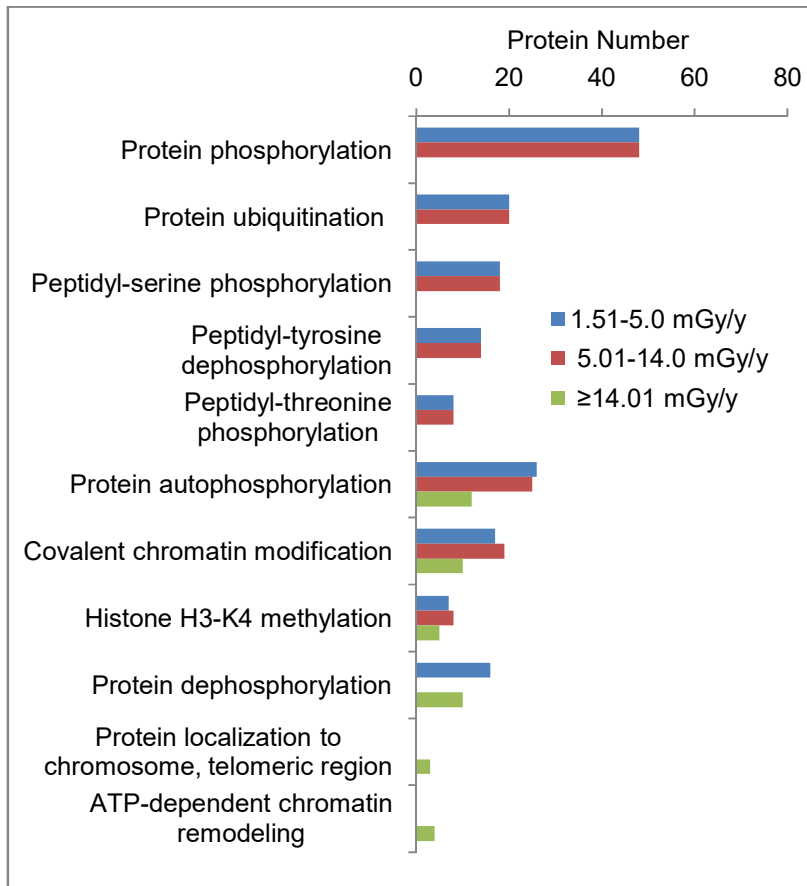
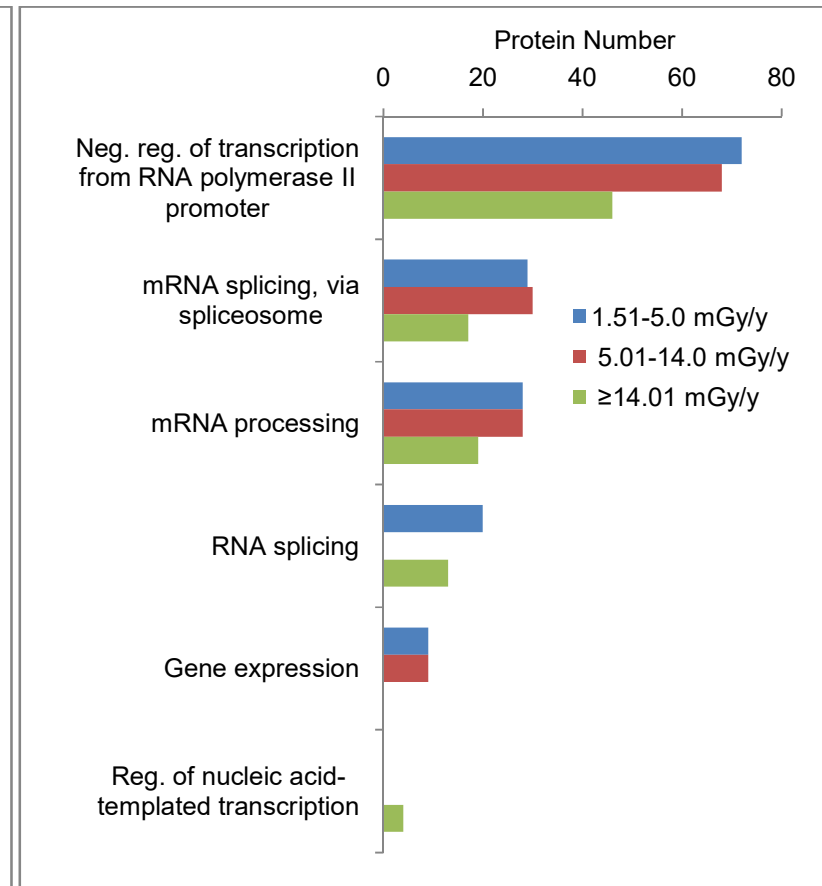


Fig.3.45. Distribution pattern of biological processes enriched in HLNRA dose groups.

3.2.2.6. Key radiation related biological processes enriched in HLNRA groups

The biological processes enriched by low dose chronic radiation could be broadly grouped into following major categories: (1) DNA repair and cell division, (2) Signaling networks, (3) Protein and chromatin modifications, (4) Gene regulation and RNA processing, (5) Cytoskeletal organization, and (6) Apoptosis and angiogenesis (**Fig.3.46A-F**).



C**D**

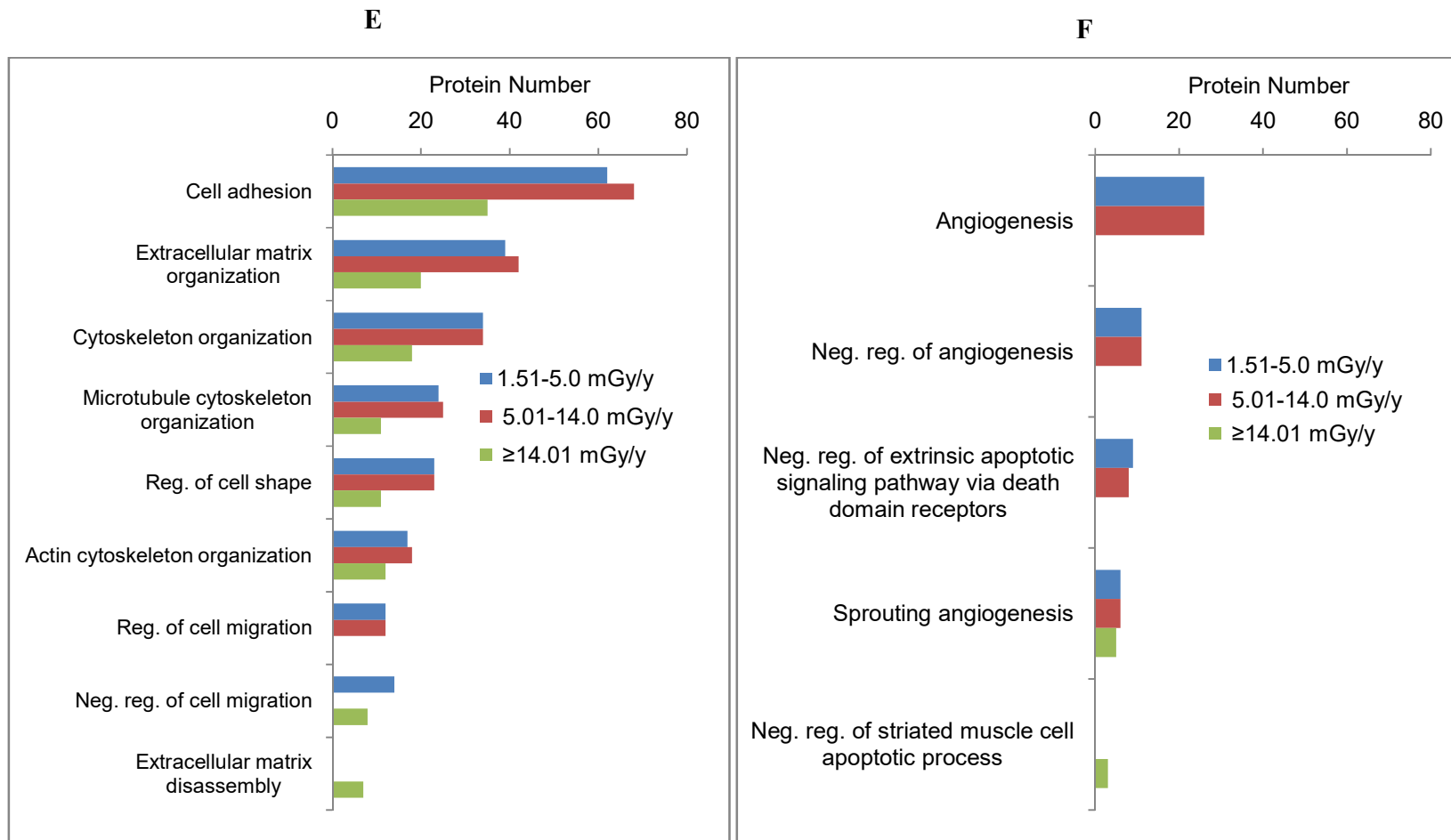


Fig.3.46. Important radiation related biological processes enriched in HLNRA dose groups (A) DNA repair and cell division (B) Signaling networks (C) Protein and chromatin modifications (D) Gene regulation & RNA processing (E) Cytoskeletal organization (F) Apoptosis & angiogenesis.

3.2.2.6.1. Proteins involved in DNA damage repair and DNA damage response signaling

A large number of proteins associated with DNA damage repair (Group II vs Group I: 22 proteins, Group III vs Group I: 22 proteins, Group IV vs Group I: 12 proteins) were identified in HLNRA subjects. This included biological processes with GO:0006281~DNA repair, GO:0006974~cellular response to DNA damage stimulus and GO:2000780~negative regulation of DSB repair (**Fig.3.46A**). HLNRA groups showed over-expression of proteins involved in all major DNA repair processes: Base excision repair (APEX2, MBD4, HUWE1), Nucleotide excision repair (XPF, RPA1, CUL4A), Mismatch repair (MSH3, MLH1), Homologous recombination repair (BLM, BRCA2, FANCI, FANCA, FANCM, RA54B, RMI2, PARI), Non-homologous end joining (XRCC6, PRKDC, UVRAG, SFPQ) and Translesion synthesis (DPOLQ, DPOLN) (**Fig.3.47A**). Highest relative fold changes were seen for proteins involved in homologous recombination. These included BLM protein (2.37 fold in Group II, 3.83 fold in Group III, 4.12 in Group IV), RMI2 (1.78 fold in Group II, 2.65 fold in Group III, 3.1 in Group IV), PARI (1.54 fold in Group II, 1.96 fold in Group III, 1.61 in Group IV) and FANCI (1.57 fold in Group II, 1.75 fold in Group III, 1.42 in Group IV). Several radiation response proteins involved in DDR signaling were also differentially modulated in three HLNRA dose groups: Group II vs Group I: 43 proteins, Group III vs Group I: 43 proteins, Group IV vs Group I: 21 proteins, respectively (**Fig.3.47B-C**). Majority of the proteins showed over-expression in HLNRA subjects. Exceptions were seen for CDK2 which was under-expressed in all three HLNRA groups and for HERC2 that showed down regulation in Group IV.

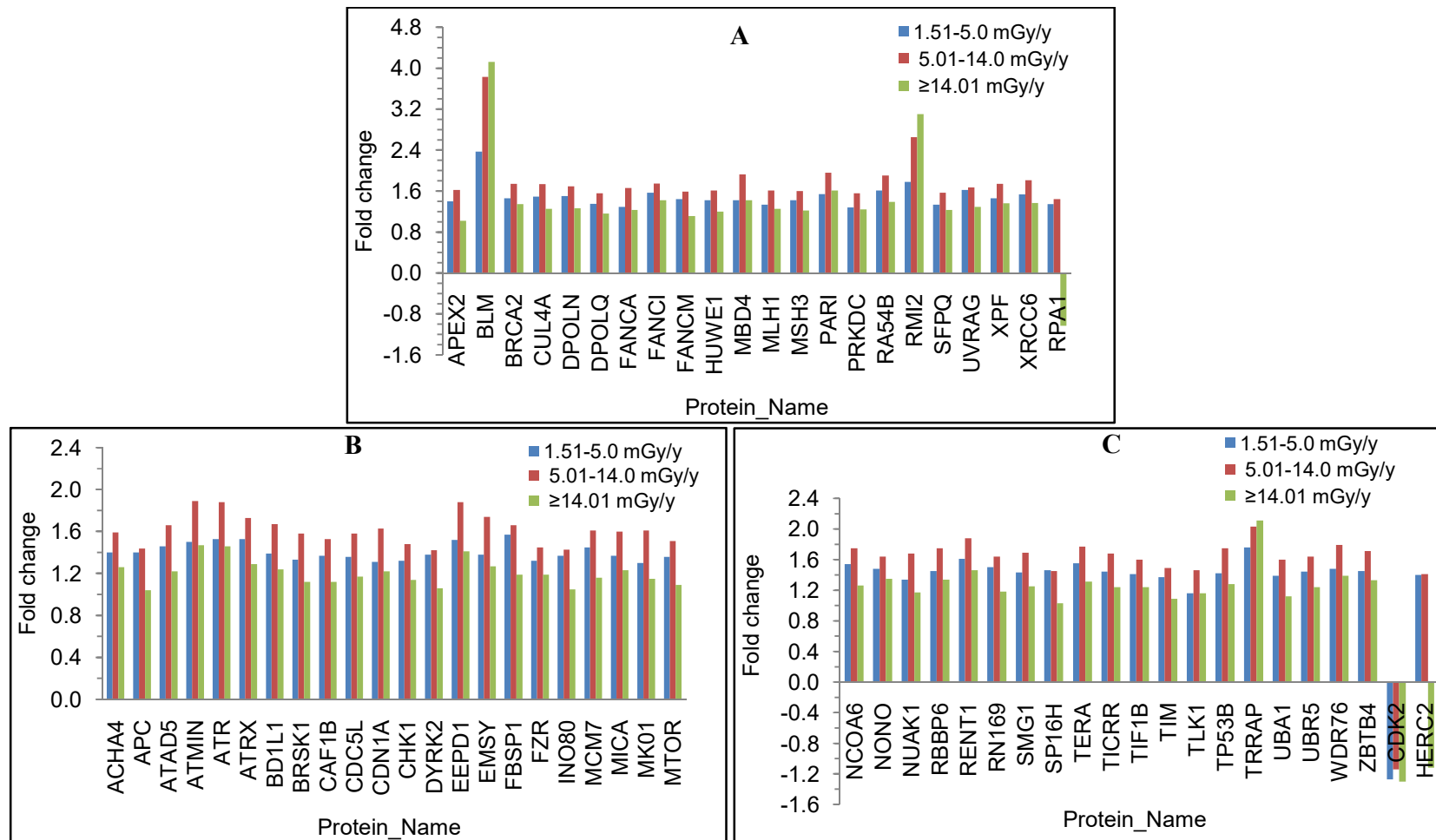


Fig.3.47. Relative fold changes of proteins enriched in HLNRA dose groups compared to NLNRA for (A) DNA damage repair and (B, C) DDR signaling process. The proteins are abbreviated as listed in **Appendix A**.

3.2.2.6.2. Proteins involved in signaling pathways

HLNRA subjects showed enrichment of several types of radiation induced signaling processes with many activated signalling processes showing a radiation dose specific activation (**Fig.3.46C**). The proteins involved in intracellular signal transduction (GO:0035556) was expressed in Group II (42 proteins) and Group III (41 proteins) of HLNRA (**Fig.3.48 A-D**). The enrichment of different Wnt signaling pathways (GO:0060070, GO:0060828, GO:0090090, GO:0016055) was also confined to Group II (44 proteins) and Group III (42 proteins) of HLNRA (**Fig.3.48 E-H**). The dose specific enrichment of phosphatidylinositol-mediated signaling (GO:0048015) was observed only in Group III (15 proteins) subjects (**Fig.3.48 I-J**), where as calcium-mediated signaling using intracellular calcium source (GO:0035584) was seen only in Group IV (4 proteins) (**Fig.3.48 K**).

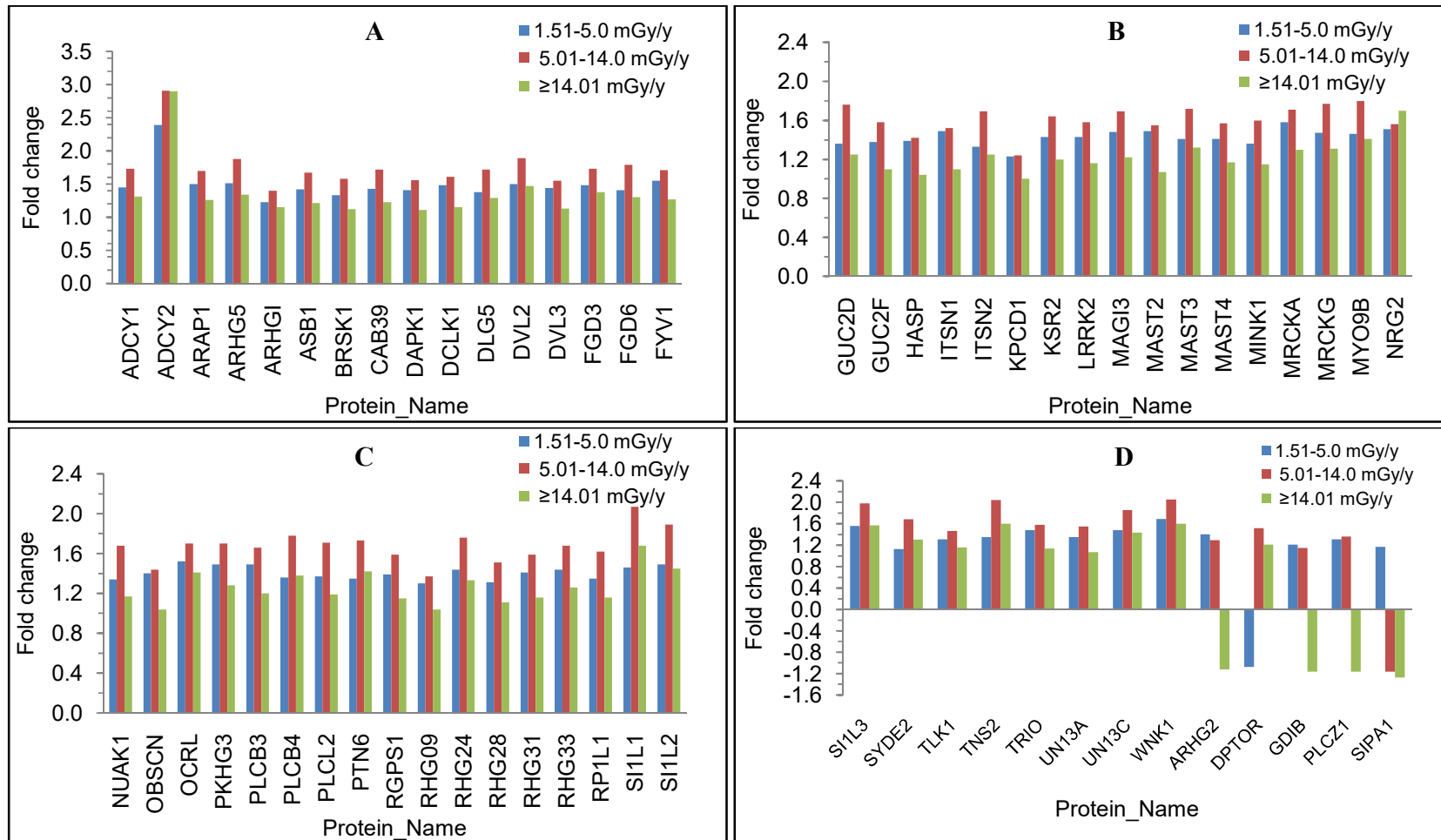


Fig.3.48A-D: Relative fold changes of proteins enriched in HLNRA dose groups compared to NLNRA for intracellular signal transduction biological process. The proteins are abbreviated as listed in **Appendix A**.

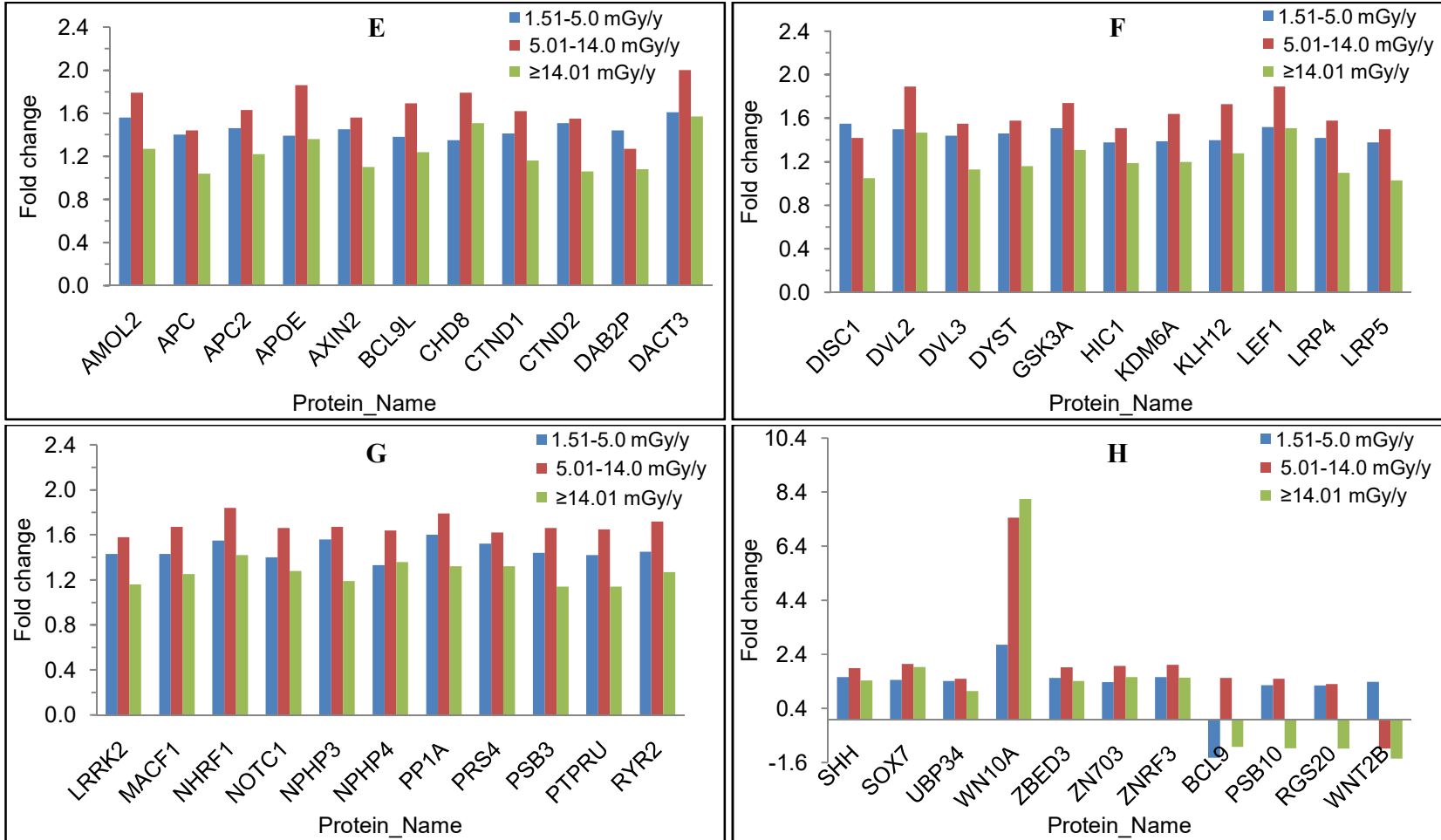


Fig.3.48 E-H: Relative fold changes of proteins enriched in HLNRA dose groups compared to NLNRA for canonical Wnt signaling pathway biological process. The proteins are abbreviated as listed in **Appendix A**.

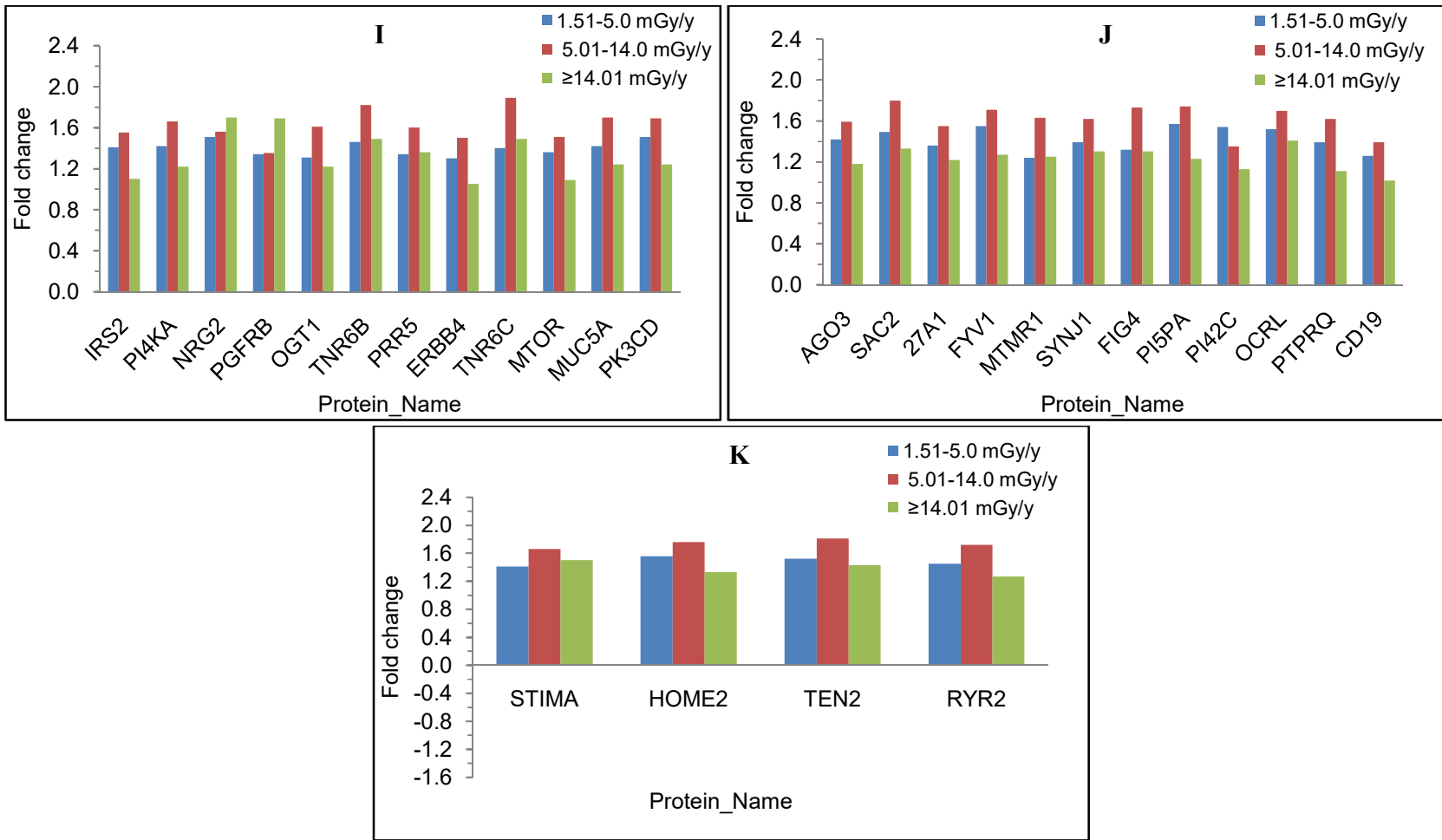


Fig.3.48. Relative fold changes of proteins enriched in HLNRA dose groups compared to NLNRA for (I-J) Phosphatidylinositol-mediated signaling (K) calcium-mediated signaling biological processes. The proteins are abbreviated as listed in **Appendix A**.

3.2.2.6.3. Proteins involved in stress activated protein kinase pathways

Chronic low dose radiation activated signaling of many mitogen activated protein kinases (GO:0000165~MAPK cascade), c-Jun amino-terminal kinases (JNK) (GO:0046328~regulation of JNK cascade) and p38 MAPKs (GO:1900744~regulation of p38MAPK cascade) in HLNRA subjects (**Fig.3.46B**). A clear distinction of biological processes was observed based on the annual radiation dose received by the HLNRA individuals. MAPK cascade and p38-MAPK signaling proteins were significantly enriched only in Group II subjects while. JNK cascade was enriched in both Group II and Group III HLNRA subjects. Group IV individuals showed a small, but statistically insignificant expression of some of these proteins (**Fig.3.49A-D**).

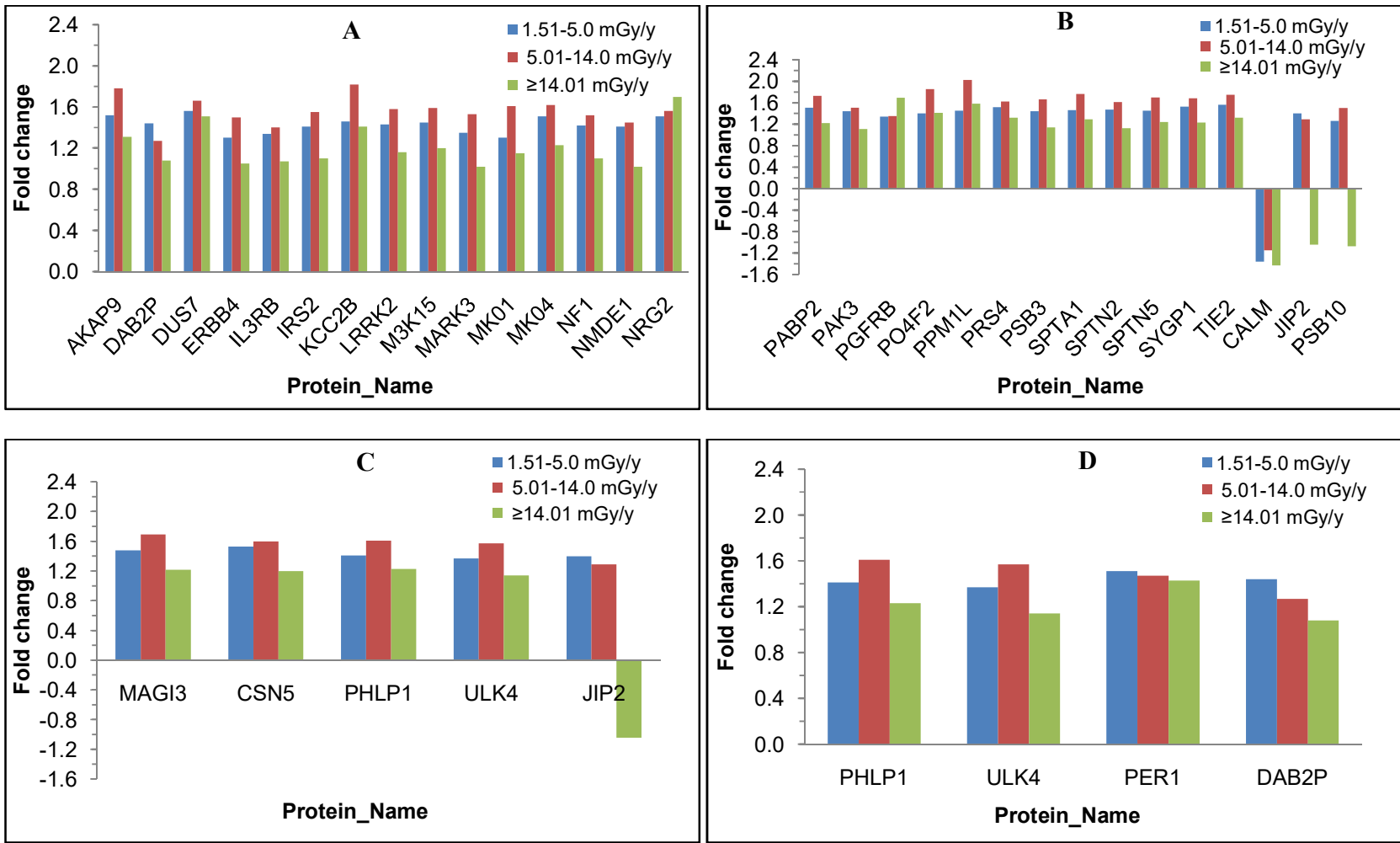
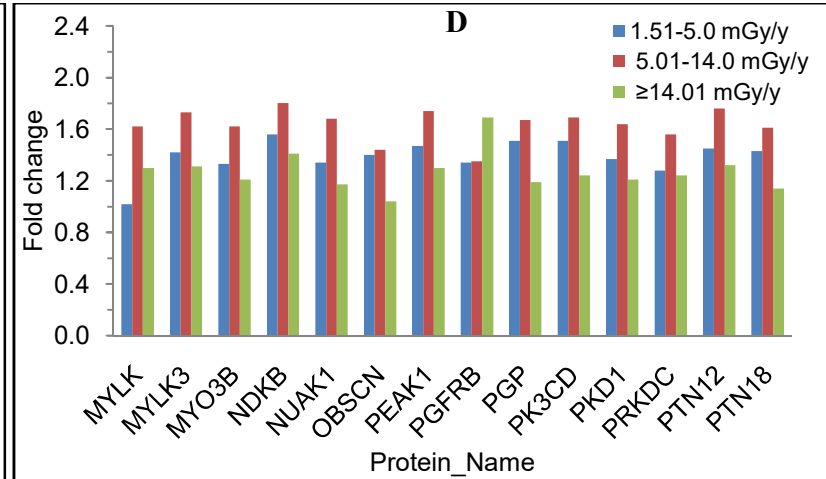
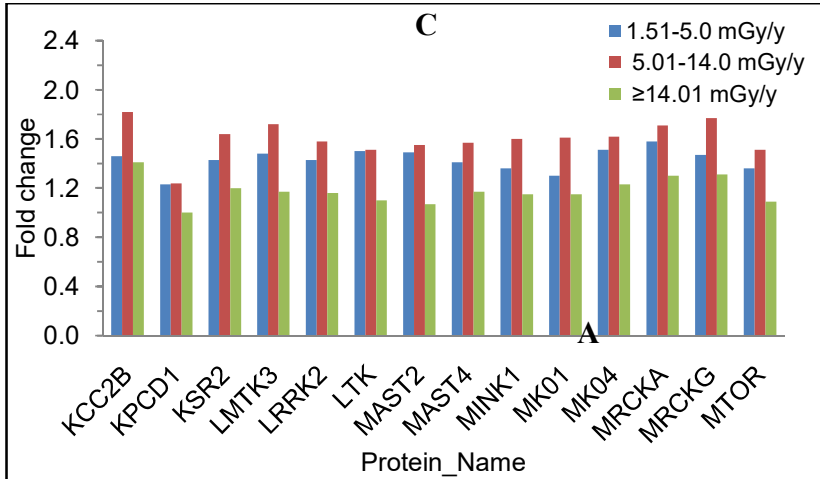
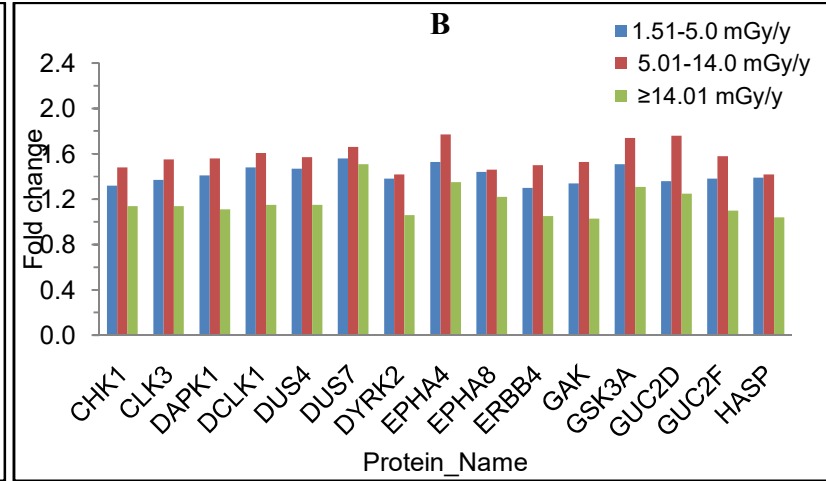
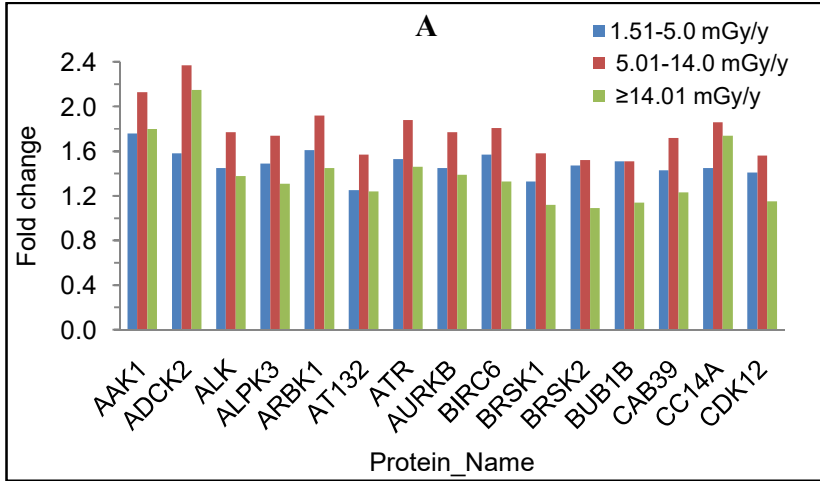


Fig.3.49. Relative fold changes of proteins enriched in HLNRA dose groups compared to NLNRA for (A, B) MAP Kinase cascade (C) JNK cascade (D) p38-MAP Kinase cascade biological processes. The proteins are abbreviated as listed in **Appendix A**.

3.2.2.6.4. Proteins involved in post-translational modifications

Proteins associated with the process of protein phosphorylation (**Fig.3.50A-F**) and protein ubiquitination of target proteins (**Fig.3.50G-H**) formed a major category of proteins altered in HLNRA individuals as compared to NLNRA. The GO biological process of protein autophosphorylation (GO:0046777) was enriched in all HLNRA groups. The biological process of peptidyl-serine phosphorylation (GO:0018105), protein phosphorylation (GO:0006468), peptidyl-threonine phosphorylation (GO:0018107), peptidyl-tyrosine dephosphorylation (GO:0035335) and protein ubiquitination involved in ubiquitin-dependent protein catabolic process (GO:0042787) were enriched only in Group II and III of HLNRA (**Fig.3.46C**). On the other hand, proteins involved in protein dephosphorylation (GO:0006470) were identified only in Group II and IV dose groups of HLNRA (**Fig.3.46C**). For the biological process of protein phosphorylation as many as 82 proteins from Group II, 84 proteins from Group III and 35 proteins from Group IV were significantly changed. For protein ubiquitination process, 20 proteins each from Group II and 11 proteins from Group IV were enriched.



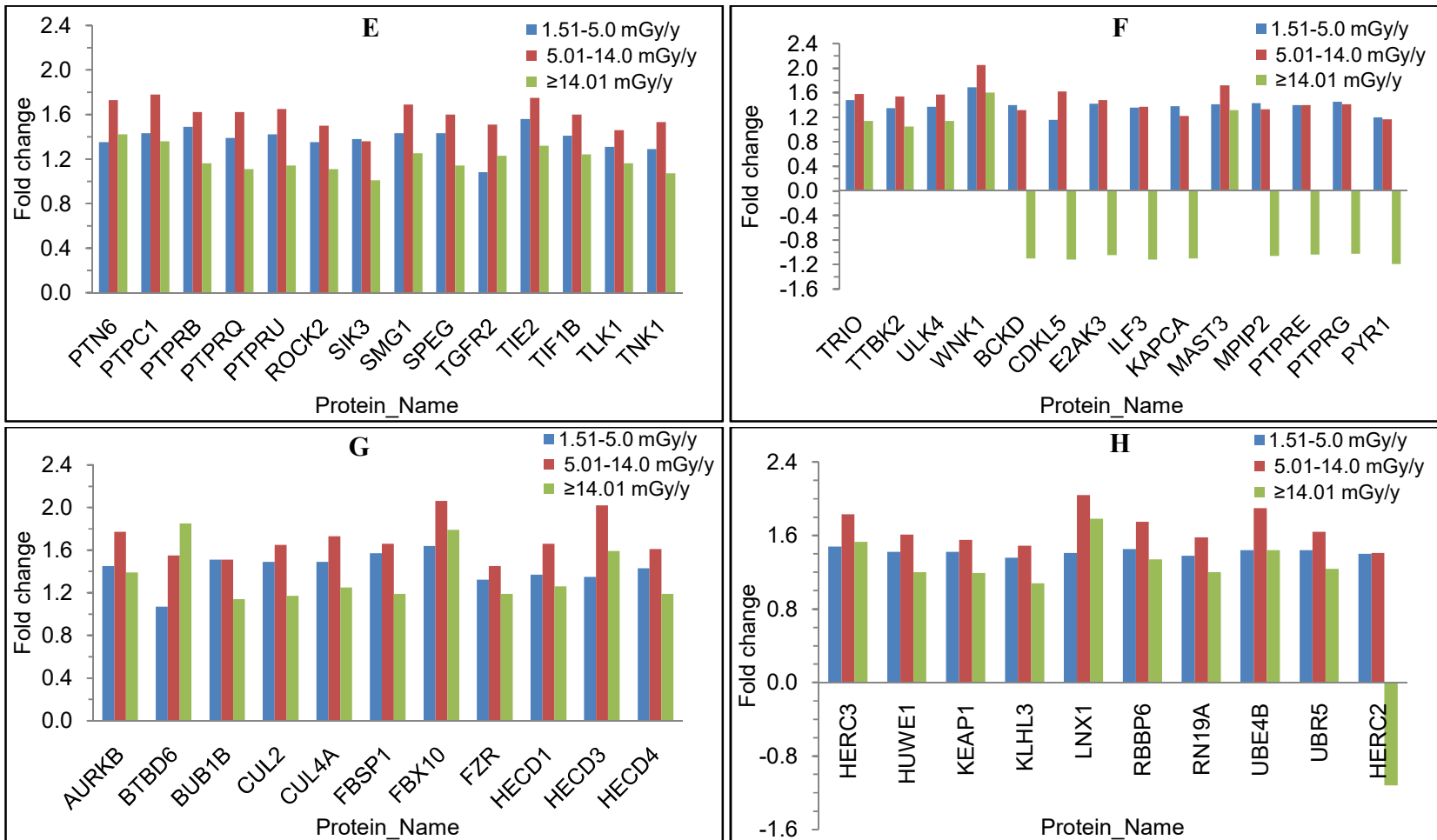


Fig.3.50. Relative fold changes of proteins enriched in HLNRA dose groups compared to NLNRA for (A-F) Protein phosphorylation (G-H) Protein ubiquitination biological processes. The proteins are abbreviated as listed in **Appendix A**.

3.2.2.6.5. Proteins involved in chromatin modifications

Another important category of biological process enriched in HLNRA subjects were proteins involved in modification of chromatin structure (Group II vs Group I: 27 proteins, Group III vs Group I: 31 proteins, Group IV vs Group I: 15 proteins) (**Fig.3.51**). The different dose groups of HLNRA showed enrichment of characteristic chromatin modification related biological processes. For example, processes like histone H3-K4 methylation (GO:0051568) and covalent chromatin modification (GO:0016569) were enriched among all HLNRA groups (**Fig.3.46C**). The Group III HLNRA subjects specifically showed modulation of proteins involved in histone H3-K4 trimethylation (GO:0080182) and chromatin-mediated maintenance of transcription (GO:0048096), whereas Group IV samples were enriched with proteins involved in ATP-dependent chromatin remodeling (GO:0043044) and protein localization to chromosome-telomeric region (GO:0070198) (**Fig.3.46C**).

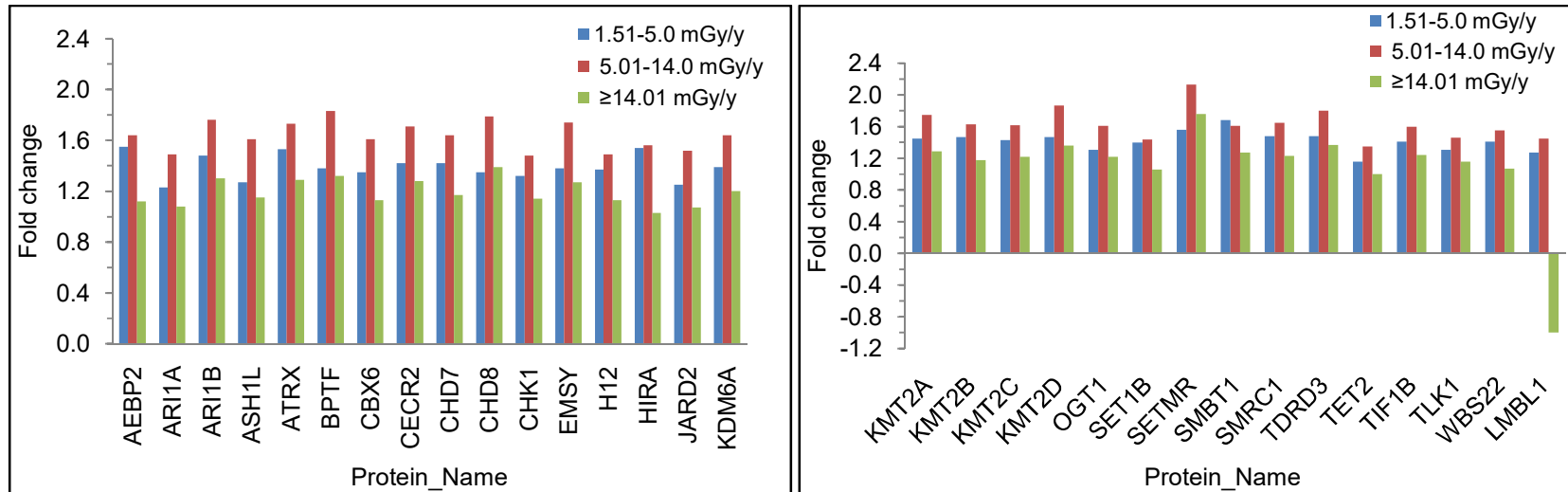
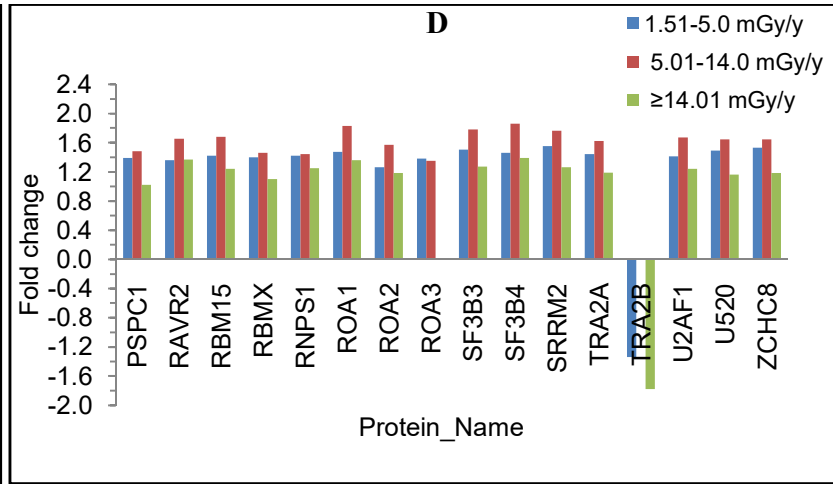
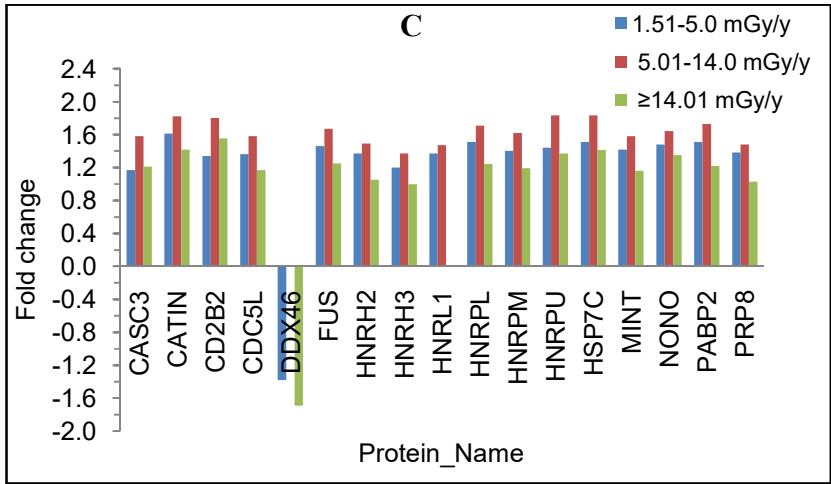
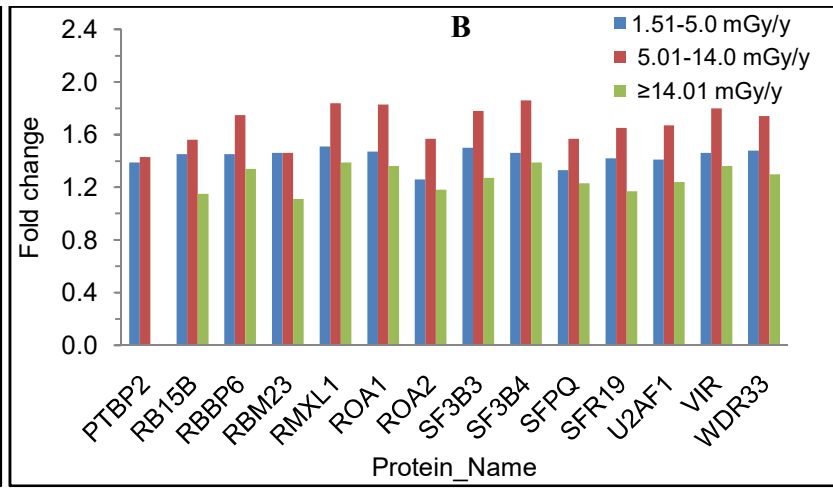
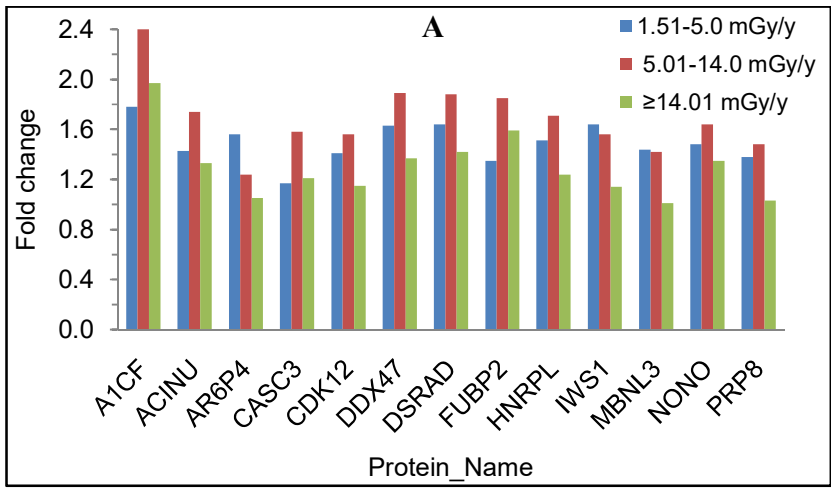


Fig.3.51. Relative fold changes of proteins enriched in HLNRA dose groups compared to NLNRA for chromatin modification biological process. The proteins are abbreviated as listed in **Appendix A**.

3.2.2.6.6. Proteins involved in RNA processing and splicing

The proteins involved in processing and splicing of RNA were another important biological process identified in HLNRA dose groups. The biological process of mRNA processing (GO:0006397) and mRNA splicing, via spliceosome (GO:0000398) were enriched among all studied dose groups (**Fig.3.46C**). The process of mRNA processing (GO:0006397) showed significant proteins alterations for 28 proteins in Group II, 28 proteins in Group III and 19 proteins in Group IV (**Fig.3.52A-B**). The number of proteins involved in biological process of mRNA splicing, via spliceosome (GO:0000398) was 29 proteins in Group II , 30 proteins in Group III and 17 proteins in Group IV (**Fig.3.52C-D**). The GO term process of RNA splicing (GO:0008380) was observed in Group II and IV (**Fig.3.52E**), whereas RNA processing (GO:0006396) biological process showed characteristic enrichment only in Group III (**Fig.3.52F**).



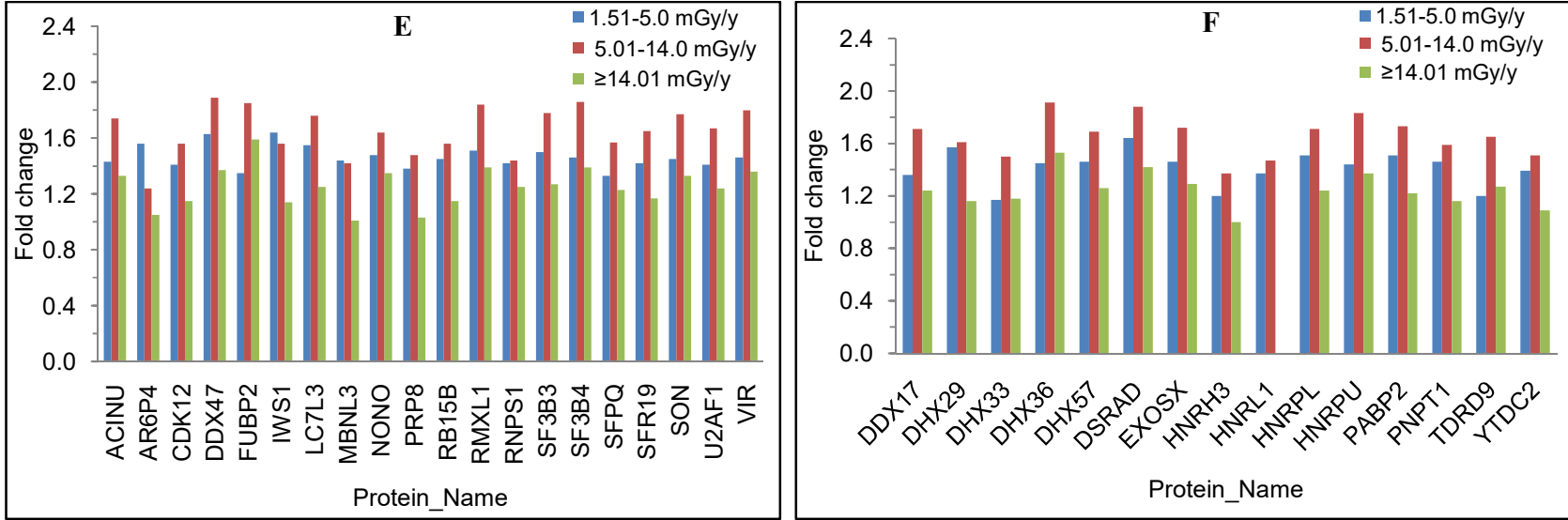


Fig.3.52. Relative fold changes of proteins enriched in HLNRA dose groups compared to NLNRA for (A-B) mRNA processing, (C-D) mRNA splicing, via spliceosome, (E) RNA splicing (F) RNA processing. The proteins are abbreviated as listed in **Appendix A**.

3.2.2.7. Classification of differentially expressed proteins by gene ontology (GO) based on molecular function

In the molecular function (MF) ontology, 93 categories were significantly ($P \leq 0.05$) enriched in HLNRA dose groups (Fig.3.53). The binding to protein, RNA, DNA and chromatin was the major category with 75% proteins of Group I, 76% proteins of Group II and 85% proteins of Group III belonging to this molecular function. The other MF categories represented were cytoskeletal structure (9%) ATPase activity (5%), kinase activity (4%), phosphatase activity (1%) and gated channel activity (1%). Out of these, MFs related to kinase activity, phosphatase activity and gated channel activity were not observed in Group IV subjects (Fig.3.54).

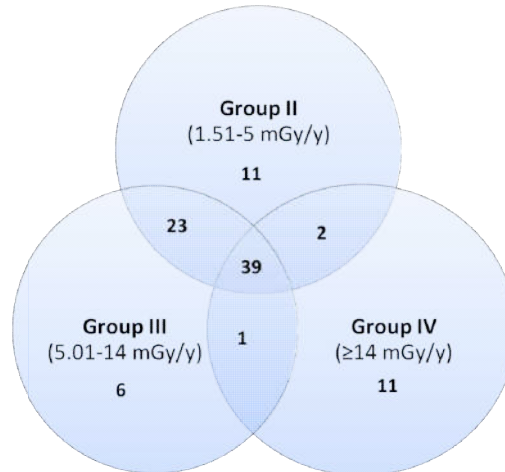


Fig.3.53. Distribution pattern of molecular function ontology enriched in HLNRA dose groups.

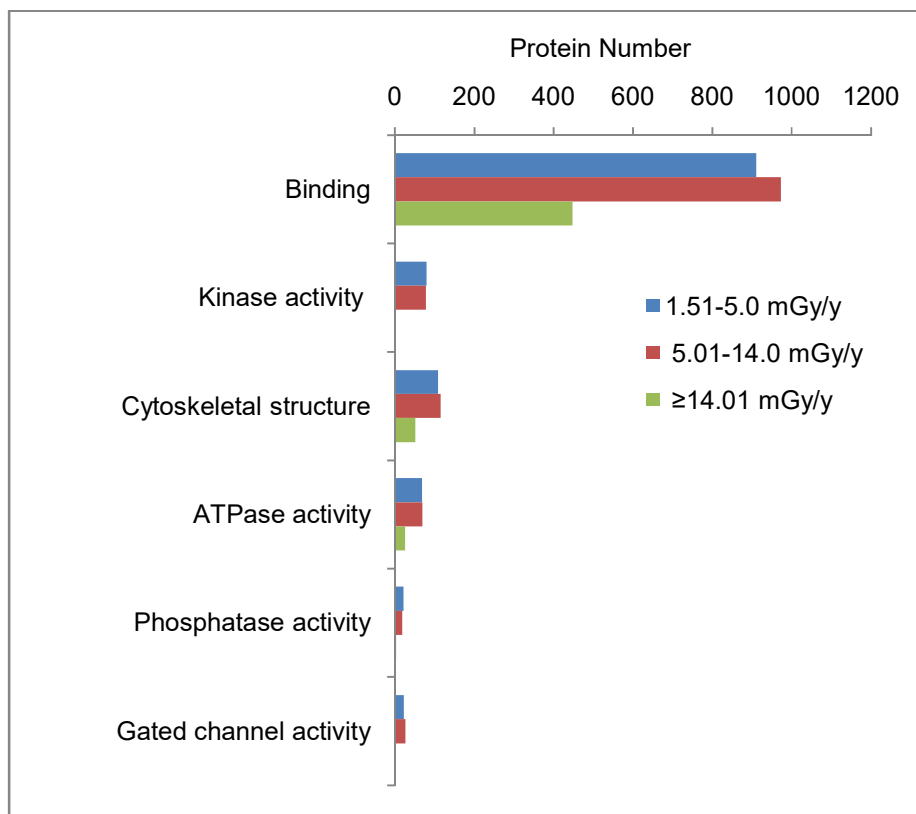


Fig.3.54. Key molecular function categories enriched in Group II, Group III and Group IV individuals of HLNRA dose groups.

3.2.2.8. Classification of differentially expressed proteins by gene ontology (GO) based on cellular component

Enrichment of 110 cellular component (CC) categories was observed in three HLNRA dose groups. The localization to cytoplasm was the major category enriched. Almost 27% proteins of Group II, an equal proportion of Group III and 33% proteins of Group IV localized to cytoplasm. Nuclear proteins were found in almost similar proportions. A smaller percentage of differentially expressed proteins localized to membrane (12%), cytoskeleton (8%), exosome (7%), organelle (7%), extracellular matrix (6%) and cell junction (5%) (Fig.3.55).

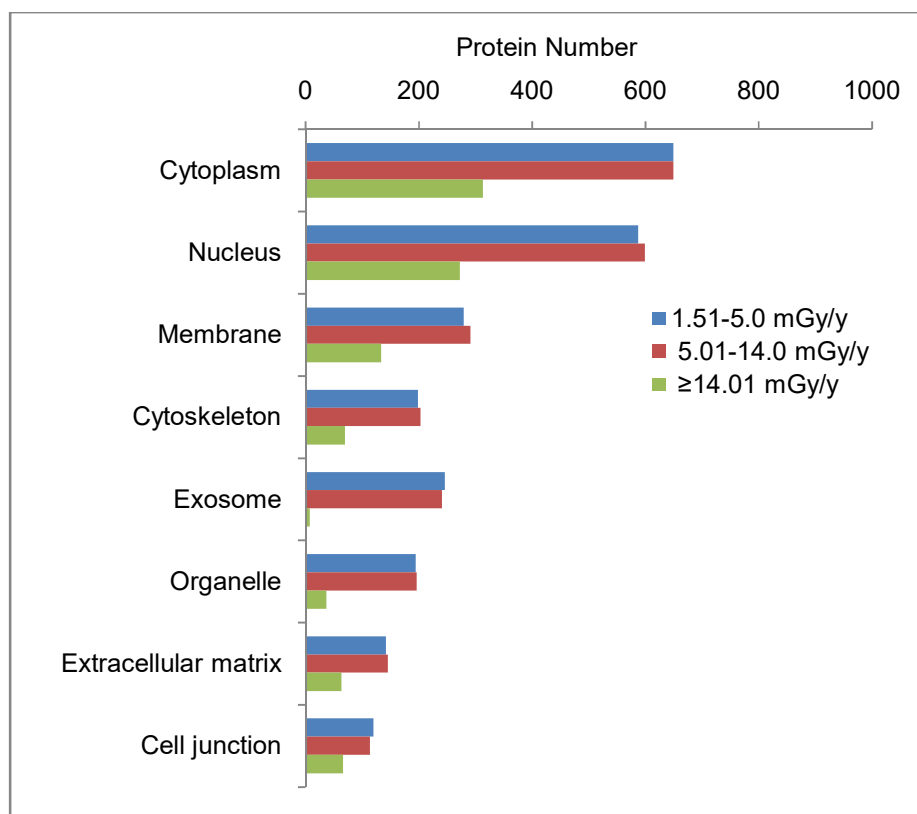


Fig.3.55. Key cellular component categories enriched in Group II, Group III and Group IV individuals of HLNRA dose groups.

3.2.2.9. KEGG pathways affected by chronic low dose radiation exposure

The molecular pathways associated with the differentially expressed proteins were identified using Kyoto Encyclopedia of Genes and Genomes (KEGG: <http://www.genome.jp/kegg/> or <http://www.kegg.jp>) analysis tool of DAVID software. Only significantly enriched categories with their *P*-value lower than 0.05 were selected. The analysis identified enrichment of 41 KEGG pathways in HLNRA individuals. Out of these, 16 pathways were shared among all three HLNRA dose groups while others showed a radiation dose specific enrichment (**Fig.3.56**). There were 30 enriched KEGG pathways in Group II individuals (**Appendix C1**), 27 in Group III individuals (**Appendix C2**) and 28 in Group IV individuals (**Appendix C3**). Again, the number of proteins involved in each KEGG pathway and their relative protein expression differed among the three HLNRA groups.

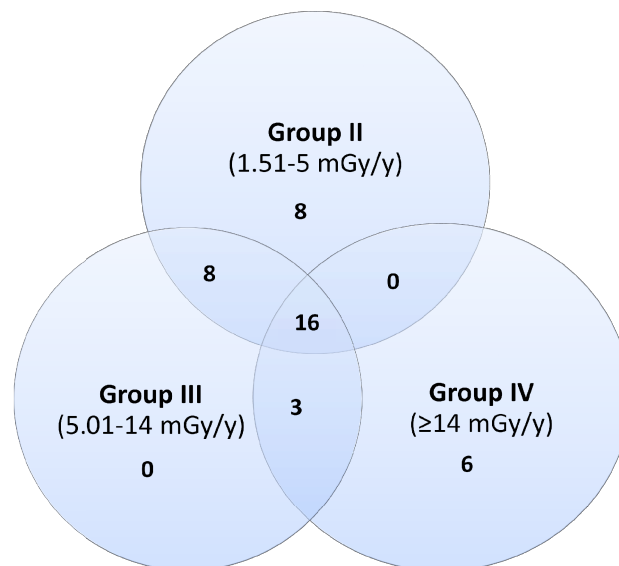


Fig.3.56. Distribution pattern of KEGG pathways enriched in HLNRA dose groups.

3.2.2.10. Key radiation related KEGG pathways enriched in HLNRA groups

Many important pathways related to cell-matrix interaction, DNA repair and signaling showed enrichment in subjects of HLNRA dose groups.

The important cell-matrix interaction related pathways enriched in all the three HLNRA groups were focal adhesion (hsa04510), ECM-receptor interaction (hsa04512), and regulation of actin cytoskeleton (hsa04810) (**Fig.3.57**). For focal adhesion, 45 proteins from Group II, 48 proteins from Group III and 28 proteins from Group IV showed significant changes (**Fig.3.58A-D**). For ECM-receptor interaction 28 proteins from Group II, 30 proteins from Group III and 15 proteins from Group IV were significantly altered (**Fig.3.58E-F**). For regulation of actin cytoskeleton, 25 proteins from Group II, 28 proteins from Group III and 16 proteins from Group IV showed significant modulation (**Fig.3.58G-H**).

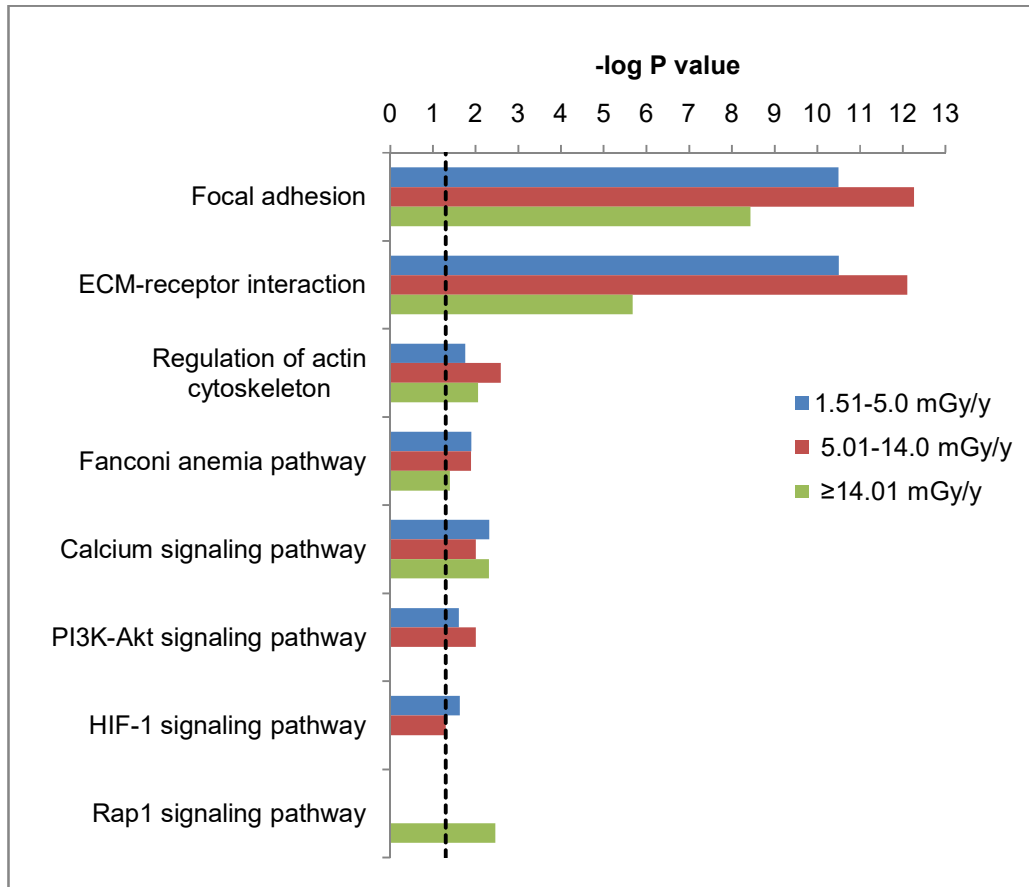


Fig.3.57. Key radiation altered KEGG pathways enriched in Group II, Group III and Group IV individuals of HLNRA dose groups.

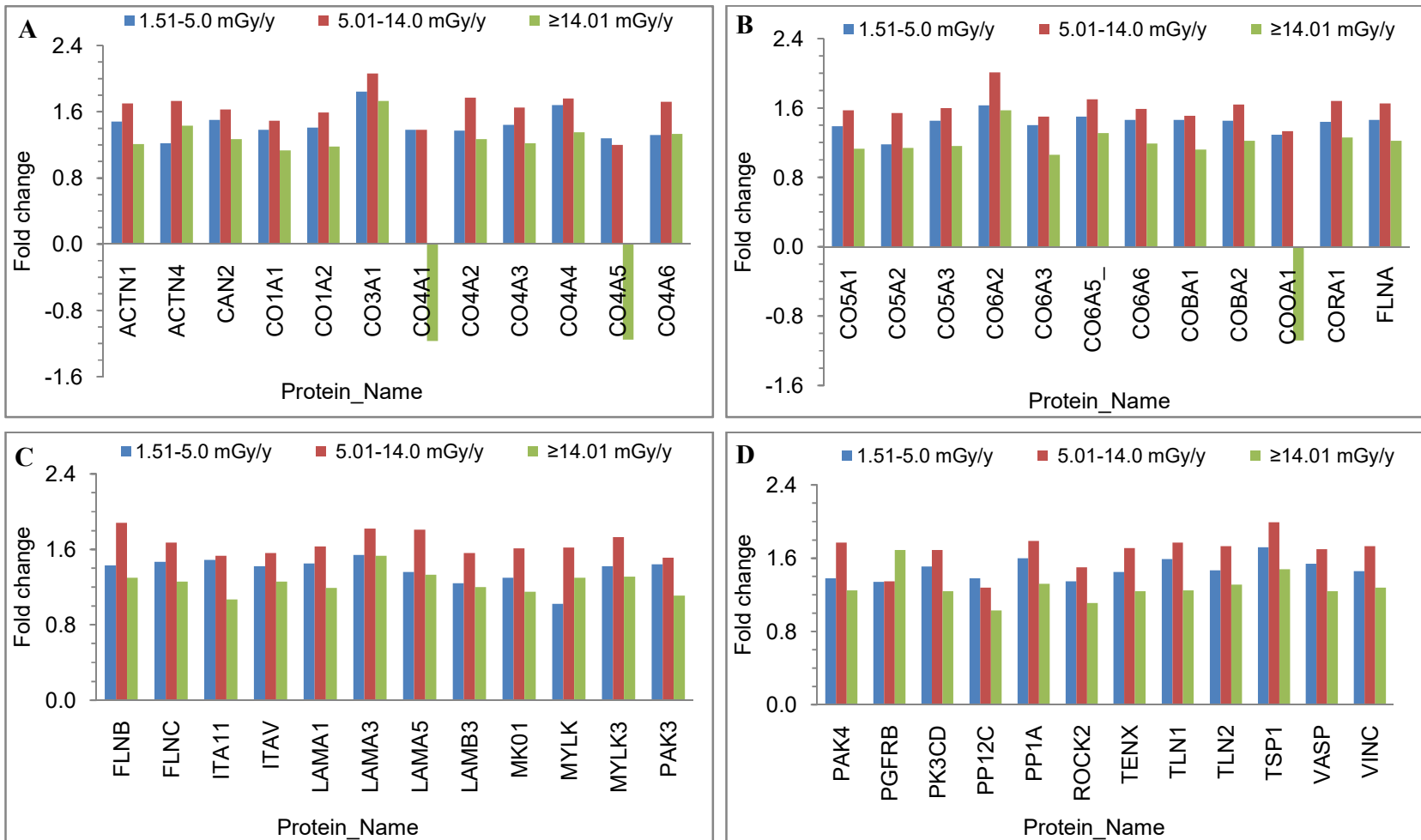


Fig.3.58A-D. Relative fold changes of proteins enriched in HLNRA groups compared to NLNRA for focal adhesion KEGG pathway. The proteins are abbreviated as listed in **Appendix A**.

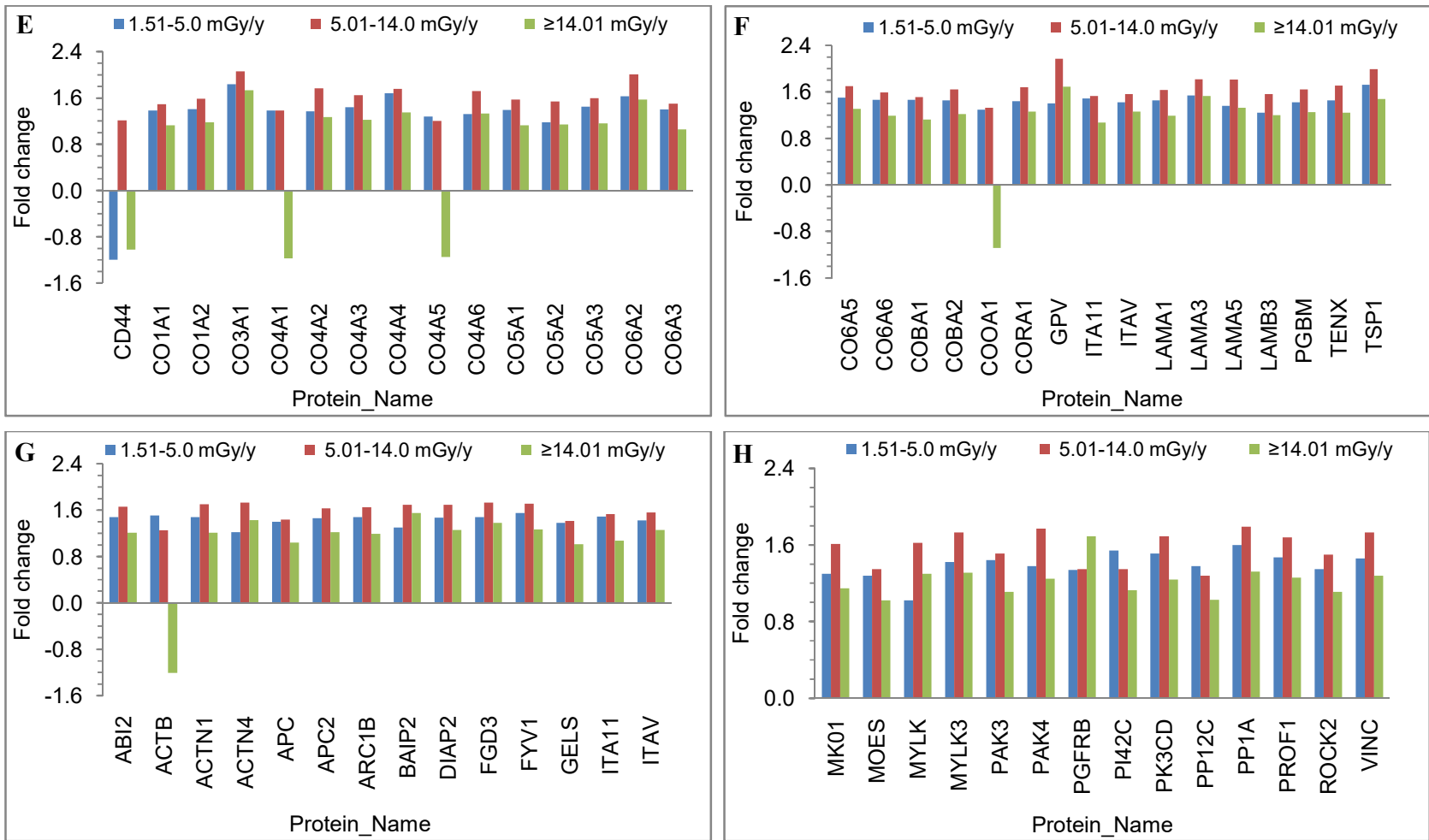


Fig.3.58. Relative fold changes of proteins enriched in HLNRA groups compared to NLNRA for (E-F) ECM-receptor interaction and (G-H) regulation of actin cytoskeleton KEGG pathway. The proteins are abbreviated as listed in **Appendix A**.

A crucial DNA repair related KEGG pathway over-expressed in the HLNRA individuals was the Fanconi anemia (FA) pathway (hsa03460), typically involved in the repair of DNA interstrand crosslinks (ICLs) in the genome (**Fig.3.57**). FA pathway proteins also coordinate the repair of DNA strand breaks through proteins of all the major DNA repair pathways. Over expression of ten FA pathway proteins (ATR, BLM, BRCA2, DPOLN, FANCA, FANCI, FANCM, MLH, RMI2, XPF) were identified in the Group II and Group III HLNRA dose groups. The Group IV individuals showed significant expression of six FA pathway proteins (ATR, DPOLN, FANCI, MLH1, RMI2, XPF) (**Fig.3.59**).

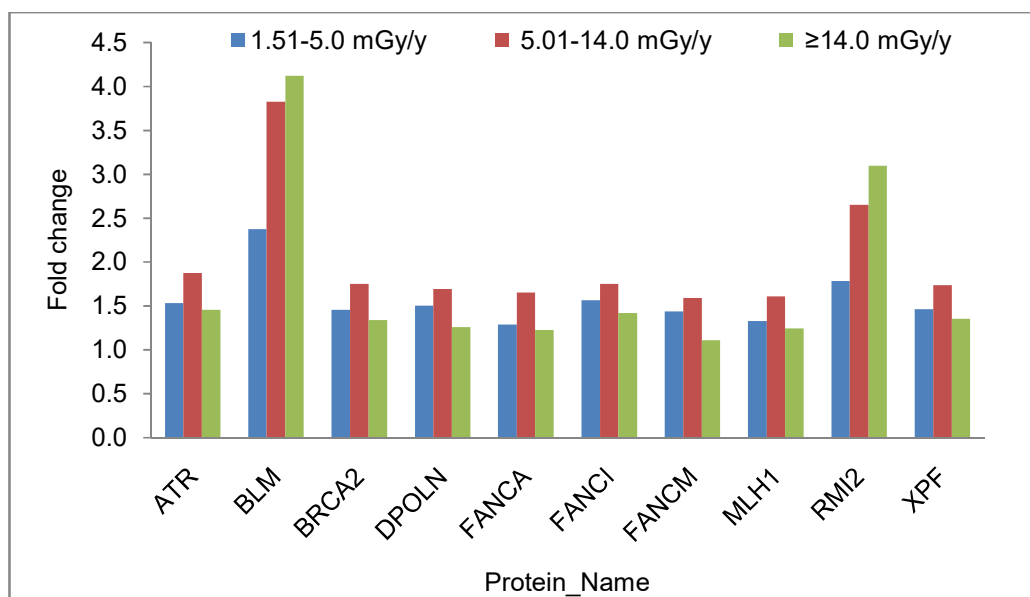


Fig.3.59. Relative fold changes of proteins enriched in HLNRA groups compared to NLNRA for Fanconi anemia DNA repair KEGG pathway. The proteins are abbreviated as listed in **Appendix A**.

Many KEGG pathways showed radiation dose dependent enrichment when compared with NLNRA individuals. Radiation induced signaling pathways involved in pro-survival were the major category of process which showed dose specific enrichment (**Fig.3.57**). The important KEGG signaling pathways enriched in HLNRA dose groups were calcium signaling pathway (hsa04020), PI3K-Akt signalling pathway (hsa04151), HIF-1 signaling pathway (hsa04066) and Rap1 signaling pathway (hsa04015). The calcium signaling KEGG pathway was enriched in all three dose groups of HLNRA (Group II vs Group I: 24 proteins, Group III vs Group I: 23 proteins, Group IV vs Group I: 15 proteins). The relative abundances of the altered proteins are given in the **Fig.3.60**. Group II and Group III individuals showed specific activation of pro-survival pathways such as PI3K-Akt signaling pathway (Group II vs Group I: 36 proteins, Group III vs Group I: 38 proteins,) and HIF-1 signaling pathway (Group II vs Group I: 14 proteins, Group III vs Group I: 13 proteins) (**Fig.3.61A-D**). A low dose radiation induced enrichment of Rap1 signaling pathway was seen only in Group IV individuals (**Fig.3.62**).

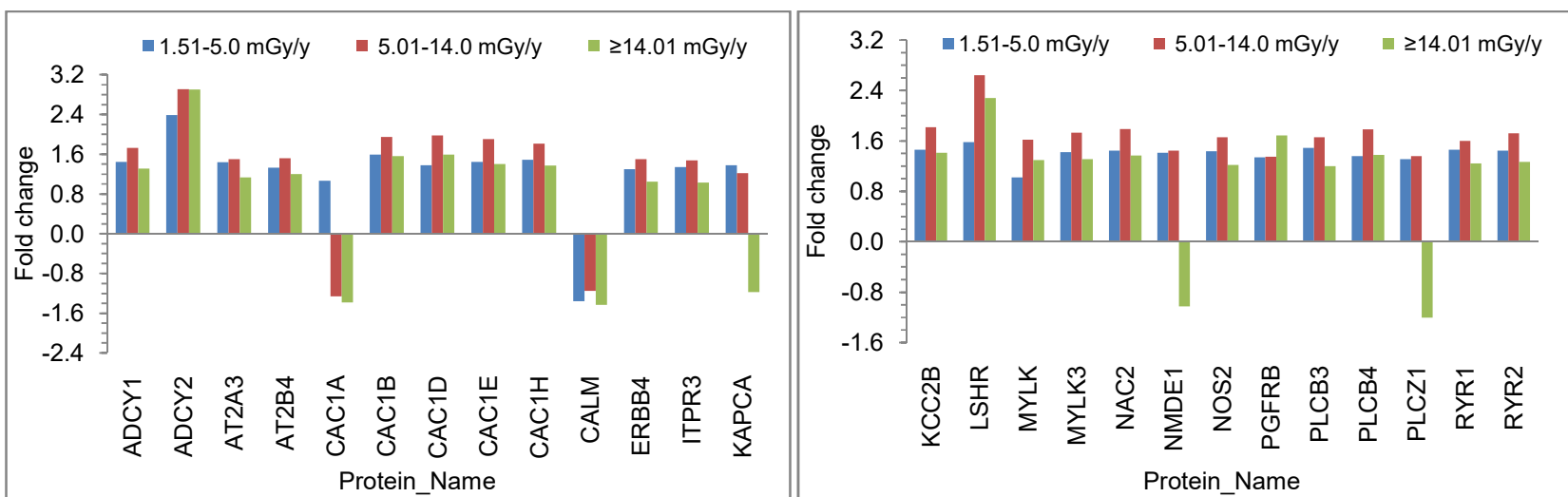


Fig.3.60. Relative fold changes of proteins enriched in HLNRA groups compared to NLNRA for calcium signaling KEGG pathway. The proteins are abbreviated as listed in **Appendix A**.

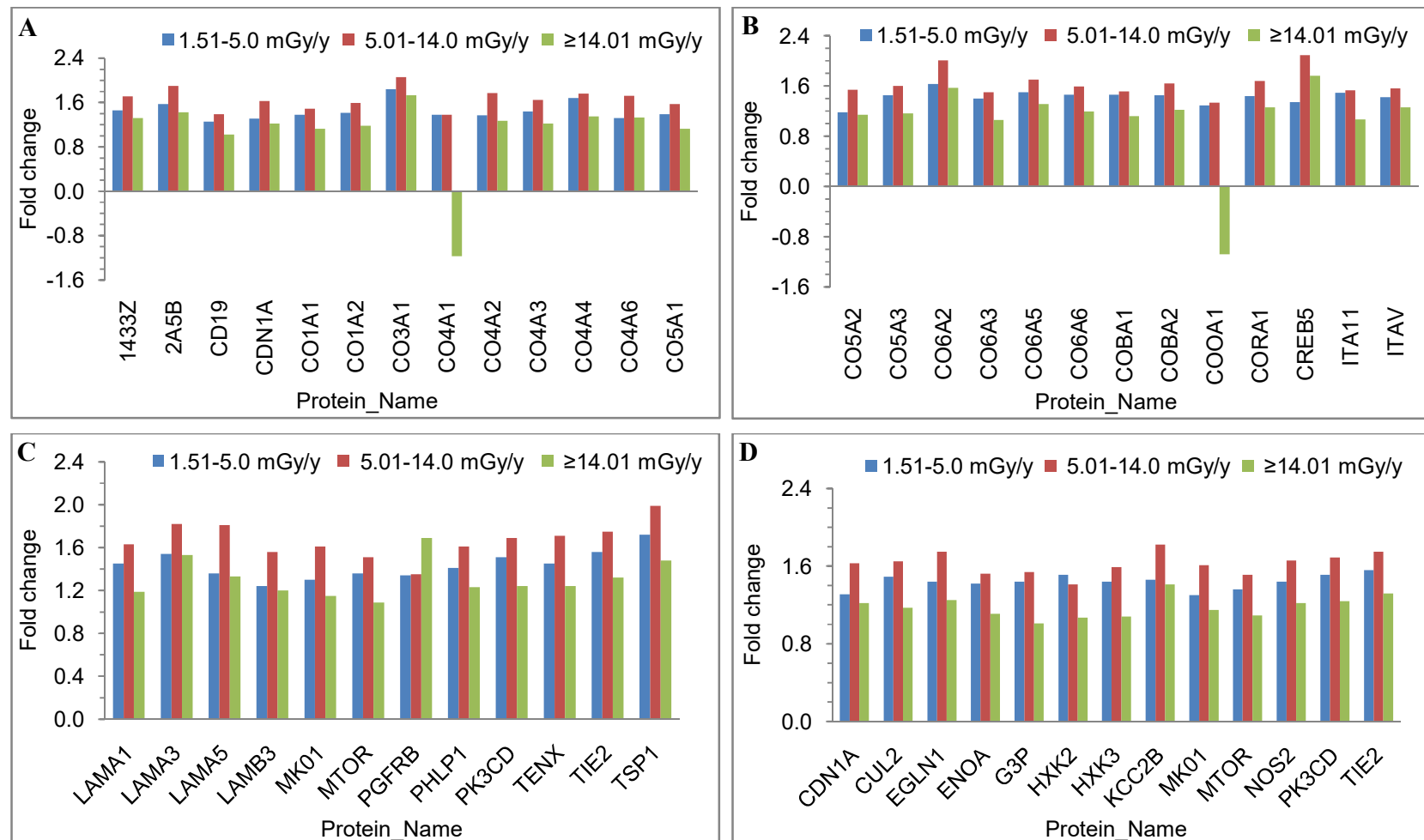


Fig.3.61. Relative fold changes of proteins enriched in HLNRA groups compared to NLNRA for (A-C) PI3K-Akt signaling KEGG pathway and (D) HIF-1 signaling KEGG pathway. The proteins are abbreviated as listed in **Appendix A**.

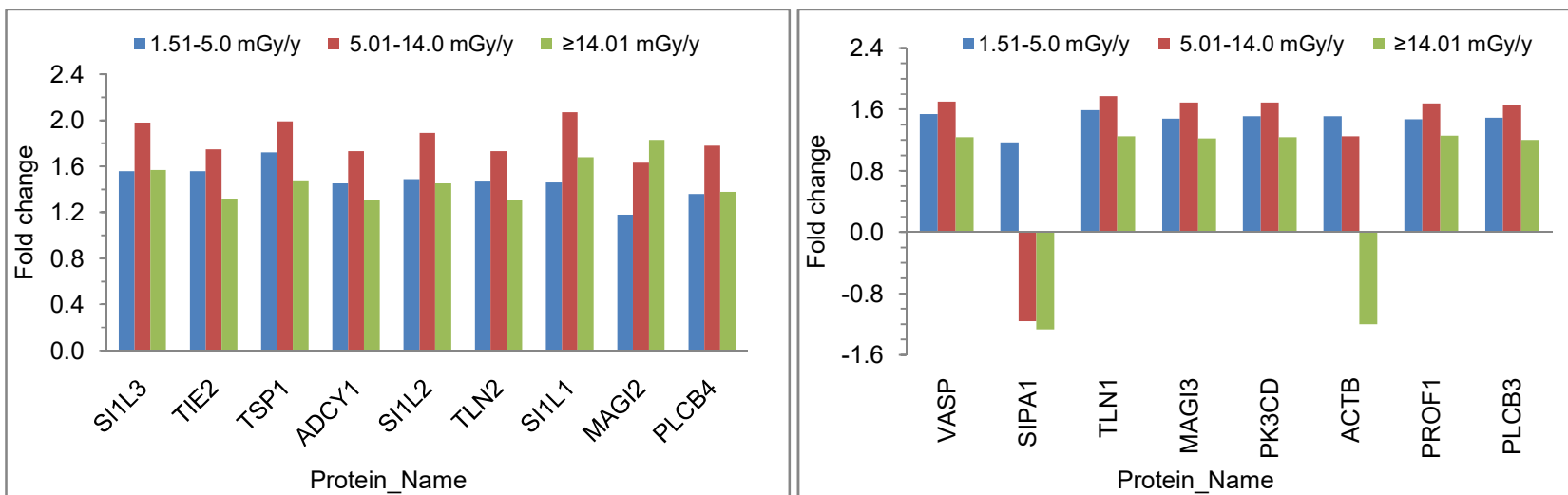


Fig.3.62. Relative fold changes of proteins enriched in HLNRA groups compared to NLNRA for Rap1 signaling KEGG pathway. The proteins are abbreviated as listed in **Appendix A**.

3.2.2.11. Real Time PCR analysis of selected radiation responsive proteins

The expression levels of selected radiation responsive proteins were analyzed at the mRNA level using RT-PCR on an additional set of samples collected from NLNRA and HLNRA. The average background dose of the collected samples varied from 1.25 ± 0.03 mGy/y (range: 1.23-1.30 mGy/y, N=5) in NLNRA, 3.30 ± 0.19 mGy/y (range: 3.11-3.53 mGy/y, N=5) in Group II and 10.98 ± 2.58 mGy/y (range: 7.98-13.69 mGy/y, N=5) in Group III dose groups of HLNRA, respectively. Samples from HLNRA Group IV could not be collected. The selected 18 candidate genes belonged to several important biological processes such as DNA repair (*ATR*, *BLM*, *ERCC4*, *FANCA*, *FANCI*, *FANCM*, *MLH1*), chromatin modifications (*ATRX*, *CHD8*, *EMSY*), MAP kinase cascade (*COP55*, *MAPK1*), post-translational modifications (*MINK1*, *SMG1*), apoptosis (*BIRC6*, *DAPK1*) and WNT signaling (*DVL2*, *ZNFR3*). Analysis was performed with the SYBR green based method.

For quantitative analysis, two endogenous reference genes *β -actin* and *GAPDH* were used to normalize the expression of target genes. The threshold cycle values (C_T) for both reference genes (*β -actin* and *GAPDH*) were first analyzed to validate the stability of expression. Both genes were found to be highly expressed, and showed good stability and minimal variation in PBMCs. The mean C_T values of *β -actin* was 23.1 ± 0.07 for NLNRA (range: 23.0-23.2), 23.7 ± 0.1 for Group II (range: 23.5 - 23.8) and 22.7 ± 0.33 for Group III (range: 22.2-23.0) HLNRA groups (**Fig.3.63A**). *GAPDH* endogenous control gene was also found to be highly stable with mean C_T values of 24.7 ± 0.3 for NLNRA (range: 24.2-25.2), 25.3 ± 0.6 for Group II (range: 24.5 - 25.8) and 24.6 ± 0.5 for Group III (range: 23.9-24.9) HLNRA groups (**Fig.3.63B**).

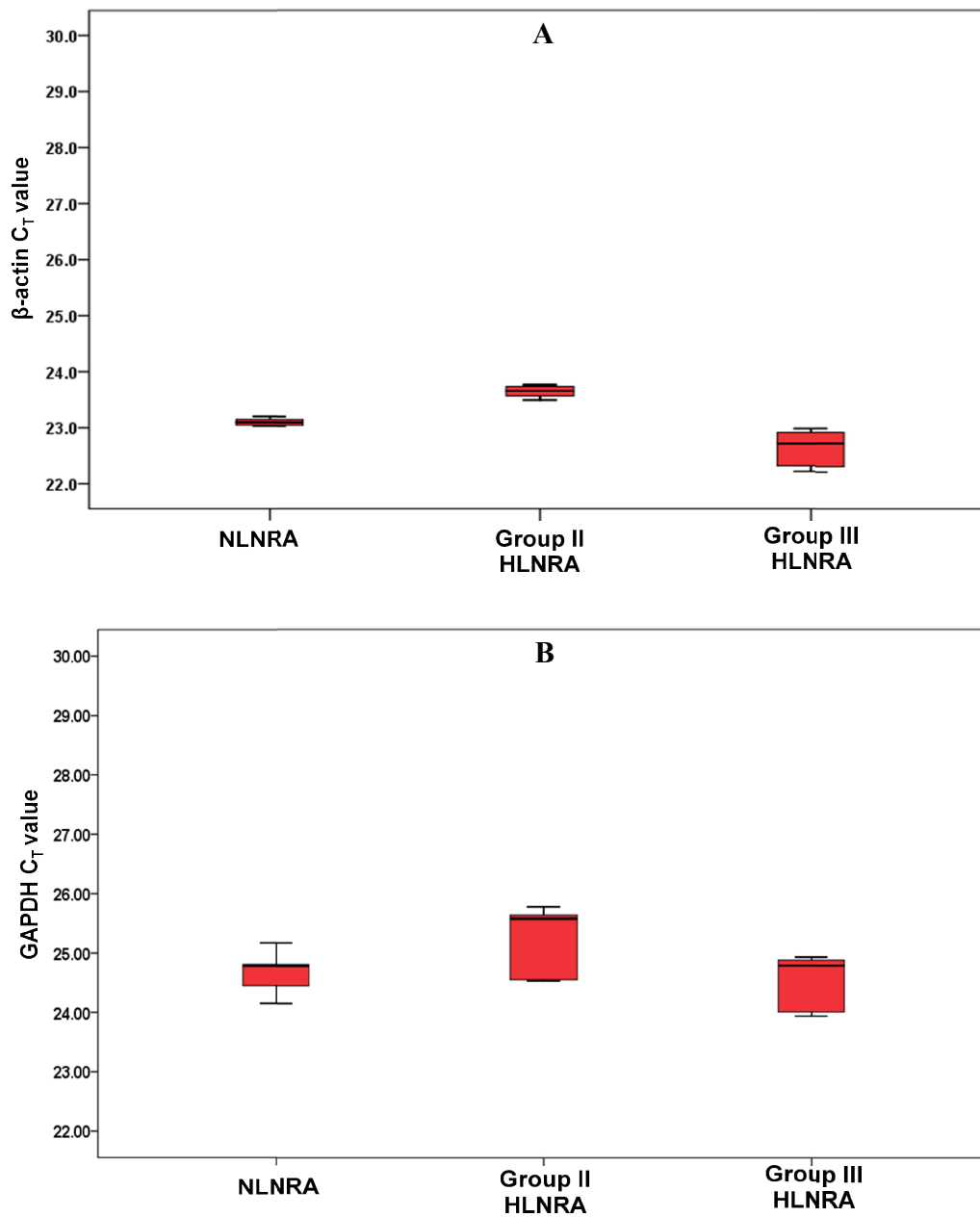


Fig.3.63. Threshold cycle (C_T) values for endogenous control genes in human PBMCs of NLNRA and HLNRA dose groups. Each box represents C_T values of five individuals for (A) β -actin and (B) GAPDH. The middle horizontal line is the median, the top and bottom of the boxes are the 25th and 75th percentiles, and the upper and lower horizontal lines (whiskers) indicate the ranges.

All the seven DNA repair genes showed significant up-regulation in both Group II and Group III HLNRA individuals and transcriptional response exhibited good correlation with the iTRAQ proteomic data. The fold changes observed in Group II individuals, as compared to NLNRA individuals, were *ATR* (1.03 fold), *BLM* (2.4 fold), *ERCC4* (1.7 fold), *FANCA* (3.1 fold), *FANCI* (1.5 fold), *FANCM* (2.6 fold) and *MLH1* (2.4 fold), The Group III subjects showed similar pattern of expression with relative expression of *ATR* (1.2 fold), *BLM* (1.8 fold), *ERCC4* (1.1 fold), *FANCA* (1.9 fold), *FANCI* (1.4 fold), *FANCM* (1.7 fold) and *MLH1* (1.4 fold) (**Fig.3.64**).

Among the other genes that showed significant increase in transcript levels in Group II individuals in accordance with the proteomic data included *ATRX*: 1.1 fold and *CHD8*: 1.5 fold; *MAPK1*: 2.0 fold; *MINK1*: 2.2 fold; *SMG1*: 1.1 fold; *DVL2*: 15.5 fold. On the other hand, expression of genes such as *EMSY* (-1.3 fold), *COPS5* (-1.4), *DAPK1* (-2.0), *ZNRF3* (-1.7) and *BIRC6* (-1.7) showed under-expression and poor correlation with the iTRAQ data. Interestingly, Group III individuals showed a poor correlation between mRNA and protein expression for majority of the genes. Genes that showed down-regulation as opposed to up-regulation in iTRAQ included *ATRX* (-3.6 fold), *CHD8* (-2.2 fold), *EMSY* (-6.3 fold), *COPS5* (-4.7fold), *MAPK1* (-6.9 fold), *MINK1* (-1.2 fold), *SMG1* (-7.4 fold), *DAPK1* (-7.1 fold) and *ZNRF3* (-3.9 fold). There were two genes *BIRC6* (20.1 fold) and *DVL2* (2.8 fold) that showed good correlation with iTRAQ data for Group II individuals (**Fig.3.64**).

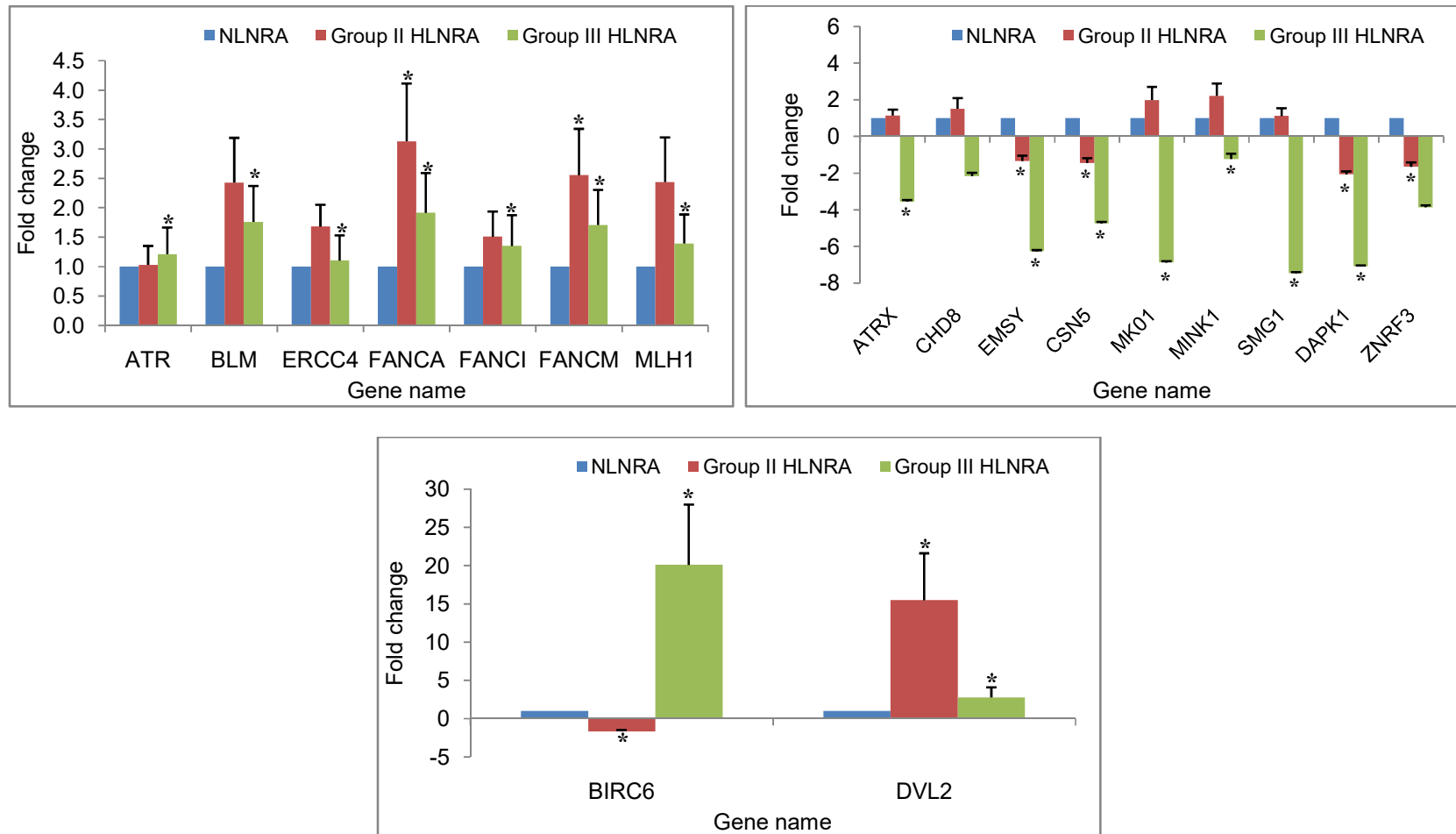


Fig.3.64. Gene expression data of 18 candidate genes belonging to different biological processes in HLNRA dose groups, as compared to NLNRA individuals. The bars correspond to the mean fold change values of five biological replicates \pm SEM. Symbol (*) represents statistical significance calculated by Student's t-test significance ($P \leq 0.05$).

3.2.2.12. Transcription factors differentially expressed in HLNRA individuals

The iTRAQ analysis identified differential alteration of 36 transcription factors in HLNRA individuals. Out of these 17 proteins were common between the three HLNRA groups (AKNA, CNOT1, COE1, COE4, DMRT2, E2F8, PO4F2, RUNX1, SLTM, SOX7, SPT5H, TCF20, TCF24, TEAN2, TF3C1, TIF1B, ZEP3). Group II and III additionally showed up-regulation of 12 TFs which included BCLF1, CMTA1, E2F1, GTF2I, RELB, SOX12, SOX3, TAF8, TCF23, TRRAP, UTF1 and NFAC4. The GATA6 protein was up-regulated only in Group II individuals. The up-regulated TFs PBX3 was observed only in Group II and IV individuals. The TBX2 protein was up-regulated in Group II individuals, and down-regulated in Group IV (**Table 3.12**).

Sl. NO	Accession No	Protein Description	Mean FC Group II	Adj P-value	Mean FC Group III	Adj P-value	Mean FC Group IV	Adj P-value	Biological function
1	AKNA	AT-hook-containing transcription factor	1.5	0.010	1.9	<0.001	1.4	0.008	Involved in antigen-dependent-B-cell development.
2	BCLF1	Bcl-2-associated transcription factor 1	1.5	0.020	1.7	0.042	1.3	0.293	Involved in regulation of DNA-templated transcription in response to stress.
3	CMTA1	Calmodulin-binding transcription activator 1	1.5	<0.001	1.8	0.005	1.3	0.113	Transcriptional activator. Functions as a tumor suppressor.
4	CNOT1	CCR4-NOT transcription complex subunit 1	1.7	<0.001	2.1	0.001	1.7	0.014	Transcriptional repressor.
5	COE1	Transcription factor COE1	1.5	<0.001	1.6	0.001	1.1	0.007	Transcriptional activator recognizes 5'-ATTCCCNNGGAATT-3' sequence
6	COE4	Transcription factor COE4	1.6	<0.001	1.7	<0.001	1.3	0.006	Binds to the 5'-ATTCCCNNGGAATT-3' palindromic DNA sequence
7	DMRT2	Doublesex- and mab-3-related transcription factor 2	1.4	<0.001	1.7	<0.001	1.3	<0.001	Transcriptional activator.
8	DMRTA	Doublesex- and mab-3-related transcription factor A1	1.0	0.956	2.8	0.118	2.2	0.191	Involved in regulation of DNA-templated transcription
9	E2F1	Transcription factor E2F1	1.4	<0.001	1.6	0.002	1.1	0.192	Regulation of cell cycle progression, DNA-damage response and apoptosis.
10	E2F8	Transcription factor E2F8	1.5	<0.001	1.8	<0.001	1.3	<0.001	Regulation of cell cycle progression, DNA-damage response and apoptosis.
11	GATA6	Transcription factor GATA-6	1.1	0.199	1.3	0.001	1.1	0.230	Transcriptional activator involved in cardiac hypertrophic response.
12	GTF2I	General transcription factor II-I	1.6	0.029	2.4	0.037	2.0	0.131	Regulation of cellular stress and activation of c-FOS promoter.
13	LBX2	Transcription factor LBX2	1.2	0.516	1.2	0.460	0.9	0.697	Putative transcription factor.
14	PBX3	Pre-B-cell leukemia transcription factor 3	1.0	0.868	1.4	<0.001	1.2	0.004	Transcriptional activator recognizes 5'-ATCAATCAA-3' DNA sequence.
15	PHTF1	Putative homeodomain transcription factor 1	1.3	0.223	1.1	0.615	0.9	0.447	Regulation transcription.
16	PO4F2	POU domain; class 4; transcription factor 2	1.4	<0.001	1.9	<0.001	1.4	0.006	TF involved in development and differentiation of target cells

17	RELB	Transcription factor RelB	1.5	0.002	1.7	0.011	1.3	0.173	NF-kappa-B complex is formed by the Rel-like domain-containing proteins
18	RUNX1	Runt-related transcription factor 1	1.6	<0.001	1.7	<0.001	1.3	0.001	Recognizes the DNA sequence 5'-TGTTGGT-3'. Role in the development of normal hematopoiesis.
19	SLTM	SAFB-like transcription modulator	1.5	0.002	1.5	<0.001	1.1	0.081	Transcription inhibitor. Role in apoptosis
20	SOX12	Transcription factor SOX-12	1.5	0.002	1.8	0.005	1.3	0.140	Recognizes the 5'-AACAAAT-3' DNA sequence.
21	SOX3	Transcription factor SOX-3	1.3	0.001	1.4	<0.001	1.0	0.903	Involved in neurogenesis
22	SOX7	Transcription factor SOX-7	1.5	<0.001	2.1	<0.001	1.9	0.024	Recognizes the 5'-AACAAAT-3' DNA sequence. Active role in the survival of hematopoietic and endothelial precursors during specification.
23	SPT5H	Transcription elongation factor SPT5	1.3	0.001	1.6	<0.001	1.3	0.026	Regulation of mRNA processing and transcription elongation by RNA pol II.
24	TAF8	Transcription initiation factor TFIID subunit 8	1.5	0.001	1.6	0.008	1.2	0.178	General transcription factor required for regulated initiation by RNA pol II. Regulates both basal and activator-dependent transcription
25	TBX2	T-box transcription factor TBX2	1.3	<0.001	1.0	0.304	0.5	0.017	Transcriptional regulation of genes involved in mesoderm differentiation.
26	TCF20	Transcription factor 20	1.6	0.011	1.8	0.002	1.4	0.088	Transcriptional co-activator stimulates transcriptional activity of JUN, SP1, PAX6 and ETS.
27	TCF23	Transcription factor 23	1.8	0.033	2.2	0.088	1.9	0.259	Inhibits E-box-mediated binding and transactivation of bHLH factors.
28	TCF24	Transcription factor 24	1.4	0.002	1.6	<0.001	1.2	0.065	Putative transcription factor.
29	TEAN2	Transcription elongation factor A N-terminal and central domain-containing protein 2	1.5	<0.001	1.7	<0.001	1.3	<0.001	Involved in regulation of DNA-templated transcription.
30	TF3C1	General transcription factor 3C polypeptide 1	1.6	<0.001	1.9	0.003	1.4	0.019	Involved in RNA pol III-mediated transcription. Mediates transcription of 5S rRNA and other stable nuclear and cytoplasmic RNAs.
31	TIF1B	Transcription intermediary factor 1-	1.4	0.001	1.6	0.007	1.2	0.043	Regulates gene silencing by recruiting

		beta							CHD3 and SETDB1 to the promoter regions of KRAB target genes.
32	TRRAP	Transformation/transcription domain-associated protein	1.8	0.016	2.0	0.010	2.1	0.148	Epigenetic transcription activation
33	TTF1	Transcription termination factor 1	0.8	0.694	1.1	0.867	0.9	0.890	Mediates termination of ribosomal gene transcription. Regulation of replication fork arrest and RNA pol I transcription.
34	UTF1	Undifferentiated embryonic cell transcription factor 1	1.5	0.085	1.5	0.017	1.1	0.796	Transcriptional co-activator of ATF2.
35	ZEP3	Transcription factor HIVEP3	1.4	0.003	1.7	0.005	1.4	0.064	Regulation of nuclear factor NF-kappa-B
36	NFAC4	Nuclear factor of activated T-cells; cytoplasmic 4	1.4	0.004	1.6	0.020	1.2	0.407	Ca ²⁺ regulated TF involved in cellular functions of the immune, cardiovascular, musculoskeletal, and nervous systems.

Table 3.12. Transcription factors differentially expressed in HLNRA dose groups. The mean changes in protein abundance in HLNRA individuals relative to NLNRA individuals are represented as fold change. The adjusted *P*-values in ‘**bold**’ represent significant ($P \leq 0.1$) changes in the expression.

3.2.2.13. Cell redox homeostasis proteins differentially expressed in HLNRA individuals

iTRAQ analysis identified alteration of 7 proteins involved in maintenance of the cell redox homeostasis. Both Group II and Group III individuals showed over expression of same six proteins: TRXR2, QSOX2, PDIA1, PDIA3, NOX5 and GSTO1 with very similar fold changes. In contrast, Group IV individuals showed up-regulation of only three such proteins QSOX2 (1.2 fold), PDIA3 (1.3 fold) and GSTO1 (1.3 fold) (**Table 3.13**).

Sl. No.	Accession No	Protein Description	Mean FC Group II	Adj P-value	Mean FC Group III	Adj P-value	Mean FC Group IV	Adj P-value	Biological function
1	SELO	Selenoprotein O	0.6	0.298	0.7	0.530	0.5	0.208	Involved in regulation of mitochondrial redox homeostasis.
2	TRXR2	Thioredoxin reductase 2; mitochondrial	1.3	<0.001	1.2	0.080	0.9	0.128	Mediates regulation of ROS and mitochondrial redox homeostasis. Required to maintain thioredoxin in a reduced state.
3	QSOX2	Sulfhydryl oxidase 2	1.5	<0.001	1.7	<0.001	1.2	0.017	Cell redox homeostasis
4	PDIA1	Protein disulfide-isomerase	1.3	<0.001	1.6	<0.001	1.1	0.199	Protein folding and redox regulation
5	PDIA3	Protein disulfide-isomerase A3	1.5	<0.001	1.7	<0.001	1.3	0.007	Protein folding and redox regulation
6	NOX5	NADPH oxidase 5	1.4	0.054	1.5	<0.001	1.1	0.001	Cellular response to oxidative stress
7	GSTO1	Glutathione S-transferase omega-1	1.5	<0.001	1.7	<0.001	1.3	<0.001	Oxidation-reduction process

Table 3.13. Cell redox homeostasis proteins differentially expressed in HLNRA dose groups. The mean changes in protein abundance in HLNRA individuals relative to NLNRA individuals are represented as fold change. The adjusted *P*-values in ‘**bold**’ represent significant ($P \leq 0.1$) changes in the expression.

3.2.3. Comparison of 2DE-MS and iTRAQ protein profiles in HLNRA individuals

As expected, high-resolution gel-free technique using iTRAQ labeling identified significantly more number of differentially expressed proteins between HLNRA and NLNRA than the 2DE-MS method. Differential modulation of ~1700 proteins was identified by iTRAQ methods as compared to 33 proteins by 2DE-MS. Out of the 33 proteins detected by 2DE-MS, 26 proteins (including isoforms) were also represented by the iTRAQ method. The proteins such as ACTB (2DE: 1.3 fold; iTRAQ: 1.2 fold), ALBU (2DE: 1.1 fold; iTRAQ: 1.7 fold), FIBB (2DE: 1.4 fold; iTRAQ: 1.2 fold), FIBG (2DE: 1.4 fold; iTRAQ: 1.6 fold), F13A (2DE: 1.1 fold; iTRAQ: 1.4 fold), GRP78 (2DE: 1.5 fold; iTRAQ: 1.3 fold), PDIA1(2DE: 1.3 fold; iTRAQ: 1.3 fold), PSME1(2DE: 1.1 fold; iTRAQ: 1.2 fold), TUBA (2DE: 1.3 fold; iTRAQ: 1.4 fold) were up-regulated and showed similar trend in expression pattern in the studied HLNRA individuals (**Fig.3.65**). However, many other proteins showed the reverse trend in HLNRA individuals: RAP1B (2DE: -1.4 fold; iTRAQ: +1.5 fold), TPM2 (2DE: -1.2 fold; iTRAQ: +2.0 fold), ATPB (2DE: -1.4 fold; iTRAQ: +1.4 fold), TPM4 (2DE: -1.3 fold; iTRAQ: +1.5 fold), CALR (2DE: -1.4 fold; iTRAQ: +1.4 fold), HSP70 (2DE: -1.1 fold; iTRAQ: +1.6 fold), PLS2 (2DE: -1.1 fold; iTRAQ: +1.0 fold), PDIA3 (2DE: -1.1 fold; iTRAQ: +1.5 fold), TUBB (2DE: -1.8 fold; iTRAQ: +1.5 fold), MV (2DE: -1.1 fold; iTRAQ: +1.5 fold) (**Fig.3.65**).

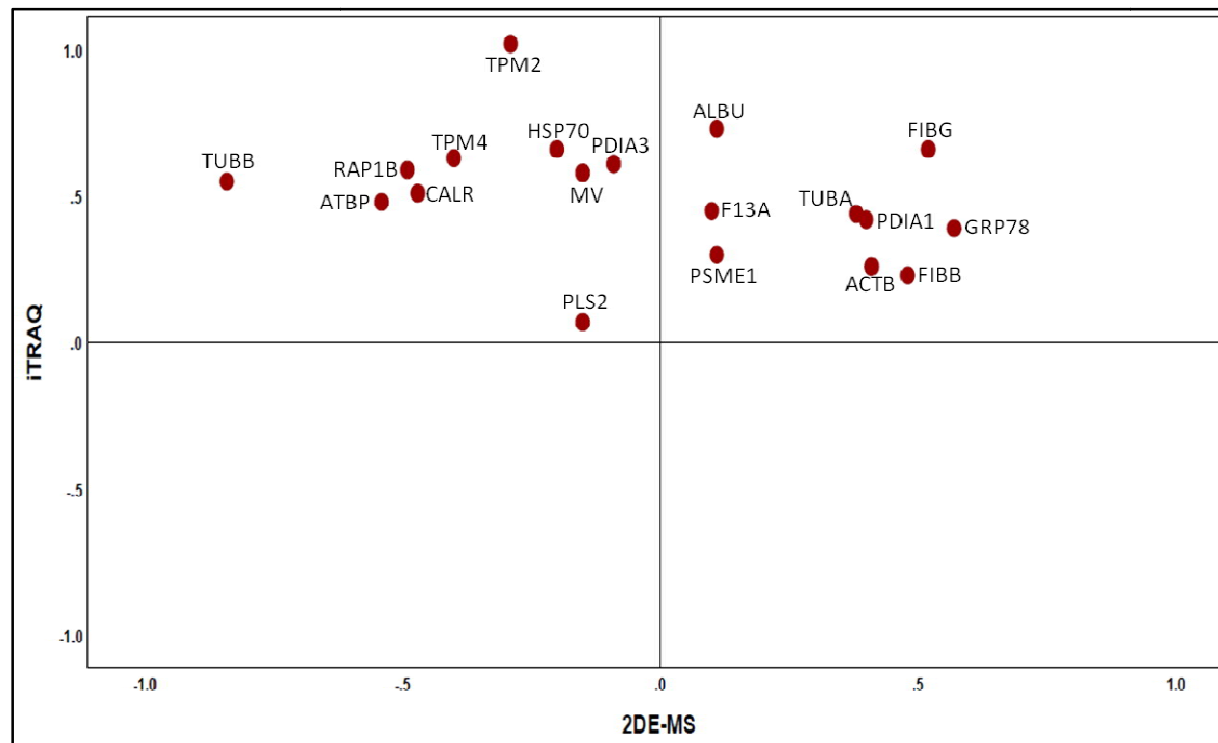


Fig.3.65. Scatter plot showing comparison of differential expression of proteins as measured by 2DE-MS and iTRAQ in HLNRA individuals, as compared to NLNRA individuals. Each point corresponds to the log2 transformed fold change of a single protein. The proteins are abbreviated as listed in **Table 3.9**.

3.2.4. Comparison of protein expression profiles with acute and chronic radiation in human PBMCs

The 2DE-MS method identified differential modulation of 23 proteins with acute radiation exposure of 300 mGy or 1 Gy, compared to sham irradiated cells. In contrast, a total of 33 proteins were found to be differentially modulated with chronic low dose in HLNRA individuals when compared to respective NLNRA group. Seventeen of these modulated proteins [ACT (3), ACT (4), CLIC, FIBB, FIBG, GRP78, HSP90, LDHB, LEI, MV, PDIA1, PLS2 (1), PRDX6, RAP1B, RhoGDI β , TUBA, TUBB] were common between the acute and chronic radiation exposure. There were 16 proteins [ACT (1), ACT (2), ACT (5), ALBU (1), ALBU (2), ATPB, CALR, F13A, HSP70, PDIA3, PSME1, Ssp2801, TMP4, TPM2 (1), TPM2 (2), VIME] that showed differential alterations only with chronic radiation exposure and 6 proteins (PDLIM1, WDR1, TCP1, RabGDI α , PNP, THBS1) that showed modulations only with acute radiation exposure. Most proteome alterations in human PBMCs were characterized by small fold changes in both acute and chronic radiation. In both the cases, these proteins could be broadly classified into processes such as cytoskeleton-associated proteins, molecular chaperones, cellular redox homeostasis, signalling, cellular metabolic process, and protein and peptide processing using UniProt/SwissProt protein database (**Fig.3.66 A-D**).

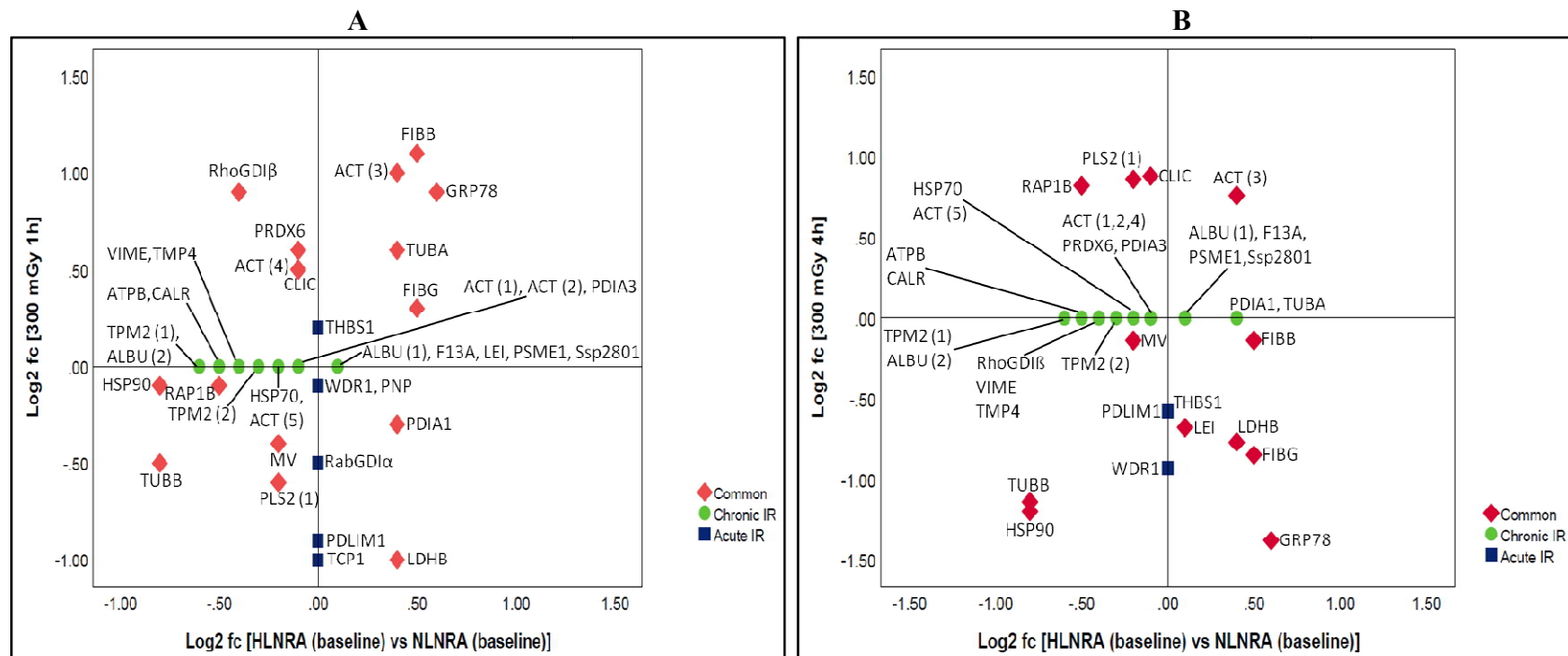


Fig.3.66 A-B. Scatter plot showing comparison of acute [(A) 300 mGy 1 h (B) 300 mGy 4 h] and chronic IR induced proteome expression profiles measured by 2DE-MS in human PBMCS. Each point corresponds to the log2 transformed fold change of a single protein. The green polygonals represent significant variation with chronic IR exposures. The blue polygonals represent significant variation with acute IR exposures. The red polygonals represent proteins common between acute and chronic IR. The proteins are abbreviated as listed in **Table 3.9**.

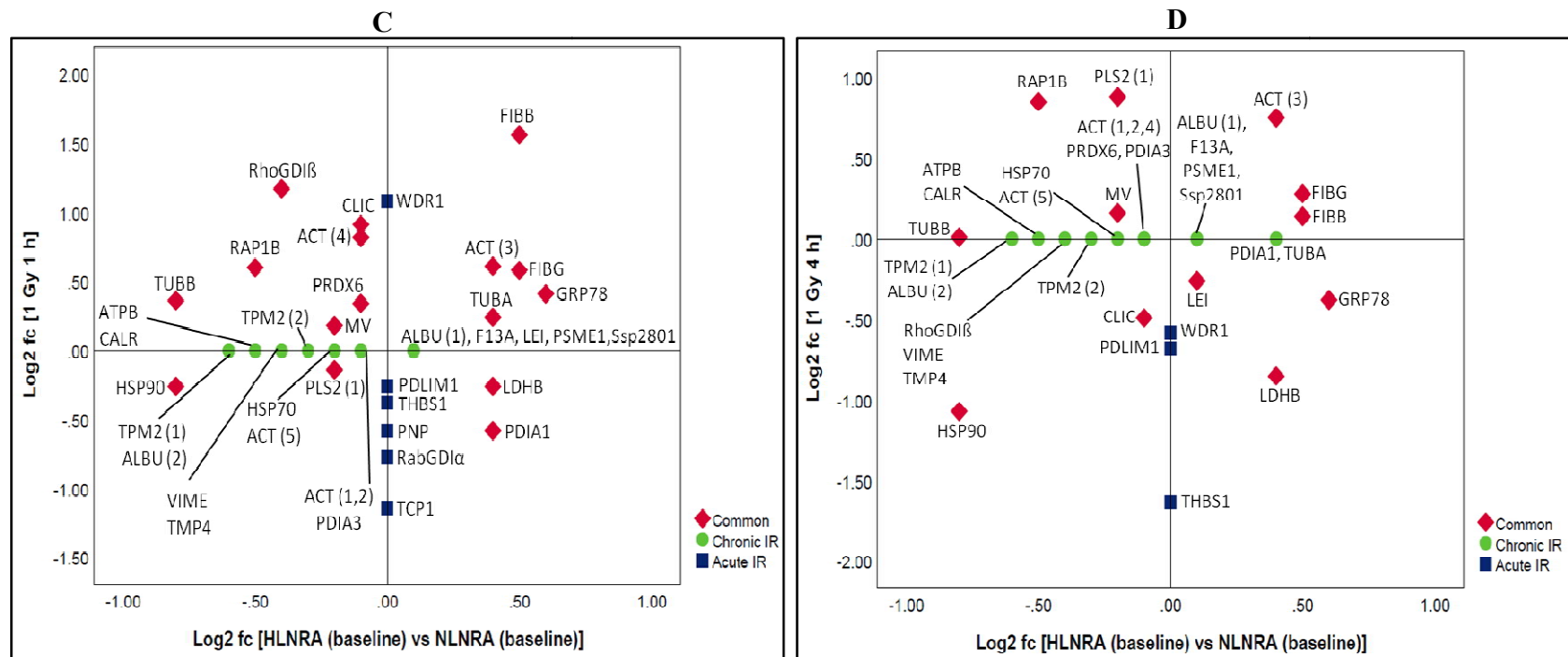


Fig.3.66 C-D. Scatter plot showing comparison of acute [(C) 1 Gy 1 h (D) 1 Gy 4 h] and chronic IR induced proteome expression profiles measured by 2DE-MS in human PBMCS. Each point corresponds to the log₂ transformed fold change of a single protein. The green polygonals represent significant variation with chronic IR exposures. The blue polygonals represent significant variation with acute IR exposures. The red polygonals represent proteins common between acute and chronic IR. The proteins are abbreviated as listed in **Table 3.9**.

CHAPTER 4

DISCUSSION

Understanding the cellular and molecular effects of low dose IR (below 100 mSv) is important since environmental, medical diagnostic and occupational exposure with IR generally lie in this region. The effects of these low dose and low dose rate radiation on human health are not well understood. Most molecular studies of radiation effects have been carried out using isolated cells in monolayer culture, and the responses extrapolated to mammalian tissues and organisms. Many studies have now indicated that different levels of biological organization (cells, tissues, or whole organisms) respond differentially to radiation. On the other extreme, epidemiological research on low dose and low dose-rate radiation has proven to be onerous due to the fact that the biological responses are generally subtle and are sometimes obscured by inter-individual variation. Researchers have attempted to overcome this limitation by studies on animals, particularly inbred mice exposed to very low continuous radiation over long time [178]. However, due to differences in anatomy, metabolic rates, DNA repair, life span etc., much of the animal data cannot be compared directly with humans [163]. Further, there are only a few studies that address the question whether low dose delivered at low dose rate results in lower biological response, and consequently lower risk, than when the same dose is delivered at a high dose rate [179-181].

Due to lack of direct data, most current knowledge of risks of low dose/low dose rate radiation exposures on humans is derived through extrapolation of the data obtained at high doses/dose rates using the LNT model [40]. For low-LET radiation, the shape of the dose-response curve in the region of low dose or dose rate exposures is continually debated [12]. Although the risk estimation at low dose region of ≤ 100 mSv remains highly uncertain, the human radiation exposure limits are legally regulated with the LNT

model. The French Academy of Sciences and French National Academy of Medicine report published in 2005 opposed the use of LNT model for radiation risk estimation based on analysis of large number of experimental data [5, 32]. One of the major radiobiological limitations of LNT model is that it does not consider immediate cellular defence mechanisms activated in response to IR against the ROS, DNA damage and elimination of damaged cells by apoptosis [23, 31, 182, 183]. Also, the LNT model takes into consideration only direct irradiation of cells. Emerging data have shown an important role of non-targeted effects like the adaptive responses, and bystander effects in cellular responses to low dose radiation. Many in the scientific community have expressed concerns that over-estimation of radiation risks by LNT model may lead to public fear about radiation and restrict beneficial applications of radiation in many fields, including justifiable medical procedures. It may also lead to severe economic loss, traumatic shock and loss of human life during avoidable evacuation procedures [184]. New research is therefore, needed to explore and understand low dose radiation-induced molecular and cellular responses, and subsequent health outcomes, for higher levels of biological organization, and more precisely for humans.

The population living in the monazite bearing coastal belt of Kerala offers one-of-a-kind opportunity to understand effects of low dose radiation directly on humans. The natural background radiation levels in this densely populated area vary from ≤ 1 mGy to ≥ 45 mGy and are mainly due to thorium and its decay products. This broad range of background dose which occurs due to non-uniform distribution of monazite sand provides an excellent opportunity for dose-response studies. The areas adjoining these HLNRA with annual background radiation dose ≤ 1.5 mGy are considered NLNRA.

Various biological studies conducted over several years in this area using different endpoints have not shown any adverse health effects in individuals residing in HLNRA [16, 59, 61, 63, 66]. Rather, there are reports of lower induction of DNA damage, activation of better repair, transcriptional changes and radioadaptive response in these individuals [68-73].

Over the last few years, radiation proteomics has emerged as a powerful approach to study the cellular effects and molecular targets of IR [7]. Proteins are considered the key functional molecules of the cell that drive cellular responses. Proteomic analysis thus, offers great promise to understand radiation induced molecular responses that may be activated to maintain homeostasis in the cellular system. Although a limited number of proteomics studies established the proteomic alterations with acute *in vitro* radiation exposures in human cells, the data on time and dose response is scarce [165-167]. Besides, there is no information about the effects of chronic low dose exposures on human proteome. Hence, in order to gain further insight on the molecular processes altered with low dose radiation, the present study focused on the proteomic responses of human PBMCs to acute and chronic radiation. PBMCs are considered an ideal cell system for human studies because of low inter-individual variation as compared to various biofluids and also because they effectively mimic the *in vivo* environment.

Proteomic responses of human PBMCs to acute *in vitro* IR

For applications like protein expression profiling to compare and contrast expression of any two samples, 2DE-MS still remains a powerful tool successfully employed by many researchers. Most studies used high dose of radiation delivered

acutely. A 2DE-MS based global proteomic profiling of MCF-7 breast cancer cells exposed to high dose of 20 Gy γ -radiation identified alteration of many proteins involved in cellular pathways of cell cycle control, apoptosis, DNA repair, signalling pathways and cell proliferation [185]. Another 2DE based proteomic analysis identified time (2, 5 and 12 h) induced protein expression changes of 14 proteins involved in several signalling pathways in human T-lymphocyte leukemia cells with a high radiation dose of 7.5 Gy [186]. In another study, the radiation stress induced effects were investigated with 2DE-MS in genetically modified fibroblast cells using a γ -radiation dose of 5 Gy at four time points (0.5, 1, 3 and 24 h) post-irradiation. The functional pathway analysis identified many proteins of cytoskeleton, signalling, transcription or translation, DNA repair, cell cycle and apoptosis [187]. Sriharshan et al. (2012) studied radiation induced proteomic changes in the human endothelial cell line EA.hy926 with a single acute dose of 2.5 Gy γ -radiation using SILAC and 2D-DIGE [188]. Proteins involved in metabolic activity, stress response and apoptosis were shown to be altered 4 h after irradiation whereas proteins corresponding to cellular signaling and transcriptional activity were mainly affected after 24 h.

There are only a few published reports on mammalian cell lines that studied proteomic responses with low dose/dose rate radiation exposures. Low dose IR (10, 30, 100 mGy) on the neuronal cells differentiation characterized many proteins involved in pathways of neuronal development, differentiation, oxidative stress, cell cycle and cell proliferation [189]. Pluder et al. (2011) investigated the proteome alterations in human endothelial cell line EA.hy926 using a low dose of 200 mGy γ -radiation after two time points (4 and 24 h) by 2D-DIGE. Proteins involved in Ran and RhoA mediated signaling

pathways, fatty acid metabolism and stress responses were affected in the study [190]. However, another 2D-DIGE based study on the same tumor model showed contradictory results, where no time dependent protein expression changes (10 min, 30 min and 4 h) with two doses (200 mGy and 1 Gy) of γ -rays were observed [191]. Another 2D-DIGE proteomic study using human coronary artery primary endothelial cells with a single low dose exposure of 200 mGy identified 28 deregulated proteins involved in radiation-responsive network of molecular transport, signaling, transcription and translation, metabolism, and cytoskeletal structure [192].

There are some radiation proteomics reports using 2DE-MS on mouse models to predict the molecular effects of whole/partial body radiation on animal systems, though with high doses. Guipaud et al. (2007) identified radiation induced alteration of 20 distinct proteins in the serum of mouse models after a single high dose exposure of 40 Gy at different time points (1, 5, 14, 21, and 33 days) after irradiation [193]. In another study, the effect of local irradiation on the serum proteome and N-glycome post-translational modifications was studied in murine models with 2D-DIGE proteomic approach. Modulation of many glycan structures and glycan families of serum proteins following high doses (20, 40, and 80 Gy) of γ -irradiation was reported [194, 195]. The proteomic alterations of mouse blood-plasma to the single dose acute γ -ray exposure (3 Gy) at two time points (2 day and 7 day) post-irradiation was studied using 2DE-MS approach. The study identified many proteins involved in inflammatory responses indicative of radiation-exposure [196]. A comparative proteomic study was performed to characterise the proteins involved in radiation damage of mouse intestinal epithelia using 2DE-MS. The study showed alterations of many biological processes involved in cellular

redox homeostasis, metabolism, signal transduction and post-translational processes [197]. Another study identified modulation of 25 proteins in various tissues (brain, lung, spleen, and intestine) of mouse models with 1 Gy γ -irradiation using 2DE-MS approach [198].

In the field of radiation proteomics, there have been only limited data on time and dose dependent differential expression in healthy human subjects using 2DE [165, 166, 199, 200]. These studies are important since the extrapolation of results obtained with mammalian cell lines or mouse models to humans is highly debated. In this regard, proteomic studies using the biological fluids of patients undergoing radiotherapy and accidentally exposed individuals represent a unique opportunity for the discovery of biomarkers of radiation exposure [201]. Nylund et al (2014) studied the proteome changes in the plasma of radiotherapy patients and radiation accident victims using 2DE-MS. The plasma samples were collected from thirty cancer patients under radiation treatment and three victims of the 1994 Kiisa, Estonia radiation accident. The analysis identified no differential modulation of proteins in radiotherapy patients (pre- vs post-treatment), but showed alteration of 18 proteins in accident victims as compared to control subjects [200]. In another study, 2D-DIGE based comparative proteomic analysis of serum samples collected from an accidentally overexposed Chilean man (22 days post-irradiation) identified abundance of serum protein glycosylation based protein translational modification in response to radiation exposure [194].

Very few studies are available which discuss whole proteome changes in human PBMCs with radiation under *in vitro* conditions. In one study, alteration of 11 proteins was reported with 2DE-MS in human PBMCs after acute IR (γ -rays) exposures where

three dose points of 1, 2 and 4 Gy were used. Most of the modulated proteins were structural proteins like beta-actin, talin-1, talin-2 and zyxin-2 [165, 166]. Skiold et al. (2011) studied proteomic modulations in human PBMCs isolated from two healthy individuals by 2DE-MS. Two doses of γ -radiation (1 mGy and 150 mGy) were used and the effects were studied after a time period of 3 h. They reported significant changes in the proteins involved in oxidative stress, fibrinolytic system and cytoskeletal modifications.

We first validated the cell system used for our work by measuring intra-individual variability in the PBMC proteome in three individuals 15 days apart. The PBMC proteome was found to be stable over time with very little variability within a subject. Among the proteins that showed variability were various isoforms of cytoskeletal protein actin and the most abundant circulating protein albumin. Dose and time dependent proteomic responses were then studied in human PBMCs exposed *ex-vivo*. The radiation doses selected for the present study were according to the assumed life time accumulated doses to the human population in the HLNRA of Kerala, India. The per capita average dose received by the human population residing in these areas is ~ 4 mGy/y. Assuming a life expectancy of 60-70 y, the life time accumulated doses to individuals will be in the range of 250-300mGy [48]. The dose of 1 Gy was selected for comparative purposes (moderately low vs moderately high dose). It was seen that radiation exposure caused rapid alterations in the PBMC proteome, even at the moderately low dose of 300 mGy, indicating an active cellular response, which however did not involve apoptosis. When DNA damage was studied using alkaline comet assay, a dose dependent increase was observed immediately following radiation (5 min), which returned to basal level within 1

h, which is the earliest time point considered for proteomic analysis. This initial DNA damage showed significant differences among the studied individuals. However, the level of residual damage was found to be similar in all individuals after 1 h, suggesting active repair and stability of the genome. Thus, the early DNA damage responses in human PBMCs may be highly heterogeneous and should be carefully taken into account. Our study identified a total of 23 proteins spots significantly altered in irradiated cells (fold change in intensity ≥ 1.5 -fold, $P \leq 0.05$) either with dose or with time, compared to sham irradiated cells. The observed CV values (33.7% at 300 mGy and 48.3% at 1 Gy) indicate that these radiation response proteins have good stability of expression at both the time points with low inter-individual variation [175, 202]. Moreover, the proportion of technical variation assessed in the study correlated well with other published reports [175, 203]. This further suggests that the inter-individual variations in human PBMC proteome maybe not be very high, especially at low doses.

The identified proteins were clustered into seven major groups based on their biological function using information available in Uniprot/Swissprot database: cytoskeleton-associated proteins, molecular chaperones, cellular redox homeostasis, signaling, cellular metabolic process, and protein and peptide processing. Among them, the cytoskeleton and associated proteins formed the largest group with eight proteins. This indicates that there may be an active reorganization of various members of cytoskeletal and its associated proteins in human PBMCs under radiation stress. The radiation stress induced alterations of cytoskeletal proteins have been reported in several cell models, including PBMCs [165-167, 187]. The cytoskeleton and associated family proteins are one of the ubiquitously expressed, highly conserved proteins among

eukaryotes. In addition to its role in maintaining cell shape and to drive cell movements, it has also been shown to associate with chromatin remodeling enzymes and all three RNA polymerases, thus indicating an important role in gene transcription [204]. More recently, tubulin proteins have also been reported to be involved in transport of DNA repair proteins in response to DNA damage [205].

Another group of proteins that showed significant alterations were the three molecular chaperones, namely TCP1, HSP 90 and GRP78; and two proteins with specific role in 'protein and peptide processing' namely, PDIA1 and LEI. There was a decrease in abundance of TCP1 at 1 h and Hsp90 at 4 h at both the doses (300 mGy and 1 Gy). These evolutionary conserved chaperone proteins play a critical role in maintaining a fine balance between protein folding, stability and degradation (proteostasis) through a small family of transcription factors called heat shock factors (HSFs), primarily HSF1 which is called the master regulator. Under basal conditions, HSF1 is maintained in the latent state by forming a complex with HSP90, either alone or as multichaperone complexes. Inhibition of HSP90 has been shown to activate HSF1 leading to alleviation of proteotoxic stress [206]. Hsp90 is considered to be the focal point for an extensive network of molecular chaperones that maintain this process of proteome homeostasis, or proteostasis.

Hsp90 is also an important component of the transcriptional arm of the unfolded protein response (UPR) since it has been shown to associate with ER stress sensors, inositol-requiring enzyme 1 (IRE1), and PKR-like ER kinase (PERK) to maintain their stability. Concomitant with this postulation we saw an increase of expression of GRP78 protein, the key regulator of ER homeostasis, at the low dose of 300 mGy. Due to its

antiapoptotic property, stress induction of GRP78 represents an important prosurvival arm of UPR. Various conditions including glucose deprivation, oxidative stress and hypoxia have been reported to augment GRP78 expression significantly [207]. The induction of GRP78 has been shown to protect the cells by suppressing oxidative damage and stabilizing calcium homeostasis [208] and is vital for maintaining the viability of cells that are subjected to such stresses [209]. Thus, it can be postulated that exposure of peripheral cells to even a low dose of 300 mGy can trigger the self-defence mechanism against oxidative stress and activate the adaptive signaling UPR pathway to promote cell survival. At 1 Gy, however, both Hsp90 and GRP78 were suppressed which might indicate that as ER stress expands and remains unresolved, additional mechanisms may set in to monitor protein folding and to control cellular homeostasis at high doses. Simultaneously, a down-regulation of pro-apoptotic enzymes, PDIA1 and LEI also may be indicative that low dose radiation stimulates cells to mount protective responses [210, 211].

The oxidative stress homeostasis proteins, PRDX6 and CLIC-1 constituted another important category of proteins that changed in abundance in human PBMCs with IR. Over-expression of PRDX6 protein was observed with 300 mGy and at an early time point of 1 h, suggesting its role in human PBMCs may be limited to early responses at low doses. Other reports have also shown oxidative stress induced expression of antioxidant proteins with IR in lymphocytes from human donors [212] and in mouse model [213]. In agreement with this observation, an increase in abundance was observed for CLIC-1 protein at both the radiation doses. Though not significant at 1 h after 300 mGy, a very strong up-regulation was seen after 4 h (~1.84 fold, $P < 0.001$). CLIC-1 is a

highly conserved protein in chordates and is believed to act as a redox sensor under external stimuli like oxidative stress that modify the redox state of the cytoplasm [214].

IR induced modulation of many signaling networks were evident in our study. Three signaling proteins (RAP1B, RhoGDI β and RabGDI α) were altered at an early time point of 1 h post-irradiation. Interplay of these signaling proteins by IR may be important to maintain genomic stability by affecting various cellular homeostatic processes [215-217]. In addition, two enzymes involved in cellular metabolism, LDHB, which is the final enzyme of anaerobic glycolysis and PNP, which acts as an alternative to *de novo* purine biosynthetic pathway [218] were broadly found to be negatively correlated with radiation, albeit at different dose/time points.

In the next step, PCA was performed. This statistical tool based on multivariate analysis was useful to analyze the multidimensional dataset and revealed well-differentiated experimental groups based on radiation dose (300 mGy and 1 Gy) and time (1 h and 4 h) expression with small overlaps. There was greater variance based on radiation dose/time than between male and female samples, which were very close to each other and could not be differentiated with PCA. Some of the key proteins which showed dose or temporal differential expression when validated with western blot showed broad agreement with 2DE data. However, the gene expression profiles measured with RT-PCR correlated poorly with the 2D data.

Our data illustrated that radiation response in human PBMCs is characterized by small fold changes and that only a small fraction of detected spots are significantly altered after irradiation when compared with sham irradiated cells. These seemingly minor time- or dose-dependent changes of protein expression in human PBMCs are in

agreement with published reports [202]. Notably, this study showed distinct effects of low dose radiation stress on PBMC proteostasis. Up-regulation of key pro-survival proteins indicated that human lymphocytes could effectively deal with these changes, probably through adaptive mechanisms, to maintain cellular homeostasis. However, it should be stressed here that the proteome is dynamic and reflects only the snap-shot taken at a given time point with a specific radiation exposure. Furthermore, in response to external stress, proteins can be modified by several additional mechanisms like post-translational modifications or miRNA regulation which too, need to be addressed. Nevertheless, this comparative proteomic analysis of human PBMCs with acute radiation exposure should prove useful to understand molecular mechanisms of cellular effects with chronic low dose radiation exposures for human population residing in HLNRA of Kerala, India.

Gene expression of AP1 family genes

Differential proteomic response with acute radiation exposure implied that human PBMCs actively respond to radiation stress. Diverse biological outcomes of radiation are known to result from activation of complex network of signaling pathways triggered through transcription factors. An over-expression of many pro-survival proteins involved in cellular defense against oxidative stress, as observed in our previous study described in section 3.1.1, prompted further analysis on one such transcription factor, activator protein 1 (AP-1). ROS and other radiation induced free radicals are known to stimulate AP-1 activity. Thus, AP-1 might be relevant in low dose radiation exposure response of human PBMCs by enhancing the cellular response against ROS. We therefore, studied mRNA

profiles of various members of AP-1, specifically the Jun family members (*c-Jun*, *JunB*, and *JunD*) and the Fos family members (*c-Fos*, *FosB*, *FosL1*, and *FosL2*).

The Jun family members can form homodimers between themselves or form heterodimers with any of the four known members of the Fos family. The Fos family members are not known to form homodimers among themselves. Hypothetically thus, these proteins can form myriad dimers, all of which are capable of interacting with specific DNA sequences known as AP-1 sites (tetradecanoylphorbol acetate-responsive elements). In addition, the Fos and Jun family members can also interact with other IEG members of leucine zipper proteins, like the CREB/ATF family (*ATF1-4*, *ATF-6*, *b-ATF*, *ATFx*). The AP-1 binding sites have been identified in large number of cellular genes, including AP-1 genes themselves. The AP-1 proteins are often the final targets of the stress activated protein kinase cascades (JNK and p38 cascades) in response to extra cellular stimuli. AP-1 transcription factors are involved in regulation of various cellular functions including cell proliferation, cell differentiation, cell growth, DNA repair, cell cycle and apoptosis.

The AP1 family genes has been shown to be expressed by IR in actively dividing human cancer cell lines, but almost no information exists for the low radiation induced transcriptional modulation of these genes in non-proliferating G₀ lymphocytes [219-221]. We thus, focused on the differential gene expression profile of various members of AP-1 complex in response to IR, both as a function of time as well as dose in non-dividing human PBMCs. Our study showed time- and dose-specific activation of various members of *fos* and *jun* family genes in human PBMCs. The observed transcriptional responses were modest and immediate. Unlike bacteria, most biologically significant changes in

mammalian systems in response to a genotoxic stress like IR, are manifested at low fold changes and cannot be ignored [222]. For example, the activation of nucleotide excision repair system in normal cells was reported even with a slight modulation of *c-fos*/AP-1 after UV radiation [223].

Interestingly, PBMCs generated a transcriptional response for supposedly minor members of the *fos* family rather than the more ubiquitous *c-fos*. Among the *jun* family members, *c-jun* was the major player that was transcriptionally activated. Different AP-1 dimers differ not only in their efficacy of binding to DNA but also in stability of binding and transcriptional activation of target gene. This difference may be dependent both on the type and dose of radiation. *Jun*, *Fos* and *FosB* are considered to be strong transactivators, while *JunB*, *JunD*, *FosL1* and *FosL2* are regarded as weak transactivators [224, 225]. The heterodimers of *Fos-Jun* have been known to bind to DNA much more strongly than homodimers [224, 225]. *In vitro* analysis using recombinant proteins have also shown that among the Jun family, complexes containing *c-Jun* bind more strongly than complexes containing *JunB* or *JunD*. Among the Fos family members, heterodimers consisting of *FosB* show greater stability in binding to DNA as compared to heterodimers of *FosL1* or *c-Fos* [226]. The present study thus suggested that low to moderately high doses of radiation may elicit a defined transcriptional response of specific members of AP-1 leading to discrete dimerization in a cell type-specific manner. Several reports have shown similar pattern of transcript response for many other genes [227]. Transcriptional modulation of genes that encode AP-1 subunits may, thus provide a fine tuning mechanism to the cells to regulate net activity after IR after specific environmental signals in a cell type specific manner.

The multivariate PCA clearly distinguished clusters of Group I and Group II responders (as described in section 3.1.2.5) at 5 min post-irradiation time point for both doses. Exposure to relatively low dose of 300 mGy generated best separated and tightly clustered groups (score, 98.75 %). On the other hand, clusters of Group I and Group II responders at early time point were not very distinct at the relatively high dose of 1 Gy, indicating a higher variance. This also suggested that inter-individual differences in early transcript response may be more subtle at low doses of radiation, as compared to radiation sensitivities at high doses. The inter-individual variation in responses to IR may result from gene polymorphisms or may be due to variations in baseline gene expression. Many other studies have also reported inter-individual differences in radiation-induced human gene expression [228].

The coordinated radiation induced transcriptional response of AP-1 family genes has not been investigated in human PBMCs and a direct comparison of our results is not possible due to the lack of data. However, radiation induced gene expression of single IEGs has been reported in various cell lines. The radiation dose dependent up-regulation of *c-fos* with 250 mGy and *c-jun* with 0.5 Gy was observed in Epstein–Barr virus transformed human lymphoblastoid 244B cells, with a peak at 1 h post-irradiation [93]. Similar over-expression of *c-fos* gene was reported in Syrian hamster embryo (SHE) cells with either 90 cGy of γ -rays or 75 cGy of X-rays within 3 h time point. However, high LET irradiation with fission spectrum neutrons did not activate *c-fos* in SHE cells [229]. Another study reported up-regulation of *fosB* and *junD* with 5 Gy of IR in human HL-60 human promyelocytic leukemia cells [230].

Responses of human PBMCs to chronic low dose IR

There are no clear answers on whether the radiation dose delivered at low dose rates leads to similar biological responses, and consequently similar health effects, as the same dose delivered acutely in a short time, specifically in humans. Studies for characterization of molecular events after low dose rate radiation therefore, become pertinent. In the present study we used global proteomic approach to identify proteins that change significantly in abundance, reflecting either synthesis or degradation, in response to well defined doses of chronic low dose radiation. The objective was to establish a benchmark dataset of proteins to evaluate true responses of chronic radiation directly in human cells with no '*a priori*' hypothesis. The radiation response was studied using PBMC samples collected from HLNRA of Kerala with gel-based (2DE-MS) and gel-free chemical labelling (iTRAQ) based quantitative proteomic methods.

Basal and induced proteome analysis with 2DE-MS in HLNRA and NLNRA individuals

Initially, a gel-based 2DE-MS method was used to compare the PBMC proteome of individuals from HLNRA and NLNRA, and also the differences in response when PBMCs from these individuals were challenged with a high dose of 2 Gy. We selected only healthy individuals so that the radiation profile most likely represents a potential bio-signature that can be generalized to human population. The HLNRA individuals *vis-à-vis* NLNRA individuals showed a moderate but distinct baseline differences in PBMC proteome. Differential alterations of 15 proteins were found in individuals from HLNRA when compared to NLNRA ($P \leq 0.05$), indicating detectable radiation-specific responses even for very low doses in the range of 1.5 mGy to 20 mGy. As we saw with proteomic

responses of acute radiation, the responses with chronic radiation were also subtle, characterized by small fold changes. As hypothesized by other researchers, significant cellular responses in mammalian systems can be regulated by subtle changes in protein abundance [177, 222]. The *ex vivo* dose of 2-Gy gamma radiation induced distinct changes in expression of as many as 24 proteins in HLNRA (2 Gy), providing a clear evidence of radio-adaptive response.

These modulated proteins were grouped into 44 biological processes by the functional pathway analysis performed with DAVID. The cytoskeleton and associated proteins involved in cell movement, cell-cell adhesion, cell-matrix adhesion and cell junction assembly was the major protein group altered by chronic low-dose radiation. In HLNRA individuals, under-expression of three actin isoforms [ACT (1): -1.10 fold, $P = 0.36$; ACT (2): -1.04 fold, $P = 0.82$; ACT (4): -1.09 fold, $P = 0.76$], RhoGDI β (-1.28 fold, $P = 0.04$), tropomyosin beta isoforms [TPM2 (1): -1.49 fold, $P = 0.05$; TPM2 (2): -1.22 $P = 0.05$], VIME (-1.32 fold, $P = 0.02$), TMP4 (-1.32 fold, $P < 0.001$), PLS2 (-1.11 fold, $P = 0.63$), TUBB (-1.79 fold, $P = 0.10$) and MV (-1.11 fold, $P = 0.47$) was observed at the baseline level as compared to NLNRA. On the other hand, baseline expression of structural proteins such as ACT (3) [1.33 fold, $P = 0.05$], FIBB (1.39, $P = 0.03$) and FIBG (1.43 fold, $P = 0.04$) showed significant over-expression in HLNRA individuals. When an *ex vivo* 2 Gy radiation dose was given to HLNRA samples, 8 structural proteins showed a reverse expression as compared to unchallenged HLNRA samples. Actin isoforms-ACT (1) and ACT (2), RhoGDI β , TPM2 (1), TMP4, PLS2, MV showed up-regulation, while ACT (3) showed down-regulation. Other proteins like TMP2 (2),

VIME, FIBB and FIBG showed similar trend in challenged HLNRA as HLNRA (2Gy) samples. Actin isoform ACT (4) was observed only in 2 Gy challenged PBMCs.

Another important group of proteins that showed alterations in expression in HLNRA samples were those involved in cell redox homeostasis and response to ROS. Proteins such as PDIA1 showed similar high expression both at the baseline (1.32 fold; $P < 0.001$) and 2 Gy-challenged (1.39 fold; $P < 0.001$) conditions in HLNRA samples. Other proteins such as PDIA3 remained consistently down-regulated in HLNRA samples at baseline (-1.06 fold; $P = 0.57$) and when challenged with 2 Gy (-1.52; $P = 0.03$). On the other hand, PRDX6 showed significant down-regulation (-1.10 fold; $P = 0.05$) under basal conditions in HLNRA samples, but was significantly up-regulated (1.38 fold; $P = 0.05$) with *ex vivo* radiation stress in HLNRA (2 Gy) samples. PRDX6 is a non-seleno peroxidase with a single redox-active cysteine. It uses glutathione to catalyze the reduction of H₂O₂ and other hydroperoxides. Over-expression of PRDX6 has been shown to reduce cell apoptosis and radiation-induced ROS, and maintain integrity of mitochondria [231, 232].

Proteins such as ATPB and TPM4 exhibited similar trend in protein abundance alteration as PRDX6, *viz* down-regulation under basal conditions and up-regulation with the *ex vivo* radiation stress. ATPB protein has dual cellular functions of ATP synthesis/hydrolysis and acts as a reversible ‘molecular switch’. The ATP hydrolysis function of ATPB has a significant role in maintenance of IR modulated mitochondrial membrane potential ($\Delta\Psi_m$) and is involved in cell survival. Restoration of $\Delta\Psi_m$ in human PBMCs during RI-AR was reported by an earlier study from our group [120]. Here, ATPB showed a strong down-regulation under basal conditions (-1.45 fold, $P =$

0.05) and up-regulation (1.38 fold, $P = 0.04$) in (2 Gy) HLNRA samples. Similarly, the cytoskeletal protein TPM4, which connects with actin filaments actively participates in the ER-to-Golgi trafficking [233], showed very low expression under basal conditions in HLNRA samples (-1.32 fold, $P < 0.001$) but was up-regulated in HLNRA (2 Gy) samples (-1.3 fold, $P = 0.05$).

Other key proteins that showed differential expression in HLNRA samples were the 78-kDa glucose-regulated protein (GRP78) and the L-lactate dehydrogenase B chain (LDHB). The endoplasmic reticulum (ER) serves as the primary site for protein synthesis, folding and trafficking. It also serves as a dynamic calcium storage organelle important for cell survival, adaptive response to stress and apoptosis. Under conditions that dysregulate ER function, cells respond through a general cellular defense mechanism known as the unfolded protein response (UPR). GRP78 is one of the key player of UPR and an important stress inducible molecular chaperone of ER [234]. Significant over-expression of GRP78 was observed both under basal conditions in HLNRA samples (1.48 fold, $P = 0.01$) as well as in challenged PBMCs from HLNRA (1.52 fold, $P = 0.01$). With its known antiapoptotic and cytoprotective activity, over-expression of GRP78 indicates a protective survival advantage to human PBMCs against radiation stress that serves to maintain homeostasis. The pro-survival protein LDHB also presented with high protein abundance [1.34-fold, $P = 0.05$ as baseline expression in HLNRA and 1.2 fold, $P = 0.05$ in HLNRA (2 Gy) samples]. Earlier reports showed that the production of pyruvate from lactate by LDHB protects the cells from multiple stresses and inhibit stress-mediated cell death in yeast [235].

The intra-group comparison of individuals from NLNRA or HLNRA with their respective *ex vivo* 2 Gy irradiated PBMCs (NLNRA vs NLNRA + 2 Gy and HLNRA vs HLNRA + 2 Gy) showed differential expression of 26 proteins ($P \leq 0.05$). The pathway analysis using the UniProt/SwissProt protein database classified these proteins into processes such as cytoskeleton-associated proteins, molecular chaperones, cellular redox homeostasis, signalling, cellular metabolic process, and protein and peptide processing. The modulated biological processes observed with the intra-group comparison of 2 Gy irradiated PBMCs from HLNRA were similar to that observed from random healthy adults, irradiated *ex vivo* with 1 Gy (as described in section 3.1). The largest enriched group in both the studies was cytoskeleton and associated structural proteins.

The observed CV values for basal protein expression were 35.6% in NLNRA and 33.3% in HLNRA. PBMCs irradiated *ex vivo* with 2 Gy showed comparable CV values [32.3% in NLNRA (2 Gy) and 38.8% in HLNRA (2 Gy)]. For majority of the protein spots, calculated CV values was <50%, at both basal level (in 80.6% of proteins from NLNRA and 83.9% of protein from HLNRA samples) and challenged dose [for 93.6% of proteins from NLNRA (2 Gy) and 71 % of proteins from HLNRA (2 Gy) samples]. The cytoskeletal and extracellular proteins showed broader CV value ranges (>50%) in HLNRA samples. The overall mean CV was ~34% indicating that majority of the radiation response proteins have good stability of expression with low inter-individual variation. Further, the present study was able to detect 1.5-fold change in mean protein expression with 80% statistical power at 5% level of significance.

The correlation analysis showed significant positive correlation of two proteins (ACT3, $r = 0.78$ and ALBU1, $r = 0.84$) with the annual dose received by individuals,

while two proteins (TMP4, $r = -0.74$) and PSME1, $r = -0.82$) showed negative correlation. The actin cytoskeleton is highly dynamic network involved in many cellular processes of signal transduction, cell division, cell adhesion, cell migration, chromatin remodelling, apoptosis, gene expression and contractility in muscle and non-muscle cells [236]. The positive correlation of ACT3 protein with radiation stress further reaffirms the key role of actin cytoskeleton in the adaptation of the cell to its microenvironment or internal signals. Although, albumin is the most abundant circulating protein in plasma, human lymphocytes are known to have membrane-bound albumin. The antioxidant activities of PBMC albumin is also suggested by several reports [237, 238]. However, further investigations are required to understand the functional role of PBMC albumin in radiation stress response. The inverse relationship showed by the cytoskeletal associated protein TMP4 indicates altered stability and rearrangement of cytoskeleton with radiation stress [167, 187, 239]. The PSME1 protein, which encodes a subunit of multicatalytic endoprotease complex required by MHC class I molecule for the efficient presentation of tumour antigens also showed inverse relationship with radiation. The association of increased expression of PSME1 with diagnosis and prognosis of various tumour types is known [240]. However, the functional significance of PSME1 protein abundance alteration with chronic radiation stress needs to be analysed further.

The PCA analysis performed on the raw spot densities of all quantified proteins clearly clustered the individuals based on the radiation dose. Interestingly, the clustering was tighter for the *ex vivo* 2 Gy irradiated PBMC samples indicating evidence of RI-AR with HLNRA individuals responding uniquely to the 2 Gy challenge dose. The western

blot validation experiments performed with some of the key proteins modulated with radiation were found to be broadly in agreement with 2DE data.

There are only few studies which have used proteomics to investigate effects of chronic low dose radiation. Most of these works are based on immortal mammalian cell lines or mouse models. Loseva et al., (2014) studied chronic low dose rate exposure (5 or 15 mGy/h) induced premature senescence in human fibroblasts by 2DE-MS approach. The accumulated dose with the dose rate of 5 mGy/h (80 days) and 15 mGy/h (65 days) was 23.4 Gy and 9.6 Gy, respectively. The proteomic analysis proposed differential modulation of many oxidative stress mediated proteins involved in regulation of ROS as probable mechanism [241]. Another study reported alterations of proteins related to inflammation and apoptosis in the liver of mouse models after chronic γ -ray exposure with a dose rate of 20 mGy/day for 400 days (total dose delivered was 8 Gy). However, the study used antibody array based proteomic methodology and failed to generate the global proteomic profile of low dose radiation exposure [242].

The present work is in line with the earlier reports on RI-AR with chronic low dose [70, 71]. In a report by Ramachandran et al., the human PBMCs from HLNRA of Kerala showed lower frequency of micronuclei when challenged with a high dose, but only in individuals older than 40 y of age [72]. The PBMC samples from individuals residing in HLNRA of Ramsar, Iran, also showed similar decrease in micronuclei frequency after a high challenge dose, as compared to control subjects [115]. These individuals however, showed higher levels of initial DNA damage as measured using comet assay [243]. Further evidence of AR in human lymphocytes with micronuclei frequency was reported from radiology and radiotherapy workers [117].

Our data showed that several protein response pathways were significantly altered when the PBMCs from HLNRA and NLNRA (assumed to be primed with background radiation) were challenged with an *ex vivo* radiation dose, suggesting a dynamic proteome. The number and the fold changes, of differentially up- and down-regulated proteins differed in HLNRA compared to NLNRA individuals, indicating different thresholds of stress response pathways. The data though preliminary, support the idea that radiation proteomics can provide new insights into cellular responses, both basal and induced, to low doses of radiation. In future, the studies will be complemented with additional analysis using high-resolution gel-free techniques.

Basal proteome analysis with iTRAQ in HLNRA and NLNRA individuals

MS-based technologies have become indispensable for “global” proteomics or the broad discovery-based quantitative proteomics measurements. Among the various gel-free mass spectrometry methods, iTRAQ offers great versatility and multiplexing. One of the major advantages of iTRAQ method over conventional mass spectrometry is the ability to actually determine the relative abundance of proteins in comparative proteomics.

There are only a few iTRAQ based proteomic studies that have been used to unravel biological pathways related to acute IR exposures and none for chronic low dose radiation exposures. Almost all of these reports are based on cell lines, animal models, radiotherapy patients or patients with other diseased conditions. An iTRAQ based proteomic study on the secretome profiling of human skin tissue after single exposure to IR (3 cGy, 10 cGy and 200 cGy of X-rays) identified significant modulation of 135

proteins involved in cellular signaling, stress response, protein binding, cell movement, inflammation and ROS scavenging [244]. A similar iTRAQ based study on human skin tissue model irradiated with 0.1 Gy of X-ray radiation detected alteration of 107 proteins involved in actin cytoskeleton regulation, organ development, post-transcriptional regulation of protein abundance and proteolytic processing [245]. Another low dose study performed on human primary keratinocytes and monocytes-like cell lines (U937 cells) with iTRAQ methodology detected IR (0.1 Gy of X-ray) induced direct and bystander effects, mediated through inhibition of protein synthesis and cytokines activation [246]. The long-term risk of radiation induced cardiovascular disease was investigated using murine cardiac proteome with Isotope coded protein label (ICPL) based LC-MS technique. Significant radiation dose dependent alterations in protein levels were found for cytoskeleton, ion transport, respiratory chain, inflammatory response and metabolic processes [247, 248]. The MS analysis of plasma or serum protein samples from cancer patients undergoing radiotherapy identified several radiation specific spectral components. These spectral components were able to discriminate cancer patients from the healthy subjects with high specificity and sensitivity [199, 249-251].

In the present study, iTRAQ based gel-free method was used to study the chronic low dose/dose rate induced proteomic responses in pooled human PBMCs collected from individuals residing in HLNRA *vis-à-vis* NLNRA. As discussed earlier in section 1.9, PBMCs serve as an important resource to study cellular perturbations in response to stress. Though several proteomic studies have discussed the utility of these cell types, none of these studies used gel-free iTRAQ analysis for radiation exposure analysis [174,

175, 252, 253]. The design of experiment was crucial to address the question of subtle variations in radiation responses between different dose groups and for the robustness of the results. Pooling of PBMCs from randomly selected healthy individuals allowed us to not only overcome resource constraints of analyzing large number of samples, it also reduced random biological variance and offered increased power to detect fine changes in expression in the average sample formed [254].

The samples collected from HLNRA were stratified into different groups based on annual radiation dose received by the individuals (Group II: 1.5-5.0 mGy/y; Group III: 5.01-14.0 mGy/y; Group IV: ≥ 14.01 mGy/y) to evaluate dose response, if any. A total of 4166 proteins were identified in PBMCs of HLNRA individuals. This is comparable to an earlier PBMC map of 4129 proteins generated with a TMT based LC-MS/MS gel-free proteomics approach [164]. The number of total identified PBMC proteins, thus expanded almost 16 times with gel-free proteomics as compared to gel-based proteomics approaches used earlier [174, 255, 256]. This being the pilot study on chronic radiation proteomic responses, we used a lower threshold (significance criteria ± 1.2 -fold, adjusted $P \leq 0.1$ with Benjamini-Hochberg correction) to detect small biologically relevant changes and to maximize the information gained. We are aware that this might also risk increase in false positives, which we intend to balance by using more stringent criteria in our future targeted proteomics work. Three technical replicates of same pooled biological samples were used for each dose group which helped us to establish true significance in protein expression levels. Thus, the number of proteins differentially expressed in HLNRA relative to NLNRA increased many fold with iTRAQ as compared to 2DE-MS: 1460 proteins in Group II, 1471 proteins in Group III and 692

proteins in Group IV. This was suggestive of radiation dose dependent alterations in human PBMCs. As quality control, an assessment of experimental variation among the technical replicates was performed by calculating CV. More than 80% of the identified proteins showed a $CV \leq 20\%$, indicating good assay reproducibility, minimum variation between experimental replicates and good stability of expression. The data quality was further assured since a high 72% of identified proteins showed ≥ 2 peptide matches and ~61% proteins showed $\geq 5\%$ peptide sequence coverage.

To identify potential pathways and functions affected by low dose radiation exposure, functional annotation of the differentially expressed proteins was performed with DAVID Bioinformatics Resource. GO annotation classified the differentially expressed proteins into 204 biological process categories, 93 molecular function categories and 110 cellular component categories. The GO term enrichment analysis indicated that many proteins that changed expression in HLNRA individuals were associated with stress response categories, including DNA damage repair, RNA processing, chromatin modifications, cytoskeletal organization, signalling and protein modifications. More than 75% of the proteins belonged to the molecular function of protein, RNA, DNA and chromatin binding. Almost 50% of the enriched proteins were localized to either cytoplasm or nucleus. Though the biological processes remained the same, each dose group differed not only in the number of proteins but also in the relative expression levels of proteins in each process.

The results showed that low dose radiation activated many proteins of the DDR including DNA signalling and DNA repair pathways. There was a distinct over-expression of proteins from all the six major DNA repair pathways that process different

types of DNA lesions, namely BER, NER, MMR, HRR, NHEJ and TLS. There was an indication of dose response with higher expression of all but four proteins (BLM, RMI2, SP16H, TRRAP) in Group III individuals as compared to Group II individuals. The expression of most proteins decreased in Group IV individuals, as compared to expression in group I or Group II individuals. DNA repair processes are crucial for maintaining genome stability and cell survival. Earlier, Jain et al. (2016) and Jain et al. (2017) found lower spontaneous frequency of γ -H2AX foci per cell, and lower induced damage with an *ex vivo* challenge dose of 0.25 Gy, in PBMCs of HLNRA individuals in the dose group >5.0 mGy/y as compared to HLNRA individuals in the dose group 1.51–5.0 mGy/y [69, 71]. Also, an enrichment of DNA repair genes was reported in HLNRA individuals [73]. Our study thus, provides a mechanism for better repair of DNA damage observed in HLNRA individuals and identifies specific proteins involved in the process.

The DDR is also known to bring about wide-ranging alterations in the gene expression program of the damaged cells for sustaining expression of genes involved in DNA repair, cell cycle regulation and/or apoptosis [73]. Recently, there have been many reports that show that a large part of these alterations occur through post-transcriptional mechanisms that regulate RNA processing. More specifically, regulation of expression of many DDR genes has been shown to be mediated through mechanisms that govern splicing or influence stability/utilization of transcripts [257, 258]. Studies have shown that genotoxic stresses like radiation not only induces alternative splicing of precursor mRNA, but also results in preferential recruitment of specific mRNA isoforms with polysomes, indicating translational control of gene expression. The regulation of alternate splicing is mediated through expression and binding of several RNA binding

proteins [259]. Various global proteomic studies have identified proteins involved in RNA metabolism, including various splicing factors, as targets for DDR kinases. These kinases either influence alternative splicing of downstream DDR genes, or splicing may allow feedback regulation of signalling genes themselves for processes that impact cell recovery. Mounting evidence thus, points towards an intricate functional link between DNA repair and RNA metabolism that impact both transcription and splicing machinery. While some studies show that DNA damage prevents association of splicing components with the chromatin, other reports suggest recruitment of splicing factors at sites of damage. In the present study, global proteomic profiling showed enrichment of a large number of proteins involved in splicing and RNA processing in response to low dose radiation in HLNRA individuals. Among them were the splicing regulators RBMX (RNA-binding motif protein, X chromosome) and the FUS (Fused in sarcoma, also called Translocated in liposarcoma, TLS) that have been shown to associate with DSBs in a PAR-dependent manner. RBMX has been implicated in HR repair in response to many DNA damaging agents including IR [260, 261]. We also observed enrichment of splicing regulator hnRNP A1 that has been implicated in telomere capping contributing to genomic integrity [262]. Similarly, HLNRA individuals showed an enrichment of three key nuclear proteins involved in various aspects of RNA metabolism: SFPQ (Splicing Factor Proline and Glutamine Rich), p54^{nrb}/NONO (non-POU domain-containing octamer-binding protein (p54) and MATR3 (Matrin 3). These proteins have been shown to be important in the early phases of DSB response [263, 264]. SFPQ has a more direct role in DDR since it can bind and modulate the function of RAD51, a key component of HR pathway [265]. We also observed enrichment of RNA binding protein EWS (Ewing

Sarcoma Protein) that works at the interface of transcription and RNA processing to regulate DNA damage-induced alternative splicing. Knockdown of EWS was shown to increase sensitivity to UV radiation [266].

In eukaryotic cells, genomic DNA is organized into chromatin through association with histone and non-histone proteins. Chromatin is considered a dynamic participant in all processes that use DNA as the template to facilitate, regulate or terminate cellular responses. Chromatin architecture influences both damage formation as well as repair of DNA. DNA lesions trigger chromatin reorganization at several levels like post-translational modification of histones, nucleosome repositioning and changes in higher-order folding of the chromatin fibre. Our data revealed chromatin modifications as one of the major processes affected with low dose radiation in HLNRA individuals. Among the proteins that showed changes in expression were several members of the SWI/SNF chromatin-remodelling family which are the ATP-dependent chromatin-remodelling enzymes. These included nucleosome repositioning enzymes like SMRC1, CHD4, CHD7, CHD8 and CHD9. Changes in abundance was also seen for the chromatin remodelling protein INO80, which is recruited to the DNA damage sites through an interaction with phosphorylated H2AX during DDR. INO80 complex has been found to be involved in many distinct activities of DDR including repair of DSBs and regulation of replication checkpoint responses [267]. In addition, we observed enrichment of several zinc finger (ZnF) domain-containing proteins that have been implicated in telomere maintenance and DNA repair. ZnF domain is one of the most abundant DNA-binding motif found in eukaryotic transcriptional factors [268].

iTRAQ analysis also showed differential modulation of a large number of cytoskeletal proteins (Group II vs Group I: 225 proteins, Group III vs Group I: 222 proteins, Group IV vs Group I: 122 proteins) in HLNRA samples. As discussed earlier, this group of proteins formed the largest protein group (13 proteins) identified with 2DE-MS method in HLNRA individuals of Kerala (section 3.2.1) and also with acute radiation (section 3.1.1). This indicates active cytoskeletal reorganization in human PBMCs under both acute and chronic radiation stress. However, specific role of cytoskeleton in low dose radiation stress remains unclear and needs to be investigated further.

There were several biological processes which showed unique expression among the three radiation dose groups of HLNRA. This was especially evident for proteins involved in signaling and protein modifications. Among them were mitogen-activated protein kinases (MAPKs) which are important signal transducers that regulate diverse cellular functions. The MAPK family consists of three well characterized subfamilies; the extracellular signal-regulated kinases (ERKs), the c-Jun N-terminal kinases (JNKs), and the p38 MAPKs. These kinases are known to be activated by a wide range of environmental stresses and transmit extracellular signals to changes in gene expression through signal responsive transcription factors like AP-1, ATF-2, and TCF/Elk-1 [75, 269, 270]. In our study, enrichment of p38-MAPK signaling proteins was observed only in the lowest radiation dose group of Group II individuals, whereas the JNK cascade was enriched in both Group II and Group III HLNRA individuals. A transient induction of MAPK pathways has been shown to promote cell survival, whereas prolonged activation promote cell death in a cell type dependent manner [75]. In an earlier study, whole transcriptome analysis showed low dose radiation induced enrichment of many members

of AP-1 family in HLNRA individuals of Kerala [73]. The Group IV individuals showed a small, but statistically insignificant expression of some of the MAPK pathway proteins. On the other hand, proteins involved in calcium signaling were enriched only in Group IV individuals. Among the proteins that showed enrichment were vital signal transduction protein calmodulin, calcium binding chaperone calreticulin involved in protein folding and oligomeric assembly, calcium/calmodulin-dependent protein kinase CamKII, transcription factor CREB5 and the Rho-associated coiled-coil containing protein kinase ROCK5. Calcium signaling has important role in several cellular functions such as secretion, enzyme activation, cell cycle regulation, unfolded protein response and apoptosis [271]. Proteins associated with the process of phosphorylation and ubiquitination of target proteins showed significant activation in Group II and III individuals only as compared to NLNRA, indicating important role of active post-translational modifications under radiation stress.

To further characterize the functions of differentially expressed radiation responsive proteins, the Kyoto Encyclopedia of Genes and Genomes (KEGG) pathway mapping based on KEGG orthology terms was performed. The analysis identified statistical enrichment ($P \leq 0.05$) of 41 pathways in individuals of three HLNRA groups. Various pathways related to cell-matrix interaction, DNA repair and signaling showed up-regulation in PBMCs of HLNRA individuals compared to NLNRA individuals.

Three cell-matrix interactions related pathways namely focal adhesion, ECM-receptor interaction and regulation of actin cytoskeleton were found to be over-expressed in all the three HLNRA dose groups. The physical interaction between the extracellular matrix (ECM) and cytoskeletal network is mediated through the transmembrane family

of integrin receptors at specific membrane areas termed as focal adhesion points. These focal adhesion points, regulated by integrin signaling pathway, serve as active regions of many signal transduction molecules like the Src-family kinases, guanine nucleotide exchange factors, Ras-family proteins, and MAP kinases. The transmission of signals is generally mediated through cytoplasmic interacting protein kinases like focal adhesion kinase (FAK), integrin-linked kinase (ILK) and Rho family members [272, 273]. However, many other studies have indicated that the regulations of cytoskeletal organization and focal adhesion formation, and subsequently, activation of MEK and MAP kinase, are independent of FAK [274, 275]. Integrin-mediated adhesion to extracellular matrix proteins has been shown to provide resistance against radiation induced genotoxic injury and regulate many cellular processes like proliferation, adhesion and migration. In addition, the role of ATM/ATR for the IR induced over-expression of integrin isoforms was demonstrated in human breast cancer cells [22].

Our results showed that many proteins (integrin, collagens, laminin, protein kinases, filamins, talin, vinculin, etc) associated with ECM-receptor interaction, FA and actin cytoskeleton regulation are altered in HLNRA individuals. HLNRA groups showed significant over-expression of two integrin receptors namely, integrin alpha-V (ITV) receptor (Group II: 1.4 fold; Group III: 1.6 fold; Group IV: 1.3 fold) and Integrin alpha-11 (ITA11) receptor (Group II: 1.5 fold; Group III: 1.5 fold; Group IV: 1.1 fold). While protein kinase FAK showed non-significant changes in expression in HLNRA individuals, several Rho GTPases showed significant changes in abundance. HLNRA individuals also showed significant up-regulation of phosphatidylinositol-4,5-bisphosphate 3-kinase catalytic subunit protein (PK3CD) and other members of

phosphatidylinositol-3 kinase (PI3K)/Akt. This is in line with the earlier evidence that integrins activate pro-survival PI3K/Akt signaling axis independent of FAK [276]. Thus, our data suggests that integrin mediated signalling via PI3K/Akt and MAP kinase may be critical regulators of cell survival in response to low dose radiation in human PBMCs.

KEGG analysis showed that the other major group of proteins that showed significant over-expression was the Fanconi-anemia (FA) pathway proteins. FA proteins are mainly involved in coordinating repair of DNA strand breaks through proteins of all the major DNA repair pathways. There are also 19 unique FA proteins in mammalian system labeled as FANCA to FANCT, which are identified as essential part of DDR. In non-replicating cells, these proteins promote alternate end joining repair over classical NHEJ. They are also involved in processing of transcription associated R-loops and stabilization of replication forks. [87, 88, 277-279]. Additional cytoprotective roles of FA pathway proteins from cell death induced by ROS and pro-inflammatory cytokines is also reported [280]. Present study showed an over expression of ten FA pathway proteins (ATR, BLM, BRCA2, DPOLN, FANCA, FANCI, FANCM, MLH, RMI2, XPF) in HLNRA individuals. All the HLNRA groups showed over-expression of ATR (Group II: 1.5 fold; Group III: 1.9 fold; Group IV: 1.5 fold), BLM (Group II: 2.4 fold; Group III: 3.8 fold; Group IV: 4.1 fold), BRCA2 (Group II: 1.5 fold; Group III: 1.8 fold; Group IV: 1.3 fold), DPOLN (Group II: 1.5 fold; Group III: 1.7 fold; Group IV: 1.3 fold), FANCA (Group II: 1.3 fold; Group III: 1.7 fold; Group IV: 1.2 fold), FANCI (Group II: 1.6 fold; Group III: 1.8 fold; Group IV: 1.4 fold), FANCM (Group II: 1.4 fold; Group III: 1.6 fold; Group IV: 1.1 fold), MLH1 (Group II: 1.3 fold; Group III: 1.6 fold; Group IV: 1.2 fold),

RMI2 (Group II: 1.8 fold; Group III: 2.6 fold; Group IV: 3.1 fold) and XPF (Group II: 1.5 fold; Group III: 1.7 fold; Group IV: 1.4 fold). Among these, the RecQ helicase protein BLM was one the most strongly expressed protein in our study. BLM is considered an early responder both to the stalled replication forks as well as to double strand breaks. Tripathi et al. (2018) showed that BLM plays a central role in optimal recruitment of multiple HR and c-NHEJ factors to the chromatin in a cell cycle-specific manner [281]. Earlier, Bosch et al., reported dose dependent activation of FA pathway proteins in primary fibroblasts for radiation doses 0.1 Gy to 5 Gy. The study showed activation and recruitment of FANCD2 to the stalled replication forks even for doses as low dose as 0.1 Gy [282]. In another study, deficiency of FA proteins led to higher baseline and IR-induced residual DNA damage with slower repair efficiency in the leukocytes of FA patients as compared to the controls [283]. Upregulation of several canonical and non-canonical FA proteins seen in the present work may thus, provide a rationale for lower incidence of basal level DNA damage in lymphocytes of HLNRA individuals from Kerala as seen with earlier studies [68, 69]. This is however, in contrast with the higher level of basal DNA damage seen in individuals residing in HLNRA of Ramsar, Iran [243].

The KEGG pathways revealed radiation dose specific response for many signaling pathways in HLNRA groups, similar to the trend shown by enriched biological processes with GO analysis. Modulation of four important pro-survival signaling pathways namely, calcium signaling pathway, PI3K-Akt signaling pathway, HIF-1 signaling pathway and Rap1 signaling pathway were observed. The proteins associated with calcium signaling pathway were enriched in all the three HLNRA groups. Calcium

is a versatile secondary messenger and the alteration of the intracellular calcium levels affects several cellular functions such as secretion, enzyme activation, exocytosis, cell cycle regulation, unfolded protein response, apoptosis and gene transcription [271, 284]. It is also intimately integrated with ROS signaling in the cell. On one hand, calcium affects ROS homeostasis by regulating both ROS generation and many antioxidant systems, while on the other hand regulation of calcium signals themselves can be redox-dependent. Many proteins such as kinases, phosphatases, transcription factors and calcium-binding proteins are modulated directly or indirectly by intracellular calcium [285]. Unlike calcium signaling, the PI3K-Akt signaling and HIF-1 signaling pathways were observed only in Group II and Group III HLNRA individuals. The PI3K-Akt signaling actively promotes the cell survival by activating many pro-survival proteins and inhibiting pro-apoptotic proteins. The IR activated PI3K-Akt signaling has been widely reported in different cell types [286, 287]. The HIF signaling is modulated by cellular redox conditions and it regulates many pro-survival or pro-death factors depending on the cellular stress conditions [75]. As opposed to HIF and PI3k-Akt, Rap1 signaling pathway was observed only in Group IV individuals. Rap1 is a ubiquitous protein that belongs to the Ras family of small molecular weight GTPases. Mammalian Rap1 isoforms are best known for regulating integrin-based cell matrix adhesion but it also regulates cytoskeleton remodeling, invasion, metastasis and MAP kinase activity [288]. However, the significance of Rap1 enrichment only in individuals in radiation dose range >14 mGy and not at lower doses need to be probed further.

Transcript profiles were studied for few key proteins belonging to major biological processes such as DNA repair, chromatin modifications, MAP kinase cascade,

post-translational modifications, apoptosis and WNT signalling in Group II and Group III individuals of HLNRA. All the seven DNA repair genes showed good correlation between mRNA as measured using RT-PCR and protein expression as observed with iTRAQ. Interestingly, for many other genes, though Group II individual showed good correlation, Group III individuals showed very poor correlation. In mammalian cells, global correlation between protein and mRNA concentration remain notoriously poor, sometimes as low as 40%. Multiple processes like the stability of mRNA, half-life of protein, translation rates, post-transcriptional and post-translational mechanisms, miRNA regulation etc may contribute to this lack of correlation.

Our study identified radiation stress induced activation of as many as 36 transcription factors (TFs) in the HLNRA individuals. TFs are considered key regulators of gene expression and play an important role in coordinating important cellular processes. Among the TFs that showed chronic radiation induced alterations were E2F1, E2F8, TRRAP, BCLAF1, RELB and GTF2I. Many of these have identified to be involved in regulation of genotoxic stress and promote cell survival. Several reports suggest that E2F family proteins coordinate the progression of cell cycle and apoptosis in response to DNA damage through ATM/ATR activation [289-292]. Over-expression of E2F1 protein was observed only in Group II (1.4 fold) and Group III (1.6 fold) individuals, while E2F8 protein was observed in all three HLNRA dose groups (Group II: 1.5 fold; Group III: 1.8 fold; Group IV: 1.3 fold). In addition, Group II (1.8 fold) and Group III (2.0 fold) individuals also showed up-regulation of E2F co-factor protein TRRAP. The γ -H2AX interacting protein BCLAF1 that facilitate DSB repair by NHEJ pathway was found to be up-regulated only in Group II (1.5 fold) and Group III (1.7 fold)

individuals [293]. The study also showed over-expression of some redox-sensitive transcription factors in HLNRA dose groups. The RELB protein of the NF- κ B protein family actively involved in cell growth and survival was up-regulated in Group II (1.5 fold) and Group III (1.7 fold) individuals [75, 294]. Furthermore, an up-regulation of GTF2I and TCF20 involved in positive regulation of AP-1 family genes was also seen thus indicating the unique role of TFs in cellular redox homeostasis with low dose IR [295-297]. The specific role of other TFs in chronic low dose radiation stress needs to be investigated further.

Human cells maintain a delicate balance between production of ROS and antioxidant defence system. This balance when disturbed by IR can lead to oxidative stress in the cells. In our study, a change in protein abundance of seven proteins (TRXR2, SELO, QSOX2, PDIA1, PDIA3, NOX5 and GSTO1) involved in regulation of ROS was observed in HLNRA individuals. These included differential alterations of two selenium dependent antioxidants (SELO and TRXR2) involved in mitochondrial redox homeostasis. TRXR2 mediate NADPH dependent reduction of oxidized thioredoxin and is required to maintain thioredoxin in the reduced state inside the cells [298, 299]. It showed significant up-regulation in Group II (1.3 fold) and Group III (1.2 fold) individuals. In contrast, the redox-active mitochondrial selenoprotein SELO showed non-significant down regulation in all the HLNRA individuals. The HLNRA subjects also showed over-expression of three antioxidants that catalyze oxidative protein folding of newly synthesised proteins in ER (PDIA1, PDIA3, QSOX2). The PDI proteins belong to thioredoxin superfamily of antioxidants, while the sulfhydryl oxidases are represented by flavoproteins superfamily [300, 301].

Dose rate at which radiation is delivered plays an important role in defining biological responses. For our study, though a direct comparison between proteomic responses with acute *vis-à-vis* chronic dose is not possible since the total dose received by individuals in both cases is very different, still few trends were evident. Chronic radiation caused alterations of more number of proteins than acute radiation. Many key proteins like GRP70, HSP90 and PDIA1 showed changes in expression in both the cases. Other proteins like the calcium binding chaperone calreticulin (CALR), radiation-induced immunomodulator HSP90 and vimentin that provides mechanical support to protect the nucleus, are activated only with chronic radiation. Among the proteins uniquely altered with acute radiation is the signalling molecule RabGDI α .

In summary, an integrated approach based on 2DE gel-based and iTRAQ gel-free method allowed comprehensive profiling of chronic low dose radiation altered proteins in HLNRA individuals. The use of 2DE gel based method allowed separation of proteins based on their charge, isoelectric point and molecular weight, and separation of various isoforms of thousands of proteins in a single run. A differential expression of isoforms of many proteins such as actin (five isoforms), tropomyosin beta chain (two isoforms) and serum albumin (two isoforms) were detected in HLNRA individuals. In comparison, the high resolution gel-free method offered improved dynamic range, accuracy and throughput. Furthermore, it allowed multiplex experiments to compare more than one treatment conditions in a single LC-MS analysis. As expected, iTRAQ analysis identified significant baseline modulation of larger number of proteins (~1700 proteins) in HLNRA samples as compared to the 2DE-MS (33 proteins) method. Approximately 79% of the proteins identified by the 2DE-MS method were also represented by the iTRAQ method

in different set of HLNRA individuals emphasizing the consistency of IR induced proteomic changes. There were few proteins that were not detected with the iTRAQ method (RhoGDI β , VIME, HSP90, LDHB, PRDX6, CLIC, LEI). This could be due to the technical limitation of chemical labelling associated with the iTRAQ reagents.

This work thus, presents for the first time a comprehensive list of human proteins altered in abundance with low dose chronic radiation. There was a distinct up-regulation of proteins involved in DNA damage signaling, DNA repair, chromatin modifications and RNA processing, among others. It also identified several proteins that provide genomic stability and survival advantage leading to radio-adaptive response. Comparison of data between human populations exposed to chronic and acute irradiation will offer critical information for understanding long term health effects of radiation. This will impact key decisions on radiation risk estimation for humans.

CHAPTER 5
KEY CONCLUSIONS
AND
FUTURE DIRECTIONS

New advances in technology and high throughput profiling techniques are now enabling a better understanding of cellular processes even at very low doses of radiation. In this context, proteomics too, has developed as a mature biological tool and is slowly gaining support among the radiation biologists. Proteins are the key effector molecules through which the cell coordinates all its functions. Analysis of alterations in protein abundance can hence, provide useful information on biological functions, and consequently on health effects associated with low doses of radiation. In this work, we studied effect of acute as well as chronic radiation on the proteome of human PBMCs in healthy individuals.

For acute radiation effects, PBMCs were exposed to two doses 300 mGy and 1 Gy of gamma rays '*ex vivo*' and proteomic responses studied at 1 h and 4 h post irradiation with 2DE. Mass spectrometry analyses identified redox sensor protein, chloride intracellular channel protein 1 (CLIC-1), the antioxidant protein, peroxiredoxin-6 and the pro-survival molecular chaperone 78 KDa glucose regulated protein (GRP78) among the 23 modulated proteins. The multivariate principal component analysis clearly differentiated experimental groups based on radiation dose and time. We thus, concluded that the radiation proteomic response of G₀ human PBMCs involves moderate up-regulation of protective mechanisms, with low inter-individual variability. Alteration of many proteins involved in cellular defense against oxidative stress, prompted analysis on one such redox sensitive transcription factor, AP-1. Coordinated transcript response of fos and jun family members which constitute AP-1 factor was studied 5 min, 1 h and 4 h post-irradiation with same two doses 300 mGy and 1 Gy in human PBMCs. The results suggested that human G₀ PBMCs respond to low and moderate gamma radiation through

transcriptional response of minor members (*FosB*, *FosL1*, and *FosL2*) of the *fos* family rather than the more ubiquitous *c-fos*. Among the *jun* family members (*c-Jun*, *JunB*, and *JunD*), *c-jun* appeared to be the more global player that is transcriptionally activated in PBMCs.

The baseline PBMC proteome was compared between individuals from HLNRA and NLNRA of Kerala, India using an integrated gel-based (2DE-MS) and gel-free (iTRAQ) method to understand effects of chronic radiation, if any. Further, differential changes in proteome when the PBMCs of individuals from HLNRA and NLNRA were challenged with a high dose of 2 Gy were also studied. The 2DE-MS method identified differences in baseline expression of 15 proteins in HLNRA individuals when compared to NLNRA ($P \leq 0.05$). However, only four proteins (ACT3, ALBU1, TMP4 and PSME1) showed significant correlation with the annual dose received by individuals. When the samples were challenged with 2 Gy gamma radiation, 24 proteins were significantly altered in HLNRA (2 Gy) as compared to NLNRA (2 Gy) samples. The pathway analysis distinguished 44 biological processes significantly ($P \leq 0.05$) modulated in HLNRA. More importantly, when challenged with an *ex vivo* dose of 2 Gy, HLNRA PBMCs responded with an up-regulation of many protective pro-survival proteins such as the redox homeostasis proteins PDIA1 and PRDX6, and the master regulator of unfolded protein response GRP78 protein. Thus, there was a clear evidence of radiation induced adaptive response in HLNRA individuals.

For iTRAQ analysis, HLNRA samples were classified into three dose groups (Group II: 1.5-5.0 mGy/y; Group III: 5.01-14.0 mGy/y; Group IV: ≥ 14.01 mGy/y; N=10 for each dose group). The analysis identified significant differential expression (± 1.2 -

fold, adjusted $P \leq 0.1$ using Benjamini-Hochberg correction) of more than 1450 proteins in Group II and Group III each when compared to Group I (NLNRA), and a smaller subset of 692 proteins in Group IV compared to Group I. The pathway analysis identified 204 biological processes significantly ($P \leq 0.05$) enriched in three HLNRA dose groups. Out of these, 57 processes involved in DNA damage repair, RNA processing, chromatin modifications and cytoskeletal organization were common among all three dose groups of HLNRA samples. In contrast, radiation induced signaling pathways showed a dose specific enrichment. Further analysis with KEGG identified enrichment ($P \leq 0.05$) of 41 pathways affected in HLNRA dose groups, although the number of proteins involved in each pathway varied among the dose groups. The important radiation altered pathways included cell-matrix interaction, signaling and DNA repair pathways. Among the repair pathways, enrichment of Fanconi anemia pathway proteins was especially evident. FA proteins are mainly involved in coordinating repair of DNA strand breaks through proteins of all the major DNA repair pathways. In non-replicating cells, these proteins promote alternate end joining repair over classical NHEJ. They are also involved in processing of transcription associated R-loops and stabilization of replication forks.

This is the first report to provide a comprehensive baseline list of human proteins expressed in individuals exposed to very low dose chronic radiation. It also revealed probable 'pro-survival' proteins that may be involved in providing an adaptive advantage to these individuals. The findings echoed the growing predilection among the scientific community that the shape of the dose-response curve in the area of low dose/dose rate exposures may not be linear. It is definitely time to incorporate the latest scientific findings into the regulatory process of risk assessment for low doses.

The present discovery proteomic analysis identified common and unique proteins in PBMCs of HLNRA individuals. In the follow-up approach, candidate proteins from processes like DNA repair or signaling need to be verified using targeted proteomics to develop potential signatures of low dose radiation. Study of low dose radiation induced alterations at the post-translational levels will be further informative. Additionally, there were more than 30 transcription factors that showed differences in expression in HLNRA individuals. Understanding the functional role of these factors in low dose radiation should be interesting.

We however, recognize the limitation of the small sample set analyzed in this study which limits understanding role of individual variations in radiation sensitivity. Using less rigorous fold change cut-off was a conscious decision which allowed generation of a comprehensive list of resource protein set which can be now put to more stringent testing for identifying small subsets of radiation-responsive candidate proteins. Relating the proteomic signatures to consequent health effects in a larger population set is part of an ongoing project.

REFERENCES

- [1] UNSCEAR, United Nations Scientific Committee on the Effects of Atomic Radiations (UNSCEAR). Sources and Effects of Ionising Radiation Annex B Exposures from Natural Radiation Sources. New York:United Nations., 2000.
- [2] ICRP, International Commission on Radiological Protection. The 2007 Recommendations of the International Commission on Radiological Protection. ICRP Publication 103., Annals of the ICRP 37 (2007) 9-34.
- [3] UNSCEAR, United Nations Scientific Committee on the Effects of Atomic Radiation (UNSCEAR). Biological mechanisms of radiation actions at low doses. A white paper to guide the Scientific Committee's future programme of work. New York:United Nations, (2012).
- [4] BEIR, Health Risks from Exposure to Low Levels of Ionizing Radiation; BEIR VII – Phase 2., (2006).
- [5] M. Tubiana, Dose–effect relationship and estimation of the carcinogenic effects of low doses of ionizing radiation: The joint report of the Académie des Sciences (Paris) and of the Académie Nationale de Médecine, International Journal of Radiation Oncology*Biology*Physics, 63 (2005) 317-319.
- [6] F. Marchetti, M.A. Coleman, I.M. Jones, A.J. Wyrobek, Candidate protein biosimulators of human exposure to ionizing radiation, Int J Radiat Biol, 82 (2006) 605-639.
- [7] D. Leszczynski, Radiation proteomics: a brief overview, Proteomics, 14 (2014) 481-488.
- [8] M.J.A. Omid Azimzadeh, Soile Tapio, Proteomics in radiation research: present status and future perspectives, Radiat Environ Biophys, 53 (2014) 31-38.

- [9] S.A. Amundson, R.A. Lee, C.A. Koch-Paiz, M.L. Bittner, P. Meltzer, J.M. Trent, A.J. Fornace, Jr., Differential responses of stress genes to low dose-rate gamma irradiation, *Mol Cancer Res*, 1 (2003) 445-452.
- [10] S. Grudzenski, A. Raths, S. Conrad, C.E. Rube, M. Lobrich, Inducible response required for repair of low-dose radiation damage in human fibroblasts, *Proc Natl Acad Sci U S A*, 107 (2010) 14205-14210.
- [11] L.H. Ding, M. Shingyoji, F. Chen, J.J. Hwang, S. Burma, C. Lee, J.F. Cheng, D.J. Chen, Gene expression profiles of normal human fibroblasts after exposure to ionizing radiation: a comparative study of low and high doses, *Radiat Res*, 164 (2005) 17-26.
- [12] R.E. Shore, H.L. Beck, J.D. Boice, E.A. Caffrey, S. Davis, H.A. Grogan, F.A. Mettler, R.J. Preston, J.E. Till, R. Wakeford, L. Walsh, L.T. Dauer, Implications of recent epidemiologic studies for the linear nonthreshold model and radiation protection, *J Radiol Prot*, 38 (2018) 1217-1233.
- [13] WHO, World Health Organization. Effects of radiation on human heredity: investigations of areas of high natural radiation. WHO Technical Report Series No. 166, Geneva., (1959).
- [14] K. Ozasa, Y. Shimizu, A. Suyama, F. Kasagi, M. Soda, E.J. Grant, R. Sakata, H. Sugiyama, K. Kodama, Studies of the mortality of atomic bomb survivors, Report 14, 1950-2003: an overview of cancer and noncancer diseases, *Radiat Res*, 177 (2012) 229-243.
- [15] N. 2012, Uncertainties in the Estimation of Radiation Risks and Probability of Disease Causation, Report No. 171 Bethesda, MD: National Council on Radiation Protection and Measurements, (2012).

- [16] R.R. Nair, B. Rajan, S. Akiba, P. Jayalekshmi, M.K. Nair, P. Gangadharan, T. Koga, H. Morishima, S. Nakamura, T. Sugahara, Background radiation and cancer incidence in Kerala, India-Karanagappally cohort study, *Health Phys*, 96 (2009) 55-66.
- [17] Z. Tao, S. Akiba, Y. Zha, Q. Sun, J. Zou, J. Li, Y. Liu, Y. Yuan, S. Tokonami, H. Morishoma, T. Koga, S. Nakamura, T. Sugahara, L. Wei, Cancer and non-cancer mortality among Inhabitants in the high background radiation area of Yangjiang, China (1979-1998), *Health Phys*, 102 (2012) 173-181.
- [18] A. Akleyev, I. Deltour, L. Krestinina, M. Sokolnikov, Y. Tsareva, E. Tolstykh, J. Schuz, Incidence and Mortality of Solid Cancers in People Exposed In Utero to Ionizing Radiation: Pooled Analyses of Two Cohorts from the Southern Urals, Russia, *PLoS One*, 11 (2016) e0160372.
- [19] S. Davis, K.J. Kopecky, T.E. Hamilton, L. Onstad, T. Hanford Thyroid Disease Study, Thyroid neoplasia, autoimmune thyroiditis, and hypothyroidism in persons exposed to iodine 131 from the hanford nuclear site, *JAMA*, 292 (2004) 2600-2613.
- [20] L.B. Zablotska, R.S. Lane, P.A. Thompson, A reanalysis of cancer mortality in Canadian nuclear workers (1956-1994) based on revised exposure and cohort data, *Br J Cancer*, 110 (2014) 214-223.
- [21] G.G. Caldwell, M.M. Zack, M.T. Mumma, H. Falk, C.W. Heath, J.E. Till, H. Chen, J.D. Boice, Mortality among military participants at the 1957 PLUMBBOB nuclear weapons test series and from leukemia among participants at the SMOKY test, *J Radiol Prot*, 36 (2016) 474-489.
- [22] J.L. Lyon, S.C. Alder, M.B. Stone, A. Scholl, J.C. Reading, R. Holubkov, X. Sheng, G.L. White, Jr., K.T. Hegmann, L. Anspaugh, F.O. Hoffman, S.L. Simon, B. Thomas, R.

Carroll, A.W. Meikle, Thyroid disease associated with exposure to the Nevada nuclear weapons test site radiation: a reevaluation based on corrected dosimetry and examination data, *Epidemiology*, 17 (2006) 604-614.

[23] M. Doss, Linear No-Threshold Model VS. Radiation Hormesis, Dose-response : a publication of International Hormesis Society, 11 (2013) 480-497.

[24] J.M. Cuttler, Evidence of a Dose Threshold for Radiation-Induced Leukemia, Dose-Response, 16 (2018) 1559325818811537.

[25] K.M. Seong, S. Seo, D. Lee, M.-J. Kim, S.-S. Lee, S. Park, Y.W. Jin, Is the Linear No-Threshold Dose-Response Paradigm Still Necessary for the Assessment of Health Effects of Low Dose Radiation?, *Journal of Korean medical science*, 31 Suppl 1 (2016) S10-S23.

[26] D. Jolly, J. Meyer, A brief review of radiation hormesis, *Australasian Physical & Engineering Sciences in Medicine*, 32 (2009) 180-187.

[27] E.J. Calabrese, Getting the dose-response wrong: why hormesis became marginalized and the threshold model accepted, *Arch Toxicol*, 83 (2009) 227-247.

[28] E.J. Calabrese, M.K. O'Connor, Estimating Risk of Low Radiation Doses – A Critical Review of the BEIR VII Report and its Use of the Linear No-Threshold (LNT) Hypothesis, *Radiation Research*, 182 (2014) 463-474.

[29] T.D. Luckey, Radiation hormesis: the good, the bad, and the ugly, Dose-response : a publication of International Hormesis Society, 4 (2006) 169-190.

[30] J. Baldwin, V. Grantham, Radiation Hormesis: Historical and Current Perspectives, *Journal of Nuclear Medicine Technology*, 43 (2015) 242-246.

- [31] J.M. Cuttler, Commentary on Using LNT for Radiation Protection and Risk Assessment, Dose-response : a publication of International Hormesis Society, 8 (2010) 378-383.
- [32] A. Aurengo, Averbeck, D., Bonnin, A., LeGuen, B., Masse, R., Monier, R., Tubiana, M., Valleron, A. J., and de Vathaire, F, Dose-Effect Relationships and Estimation of the Carcinogenic Effects of Low Doses of Ionizing Radiation, Academies of Sciences and Medicine, Paris., (2005).
- [33] K.W. Fornalski, L. Dobrzyński, The Healthy Worker Effect and Nuclear Industry Workers, Dose-Response, 8 (2010) dose-response.09-019.Fornalski.
- [34] O. Desouky, N. Ding, G. Zhou, Targeted and non-targeted effects of ionizing radiation, Journal of Radiation Research and Applied Sciences, 8 (2015) 247-254.
- [35] R. Baskar, Emerging role of radiation induced bystander effects: Cell communications and carcinogenesis, Genome Integrity, 1 (2010) 13.
- [36] J.J. Burt, P.A. Thompson, R.M. Lafrenie, Non-targeted effects and radiation-induced carcinogenesis: a review, Journal of Radiological Protection, 36 (2016) R23-R35.
- [37] E.G. Wright, Manifestations and mechanisms of non-targeted effects of ionizing radiation, Mutation Research/Fundamental and Molecular Mechanisms of Mutagenesis, 687 (2010) 28-33.
- [38] H. Nagasawa, J.B. Little, Induction of Sister Chromatid Exchanges by Extremely Low Doses of α -Particles, Cancer Research, 52 (1992) 6394-6396.
- [39] S.A. Krueger, S.J. Collis, M.C. Joiner, G.D. Wilson, B. Marples, Transition in survival from low-dose hyper-radiosensitivity to increased radioresistance is independent

of activation of ATM Ser1981 activity, *Int J Radiat Oncol Biol Phys*, 69 (2007) 1262-1271.

[40] ICRP, International Commission on Radiological Protection (ICRP). Recommendations of the ICRP. ICRP Publication 9., (1966).

[41] J.D.B. Jr, The linear nonthreshold (LNT) model as used in radiation protection: an NCRP update AU - Boice, John D, *International Journal of Radiation Biology*, 93 (2017) 1079-1092.

[42] J.H. Hendry, S.L. Simon, A. Wojcik, M. Sohrabi, W. Burkart, E. Cardis, D. Laurier, M. Tirmarche, I. Hayata, Human exposure to high natural background radiation: what can it teach us about radiation risks?, *Journal of radiological protection : official journal of the Society for Radiological Protection*, 29 (2009) A29-A42.

[43] J.H. Hendry, S.L. Simon, A. Wojcik, M. Sohrabi, W. Burkart, E. Cardis, D. Laurier, M. Tirmarche, I. Hayata, Human exposure to high natural background radiation: what can it teach us about radiation risks?, *J Radiol Prot*, 29 (2009) A29-42.

[44] M. Sohrabi, World high background natural radiation areas: Need to protect public from radiation exposure, *Radiation Measurements*, 50 (2013) 166-171.

[45] V. Valković, CHAPTER 2 - Radioactive Nuclides in Nature, in: V. Valković (Ed.) *Radioactivity in the Environment*, Elsevier Science, Amsterdam, 2000, pp. 5-32.

[46] H.C. Griffin, Natural Radioactive Decay Chains, in: A. Vértes, S. Nagy, Z. Klencsár, R.G. Lovas, F. Rösch (Eds.) *Handbook of Nuclear Chemistry*, Springer US, Boston, MA, 2011, pp. 667-687.

[47] K.S. K.P. George, K.B. Mistry, G. Ayenger, Investigations on human population residing in high background radiation areas of Kerala and adjoining regions, in:

Proceedings of Symposium on Biological and Environmental Effects of low level Radiation. I.A.E.A, 2 (1976) 325–329.

[48] G.H.V. D.S. Bharatwal, Radiation dose measurements in the monazite areas of Kerala state in India., Proceedings of the 2nd UN International conference on Peaceful uses of Atomic energy. United Nations, NewYork 23 (1958) 156.

[49] C. Sunta, A review of the studies of high background areas of the S-W coast of India. In: Sohrabi M, Ahmed JU, Durani SA, editors. Proceedings of the International conference on high levels of natural radiation, Atomic Energy Organization of Iran, Tehran, (1993).

[50] C.E. Pereira, V.K. Vaidyan, M.P. Chougaonkar, Y.S. Mayya, B.K. Sahoo, P.J. Jojo, Indoor radon and thoron levels in Neendakara and Chavara regions of southern coastal Kerala, India, Radiat Prot Dosimetry, 150 (2012) 385-390.

[51] S. Ben Byju, P.K. Koya, B.K. Sahoo, P.J. Jojo, M.P. Chougaonkar, Y.S. Mayya, Inhalation and external doses in coastal villages of high background radiation area in Kollam, India, Radiat Prot Dosimetry, 152 (2012) 154-158.

[52] Y. Omori, S. Tokonami, S.K. Sahoo, T. Ishikawa, A. Sorimachi, M. Hosoda, H. Kudo, C. Pornnumpa, R.R. Nair, P.A. Jayalekshmi, P. Sebastian, S. Akiba, Radiation dose due to radon and thoron progeny inhalation in high-level natural radiation areas of Kerala, India, J Radiol Prot, 37 (2017) 111-126.

[53] B.G. Gruneberg H , Berry RJ , Riles LL , Smith CAB , Weiss RA, A search for genetic effects of high natural radioactivity in South India . Special Report Series No. 307 . London: Medical Research Council., (1966).

- [54] S.K. Ayengar ARG, Mistry KB, Suntha CM, Nambi CSV, Kaithuria SP et al, Evaluation of the long term effects of high background radiation on selected population groups of Kerala coasts. In: Proceedings of 4th UN International Conference on Peaceful Uses of Atomic Energy. United Nations, New York, pp (1972) 31–51.
- [55] N. Kochupillai, I.C. Verma, M.S. Grewal, V. Ramalingaswami, Down's syndrome and related abnormalities in an area of high background radiation in coastal Kerala, *Nature*, 262 (1976) 60-61.
- [56] S. K, Down's syndrome in Kerala [letter], *Nature* (1977) 267:728.
- [57] P.K. Koya, M.P. Chougankar, P. Predeep, P.J. Jojo, V.D. Cheriyan, Y.S. Mayya, M. Seshadri, Effect of low and chronic radiation exposure: a case-control study of mental retardation and cleft lip/palate in the monazite-bearing coastal areas of southern Kerala, *Radiat Res*, 177 (2012) 109-116.
- [58] P.K. Koya, G. Jaikrishan, K.R. Sudheer, V.J. Andrews, M. Madhusoodhanan, C.K. Jagadeesan, B. Das, Sex ratio at birth: scenario from normal- and high-level natural radiation areas of Kerala coast in south-west India, *Radiat Environ Biophys*, 54 (2015) 453-463.
- [59] E.N. Ramachandran, C.V. Karuppasamy, V.D. Cheriyan, D.C. Soren, B. Das, V. Anilkumar, P.K. Koya, M. Seshadri, Cytogenetic studies on newborns from high and normal level natural radiation areas of Kerala in southwest coast of India, *Int J Radiat Biol*, 89 (2013) 259-267.
- [60] C.V. Karuppasamy, E.N. Ramachandran, V. Anil Kumar, P.R. Vivek Kumar, P.K.M. Koya, G. Jaikrishan, B. Das, Frequency of chromosome aberrations among adult

male individuals from high and normal level natural radiation areas of Kerala in the southwest coast of India, *Mutat Res*, 828 (2018) 23-29.

[61] B. Das, C.V. Karuppasamy, Spontaneous frequency of micronuclei among the newborns from high level natural radiation areas of Kerala in the southwest coast of India, *Int J Radiat Biol*, 85 (2009) 272-280.

[62] C.V. Karuppasamy, E.N. Ramachandran, V.A. Kumar, P.R. Kumar, P.K. Koya, G. Jaikrishan, B. Das, Peripheral blood lymphocyte micronucleus frequencies in men from areas of Kerala, India, with high vs normal levels of natural background ionizing radiation, *Mutat Res Genet Toxicol Environ Mutagen*, 800-801 (2016) 40-45.

[63] B. Das, D. Saini, M. Seshadri, Telomere length in human adults and high level natural background radiation, *PLoS One*, 4 (2009) e8440.

[64] B. Das, D. Saini, M. Seshadri, No evidence of telomere length attrition in newborns from high level natural background radiation areas in Kerala coast, south west India, *Int J Radiat Biol*, 88 (2012) 642-647.

[65] L. Forster, P. Forster, S. Lutz-Bonengel, H. Willkomm, B. Brinkmann, Natural radioactivity and human mitochondrial DNA mutations, *Proc Natl Acad Sci U S A*, 99 (2002) 13950-13954.

[66] G. Jaikrishan, K.R. Sudheer, V.J. Andrews, P.K. Koya, M. Madhusoodhanan, C.K. Jagadeesan, M. Seshadri, Study of stillbirth and major congenital anomaly among newborns in the high-level natural radiation areas of Kerala, India, *J Community Genet*, 4 (2013) 21-31.

- [67] S. Ahmad, P.K. Koya, M. Seshadri, Effects of chronic low level radiation in the population residing in the high level natural radiation area in Kerala, India: employing heritable DNA mutation studies, *Mutat Res*, 751 (2013) 91-95.
- [68] P.R. Kumar, V.D. Cheriyan, M. Seshadri, Evaluation of spontaneous DNA damage in lymphocytes of healthy adult individuals from high-level natural radiation areas of Kerala in India, *Radiat Res*, 177 (2012) 643-650.
- [69] V. Jain, P.R. Kumar, P.K. Koya, G. Jaikrishan, B. Das, Lack of increased DNA double-strand breaks in peripheral blood mononuclear cells of individuals from high level natural radiation areas of Kerala coast in India, *Mutat Res*, 788 (2016) 50-57.
- [70] P.R. Kumar, M. Seshadri, G. Jaikrishan, B. Das, Effect of chronic low dose natural radiation in human peripheral blood mononuclear cells: Evaluation of DNA damage and repair using the alkaline comet assay, *Mutat Res*, 775 (2015) 59-65.
- [71] Vinay Jain, Divyalakshmi Saini, P.R. Vivek Kumar, G. Jaikrishan, B. Das, Efficient repair of DNA double strand breaks in individuals from high level natural radiation areas of Kerala coast, south-west India, *Mutat Res Fund Mol Mech Mutagen* 806 (2017) 39–50.
- [72] E. N. Ramachandran, C. V. Karuppasamy, D.C.S. V. Anil Kumar, P. R. Vivek Kumar, P. K. M. Koya, G. Jaikrishan, B. Das., Radio-adaptive response in peripheral blood lymphocytes of individuals residing in high-level natural radiation areas of Kerala in the southwest coast of India, *Mutagenesis*, 32 (2017) 267-273.
- [73] V. Jain, B. Das, Global transcriptome profile reveals abundance of DNA damage response and repair genes in individuals from high level natural radiation areas of Kerala coast, *PLoS One*, 12 (2017) e0187274.

- [74] E.I. Azzam, J.-P. Jay-Gerin, D. Pain, Ionizing radiation-induced metabolic oxidative stress and prolonged cell injury, *Cancer letters*, 327 (2012) 48-60.
- [75] D. Trachootham, W. Lu, M.A. Ogasawara, R.-D.V. Nilsa, P. Huang, Redox regulation of cell survival, *Antioxidants & Redox Signaling*, 10 (2008) 1343-1374.
- [76] R.T. Dean, S. Fu, R. Stocker, M.J. Davies, Biochemistry and pathology of radical-mediated protein oxidation, *The Biochemical journal*, 324 (Pt 1) (1997) 1-18.
- [77] D. Poppek, T. Grune, Proteasomal Defense of Oxidative Protein Modifications, *Antioxidants & Redox Signaling*, 8 (2006) 173-184.
- [78] X. Li, W.-D. Heyer, Homologous recombination in DNA repair and DNA damage tolerance, *Cell research*, 18 (2008) 99-113.
- [79] A. Ciccia, S.J. Elledge, The DNA Damage Response: Making It Safe to Play with Knives, *Molecular Cell*, 40 (2010) 179-204.
- [80] J. Jiricny, The multifaceted mismatch-repair system, *Nature Reviews Molecular Cell Biology*, 7 (2006) 335.
- [81] H.E. Krokan, M. Bjørås, Base Excision Repair, *Cold Spring Harbor Perspectives in Biology*, 5 (2013).
- [82] S.S. Wallace, Base excision repair: a critical player in many games, *DNA Repair*, 19 (2014) 14-26.
- [83] G. Spivak, Nucleotide excision repair in humans, *DNA Repair*, 36 (2015) 13-18.
- [84] H.H.Y. Chang, N.R. Pannunzio, N. Adachi, M.R. Lieber, Non-homologous DNA end joining and alternative pathways to double-strand break repair, *Nature Reviews Molecular Cell Biology*, 18 (2017) 495.

- [85] A.J. Davis, D.J. Chen, DNA double strand break repair via non-homologous end-joining, *Translational cancer research*, 2 (2013) 130-143.
- [86] M.-E. Dextraze, T. Gantchev, S. Girouard, D. Hunting, DNA interstrand cross-links induced by ionizing radiation: An unsung lesion, *Mutation Research/Reviews in Mutation Research*, 704 (2010) 101-107.
- [87] G.-L. Moldovan, A.D. D'Andrea, How the fanconi anemia pathway guards the genome, *Annual review of genetics*, 43 (2009) 223-249.
- [88] R. Ceccaldi, P. Sarangi, A.D. D'Andrea, The Fanconi anaemia pathway: new players and new functions, *Nature Reviews Molecular Cell Biology*, 17 (2016) 337.
- [89] B. Marengo, M. Nitti, A.L. Furfaro, R. Colla, C.D. Ciucis, U.M. Marinari, M.A. Pronzato, N. Traverso, C. Domenicotti, Redox Homeostasis and Cellular Antioxidant Systems: Crucial Players in Cancer Growth and Therapy, *Oxidative medicine and cellular longevity*, 2016 (2016) 6235641-6235641.
- [90] J.A. Reisz, N. Bansal, J. Qian, W. Zhao, C.M. Furdui, Effects of ionizing radiation on biological molecules--mechanisms of damage and emerging methods of detection, *Antioxidants & Redox Signaling*, 21 (2014) 260-292.
- [91] W. Kruijer, J.A. Cooper, T. Hunter, I.M. Verma, Platelet-derived growth factor induces rapid but transient expression of the c-fos gene and protein, *Nature*, 312 (1984) 711-716.
- [92] L.F. Lau, D. Nathans, Expression of a set of growth-related immediate early genes in BALB/c 3T3 cells: coordinate regulation with c-fos or c-myc, *Proceedings of the National Academy of Sciences of the United States of America*, 84 (1987) 1182-1186.

- [93] A.V. Prasad, N. Mohan, B. Chandrasekar, M.L. Meltz, Induction of Transcription of "Immediate Early Genes" by Low-Dose Ionizing Radiation, *Radiation Research*, 143 (1995) 263-272.
- [94] T. Fowler, R. Sen, A.L. Roy, Regulation of primary response genes, *Molecular Cell*, 44 (2011) 348-360.
- [95] Y.M.W. Janssen-Heininger, B.T. Mossman, N.H. Heintz, H.J. Forman, B. Kalyanaraman, T. Finkel, J.S. Stamler, S.G. Rhee, A. van der Vliet, Redox-based regulation of signal transduction: principles, pitfalls, and promises, *Free radical biology & medicine*, 45 (2008) 1-17.
- [96] A.C. UNSCEAR, Non-targeted and Delayed Effects of Exposure to Ionizing Radiations, UNSCEAR, (2006).
- [97] O.V. Belyakov, A.M. Malcolmson, M. Folkard, K.M. Prise, B.D. Michael, Direct evidence for a bystander effect of ionizing radiation in primary human fibroblasts, *British journal of cancer*, 84 (2001) 674-679.
- [98] B.D. Michael, Non-DNA-Targeted Effects and Low-Dose Radiation Risk, in: M. Nakashima, N. Takamura, K. Tsukasaki, Y. Nagayama, S. Yamashita (Eds.) *Radiation Health Risk Sciences*, Springer Japan, Tokyo, 2009, pp. 29-33.
- [99] M. Kadhim, S. Salomaa, E. Wright, G. Hildebrandt, O.V. Belyakov, K.M. Prise, M.P. Little, Non-targeted effects of ionising radiation--implications for low dose risk, *Mutation research*, 752 (2013) 84-98.
- [100] W.F. Morgan, M.B. Sowa, Non-targeted effects induced by ionizing radiation: Mechanisms and potential impact on radiation induced health effects, *Cancer letters*, 356 (2015) 17-21.

- [101] S. Bright, M. Kadhim, The future impacts of non-targeted effects, *International Journal of Radiation Biology*, 94 (2018) 727-736.
- [102] E.G. Wright, P.J. Coates, Untargeted effects of ionizing radiation: Implications for radiation pathology, *Mutation Research/Fundamental and Molecular Mechanisms of Mutagenesis*, 597 (2006) 119-132.
- [103] S. Tapio, V. Jacob, Radioadaptive response revisited, *Radiation and Environmental Biophysics*, 46 (2007) 1-12.
- [104] W.F. Morgan, M.B. Sowa, Effects of ionizing radiation in nonirradiated cells, *Proceedings of the National Academy of Sciences of the United States of America*, 102 (2005) 14127.
- [105] L.T. Dauer, A.L. Brooks, D.G. Hoel, W.F. Morgan, D. Stram, P. Tran, Review and evaluation of updated research on the health effects associated with low-dose ionising radiation, *Radiation Protection Dosimetry*, 140 (2010) 103-136.
- [106] E.J. Tawn, C.A. Whitehouse, F.A. Martin, Sequential chromosome aberration analysis following radiotherapy — no evidence for enhanced genomic instability, *Mutation Research/Genetic Toxicology and Environmental Mutagenesis*, 465 (2000) 45-51.
- [107] E.J. Tawn, C.A. Whitehouse, J.F. Winther, G.B. Curwen, G.S. Rees, M. Stovall, J.H. Olsen, P. Guldberg, C. Rechnitzer, H. Schröder, J.D. Boice, Chromosome analysis in childhood cancer survivors and their offspring—No evidence for radiotherapy-induced persistent genomic instability, *Mutation Research/Genetic Toxicology and Environmental Mutagenesis*, 583 (2005) 198-206.

- [108] S.-H. Lefèvre, N. Vogt, A.-M. Dutrillaux, L. Chauveinc, D. Stoppa-Lyonnet, F. Doz, L. Desjardins, B. Dutrillaux, S. Chevillard, B. Malfoy, Genome instability in secondary solid tumors developing after radiotherapy of bilateral retinoblastoma, *Oncogene*, 20 (2001) 8092.
- [109] S. Salomaa, Chromosomal instability in in vivo radiation exposed subjects, *International Journal of Radiation Biology*, 74 (1998) 771-779.
- [110] M. Nakanishi, K. Tanaka, T. Takahashi, T. Kyo, H. Dohy, M. Fujiwara, N. Kamada, Microsatellite instability in acute myelocytic leukaemia developed from A-bomb survivors, *International Journal of Radiation Biology*, 77 (2001) 687-694.
- [111] C.A. Whitehouse, E.J. Tawn, No Evidence for Chromosomal Instability in Radiation Workers with *In Vivo* Exposure to Plutonium, BIIONE2001.
- [112] D. Frankenberg, K.-D. Greif, U. Giesen, Radiation response of primary human skin fibroblasts and their bystander cells after exposure to counted particles at low and high LET, *International Journal of Radiation Biology*, 82 (2006) 59-67.
- [113] W. Tu, C. Dong, J. Fu, Y. Pan, A. Kobayashi, Y. Furusawa, T. Konishi, C. Shao, Both irradiated and bystander effects link with DNA repair capacity and the linear energy transfer, *Life Sciences*, 222 (2019) 228-234.
- [114] G. Olivieri, J. Bodycote, S. Wolff, Adaptive response of human lymphocytes to low concentrations of radioactive thymidine, *Science*, 223 (1984) 594.
- [115] Shahla Mohammadi, Mahnaz Taghavi-Dehaghani, Mohammad R. Gharaati, R. Masoomi, M. Ghiassi-Nejad., Adaptive response of blood lymphocytes of inhabitants residing in high background radiation areas of ramsar- micronuclei, apoptosis and comet assays., *J. Radiat. Res.*, 47 (2006) 279–285.

- [116] M. Ghiassi-nejad, S.M. Mortazavi, J.R. Cameron, A. Niroomand-rad, P.A. Karam, Very high background radiation areas of Ramsar, Iran: preliminary biological studies, *Health Phys*, 82 (2002) 87-93.
- [117] H. Gourabi, H. Mozdarani, A cytokinesis-blocked micronucleus study of the radioadaptive response of lymphocytes of individuals occupationally exposed to chronic doses of radiation., *Mutagenesis*, 13 (1998) 475-480.
- [118] H. Thierens, A. Vral, M. Barbé, M. Meijlaers, A. Baeyens, L.D. Ridder, Chromosomal radiosensitivity study of temporary nuclear workers and the support of the adaptive response induced by occupational exposure, *International Journal of Radiation Biology*, 78 (2002) 1117-1126.
- [119] L. Padovani, M. Appolloni, P. Anzidei, B. Tedeschi, D. Caporossi, P. Vernole, F. Mauro, Do human lymphocytes exposed to the fallout of the Chernobyl accident exhibit an adaptive response? 1. Challenge with ionizing radiation, *Mutation Research/Fundamental and Molecular Mechanisms of Mutagenesis*, 332 (1995) 33-38.
- [120] Neha Paraswani, Maikho Thoh, Hari N. Bhilwade, A. Ghosh., Early antioxidant responses through concerted activation of NF- κ B and Nrf2 characterize gamma radiation induced-adaptive response in quiescent human peripheral blood mononuclear cells, *Mutat Res Genet Toxicol Environ Mutagen.*, 831 (2018) 50-61.
- [121] E.G. Dimova, P.E. Bryant, S.G. Chankova, Adaptive response: some underlying mechanisms and open questions, *Genetics and Molecular Biology*, 31 (2008) 396-408.
- [122] S.M. Toprani, B. Das, Radio-adaptive response of base excision repair genes and proteins in human peripheral blood mononuclear cells exposed to gamma radiation, *Mutagenesis*, 30 (2015) 663-676.

- [123] S. Shelke, B. Das, Dose response and adaptive response of non-homologous end joining repair genes and proteins in resting human peripheral blood mononuclear cells exposed to γ radiation, *Mutagenesis*, 30 (2014) 365-379.
- [124] M.R. Wilkins, J.-C. Sanchez, A.A. Gooley, R.D. Appel, I. Humphery-Smith, D.F. Hochstrasser, K.L. Williams, Progress with Proteome Projects: Why all Proteins Expressed by a Genome Should be Identified and How To Do It, *Biotechnology and Genetic Engineering Reviews*, 13 (1996) 19-50.
- [125] C. Abdallah, E. Dumas-Gaudot, J. Renaut, K. Sergeant, Gel-Based and Gel-Free Quantitative Proteomics Approaches at a Glance, *International Journal of Plant Genomics*, 2012 (2012) 17.
- [126] S. Tapio, S. Hornhardt, M. Gomolka, D. Leszczynski, A. Posch, S. Thalhammer, M.J. Atkinson, Use of proteomics in radiobiological research: current state of the art, *Radiation and Environmental Biophysics*, 49 (2010) 1-4.
- [127] S.-E. Ong, M. Mann, Mass spectrometry-based proteomics turns quantitative, *Nature Chemical Biology*, 1 (2005) 252.
- [128] H. Baharvand, A. Fathi, D. van Hoof, G.H. Salekdeh, Concise Review: Trends in Stem Cell Proteomics, *STEM CELLS*, 25 (2007) 1888-1903.
- [129] L. Monteoliva, J.P. Albar, Differential proteomics: an overview of gel and non-gel based approaches, *Brief Funct Genomic Proteomic*, 3 (2004) 220-239.
- [130] A. Rogowska-Wrzesinska, M.C. Le Bihan, M. Thaysen-Andersen, P. Roepstorff, 2D gels still have a niche in proteomics, *J Proteomics*, 88 (2013) 4-13.
- [131] T. Rabilloud, C. Lelong, Two-dimensional gel electrophoresis in proteomics: A tutorial, *Journal of Proteomics*, 74 (2011) 1829-1841.

- [132] F. Chevalier, Highlights on the capacities of "Gel-based" proteomics, *Proteome science*, 8 (2010) 23-23.
- [133] T. Rabilloud, M. Chevallet, S. Luche, C. Lelong, Two-dimensional gel electrophoresis in proteomics: Past, present and future, *Journal of Proteomics*, 73 (2010) 2064-2077.
- [134] S. Beranova-Giorgianni, Proteome analysis by two-dimensional gel electrophoresis and mass spectrometry: strengths and limitations, *TrAC Trends in Analytical Chemistry*, 22 (2003) 273-281.
- [135] J.L. López, Two-dimensional electrophoresis in proteome expression analysis, *Journal of Chromatography B*, 849 (2007) 190-202.
- [136] P. Pomastowski, B. Buszewski, Two-dimensional gel electrophoresis in the light of new developments, *TrAC Trends in Analytical Chemistry*, 53 (2014) 167-177.
- [137] S. Garbis, G. Lubec, M. Fountoulakis, Limitations of current proteomics technologies, *Journal of Chromatography A*, 1077 (2005) 1-18.
- [138] B.M. Oliveira, J.R. Coorsen, D. Martins-de-Souza, 2DE: The Phoenix of Proteomics, *Journal of Proteomics*, 104 (2014) 140-150.
- [139] P. Meleady, Two-Dimensional Gel Electrophoresis and 2D-DIGE, in: K. Ohlendieck (Ed.) *Difference Gel Electrophoresis: Methods and Protocols*, Springer New York, New York, NY, 2018, pp. 3-14.
- [140] H.J. Issaq, T.D. Veenstra, Two-dimensional polyacrylamide gel electrophoresis (2D-PAGE): advances and perspectives, *BioTechniques*, 44 (2008) 697-700.
- [141] G. Arentz, F. Weiland, M.K. Oehler, P. Hoffmann, State of the art of 2D DIGE, *PROTEOMICS – Clinical Applications*, 9 (2015) 277-288.

- [142] K.S. Lilley, D.B. Friedman, All about DIGE: quantification technology for differential-display 2D-gel proteomics, *Expert Review of Proteomics*, 1 (2004) 401-409.
- [143] J. Minden, Comparative Proteomics and Difference Gel Electrophoresis, *BioTechniques*, 43 (2007) 739-745.
- [144] H. Baharvand, A. Fathi, D. van Hoof, G.H. Salekdeh, Concise Review: Trends in Stem Cell Proteomics, 2007.
- [145] T.J. Griffin, H. Xie, S. Bandhakavi, J. Popko, A. Mohan, J.V. Carlis, L. Higgins, iTRAQ reagent-based quantitative proteomic analysis on a linear ion trap mass spectrometer, *Journal of Proteome Research*, 6 (2007) 4200-4209.
- [146] N. Rauniyar, J.R. Yates, Isobaric Labeling-Based Relative Quantification in Shotgun Proteomics, *Journal of Proteome Research*, 13 (2014) 5293-5309.
- [147] O. Chahrour, D. Cobice, J. Malone, Stable isotope labelling methods in mass spectrometry-based quantitative proteomics, *Journal of Pharmaceutical and Biomedical Analysis*, 113 (2015) 2-20.
- [148] I.A. Brewis, P. Brennan, Chapter 1 - Proteomics technologies for the global identification and quantification of proteins, in: R. Donev (Ed.) *Advances in Protein Chemistry and Structural Biology*, Academic Press 2010, pp. 1-44.
- [149] M. Bantscheff, S. Lemeer, M.M. Savitski, B. Kuster, Quantitative mass spectrometry in proteomics: critical review update from 2007 to the present, *Analytical and Bioanalytical Chemistry*, 404 (2012) 939-965.
- [150] J.R. Wiśniewski, *Mass Spectrometry-Based Proteomics: Principles, Perspectives, and Challenges*, *Archives of Pathology & Laboratory Medicine*, 132 (2008) 1566-1569.

- [151] S.K. Van Riper, E.P. de Jong, J.V. Carlis, T.J. Griffin, Mass Spectrometry-Based Proteomics: Basic Principles and Emerging Technologies and Directions, in: D. Leszczynski (Ed.) Radiation Proteomics: The effects of ionizing and non-ionizing radiation on cells and tissues, Springer Netherlands, Dordrecht, 2013, pp. 1-35.
- [152] D. Lin, D.L. Tabb, J.R. Yates, Large-scale protein identification using mass spectrometry, *Biochimica et Biophysica Acta (BBA) - Proteins and Proteomics*, 1646 (2003) 1-10.
- [153] F. Xie, T. Liu, W.-J. Qian, V.A. Petyuk, R.D. Smith, Liquid chromatography-mass spectrometry-based quantitative proteomics, *The Journal of biological chemistry*, 286 (2011) 25443-25449.
- [154] M. Bantscheff, M. Schirle, G. Sweetman, J. Rick, B. Kuster, Quantitative mass spectrometry in proteomics: a critical review, *Analytical and Bioanalytical Chemistry*, 389 (2007) 1017-1031.
- [155] S.-E. Ong, B. Blagoev, I. Kratchmarova, D.B. Kristensen, H. Steen, A. Pandey, M. Mann, Stable Isotope Labeling by Amino Acids in Cell Culture, SILAC, as a Simple and Accurate Approach to Expression Proteomics, *Molecular & Cellular Proteomics*, 1 (2002) 376.
- [156] M. Mann, Functional and quantitative proteomics using SILAC, *Nature Reviews Molecular Cell Biology*, 7 (2006) 952.
- [157] W.A. Tao, R. Aebersold, Advances in quantitative proteomics via stable isotope tagging and mass spectrometry, *Curr Opin Biotechnol*, 14 (2003) 110-118.
- [158] P.L. Ross, Y.N. Huang, J.N. Marchese, B. Williamson, K. Parker, S. Hattan, N. Khainovski, S. Pillai, S. Dey, S. Daniels, S. Purkayastha, P. Juhasz, S. Martin, M.

- Bartlet-Jones, F. He, A. Jacobson, D.J. Pappin, Multiplexed Protein Quantitation in *Saccharomyces cerevisiae*; Using Amine-reactive Isobaric Tagging Reagents, *Molecular & Cellular Proteomics*, 3 (2004) 1154.
- [159] V.C. Wasinger, M. Zeng, Y. Yau, Current Status and Advances in Quantitative Proteomic Mass Spectrometry, *International Journal of Proteomics*, 2013 (2013) 12.
- [160] C. Evans, J. Noirel, S.Y. Ow, M. Salim, A.G. Pereira-Medrano, N. Couto, J. Pandhal, D. Smith, T.K. Pham, E. Karunakaran, X. Zou, C.A. Biggs, P.C. Wright, An insight into iTRAQ: where do we stand now?, *Analytical and Bioanalytical Chemistry*, 404 (2012) 1011-1027.
- [161] D.P.G. Brown, J. You, K.G. Bemis, M. Wang, T.J. Tegeler, Label-free mass spectrometry-based protein quantification technologies in proteomic analysis, *Briefings in Functional Genomics*, 7 (2008) 329-339.
- [162] D. Leszczynski, Radiation proteomics: A brief overview, *Proteomics*, 14 (2014) 481-488.
- [163] A. Monro, J. Mordenti, Expression of Exposure in Negative Carcinogenicity Studies: Dose/Body Weight, Dose/Body Surface Area, or Plasma Concentrations?, *Toxicologic Pathology*, 23 (1995) 187-198.
- [164] S. Koncarevic, C. Lossner, K. Kuhn, T. Prinz, I. Pike, H.D. Zucht, In-depth profiling of the peripheral blood mononuclear cells proteome for clinical blood proteomics, *Int J Proteomics*, 2014 (2014) 129259.
- [165] A. Turtoi, R.N. Sharan, A. Srivastava, F.H. Schneeweiss, Proteomic and genomic modulations induced by gamma-irradiation of human blood lymphocytes, *Int J Radiat Biol*, 86 (2010) 888-904.

- [166] A.S. A. Turtoi, R. N. Sharan, D. Oskamp, R. Hille, F. H. A. Schneeweiss, Early response of lymphocyte proteins after gamma-radiation, *Journal of Radioanalytical and Nuclear Chemistry*, 274 (2007) 435–439.
- [167] B.S. Skiöld S, Hellman U, Auer G, Näslund I, Low doses of γ -radiation induce consistent protein expression changes in human leukocytes, *Int. J. Low Radiation*, 8 (2011) 374-387.
- [168] C. Riccardi, I. Nicoletti, Analysis of apoptosis by propidium iodide staining and flow cytometry, *Nat Protoc*, 1 (2006) 1458-1461.
- [169] R.C. Chaubey, Computerized image analysis software for the comet assay, *Methods Mol Biol*, 291 (2005) 97-106.
- [170] K.J. Livak, T.D. Schmittgen, Analysis of relative gene expression data using real-time quantitative PCR and the $2^{-\Delta\Delta C(T)}$ Method, *Methods (San Diego, Calif.)*, 25 (2001) 402-408.
- [171] Y. Benjamini, Y. Hochberg, Controlling the False Discovery Rate: A Practical and Powerful Approach to Multiple Testing, *Journal of the Royal Statistical Society. Series B (Methodological)*, 57 (1995) 289-300.
- [172] D.W. Huang, B.T. Sherman, R.A. Lempicki, Bioinformatics enrichment tools: paths toward the comprehensive functional analysis of large gene lists, *Nucleic Acids Research*, 37 (2009) 1-13.
- [173] D.W. Huang, B.T. Sherman, R.A. Lempicki, Systematic and integrative analysis of large gene lists using DAVID bioinformatics resources, *Nature Protocols*, 4 (2008) 44.
- [174] D. Vergara, F. Chiriaco, R. Acierno, M. Maffia, Proteomic map of peripheral blood mononuclear cells, *Proteomics*, 8 (2008) 2045-2051.

- [175] E. Maes, B. Landuyt, I. Mertens, L. Schoofs, Interindividual variation in the proteome of human peripheral blood mononuclear cells, *PLoS One*, 8 (2013) e61933.
- [176] G. Van Belle, D.C. Martin, Sample Size as a Function of Coefficient of Variation and Ratio of Means, *The American Statistician*, 47 (1993) 165-167.
- [177] G.M. Silva, C. Vogel, Quantifying gene expression: the importance of being subtle, *Mol Syst Biol*, 12 (2016) 885.
- [178] I. Braga-Tanaka, S. Tanaka, A. Kohda, D. Takai, S. Nakamura, T. Ono, K. Tanaka, J.-i. Komura, Experimental studies on the biological effects of chronic low dose-rate radiation exposure in mice: overview of the studies at the Institute for Environmental Sciences, *International Journal of Radiation Biology*, 94 (2018) 423-433.
- [179] A.L. Brooks, D.G. Hoel, R.J. Preston, The role of dose rate in radiation cancer risk: evaluating the effect of dose rate at the molecular, cellular and tissue levels using key events in critical pathways following exposure to low LET radiation, *International Journal of Radiation Biology*, 92 (2016) 405-426.
- [180] W. Olipitz, D. Wiktor-Brown, J. Shuga, B. Pang, J. McFaline, P. Lonkar, A. Thomas, T. Mutamba James, S. Greenberger Joel, D. Samson Leona, C. Dedon Peter, C. Yanch Jacquelyn, P. Engelward Bevin, Integrated Molecular Analysis Indicates Undetectable Change in DNA Damage in Mice after Continuous Irradiation at ~ 400-fold Natural Background Radiation, *Environmental Health Perspectives*, 120 (2012) 1130-1136.
- [181] T. Nakajima, B. Wang, T. Ono, Y. Uehara, S. Nakamura, K. Ichinohe, I. Braga-Tanaka, III, S. Tanaka, K. Tanaka, M. Neno, Differences in sustained alterations in

protein expression between livers of mice exposed to high-dose-rate and low-dose-rate radiation, *Journal of Radiation Research*, 58 (2017) 421-429.

[182] K. Rothkamm, M. Lobrich, Evidence for a lack of DNA double-strand break repair in human cells exposed to very low x-ray doses, *Proc Natl Acad Sci U S A*, 100 (2003) 5057-5062.

[183] J.A. Siegel, M.G. Stabin, Radar commentary: Use of linear no-threshold hypothesis in radiation protection regulation in the United States, *Health Phys*, 102 (2012) 90-99.

[184] M. Tubiana, L.E. Feinendegen, C. Yang, J.M. Kaminski, The linear no-threshold relationship is inconsistent with radiation biologic and experimental data, *Radiology*, 251 (2009) 13-22.

[185] S. Jung, S. Lee, J. Lee, C. Li, J.-Y. Ohk, H.-K. Jeong, S. Lee, S. Kim, Y. Choi, S. Kim, H. Lee, M.-S. Lee, Protein expression pattern in response to ionizing radiation in MCF-7 human breast cancer cells, *Oncology letters*, 3 (2012) 147-154.

[186] S. Szkanderova, J. Vavrova, L. Hernychova, V. Neubauerova, J. Lenco, J. Stulik, Proteome alterations in gamma-irradiated human T-lymphocyte leukemia cells, *Radiat Res*, 163 (2005) 307-315.

[187] A.K. Cheema, R.S. Varghese, O. Timofeeva, L. Zhang, A. Kirilyuk, F. Zandkarimi, P. Kaur, H.W. Resson, M. Jung, A. Dritschilo, Functional proteomics analysis to study ATM dependent signaling in response to ionizing radiation, *Radiat Res*, 179 (2013) 674-683.

[188] A. Sriharshan, K. Boldt, H. Sarioglu, Z. Barjaktarovic, O. Azimzadeh, L. Hieber, H. Zitzelsberger, M. Ueffing, M.J. Atkinson, S. Tapio, Proteomic analysis by SILAC and

2D-DIGE reveals radiation-induced endothelial response: four key pathways, *J Proteomics*, 75 (2012) 2319-2330.

[189] A. Bajinskis, H. Lindegren, L. Johansson, M. Harms-Ringdahl, A. Forsby, Low-dose/dose-rate gamma radiation depresses neural differentiation and alters protein expression profiles in neuroblastoma SH-SY5Y cells and C17.2 neural stem cells, *Radiat Res*, 175 (2011) 185-192.

[190] F. Pluder, Z. Barjaktarovic, O. Azimzadeh, S. Mortl, A. Kramer, S. Steininger, H. Sarioglu, D. Leszczynski, R. Nylund, A. Hakanen, A. Sriharshan, M.J. Atkinson, S. Tapio, Low-dose irradiation causes rapid alterations to the proteome of the human endothelial cell line EA.hy926, *Radiat Environ Biophys*, 50 (2011) 155-166.

[191] L.E. Nylund R, Eklund E, Hakanen A and Leszczynski A The lack of acute effect of low-to-moderate-dose ionising radiation on endothelial proteome, *Int. J. Low Radiation.*, 9 (2013) 127-137.

[192] Z. Barjaktarovic, N. Anastasov, O. Azimzadeh, A. Sriharshan, H. Sarioglu, M. Ueffing, H. Tammio, A. Hakanen, D. Leszczynski, M.J. Atkinson, S. Tapio, Integrative proteomic and microRNA analysis of primary human coronary artery endothelial cells exposed to low-dose gamma radiation, *Radiat Environ Biophys*, 52 (2013) 87-98.

[193] O. Guipaud, V. Holler, V. Buard, G. Tarlet, N. Royer, J. Vinh, M. Benderitter, Time-course analysis of mouse serum proteome changes following exposure of the skin to ionizing radiation, *Proteomics*, 7 (2007) 3992-4002.

[194] T. Chaze, M.-C. Slomianny, F. Milliat, G. Tarlet, T. Lefebvre-Darroman, P. Gourmelon, E. Bey, M. Benderitter, J.-C. Michalski, O. Guipaud, Alteration of the serum

N-glycome of mice locally exposed to high doses of ionizing radiation, *Molecular & cellular proteomics* : MCP, 12 (2013) 283-301.

[195] T. Chaze, L. Hornez, C. Chambon, I. Haddad, J. Vinh, J.-P. Peyrat, M. Benderitter, O. Guipaud, Serum Proteome Analysis for Profiling Predictive Protein Markers Associated with the Severity of Skin Lesions Induced by Ionizing Radiation, *Proteomes*, 1 (2013).

[196] K.N. Rithidech, L. Honikel, R. Rieger, W. Xie, T. Fischer, S.R. Simon, Protein-expression profiles in mouse blood-plasma following acute whole-body exposure to ^{137}Cs γ rays, *International Journal of Radiation Biology*, 85 (2009) 432-447.

[197] B. Zhang, Y.-P. Su, G.-P. Ai, X.-H. Liu, F.-C. Wang, T.-M. Cheng, Differentially expressed proteins of gamma-ray irradiated mouse intestinal epithelial cells by two-dimensional electrophoresis and MALDI-TOF mass spectrometry, *World journal of gastroenterology*, 9 (2003) 2726-2731.

[198] Y.-B. Lim, B.-J. Pyun, H.-J. Lee, S.-R. Jeon, Y.B. Jin, Y.-S. Lee, Proteomic identification of radiation response markers in mouse intestine and brain, *Proteomics*, 11 (2011) 1254-1263.

[199] C. Menard, D. Johann, M. Lowenthal, T. Muanza, M. Sproull, S. Ross, J. Gulley, E. Petricoin, C.N. Coleman, G. Whiteley, L. Liotta, K. Camphausen, Discovering clinical biomarkers of ionizing radiation exposure with serum proteomic analysis, *Cancer Res*, 66 (2006) 1844-1850.

[200] R. Nylund, E. Lemola, S. Hartwig, S. Lehr, A. Acheva, J. Jahns, G. Hildebrandt, C. Lindholm, Profiling of low molecular weight proteins in plasma from locally irradiated individuals, *J Radiat Res*, 55 (2014) 674-682.

- [201] K. Jelonek, M. Pietrowska, P. Widlak, Systemic effects of ionizing radiation at the proteome and metabolome levels in the blood of cancer patients treated with radiotherapy: the influence of inflammation and radiation toxicity, *International Journal of Radiation Biology*, 93 (2017) 683-696.
- [202] A. Gurtler, M. Hauptmann, S. Pautz, U. Kulka, A.A. Friedl, S. Lehr, S. Hornhardt, M. Gomolka, The inter-individual variability outperforms the intra-individual variability of differentially expressed proteins prior and post irradiation in lymphoblastoid cell lines, *Arch Physiol Biochem*, 120 (2014) 198-207.
- [203] B. de Roos, S.J. Duthie, A.C. Polley, F. Mulholland, F.G. Bouwman, C. Heim, G.J. Rucklidge, I.T. Johnson, E.C. Mariman, H. Daniel, R.M. Elliott, Proteomic methodological recommendations for studies involving human plasma, platelets, and peripheral blood mononuclear cells, *J Proteome Res*, 7 (2008) 2280-2290.
- [204] P. de Lanerolle, Nuclear actin and myosins at a glance, *J Cell Sci*, 125 (2012) 4945-4949.
- [205] M.S. Poruchynsky, E. Komlodi-Pasztor, S. Trostel, J. Wilkerson, M. Regairaz, Y. Pommier, X. Zhang, T. Kumar Maity, R. Robey, M. Burotto, D. Sackett, U. Guha, A.T. Fojo, Microtubule-targeting agents augment the toxicity of DNA-damaging agents by disrupting intracellular trafficking of DNA repair proteins, *Proc Natl Acad Sci U S A*, 112 (2015) 1571-1576.
- [206] J. Zou, Y. Guo, T. Guettouche, D.F. Smith, R. Voellmy, Repression of Heat Shock Transcription Factor HSF1 Activation by HSP90 (HSP90 Complex) that Forms a Stress-Sensitive Complex with HSF1, *Cell*, 94 (1998) 471-480.

- [207] R.J. Kaufman, Stress signaling from the lumen of the endoplasmic reticulum: coordination of gene transcriptional and translational controls. , *Genes Dev*, 13 (1999) 1211–1233.
- [208] Z. Yu, H. Luo, W. Fu, M.P. Mattson, The endoplasmic reticulum stress-responsive protein GRP78 protects neurons against excitotoxicity and apoptosis: suppression of oxidative stress and stabilization of calcium homeostasis, *Exp Neurol*, 155 (1999) 302-314.
- [209] H. Liu, R.C. Bowes, 3rd, B. van de Water, C. Sillence, J.F. Nagelkerke, J.L. Stevens, Endoplasmic reticulum chaperones GRP78 and calreticulin prevent oxidative stress, Ca²⁺ disturbances, and cell death in renal epithelial cells, *J Biol Chem*, 272 (1997) 21751-21759.
- [210] G. Zhao, H. Lu, C. Li, Proapoptotic activities of protein disulfide isomerase (PDI) and PDIA3 protein, a role of the Bcl-2 protein Bak, *The Journal of biological chemistry*, 290 (2015) 8949-8963.
- [211] I. Jaadane, A. Nagbou, F. Behar-Cohen, A. Torriglia, Interaction of Leukocyte Elastase Inhibitor/L-DNase II with BCL-2 and BAX, *Biochimica et Biophysica Acta (BBA) - Molecular Cell Research*, 1843 (2014) 2807-2815.
- [212] Y. Hoshi, H. Tanooka, K. Miyazaki, H. Wakasugi, Induction of thioredoxin in human lymphocytes with low-dose ionizing radiation, *Biochim Biophys Acta*, 1359 (1997) 65-70.
- [213] S. Zhang, W. Wang, Q. Gu, J. Xue, H. Cao, Y. Tang, X. Xu, J. Cao, J. Zhou, J. Wu, W.Q. Ding, Protein and miRNA profiling of radiation-induced skin injury in rats:

the protective role of peroxiredoxin-6 against ionizing radiation, *Free Radic Biol Med*, 69 (2014) 96-107.

[214] S. Averaimo, R.H. Milton, M.R. Duchon, M. Mazzanti, Chloride intracellular channel 1 (CLIC1): Sensor and effector during oxidative stress, *FEBS Letters*, 584 (2010) 2076-2084.

[215] A. Minden, A. Lin, F.X. Claret, A. Abo, M. Karin, Selective activation of the JNK signaling cascade and c-Jun transcriptional activity by the small GTPases Rac and Cdc42Hs, *Cell*, 81 (1995) 1147-1157.

[216] B. Olofsson, Rho guanine dissociation inhibitors: pivotal molecules in cellular signalling, *Cell Signal*, 11 (1999) 545-554.

[217] A. Morin, F.P. Cordelieres, J. Cherfils, B. Olofsson, RhoGDI3 and RhoG: Vesicular trafficking and interactions with the Sec3 Exocyst subunit, *Small GTPases*, 1 (2010) 142-156.

[218] F. Canduri, D.M. dos Santos, R.G. Silva, M.A. Mendes, L.A. Basso, M.S. Palma, W.F. de Azevedo, D.S. Santos, Structures of human purine nucleoside phosphorylase complexed with inosine and ddI, *Biochem Biophys Res Commun*, 313 (2004) 907-914.

[219] S.A. Lee, A. Dritschilo, M. Jung, Impaired Ionizing Radiation-induced Activation of a Nuclear Signal Essential for Phosphorylation of c-Jun by Dually Phosphorylated c-Jun Amino-terminal Kinases in Ataxia Telangiectasia Fibroblasts, *Journal of Biological Chemistry*, 273 (1998) 32889-32894.

[220] A. Turtoi, F.H.A. Schneeweiss, Effect of ²¹¹At α -particle irradiation on expression of selected radiation responsive genes in human lymphocytes, *International Journal of Radiation Biology*, 85 (2009) 403-412.

- [221] A. Morales, M. Miranda, A. Sanchez-Reyes, A. Colell, A. Biete, J.C. Fernández-Checa, Transcriptional regulation of the heavy subunit chain of γ -glutamylcysteine synthetase by ionizing radiation, *FEBS Letters*, 427 (1998) 15-20.
- [222] G. St Laurent, D. Shtokalo, M.R. Tackett, Z. Yang, Y. Vyatkin, P.M. Milos, B. Seilheimer, T.A. McCaffrey, P. Kapranov, On the importance of small changes in RNA expression, *Methods*, 63 (2013) 18-24.
- [223] M. Christmann, B. Kaina, Transcriptional regulation of human DNA repair genes following genotoxic stress: trigger mechanisms, inducible responses and genotoxic adaptation, *Nucleic acids research*, 41 (2013) 8403-8420.
- [224] C. Abate, D. Luk, T. Curran, Transcriptional regulation by Fos and Jun in vitro: interaction among multiple activator and regulatory domains, *Molecular and cellular biology*, 11 (1991) 3624-3632.
- [225] T.D. Halazonetis, K. Georgopoulos, M.E. Greenberg, P. Leder, c-Jun dimerizes with itself and with c-Fos, forming complexes of different DNA binding affinities, *Cell*, 55 (1988) 917-924.
- [226] R.P. Ryseck, R. Bravo, c-JUN, JUN B, and JUN D differ in their binding affinities to AP-1 and CRE consensus sequences: effect of FOS proteins, *Oncogene*, 6 (1991) 533-542.
- [227] G. Manning, S. Kabacik, P. Finnon, S. Bouffler, C. Badie, High and low dose responses of transcriptional biomarkers in ex vivo X-irradiated human blood, *International Journal of Radiation Biology*, 89 (2013) 512-522.
- [228] D.A. Smirnov, M. Morley, E. Shin, R.S. Spielman, V.G. Cheung, Genetic analysis of radiation-induced changes in human gene expression, *Nature*, 459 (2009) 587.

- [229] G.E. Woloschak, C.-M. Chang-Liu, Differential Modulation of Specific Gene Expression Following High- and Low-LET Radiations, *Radiation Research*, 124 (1990) 183-187.
- [230] R. Datta, D.E. Hallahan, S.M. Kharbanda, E. Rubin, M.L. Sherman, E. Huberman, R.R. Weichselbaum, D.W. Kufe, Involvement of reactive oxygen intermediates in the induction of c-jun gene transcription by ionizing radiation, *Biochemistry*, 31 (1992) 8300-8306.
- [231] S. Zhang, W. Wang, Q. Gu, J. Xue, H. Cao, Y. Tang, X. Xu, J. Cao, J. Zhou, J. Wu, W.-Q. Ding, Protein and miRNA profiling of radiation-induced skin injury in rats: the protective role of peroxiredoxin-6 against ionizing radiation, *Free radical biology & medicine*, 69 (2014) 96-107.
- [232] Y. Wang, S.I. Feinstein, A.B. Fisher, Peroxiredoxin 6 as an antioxidant enzyme: protection of lung alveolar epithelial type II cells from H₂O₂-induced oxidative stress, *J Cell Biochem*, 104 (2008) 1274-1285.
- [233] A.J. Kee, N.S. Bryce, L. Yang, E. Polishchuk, G. Schevzov, R. Weigert, R. Polishchuk, P.W. Gunning, E.C. Hardeman, ER/Golgi trafficking is facilitated by unbranched actin filaments containing Tpm4.2, *Cytoskeleton (Hoboken)*, 74 (2017) 379-389.
- [234] A.S. Lee, Glucose-regulated proteins in cancer: molecular mechanisms and therapeutic potential, *Nat Rev Cancer*, 14 (2014) 263-276.
- [235] S. Sheibani, N.K. Jones, R. Eid, N. Gharib, N.T. Arab, V. Titorenko, H. Vali, P.A. Young, M.T. Greenwood, Inhibition of stress mediated cell death by human lactate dehydrogenase B in yeast, *FEMS Yeast Res*, 15 (2015) fov032.

- [236] P. Vedula, A. Kashina, The makings of the 'actin code': regulation of actin's biological function at the amino acid and nucleotide level, *Journal of Cell Science*, 131 (2018).
- [237] M. Roche, P. Rondeau, N.R. Singh, E. Tarnus, E. Bourdon, The antioxidant properties of serum albumin, *FEBS Letters*, 582 (2008) 1783-1787.
- [238] K.T. Park, C.-H. Yun, C.-S. Bae, T. Ahn, Decreased Level of Albumin in Peripheral Blood Mononuclear Cells of Streptozotocin-Induced Diabetic Rats, *The Journal of Veterinary Medical Science*, 76 (2014) 1087-1092.
- [239] J.J.-C. Lin, R.D. Eppinga, K.S. Warren, K.R. McCrae, Human Tropomyosin Isoforms in the Regulation of Cytoskeleton Functions, in: P. Gunning (Ed.) *Tropomyosin*, Springer New York, New York, NY, 2008, pp. 201-222.
- [240] S. Lou, A.H.G. Cleven, B. Balluff, M. de Graaff, M. Kostine, I. Briaire-de Bruijn, L.A. McDonnell, J.V.M.G. Bovée, High nuclear expression of proteasome activator complex subunit 1 predicts poor survival in soft tissue leiomyosarcomas, *Clinical Sarcoma Research*, 6 (2016) 17.
- [241] O. Loseva, E. Shubbar, S. Haghdooost, B. Evers, T. Helleday, M. Harms-Ringdahl, Chronic Low Dose Rate Ionizing Radiation Exposure Induces Premature Senescence in Human Fibroblasts that Correlates with Up Regulation of Proteins Involved in Protection against Oxidative Stress, *Proteomes*, 2 (2014).
- [242] B. Wang, M. Nenoï, T. Nakajima, I. Braga-Tanaka, III, K. Ichinohe, K. Tanaka, S. Tanaka, S. Nakamura, T. Ono, Y. Uehara, Differences in sustained alterations in protein expression between livers of mice exposed to high-dose-rate and low-dose-rate radiation, *Journal of Radiation Research*, 58 (2017) 421-429.

- [243] J.R. Masoomi, Sh. Mohammadi, M. Amini, M. Ghiassi-Nejad, High background radiation areas of Ramsar in Iran: evaluation of DNA damage by alkaline single cell gel electrophoresis (SCGE), *J Environ Radioact.*, 86 (2006) 176-186.
- [244] Q. Zhang, M. Matzke, A.A. Schepmoes, R.J. Moore, B.J. Webb-Robertson, Z. Hu, M.E. Monroe, W.J. Qian, R.D. Smith, W.F. Morgan, High and low doses of ionizing radiation induce different secretome profiles in a human skin model, *PLoS One*, 9 (2014) e92332.
- [245] M.S. Hengel, T.J. Aldrich, M.K. Waters, L. Pasa-Tolic, L.D. Stenoien, Quantitative Proteomic Profiling of Low-Dose Ionizing Radiation Effects in a Human Skin Model, *Proteomes*, 2 (2014).
- [246] K. Sekihara, K. Saitoh, H. Yang, H. Kawashima, S. Kazuno, M. Kikkawa, H. Arai, T. Miida, N. Hayashi, K. Sasai, Y. Tabe, Low-dose ionizing radiation exposure represses the cell cycle and protein synthesis pathways in in vitro human primary keratinocytes and U937 cell lines, *PLoS One*, 13 (2018) e0199117.
- [247] Z. Barjaktarovic, A. Shyla, O. Azimzadeh, S. Schulz, J. Haagen, W. Dörr, H. Sarioglu, M.J. Atkinson, H. Zischka, S. Tapio, Ionising radiation induces persistent alterations in the cardiac mitochondrial function of C57BL/6 mice 40weeks after local heart exposure, *Radiotherapy and Oncology*, 106 (2013) 404-410.
- [248] M.V. Bakshi, Z. Barjaktarovic, O. Azimzadeh, S.J. Kempf, J. Merl, S.M. Hauck, P. Eriksson, S. Buratovic, M.J. Atkinson, S. Tapio, Long-term effects of acute low-dose ionizing radiation on the neonatal mouse heart: a proteomic study, *Radiation and Environmental Biophysics*, 52 (2013) 451-461.

- [249] M. Pietrowska, J. Polańska, A. Walaszczyk, A. Wygoda, T. Rutkowski, K. Składowski, Ł. Marczak, M. Stobiecki, M. Marczyk, A. Polański, P. Widłak, Association between plasma proteome profiles analysed by mass spectrometry, a lymphocyte-based DNA-break repair assay and radiotherapy-induced acute mucosal reaction in head and neck cancer patients, *International Journal of Radiation Biology*, 87 (2011) 711-719.
- [250] P. Widłak, M. Pietrowska, J. Polańska, T. Rutkowski, K. Jelonek, M. Kalinowska-Herok, A. Gdowicz-Kłosok, A. Wygoda, R. Tarnawski, K. Składowski, Radiotherapy-related changes in serum proteome patterns of head and neck cancer patients; the effect of low and medium doses of radiation delivered to large volumes of normal tissue, *Journal of translational medicine*, 11 (2013) 299-299.
- [251] M. Pietrowska, K. Jelonek, J. Polanska, A. Wojakowska, L. Marczak, E. Chawinska, A. Chmura, W. Majewski, L. Miszczyk, P. Widlak, Partial-Body Irradiation in Patients with Prostate Cancer Treated with IMRT Has Little Effect on the Composition of Serum Proteome, *Proteomes*, 3 (2015) 117.
- [252] L. Wang, Y. Dai, S. Qi, B. Sun, J. Wen, L. Zhang, Z. Tu, Comparative proteome analysis of peripheral blood mononuclear cells in systemic lupus erythematosus with iTRAQ quantitative proteomics, *Rheumatology International*, 32 (2012) 585-593.
- [253] D. Cigna, C. D'Anna, C. Zizzo, D. Francofonte, I. Sorrentino, P. Colomba, G. Albeggiani, A. Armini, L. Bianchi, L. Bini, G. Duro, Alteration of proteomic profiles in PBMC isolated from patients with Fabry disease: preliminary findings, *Molecular BioSystems*, 9 (2013) 1162-1168.

- [254] E. Maes, D. Valkenburg, G. Baggerman, H. Willems, B. Landuyt, L. Schoofs, I. Mertens, Determination of variation parameters as a crucial step in designing TMT-based clinical proteomics experiments, *PLoS One*, 10 (2015) e0120115-e0120115.
- [255] S. Nishad, A. Ghosh, Dynamic changes in the proteome of human peripheral blood mononuclear cells with low dose ionizing radiation, *Mutat Res Genet Toxicol Environ Mutagen*, 797 (2016) 9-20.
- [256] S. Nishad, A. Ghosh, Comparative proteomic analysis of human peripheral blood mononuclear cells indicates adaptive response to low-dose radiation in individuals from high background radiation areas of Kerala, *Mutagenesis*, 33 (2018) 359-370.
- [257] J. Boucas, A. Riabinska, M. Jokic, G.S. Herter-Sprie, S. Chen, K. Höpker, H.C. Reinhardt, Posttranscriptional regulation of gene expression-adding another layer of complexity to the DNA damage response, *Front Genet*, 3 (2012) 159-159.
- [258] M. Dutertre, G. Sanchez, J. Barbier, L. Corcos, D. Auboeuf, The emerging role of pre-messenger RNA splicing in stress responses: Sending alternative messages and silent messengers, *RNA Biology*, 8 (2011) 740-747.
- [259] A. Wahba, M.C. Ryan, U.T. Shankavaram, K. Camphausen, P.J. Tofilon, Radiation-induced alternative transcripts as detected in total and polysome-bound mRNA, *Oncotarget*, 9 (2017) 691-705.
- [260] B. Adamson, A. Smogorzewska, F.D. Sigoillot, R.W. King, S.J. Elledge, A genome-wide homologous recombination screen identifies the RNA-binding protein RBMX as a component of the DNA-damage response, *Nature Cell Biology*, 14 (2012) 318-328.

- [261] B. Rogelj, L.E. Easton, G.K. Bogu, L.W. Stanton, G. Rot, T. Curk, B. Zupan, Y. Sugimoto, M. Modic, N. Haberman, J. Tollervery, R. Fujii, T. Takumi, C.E. Shaw, J. Ule, Widespread binding of FUS along nascent RNA regulates alternative splicing in the brain, *Scientific Reports*, 2 (2012) 603.
- [262] Q.-S. Zhang, L. Manche, R.-M. Xu, A.R. Krainer, hnRNP A1 associates with telomere ends and stimulates telomerase activity, *RNA*, 12 (2006) 1116-1128.
- [263] M. Salton, Y. Lerenthal, S.-Y. Wang, D.J. Chen, Y. Shiloh, Involvement of Matrin 3 and SFPQ/NONO in the DNA damage response, *Cell Cycle*, 9 (2010) 1568-1576.
- [264] S. Li, W.W. Kuhne, A. Kulharya, F.Z. Hudson, K. Ha, Z. Cao, W.S. Dynan, Involvement of p54(nrb), a PSF partner protein, in DNA double-strand break repair and radioresistance, *Nucleic acids research*, 37 (2009) 6746-6753.
- [265] C. Rajesh, D.K. Baker, A.J. Pierce, D.L. Pittman, The splicing-factor related protein SFPQ/PSF interacts with RAD51D and is necessary for homology-directed repair and sister chromatid cohesion, *Nucleic acids research*, 39 (2011) 132-145.
- [266] Maria P. Paronetto, B. Miñana, J. Valcárcel, The Ewing Sarcoma Protein Regulates DNA Damage-Induced Alternative Splicing, *Molecular Cell*, 43 (2011) 353-368.
- [267] Geeta J. Narlikar, R. Sundaramoorthy, T. Owen-Hughes, Mechanisms and Functions of ATP-Dependent Chromatin-Remodeling Enzymes, *Cell*, 154 (2013) 490-503.
- [268] C.K. Vilas, L.E. Emery, E.L. Denchi, K.M. Miller, Caught with One's Zinc Fingers in the Genome Integrity Cookie Jar, *Trends in Genetics*, 34 (2018) 313-325.
- [269] P. Dent, A. Yacoub, P.B. Fisher, M.P. Hagan, S. Grant, MAPK pathways in radiation responses, *Oncogene*, 22 (2003) 5885-5896.

- [270] A. Munshi, R. Ramesh, Mitogen-activated protein kinases and their role in radiation response, *Genes Cancer*, 4 (2013) 401-408.
- [271] D.E. Clapham, Calcium Signaling, *Cell*, 131 (2007) 1047-1058.
- [272] K. Burridge, M. Chrzanowska-Wodnicka, FOCAL ADHESIONS, CONTRACTILITY, AND SIGNALING, *Annual Review of Cell and Developmental Biology*, 12 (1996) 463-519.
- [273] H. Jyrki, K. Jarmo, Cellular Receptors of Extracellular Matrix Molecules, *Current Pharmaceutical Design*, 15 (2009) 1309-1317.
- [274] T.H. Lin, A.E. Aplin, Y. Shen, Q. Chen, M. Schaller, L. Romer, I. Aukhil, R.L. Juliano, Integrin-mediated activation of MAP kinase is independent of FAK: evidence for dual integrin signaling pathways in fibroblasts, *The Journal of Cell Biology*, 136 (1997) 1385-1395.
- [275] M.W. Renshaw, D. Toksoz, M.A. Schwartz, Involvement of the Small GTPase Rho in Integrin-mediated Activation of Mitogen-activated Protein Kinase, *Journal of Biological Chemistry*, 271 (1996) 21691-21694.
- [276] T. Velling, S. Nilsson, A. Stefansson, S. Johansson, beta1-Integrins induce phosphorylation of Akt on serine 473 independently of focal adhesion kinase and Src family kinases, *EMBO Rep*, 5 (2004) 901-905.
- [277] R. Che, J. Zhang, M. Nepal, B. Han, P. Fei, Multifaceted Fanconi Anemia Signaling, *Trends Genet*, 34 (2018) 171-183.
- [278] A. Datta, R.M. Brosh, Jr., Holding All the Cards-How Fanconi Anemia Proteins Deal with Replication Stress and Preserve Genomic Stability, *Genes (Basel)*, 10 (2019) 170.

- [279] M. Levitus, H. Joenje, J.P. de Winter, The Fanconi anemia pathway of genomic maintenance, *Cell Oncol*, 28 (2006) 3-29.
- [280] R. Sumpter, Jr., B. Levine, Emerging functions of the Fanconi anemia pathway at a glance, *Journal of Cell Science*, 130 (2017) 2657-2662.
- [281] V. Tripathi, H. Agarwal, S. Priya, H. Batra, P. Modi, M. Pandey, D. Saha, S.C. Raghavan, S. Sengupta, MRN complex-dependent recruitment of ubiquitylated BLM helicase to DSBs negatively regulates DNA repair pathways, *Nature Communications*, 9 (2018) 1016.
- [282] P.C. Bosch, M. Bogliolo, J. Surrallés, Activation of the Fanconi anemia/BRCA pathway at low doses of ionization radiation, *Mutation Research/Genetic Toxicology and Environmental Mutagenesis*, 793 (2015) 9-13.
- [283] A. Mohseni-Meybodi, H. Mozdarani, S. Mozdarani, DNA damage and repair of leukocytes from Fanconi anaemia patients, carriers and healthy individuals as measured by the alkaline comet assay, *Mutagenesis*, 24 (2008) 67-73.
- [284] M.C. Nowycky, A.P. Thomas, Intracellular calcium signaling, *Journal of Cell Science*, 115 (2002) 3715.
- [285] M.D. Bootman, *Calcium Signaling*, Cold Spring Harbor Perspectives in Biology, 4 (2012).
- [286] K. Valerie, A. Yacoub, M.P. Hagan, D.T. Curiel, P.B. Fisher, S. Grant, P. Dent, Radiation-induced cell signaling: inside-out and outside-in, *Mol Cancer Ther*, 6 (2007) 789-801.

- [287] A.L. Hein, M.M. Ouellette, Y. Yan, Radiation-induced signaling pathways that promote cancer cell survival (review), *International journal of oncology*, 45 (2014) 1813-1819.
- [288] Y.-L. Zhang, R.-C. Wang, K. Cheng, B.Z. Ring, L. Su, Roles of Rap1 signaling in tumor cell migration and invasion, *Cancer Biol Med*, 14 (2017) 90-99.
- [289] A.L. Carcagno, M.F. Ogara, S.V. Sonzogni, M.C. Marazita, P.F. Sirkin, J.M. Ceruti, E.T. Cánepa, E2F1 transcription is induced by genotoxic stress through ATM/ATR activation, *IUBMB Life*, 61 (2009) 537-543.
- [290] V. Pagliarini, P. Giglio, P. Bernardoni, D. De Zio, G.M. Fimia, M. Piacentini, M. Corazzari, Downregulation of E2F1 during ER stress is required to induce apoptosis, *Journal of Cell Science*, 128 (2015) 1166.
- [291] I. Thurlings, L.M. Martínez-López, B. Westendorp, M. Zijp, R. Kuiper, P. Tooten, L.N. Kent, G. Leone, H.J. Vos, B. Burgering, A. de Bruin, Synergistic functions of E2F7 and E2F8 are critical to suppress stress-induced skin cancer, *Oncogene*, 36 (2017) 829-839.
- [292] S.B. McMahon, H.A. Van Buskirk, K.A. Dugan, T.D. Copeland, M.D. Cole, The Novel ATM-Related Protein TRRAP Is an Essential Cofactor for the c-Myc and E2F Oncoproteins, *Cell*, 94 (1998) 363-374.
- [293] Y.Y. Lee, Y.B. Yu, H.P. Gunawardena, L. Xie, X. Chen, BCLAF1 is a radiation-induced H2AX-interacting partner involved in γ H2AX-mediated regulation of apoptosis and DNA repair, *Cell Death Dis*, 3 (2012) e359-e359.

- [294] C.E. Hellweg, L.F. Spitta, B. Henschenmacher, S. Diegeler, C. Baumstark-Khan, Transcription Factors in the Cellular Response to Charged Particle Exposure, *Frontiers in oncology*, 6 (2016) 61-61.
- [295] A.X. Fan, G.L. Papadopoulos, M.A. Hossain, I.J. Lin, J. Hu, T.M. Tang, M.S. Kilberg, R. Renne, J. Strouboulis, J. Bungert, Genomic and proteomic analysis of transcription factor TFII-I reveals insight into the response to cellular stress, *Nucleic acids research*, 42 (2014) 7625-7641.
- [296] Y. Bu, L. Gao, I.H. Gelman, Role for transcription factor TFII-I in the suppression of SSeCKS/Gravin/Akap12 transcription by Src, *Int J Cancer*, 128 (2011) 1836-1842.
- [297] A.L. Roy, Pathophysiology of TFII-I: Old Guard Wearing New Hats, *Trends Mol Med*, 23 (2017) 501-511.
- [298] E. Zoidis, I. Seremelis, N. Kontopoulos, G.P. Danezis, Selenium-Dependent Antioxidant Enzymes: Actions and Properties of Selenoproteins, *Antioxidants (Basel)*, 7 (2018) 66.
- [299] K.M. Brown, J.R. Arthur, Selenium, selenoproteins and human health: a review, *Public Health Nutrition*, 4 (2001) 593-599.
- [300] H. Ali Khan, B. Mutus, Protein disulfide isomerase a multifunctional protein with multiple physiological roles, *Front Chem*, 2 (2014) 70-70.
- [301] V.K. Kodali, C. Thorpe, Oxidative Protein Folding and the Quiescin–Sulfhydryl Oxidase Family of Flavoproteins, *Antioxidants & Redox Signaling*, 13 (2010) 1217-1230.

APPENDIX

Appendix A

Accession No	Protein Description	Peptide Matches	Protein % Coverage	Group II			Group III			Group IV		
				Mean FC	SD	Adj. P-value	Mean FC	SD	Adj. P-value	Mean FC	SD	Adj. P-value
1433Z_HUMAN	14-3-3 protein zeta/delta	12	20.8	1.46	0.05	<0.001	1.71	0.02	<0.001	1.32	0.03	<0.001
2A5B_HUMAN	Serine/threonine-protein phosphatase 2A 56 kDa regulatory subunit beta isoform	5	9.5	1.57	0.05	<0.001	1.9	0.03	<0.001	1.42	0.01	<0.001
3BP1_HUMAN	SH3 domain-binding protein 1	12	21.7	1.46	0.13	0.005	1.73	0.04	<0.001	1.29	0	<0.001
A1CF_HUMAN	APOBEC1 complementation factor	7	15.8	1.78	0.05	<0.001	2.58	0.05	<0.001	1.97	0.1	0.001
AAK1_HUMAN	AP2-associated protein kinase 1	4	5.3	1.76	0.25	0.009	2.13	0.27	0.003	1.8	0.37	0.046
ACHA4_HUMAN	Neuronal acetylcholine receptor subunit alpha-4	3	6.1	1.4	0.06	<0.001	1.59	0.13	0.003	1.26	0.04	0.002
ACINU_HUMAN	Apoptotic chromatin condensation inducer in the nucleus	8	3	1.43	0.01	<0.001	1.74	0.11	0.001	1.33	0.08	0.008
ACTB_HUMAN	Actin; cytoplasmic 1	36	35.2	1.51	0.07	<0.001	1.25	0.01	<0.001	0.83	0.02	0.001
ACTN1_HUMAN	Alpha-actinin-1	11	14.3	1.48	0.04	<0.001	1.7	0.03	<0.001	1.21	0.06	0.012
ADA22_HUMAN	Disintegrin and metalloproteinase domain-containing protein 22	9	6.7	1.42	0.01	<0.001	1.69	0.01	<0.001	1.22	0.02	<0.001
ADCK2_HUMAN	Uncharacterized aarF domain-containing protein kinase 2	2	5.1	1.58	0.34	0.051	2.37	0.77	0.046	2.15	1.12	0.213
ADCY1_HUMAN	Adenylate cyclase type 1	6	8	1.45	0.02	<0.001	1.73	0.06	<0.001	1.31	0.04	0.001
ADCY2_HUMAN	Adenylate cyclase type 2	3	5.6	2.39	1	0.086	2.91	1.52	0.109	2.9	1.91	0.225
ADIPO_HUMAN	Adiponectin	4	28.3	1.43	0.04	<0.001	1.95	0.36	0.015	1.52	0.31	0.082
AEBP2_HUMAN	Zinc finger protein AEBP2	3	14.1	1.55	0.02	<0.001	1.64	0	<0.001	1.12	0.04	0.023
AGO3_HUMAN	Protein argonaute-3	6	6.7	1.42	0.02	<0.001	1.59	0.01	<0.001	1.18	0.01	<0.001
AGRB2_HUMAN	Adhesion G protein-coupled receptor B2	7	6.5	1.51	0.09	0.001	1.46	0.1	0.002	1.07	0.13	0.485
AGRB3_HUMAN	Adhesion G protein-coupled receptor B3	4	4.4	1.25	0.32	0.272	1.58	0.17	0.006	1.27	0.21	0.140
AHNK_HUMAN	Neuroblast differentiation-associated protein AHNAK	17	3.1	1.35	0.08	0.002	1.5	0.14	0.006	1	0.16	0.977
AKAP9_HUMAN	A-kinase anchor protein 9	13	4.6	1.52	0.08	0.001	1.78	0.13	0.001	1.31	0.14	0.043
AKNA_HUMAN	AT-hook-containing transcription factor	4	3.6	1.51	0.17	0.010	1.93	0.09	<0.001	1.44	0.11	0.008
ALDOA_HUMAN	Fructose-bisphosphate aldolase A	5	12.9	1.74	0.02	<0.001	2.12	0.02	<0.001	1.59	0.13	0.006
ALK_HUMAN	ALK tyrosine kinase receptor	11	7.3	1.45	0.01	<0.001	1.77	0.04	<0.001	1.38	0.04	0.001

ALPK3_HUMAN	Alpha-protein kinase 3	6	3.3	1.49	0.04	<0.001	1.74	0.01	<0.001	1.31	0.01	<0.001
AMOL2_HUMAN	Angiotensin-like protein 2	7	18	1.56	0.05	<0.001	1.79	0.05	<0.001	1.27	0.11	0.037
ANK2_HUMAN	Ankyrin-2	14	5.1	1.49	0.04	<0.001	1.75	0.12	0.001	1.38	0.12	0.015
ANK3_HUMAN	Ankyrin-3	15	4.3	1.49	0.02	<0.001	1.84	0.1	<0.001	1.38	0.08	0.006
ANR33_HUMAN	Ankyrin repeat domain-containing protein 33	5	26.5	1.48	0.06	<0.001	1.58	0.36	0.057	1.11	0.28	0.622
APBA1_HUMAN	Amyloid beta A4 precursor protein-binding family A member 1	4	7.9	1.34	0.16	0.028	1.4	0.2	0.033	1.13	0.02	0.001
APC_HUMAN	Adenomatous polyposis coli protein	19	9.7	1.4	0.04	<0.001	1.44	0.19	0.022	1.04	0.2	0.808
APC2_HUMAN	Adenomatous polyposis coli protein 2	4	6.9	1.46	0.01	<0.001	1.63	0.03	<0.001	1.22	0.01	<0.001
APEX2_HUMAN	DNA-(apurinic or apyrimidinic site) lyase 2	2	6	1.4	0.09	0.002	1.62	0.01	<0.001	1.02	0.07	0.679
APOE_HUMAN	Apolipoprotein E	2	9.1	1.39	0.12	0.008	1.86	0.09	<0.001	1.36	0.27	0.135
AR6P4_HUMAN	ADP-ribosylation factor-like protein 6-interacting protein 4	7	10.9	1.56	0.08	0.001	1.24	0.47	0.451	1.05	0.18	0.706
ARAP1_HUMAN	Arf-GAP with Rho-GAP domain; ANK repeat and PH domain-containing protein 1	5	3	1.5	0.07	<0.001	1.7	0.03	<0.001	1.26	0.02	<0.001
ARBK1_HUMAN	Beta-adrenergic receptor kinase 1	7	9.7	1.61	0.09	<0.001	1.92	0.05	<0.001	1.45	0.01	<0.001
ARHG2_HUMAN	Rho guanine nucleotide exchange factor 2	5	7.8	1.4	0.15	0.012	1.29	0.22	0.096	0.89	0.24	0.558
ARHG5_HUMAN	Rho guanine nucleotide exchange factor 5	7	3.8	1.51	0.12	0.002	1.88	0.08	<0.001	1.34	0	<0.001
ARHG1_HUMAN	Rho guanine nucleotide exchange factor 18	5	3.8	1.23	0.13	0.052	1.4	0.19	0.027	1.15	0.01	<0.001
ARI1A_HUMAN	AT-rich interactive domain-containing protein 1A	26	17	1.23	0.24	0.189	1.49	0.07	0.001	1.08	0	<0.001
ARI1B_HUMAN	AT-rich interactive domain-containing protein 1B	27	8.3	1.48	0.01	<0.001	1.76	0.06	<0.001	1.3	0.05	0.003
ARI3A_HUMAN	AT-rich interactive domain-containing protein 3A	6	16.9	1.56	0	<0.001	1.74	0.01	<0.001	1.25	0.02	<0.001
ARVC_HUMAN	Armadillo repeat protein deleted in velo-cardio-facial syndrome	5	7.9	1.65	0.21	0.009	2.02	0.12	<0.001	1.64	0.06	0.001
ASB1_HUMAN	Ankyrin repeat and SOCS box protein 1	8	12.2	1.42	0.07	0.001	1.67	0.23	0.011	1.21	0.26	0.313
ASH1L_HUMAN	Histone-lysine N-methyltransferase ASH1L	8	2.8	1.27	0.26	0.157	1.61	0.06	<0.001	1.15	0.01	<0.001
ASXL1_HUMAN	Putative Polycomb group protein ASXL1	9	9.5	1.44	0.03	<0.001	1.6	0.06	<0.001	1.17	0.14	0.163
AT10A_HUMAN	Probable phospholipid-transporting ATPase VA	8	5.9	1.42	0.02	<0.001	1.56	0.04	<0.001	1.12	0.03	0.008
AT132_HUMAN	Probable cation-transporting ATPase 13A2	3	3.2	1.25	0.26	0.193	1.57	0.04	<0.001	1.24	0.18	0.142
ATAD5_HUMAN	ATPase family AAA domain-containing protein 5	11	5.4	1.46	0.02	<0.001	1.66	0.12	0.001	1.22	0.12	0.071
ATMIN_HUMAN	ATM interactor	6	7.8	1.5	0.02	<0.001	1.89	0.06	<0.001	1.47	0.05	0.001

ATP7A_HUMAN	Copper-transporting ATPase 1	6	4.1	1.5	0.09	0.001	1.81	0.25	0.007	1.34	0.22	0.103
ATPB_HUMAN	ATP synthase subunit beta; mitochondrial	5	8.5	1.45	0.05	<0.001	1.56	0	<0.001	1.18	0.04	0.004
ATR_HUMAN	Serine/threonine-protein kinase ATR	19	3.2	1.53	0	<0.001	1.88	0.05	<0.001	1.46	0.02	<0.001
ATRX_HUMAN	Transcriptional regulator ATRX	7	3.9	1.53	0.14	0.003	1.73	0.24	0.009	1.29	0.19	0.099
AURKB_HUMAN	Aurora kinase B	4	7.8	1.45	0.05	<0.001	1.77	0.07	<0.001	1.39	0.06	0.002
AXIN2_HUMAN	Axin-2	9	4.5	1.45	0.03	<0.001	1.56	0.03	<0.001	1.1	0.03	0.017
BAG3_HUMAN	BAG family molecular chaperone regulator 3	9	14.1	1.39	0	<0.001	1.8	0.06	<0.001	1.44	0.21	0.049
BAIP2_HUMAN	Brain-specific angiogenesis inhibitor 1-associated protein 2	5	13.6	1.3	0.24	0.106	1.69	0.11	0.001	1.55	0.31	0.076
BC11A_HUMAN	B-cell lymphoma/leukemia 11A	5	7.5	1.32	0.04	<0.001	1.3	0.04	0.001	0.92	0.07	0.160
BCAS3_HUMAN	Breast carcinoma-amplified sequence 3	4	8.3	1.68	0.2	0.006	2.18	0.47	0.017	1.59	0.24	0.034
BCKD_HUMAN	[3-methyl-2-oxobutanoate dehydrogenase [lipoamide]] kinase; mitochondrial	6	6.8	1.4	0.01	<0.001	1.32	0.08	0.004	0.91	0.04	0.053
BCL9_HUMAN	B-cell CLL/lymphoma 9 protein	12	15.1	0.7	0.22	0.085	1.53	0.18	0.011	0.98	0.52	0.951
BCL9L_HUMAN	B-cell CLL/lymphoma 9-like protein	18	9.1	1.38	0.13	0.009	1.69	0.03	<0.001	1.24	0.01	<0.001
BD1L1_HUMAN	Biorientation of chromosomes in cell division protein 1-like 1	8	3	1.39	0.01	<0.001	1.67	0.01	<0.001	1.24	0.02	<0.001
BIRC6_HUMAN	Baculoviral IAP repeat-containing protein 6	7	1.8	1.57	0.01	<0.001	1.81	0.13	0.001	1.33	0.11	0.020
BLM_HUMAN	Bloom syndrome protein	7	3.7	2.37	0.87	0.063	3.83	1.74	0.058	4.12	2.46	0.148
BORG5_HUMAN	Cdc42 effector protein 1	5	21.2	1.42	0.05	<0.001	1.5	0.01	<0.001	1.03	0.02	0.111
BPTF_HUMAN	Nucleosome-remodeling factor subunit BPTF	7	3.4	1.38	0.01	<0.001	1.83	0.08	<0.001	1.32	0.09	0.013
BRSK1_HUMAN	Serine/threonine-protein kinase BRSK1	5	15	1.33	0.19	0.044	1.58	0.19	0.010	1.12	0.19	0.434
BRSK2_HUMAN	Serine/threonine-protein kinase BRSK2	5	2.3	1.47	0.07	0.001	1.52	0.15	0.006	1.09	0.03	0.012
BRWD1_HUMAN	Bromodomain and WD repeat-containing protein 1	11	4.4	1.46	0.05	<0.001	1.74	0.04	<0.001	1.3	0.02	<0.001
BRWD3_HUMAN	Bromodomain and WD repeat-containing protein 3	4	3.5	1.33	0.15	0.023	1.77	0.06	<0.001	1.32	0	<0.001
BTBD6_HUMAN	BTB/POZ domain-containing protein 6	3	8.9	1.07	0.5	0.834	1.55	0.19	0.011	1.85	0.6	0.122
BZW2_HUMAN	Basic leucine zipper and W2 domain-containing protein 2	1	4.5	1.5	0.01	<0.001	1.83	0.37	0.024	1.37	0.38	0.231
CAB39_HUMAN	Calcium-binding protein 39	5	13.5	1.43	0.06	<0.001	1.72	0	<0.001	1.23	0.02	0.001
CAF1B_HUMAN	Chromatin assembly factor 1 subunit B	5	7	1.37	0.03	<0.001	1.53	0.09	0.001	1.12	0.03	0.005
CALM_HUMAN	Calmodulin OS=Homo sapiens GN=CALM1 PE=1 SV=2	12	33.6	0.74	0.08	0.008	0.87	0.59	0.742	0.7	0.48	0.420

CALR_HUMAN	Calreticulin	4	12.9	1.48	0.01	<0.001	1.62	0.13	0.002	1.18	0.16	0.181
CAMP3_HUMAN	Calmodulin-regulated spectrin-associated protein 3	9	4.7	1.42	0.01	<0.001	1.51	0.16	0.008	1.02	0.13	0.808
CAN2_HUMAN	Calpain-2 catalytic subunit	4	3.7	1.5	0	<0.001	1.63	0.01	<0.001	1.27	0.13	0.047
CAN3_HUMAN	Calpain-3	2	3	1.5	0.12	0.002	1.75	0.1	0.001	1.24	0.01	<0.001
CASC3_HUMAN	Protein CASC3	7	10.5	1.17	0.23	0.296	1.58	0.22	0.015	1.21	0.11	0.063
CATIN_HUMAN	Cactin	3	5.3	1.61	0.09	<0.001	1.82	0.1	<0.001	1.42	0.01	<0.001
CBX6_HUMAN	Chromobox protein homolog 6	4	10	1.35	0.11	0.008	1.61	0.43	0.083	1.13	0.41	0.681
CC14A_HUMAN	Dual specificity protein phosphatase CDC14A	7	17.3	1.45	0.02	<0.001	1.86	0.01	<0.001	1.74	0.26	0.021
CD19_HUMAN	B-lymphocyte antigen CD19	2	2.9	1.26	0.21	0.111	1.39	0.21	0.041	1.02	0.1	0.798
CD2B2_HUMAN	CD2 antigen cytoplasmic tail-binding protein 2	2	2.3	1.34	0.09	0.005	1.8	0.02	<0.001	1.55	0.27	0.051
CD44_HUMAN	CD44 antigen	1	1.3	0.83	0.39	0.515	1.21	0.14	0.072	0.98	0.23	0.903
CDC5L_HUMAN	Cell division cycle 5-like protein	5	6.7	1.36	0.03	<0.001	1.58	0.05	<0.001	1.17	0.03	0.002
CDHR5_HUMAN	Cadherin-related family member 5	4	5.2	1.4	0.04	<0.001	1.7	0.02	<0.001	1.26	0.04	0.002
CDK12_HUMAN	Cyclin-dependent kinase 12	4	3.2	1.41	0.14	0.010	1.56	0.18	0.009	1.15	0.1	0.118
CDKL5_HUMAN	Cyclin-dependent kinase-like 5	4	5	1.16	0.25	0.366	1.62	0.15	0.004	0.89	0.15	0.356
CDN1A_HUMAN	Cyclin-dependent kinase inhibitor 1	1	17.7	1.31	0.08	0.003	1.63	0.05	<0.001	1.22	0.02	<0.001
CDSN_HUMAN	Corneodesmosin	5	7.9	1.47	0.25	0.036	1.34	0.13	0.016	1.11	0.33	0.658
CECR2_HUMAN	Cat eye syndrome critical region protein 2	11	6.9	1.42	0.07	0.001	1.71	0.11	0.001	1.28	0.08	0.012
CELR1_HUMAN	Cadherin EGF LAG seven-pass G-type receptor 1	8	3.7	1.45	0.02	<0.001	1.77	0.2	0.004	1.33	0.1	0.015
CHD7_HUMAN	Chromodomain-helicase-DNA-binding protein 7	9	5	1.42	0.07	0.001	1.64	0.29	0.024	1.17	0.22	0.320
CHD8_HUMAN	Chromodomain-helicase-DNA-binding protein 8	5	3.4	1.35	0.26	0.093	1.79	0.18	0.003	1.39	0.16	0.034
CHK1_HUMAN	Serine/threonine-protein kinase Chk1	3	12.8	1.32	0.19	0.054	1.48	0.16	0.010	1.14	0.1	0.141
CHP2_HUMAN	Calcineurin B homologous protein 2	2	17.9	1.74	0.21	0.005	2.31	0.4	0.007	1.88	0.45	0.058
CHST4_HUMAN	Carbohydrate sulfotransferase 4	1	3.6	1.2	0.43	0.489	1.64	0.09	0.001	1.47	0.12	0.009
CLAP1_HUMAN	CLIP-associating protein 1	15	8.1	1.44	0.15	0.010	1.79	0.09	<0.001	1.34	0.1	0.012
CLAP2_HUMAN	CLIP-associating protein 2	15	14.6	1.4	0.03	<0.001	1.62	0.03	<0.001	1.15	0.04	0.008
CLK3_HUMAN	Dual specificity protein kinase CLK3	5	2.8	1.37	0.23	0.057	1.55	0.26	0.028	1.14	0.18	0.325
CNOT1_HUMAN	CCR4-NOT transcription complex subunit 1	12	2	1.73	0.08	<0.001	2.08	0.18	0.001	1.68	0.2	0.014

CNT3B_HUMAN	Contactin-associated protein-like 3B	3	3.3	0.95	0.28	0.780	1.09	0.13	0.308	0.58	0.25	0.080
CNTN5_HUMAN	Contactin-5	3	4.6	1.75	0.34	0.024	1.75	0.31	0.018	1.29	0.32	0.260
CNTN6_HUMAN	Contactin-6	3	3.8	1.38	0.02	<0.001	1.52	0.09	0.001	1.11	0.16	0.395
CNTP3_HUMAN	Contactin-associated protein-like 3	7	6	1.48	0.01	<0.001	1.74	0.1	0.001	1.27	0.06	0.006
CO1A1_HUMAN	Collagen alpha-1(I) chain	15	18.8	1.38	0.01	<0.001	1.49	0.08	0.001	1.13	0.06	0.050
CO1A2_HUMAN	Collagen alpha-2(I) chain	23	30.8	1.41	0.03	<0.001	1.59	0.06	<0.001	1.18	0.05	0.013
CO3A1_HUMAN	Collagen alpha-1(III) chain	13	21.7	1.84	0.13	0.001	2.06	0.07	<0.001	1.73	0.12	0.002
CO4A1_HUMAN	Collagen alpha-1(IV) chain	6	6.5	1.38	0.08	0.001	1.38	0.16	0.021	0.86	0.23	0.413
CO4A2_HUMAN	Collagen alpha-2(IV) chain	21	15.7	1.37	0.02	<0.001	1.77	0.14	0.002	1.27	0.07	0.008
CO4A3_HUMAN	Collagen alpha-3(IV) chain	18	15	1.44	0.03	<0.001	1.65	0.06	<0.001	1.22	0.07	0.014
CO4A4_HUMAN	Collagen alpha-4(IV) chain	21	21.6	1.68	0.11	0.001	1.76	0.15	0.002	1.35	0.25	0.126
CO4A5_HUMAN	Collagen alpha-5(IV) chain	16	13	1.28	0.15	0.039	1.2	0.26	0.280	0.87	0.08	0.085
CO4A6_HUMAN	Collagen alpha-6(IV) chain	16	14.8	1.32	0.23	0.089	1.72	0.02	<0.001	1.33	0.03	<0.001
CO5A1_HUMAN	Collagen alpha-1(V) chain	9	9.4	1.39	0.03	<0.001	1.57	0.1	0.001	1.13	0	<0.001
CO5A2_HUMAN	Collagen alpha-2(V) chain	18	18.3	1.18	0.09	0.028	1.54	0.05	<0.001	1.14	0.09	0.088
CO5A3_HUMAN	Collagen alpha-3(V) chain	14	12.3	1.45	0	<0.001	1.6	0.02	<0.001	1.16	0.04	0.006
CO6A2_HUMAN	Collagen alpha-2(VI) chain	5	7.1	1.63	0.03	<0.001	2.01	0.17	0.001	1.57	0.11	0.004
CO6A3_HUMAN	Collagen alpha-3(VI) chain	8	3.2	1.4	0.02	<0.001	1.5	0.02	<0.001	1.06	0.05	0.186
CO6A5_HUMAN	Collagen alpha-5(VI) chain	9	4.8	1.5	0.01	<0.001	1.7	0.03	<0.001	1.31	0.01	<0.001
CO6A6_HUMAN	Collagen alpha-6(VI) chain	9	5.6	1.46	0	<0.001	1.59	0.02	<0.001	1.19	0.02	0.001
CO7A1_HUMAN	Collagen alpha-1(VII) chain	28	13.8	1.5	0.06	<0.001	1.69	0.06	<0.001	1.23	0.04	0.003
CO8A2_HUMAN	Collagen alpha-2(VIII) chain	5	9.2	1.05	0.38	0.832	1.8	0.35	0.023	1.55	0.14	0.009
CO9A1_HUMAN	Collagen alpha-1(IX) chain	12	24.1	1.42	0.08	0.001	1.7	0.17	0.004	1.18	0.19	0.245
CO9A2_HUMAN	Collagen alpha-2(IX) chain	7	25	1.43	0.03	<0.001	1.64	0	<0.001	1.26	0	<0.001
COBA1_HUMAN	Collagen alpha-1(XI) chain	15	15.4	1.46	0.08	0.001	1.51	0.03	<0.001	1.12	0	<0.001
COBL1_HUMAN	Cordon-bleu protein-like 1	9	6.9	1.19	0.28	0.341	1.64	0.24	0.015	1.26	0.18	0.110
COCA1_HUMAN	Collagen alpha-1(XII) chain	6	2.3	1.43	0.06	<0.001	1.48	0.05	<0.001	1.14	0.03	0.003
COE4_HUMAN	Transcription factor COE4	8	7.5	1.59	0.05	<0.001	1.71	0.06	<0.001	1.3	0.07	0.006

COEA1_HUMAN	Collagen alpha-1(XIV) chain	6	3.3	1.33	0.15	0.026	1.35	0.26	0.094	0.95	0.23	0.764
COFA1_HUMAN	Collagen alpha-1(XV) chain	5	3.3	1.31	0.28	0.144	1.56	0.25	0.023	1.15	0.2	0.338
COGA1_HUMAN	Collagen alpha-1(XVI) chain	15	8.7	1.47	0	<0.001	1.79	0.06	<0.001	1.37	0.02	<0.001
COHA1_HUMAN	Collagen alpha-1(XVII) chain	11	10.6	1.41	0.01	<0.001	1.79	0.17	0.003	1.35	0.08	0.008
COIA1_HUMAN	Collagen alpha-1(XVIII) chain	12	10.5	1.45	0.05	<0.001	1.66	0.03	<0.001	1.18	0.03	0.002
COJA1_HUMAN	Collagen alpha-1(XIX) chain	6	7.7	1.32	0	<0.001	1.61	0.01	<0.001	1.21	0.04	0.003
CORA1_HUMAN	Collagen alpha-1(XXVII) chain	26	18	1.44	0.01	<0.001	1.68	0.03	<0.001	1.26	0.01	<0.001
COSA1_HUMAN	Collagen alpha-1(XXVIII) chain	9	8.3	1.44	0.01	<0.001	1.42	0.23	0.040	0.99	0.19	0.951
CSN5_HUMAN	COP9 signalosome complex subunit 5	3	7.5	1.53	0.07	<0.001	1.6	0.06	<0.001	1.2	0.04	0.005
CTND1_HUMAN	Catenin delta-1	6	12.7	1.41	0.01	<0.001	1.62	0.09	0.001	1.16	0.07	0.038
CTND2_HUMAN	Catenin delta-2	11	5.9	1.51	0.1	0.001	1.55	0.07	<0.001	1.06	0.06	0.243
CTTB2_HUMAN	Cortactin-binding protein 2	5	2.9	1.32	0.08	0.003	1.43	0.28	0.068	0.99	0.17	0.939
CUL2_HUMAN	Cullin-2	4	7.7	1.49	0.04	<0.001	1.65	0.08	<0.001	1.17	0.09	0.072
CUL4A_HUMAN	Cullin-4A	7	5.7	1.49	0.02	<0.001	1.73	0.02	<0.001	1.25	0.05	0.004
CUL9_HUMAN	Cullin-9	11	6.9	1.44	0.05	<0.001	1.86	0.16	0.002	1.36	0.12	0.017
CUX1_HUMAN	Homeobox protein cut-like 1	9	6	1.41	0.1	0.003	1.71	0.02	<0.001	1.27	0.04	0.002
CYC_HUMAN	Cytochrome c	2	14.3	1.46	0.01	<0.001	1.76	0.01	<0.001	1.28	0.04	0.002
CYTSA_HUMAN	Cytospin-A	10	11.6	1.38	0.05	<0.001	1.43	0.1	0.003	1.02	0.15	0.841
DAB2P_HUMAN	Disabled homolog 2-interacting protein	5	5.2	1.44	0.07	0.001	1.27	0.47	0.393	1.08	0.19	0.590
DACT3_HUMAN	Dapper homolog 3	4	5.6	1.61	0.15	0.003	2	0.28	0.006	1.57	0.3	0.061
DAPK1_HUMAN	Death-associated protein kinase 1	7	3.4	1.41	0.04	<0.001	1.56	0.08	0.001	1.11	0.12	0.259
DCLK1_HUMAN	Serine/threonine-protein kinase DCLK1	6	8.2	1.48	0.06	<0.001	1.61	0.08	0.001	1.15	0.08	0.075
DDX17_HUMAN	Probable ATP-dependent RNA helicase DDX17	10	2.3	1.36	0.09	0.002	1.71	0.13	0.001	1.24	0.08	0.016
DDX47_HUMAN	Probable ATP-dependent RNA helicase DDX47	2	6.4	1.63	0.04	<0.001	1.89	0.07	<0.001	1.37	0.08	0.005
DEN2A_HUMAN	DENN domain-containing protein 2A	4	5.6	1.21	0.09	0.020	1.27	0.05	0.002	0.91	0.12	0.364
DEN5A_HUMAN	DENN domain-containing protein 5A	10	2.8	1.45	0.05	<0.001	1.73	0.01	<0.001	1.3	0.01	<0.001
DESP_HUMAN	Desmoplakin	8	2.9	1.24	0.17	0.086	1.25	0.04	0.001	0.92	0.09	0.269
DHX29_HUMAN	ATP-dependent RNA helicase DHX29	4	4.6	1.57	0.18	0.008	1.61	0.08	0.001	1.16	0.02	0.002

DHX33_HUMAN	Putative ATP-dependent RNA helicase DHX33	7	5.5	1.17	0.05	0.006	1.5	0.05	<0.001	1.18	0.11	0.098
DHX36_HUMAN	ATP-dependent RNA helicase DHX36	10	5	1.45	0	<0.001	1.91	0.09	<0.001	1.53	0.11	0.005
DHX57_HUMAN	Putative ATP-dependent RNA helicase DHX57	15	4.3	1.46	0.04	<0.001	1.69	0.14	0.002	1.26	0.14	0.067
DIAP2_HUMAN	Protein diaphanous homolog 2	13	5.1	1.47	0.02	<0.001	1.69	0.02	<0.001	1.26	0.02	<0.001
DISC1_HUMAN	Disrupted in schizophrenia 1 protein	5	4.8	1.55	0	<0.001	1.42	0.29	0.076	1.05	0.13	0.653
DLG5_HUMAN	Disks large homolog 5	8	6.1	1.38	0.14	0.012	1.72	0.07	<0.001	1.29	0.06	0.005
DLX1_HUMAN	Homeobox protein DLX-1	8	17.6	1.42	0.07	0.001	1.71	0.17	0.003	1.22	0.19	0.174
DMRT2_HUMAN	Doublesex- and mab-3-related transcription factor 2	4	7.8	1.4	0.02	<0.001	1.7	0.05	<0.001	1.3	0.02	<0.001
DOC11_HUMAN	Dedicator of cytokinesis protein 11	10	4.1	1.48	0.01	<0.001	1.69	0.05	<0.001	1.25	0	<0.001
DOCK3_HUMAN	Dedicator of cytokinesis protein 3	5	3	1.3	0.01	<0.001	1.73	0.17	0.003	1.18	0.11	0.102
DOCK6_HUMAN	Dedicator of cytokinesis protein 6	9	7.3	1.36	0.02	<0.001	1.64	0.09	0.001	1.23	0.13	0.068
DOCK7_HUMAN	Dedicator of cytokinesis protein 7	11	6.2	1.43	0.01	<0.001	1.87	0.14	0.001	1.4	0.13	0.019
DOCK9_HUMAN	Dedicator of cytokinesis protein 9	6	2.9	1.45	0.02	<0.001	1.69	0.25	0.012	1.23	0.28	0.304
DPOLQ_HUMAN	DNA polymerase theta	6	3.1	1.35	0.1	0.006	1.56	0.12	0.002	1.16	0.1	0.096
DPTOR_HUMAN	DEP domain-containing mTOR-interacting protein	5	18.1	0.93	0.07	0.158	1.52	0.38	0.090	1.21	0.42	0.516
DSCL1_HUMAN	Down syndrome cell adhesion molecule-like protein 1	9	4.1	1.53	0.09	0.001	1.64	0.05	<0.001	1.21	0.04	0.005
DSG2_HUMAN	Desmoglein-2	9	9.9	1.47	0.04	<0.001	1.69	0.05	<0.001	1.26	0.01	<0.001
DSRAD_HUMAN	Double-stranded RNA-specific adenosine deaminase	7	5.5	1.64	0.23	0.012	1.88	0.39	0.023	1.42	0.31	0.126
DUS4_HUMAN	Dual specificity protein phosphatase 4	3	6.3	1.47	0.03	<0.001	1.57	0.26	0.027	1.15	0.28	0.500
DUS7_HUMAN	Dual specificity protein phosphatase 7	7	6.9	1.56	0.09	0.001	1.66	0.09	0.001	1.51	0.27	0.061
DVL2_HUMAN	Segment polarity protein dishevelled homolog DVL-2	3	6.9	1.5	0.15	0.006	1.89	0.31	0.011	1.47	0.28	0.084
DVL3_HUMAN	Segment polarity protein dishevelled homolog DVL-3	4	6.8	1.44	0.05	<0.001	1.55	0.18	0.009	1.13	0.15	0.279
DYRK2_HUMAN	Dual specificity tyrosine-phosphorylation-regulated kinase 2	3	4.8	1.38	0.08	0.002	1.42	0.11	0.004	1.06	0.1	0.492
DYST_HUMAN	Dystonin	12	2.3	1.46	0.05	<0.001	1.58	0.08	<0.001	1.16	0.05	0.015
E2AK3_HUMAN	Eukaryotic translation initiation factor 2-alpha kinase 3	5	4.8	1.42	0.01	<0.001	1.48	0.13	0.005	0.95	0.04	0.185
E2F1_HUMAN	Transcription factor E2F1	3	5.9	1.43	0.03	<0.001	1.55	0.11	0.002	1.09	0.09	0.192

E2F8_HUMAN	Transcription factor E2F8	3	3.9	1.5	0.03	<0.001	1.78	0	<0.001	1.34	0.02	<0.001
E41L1_HUMAN	Band 4.1-like protein 1	5	5.3	1.41	0.08	0.001	1.75	0.04	<0.001	1.36	0.03	<0.001
EEPD1_HUMAN	Endonuclease/exonuclease/phosphatase family domain-containing protein 1	7	12.7	1.52	0.01	<0.001	1.88	0.07	<0.001	1.41	0.08	0.004
EGLN1_HUMAN	Egl nine homolog 1	7	11.5	1.44	0.02	<0.001	1.75	0.04	<0.001	1.25	0.08	0.019
EID2_HUMAN	EP300-interacting inhibitor of differentiation 2	7	30.5	1.4	0.01	<0.001	1.68	0.11	0.001	1.26	0.13	0.050
ELN_HUMAN	Elastin	6	10.2	1.48	0.02	<0.001	1.67	0.04	<0.001	1.22	0.02	<0.001
EMAL3_HUMAN	Echinoderm microtubule-associated protein-like 3	6	5.8	1.55	0.04	<0.001	1.88	0.02	<0.001	1.21	0.18	0.170
EMAL4_HUMAN	Echinoderm microtubule-associated protein-like 4	4	6.6	1.53	0.03	<0.001	1.83	0.11	<0.001	1.34	0.09	0.011
EMIL1_HUMAN	EMILIN-1	5	9.8	1.27	0.23	0.124	1.69	0.03	<0.001	1.22	0.02	0.001
EMIL2_HUMAN	EMILIN-2	6	8.5	1.56	0.07	<0.001	1.7	0.08	<0.001	1.24	0.12	0.051
EMSY_HUMAN	BRCA2-interacting transcriptional repressor EMSY	4	3.6	1.38	0	<0.001	1.74	0.08	<0.001	1.27	0.02	<0.001
ENOA_HUMAN	Alpha-enolase	8	13.1	1.42	0.06	0.001	1.52	0.06	<0.001	1.11	0.06	0.081
EP2A2_HUMAN	Laforin; isoform 9	5	22.7	1.42	0.05	<0.001	1.61	0.05	<0.001	1.07	0.13	0.486
EPHA4_HUMAN	Ephrin type-A receptor 4	8	7.9	1.53	0.02	<0.001	1.77	0.09	<0.001	1.35	0.07	0.004
EPHA8_HUMAN	Ephrin type-A receptor	6	4.9	1.44	0	<0.001	1.46	0.09	0.002	1.22	0.08	0.021
EPIPL_HUMAN	Epiplakin	8	1.3	1.48	0.02	<0.001	1.63	0.08	<0.001	1.19	0.06	0.017
ERBB4_HUMAN	Receptor tyrosine-protein kinase erbB-4	5	7	1.3	0.18	0.053	1.5	0.1	0.002	1.05	0.03	0.131
ESYT2_HUMAN	Extended synaptotagmin-2	3	3.7	1.36	0.07	0.001	1.57	0.01	<0.001	1.24	0.22	0.201
EXOC8_HUMAN	Exocyst complex component 8	2	3.6	1.43	0.08	0.001	1.67	0.07	<0.001	1.36	0.09	0.008
EXOSX_HUMAN	Exosome component 10	3	4.1	1.46	0.05	<0.001	1.72	0.03	<0.001	1.29	0.06	0.004
FANCA_HUMAN	Fanconi anemia group A protein	2	3.2	1.29	0.09	0.006	1.66	0.22	0.010	1.23	0.17	0.136
FANCI_HUMAN	Fanconi anemia group I protein	8	3.4	1.57	0.09	0.001	1.75	0.1	0.001	1.42	0.1	0.006
FAT1_HUMAN	Protocadherin Fat 1	7	1.9	1.43	0.02	<0.001	1.56	0.05	<0.001	1.15	0.05	0.021
FAT4_HUMAN	Protocadherin Fat 4	7	1.9	1.42	0.01	<0.001	1.55	0.01	<0.001	1.21	0.07	0.018
FBSP1_HUMAN	F-box/SPRY domain-containing protein 1	10	13.3	1.57	0.05	<0.001	1.66	0.07	<0.001	1.19	0.05	0.009
FBX10_HUMAN	F-box only protein 10	5	7	1.64	0.12	0.001	2.06	0.06	<0.001	1.79	0.11	0.002
FGD3_HUMAN	FYVE; RhoGEF and PH domain-containing protein	3	5.1	1.48	0.17	0.011	1.73	0.14	0.002	1.38	0.02	<0.001

FGD6_HUMAN	FYVE; RhoGEF and PH domain-containing protein	3	1.5	1.41	0.01	<0.001	1.79	0	<0.001	1.3	0.02	<0.001
FIBA_HUMAN	Fibrinogen alpha chain	9	7.7	1.37	0.04	<0.001	1.4	0.14	0.011	1.05	0.08	0.451
FIBB_HUMAN	Fibrinogen beta chain	4	7.3	1.32	0.05	0.001	1.32	0.06	0.002	0.89	0.04	0.021
FIBG_HUMAN	Fibrinogen gamma chain	3	2.9	1.53	0.02	<0.001	1.78	0.01	<0.001	1.42	0.06	0.002
FIG4_HUMAN	Polyphosphoinositide phosphatase	6	6	1.32	0.02	<0.001	1.73	0.14	0.002	1.3	0.15	0.058
FLNA_HUMAN	Filamin-A	28	9.8	1.46	0.02	<0.001	1.65	0.07	<0.001	1.22	0.05	0.005
FLNB_HUMAN	Filamin-B	10	4	1.43	0.07	0.001	1.88	0.01	<0.001	1.3	0.05	0.002
FLOT2_HUMAN	Flotillin-2	4	7.2	1.55	0.15	0.004	1.73	0.26	0.012	1.27	0.19	0.117
FMN1_HUMAN	Formin-1	13	10.3	1.47	0.11	0.003	1.71	0.16	0.003	1.29	0.09	0.016
FMNL1_HUMAN	Formin-like protein 1	6	4.3	1.54	0.02	<0.001	1.84	0.03	<0.001	1.39	0.02	<0.001
FNIP1_HUMAN	Folliculin-interacting protein 1	5	5.7	1.4	0.04	<0.001	1.68	0.08	<0.001	1.19	0.1	0.071
FOG1_HUMAN	Zinc finger protein ZFPM1	5	8.1	1.32	0.06	0.001	1.41	0.17	0.018	0.9	0.11	0.239
FOG2_HUMAN	Zinc finger protein ZFPM2	3	3.3	1.38	0.12	0.008	1.42	0.2	0.029	1.12	0.19	0.433
FREM2_HUMAN	FRAS1-related extracellular matrix protein 2	8	3.6	1.45	0.01	<0.001	1.76	0.13	0.001	1.27	0.1	0.027
FTCD_HUMAN	Formimidoyltransferase-cyclodeaminase	14	9.4	1.4	0.04	<0.001	1.68	0.1	0.001	1.26	0.11	0.038
FUBP2_HUMAN	Far upstream element-binding protein 2	9	12.7	1.35	0.1	0.005	1.85	0.02	<0.001	1.59	0.19	0.018
FURIN_HUMAN	Furin	4	7.3	1.58	0.09	<0.001	2.21	0.57	0.027	1.82	0.6	0.127
FUS_HUMAN	RNA-binding protein FUS	20	16.2	1.46	0.03	<0.001	1.67	0	<0.001	1.25	0.03	0.001
FYV1_HUMAN	1-phosphatidylinositol 3-phosphate 5-kinase	10	3.5	1.55	0.03	<0.001	1.71	0.05	<0.001	1.27	0	<0.001
FZR_HUMAN	Fizzy-related protein homolog	3	11.9	1.32	0.18	0.047	1.45	0.3	0.075	1.19	0.13	0.102
G3P_HUMAN	Glyceraldehyde-3-phosphate dehydrogenase	10	10.7	1.44	0.05	<0.001	1.54	0.16	0.006	1.01	0.16	0.940
GAK_HUMAN	Cyclin-G-associated kinase	4	3.2	1.34	0.03	<0.001	1.53	0.05	<0.001	1.03	0	<0.001
GATA6_HUMAN	Transcription factor GATA-6	14	9.6	1.14	0.15	0.199	1.34	0.05	0.001	1.11	0.11	0.230
GCN1_HUMAN	eIF-2-alpha kinase activator GCN1	19	7	1.5	0.03	<0.001	1.95	0	<0.001	1.49	0	<0.001
GDIB_HUMAN	Rab GDP dissociation inhibitor beta	4	2.5	1.21	0.06	0.005	1.15	0.05	0.012	0.86	0.1	0.119
GDS1_HUMAN	Rap1 GTPase-GDP dissociation stimulator 1	2	4.9	1.27	0.1	0.012	1.45	0.12	0.005	1.08	0.13	0.424
GFAP_HUMAN	Glial fibrillary acidic protein	13	12	1.45	0.03	<0.001	1.51	0.07	0.001	1.08	0.04	0.061
GLCNE_HUMAN	Bifunctional UDP-N-acetylglucosamine 2-	5	4.8	1.33	0.12	0.013	1.22	0.26	0.229	0.86	0.19	0.329

	epimerase/N-acetylmannosamine kinase											
GPV_HUMAN	Platelet glycoprotein V	3	6.3	1.4	0.19	0.025	2.17	0.4	0.011	1.69	0.3	0.039
GRHL3_HUMAN	Grainyhead-like protein 3 homolog	3	4.3	1.47	0.03	<0.001	1.89	0.16	0.001	1.52	0.15	0.014
GRP78_HUMAN	78 kDa glucose-regulated protein	7	8.6	1.35	0.03	<0.001	1.51	0.01	<0.001	1.08	0.03	0.018
GSK3A_HUMAN	Glycogen synthase kinase-3 alpha	11	19	1.51	0.02	<0.001	1.74	0.04	<0.001	1.31	0.04	0.001
GTF2I_HUMAN	General transcription factor II-I	6	9.2	1.64	0.31	0.029	2.41	0.74	0.037	2.01	0.75	0.131
GUC2D_HUMAN	Retinal guanylyl cyclase 1	8	6.1	1.36	0.19	0.040	1.76	0.35	0.027	1.25	0.35	0.358
GUC2F_HUMAN	Retinal guanylyl cyclase 2	3	3.7	1.38	0.02	<0.001	1.58	0.09	0.001	1.1	0.07	0.115
H12_HUMAN	Histone H1.2	4	11.7	1.37	0.15	0.016	1.49	0.1	0.002	1.13	0.14	0.247
H13_HUMAN	Histone H1.3	5	19.9	1.3	0	<0.001	0.9	0.13	0.280	0.71	0.11	0.029
HASP_HUMAN	Serine/threonine-protein kinase haspin	2	2.1	1.39	0.03	<0.001	1.42	0.08	0.002	1.04	0.02	0.050
HDAC9_HUMAN	Histone deacetylase 9	2	1.1	1.46	0.1	0.002	1.56	0.15	0.005	1.12	0.08	0.129
HECD1_HUMAN	E3 ubiquitin-protein ligase HECTD1	11	5.5	1.37	0.04	<0.001	1.66	0.04	<0.001	1.26	0.09	0.023
HECD4_HUMAN	Probable E3 ubiquitin-protein ligase HECTD4	13	2.3	1.43	0.1	0.002	1.61	0.32	0.037	1.19	0.3	0.421
HERC1_HUMAN	Probable E3 ubiquitin-protein ligase HERC1	11	2.4	1.43	0.15	0.010	1.61	0.18	0.006	1.19	0.2	0.254
HERC2_HUMAN	E3 ubiquitin-protein ligase HERC2	7	2.1	1.4	0.05	<0.001	1.41	0.04	<0.001	0.89	0.07	0.090
HERC3_HUMAN	Probable E3 ubiquitin-protein ligase HERC3	2	1	1.48	0.27	0.046	1.83	0.66	0.107	1.53	0.8	0.394
HEY1_HUMAN	Hairy/enhancer-of-split related with YRPW motif protein 1	2	13.8	1.29	0.01	<0.001	1.37	0.03	<0.001	0.9	0	<0.001
HEYL_HUMAN	Hairy/enhancer-of-split related with YRPW motif-like protein	1	6.4	1.32	0.19	0.054	1.55	0.62	0.215	1.16	0.71	0.772
HIC1_HUMAN	Hypermethylated in cancer 1 protein	4	14.7	1.38	0.11	0.006	1.51	0.07	0.001	1.19	0.11	0.073
HIRA_HUMAN	Protein HIRA	9	11	1.54	0.04	<0.001	1.56	0.1	0.001	1.03	0.08	0.672
HMCN2_HUMAN	Hemicentin-2	17	4.5	1.43	0.03	<0.001	1.44	0.05	<0.001	1.1	0.02	0.002
HMDH_HUMAN	3-hydroxy-3-methylglutaryl-coenzyme A reductase	6	2.3	1.43	0.01	<0.001	1.89	0.16	0.001	1.43	0.15	0.019
HNRH2_HUMAN	Heterogeneous nuclear ribonucleoprotein H2	4	15.1	1.37	0.1	0.005	1.49	0.12	0.004	1.05	0.18	0.723
HNRL1_HUMAN	Heterogeneous nuclear ribonucleoprotein U-like protein 1	3	5.6	1.37	0.15	0.017	1.47	0.23	0.033	0.97	0.19	0.840
HNRPL_HUMAN	Heterogeneous nuclear ribonucleoprotein L	20	18	1.51	0.01	<0.001	1.71	0.03	<0.001	1.24	0.02	0.001
HNRPM_HUMAN	Heterogeneous nuclear ribonucleoprotein M	41	31.9	1.4	0.04	<0.001	1.62	0.04	<0.001	1.19	0.04	0.007

HNRPU_HUMAN	Heterogeneous nuclear ribonucleoprotein U	11	8.7	1.44	0.07	0.001	1.83	0.02	<0.001	1.37	0.04	0.001
HOME2_HUMAN	Homer protein homolog 2	2	9.3	1.56	0.05	<0.001	1.76	0.11	0.001	1.33	0.06	0.003
HSP7C_HUMAN	Heat shock cognate 71 kDa protein	12	17.3	1.51	0.01	<0.001	1.83	0.02	<0.001	1.41	0.04	0.001
HUWE1_HUMAN	E3 ubiquitin-protein ligase HUWE1	11	3.3	1.42	0.06	<0.001	1.61	0.17	0.006	1.2	0.16	0.145
ID4_HUMAN	DNA-binding protein inhibitor ID-4	2	14.3	1.42	0.07	0.001	1.48	0.01	<0.001	1.06	0.01	0.001
IF4G1_HUMAN	Eukaryotic translation initiation factor 4 gamma 1	5	2.4	1.49	0.13	0.003	1.5	0.14	0.006	1	0.08	0.988
IF4H_HUMAN	Eukaryotic translation initiation factor 4H	4	7.3	1.23	0.07	0.006	1.41	0.24	0.050	1	0.24	0.986
IL3RB_HUMAN	Cytokine receptor common subunit beta	1	1.8	1.34	0.03	<0.001	1.4	0.1	0.004	1.07	0.01	<0.001
ILF3_HUMAN	Interleukin enhancer-binding factor 3	5	5.3	1.36	0.26	0.090	1.37	0.22	0.049	0.89	0.16	0.401
INO80_HUMAN	DNA helicase INO80	3	2.4	1.37	0.01	<0.001	1.43	0.25	0.051	1.05	0.13	0.613
IQEC2_HUMAN	IQ motif and SEC7 domain-containing protein 2	7	4.1	1.47	0.02	<0.001	1.87	0.07	<0.001	1.42	0.04	0.001
IQEC3_HUMAN	IQ motif and SEC7 domain-containing protein 3	4	3.7	1.52	0.1	0.001	1.53	0	<0.001	1.11	0.01	0.001
IRS2_HUMAN	Insulin receptor substrate 2	9	11.8	1.41	0.08	0.002	1.55	0.23	0.019	1.1	0.24	0.604
ITA11_HUMAN	Integrin alpha-11	4	3.6	1.49	0.03	<0.001	1.53	0.3	0.046	1.07	0.28	0.742
ITAV_HUMAN	Integrin alpha-V	3	3.8	1.42	0.15	0.011	1.56	0.09	0.001	1.26	0.11	0.032
ITPR3_HUMAN	Inositol 1;4;5-trisphosphate receptor type 3	9	2.4	1.34	0.01	<0.001	1.48	0.1	0.002	1.03	0.09	0.658
ITSN1_HUMAN	Intersectin-1	5	4.4	1.49	0.05	<0.001	1.52	0.07	0.001	1.1	0.03	0.015
ITSN2_HUMAN	Intersectin-2	6	5.2	1.33	0.04	<0.001	1.69	0	<0.001	1.25	0.07	0.014
IWS1_HUMAN	Protein IWS1 homolog	3	4.8	1.64	0.35	0.041	1.56	0.25	0.022	1.14	0.19	0.326
JARD2_HUMAN	Protein Jumonji	3	2.6	1.25	0	<0.001	1.52	0.12	0.003	1.07	0.15	0.518
JIP2_HUMAN	C-Jun-amino-terminal kinase-interacting protein 2	4	9.2	1.4	0	<0.001	1.29	0.03	<0.001	0.96	0.04	0.224
K22E_HUMAN	Keratin; type II cytoskeletal 2 epidermal	14	20	1.44	0	<0.001	1.57	0	<0.001	1.11	0.05	0.034
K22O_HUMAN	Keratin; type II cytoskeletal 2 oral	11	19.1	1.4	0.07	0.001	1.47	0.12	0.004	1.1	0.06	0.086
K2C4_HUMAN	Keratin; type II cytoskeletal 4	3	12	1.4	0.1	0.002	1.59	0.16	0.005	1.16	0.19	0.291
KANK1_HUMAN	KN motif and ankyrin repeat domain-containing protein 1	9	8.7	1.4	0.06	0.001	1.34	0.12	0.010	0.98	0.04	0.635
KAPCA_HUMAN	cAMP-dependent protein kinase catalytic subunit alpha	1	2.3	1.38	0.14	0.011	1.22	0.02	<0.001	0.91	0.11	0.310
KASH5_HUMAN	Protein KASH5	3	5.2	1.47	0.02	<0.001	1.5	0.04	<0.001	1.04	0.02	0.053

KCC2B_HUMAN	Calcium/calmodulin-dependent protein kinase type II subunit beta	5	6.8	1.46	0.03	<0.001	1.82	0.09	<0.001	1.41	0.05	0.001
KCMA1_HUMAN	Calcium-activated potassium channel subunit alpha-1	22	5.2	1.45	0.2	0.023	1.55	0.36	0.067	1.12	0.25	0.541
KDM2B_HUMAN	Lysine-specific demethylase 2B	9	5.5	1.47	0.01	<0.001	1.65	0.12	0.002	1.21	0.17	0.163
KDM6A_HUMAN	Lysine-specific demethylase 6A	6	6.9	1.39	0.05	<0.001	1.64	0.08	<0.001	1.2	0.07	0.025
KIBRA_HUMAN	Protein KIBRA	4	2.5	1.38	0	<0.001	1.57	0.08	0.001	1.28	0.2	0.126
KIF14_HUMAN	Kinesin-like protein KIF14	4	2.5	1.44	0.04	<0.001	1.72	0.01	<0.001	1.29	0.03	0.001
KLH12_HUMAN	Kelch-like protein 12	5	7.9	1.4	0.1	0.004	1.73	0.16	0.003	1.28	0.21	0.141
KLHL3_HUMAN	Kelch-like protein 3	4	8.3	1.36	0.01	<0.001	1.49	0.21	0.022	1.08	0.33	0.737
KMT2A_HUMAN	Histone-lysine N-methyltransferase 2A	26	6	1.45	0.05	<0.001	1.75	0.18	0.003	1.29	0.13	0.043
KMT2B_HUMAN	Histone-lysine N-methyltransferase 2B	18	6.6	1.47	0.03	<0.001	1.63	0	<0.001	1.18	0.03	0.002
KMT2C_HUMAN	Histone-lysine N-methyltransferase 2C	14	3.5	1.43	0.08	0.001	1.62	0.13	0.002	1.22	0.1	0.045
KMT2D_HUMAN	Histone-lysine N-methyltransferase 2D	11	2.1	1.47	0.08	0.001	1.87	0.06	<0.001	1.36	0.08	0.005
KPCD1_HUMAN	Serine/threonine-protein kinase D1	3	8.1	1.23	0.15	0.075	1.24	0.32	0.286	1	0.14	0.969
KPTN_HUMAN	Kaptin	2	8	1.7	0.22	0.008	2.22	0.61	0.032	1.96	0.67	0.115
KSR2_HUMAN	Kinase suppressor of Ras 2	5	6	1.43	0.03	<0.001	1.64	0.03	<0.001	1.2	0.02	0.001
LAMA1_HUMAN	Laminin subunit alpha-1	4	1.5	1.45	0.1	0.002	1.63	0.15	0.004	1.19	0.08	0.037
LAMA3_HUMAN	Laminin subunit alpha-3	4	1.5	1.54	0.11	0.002	1.82	0.31	0.015	1.53	0.05	0.001
LAMA5_HUMAN	Laminin subunit alpha-5	7	3.6	1.36	0.1	0.005	1.81	0.39	0.029	1.33	0.39	0.296
LAMB3_HUMAN	Laminin subunit beta-3	9	10.4	1.24	0.31	0.267	1.56	0.22	0.015	1.2	0.07	0.020
LC7L3_HUMAN	Luc7-like protein 3	2	3.7	1.55	0	<0.001	1.76	0.02	<0.001	1.25	0.03	0.001
LEF1_HUMAN	Lymphoid enhancer-binding factor 1	4	16.3	1.52	0.05	<0.001	1.89	0.04	<0.001	1.51	0.08	0.002
LIPA2_HUMAN	Liprin-alpha-2	9	8.7	1.44	0.17	0.016	1.75	0.27	0.012	1.35	0.27	0.144
LIPB1_HUMAN	Liprin-beta-1	5	8.2	1.38	0.08	0.001	1.56	0.27	0.029	1.11	0.23	0.517
LMBL1_HUMAN	Lethal(3)malignant brain tumor-like protein 1	4	9.6	1.27	0.24	0.136	1.45	0.18	0.018	1	0.09	0.996
LMLN_HUMAN	Leishmanolysin-like peptidase	4	3.1	1.51	0.01	<0.001	1.43	0.19	0.022	1.33	0.02	<0.001
LMTK3_HUMAN	Serine/threonine-protein kinase LMTK3	4	5.1	1.48	0.01	<0.001	1.72	0.12	0.001	1.17	0.11	0.100
LRP1_HUMAN	Prolow-density lipoprotein receptor-related protein	11	3.7	1.39	0.01	<0.001	1.56	0.01	<0.001	1.09	0.02	0.003

LRP4_HUMAN	Low-density lipoprotein receptor-related protein 4	6	2.9	1.42	0.03	<0.001	1.58	0.03	<0.001	1.1	0.01	0.001
LRP5_HUMAN	Low-density lipoprotein receptor-related protein 5	19	8.2	1.38	0.22	0.049	1.5	0.21	0.021	1.03	0.21	0.827
LRRK2_HUMAN	Leucine-rich repeat serine/threonine-protein kinase 2	2	1	1.43	0.01	<0.001	1.58	0.11	0.002	1.16	0.09	0.067
LTK_HUMAN	Leukocyte tyrosine kinase receptor	9	4.6	1.5	0.03	<0.001	1.51	0.28	0.042	1.1	0.29	0.650
M3K15_HUMAN	Mitogen-activated protein kinase kinase kinase 15	4	5.1	1.45	0.08	0.001	1.59	0.11	0.002	1.2	0.17	0.169
MA7D3_HUMAN	MAP7 domain-containing protein 3	5	1.9	1.44	0.14	0.009	1.62	0.23	0.014	1.18	0.16	0.178
MACF1_HUMAN	Microtubule-actin cross-linking factor 1; isoforms 1/2/3/5	15	2.9	1.43	0.01	<0.001	1.67	0.01	<0.001	1.25	0.03	0.001
MAGI2_HUMAN	Membrane-associated guanylate kinase; WW and PDZ domain-containing protein 2	9	7.3	1.18	0.29	0.357	1.63	0.27	0.022	1.83	0.43	0.059
MAGI3_HUMAN	Membrane-associated guanylate kinase; WW and PDZ domain-containing protein 3	3	3.3	1.48	0.06	<0.001	1.69	0.01	<0.001	1.22	0.02	<0.001
MAP1B_HUMAN	Microtubule-associated protein 1B	7	4.3	1.43	0.05	<0.001	1.55	0.12	0.003	1.14	0.16	0.296
MAP6_HUMAN	Microtubule-associated protein 6	7	7.9	1.47	0.06	<0.001	1.68	0.11	0.001	1.25	0.21	0.160
MARK3_HUMAN	MAP/microtubule affinity-regulating kinase 3	7	8.9	1.35	0.02	<0.001	1.53	0.24	0.023	1.02	0.15	0.893
MAST2_HUMAN	Microtubule-associated serine/threonine-protein kinase 2	4	3.9	1.49	0.09	0.001	1.55	0.14	0.005	1.07	0.07	0.262
MAST3_HUMAN	Microtubule-associated serine/threonine-protein kinase 3	18	8.5	1.41	0.06	<0.001	1.72	0.11	0.001	1.32	0.07	0.006
MAST4_HUMAN	Microtubule-associated serine/threonine-protein kinase 4	8	1.6	1.41	0.01	<0.001	1.57	0.02	<0.001	1.17	0.02	0.001
MBD4_HUMAN	Methyl-CpG-binding domain protein 4	5	2.4	1.42	0.03	<0.001	1.92	0.4	0.021	1.42	0.36	0.172
MBNL3_HUMAN	Muscleblind-like protein 3	3	11.6	1.44	0.05	<0.001	1.42	0.01	<0.001	1.01	0.07	0.847
MCM7_HUMAN	DNA replication licensing factor MCM7	5	11.3	1.45	0.04	<0.001	1.61	0.07	<0.001	1.16	0.08	0.051
MED1_HUMAN	Mediator of RNA polymerase II transcription subunit 1	11	10.2	1.2	0	<0.001	1.66	0.36	0.041	1.21	0.41	0.508
MED14_HUMAN	Mediator of RNA polymerase II transcription subunit 14	4	2.7	1.54	0.02	<0.001	1.94	0.23	0.003	1.43	0.16	0.028
MIA3_HUMAN	Melanoma inhibitory activity protein 3	8	5.7	1.46	0.01	<0.001	1.81	0.02	<0.001	1.36	0.04	0.001
MICA_HUMAN	MHC class I polypeptide-related sequence A	1	2.6	1.37	0.03	<0.001	1.6	0.15	0.004	1.23	0.2	0.171
MICA2_HUMAN	Protein-methionine sulfoxide oxidase MICAL2	5	4.7	1.34	0.11	0.008	1.59	0.17	0.006	1.18	0.18	0.230
MINK1_HUMAN	Misshapen-like kinase 1	11	9.8	1.36	0	<0.001	1.6	0.06	<0.001	1.15	0.07	0.042
MINT_HUMAN	Msx2-interacting protein	10	3.1	1.42	0.04	<0.001	1.58	0.02	<0.001	1.16	0.01	<0.001
MK01_HUMAN	Mitogen-activated protein kinase 1	8	6.7	1.3	0.11	0.013	1.61	0.32	0.037	1.15	0.32	0.531

MK04_HUMAN	Mitogen-activated protein kinase 4	4	9.9	1.51	0.01	<0.001	1.62	0.05	<0.001	1.23	0.03	0.002
MMRN1_HUMAN	Multimerin-1	8	10.5	1.38	0.04	<0.001	1.81	0.49	0.056	1.36	0.51	0.372
MOES_HUMAN	Moesin	4	6.6	1.28	0.19	0.074	1.35	0.22	0.068	1.02	0.09	0.762
MPDZ_HUMAN	Multiple PDZ domain protein	6	2.2	1.37	0.07	0.001	2.07	0.69	0.067	1.54	0.66	0.308
MPIP2_HUMAN	M-phase inducer phosphatase 2	3	2.6	1.43	0.24	0.046	1.33	0.47	0.305	0.94	0.36	0.828
MPRIP_HUMAN	Myosin phosphatase Rho-interacting protein	7	7.3	1.57	0.12	0.002	1.6	0.11	0.001	1.27	0	<0.001
MRCKA_HUMAN	Serine/threonine-protein kinase MRCK alpha	5	2.5	1.58	0.04	<0.001	1.71	0.18	0.004	1.3	0.2	0.111
MRCKG_HUMAN	Serine/threonine-protein kinase MRCK gamma	8	5.6	1.47	0.01	<0.001	1.77	0	<0.001	1.31	0.04	0.002
MSH3_HUMAN	DNA mismatch repair protein Msh3	7	6.8	1.42	0.12	0.005	1.6	0.08	<0.001	1.22	0.05	0.005
MTAP2_HUMAN	Microtubule-associated protein 2	14	8.8	1.47	0.02	<0.001	1.5	0.26	0.036	1.05	0.24	0.772
MTMR1_HUMAN	Myotubularin-related protein 1	5	9.5	1.24	0.2	0.114	1.63	0.19	0.007	1.25	0.15	0.089
MTMR5_HUMAN	Myotubularin-related protein 5	5	3.6	1.78	0.01	<0.001	2.53	0.38	0.004	2.09	0.42	0.027
MTOR_HUMAN	Serine/threonine-protein kinase mTOR	14	6.3	1.36	0.19	0.038	1.51	0.3	0.049	1.09	0.28	0.663
MTP_HUMAN	Microsomal triglyceride transfer protein large subunit	4	6.3	1.4	0.04	<0.001	1.68	0.07	<0.001	1.29	0.06	0.004
MUC16_HUMAN	Mucin-16	51	3.2	1.5	0.02	<0.001	1.75	0.14	0.002	1.33	0.14	0.036
MUC4_HUMAN	Mucin-4	5	3.4	1.39	0.02	<0.001	1.43	0.06	0.001	1.02	0.04	0.650
MUC5A_HUMAN	Mucin-5AC	15	3.7	1.42	0.11	0.004	1.7	0.03	<0.001	1.24	0.07	0.014
MYH14_HUMAN	Myosin-14	15	6.5	1.48	0.01	<0.001	1.55	0.18	0.010	1.1	0.18	0.445
MYH3_HUMAN	Myosin-3	4	3.2	1.48	0.1	0.002	1.49	0.51	0.186	1.06	0.39	0.841
MYH9_HUMAN	Myosin-9	18	4.2	1.51	0.06	<0.001	1.73	0.16	0.002	1.26	0.14	0.064
MYLK_HUMAN	Myosin light chain kinase; smooth muscle	5	2.4	1.02	0.41	0.937	1.62	0.06	<0.001	1.3	0.11	0.021
MYLK3_HUMAN	Myosin light chain kinase 3	5	5.9	1.42	0.02	<0.001	1.73	0.14	0.002	1.31	0.16	0.058
MYO3B_HUMAN	Myosin-IIIb	5	2.5	1.33	0.04	<0.001	1.62	0.12	0.002	1.21	0.09	0.038
MYO9B_HUMAN	Unconventional myosin-IXb	6	3.8	1.46	0.11	0.003	1.8	0.01	<0.001	1.41	0.01	<0.001
NACAM_HUMAN	Nascent polypeptide-associated complex subunit alpha; muscle-specific form	7	4.3	1.42	0.1	0.002	1.55	0.01	<0.001	1.25	0.12	0.050
NCOA2_HUMAN	Nuclear receptor coactivator 2	6	5.1	1.4	0.07	0.001	1.53	0	<0.001	1.08	0.06	0.105
NCOA6_HUMAN	Nuclear receptor coactivator 6	13	6.1	1.54	0.11	0.001	1.75	0.32	0.021	1.26	0.28	0.250

NCOR2_HUMAN	Nuclear receptor corepressor 2	6	4.6	1.46	0.04	<0.001	1.63	0.1	0.001	1.18	0.04	0.007
NDKB_HUMAN	Nucleoside diphosphate kinase B	3	19.1	1.56	0.04	<0.001	1.8	0.01	<0.001	1.41	0.08	0.004
NF1_HUMAN	Neurofibromin	6	1.3	1.42	0.11	0.003	1.52	0.13	0.004	1.1	0.09	0.181
NF2IP_HUMAN	NFATC2-interacting protein	1	4.8	0.54	0.54	0.233	0.57	0.57	0.285	0.23	0.23	0.015
NFH_HUMAN	Neurofilament heavy polypeptide	4	5.3	1.16	0.27	0.375	1.76	0.28	0.013	1.02	0.01	0.030
NFX1_HUMAN	Transcriptional repressor NF-X1	2	2.5	1.44	0.02	<0.001	1.45	0.02	<0.001	1.11	0.14	0.322
NGN3_HUMAN	Neurogenin-3	2	7	1.67	0.12	0.001	1.59	0.5	0.125	1.54	0.29	0.065
NHRF1_HUMAN	Na(+)/H(+) exchange regulatory cofactor NHE-RF1	4	17.3	1.55	0.16	0.006	1.84	0.23	0.005	1.42	0.27	0.099
NKAP_HUMAN	NF-kappa-B-activating protein	5	7.2	1.48	0.02	<0.001	1.64	0	<0.001	1.24	0	<0.001
NMDE1_HUMAN	Glutamate receptor ionotropic; NMDA 2A	8	4.7	1.41	0.19	0.025	1.45	0.13	0.006	0.98	0.11	0.818
NONO_HUMAN	Non-POU domain-containing octamer-binding protein	8	10.6	1.48	0.06	<0.001	1.64	0.09	0.001	1.35	0.01	<0.001
NOTC1_HUMAN	Neurogenic locus notch homolog protein 1	5	2.2	1.4	0.04	<0.001	1.66	0.01	<0.001	1.28	0.11	0.032
NOX5_HUMAN	NADPH oxidase 5	3	5.2	1.4	0.24	0.054	1.47	0.03	<0.001	1.07	0.01	0.001
NPHP4_HUMAN	Nephrocystin-4	3	3	1.33	0.43	0.276	1.64	0.13	0.002	1.36	0.02	<0.001
NR2E3_HUMAN	Photoreceptor-specific nuclear receptor	6	11.5	1.4	0.15	0.012	1.39	0.44	0.215	1.03	0.34	0.907
NR2F6_HUMAN	Nuclear receptor subfamily 2 group F member 6	3	10.6	1.24	0.35	0.317	1.72	0.54	0.093	1.37	0.37	0.224
NRG2_HUMAN	Pro-neuregulin-2; membrane-bound isoform	6	8.2	1.51	0.08	0.001	1.56	0	<0.001	1.7	0.56	0.154
NRP2_HUMAN	Neuropilin-2	3	2.9	1.41	0.01	<0.001	1.42	0	<0.001	1	0	0.144
NRX1B_HUMAN	Neurexin-1-beta	6	5.9	1.2	0.3	0.340	1.48	0.32	0.068	1.17	0.21	0.308
NUAK1_HUMAN	NUAK family SNF1-like kinase 1	4	9.4	1.34	0.05	<0.001	1.68	0.23	0.011	1.17	0.17	0.228
NUCL_HUMAN	Nucleolin	5	4.9	1.51	0.01	<0.001	1.65	0.17	0.004	1.22	0.16	0.132
OBSCN_HUMAN	Obscurin	30	5.1	1.4	0.05	<0.001	1.44	0.05	<0.001	1.04	0.07	0.484
OBSL1_HUMAN	Obscurin-like protein 1	6	4.3	1.49	0.03	<0.001	1.83	0.17	0.002	1.37	0.21	0.072
OCRL_HUMAN	Inositol polyphosphate 5-phosphatase OCRL-1	4	7.3	1.52	0.06	<0.001	1.7	0.09	0.001	1.41	0.04	0.001
OGT1_HUMAN	UDP-N-acetylglucosamine--peptide N-acetylglucosaminyltransferase 110 kDa subunit	2	4.1	1.31	0.31	0.174	1.61	0.44	0.087	1.22	0.51	0.566
OTU7B_HUMAN	OTU domain-containing protein 7B	6	10.4	1.38	0.08	0.002	1.57	0.1	0.001	1.09	0.1	0.249
PABP2_HUMAN	Polyadenylate-binding protein 2	8	7.5	1.51	0.08	0.001	1.73	0.26	0.011	1.22	0.22	0.225

PAI1_HUMAN	Plasminogen activator inhibitor 1	5	16.7	1.23	0.04	0.001	1.28	0.29	0.183	1.03	0.27	0.890
PAK3_HUMAN	Serine/threonine-protein kinase PAK 3	4	7.7	1.44	0.01	<0.001	1.51	0.11	0.002	1.11	0.04	0.020
PAK4_HUMAN	Serine/threonine-protein kinase PAK 4	4	4.9	1.38	0.07	0.001	1.77	0.26	0.010	1.25	0.24	0.213
PARI_HUMAN	PCNA-interacting partner	2	6.2	1.54	0.1	0.001	1.96	0.09	<0.001	1.61	0.01	<0.001
PBX3_HUMAN	Pre-B-cell leukemia transcription factor 3	2	16.6	0.97	0.3	0.868	1.43	0.02	<0.001	1.22	0.04	0.004
PCD16_HUMAN	Protocadherin-16	5	2.9	1.46	0.04	<0.001	1.6	0.08	0.001	1.19	0.09	0.052
PCDA8_HUMAN	Protocadherin alpha-8	4	5.9	1.34	0.01	<0.001	1.41	0.01	<0.001	1.07	0.06	0.171
PCGF6_HUMAN	Polycomb group RING finger protein 6	3	4.6	1.41	0.06	0.001	1.53	0.1	0.002	1.09	0.03	0.016
PCLO_HUMAN	Protein piccolo	18	5.9	1.43	0	<0.001	1.63	0.01	<0.001	1.18	0.01	<0.001
PDE3A_HUMAN	cGMP-inhibited 3~,5~-cyclic phosphodiesterase A	2	3.2	1.36	0.01	<0.001	1.32	0.12	0.015	0.96	0.08	0.517
PDE3B_HUMAN	cGMP-inhibited 3~,5~-cyclic phosphodiesterase B	1	1.4	1.66	0.27	0.018	1.74	0.75	0.185	1.38	0.78	0.525
PDZD2_HUMAN	PDZ domain-containing protein 2	21	10.4	1.35	0.02	<0.001	1.55	0.18	0.010	1.1	0.2	0.502
PEAK1_HUMAN	Pseudopodium-enriched atypical kinase 1	7	5	1.47	0.02	<0.001	1.74	0.05	<0.001	1.3	0.04	0.001
PEG3_HUMAN	Paternally-expressed gene 3 protein	6	2.6	1.49	0.01	<0.001	1.62	0.03	<0.001	1.2	0.06	0.013
PEPL_HUMAN	Periplakin	5	2.3	1.46	0.02	<0.001	1.69	0.1	0.001	1.21	0.11	0.063
PER1_HUMAN	Period circadian protein homolog 1	4	1.6	1.51	0.01	<0.001	1.47	0.51	0.201	1.43	0.09	0.005
PGBM_HUMAN	Basement membrane-specific heparan sulfate proteoglycan core protein	11	3.4	1.42	0.01	<0.001	1.64	0.12	0.002	1.25	0.12	0.049
PGFRB_HUMAN	Platelet-derived growth factor receptor beta	6	4.8	1.34	0.16	0.024	1.35	0.23	0.071	1.69	0.58	0.167
PGP_HUMAN	Glycerol-3-phosphate phosphatase	4	16.5	1.51	0.02	<0.001	1.67	0.01	<0.001	1.19	0.06	0.016
PHAR4_HUMAN	Phosphatase and actin regulator 4	9	9.7	1.51	0.04	<0.001	1.57	0.11	0.002	1.06	0.14	0.598
PHF14_HUMAN	PHD finger protein 14	5	6.1	1.42	0.05	<0.001	1.65	0.15	0.003	1.22	0.13	0.081
PHLB2_HUMAN	Pleckstrin homology-like domain family B member 2	5	5.6	1.59	0.18	0.007	2.09	0.45	0.019	1.66	0.36	0.067
PHLP1_HUMAN	PH domain leucine-rich repeat-containing protein phosphatase 1	6	3.2	1.41	0.07	0.001	1.61	0.16	0.005	1.23	0.14	0.087
PI42C_HUMAN	Phosphatidylinositol 5-phosphate 4-kinase type-2 gamma	3	11.2	1.54	0.15	0.005	1.35	0.01	<0.001	1.13	0.08	0.084
PI4KA_HUMAN	Phosphatidylinositol 4-kinase alpha	8	3.8	1.42	0.03	<0.001	1.66	0	<0.001	1.22	0	<0.001
PI5PA_HUMAN	Phosphatidylinositol 4;5-bisphosphate 5-phosphatase A	6	4.4	1.57	0.01	<0.001	1.74	0.02	<0.001	1.23	0.02	<0.001
PK3CD_HUMAN	Phosphatidylinositol 4;5-bisphosphate 3-kinase	8	4.6	1.51	0.05	<0.001	1.69	0.18	0.004	1.24	0.15	0.095

	catalytic subunit delta isoform											
PKD1_HUMAN	Polycystin-1	19	4.3	1.37	0.1	0.005	1.64	0.01	<0.001	1.21	0.01	<0.001
PKHG3_HUMAN	Pleckstrin homology domain-containing family G member 3	6	4.1	1.49	0.02	<0.001	1.7	0.02	<0.001	1.28	0.05	0.003
PKP1_HUMAN	Plakophilin-1	5	7.8	1.33	0.14	0.020	1.53	0.11	0.002	1.04	0.07	0.466
PLCB3_HUMAN	1-phosphatidylinositol 4;5-bisphosphate phosphodiesterase beta-3	6	4.5	1.49	0.04	<0.001	1.66	0.03	<0.001	1.2	0.02	0.001
PLCB4_HUMAN	1-phosphatidylinositol 4;5-bisphosphate phosphodiesterase beta-4	4	4.2	1.36	0.18	0.031	1.78	0.18	0.003	1.38	0.18	0.052
PLCL2_HUMAN	Inactive phospholipase C-like protein 2	5	2.6	1.37	0.07	0.001	1.71	0.28	0.017	1.19	0.33	0.470
PLCZ1_HUMAN	1-phosphatidylinositol 4;5-bisphosphate phosphodiesterase zeta-1	2	5.3	1.31	0.2	0.066	1.36	0.26	0.087	0.86	0.26	0.497
PLEC_HUMAN	Plectin	16	3.6	1.42	0.11	0.003	1.6	0.16	0.005	1.17	0.09	0.066
PLSL_HUMAN	Plastin-2	12	13.7	1.32	0.04	<0.001	1.08	0.05	0.059	0.74	0.07	0.011
PLXA4_HUMAN	Plexin-A4	7	6.4	1.43	0.03	<0.001	1.58	0.01	<0.001	1.13	0.1	0.145
PLXB3_HUMAN	Plexin-B3	2	1.9	1.48	0.21	0.022	1.7	0.66	0.154	1.35	0.58	0.434
PLXD1_HUMAN	Plexin-D1	4	2.6	1.47	0.06	<0.001	1.62	0.01	<0.001	1.1	0.05	0.065
PNPT1_HUMAN	Polyribonucleotide nucleotidyltransferase 1; mitochondrial	6	5.4	1.46	0.04	<0.001	1.59	0.26	0.023	1.16	0.21	0.342
PO4F2_HUMAN	POU domain; class 4; transcription factor 2	13	19.8	1.4	0.01	<0.001	1.85	0.03	<0.001	1.41	0.09	0.006
PP1A_HUMAN	Serine/threonine-protein phosphatase PP1-alpha catalytic subunit	8	11.2	1.6	0.12	0.002	1.79	0.17	0.003	1.32	0.13	0.035
PPM1B_HUMAN	Protein phosphatase 1B	7	2.9	1.63	0.01	<0.001	1.75	0.02	<0.001	1.28	0.02	<0.001
PPM1H_HUMAN	Protein phosphatase 1H	4	15.2	1.3	0.13	0.018	1.61	0.04	<0.001	1.1	0.13	0.346
PPM1L_HUMAN	Protein phosphatase 1L	3	11.4	1.45	0.02	<0.001	2.02	0.06	<0.001	1.58	0.11	0.004
PRGR_HUMAN	Progesterone receptor	7	10	1.54	0.09	0.001	1.97	0.16	0.001	1.58	0.28	0.051
PRKDC_HUMAN	DNA-dependent protein kinase catalytic subunit	16	4.4	1.28	0.18	0.060	1.56	0.08	0.001	1.24	0.19	0.156
PRP8_HUMAN	Pre-mRNA-processing-splicing factor 8	6	3.3	1.38	0.01	<0.001	1.48	0.01	<0.001	1.03	0.01	0.004
PRR5_HUMAN	Proline-rich protein 5	3	7	1.34	0.03	<0.001	1.6	0.11	0.002	1.36	0.2	0.072
PRS4_HUMAN	26S protease regulatory subunit 4	6	3.4	1.52	0.2	0.015	1.62	0.2	0.009	1.32	0.19	0.083
PSB10_HUMAN	Proteasome subunit beta type-10	4	6.6	1.26	0.02	<0.001	1.5	0.04	<0.001	0.93	0.03	0.021
PSB3_HUMAN	Proteasome subunit beta type-3	13	13.2	1.44	0.01	<0.001	1.66	0	<0.001	1.14	0.03	0.003

PSPC1_HUMAN	Paraspeckle component 1	4	15.1	1.39	0.05	<0.001	1.48	0.11	0.003	1.02	0.05	0.585
PTBP2_HUMAN	Polypyrimidine tract-binding protein 2	3	3.8	1.39	0.01	<0.001	1.43	0.06	0.001	0.98	0.02	0.183
PTN1_HUMAN	Tyrosine-protein phosphatase non-receptor type 1	1	2.5	1.05	0.27	0.795	1.06	0.14	0.489	0.78	0.1	0.040
PTN12_HUMAN	Tyrosine-protein phosphatase non-receptor type 12	5	9	1.45	0.03	<0.001	1.76	0.03	<0.001	1.32	0.1	0.018
PTN18_HUMAN	Tyrosine-protein phosphatase non-receptor type 18	3	8.5	1.43	0.06	<0.001	1.61	0.06	<0.001	1.14	0.03	0.004
PTN6_HUMAN	Tyrosine-protein phosphatase non-receptor type 6	4	5.2	1.35	0.21	0.053	1.73	0.21	0.006	1.42	0.09	0.005
PTPC1_HUMAN	Protein tyrosine phosphatase domain-containing protein 1	2	2.9	1.43	0.04	<0.001	1.78	0.19	0.004	1.36	0.22	0.084
PTPRB_HUMAN	Receptor-type tyrosine-protein phosphatase beta	17	9.5	1.49	0.04	<0.001	1.62	0.06	<0.001	1.16	0.02	0.001
PTPRE_HUMAN	Receptor-type tyrosine-protein phosphatase epsilon	4	9.6	1.4	0.1	0.004	1.4	0.07	0.002	0.96	0.08	0.527
PTPRG_HUMAN	Receptor-type tyrosine-protein phosphatase gamma	6	2.2	1.45	0.09	0.002	1.41	0.09	0.003	0.98	0.11	0.823
PTPRQ_HUMAN	Phosphatidylinositol phosphatase PTPRQ	5	3.4	1.39	0.02	<0.001	1.62	0.06	<0.001	1.11	0.06	0.071
PTPRU_HUMAN	Receptor-type tyrosine-protein phosphatase U	4	4.7	1.42	0.01	<0.001	1.65	0.08	<0.001	1.14	0	<0.001
PYR1_HUMAN	CAD protein	4	3.3	1.2	0.14	0.085	1.17	0.13	0.106	0.84	0.06	0.031
RAB1A_HUMAN	Ras-related protein Rab-1A	6	12.2	1.45	0.03	<0.001	1.74	0.03	<0.001	1.32	0	<0.001
RABE2_HUMAN	Rab GTPase-binding effector protein 2	3	3.9	1.5	0.04	<0.001	1.79	0.06	<0.001	1.34	0.09	0.010
RAVR2_HUMAN	Ribonucleoprotein PTB-binding 2	4	5.8	1.36	0.15	0.018	1.65	0.02	<0.001	1.37	0.16	0.037
RB15B_HUMAN	Putative RNA-binding protein 15B	9	9.7	1.45	0.02	<0.001	1.56	0.12	0.002	1.15	0.12	0.158
RBBP6_HUMAN	E3 ubiquitin-protein ligase RBBP6	5	3.9	1.45	0.12	0.004	1.75	0.09	<0.001	1.34	0.02	<0.001
RBM15_HUMAN	Putative RNA-binding protein 15	17	10.3	1.42	0.05	<0.001	1.68	0.1	0.001	1.24	0.09	0.024
RBM23_HUMAN	Probable RNA-binding protein 23	4	8.7	1.46	0.1	0.002	1.46	0.31	0.075	1.11	0.31	0.650
RBMX_HUMAN	RNA-binding motif protein; X chromosome	6	9.7	1.4	0.09	0.002	1.46	0.19	0.018	1.1	0.1	0.213
RCOR3_HUMAN	REST corepressor 3	2	6.5	1.49	0.06	<0.001	1.56	0.23	0.018	1.09	0.22	0.588
RELB_HUMAN	Transcription factor RelB	6	5.4	1.52	0.12	0.002	1.73	0.25	0.011	1.3	0.26	0.173
RENT1_HUMAN	Regulator of nonsense transcripts 1	6	3.8	1.61	0.08	<0.001	1.88	0.14	0.001	1.46	0.08	0.003
RGMC_HUMAN	Hemojuvelin	3	6.8	1.55	0	<0.001	1.72	0.03	<0.001	1.25	0.01	<0.001
RGPS1_HUMAN	Ras-specific guanine nucleotide-releasing factor RalGPS1	4	3.2	1.39	0	<0.001	1.59	0.04	<0.001	1.15	0.03	0.004
RGS20_HUMAN	Regulator of G-protein signaling 20	3	15.2	1.24	0.02	<0.001	1.3	0.02	<0.001	0.91	0.13	0.395

RGS3_HUMAN	Regulator of G-protein signaling 3	5	4.2	1.33	0.11	0.010	1.57	0.09	0.001	1.12	0.04	0.018
RHG09_HUMAN	Rho GTPase-activating protein 9	2	5.6	1.3	0.24	0.109	1.37	0.03	<0.001	1.04	0.09	0.594
RHG21_HUMAN	Rho GTPase-activating protein 21	9	4.8	1.42	0.01	<0.001	1.7	0.06	<0.001	1.3	0.01	<0.001
RHG24_HUMAN	Rho GTPase-activating protein 24	6	10.7	1.44	0.01	<0.001	1.76	0.01	<0.001	1.33	0.02	<0.001
RHG28_HUMAN	Rho GTPase-activating protein 28	4	3.7	1.31	0.23	0.087	1.51	0.25	0.031	1.11	0.12	0.271
RHG31_HUMAN	Rho GTPase-activating protein 31	7	5.9	1.41	0.02	<0.001	1.59	0.06	<0.001	1.16	0.04	0.010
RHG33_HUMAN	Rho GTPase-activating protein 33	6	5.4	1.44	0.02	<0.001	1.68	0.11	0.001	1.26	0.04	0.003
RIC8A_HUMAN	Synembryn-A	2	2.1	1.66	0.61	0.153	2.02	0.66	0.067	1.67	0.56	0.166
RIN1_HUMAN	Ras and Rab interactor 1	9	7	1.47	0.08	0.001	1.62	0.15	0.004	1.17	0.14	0.147
RMXL1_HUMAN	RNA binding motif protein; X-linked-like-1	8	14.9	1.51	0.01	<0.001	1.84	0.02	<0.001	1.39	0.01	<0.001
RN169_HUMAN	E3 ubiquitin-protein ligase RNF169	4	10.3	1.5	0.12	0.002	1.64	0.05	<0.001	1.18	0.05	0.010
RN19A_HUMAN	E3 ubiquitin-protein ligase RNF19A	11	8.1	1.38	0.09	0.003	1.58	0.03	<0.001	1.2	0	<0.001
RNPS1_HUMAN	RNA-binding protein with serine-rich domain 1	3	14.1	1.42	0.02	<0.001	1.44	0.15	0.010	1.25	0.09	0.025
ROA0_HUMAN	Heterogeneous nuclear ribonucleoprotein A0	22	19.3	1	0.23	0.991	0.86	0.01	<0.001	0.63	0.09	0.007
ROA1_HUMAN	Heterogeneous nuclear ribonucleoprotein A1	7	14.8	1.47	0.02	<0.001	1.83	0.01	<0.001	1.36	0.03	<0.001
ROA3_HUMAN	Heterogeneous nuclear ribonucleoprotein A3	8	19.8	1.38	0.01	<0.001	1.35	0.17	0.030	1	0.07	0.970
ROBO4_HUMAN	Roundabout homolog 4	6	1.2	1.45	0	<0.001	1.65	0.1	0.001	1.2	0.09	0.045
ROCK2_HUMAN	Rho-associated protein kinase 2	4	2.8	1.35	0	<0.001	1.5	0.08	0.001	1.11	0.04	0.028
RPIL1_HUMAN	Retinitis pigmentosa 1-like 1 protein	14	7.4	1.35	0.07	0.001	1.62	0.01	<0.001	1.16	0.01	<0.001
RRP5_HUMAN	Protein RRP5 homolog	3	1.5	1.1	0.01	<0.001	0.94	0.02	0.008	0.55	0.01	<0.001
RS2_HUMAN	40S ribosomal protein S2	13	11.9	1.45	0.03	<0.001	1.69	0.07	<0.001	1.12	0.02	0.005
RSSA_HUMAN	40S ribosomal protein SA	3	15.3	1.5	0.06	<0.001	1.69	0.05	<0.001	1.26	0.02	<0.001
RUNX1_HUMAN	Runt-related transcription factor 1	8	8.4	1.59	0.06	<0.001	1.73	0	<0.001	1.3	0.03	0.001
RYR2_HUMAN	Ryanodine receptor 2	16	3.6	1.45	0	<0.001	1.72	0	<0.001	1.27	0	<0.001
S27A1_HUMAN	Long-chain fatty acid transport protein 1	2	5.3	1.36	0.07	0.001	1.55	0.18	0.009	1.22	0.11	0.051
SAC2_HUMAN	Phosphatidylinositide phosphatase SAC2	3	1	1.49	0.05	<0.001	1.8	0.06	<0.001	1.33	0.06	0.004
SAFB1_HUMAN	Scaffold attachment factor B1	10	6.2	1.47	0.01	<0.001	1.64	0.05	<0.001	1.23	0.06	0.011
SAHH2_HUMAN	Adenosylhomocysteinase 2	6	8.7	1.38	0.03	<0.001	1.51	0	<0.001	1.08	0.02	0.010

SC61B_HUMAN	Protein transport protein Sec61 subunit beta	2	16.7	1.34	0.09	0.004	1.59	0.28	0.029	1.22	0.17	0.144
SCRT1_HUMAN	Transcriptional repressor scratch 1	8	27.9	1.31	0.24	0.104	1.62	0.01	<0.001	1.26	0.01	<0.001
SCRT2_HUMAN	Transcriptional repressor scratch 2	5	7.5	1.43	0.08	0.001	1.62	0.11	0.001	1.24	0.11	0.048
SET1B_HUMAN	Histone-lysine N-methyltransferase SETD1B	5	2.7	1.4	0.1	0.003	1.44	0.27	0.057	1.06	0.17	0.627
SETMR_HUMAN	Histone-lysine N-methyltransferase SETMAR	2	5.1	1.56	0.04	<0.001	2.13	0.14	<0.001	1.76	0.28	0.026
SF3B3_HUMAN	Splicing factor 3B subunit 3	2	3	1.5	0.05	<0.001	1.78	0.03	<0.001	1.27	0.03	0.001
SF3B4_HUMAN	Splicing factor 3B subunit 4	1	4.7	1.46	0.13	0.005	1.86	0.18	0.002	1.39	0.17	0.038
SF3B4_HUMAN	Splicing factor; proline- and glutamine-rich	19	14.7	1.33	0.03	<0.001	1.57	0.05	<0.001	1.23	0.01	<0.001
SFR19_HUMAN	Splicing factor; arginine/serine-rich 19	14	4.6	1.42	0.12	0.005	1.65	0.01	<0.001	1.17	0.03	0.002
SH3K1_HUMAN	SH3 domain-containing kinase-binding protein 1	5	4.7	1.44	0.12	0.005	1.6	0.04	<0.001	1.13	0.02	0.003
SHH_HUMAN	Sonic hedgehog protein	9	8.4	1.56	0.01	<0.001	1.89	0.07	<0.001	1.44	0.04	0.001
SHOT1_HUMAN	Shootin-1	1	1.4	1.43	0.01	<0.001	1.38	0.01	<0.001	0.99	0.04	0.686
SHOX2_HUMAN	Short stature homeobox protein 2	7	14.2	1.37	0.04	<0.001	1.47	0.03	<0.001	1.1	0.02	0.005
SHRM3_HUMAN	Protein Shroom3	10	3.5	1.43	0.01	<0.001	1.54	0.07	0.001	1.1	0.04	0.025
SIIL2_HUMAN	Signal-induced proliferation-associated 1-like protein 2	6	3.6	1.49	0.13	0.003	1.89	0.34	0.015	1.45	0.29	0.098
SIIL3_HUMAN	Signal-induced proliferation-associated 1-like protein 3	6	5.8	1.56	0.01	<0.001	1.98	0.13	0.001	1.57	0.2	0.020
SIG10_HUMAN	Sialic acid-binding Ig-like lectin 10	8	3.4	1.39	0.06	0.001	1.4	0.15	0.013	1.01	0.13	0.954
SIK3_HUMAN	Serine/threonine-protein kinase SIK3	7	6	1.38	0.03	<0.001	1.36	0.05	0.001	1.01	0.04	0.686
SIN3B_HUMAN	Paired amphipathic helix protein Sin3b	7	2.2	1.41	0.05	<0.001	1.72	0.11	0.001	1.45	0.25	0.067
SIPA1_HUMAN	Signal-induced proliferation-associated protein 1	3	4.7	1.17	0.19	0.223	0.86	0.36	0.563	0.79	0.09	0.036
SKOR1_HUMAN	SKI family transcriptional corepressor 1	15	11.7	1.49	0.02	<0.001	1.9	0.34	0.014	1.43	0.34	0.144
SMBT1_HUMAN	Scm-like with four MBT domains protein 1	2	4	1.68	0.17	0.003	1.61	0.15	0.003	1.27	0.07	0.009
SMG1_HUMAN	Serine/threonine-protein kinase SMG1	13	3.6	1.43	0	<0.001	1.69	0.15	0.003	1.25	0.16	0.097
SMRC1_HUMAN	SWI/SNF complex subunit SMARCC1	4	6.7	1.48	0	<0.001	1.65	0.03	<0.001	1.23	0.02	<0.001
SND1_HUMAN	Staphylococcal nuclease domain-containing protein 1	6	6.8	1.4	0.09	0.002	1.45	0.05	<0.001	1.02	0.04	0.559
SNED1_HUMAN	Sushi; nidogen and EGF-like domain-containing protein 1	9	7.1	1.5	0.01	<0.001	1.53	0.04	<0.001	1.15	0.01	<0.001
SON_HUMAN	Protein SON	37	7.5	1.45	0.01	<0.001	1.77	0.04	<0.001	1.33	0.02	<0.001

SOX3_HUMAN	Transcription factor SOX-3	9	22.4	1.25	0.05	0.001	1.4	0.04	<0.001	1.01	0.13	0.903
SOX7_HUMAN	Transcription factor SOX-7	1	3.4	1.46	0.02	<0.001	2.05	0.09	<0.001	1.93	0.34	0.024
SP16H_HUMAN	FACT complex subunit SPT16	5	6.1	1.46	0.05	<0.001	1.45	0.1	0.003	1.03	0.1	0.723
SPEG_HUMAN	Striated muscle preferentially expressed protein kinase	7	1.9	1.43	0.02	<0.001	1.6	0.01	<0.001	1.14	0.06	0.034
SPG7_HUMAN	Paraplegin	7	5	1.41	0.06	<0.001	1.45	0.01	<0.001	1.02	0.01	0.070
SPIR1_HUMAN	Protein spire homolog 1	4	3.3	1.29	0.07	0.003	1.55	0.1	0.001	1.12	0.08	0.114
SPT5H_HUMAN	Transcription elongation factor SPT5	10	5.8	1.31	0.06	0.001	1.64	0.02	<0.001	1.25	0.09	0.026
SPTA1_HUMAN	Spectrin alpha chain; erythrocytic 1	8	2.7	1.46	0.04	<0.001	1.76	0.17	0.003	1.29	0.19	0.106
SPTN2_HUMAN	Spectrin beta chain; non-erythrocytic 2	11	6.4	1.47	0.01	<0.001	1.61	0.1	0.001	1.12	0.01	0.001
SPTN5_HUMAN	Spectrin beta chain; non-erythrocytic 5	13	4.8	1.45	0.02	<0.001	1.7	0.07	<0.001	1.24	0.07	0.015
SRBS2_HUMAN	Sorbin and SH3 domain-containing protein 2	3	4.1	1.35	0.31	0.140	2.02	0.3	0.006	1.72	0.17	0.007
SRCN1_HUMAN	SRC kinase signaling inhibitor 1	5	7.4	1.23	0.13	0.046	2.2	0.64	0.039	2.42	1.22	0.172
SRF_HUMAN	Serum response factor	8	7.3	1.43	0	<0.001	1.75	0.03	<0.001	1.29	0.05	0.004
SRRM2_HUMAN	Serine/arginine repetitive matrix protein 2	24	10.9	1.55	0.03	<0.001	1.76	0.05	<0.001	1.26	0.06	0.006
SSPO_HUMAN	SCO-spondin	2	0.3	1.05	0.36	0.845	1.56	0.01	<0.001	1.22	0.14	0.102
STAB1_HUMAN	Stabilin-1	8	5.6	1.45	0.09	0.001	1.72	0.12	0.001	1.29	0.1	0.019
STB5L_HUMAN	Syntaxin-binding protein 5-like	4	4.8	1.47	0.11	0.002	1.64	0.14	0.003	1.24	0.12	0.051
STRP2_HUMAN	Striatin-interacting protein 2	8	5.8	1.47	0.13	0.005	3	1.21	0.055	2.57	1.24	0.149
SUZ12_HUMAN	Polycomb protein SUZ12	4	7.2	1.26	0.03	<0.001	1.36	0.01	<0.001	0.97	0.04	0.280
SVIL_HUMAN	Supervillin	8	3.5	1.41	0.06	<0.001	1.54	0.09	0.001	1.11	0.12	0.251
SYDE2_HUMAN	Rho GTPase-activating protein SYDE2	8	10.2	1.13	0.29	0.516	1.68	0.29	0.020	1.3	0.2	0.106
SYGP1_HUMAN	Ras/Rap GTPase-activating protein SynGAP	10	8	1.53	0.03	<0.001	1.68	0.11	0.001	1.23	0.09	0.034
SYNJ1_HUMAN	Synaptojanin-1	8	6.4	1.39	0.04	<0.001	1.62	0.05	<0.001	1.3	0.15	0.057
TACC1_HUMAN	Transforming acidic coiled-coil-containing protein 1	4	9.7	1.44	0.15	0.010	1.87	0.22	0.004	1.42	0.2	0.047
TACC2_HUMAN	Transforming acidic coiled-coil-containing protein 2	12	6.4	1.46	0.01	<0.001	1.67	0.05	<0.001	1.25	0.01	<0.001
TACC3_HUMAN	Transforming acidic coiled-coil-containing protein 3	2	3.5	1.66	0.13	0.001	2.13	0.45	0.017	1.73	0.38	0.059
TAGL2_HUMAN	Transgelin-2	10	26.6	1.5	0.09	0.001	1.74	0.04	<0.001	1.26	0.09	0.019

TAL1_HUMAN	T-cell acute lymphocytic leukemia protein 1	3	16.3	1.62	0.06	<0.001	1.94	0.1	<0.001	1.48	0.05	0.001
TARA_HUMAN	TRIO and F-actin-binding protein	5	2.7	1.32	0	<0.001	1.71	0.36	0.034	1.28	0.24	0.174
TBA1A_HUMAN	Tubulin alpha-1A chain	6	8	1.46	0.02	<0.001	1.51	0.01	<0.001	1.11	0.02	0.003
TBX2_HUMAN	T-box transcription factor TBX2	3	4.5	1.28	0.01	<0.001	0.96	0.05	0.304	0.46	0.18	0.017
TCAF1_HUMAN	TRPM8 channel-associated factor 1	4	5.5	1.28	0.04	<0.001	1.74	0.13	0.001	1.36	0	<0.001
TCF20_HUMAN	Transcription factor 20	2	1.6	1.64	0.22	0.011	1.75	0.16	0.002	1.37	0.23	0.088
TDRD3_HUMAN	Tudor domain-containing protein 3	6	9.1	1.48	0.01	<0.001	1.8	0.01	<0.001	1.37	0.03	<0.001
TDRD9_HUMAN	Putative ATP-dependent RNA helicase TDRD9	7	7.7	1.2	0.09	0.029	1.65	0.38	0.051	1.27	0.35	0.329
TEN2_HUMAN	Teneurin-2	5	1.5	1.52	0.17	0.008	1.81	0.19	0.003	1.43	0.06	0.001
TENX_HUMAN	Tenascin-X	16	4.9	1.45	0.03	<0.001	1.71	0.04	<0.001	1.24	0.06	0.008
TERA_HUMAN	Transitional endoplasmic reticulum ATPase	5	7.9	1.55	0.02	<0.001	1.77	0.15	0.002	1.31	0.12	0.028
TET2_HUMAN	Methylcytosine dioxygenase TET2	4	2.3	1.16	0.09	0.044	1.35	0.05	0.001	1	0.01	1.001
TGFR2_HUMAN	TGF-beta receptor type-2	4	8.5	1.08	0.36	0.747	1.51	0.13	0.004	1.23	0.01	<0.001
TICRR_HUMAN	Treslin	8	4.5	1.44	0.02	<0.001	1.68	0.1	0.001	1.24	0.04	0.003
TIE2_HUMAN	Angiopoietin-1 receptor	3	1.7	1.56	0.1	0.001	1.75	0.1	0.001	1.32	0.14	0.038
TIF1B_HUMAN	Transcription intermediary factor 1-beta	6	7.4	1.41	0.08	0.001	1.6	0.18	0.007	1.24	0.11	0.043
TIM_HUMAN	Protein timeless homolog	4	4.7	1.37	0.08	0.002	1.49	0.03	<0.001	1.09	0.03	0.017
TLK1_HUMAN	Serine/threonine-protein kinase tousled-like 1	6	5.1	1.31	0.08	0.003	1.46	0.05	<0.001	1.16	0.07	0.034
TLN1_HUMAN	Talin-1	56	16.6	1.59	0.04	<0.001	1.77	0.1	0.001	1.25	0.1	0.031
TLN2_HUMAN	Talin-2	8	3.4	1.47	0.03	<0.001	1.73	0.04	<0.001	1.31	0.04	0.002
TNAP3_HUMAN	Tumor necrosis factor alpha-induced protein 3	1	2.5	1.55	0.23	0.019	1.51	0.02	<0.001	1.04	0.09	0.589
TNK1_HUMAN	Non-receptor tyrosine-protein kinase TNK1	6	15.6	1.29	0.19	0.069	1.53	0.57	0.201	1.07	0.47	0.843
TNR6B_HUMAN	Trinucleotide repeat-containing gene 6B protein	3	2.3	1.46	0.07	0.001	1.82	0.11	<0.001	1.49	0.02	<0.001
TNR6C_HUMAN	Trinucleotide repeat-containing gene 6C protein	9	8.4	1.4	0.04	<0.001	1.89	0.02	<0.001	1.49	0	<0.001
TNS2_HUMAN	Tensin-2	7	7.4	1.35	0.06	0.001	2.04	0.39	0.014	1.6	0.24	0.033
TP53B_HUMAN	Tumor suppressor p53-binding protein 1	10	5.2	1.42	0.1	0.002	1.75	0.05	<0.001	1.28	0.02	<0.001
TPM1_HUMAN	Tropomyosin alpha-1 chain	7	8.8	1.24	0.04	0.001	1.29	0.14	0.031	0.89	0.11	0.209
TPM2_HUMAN	Tropomyosin beta chain	3	8.8	1.4	0.05	<0.001	2.55	0.86	0.043	2.13	0.84	0.135

TPM4_HUMAN	Tropomyosin alpha-4 chain	8	19.4	1.51	0.09	0.001	1.78	0.03	<0.001	1.35	0.06	0.003
TR10A_HUMAN	Tumor necrosis factor receptor superfamily member 10A	2	7.3	1.41	0.08	0.001	1.7	0.06	<0.001	1.2	0.07	0.023
TRA2A_HUMAN	Transformer-2 protein homolog alpha	12	15.2	1.44	0.01	<0.001	1.62	0.07	<0.001	1.19	0.06	0.013
TRIO_HUMAN	Triple functional domain protein	7	2.8	1.48	0.03	<0.001	1.58	0.18	0.008	1.14	0.2	0.364
TRRAP_HUMAN	Transformation/transcription domain-associated protein	6	1.4	1.76	0.31	0.016	2.03	0.34	0.010	2.11	0.87	0.148
TSP1_HUMAN	Thrombospondin-1	8	3.8	1.72	0.21	0.006	1.99	0.2	0.002	1.48	0.25	0.058
TTBK2_HUMAN	Tau-tubulin kinase 2	6	5.9	1.35	0.09	0.003	1.54	0.02	<0.001	1.05	0.05	0.176
TWST1_HUMAN	Twist-related protein 1	3	24.3	1.49	0.09	0.001	1.54	0.31	0.047	1.07	0.32	0.759
TYPH_HUMAN	Thymidine phosphorylase	3	10	1.42	0.01	<0.001	1.64	0.13	0.002	1.17	0.08	0.048
U520_HUMAN	U5 small nuclear ribonucleoprotein 200 kDa helicase	8	2.7	1.49	0.02	<0.001	1.64	0.07	<0.001	1.16	0.04	0.008
UBA1_HUMAN	Ubiquitin-like modifier-activating enzyme 1	5	5.2	1.39	0.05	<0.001	1.6	0.08	<0.001	1.12	0.07	0.064
UBP34_HUMAN	Ubiquitin carboxyl-terminal hydrolase 34	6	1.9	1.42	0.01	<0.001	1.5	0.06	<0.001	1.04	0.07	0.467
UBR5_HUMAN	E3 ubiquitin-protein ligase UBR5	8	3.9	1.44	0.04	<0.001	1.64	0.06	<0.001	1.24	0.07	0.013
ULK4_HUMAN	Serine/threonine-protein kinase ULK4	4	4.6	1.37	0.03	<0.001	1.57	0.09	0.001	1.14	0.04	0.016
UN13A_HUMAN	Protein unc-13 homolog A	6	1.9	1.35	0.05	<0.001	1.55	0.12	0.003	1.07	0.09	0.289
UN13C_HUMAN	Protein unc-13 homolog C	16	4.4	1.48	0.05	<0.001	1.85	0.28	0.009	1.43	0.28	0.103
UNC5D_HUMAN	Netrin receptor UNC5D	13	5.1	1.27	0.21	0.096	1.53	0.19	0.012	1.18	0.02	0.001
USP9X_HUMAN	Probable ubiquitin carboxyl-terminal hydrolase FAF-X	6	2.9	1.56	0.09	0.001	1.79	0.11	0.001	1.29	0.13	0.047
UVRAG_HUMAN	UV radiation resistance-associated gene protein	7	8.4	1.62	0.13	0.002	1.67	0.07	<0.001	1.29	0.11	0.028
VASH1_HUMAN	Vasohibin-1	3	11.2	1.15	0.4	0.579	1.78	0.33	0.019	1.36	0.25	0.115
VASP_HUMAN	Vasodilator-stimulated phosphoprotein	6	11.6	1.54	0.12	0.002	1.7	0	<0.001	1.24	0.05	0.005
VINC_HUMAN	Vinculin	32	12.5	1.46	0.09	0.001	1.73	0.13	0.001	1.28	0.1	0.021
VIR_HUMAN	Protein virilizer homolog	7	5.3	1.46	0.01	<0.001	1.8	0.07	<0.001	1.36	0.14	0.028
VPRBP_HUMAN	Protein VPRBP	3	4.4	1.29	0	<0.001	1.36	0.06	0.001	1.01	0.08	0.826
WBS22_HUMAN	Probable 18S rRNA (guanine-N(7))-methyltransferase	4	6.4	1.41	0.12	0.005	1.55	0.39	0.082	1.07	0.38	0.815
WDR33_HUMAN	pre-mRNA 3'-end processing protein WDR33	9	3.3	1.48	0.02	<0.001	1.74	0.14	0.001	1.3	0.1	0.021
WDR76_HUMAN	WD repeat-containing protein 76	6	10.5	1.48	0.03	<0.001	1.79	0.02	<0.001	1.39	0.08	0.004

WIPF1_HUMAN	WAS/WASL-interacting protein family member 1	8	25.8	1.51	0.15	0.005	1.88	0.08	<0.001	1.56	0.07	0.001
WIPF2_HUMAN	WAS/WASL-interacting protein family member	5	12	1.62	0.01	<0.001	1.83	0.36	0.021	1.39	0.38	0.221
WIZ_HUMAN	Protein Wiz	9	3.2	1.42	0.05	<0.001	1.86	0.08	<0.001	1.44	0.08	0.003
WN10A_HUMAN	Protein Wnt-10a	1	5.5	2.75	0.25	<0.001	7.46	0.51	<0.001	8.15	0.07	<0.001
WNK1_HUMAN	Serine/threonine-protein kinase WNK1	9	5.3	1.69	0.2	0.006	2.05	0.41	0.016	1.6	0.43	0.124
WNT2B_HUMAN	Protein Wnt-2b	2	8.7	1.38	0.1	0.003	0.92	0.21	0.581	0.68	0.27	0.172
WTIP_HUMAN	Wilms tumor protein 1-interacting protein	8	15.6	1.42	0.05	<0.001	1.86	0.02	<0.001	1.33	0.02	<0.001
WWC2_HUMAN	Protein WWC2	7	6.9	1.48	0.01	<0.001	1.61	0.01	<0.001	1.15	0.01	<0.001
XIRP1_HUMAN	Xin actin-binding repeat-containing protein 1	2	2.7	1.42	0.11	0.004	1.86	0.06	<0.001	1.38	0.06	0.002
XIRP2_HUMAN	Xin actin-binding repeat-containing protein 2	12	4.6	1.52	0.01	<0.001	1.82	0.05	<0.001	1.35	0.07	0.005
XPF_HUMAN	DNA repair endonuclease XPF	5	7.9	1.46	0.11	0.003	1.74	0.21	0.006	1.36	0.05	0.001
YTDC2_HUMAN	Probable ATP-dependent RNA helicase YTHDC2	12	6	1.39	0.06	0.001	1.51	0.07	0.001	1.09	0.01	0.001
ZBED3_HUMAN	Zinc finger BED domain-containing protein 3	5	16.2	1.53	0.05	<0.001	1.92	0.06	<0.001	1.42	0.03	<0.001
ZBTB4_HUMAN	Zinc finger and BTB domain-containing protein 4	10	8.1	1.45	0.04	<0.001	1.71	0.06	<0.001	1.33	0.01	<0.001
ZCHC8_HUMAN	Zinc finger CCHC domain-containing protein 8	8	11.3	1.53	0.03	<0.001	1.64	0.2	0.008	1.18	0.15	0.154
ZFHX3_HUMAN	Zinc finger homeobox protein 3	6	2.1	1.5	0.16	0.008	1.6	0.2	0.010	1.19	0.23	0.309
ZMIZ2_HUMAN	Zinc finger MIZ domain-containing protein 2	1	3.4	1.12	0.15	0.260	1.75	0.21	0.005	1.82	0.17	0.005
ZMYM3_HUMAN	Zinc finger MYM-type protein 3	3	3.7	1.52	0.17	0.008	1.74	0.11	0.001	1.46	0.2	0.040
ZN281_HUMAN	Zinc finger protein 281	3	4.2	1.34	0.01	<0.001	1.24	0.1	0.017	1.15	0.27	0.462
ZN292_HUMAN	Zinc finger protein 292	12	5.9	1.35	0.12	0.009	1.83	0.02	<0.001	1.28	0.06	0.005
ZN296_HUMAN	Zinc finger protein 296	4	9.5	1.49	0.01	<0.001	1.79	0.12	0.001	1.42	0.11	0.010
ZN462_HUMAN	Zinc finger protein 462	9	3.3	1.47	0.06	<0.001	1.78	0.16	0.002	1.3	0.14	0.050
ZN703_HUMAN	Zinc finger protein 703	2	9.8	1.37	0.03	<0.001	1.97	0.19	0.002	1.56	0.2	0.022
ZNRF3_HUMAN	E3 ubiquitin-protein ligase ZNRF3	3	3.4	1.56	0.2	0.011	2.01	0.48	0.028	1.54	0.49	0.188
ZO2_HUMAN	Tight junction protein ZO-2	6	3.4	1.52	0.07	<0.001	1.77	0.1	<0.001	1.36	0.14	0.028

Appendix A: Partial list of differentially expressed in HLNRA dose groups showing UNIPROT accession number, peptide matches, protein sequence coverage (%). The mean changes in protein abundance in HLNRA individuals relative to NLNRA individuals are represented as fold change. The adjusted *P*-values represent significant ($P \leq 0.1$) changes in the expression.

Appendix B

Sl. No	Protein ID	Protein Name	Group II		Group III		Group IV		Biological function
			Mean FC	Adj. P-value	Mean FC	Adj. P-value	Mean FC	Adj. P-value	
1.	WN10A	Protein Wnt-10a	2.75	<0.001	7.46	<0.001	8.15	<0.001	Canonical Wnt signaling pathway
2.	ATX1L	Ataxin-1-like	4.86	0.168	4.68	0.147	4.64	0.250	Regulation of HSC proliferation
3.	TRNP1	TMF-regulated nuclear protein 1	1.56	0.010	4.18	0.113	1.54	0.107	Regulation of cell cycle
4.	GSAS1	Putative uncharacterized protein GSN-AS1	2.47	0.101	4.04	0.089	3.76	0.143	Unknown function
5.	BLM	Bloom syndrome protein	2.37	0.063	3.83	0.058	4.12	0.148	DDR signaling and DNA repair
6.	T132B	Transmembrane protein 132B	1.7	0.018	3.05	0.067	2.31	0.164	Single-pass type I membrane protein
7.	TP4AP	Short transient receptor potential channel 4-associated protein	1.97	0.033	3.04	0.049	2.54	0.126	Involved in pathway protein ubiquitination.
8.	STRP2	Striatin-interacting protein 2	1.47	0.005	3	0.055	2.57	0.149	Regulation of cell morphology and cytoskeletal organization.
9.	ADCY2	Adenylate cyclase type 2	2.39	0.086	2.91	0.109	2.9	0.225	cAMP biosynthesis and cAMP signaling
10.	RMI2	RecQ-mediated genome instability protein 2	1.78	<0.001	2.65	0.006	3.1	0.082	Homologous recombination repair.
11.	DZAN1	Double zinc ribbon and ankyrin repeat-containing protein 1	-2.08	0.150	-12.50	<0.001	-9.09	0.001	Protein-protein interaction
12.	NF2IP	NFATC2-interacting protein	-1.85	0.233	-1.75	0.285	-4.35	0.015	Cytokine (IL3, IL4, IL5, IL13) production
13.	NDUA6	NADH dehydrogenase [ubiquinone] 1 alpha subcomplex subunit 6	-1.89	0.218	-1.85	0.227	-3.33	0.037	Mitochondrial electron transport
14.	UMPS	Uridine 5~monophosphate synthase	-1.35	0.107	-1.75	<0.001	-3.23	0.043	Pyrimidine nucleobase biosynthesis
15.	GIMA4	GTPase IMAP family member 4	-1.64	0.351	-1.64	0.351	-2.38	0.124	GTP binding
16.	ZC3HD	Zinc finger CCCH domain-containing protein 13	-1.54	0.435	-1.37	0.582	-2.27	0.150	mRNA processing, methylation and splicing
17.	C1QL3	Complement C1q-like protein 3	-1.06	0.002	-1.45	<0.001	-2.22	0.005	Role in glucose homeostasis.
18.	CBPC5	Cytosolic carboxypeptidase-like protein	-1.41	0.531	-1.52	0.453	-2.17	0.167	Protein deglutamylation.
19.	ECHD2	Enoyl-CoA hydratase domain-containing protein 2; mitochondrial	-2.70	0.051	-1.92	0.200	-1.89	0.269	Fatty acid beta-oxidation
20.	CERS5	Ceramide synthase 5	-2.13	0.140	-3.23	0.022	-1.82	0.302	Ceramide biosynthesis

Appendix B: Relative fold changes top ten up- and down-regulated proteins in HLNRA groups compared to NLNRA. The adjusted *P*-values represent significant ($P \leq 0.1$) changes in the expression.

Appendix C1

Sl.No.	Term	Count	P-value	Genes
1.	hsa04974:Protein digestion and absorption	29	6.78E-12	CO5A1, CO6A6, COBA1, COHA1, CORA1, CO4A3, COEA1, COBA2, COMA1, CO4A2, CO4A5, CO6A5, CO4A6, ELN, CO4A4, CO7A1, COOA1, CO4A1, NAC2, COCA1, CO1A2, CO6A3, CO6A2, CO5A3, CO3A1, CO1A1, COIA1, CO9A1, CO9A2
2.	hsa04512:ECM-receptor interaction	28	3.13E-11	CO5A1, COBA1, CO6A6, LAMA3, CORA1, CO4A3, COBA2, CO4A2, CO4A5, CO6A5, CO4A6, CO4A4, COOA1, CO4A1, TSP1, TENX, CO1A2, CO6A3, CO6A2, ITAV, CO5A3, GPV, CO3A1, CO1A1, PGBM, LAMA1, ITA11, LAMA5
3.	hsa04510:Focal adhesion	45	3.17E-11	PP1A, CO5A1, CO6A6, COBA1, LAMA3, CORA1, CO4A3, TLN2, COBA2, CO4A2, PGFRB, CO4A5, TLN1, CO6A5, FLNC, CO4A6, PAK4, CO4A4, ACTB, COOA1, CO4A1, VINC, FLNA, ACTN1, ROCK2, PAK3, TENX, TSP1, VASP, MYLK3, CO1A2, MK01, CO6A3, CO6A2, ITAV, CO5A3, PP12C, CO3A1, PK3CD, CO1A1, CAN2, LAMA1, ITA11, LAMA5, FLNB
4.	hsa05146:Amoebiasis	27	1.96E-08	CO5A1, COBA1, LAMA3, CORA1, CO4A3, COBA2, CO4A2, CO4A5, PLCB4, CO4A6, ADCY1, CO4A4, COOA1, CO4A1, VINC, ACTN1, KAPCA, CO1A2, MUC2, CO5A3, NOS2, CO3A1, PK3CD, CO1A1, LAMA1, LAMA5, PLCB3
5.	hsa04611:Platelet activation	30	2.96E-08	CO5A1, PP1A, COBA1, CORA1, TLN2, COBA2, PA24B, PLCB4, TLN1, URP2, ADCY1, ACTB, COOA1, ITPR3, ROCK2, KAPCA, VASP, ADCY2, MYLK3, CO1A2, FIBA, MK01, FIBB, CO5A3, GPV, CO3A1, PK3CD, CO1A1, PLCB3, FIBG
6.	hsa02010:ABC transporters	12	0.000218	ABCG5, MRP7, ABCA1, ABCAC, ABCA4, MRP2, ABCAD, ABCA2, ABCA7, MDR1, ABCA3, MRP9
7.	hsa04022:cGMP-PKG signaling pathway	25	0.000799	PP1A, CREB5, CNGB1, GTF2I, PLCB4, AT2B4, PDE3B, NFAC4, ADCY1, AT2A3, CALM, KCMA1, ITPR3, NAC2, ROCK2, CAC1D, IRS2, VASP, ADCY2, MYLK3, PDE3A, MK01, SRF, PK3CD, PLCB3
8.	hsa04921:Oxytocin signaling pathway	23	0.002135	ROCK2, PP1A, CAC1D, MYL6B, KAPCA, CDN1A, ADCY2, KCC2B, MYLK3, RYR2, PA24B, MK01, PLCB4, RYR1, NFAC4, ADCY1, PP12C, PK3CD, ACTB, CALM, MYL6, ITPR3, PLCB3
9.	hsa04713:Circadian entrainment	16	0.003163	CAC1D, KAPCA, ADCY2, KCC2B, GRIA1, RYR2, MK01, PER1, NMDE1, PLCB4, RYR1, ADCY1, CALM, CAC1H, ITPR3, PLCB3
10.	hsa04020:Calcium signaling pathway	24	0.004824	CAC1D, KAPCA, ADCY2, KCC2B, MYLK3, PLCZ1, RYR2, PGFRB, NMDE1, LSHR, PLCB4, CAC1E, AT2B4, RYR1, NOS2, ERBB4, ADCY1, AT2A3, CALM, CAC1B, CAC1H, ITPR3, NAC2, PLCB3
11.	hsa05205:Proteoglycans in cancer	26	0.004853	PP1A, WNT2B, ANK2, CDN1A, KCC2B, FLNC, ACTB, ANK3, WN10A, ITPR3, TWST1, FLNA, ROCK2, MOES, KAPCA, TSP1, MK01, ITAV, PDCD4, ERBB4, PP12C, MTOR, PK3CD, PTN6, PGBM, FLNB
12.	hsa04930:Type II diabetes mellitus	10	0.006676	CAC1D, IRS2, ADIPO, HXK3, MTOR, PK3CD, HXK2, CAC1B, MK01, CAC1E
13.	hsa04724:Glutamatergic synapse	17	0.007626	CAC1D, HOME2, KAPCA, EAA5, ADCY2, GRIA1, ARBK1, PA24B, NMDE1, MK01, EAA2, PLCB4, ADCY1, SHAN1, ITPR3, PLCB3, SHAN2
14.	hsa05222:Small cell lung cancer	14	0.007629	LAMA3, E2F1, CO4A3, CYC, CO4A2, CO4A5, ITAV, CO4A6, NOS2, CO4A4, PK3CD, CO4A1, LAMA1, LAMA5
15.	hsa04270:Vascular smooth muscle contraction	17	0.0114	ROCK2, PP1A, CAC1D, KAPCA, MYL6B, ADCY2, MYLK3, PA24B, MK01, PLCB4, ADCY1, PP12C, CALM, KCMA1, MYL6, ITPR3, PLCB3

16.	hsa03460:Fanconi anemia pathway	10	0.012803	BLM, XPF, FANCI, BRCA2, FANCA, MLH1, RMI2, DPOLN, FANCM, ATR
17.	hsa04725:Cholinergic synapse	16	0.013433	CAC1D, KCNQ5, KAPCA, CLAT, ADCY2, KCC2B, CREB5, MK01, PLCB4, ACHA4, ADCY1, PK3CD, KCNQ3, CAC1B, ITPR3, PLCB3
18.	hsa04810:Regulation of actin cytoskeleton	25	0.017499	PPIA, GELS, PGFRB, APC, ABI2, DIAP2, PAK4, APC2, ACTB, FYV1, VINC, ACTN1, ROCK2, PAK3, MOES, ARC1B, MYLK3, FGD3, MK01, ITAV, PP12C, PK3CD, PROF1, ITA11, PI42C
19.	hsa04720:Long-term potentiation	11	0.019308	PP1A, KAPCA, ADCY1, KCC2B, GRIA1, CALM, MK01, ITPR3, NMDE1, PLCB4, PLCB3
20.	hsa04066:HIF-1 signaling pathway	14	0.023623	TIE2, HXK3, G3P, NOS2, CDN1A, CUL2, MTOR, PK3CD, KCC2B, HXK2, MK01, ENOA, EGLN1, PAI1
21.	hsa04151:PI3K-Akt signaling pathway	36	0.024894	CO5A1, CO6A6, COBA1, LAMA3, CDN1A, CORA1, 1433Z, CO4A3, PHLP1, CREB5, COBA2, PGFRB, CO4A2, CO4A5, CO6A5, CO4A6, CO4A4, COA1, CO4A1, TSP1, TENX, CO1A2, MK01, CO6A3, CO6A2, ITAV, 2A5B, TIE2, CO5A3, CO3A1, MTOR, PK3CD, CO1A1, LAMA1, ITA11, LAMA5
22.	hsa05200:Pathways in cancer	40	0.025363	WNT2B, LAMA3, CDN1A, CYC, CO4A3, DVL2, PGFRB, CO4A2, APC, CO4A5, PLCB4, CO4A6, ADCY1, MLH1, APC2, CUL2, CO4A4, CO4A1, WN10A, DVL3, ROCK2, KAPCA, BRCA2, E2F1, ADCY2, MK01, EGLN1, ITAV, SHH, LEF1, RUNX1, NOS2, MTOR, MSH3, PK3CD, AXIN2, LAMA1, DAPK1, LAMA5, PLCB3
23.	hsa04925:Aldosterone synthesis and secretion	12	0.030639	CAC1D, KPCD1, KAPCA, ADCY1, ADCY2, KCC2B, CALM, CREB5, CAC1H, ITPR3, PLCB4, PLCB3
24.	hsa01200:Carbon metabolism	15	0.032703	ECHA, ALDOA, DHE4, CISY, HXK2, GCSP, HXK3, G3P, PGP, TKT, PYC, RPIA, PGK1, ALDOC, ENOA
25.	hsa04261:Adrenergic signaling in cardiomyocytes	18	0.034019	PPIA, CAC1D, KAPCA, ADCY2, KCC2B, RYR2, CREB5, TPM2, MK01, PLCB4, TPM4, AT2B4, 2A5B, TPM1, ADCY1, PK3CD, CALM, PLCB3
26.	hsa04919:Thyroid hormone signaling pathway	15	0.034917	NCOA1, KAPCA, MED24, NCOA2, PLCZ1, MED1, MK01, PLCB4, ITAV, MTOR, PK3CD, ACTB, NOTC1, MED14, PLCB3
27.	hsa01230:Biosynthesis of amino acids	11	0.039391	ALDOA, G3P, CISY, METH, TKT, P5CR3, PYC, RPIA, ALDOC, ENOA, PGK1
28.	hsa04911:Insulin secretion	12	0.041682	CAC1D, KAPCA, ADCY1, ADCY2, PCLO, KCC2B, KCMA1, CREB5, RYR2, ITPR3, PLCB4, PLCB3
29.	hsa05217:Basal cell carcinoma	9	0.042712	SHH, LEF1, WNT2B, APC2, AXIN2, DVL2, WN10A, APC, DVL3
30.	hsa00670:One carbon pool by folate	5	0.051932	MTDC, FTCD, C1TM, METH, AL1L1

Appendix C1: Radiation altered KEGG pathways enriched in Group II individuals of HLNRA dose groups compared to NLNRA individuals.

Appendix C2

Sl.No.	Term	Count	P-value	Genes
1.	hsa04510:Focal adhesion	48	5.48E-13	PP1A, CO5A1, CO5A2, CO6A6, COBA1, LAMA3, CORA1, CO4A3, TLN2, COBA2, CO4A2, PGFRB, TLN1, CO6A5, FLNC, CO4A6, PAK4, CO4A4, ACTB, COOA1, CO4A1, VINC, FLNA, ACTN1, ROCK2, PAK3, ACTN4, TENX, TSP1, LAMB3, VASP, MYLK3, CO1A2, MK01, CO6A3, CO6A2, ITAV, CO5A3, PP12C, CO3A1, PK3CD, MYLK, CO1A1, CAN2, LAMA1, ITA11, LAMA5, FLNB
2.	hsa04512:ECM-receptor interaction	30	7.8E-13	CO5A1, CO5A2, CO6A6, COBA1, LAMA3, CORA1, CO4A3, COBA2, CO4A2, CO6A5, CO4A6, CO4A4, COOA1, CO4A1, TSP1, TENX, LAMB3, CO1A2, CD44, CO6A3, CO6A2, ITAV, CO5A3, GPV, CO3A1, CO1A1, PGBM, LAMA1, ITA11, LAMA5
3.	hsa04974:Protein digestion and absorption	30	1.09E-12	CO5A1, CO5A2, CO6A6, COBA1, COHA1, CORA1, CO4A3, COEA1, COBA2, COMA1, CO4A2, CO6A5, CO4A6, ELN, CO4A4, CO7A1, COOA1, CO4A1, NAC2, COFA1, COCA1, CO1A2, CO6A3, CO6A2, CO5A3, CO3A1, CO1A1, COIA1, CO9A1, CO9A2
4.	hsa05146:Amoebiasis	29	9.36E-10	CO5A1, CO5A2, COBA1, LAMA3, CORA1, CO4A3, COBA2, CO4A2, PLCB4, CO4A6, ADCY1, CO4A4, COOA1, CO4A1, VINC, ACTN1, ACTN4, KAPCA, LAMB3, CO1A2, MUC2, CO5A3, NOS2, CO3A1, PK3CD, CO1A1, LAMA1, LAMA5, PLCB3
5.	hsa04611:Platelet activation	31	7.68E-09	PP1A, CO5A1, CO5A2, COBA1, CORA1, TLN2, COBA2, PA24B, PLCB4, TLN1, URP2, ADCY1, ACTB, COOA1, ITPR3, ROCK2, KAPCA, VASP, MYLK3, CO1A2, FIBA, MK01, FIBB, CO5A3, GPV, CO3A1, PK3CD, MYLK, CO1A1, PLCB3, FIBG
6.	hsa02010:ABC transporters	11	0.000962	ABCG5, MRP7, ABCAC, ABCA4, MRP2, ABCAD, ABCA2, ABCA7, MDR1, ABCA3, MRP9
7.	hsa05205:Proteoglycans in cancer	27	0.00246	PP1A, ANK2, CDN1A, KCC2B, FLNC, ACTB, ANK3, WN10A, ITPR3, TWST1, RNC, FLNA, ROCK2, MOES, KAPCA, TSP1, MK01, CD44, ITAV, PDCC4, ERBB4, PP12C, MTOR, PK3CD, PTN6, PGBM, FLNB
8.	hsa04810:Regulation of actin cytoskeleton	28	0.002573	PP1A, BAIP2, GELS, PGFRB, APC, ABI2, DIAP2, PAK4, APC2, ACTB, FYV1, VINC, ACTN1, ROCK2, ACTN4, PAK3, MOES, ARC1B, FGD3, MYLK3, MK01, ITAV, PP12C, PK3CD, PROF1, MYLK, ITA11, PI42C
9.	hsa05222:Small cell lung cancer	15	0.002935	LAMA3, LAMB3, E2F1, CO4A3, CYC, CO4A2, TRAF1, ITAV, CO4A6, NOS2, CO4A4, PK3CD, CO4A1, LAMA1, LAMA5
10.	hsa04022:cGMP-PKG signaling pathway	23	0.00407	ROCK2, PP1A, CAC1D, IRS2, VASP, MYLK3, CREB5, PDE3A, GTF2I, CNGB1, MK01, SRF, PLCB4, AT2B4, NFAC4, ADCY1, AT2A3, PK3CD, MYLK, KCMA1, ITPR3, NAC2, PLCB3
11.	hsa04921:Oxytocin signaling pathway	22	0.004784	ROCK2, PP1A, CAC1D, MYL6B, KAPCA, CDN1A, KCC2B, MYLK3, RYR2, PA24B, MK01, PLCB4, RYR1, NFAC4, ADCY1, PP12C, PK3CD, ACTB, MYLK, MYL6, ITPR3, PLCB3
12.	hsa04930:Type II diabetes mellitus	10	0.006763	CAC1D, IRS2, ADIPO, HXK3, MTOR, PK3CD, HXK2, CAC1B, MK01, CAC1E
13.	hsa04020:Calcium signaling pathway	23	0.009883	CAC1D, KAPCA, KCC2B, MYLK3, PLCZ1, RYR2, PGFRB, NMDE1, LSHR, PLCB4, CAC1E, AT2B4, RYR1, NOS2, ERBB4, ADCY1, AT2A3, MYLK, CAC1B, CAC1H, ITPR3, NAC2, PLCB3
14.	hsa04151:PI3K-Akt signaling pathway	38	0.009904	CO5A1, CO5A2, CO6A6, COBA1, LAMA3, CDN1A, CORA1, 1433Z, CO4A3, PHLP1, CREB5, COBA2, PGFRB, CO4A2, CO6A5, CO4A6, CO4A4, COOA1, CO4A1, TENX, TSP1, LAMB3, CO1A2, MK01, CO6A3, CO6A2, ITAV, 2A5B, TIE2, CO5A3, CO3A1, MTOR, PK3CD, CO1A1,

				CD19, LAMA1, ITA11, LAMA5
15.	hsa03460:Fanconi anemia pathway	10	0.01296	BLM, XPF, FANCI, BRCA2, FANCA, MLH1, RMI2, DPOLN, FANCM, ATR
16.	hsa04724:Glutamatergic synapse	16	0.017165	CAC1D, KAPCA, HOME2, EAA5, GRIA1, PA24B, ARBK1, NMDE1, MK01, EAA2, PLCB4, ADCY1, SHAN1, ITPR3, SHAN2, PLCB3
17.	hsa04919:Thyroid hormone signaling pathway	16	0.017165	NCOA1, KAPCA, MED24, NCOA2, PLCZ1, MED1, MK01, PLCB4, ITAV, MTOR, PK3CD, ACTB, NOTC1, MED14, MED17, PLCB3
18.	hsa04713:Circadian entrainment	14	0.018952	CAC1D, KAPCA, KCC2B, GRIA1, RYR2, MK01, NMDE1, PLCB4, MTR1A, RYR1, ADCY1, CAC1H, ITPR3, PLCB3
19.	hsa04270:Vascular smooth muscle contraction	16	0.024482	ROCK2, PP1A, CAC1D, KAPCA, MYL6B, MYLK3, PA24B, MK01, PLCB4, ADCY1, PP12C, MYLK, KCMA1, MYL6, ITPR3, PLCB3
20.	hsa05200:Pathways in cancer	40	0.026342	LAMA3, CDN1A, CYC, CO4A3, DVL2, TGFR2, PGFRB, CO4A2, TRAF1, APC, PLCB4, CO4A6, ADCY1, MLH1, APC2, CUL2, CO4A4, CO4A1, WN10A, DVL3, ROCK2, KAPCA, BRCA2, E2F1, LAMB3, MK01, EGLN1, ITAV, SHH, LEF1, RUNX1, NOS2, MTOR, MSH3, PK3CD, AXIN2, LAMA1, DAPK1, LAMA5, PLCB3
21.	hsa04725:Cholinergic synapse	15	0.029011	CAC1D, KCNQ5, KAPCA, CLAT, KCC2B, CREB5, MK01, PLCB4, ACHA4, ADCY1, PK3CD, KCNQ3, CAC1B, ITPR3, PLCB3
22.	hsa00562:Inositol phosphate metabolism	11	0.031034	PI4KA, PK3CD, FYV1, MTMR1, PLCZ1, SYNJ1, PLCB4, PLCB3, PI5PA, PI42C, OCRL
23.	hsa04520:Adherens junction	11	0.031034	BAIP2, ACTN4, PTPRB, LEF1, CTND1, PTN6, ACTB, TGFR2, MK01, VINC, ACTN1
24.	hsa05210:Colorectal cancer	10	0.033419	LEF1, MLH1, APC2, MSH3, PK3CD, CYC, AXIN2, TGFR2, MK01, APC
25.	hsa04720:Long-term potentiation	10	0.047336	PP1A, KAPCA, ADCY1, KCC2B, GRIA1, MK01, ITPR3, NMDE1, PLCB4, PLCB3
26.	hsa04066:HIF-1 signaling pathway	13	0.050067	TIE2, HXK3, G3P, NOS2, CDN1A, CUL2, MTOR, PK3CD, KCC2B, HXK2, MK01, ENOA, EGLN1
27.	hsa00670:One carbon pool by folate	5	0.052251	MTDC, FTCD, C1TM, METH, AL1L1

Appendix C2: Radiation altered KEGG pathways enriched in Group III individuals of HLNRA dose groups compared to NLNRA individuals.

Appendix C3

Sl. No.	Term	Count	P-value	Genes
1.	hsa04510:Focal adhesion	28	3.69E-09	PP1A, LAMA3, CORA1, CO4A3, TLN2, COBA2, CO4A2, TLN1, CO6A5, CO4A6, FLNC, ACTB, VINC, ACTN1, FLNA, ACTN4, TSP1, TENX, VASP, LAMB3, MYLK3, CO6A2, ITAV, CO3A1, PK3CD, MYLK, CAN2, FLNB
2.	hsa05146:Amoebiasis	17	9.56E-07	ACTN4, LAMA3, LAMB3, CORA1, CO4A3, COBA2, CO4A2, PLCB4, MUC2, CO4A6, NOS2, ADCY1, CO3A1, PK3CD, VINC, PLCB3, ACTN1
3.	hsa04512:ECM-receptor interaction	15	2.12E-06	TSP1, TENX, LAMA3, LAMB3, CORA1, CO4A3, COBA2, CO4A2, CO6A2, CO6A5, ITAV, CO4A6, GPV, CO3A1, PGBM
4.	hsa04974:Protein digestion and absorption	14	1.3E-05	COHA1, CORA1, CO4A3, COBA2, CO4A2, COMA1, CO6A2, CO6A5, ELN, CO4A6, CO3A1, CO7A1, CO9A2, NAC2
5.	hsa04611:Platelet activation	17	1.46E-05	PP1A, VASP, CORA1, MYLK3, TLN2, COBA2, PA24B, PLCB4, TLN1, GPV, ADCY1, CO3A1, PK3CD, ACTB, MYLK, FIBG, PLCB3
6.	hsa04713:Circadian entrainment	12	0.000552	MTR1A, CAC1D, RYR1, ADCY1, KCC2B, GRIA3, GRIA1, RYR2, PER1, CAC1H, PLCB4, PLCB3
7.	hsa04015:Rap1 signaling pathway	17	0.003504	SI1L3, TSP1, VASP, TLN2, SI1L1, SIPA1, PLCB4, TLN1, TIE2, ADCY1, MAGI3, SI1L2, PK3CD, ACTB, PROF1, MAGI2, PLCB3
8.	hsa00562:Inositol phosphate metabolism	9	0.003703	PI4KA, PK3CD, FYV1, MTMR1, SYNJ1, PLCB4, PLCB3, PI5PA, OCRL
9.	hsa04520:Adherens junction	9	0.003703	BAIP2, ACTN4, LEF1, PTN1, PTN6, ACTB, TGFR2, VINC, ACTN1
10.	hsa04921:Oxytocin signaling pathway	14	0.004316	PP1A, CAC1D, CDN1A, KCC2B, MYLK3, RYR2, PA24B, PLCB4, RYR1, ADCY1, PK3CD, ACTB, MYLK, PLCB3
11.	hsa04020:Calcium signaling pathway	15	0.004894	CAC1D, RYR1, ADCY1, NOS2, CAC1A, MYLK3, KCC2B, MYLK, CAC1B, RYR2, CAC1H, NAC2, LSHR, PLCB4, PLCB3
12.	hsa04724:Glutamatergic synapse	11	0.007605	CAC1D, ADCY1, HOME2, CAC1A, GRIA3, GRIA1, ARBK1, PA24B, PLCB4, PLCB3, SHAN2
13.	hsa04810:Regulation of actin cytoskeleton	16	0.008713	BAIP2, PP1A, ACTN4, MYLK3, FGD3, ABI2, DIAP2, ITAV, APC2, PK3CD, ACTB, PROF1, MYLK, FYV1, VINC, ACTN1
14.	hsa05222:Small cell lung cancer	9	0.010913	LAMA3, NOS2, LAMB3, CO4A3, PK3CD, CYC, CO4A2, ITAV, CO4A6
15.	hsa05205:Proteoglycans in cancer	15	0.012579	PP1A, TSP1, ANK2, CDN1A, KCC2B, ITAV, FLNC, PK3CD, PTN6, ACTB, PGBM, ANK3, WN10A, FLNB, FLNA
16.	hsa05412:Arrhythmogenic right ventricular cardiomyopathy (ARVC)	8	0.013264	CAC1D, ACTN4, LEF1, DSG2, ACTB, RYR2, ITAV, ACTN1
17.	hsa04728:Dopaminergic synapse	11	0.016416	PP1A, CAC1D, 2A5B, GSK3A, KCC2B, CAC1A, GRIA3, GRIA1, CAC1B, PLCB4, PLCB3
18.	hsa02010:ABC transporters	6	0.019837	ABCAC, ABCA4, ABCA2, ABCA7, ABCA3, MRP9
19.	hsa04730:Long-term depression	7	0.019948	RYR1, CAC1A, GRIA3, GRIA1, PA24B, PLCB4, PLCB3

20.	hsa05210:Colorectal cancer	7	0.023095	LEF1, MLH1, APC2, MSH3, PK3CD, CYC, TGFR2
21.	hsa04070:Phosphatidylinositol signaling system	9	0.024037	PI4KA, PK3CD, FYV1, MTMR1, SYNJ1, PLCB4, PLCB3, PI5PA, OCRL
22.	hsa05200:Pathways in cancer	23	0.024427	LAMA3, LAMB3, CDN1A, CO4A3, CYC, DVL2, TGFR2, CO4A2, PLCB4, ITAV, CO4A6, EGLN1, SHH, LEF1, NOS2, MLH1, ADCY1, RUNX1, MSH3, APC2, PK3CD, WN10A, PLCB3
23.	hsa04723:Retrograde endocannabinoid signaling	9	0.02819	CAC1D, ADCY1, RIMS1, CAC1A, GRIA3, GRIA1, CAC1B, PLCB4, PLCB3
24.	hsa03460:Fanconi anemia pathway	6	0.040508	XPF, FANCI, MLH1, RMI2, DPOLN, ATR
25.	hsa03015:mRNA surveillance pathway	8	0.04442	PP1A, 2A5B, WDR33, SMG1, ACINU, CASC3, RENT1, RNPS1
26.	hsa04390:Hippo signaling pathway	11	0.044627	PP1A, GDF7, LEF1, APC2, 1433Z, ACTB, DVL2, TGFR2, WN10A, WTIP, CRUM2
27.	hsa04725:Cholinergic synapse	9	0.045559	CAC1D, ADCY1, PK3CD, KCC2B, CAC1A, CAC1B, PLCB4, ACHA4, PLCB3
28.	hsa05033:Nicotine addiction	5	0.053924	CAC1A, GRIA3, GRIA1, CAC1B, ACHA4

Appendix C3: Radiation altered KEGG pathways enriched in Group IV individuals of HLNRA dose groups compared to NLNRA individuals.

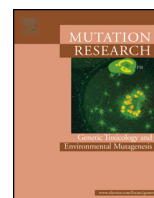
APPENDIX D
JOURNAL PUBLICATIONS



Contents lists available at [ScienceDirect](http://www.sciencedirect.com)

Mutation Research/Genetic Toxicology and Environmental Mutagenesis

journal homepage: www.elsevier.com/locate/gen tox
Community address: www.elsevier.com/locate/mutres



Dynamic changes in the proteome of human peripheral blood mononuclear cells with low dose ionizing radiation



Nishad S., Anu Ghosh*

Radiation Signaling Group, Radiation Signaling & Cancer Biology Section, Radiation Biology & Health Sciences Division, Bhabha Atomic Research Centre, Mumbai 400 085, India

ARTICLE INFO

Article history:

Received 23 July 2015
Received in revised form
30 December 2015
Accepted 5 January 2016
Available online 7 January 2016

Keywords:

Acute low dose radiation
Human peripheral blood mononuclear cells
Two dimensional gel based proteomics
(2-DE)
MALDI-TOF MS

ABSTRACT

Humans are continually exposed to ionizing radiation from natural as well as anthropogenic sources. Though biological effects of high dose radiation exposures have been well accepted, studies on low-to-moderate dose exposures (in the range of 50–500 mGy) have been strongly debated even as researchers continue to search for elusive ‘radiation signatures’ in humans. Proteins are considered as dynamic functional players that drive cellular responses. However, there is little proteomic information available in context of human exposure to ionizing radiation. In this study, we determined differential expressed proteins in G₀ peripheral blood mononuclear cells (PBMCs) from healthy individuals 1 h and 4 h after ‘*ex vivo*’ exposure with two radiation doses (300 mGy and 1 Gy). Twenty-three proteins were found to be significantly altered in irradiated cells when compared to sham irradiated cells with fold change ± 1.5 -fold ($p \leq 0.05$), with only three proteins showing ≥ 2.5 -fold change, either with dose or with time. Mass spectrometry analyses identified redox sensor protein, chloride intracellular channel protein 1 (CLIC-1), the antioxidant protein, peroxiredoxin-6 and the pro-survival molecular chaperone 78 kDa glucose regulated protein (GRP78) among the 23 modulated proteins. The mean coefficient of variation (CV) for the twenty-three radiation responsive protein spots was found to be 33.7% for 300 mGy and 48.3% for 1 Gy. We thus, conclude that the radiation proteomic response of G₀ human PBMCs, which are in the resting stage of the cell cycle, involves moderate upregulation of protective mechanisms, with low inter-individual variability. This study will help further our understanding of cellular effects of low dose acute radiation in humans and contribute toward differential biomarker discovery.

© 2016 Elsevier B.V. All rights reserved.

1. Introduction

For the past several decades, understanding cellular and biological effects of low dose radiation exposures, and to quantify risks from such exposures, has remained a scientific challenge. Biological effects at high doses of ionizing radiation, which are well above the low dose range for environmental or therapeutic radiation exposures (>1 Gy) have been clearly documented [1–3]. In recent times, due to more and more technological advances, the human genome has been increasingly threatened by low dose low-linear energy transfer radiation from environmental, medical, and in many cases, occupational sources. Understanding biological effects of low-to-moderate dose ionizing radiation (50–500 mGy),

directly on humans, is important to address key radiation protection concerns. As several recent studies have suggested, for many biological end points, the responses at low doses might be different from that of high doses [4]. The 2011 Fukushima nuclear accident of Japan has again returned the spotlight on linear no-threshold model and on the importance of validating data obtained from cell-lines or animal models, directly on humans.

Proteins are considered to be key effector molecules through which a cell enacts cellular changes and fine tunes its response to micro environmental signals. The differences found in the proteome may thus, better reflect, the global responses of cells following radiation stress with no ‘*a priori*’ hypothesis about biological mechanisms. Over the years, many studies have been published which identify radiation responsive proteins using traditional single protein approach. However, very few examine whole proteome changes in human cells exposed to IR, either *in vivo* or *in vitro* [5–7]. Moreover, most such investigations have been performed either on the biofluids of patients undergoing radiotherapy [8–11] or with human immortalized cells in culture, which may differ from

* Corresponding author at: Homi Bhabha National Institute, & Radiation Signaling Group, Radiation Signaling & Cancer Biology Section, Radiation Biology & Health Sciences Division, Bio-Science Group, Bhabha Atomic Research Centre, Mumbai 400 085, India. Fax: +91 22 2550 5326.

E-mail addresses: anugh@barc.gov.in, anug.barc@gmail.com (A. Ghosh).

responses in primary human cells [12–15]. In the recent published map of the human proteome from 32 different tissues and organs, extreme caution has been advocated while extending conclusions derived from cell line studies to the corresponding tissues. The authors reported down-regulation or complete “turn off” of many of the tissue-enriched genes in the corresponding cell lines of the normal tissues [16]. The variation in the experimental conditions and methods used for analysis in multiple studies, further limits this extrapolation [2]. Application of proteome profiling for radiation research has also been limited by lack of data on the time- and dose-dependent variation of protein expression. In addition, any attempt to identify potential biomarker in response to radiation that can be tested in molecular epidemiological studies has been constrained by inadequate information on the inherent genetic and physiological variability between individuals leading to differences in radiosensitivity which makes the interpretation of these results more challenging [17].

In this paper, we attempt to bridge this information gap by undertaking a study on human peripheral blood mononuclear cells (PBMCs), which are considered to be highly radiosensitive. Also, since these cells are in the G_0 resting stage of the cell cycle, they may effectively mimic the *in vivo* conditions. Human PBMCs are easy to collect through semi-invasive means and as some reports indicate, may hold the additional advantage of low inter-individual variation as compared to other biofluids [18]. Differential protein expression changes in G_0 PBMCs from healthy individuals were investigated after acute gamma irradiation using two dimensional gel based proteomics (2-DE) and matrix-assisted laser desorption ionization-time of flight mass spectrometry (MALDI-TOF MS). The analysis were performed after irradiation of cells with two radiation doses (300 mGy and 1 Gy) to understand relatively low and moderately high dose effects and at two time points (1 h and 4 h) to discern the early and late responses, post irradiation. The use of 2-DE method allowed direct visualization and robust detection of intact proteins, especially for the comparative experiments [19]. In addition, we determined inter-individual variations of differentially expressed proteins in the healthy volunteers which will be useful for quantitative expression studies in large epidemiological datasets.

2. Materials and methods

2.1. Ethics statement

The blood samples were collected from healthy adult volunteers with informed consent. The project has been approved by the institutional ethics committee.

2.2. PBMC isolation and irradiation

Venous blood was collected from eight random healthy individuals in the age group of 25–45 years; and a gender ratio of 4/4 (M/F) in sterile EDTA tubes (BD™ vacutainers, NJ, USA) and processed within 30 min of blood withdrawal. PBMCs were separated using Histopaque-1077 (Sigma–Aldrich Corp., MO, USA) density gradient media according to manufacturer's instructions. Cells were then counted and their viability was assessed by trypan blue exclusion. The isolated PBMCs were resuspended in RPMI-1640 media (Sigma–Aldrich Corp. MO, USA) and irradiated at room temperature using Co^{60} γ -rays (Blood irradiator, 2000, BRIT, India) at a dose rate of 0.4 Gy/min. Two radiation doses (300 mGy and 1 Gy) were used and the sham irradiated cells served as control. The irradiated cells were incubated in RPMI-1640 media at 37 °C in a humidified, 5% CO_2 atmosphere for the required time (1 h or 4 h) before analysis.

2.3. Sample preparation for proteome analysis

Cells were homogenized by sonication in 10 mM Tris Buffer, pH 7.0 containing 1X protease inhibitor cocktail (Roche Diagnostics, Mannheim, Germany). The cell extract was centrifuged at $20,000 \times g$ for 40 min at 4 °C and the clear supernatant was collected. Protein concentration of the supernatant was determined in triplicate by bicinchoninic acid (BCA) method as recommended by the manufacturer (Bangalore Genei, India). Bovine serum albumin (BSA) was used as standard. The cell lysate was treated with benzonase endonuclease (Sigma–Aldrich MO, USA) at a final concentration of 0.5 U/ μ l of protein extract and purified using a Ready Prep 2D clean up kit (Bio-Rad, CA, USA) before loading on immobilized pH gradient (IPG) strips (Bio-Rad, CA, USA). All eight samples were singularly used for 2DE.

2.4. Two-dimensional polyacrylamide gel electrophoresis (2DE)

Isoelectric focusing (IEF) was performed on 17 cm ready made IPG strips on PROTEAN IEF system (Bio-Rad, CA, USA). The strips were rehydrated with pre-estimated protein samples dissolved in rehydration buffer (7 M urea, 20 mM dithiothreitol (DTT), 4% 3-[(3-cholamidopropyl)-dimethylammonio]-1-propanesulfonate (CHAPS), 0.2% carrier ampholytes, 0.0002% bromophenol blue) by passive method. A three step program was used: 250 V for 20 min, 10,000 V for 4 h, and finally 60,000 Volt-h. After IEF, the strips were equilibrated first in an equilibration buffer I [6 M urea, 2% SDS, 0.05 M Tris-Cl (pH 6.8), 20% Glycerol and 2% DTT], then in equilibration buffer II containing 2.5% iodoacetamide instead of DTT. The second dimension electrophoresis was conducted using a PROTEAN-II vertical gel electrophoresis system on 10% SDS PAGE gels at 85 V. All the chemicals used for 2-DE were procured from Bio-Rad, CA, USA. For molecular weight range determination, molecular weight markers (Bangalore Genei, India) were applied during SDS-PAGE. After electrophoresis, gels were stained with coomassie blue R-250 and the images were acquired using a gel documentation system (Syngene, UK). Two gels were run for each sample preparation.

2.5. Image processing and analysis

2-D gel image analysis was performed with PDQuest software (ver 8, Bio-Rad, CA, USA). Each protein spot on the gel was marked by a standard spot number (SSP#), automatically assigned by the software. Manual editing was also done to correct ambiguous protein spots. Spot height (also known as peak value) of the Gaussian spot was employed to quantitate the level of each protein spot. To compensate for subtle differences in sample loading and inconsistencies in staining, sixteen gels from all the eight samples (with two gels for each sample) were normalized together. For normalization, the raw quantity of each spot in a member gel, divided by the total quantity of valid spots in the gel was used. Only the protein spot with a fold change ± 1.5 -fold change, and $p < 0.05$ were considered to be differentially expressed proteins. The fold change of protein expression between the two groups (irradiated versus sham-irradiated) was calculated by taking mean of spot intensity (measured as the relative volumes of spots) of all the gels in each group. A positive value indicates an increase in expression, and a negative value indicates a decrease in expression.

2.6. MALDI-TOF-Mass spectrometry and protein identification

Coordinates of protein spots of interest was matched and the spots were excised manually. The gel was destained by repeated washings with 50 mM NH_4HCO_3 /acetonitrile (ACN) (v/v). An enzymatic in-gel digestion was performed with trypsin (25 ng/ μ l)

overnight at 37 °C and the tryptic peptides were extracted by using a serial extraction with 0.1% trifluoroacetic acid (TFA), 0.1% TFA in 50% ACN and only ACN. All the fractions were pooled, vacuum dried and stored at –80 °C until further analysis. For the mass spectral analysis, equal quantities (v/v) of the sample and MALDI matrix (α -cyano-4-hydroxycinnamic acid or alpha-matrix) were mixed and spotted on a MALDI target plate. The spots were analyzed with MALDI TOF equipment (UltraFlexII, Bruker Daltonics, Germany) in reflector mode. The peptide calibration standard (Bruker Daltonics) contained nine standard peptides. The spectra were analyzed for peptide mass fingerprinting using MASCOT server (Matrix science, London, U.K). SWISS-PROT database was used for the identification of the proteins, specified for *Homo sapiens* taxonomy. The search parameters were set as one missed cleavage, error tolerance of ± 100 ppm for PMF and ± 0.5 Da for MS/MS ion search. Identification of proteins was based on the MASCOT score, the observed pI and molecular weight (in kDa), the number of matching peptides and the total percentage of the amino acid sequence covered by these peptides. Protein identification with a MOWSE score greater than 56 (except RhoGDI β) was considered as significant ($p \leq 0.05$).

2.7. Statistical analysis for protein expression

Four experimental groups consisting of two irradiation dose (300 mGy and 1 Gy) at each of the two time points (1 h and 4 h post irradiation) were analyzed. Each experimental group was repeated in duplicate (technical replicates). Following criteria were used to determine significantly altered proteins (I). Only those protein spots which matched across all eight samples (in both the duplicate gels) were considered. (II). Of the above spots, proteins which showed a change in spot intensity of at least ± 1.5 -fold and a statistical difference at the 95% confidence level using Student's *t*-test ($p \leq 0.05$) were considered to be differentially regulated. Spot wise standard deviation (SD), arithmetic mean and coefficient of variation (ratio of the standard deviations of normalized spot volumes to the means, expressed in percentage; CV%) values were calculated for the spots that showed differential expression. Heat map visualization was performed using Matlab software.

2.8. Determination of apoptosis by flow cytometry

The viability of cells at the doses and the time points used for 2DE was further assessed by flow cytometry. The cells were prepared for flow cytometry as described by Riccardi and Nicoletti with minor modifications [20]. Briefly, the irradiated cells (1×10^6 cells/ml) were incubated at 37 °C in a humidified, 5% CO₂ atmosphere for the required time and harvested 1 h and 4 h after irradiation to analyze the subdiploid (sub G1) peak. Sham irradiated cells incubated under similar conditions for the same duration served as control. At the respective time points, cells were washed two times in ice-cold phosphate buffered saline (PBS) buffer (pH 7.5). The cell pellets were re-suspended in PBS containing 50 μ g/ml propidium iodide (PI), 0.1% sodium citrate (wt/v) and 0.1% Triton X-100 (v/v). Following incubation for 1 h in dark, a total of 10,000 cells were acquired with a flow cytometer (Cyflow, Partec) and analyzed using FloMax[®] software.

2.9. Alkaline comet assay

Alkaline comet assay was performed to assess radiation induced DNA strand breaks at the dose points used for 2-DE. PBMCs were collected from the same 8 individual individuals analyzed for 2DE. For the assay, cells (1×10^6 cells/ml) were exposed to same radiation doses as 2DE (300 mGy and 1 Gy) and compared with sham irradiated control cells. The samples were incubated at 37 °C in a CO₂ incubator and the damage was assessed at three time points (5 min,

1 h and 4 h post-irradiation) under minimal light to prevent introduction of additional DNA damage in the cells. Cell suspension was mixed with 0.8% low-gelling-temperature agarose prepared in 0.9% saline and evenly layered onto fully frosted slides. After solidification of the agarose, slides were submerged in lysis buffer (2.5 M NaCl, 100 mM EDTA, 1% Triton X-100, 10 mM Tris-Cl, pH 10.0 and 10% DMSO) for 1 h at 4 °C. Lysis was followed by DNA unwinding and expression of alkali-labile sites by immersing the slides in alkaline buffer (300 mM NaOH, 1 mM EDTA pH ≥ 13.0) at room temperature for 20 min. Electrophoresis was performed at 25 V for 30 min. Slides were washed with neutralizing buffer (0.4 M Tris-HCl, pH 7.5) to remove alkali and detergents, stained with SYBR Green II and air dried. Images of comets were viewed with a fluorescence microscope (Carl Zeiss Axio-vision) at 40 \times magnification. A total of 50 images were acquired for each slide and two slides were prepared per experimental point for each individual. The images were analyzed for % DNA in comet tail using SCGE-PRO image analysis software [21].

2.10. Western blot analysis

40 μ g of pooled protein lysate from the same eight subjects used for 2DE were analyzed by Western blot. Briefly, proteins were resolved on 4–12% Bis-Tris NuPage gels (Invitrogen, NJ, USA) and transferred onto a PVDF membrane (Millipore Corp., MA, USA) using wet blotting system (25 V, overnight). The membrane were blocked in 5% BSA (Sigma-Aldrich) in TBS-T (Tris buffered saline containing 0.1% Tween 20) and probed with the following primary antibodies: anti-GRP78 (rabbit polyclonal, sc-13968); anti-HSP 90 α/β (Rabbit polyclonal, sc-7947); anti-PRDX6 (mouse monoclonal, sc-101522) and anti-PDI (goat polyclonal, sc-2005). After washing, the blots were incubated with horse radish peroxidase-conjugated secondary antibody (Santa Cruz Biotechnology, INC) for 1 h at room temperature and protein bands were visualized using SuperSignal West Dura Extended Duration Substrate (Thermo Scientific, IL, USA). The chemiluminescence signals were captured using gel documentation system (Syngene) and band intensity was calculated using ImageJ software. The relative intensity of the proteins obtained after irradiation with respect to sham irradiated controls was calculated after normalizing with GAPDH as the loading control.

3. Result and discussion

3.1. Human PBMCs show irradiation dose and time dependent changes in the proteome

In this study, dose and time specific effects on the proteome of G₀ PBMCs were assessed using 2D-MS proteomic approach. Initially, a pH 3–10 linear gradient IPG strips was used as the first dimension. Later, for better resolution, a pH 4–7 linear gradient was used. 2D proteome spot pattern analysis showed an average of 260 ± 26 (SE) protein spots per gel. This is comparable to 246 spots identified by coupling 2D and MS analysis to generate PBMC map by Vergara et al. [22]. At each harvest time (1 h and 4 h), 2-DE gels from eight samples were normalized together and a master gel (reference gel) was prepared using extensive matching and land-marking. The profiles of the radiation exposed replicate group (300 mGy or 1 Gy) were then compared with sham irradiated control replicate group to identify the differentially expressed proteins. The highly reproducible protein maps for the two dose points are shown in Fig. 1. A total of 23 proteins were found to be differentially expressed with radiation (either with 300 mGy or with 1 Gy when compared with sham-irradiated controls) with a fold change ± 1.5 fold and at 95% confidence level ($p \leq 0.05$). Only three proteins showed change in

Table 1

Identification of proteins differentially expressed after acute ionizing radiation in human PBMCs derived from healthy individuals. The proteins are listed 1–23 as labelled on Fig 1.

Spot no.	Protein name	SWISS PROT accession number	Mascot Score	Sequence coverage	Peptide matches	Molecular weight (kDa)/pI	
						Theoretical	Measured
1.	Plastin-2 (PLS-2)	P13796	130	31.3%	18	70.8/5.2	96.3/5.0
2.	Vinculin (MV)	P18206	116	24.3%	22	124.3/5.4	109.5/6.1
3.	PDZ and LIM domain protein 1 (PDLIM1)	O00151	96	54.1%	10	36.6/6.6	36.4/6.5
4.	WD repeat-containing protein 1 (WDR1)	O75083	57	24.6%	6	67.0/6.2	73.0/6.7
5.	Actin gamma/Actin beta (ACT)	P63261/P60709	70	28.8%	8	42.0/5.2	38.1/5.3
6.	Actin gamma/Actin beta (ACT)	P63261/P60709	88	33.9%	10	42.0/5.2	46.0/5.6
7.	Tubulin beta chain/beta2A/beta2B chain/beta4B chain (TUBB)	P07437/Q13885/Q9BVA1/P68371	69	29.5%	9	50.0/4.6	60.8/4.7
8.	Tubulin alpha-1B chain/1A chain/1C chain/4A chain/8Chain/3C/D Chain/3E chain (TUBA)	P68363/Q71U36/Q9BQE3/P68366//Q9NY65/Q13748/Q6PEY2	134	47.9%	17	50.8/4.8	62.5/5.2
9.	Heat shock protein HSP 90-alpha/beta (HSP90)	P07900/P08238	84	22.1%	17	85.0/4.8	91.6/4.8
10.	78 kDa glucose-regulated protein (GRP78)	P11021	60	20.6%	10	72.4/4.9	83.0/4.8
11.	T-complex protein 1 subunit beta (TCP1)	P78371	127	37.0%	14	57.8/6.0	63.5/6.2
12.	Protein disulfide-isomerase A1 (PDIA1)	P07237	197	40.2%	19	57.5/4.6	67.7/4.5
13.	Leukocyte elastase inhibitor (LEI)	P30740	97	32.2%	11	42.9/5.9	48.3/6.0
14.	Peroxiredoxin-6 (PRDX6)	P30041	56	38.8%	6	25.14/6.0	27.0/6.4
15.	Chloride intracellular channel protein 1 (CLIC)	O00299	149	67.6%	15	27.25/4.9	31.2/5.0
16.	Ras-related protein Rap-1b (RAP1B)	P61224	186	67.4%	14	21.0/5.5	22.0/4.9
17.	Rab GDP dissociation inhibitor alpha (RabGDI α)	P31150	88	29.3%	14	51.18/4.9	68.7/4.8
18.	Rho GDP-dissociation inhibitor 2 (RhoGDI β)	P52566	52	40.8%	7	23.0/4.9	25.5/4.9
19.	L-lactate dehydrogenase B chain (LDHB)	P07195	96	41.6%	12	37.0/5.7	36.4/5.6
20.	Purine nucleoside phosphorylase (PNP)	P00491	93	49.8%	12	32.4/6.5	27.5/6.1
21.	Fibrinogen gamma chain (FGG)	P02679	73	26.5%	8	52.10/5.3	58.6/5.4
22.	Fibrinogen beta chain (FGB)	P02675	139	42.0%	23	56.6/9.3	63.0/6.9
23.	Thrombospondin-1 (THBS1)	P07996	67	12.8%	12	133.3/4.6	29.0/6.2

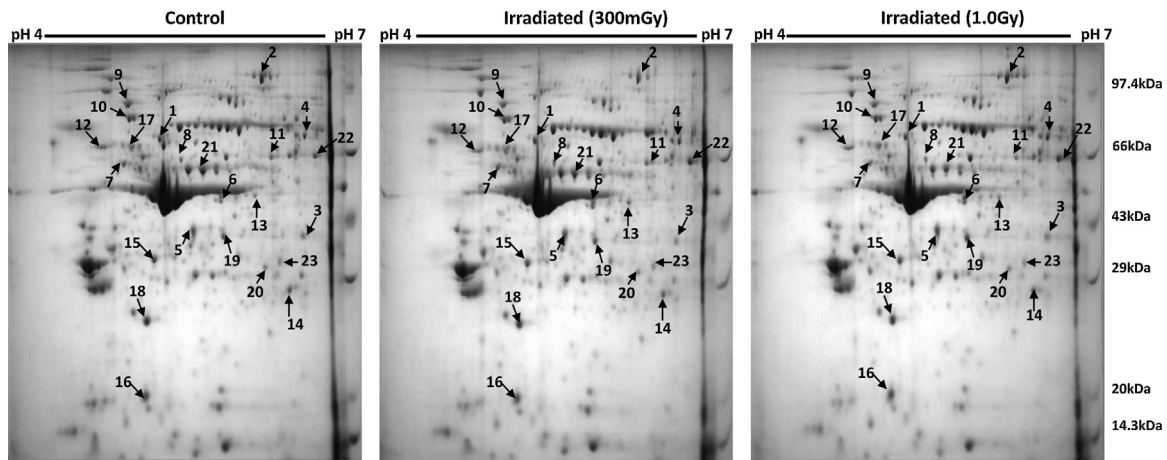


Fig. 1. Representative 2D images of proteins in sham irradiated human PBMCs from a healthy individual 1 h and 4 h after irradiation with 300 mGy and 1 Gy acute dose (dose rate 0.4 Gy/min). Proteins were separated in the first dimension by IEF on IPG strips with pH 4–7 gradient, then in the second dimension on 10% SDS-PAGE gels. Proteins were visualized by staining with coomassie blue. The proteins were identified by mass spectrometry and are numbered as listed in Table 1.

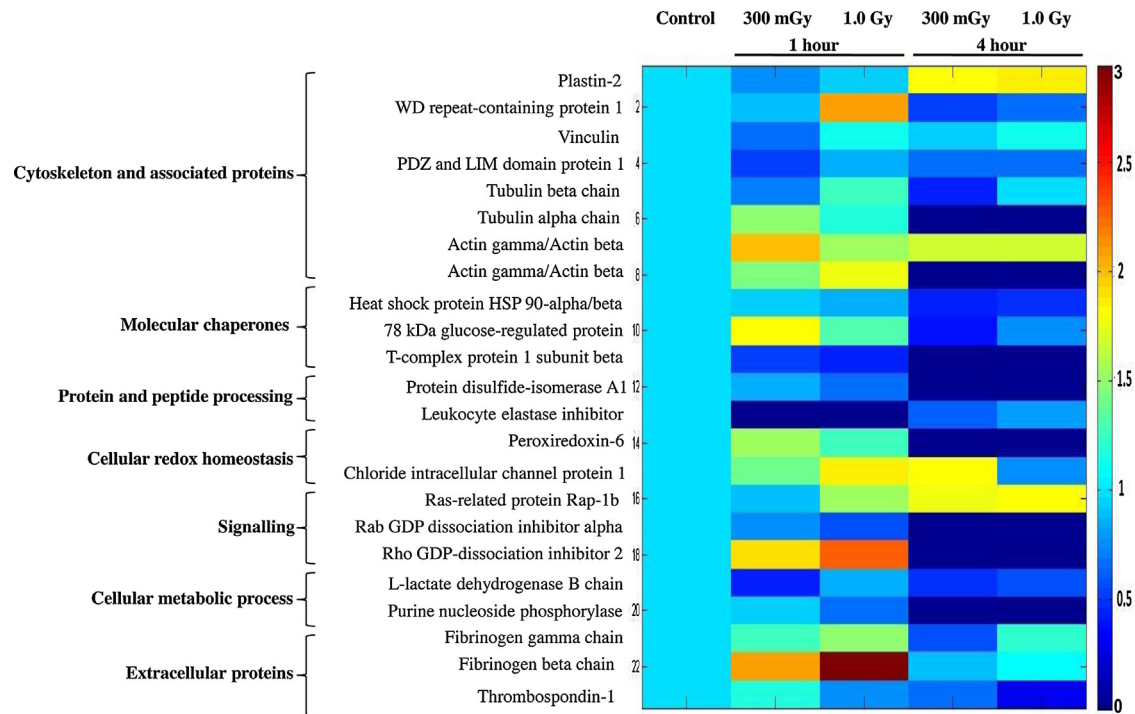


Fig. 2. Heat map showing radiation-associated changes in the relative level of differentially expressed proteins (fold change ± 1.5 fold and $p \leq 0.05$) in the sham irradiated and irradiated (300 mGy and 1 Gy) human PBMCs. Intensity of protein spots on 2 DE gels was determined by PDQuest 8.0 (Bio-Rad). Relative spot intensity of differentially regulated proteins in irradiated samples (300 mGy or 1 Gy) compared to sham irradiated control, at indicated time points (1 h and 4 h), averaged for 8 studied individuals, is shown in each column. Rows represent individual proteins grouped according to their biological function and are arranged as listed in Table 1.

intensity ≥ 2.5 -fold. Differentially expressed proteins were identified by MALDI-TOF MS (Table 1, Fig. 2).

When proteins were classified according to radiation dose, there were six proteins that showed significant up- or down regulation with only low dose and five proteins with only high dose, compared to the sham irradiated cells (Table 2). The proteins that showed significant alterations with 300 mGy included, among others, the thiol specific antioxidant, peroxiredoxin-6 and cytoskeletal proteins (vinculin, tubulin alpha and beta). Examples of proteins that displayed significant change with 1 Gy included proteins like Ras-related Rap-1b protein, enzymes involved in purine metabolism (purine nucleoside phosphorylase) and A1 isoform of protein disulfide-isomerase. On the other hand, 12 proteins were signif-

icantly up- or down regulated in PBMCs with both the doses as compared to sham irradiated control cells (Table 2).

When time dependent changes were considered, independent of the dose used, 11 proteins showed significant changes in expression when the proteome was analyzed 1 h after irradiation (Fig. 3A), but not at late time point (4 h). In contrast, only 5 proteins showed such changes 4 h post irradiation, but not when analyzed at an early time point (1 h), irrespective of the dose used (Fig. 3B). There were 7 proteins that showed significant alterations after 1 h which persisted upto 4 h (Fig. 3C). This showed that most proteome alterations were immediate and transient. The mean fold changes ranged between -3.1 fold (thrombospondin 1) and 2.94 fold (fibrinogen beta).

Table 2
Dose (300 mGy and 1 Gy) and time dependent (1 h and 4 h) changes in expression of proteins differentially modulated after acute ionizing radiation in human PBMCs. The represented fold change is mean change (\pm SD) in spot intensity in irradiated PBMCs derived from eight individuals relative to sham irradiated PBMCs. P values represent the significant of change in the expression levels of proteins after 1 h and 4 h after radiation exposure compared to the sham treated cells. The significance was determined using t test ($p \leq 0.05$). All changes in expression which passed the selection criteria (fold change ± 1.5 -fold, $p \leq 0.05$) are represented in 'bold'. The symbol (–) depicts down regulation. Coefficient of variation was calculated as the ratio of the standard deviations of normalised spot volumes to the means, expressed in percentage (CV%). The proteins are listed 1–23 as labelled on Fig 1.

Sl. no.	Protein name	300 mGy 1 h			1.0 Gy 1 h			300 mGy 4 h			1.0 Gy 4 h		
		Mean \pm SD	P value	CV%	Mean \pm SD	P value	CV%	Mean \pm SD	P value	CV%	Mean \pm SD	P value	CV%
1.	Plastin-2	–1.30 \pm 0.46	<i>P</i> =0.19	59.4	–1.10 \pm 0.47	<i>P</i> =0.82	48.8	1.82 \pm 0.31	<i>P</i> < 0.001	16.8	1.84 \pm 0.96	<i>P</i> = 0.042	52.3
2.	Vinculin	–1.50 \pm 0.20	<i>P</i> = 0.002	31.3	1.13 \pm 0.4	<i>P</i> =0.40	36.2	–1.10 \pm 0.48	<i>P</i> =0.74	50.9	1.12 \pm 1.23	<i>P</i> =0.80	110
3.	PDZ and LIM domain protein 1	–1.90 \pm 0.06	<i>P</i> < 0.001	12.1	–1.20 \pm 0.21	<i>P</i> =0.056	25.0	–1.50 \pm 0.19	<i>P</i> < 0.001	28.2	–1.60 \pm 0.31	<i>P</i> = 0.01	47.6
4.	WD repeat-containing protein 1	–1.10 \pm 0.03	<i>P</i> < 0.001	3.5	2.12 \pm 0.48	<i>P</i> < 0.001	43.1	–1.90 \pm 0.23	<i>P</i> < 0.001	22.8	–1.50 \pm 0.49	<i>P</i> =0.08	74.7
5.	Actin gamma/beta	2.02 \pm 0.77	<i>P</i> = 0.007	38.2	1.53 \pm 0.49	<i>P</i> = 0.019	31.9	1.69 \pm 0.4	<i>P</i> = 0.002	23.4	1.68 \pm 0.41	<i>P</i> = 0.002	24.6
6.	Actin gamma/beta	1.45 \pm 0.42	<i>P</i> =0.019	28.9	1.77 \pm 0.35	<i>P</i> < 0.001	20.0	No change					
7.	Tubulin beta chain	–1.40 \pm 0.39	<i>P</i> =0.07	54.4	1.28 \pm 0.39	<i>P</i> =0.081	30.5	–2.30 \pm 0.27	<i>P</i> < 0.001	61.9	1.01 \pm 1.3	<i>P</i> =0.98	129.5
8.	Tubulin alpha chain	1.52 \pm 0.14	<i>P</i> < 0.001	9.5	1.18 \pm 0.53	<i>P</i> =0.376	44.8	No change					
9.	Heat shock protein 90-alpha/beta	–1.10 \pm 0.38	<i>P</i> =0.79	39.9	–1.20 \pm 0.31	<i>P</i> =0.26	35.4	–2.20 \pm 0.29	<i>P</i> < 0.001	63.1	–2.10 \pm 0.21	<i>P</i> < 0.001	43.2
10.	78 kDa glucose-regulated protein	1.83 \pm 0.43	<i>P</i> < 0.001	23.8	1.33 \pm 0.42	<i>P</i> =0.06	31.3	–2.60 \pm 0.13	<i>P</i> < 0.001	36.0	–1.30 \pm 0.28	<i>P</i> =0.04	37.2
11.	T-complex protein 1 subunit beta	–2.0 \pm 0.14	<i>P</i> < 0.001	27.4	–2.20 \pm 0.25	<i>P</i> < 0.001	56.3	No change					
12.	Protein disulfide-isomerase A1	–1.20 \pm 0.32	<i>P</i> =0.221	37.9	–1.50 \pm 0.37	<i>P</i> = 0.047	53.9	No change					
13.	Leukocyte elastase inhibitor	No change						–1.6 \pm 0.26	<i>P</i> = 0.005	42.3	–1.2 \pm 0.02	<i>P</i> < 0.001	2.7
14.	Peroxiredoxin-6	1.54 \pm 0.23	<i>P</i> < 0.001	14.8	1.27 \pm 0.42	<i>P</i> =0.108	32.9	No change					
15.	Chloride intracellular channel protein 1	1.40 \pm 0.22	<i>P</i> < 0.001	15.8	1.88 \pm 0.67	<i>P</i> = 0.007	35.6	1.84 \pm 0.44	<i>P</i> < 0.001	23.7	–1.40 \pm 0.14	<i>P</i> < 0.001	19.4
16.	Ras-related protein Rap-1b	–1.10 \pm 0.58	<i>P</i> =0.58	66.3	1.52 \pm 0.65	<i>P</i> = 0.05	42.6	1.77 \pm 1.04	<i>P</i> =0.07	59.1	1.80 \pm 1.27	<i>P</i> =0.12	70.3
17.	Rab GDP dissociation inhibitor alpha	–1.40 \pm 0.12	<i>P</i> < 0.001	16.7	–1.70 \pm 0.11	<i>P</i> < 0.001	19.3	No change					
18.	Rho GDP-dissociation inhibitor 2	1.92 \pm 0.63	<i>P</i> = 0.004	32.7	2.25 \pm 0.28	<i>P</i> < 0.001	12.6	No change					
19.	L-lactate dehydrogenase B chain	–2.0 \pm 0.49	<i>P</i> = 0.036	97.9	–1.20 \pm 0.19	<i>P</i> =0.042	23.4	–1.70 \pm 0.33	<i>P</i> = 0.011	54.3	–1.80 \pm 0.42	<i>P</i> = 0.02	74.6
20.	Purine nucleoside phosphorylase	–1.10 \pm 0.22	<i>P</i> =0.478	23.4	–1.50 \pm 0.12	<i>P</i> < 0.001	18.3	No change					
21.	Fibrinogen gamma chain	1.24 \pm 0.63	<i>P</i> =0.31	50.9	1.50 \pm 0.21	<i>P</i> < 0.001	14.4	–1.8 \pm 0.14	<i>P</i> < 0.001	24.8	1.21 \pm 0.3	<i>P</i> =0.08	24.6
22.	Fibrinogen beta chain	2.09 \pm 0.94	<i>P</i> = 0.013	44.9	2.94 \pm 1.36	<i>P</i> = 0.005	46.2	–1.10 \pm 0.66	<i>P</i> =0.741	71.7	1.10 \pm 0.97	<i>P</i> =0.786	88.2
23.	Thrombospondin-1	1.16 \pm 0.29	<i>P</i> =0.15	25.1	–1.30 \pm 0.19	<i>P</i> =0.01	25.0	–1.50 \pm 0.33	<i>P</i> =0.02	51.4	–3.10 \pm 0.06	<i>P</i> < 0.001	19.9

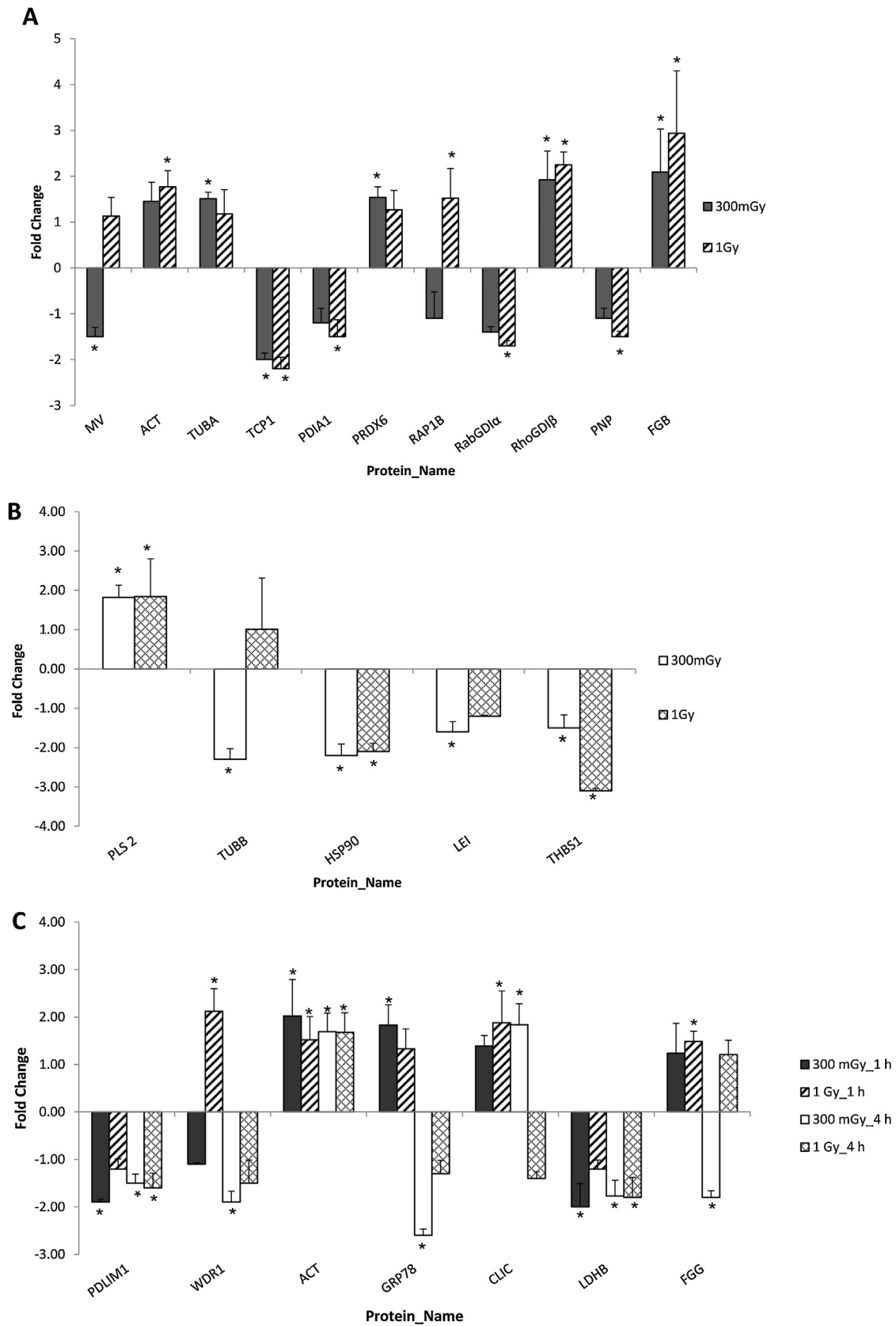


Fig. 3. Fold changes in expression of proteins in irradiated human PBMCs (300 mGy and 1 Gy) as compared to sham irradiated cells. Fold change was calculated relative to sham irradiated controls at respective time and dose point. The fold change of abundance at each dose is shown for (A) proteins that changed in expression 1 h post irradiation, (B) proteins that changed in expression 4 h post irradiation, (C) proteins which showed significant alterations both 1 h and 4 h post irradiation. Data are expressed as the mean \pm SD of 8 studied samples as given in Table 2. Symbol (*) represents significance (fold change \pm 1.5; $p \leq 0.05$) when the corresponding irradiated (either 300 mGy or 1.0 Gy as marked on the bar) cells were compared with sham irradiated control cells. These are marked in bold in Table 2. The abbreviations used are as listed in Table 1.

3.2. Analysis of viability and DNA damage in human PBMCs

Human peripheral blood lymphocytes are known to be very radiosensitive and readily undergo apoptosis. Preliminary analysis of cell viability using trypan blue exclusion showed that >90% of PBMC were viable. To further assess the viability of the human PBMCs at the irradiation doses and time points used for 2-DE, PI staining followed by measurement of DNA content using flow cytometry was performed. As shown in Fig. 4, there was only a negligible decrease in cell viability at the chosen doses and time points of proteome analysis.

In order to correlate viability of the cells with DNA damage, comet assay was performed on the PBMCs obtained from the same eight individuals as above. There was no difference in DNA damage (% Tail DNA, as compared to sham irradiated cells) when cells irradiated either with 300 mGy or 1 Gy were analyzed 1 h post irradiation, which is the earliest time point used for 2-DE analysis. Neither any difference in DNA damage (% Tail DNA, as compared to sham irradiated cells) was seen when the PBMCs were analyzed 4 h post irradiation, the time point at which late proteome alterations were studied. As many published reports have shown that most DNA strand breaks are repaired in the initial 10 min [23], comet assay was also performed at an additional time point (5 min after irradiation) to capture early DNA damage, if any, at the two doses used for 2DE. Significant increase in DNA damage, as compared to sham irradiated cells, was observed after irradiation both with 300 mGy and 1 Gy at this time point (Fig. 5A). As expected, for an individual, high dose (1 Gy) induced higher damage as compared to the low dose (300 mGy) (Fig. 5B). In addition, considerable inter-individual variation in % tail DNA was evident. Thus, though DNA damage was clearly evident immediately after irradiation, it returned to the baseline of sham-irradiated cells at the two time points used for 2DE.

3.3. Functional classification of differentially expressed proteins

The 23 identified proteins were then subdivided into seven categories according to their general biological function using the UniProt/SwissProt protein database (Fig. 2). Of these, the cytoskeleton and associated proteins formed the largest group with eight proteins (Fig. 2). This indicates that there may be an active reorganization with significant inter-dependence and cross-talk between various members of cytoskeleton in human PBMCs under radiation stress. Radiation induced perturbations of cytoskeletal proteins have been reported in various cell models, including PBMCs [7,24,25]. These disturbances may influence various actin/tubulin based cell processes including alteration of cell shape, cell mobility, intracellular trafficking, mitosis, cell signaling and apoptosis. More recently, tubulin proteins have also been reported to be involved in transport of DNA repair proteins in response to DNA damage [26].

Molecular chaperones constituted another important category of proteins that changed in abundance in human PBMCs with IR. With 300 mGy, the 78 kDa glucose-regulated protein (GRP78) showed an upregulation at 1 h, but at 4 h it showed opposite tendency and was significantly downregulated (Fig. 3C). GRP78 has been shown to represent an important pro-survival arm of the unfolded protein response (UPR) due to its antiapoptotic property. Various conditions including glucose deprivation, oxidative stress and hypoxia have been reported to augment GRP78 expression significantly [27]. The induction of GRP78 has been shown to protect the cells by suppressing oxidative damage and stabilizing calcium homeostasis [28] and is vital for maintaining the viability of cells that are subjected to such stresses [29]. Thus, exposure of peripheral cells to even a low dose of 300 mGy triggers the self-defence mechanism against oxidative stress and activates the adaptive signaling UPR pathway to promote cell survival. However,

if the damage persists for longer times, GRP78 showed downregulation indicating that as ER stress expands and remains unresolved, additional mechanisms may set in to regulate protein folding and to control cellular homeostasis. Concomitant with this postulation, the abundant molecular chaperone, heat shock protein 90 (HSP90) showed downregulation with both 300 mGy and 1 Gy at the late time point of 4 h (Fig. 3B). The down regulation was also seen at 1 h post irradiation but was not statistically significant. Inhibition of Hsp90 has been shown to have wide spread effects on various cellular functions including proteasomal regulation of signaling proteins such as proto-oncogenic kinases and activation of cytosolic stress response through HSF1, the master transcription factor [30]. Hsp90 is also an important component of the transcriptional arm of the UPR since it has been shown to associate with ER stress sensors, inositol-requiring enzyme 1 (IRE1), and PKR-like ER kinase (PERK) to maintain their stability. Association of IR with UPR was further corroborated by a significant down regulation of T-complex protein 1 subunit beta (TCP1) at 1 h with both 300 mGy and 1 Gy (Fig. 3A). Similarly, protein disulphide isomerase (PDI) which is an enzyme of a thioredoxin superfamily primarily functioning as the disulphide bond-modulating ER chaperone, was down-regulated (Fig. 3A), which again may contribute to net protective benefit [31].

Another important group of proteins that showed alterations in expression were the oxidative stress homeostasis proteins peroxiredoxin-6 (PRDX6) and chloride intracellular channel protein 1 (CLIC-1). Peroxiredoxin-6 (PRDX6) showed upregulation at the early time point of 1 h but was statistically significant only with 300 mGy, suggesting that its role in human PBMCs may be limited to early responses at low doses (Fig. 3A). Other researchers have also shown oxidative stress induced expression of antioxidant proteins with ionizing irradiation of lymphocytes from human donors [32]. Over expression of Prdx6 in irradiated rat skin cells has been shown to decrease radiation-induced ROS and cell apoptosis and maintain mitochondrial integrity [33]. In sync with this observation, an increase in abundance was observed for CLIC-1 protein at both the radiation doses, albeit after 4 h with 300 mGy and after 1 h with 1 Gy. CLIC-1 is a highly conserved protein in chordates and is believed to act as a redox sensor under external stimuli like oxidative stress that modify the redox state of the cytoplasm (Fig. 3C).

Accumulating evidences suggests that ionizing radiation modulates many signaling network pathways inside the cell to maintain cellular homeostasis [34]. Three signaling proteins were found to be differentially altered in human PBMC following gamma irradiation, Ras-related Rap-1b protein (RAP1B), Rho GDP-dissociation inhibitor 2 (RhoGDI β) and Rab GDP dissociation Inhibitor α (RabGDI α), all at the early time point of 1 h post irradiation (Fig. 3A). In addition, two enzymes involved in cellular metabolism, lactate dehydrogenase (LDHB, Fig. 3C) which is the final enzyme of anaerobic glycolysis and purine nucleoside phosphorylase (PNP, Fig. 3A) which acts as an alternative to *de novo* purine biosynthetic pathway [35] were broadly found to be negatively correlated with radiation, albeit at different dose/time points. There were three extracellular proteins, fibrinogen beta chain, fibrinogen gamma chain and thrombospondin-1 which showed significant modulation with radiation. It is possible that these proteins co-extracted with PBMC proteins during density gradient centrifugation.

To validate some of the key proteins modulated with radiation, we analyzed their expression levels 1 h post-irradiation with western blot and found them to be broadly in agreement with 2DE data (Fig. 6).

3.4. Variability in protein expression

For correct interpretation of the results obtained using differential proteomics with human samples, it is necessary to know

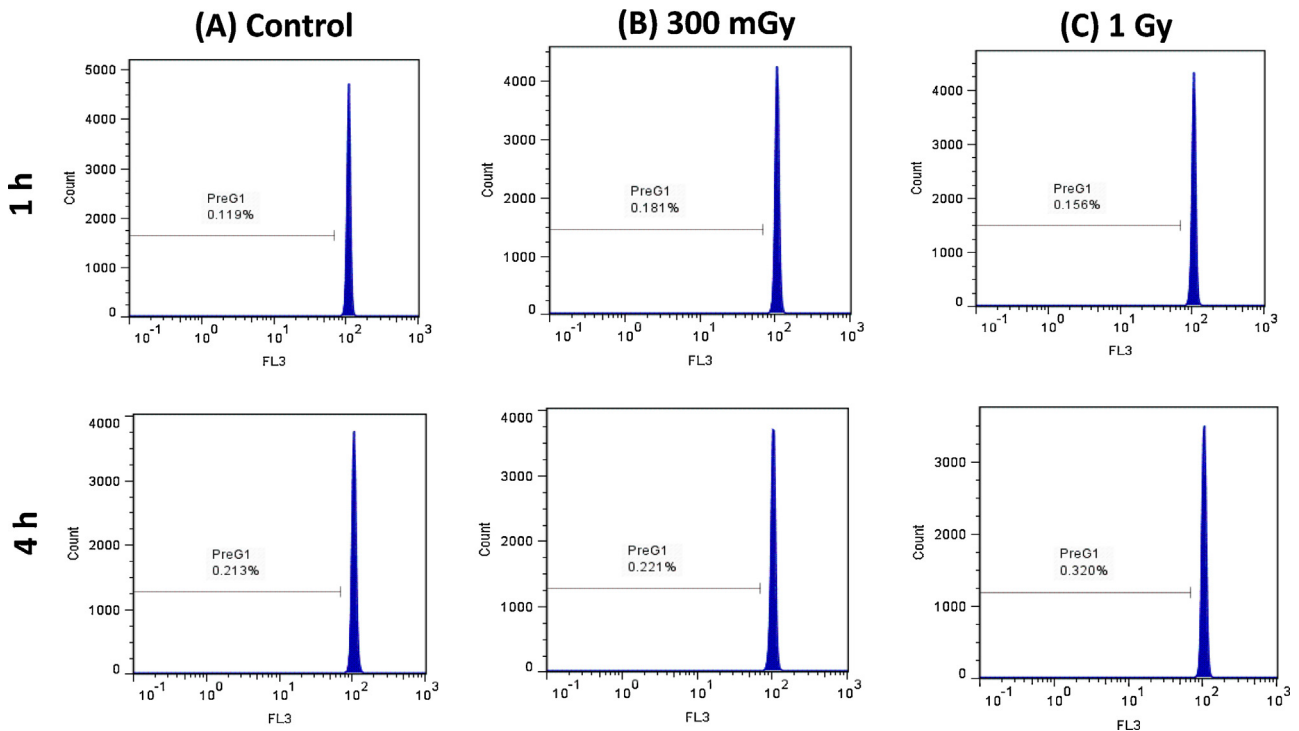


Fig. 4. Flow cytometric profile of human PBMCs from an individual with and without irradiation with PI staining. Sub-G1 peak was analyzed to measure the percentage of apoptosis in sham irradiated, 300 mGy and 1 Gy irradiated cells after 1 h (A,B,C upper panel) and 4 h (A, B, C lower panel), respectively. The peak analysis of the gated cells was from 10,000 events.

and quantify variance between individuals. To analyze the inter-individual variations, the coefficient of variation was calculated for all the 23 protein spots that showed differential expression with respect to time and/or dose among the eight studied individuals (ratio of the standard deviations of normalized spot volumes to the means, expressed in percentage; CV%). The CV of the protein spots which showed differential expression when analyzed 1 h post irradiation as compared to the sham irradiated controls ranged from 3.5% to 97.9%, with a mean of 33.7% (Table 2). According to the published studies, a CV threshold of $\geq 50\%$ is considered significant and proteins above this value are considered highly variable and uninformative as differential biomarkers [36]. Using this criteria, in our study, at the early time point of 1 h, almost 78% of the proteins that showed differential expression with 300 mGy and a high 91% of the proteins which showed differential expression with 1 Gy showed CV values less than 50%. This indicated that these radiation induced proteins have good stability of expression at the early time point with low inter-individual variation. On the other hand, the CV of the protein spots which showed differential expression when analyzed 4 h post irradiation as compared to the sham irradiated controls ranged from 2.7% to 129.5%, with a mean of 48.3% (Table 2). At this time point, almost 70% of the proteins that showed differential expression with 300 mGy and 65% of the proteins which showed differential expression with 1 Gy showed CV values less than 50%. This suggests that differences in radiation sensitivities may be more subtle at low doses of radiation, especially in early proteomic responses, as compared to inter-individual differences at high doses.

Though a direct comparison of gel based methods for inter-individual variation under radiation stress is not possible due to lack of data, when a comparison with other human variation studies were made, it showed that our data with 2DE was consistent with other studies that used 2D-DIGE (2-dimensional difference gel electrophoresis). A study on PBMC proteome from 24 elderly volunteers (15 males and 9 females), in the age group 63–86, with

2D-DIGE showed a variation of 12.99–148.45%, with a median of 28% [36]. Gurtler et al. showed similar inter-individual variability in proteomic responses in human lymphoblastoid cell lines (LCLs) following exposure with 10 Gy ^{137}Cs gamma rays [37].

Inherent variability of 2DE has been considered a bane in proteomics. To calculate the experimental variance, CV was calculated between two duplicate gels of an individual sample for all the 23 spots identified above (Supplementary Table I). To assess the proportion of technical variation to the total variation, both CV values were plotted against each other (Fig 7). The average CV from 2DE was found to be 12.66% with more variation for proteins evaluated 4 h post irradiation (9.76% versus 15.57% for 1 h and 4 h, respectively). However, for few protein spots, technical variation was seen to be a major contributor to the total variation. An earlier study by Roos et al. found technical variation within lab to range between 18–68% [38]. Another study by Maes et al. on the proteome of human PBMCs showed that the average CV from sample preparation was 32.05% [36]. Low CV values for experimental variation between gels obtained in this study thus, affirmed that the variation in 2DE due to technical reasons might only be a very small fraction, provided optimal sample size and proper replicates are maintained.

In the field of radiation proteomics, there have been only limited data on time and dose dependent differential expression in healthy individuals [5,7,9,11]. Our data indicated that radiation response in human PBMCs is characterized by small fold changes and that only a small fraction of detected spots are significantly altered after irradiation when compared with sham irradiated cells. This small change in fold intensity either with dose or with time in human lymphocytes is in agreement with published studies [37]. Notably, this study showed distinct effects of low dose radiation stress on PBMC proteostasis. Upregulation of key pro-survival proteins indicated that human lymphocytes could effectively deal with these changes, probably through adaptive mechanisms, to maintain cellular homeostasis. However, several additional mechanisms

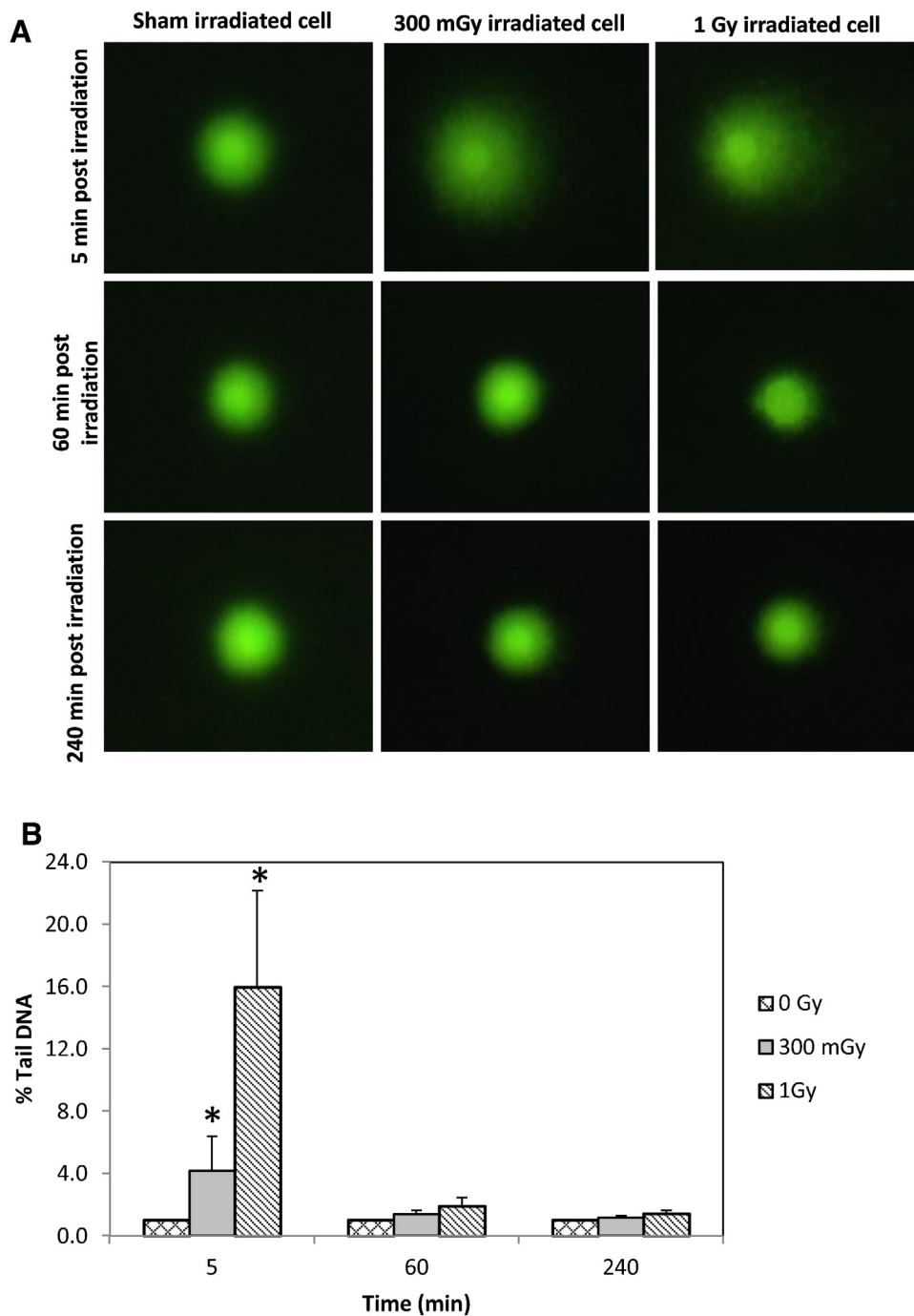


Fig. 5. Induction of DNA damage in gamma irradiated human PBMCs. DNA damage as measured by alkaline comet assay 5 min, 60 min (1 h) and 240 min (4 h) after irradiation with either 300 mGy or 1 Gy and compared with sham irradiated control. (A) Representative of SYBR green stained comets prepared from a healthy individual. (B) Mean percentage of DNA (\pm SD) in comet tails in the 8 studied samples. The significance was determined using *t* test ($*p < 0.05$).

like post translational modifications of proteins, miRNA regulation of protein expression too, need to be addressed and integrated to comprehend complex cellular responses to radiation *in vivo*. The data obtained here will serve as the baseline for our future work to understand effect of protracted low dose radiation exposures for human population residing in High Background Radiation Areas of Kerala, India, which are currently underway in the lab. The per capita average dose received by the human population residing in these areas is ~ 4 mGy/year [39] Assuming an average life expectancy of 60–70 years, life time accumulated dose to the population of this area will be ~ 250 – 300 mGy, similar to the low dose

used in the present study. The existence of variability in protein expression between individuals is a major deterrent when considering many of these proteins as potential biomarkers. This study demonstrated that the inter-individual variations in human PBMC may be not very high especially at low doses, which will help in future studies to identify potential biomarkers that may be then tested in molecular epidemiological studies.

Declaration of interest

The authors declare no conflict of interest.

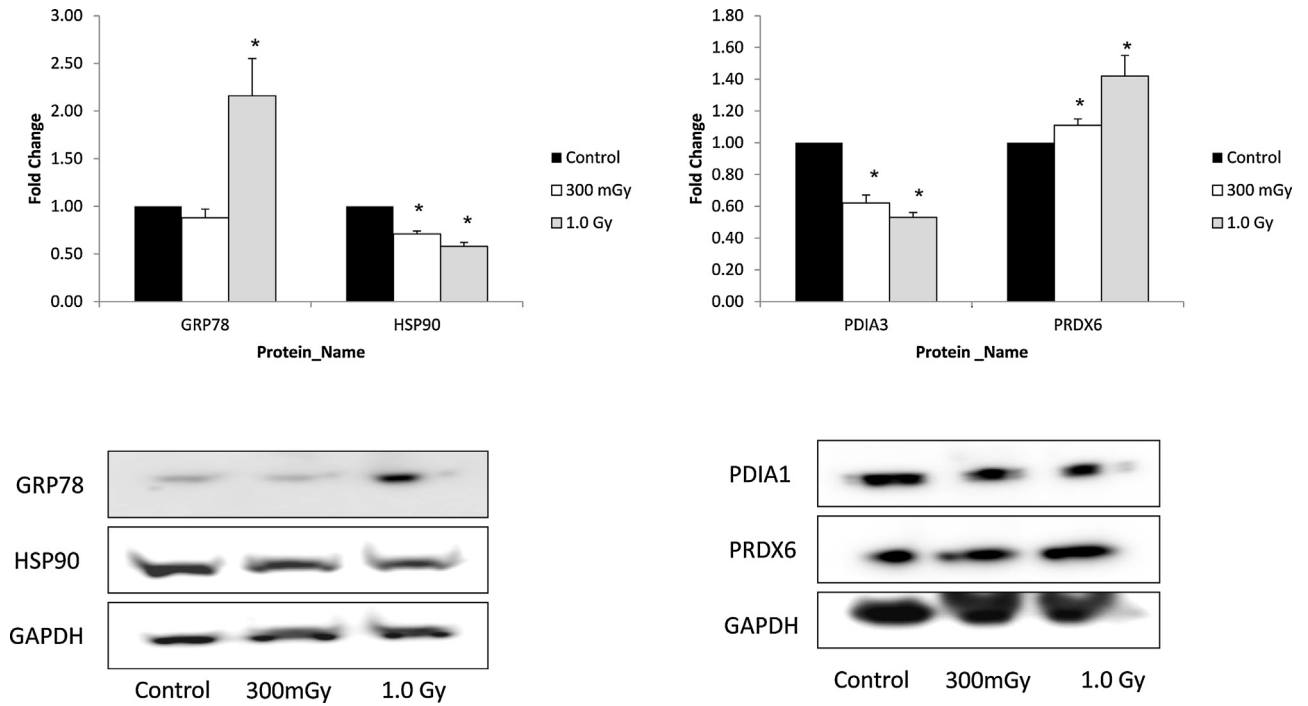


Fig. 6. Western Blot validation for differentially expressed proteins. Protein extracts were prepared, 1h post irradiation, by sonication in 10 mM Tris Buffer, pH 7.0 containing 1X protease inhibitor cocktail. Lysates of irradiated samples (300 mGy and 1 Gy) and sham irradiated control were separated on 4–12% Bis–Tris gels. Proteins were transferred onto a PVDF membranes and probed with specific antibodies. The band intensity was measured by densitometry using Image J. Fold change in expression was calculated relative to GAPDH. The bars correspond to the mean values of three technical replicates of eight pooled biological samples \pm SD. The significance was determined using *t* test ($*p < 0.05$).

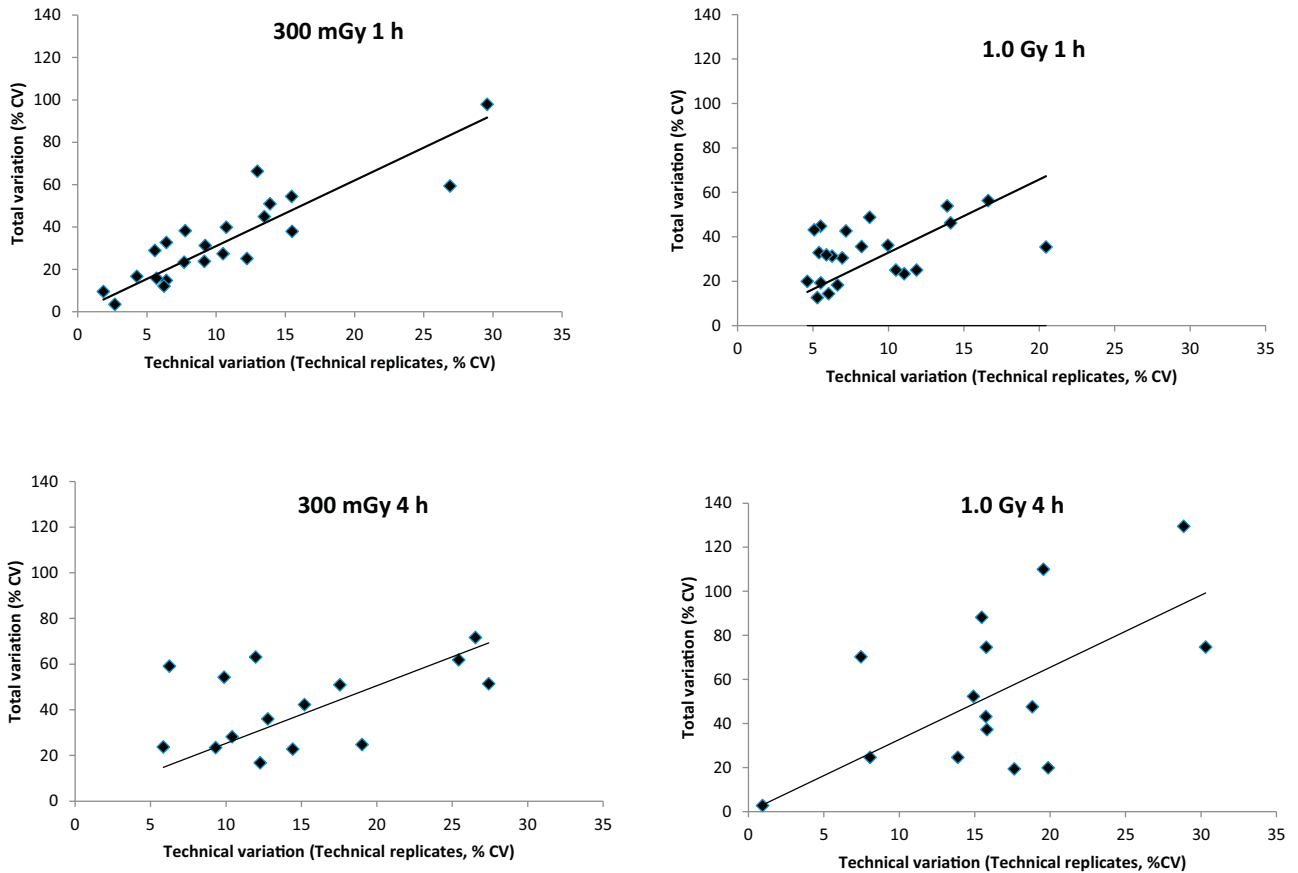


Fig. 7. The scatter plot illustrates the contribution of variance among the technical replicates for a healthy individual to the total variance. Mean fold change (\pm SD) of differentially expressed protein spots was calculated at indicated dose (300 mGy and 1 Gy) and time (1 h and 4 h) points and used to determine coefficient of variation (CV %). The scatter was found to be more at late time point of 4 h as compared to 1 h.

Acknowledgments

The authors put on record sincere thanks to all the volunteers who participated in this study. We thank Ms. J.A. Prabhu and Mr. Sangram Kamble, Trombay Dispensary, BARC for their assistance in collecting blood samples. We also thank Dr. H.N. Bhilwade, RB&HSD, BARC for his help with the comet assay, Mr. Prayag Amin, RB&HSD, BARC for technical help during flow cytometry experiments and Dr. Rukmini Govekar and Mr. S.S. Dolas, Mass Spectrometry Facility, ACTREC for their help during MALDI-TOF MS. We also wish to extend our thanks to Mr. P.K.M. Koya, LLRRL, Kollam, Kerala, for his suggestions during statistical analysis of the data. The authors express their sincere gratitude to Dr. S. Chattopadhyay, Head RB&HSD and Associate Director, Bio-Science Group for the critical review of the manuscript, valuable suggestions and comments. This work was supported by funding from Bhabha Atomic Research Centre, Government of India.

Appendix A. Supplementary data

Supplementary data associated with this article can be found, in the online version, at <http://dx.doi.org/10.1016/j.mrgentox.2016.01.001>.

References

- [1] F. Marchetti, M.A. Coleman, I.M. Jones, A.J. Wyrobek, Candidate protein biodosimeters of human exposure to ionizing radiation, *Int. J. Radiat. Biol.* 82 (2006) 605–639.
- [2] D. Leszczynski, Radiation proteomics: a brief overview, *Proteomics* 14 (2014) 481–488.
- [3] O. Azimzadeh, M.J. Atkinson, S. Tapio, Proteomics in radiation research: present status and future perspectives, *Radiat. Environ. Biophys.* 53 (2014) 31–38.
- [4] Q. Zhang, M. Matzke, A.A. Schepmoes, R.J. Moore, B.J. Webb-Robertson, Z. Hu, M.E. Monroe, W.J. Qian, R.D. Smith, W.F. Morgan, High and low doses of ionizing radiation induce different secretome profiles in a human skin model, *PLoS One* 9 (2014) e92332.
- [5] A. Turtoi, A. Srivastava, R.N. Sharan, D. Oskamp, R. Hille, F.H.A. Schneeweiss, Early response of lymphocyte proteins after gamma-radiation, *J. Radioanal. Nuclear Chem.* 274 (2007) 435–439.
- [6] O. Guipaud, M. Benderitter, Protein biomarkers for radiation exposure: towards a proteomic approach as a new investigation tool, *Ann. Ist Super Sanita* 45 (2009) 278–286.
- [7] A. Turtoi, R.N. Sharan, A. Srivastava, F.H. Schneeweiss, Proteomic and genomic modulations induced by γ -irradiation of human blood lymphocytes, *Int. J. Radiat. Biol.* 86 (2010) 888–904.
- [8] H.D. Moore, R.G. Ivey, U.J. Voytovich, C. Lin, D.L. Stirewalt, E.L. Pogosova-Agadjanian, A.G. Paulovich, The human salivary proteome is radiation responsive, *Radiat. Res.* 181 (2014) 521–530.
- [9] C. Menard, D. Johann, M. Lowenthal, T. Muanza, M. Sproull, S. Ross, J. Gulley, E. Petricoin, C.N. Coleman, G. Whiteley, L. Liotta, K. Camphausen, Discovering clinical biomarkers of ionizing radiation exposure with serum proteomic analysis, *Cancer Res.* 66 (2006) 1844–1850.
- [10] M. Sharma, J.E. Moulder, The urine proteome as a radiation biodosimeter, *Adv. Exp. Med. Biol.* 990 (2013) 87–100.
- [11] R. Nylund, E. Lemola, S. Hartwig, S. Lehr, A. Acheva, J. Jahns, G. Hildebrandt, C. Lindholm, Profiling of low molecular weight proteins in plasma from locally irradiated individuals, *J. Radiat. Res.* 55 (2014) 674–682.
- [12] Z. Barjaktarovic, N. Anastasov, O. Azimzadeh, A. Sriharshan, H. Sarioglu, M. Ueffing, H. Tammio, A. Hakanen, D. Leszczynski, M.J. Atkinson, S. Tapio, Integrative proteomic and microRNA analysis of primary human coronary artery endothelial cells exposed to low-dose gamma radiation, *Radiat. Environ. Biophys.* 52 (2013) 87–98.
- [13] A. Bajinskis, H. Lindegren, L. Johansson, M. Harms-Ringdahl, A. Forsby, Low-dose/dose-rate gamma radiation depresses neural differentiation and alters protein expression profiles in neuroblastoma SH-SY5Y cells and C17.2 neural stem cells, *Radiat. Res.* 175 (2011) 185–192.
- [14] R.G. Ivey, O. Subramanian, T.D. Lorentzen, A.G. Paulovich, Antibody-based screen for ionizing radiation-dependent changes in the Mammalian proteome for use in biodosimetry, *Radiat. Res.* 171 (2009) 549–561.
- [15] S. Szkanterova, J. Vavrova, L. Hernychova, V. Neubauerova, J. Lenco, J. Stulik, Proteome alterations in gamma-irradiated human T-lymphocyte leukemia cells, *Radiat. Res.* 163 (2005) 307–315.
- [16] M. Uhlen, L. Fagerberg, B.M. Hallstrom, C. Lindskog, P. Oksvold, A. Mardinoglu, A. Sivertsson, C. Kampf, E. Sjostedt, A. Asplund, I. Olsson, K. Edlund, E. Lundberg, S. Navani, C.A. Szijgyarto, J. Odeberg, D. Djureinovic, J.O. Takananen, S. Hober, T. Alm, P.H. Edqvist, H. Berling, H. Tegel, J. Mulder, J. Rockberg, P. Nilsson, J.M. Schwenk, M. Hamsten, K. von Feilitzen, M. Forsberg, L. Persson, F. Johansson, M. Zwahlen, G. von Heijne, J. Nielsen, F. Ponten, Proteomics. Tissue-based map of the human proteome, *Science* 347 (2015) 1260419.
- [17] O. Guipaud, Serum and plasma proteomics and its possible use as detector and predictor of radiation diseases, *Adv. Exp. Med. Biol.* 990 (2013) 61–86.
- [18] F.G. Bouwman, B. de Roos, I. Rubio-Aliaga, L.K. Crosley, S.J. Duthie, C. Mayer, G. Horgan, A.C. Polley, C. Heim, S.L. Coort, C.T. Evelo, F. Mulholland, I.T. Johnson, R.M. Elliott, H. Daniel, E.C. Mariman, 2D-electrophoresis and multiplex immunoassay proteomic analysis of different body fluids and cellular components reveal known and novel markers for extended fasting, *BMC Med. Genomics* 4 (2011) 24.
- [19] A. Rogowska-Wrzesinska, M.C. Le Bihan, M. Thaysen-Andersen, P. Roepstorff, 2D gels still have a niche in proteomics, *J. Proteomics* 88 (2013) 4–13.
- [20] C. Riccardi, I. Nicoletti, Analysis of apoptosis by propidium iodide staining and flow cytometry, *Nat. Protoc.* 1 (2006) 1458–1461.
- [21] R.C. Chaubey, Computerized image analysis software for the comet assay, *Methods Mol. Biol.* 291 (2005) 97–106.
- [22] D. Vergara, F. Chiriaco, R. Acierno, M. Maffia, Proteomic map of peripheral blood mononuclear cells, *Proteomics* 8 (2008) 2045–2051.
- [23] P.R.V. Kumar, M. Seshadri, G. Jaikrishan, B. Das, Effect of chronic low dose natural radiation in human peripheral blood mononuclear cells: evaluation of DNA damage and repair using the alkaline comet assay, *Mutat. Res.* 775 (2015) 59–65.
- [24] A.K. Cheema, R.S. Varghese, O. Timofeeva, L. Zhang, A. Kirilyuk, F. Zandkarimi, P. Kaur, H.W. Resson, M. Jung, A. Dritschilo, Functional proteomics analysis to study ATM dependent signaling in response to ionizing radiation, *Radiat. Res.* 179 (2013) 674–683.
- [25] S. Skiöld, S. Becker, U. Hellman, G. Auer, I. Näslund, Low doses of γ -radiation induce consistent protein expression changes in human leukocytes, *Int. J. Low Radiat.* 8 (2011) 374–387.
- [26] M.S. Poruchynsky, E. Komlodi-Pasztor, S. Trostel, J. Wilkerson, M. Regairaz, Y. Pommier, X. Zhang, T. Kumar Maity, R. Robey, M. Burotto, D. Sackett, U. Guha, A.T. Fojo, Microtubule-targeting agents augment the toxicity of DNA-damaging agents by disrupting intracellular trafficking of DNA repair proteins, *Proc. Natl. Acad. Sci. U. S. A.* 112 (2015) 1571–1576.
- [27] R.J. Kaufman, Stress signaling from the lumen of the endoplasmic reticulum: coordination of gene transcriptional and translational controls, *Genes Dev.* 13 (1999) 1211–1233.
- [28] Z. Yu, H. Luo, W. Fu, M.P. Mattson, The endoplasmic reticulum stress-responsive protein GRP78 protects neurons against excitotoxicity and apoptosis: suppression of oxidative stress and stabilization of calcium homeostasis, *Exp. Neurol.* 155 (1999) 302–314.
- [29] H. Liu, R.C. Bowes 3rd, C. van de Water, J.F. Nagelkerke, J.L. Stevens, Endoplasmic reticulum chaperones GRP78 and calreticulin prevent oxidative stress, Ca^{2+} disturbances, and cell death in renal epithelial cells, *J. Biol. Chem.* 272 (1997) 21751–21759.
- [30] K. Sharma, R.M. Vabulas, B. Macek, S. Pinkert, J. Cox, M. Mann, F.U. Hartl, Quantitative proteomics reveals that Hsp90 inhibition preferentially targets kinases and the DNA damage response, *Mol. Cell Proteom.* 11 (2012) 014654, M111.
- [31] B.G. Hoffstrom, A. Kaplan, R. Letso, R.S. Schmid, G.J. Turmel, D.C. Lo, B.R. Stockwell, Inhibitors of protein disulfide isomerase suppress apoptosis induced by misfolded proteins, *Nat. Chem. Biol.* 6 (2010) 900–906.
- [32] Y. Hoshi, H. Tanooka, K. Miyazaki, H. Wakasugi, Induction of thioredoxin in human lymphocytes with low-dose ionizing radiation, *Biochim. Biophys. Acta* 1359 (1997) 65–70.
- [33] S. Zhang, W. Wang, Q. Gu, J. Xue, H. Cao, Y. Tang, X. Xu, J. Cao, J. Zhou, J. Wu, W.Q. Ding, Protein and miRNA profiling of radiation-induced skin injury in rats: the protective role of peroxiredoxin-6 against ionizing radiation, *Free Radic. Biol. Med.* 69 (2014) 96–107.
- [34] K. Valerie, A. Yacoub, M.P. Hagan, D.T. Curiel, P.B. Fisher, S. Grant, P. Dent, Radiation-induced cell signaling: inside-out and outside-in, *Mol. Cancer Ther.* 6 (2007) 789–801.
- [35] F. Canduri, D.M. dos Santos, R.G. Silva, M.A. Mendes, L.A. Basso, M.S. Palma, W.F. de Azevedo, D.S. Santos, Structures of human purine nucleoside phosphorylase complexed with inosine and ddi, *Biochem. Biophys. Res. Commun.* 313 (2004) 907–914.
- [36] E. Maes, B. Landuyt, I. Mertens, L. Schoofs, Interindividual variation in the proteome of human peripheral blood mononuclear cells, *PLoS One* 8 (2013) e61933.
- [37] A. Gurtler, M. Hauptmann, S. Pautz, U. Kulka, A.A. Friedl, S. Lehr, S. Hornhardt, M. Gomolka, The inter-individual variability outperforms the intra-individual variability of differentially expressed proteins prior and post irradiation in lymphoblastoid cell lines, *Arch. Physiol. Biochem.* 120 (2014) 198–207.
- [38] B. de Roos, S.J. Duthie, A.C. Polley, F. Mulholland, F.G. Bouwman, C. Heim, G.J. Rucklidge, I.T. Johnson, E.C. Mariman, H. Daniel, R.M. Elliott, Proteomic methodological recommendations for studies involving human plasma, platelets, and peripheral blood mononuclear cells, *J. Proteom. Res.* 7 (2008) 2280–2290.
- [39] D.S. Bharatwal, G.H. Vaze, Radiation dose measurements in the monazite areas of Kerala state in India, United Nations, New York, in: *Proceedings of the 2nd UN International conference on Peaceful uses of Atomic energy*, 23, 1958, p. 156.

Gene expression of immediate early genes of AP-1 transcription factor in human peripheral blood mononuclear cells in response to ionizing radiation

S. Nishad¹ · Anu Ghosh^{1,2}

Received: 16 September 2015 / Accepted: 18 August 2016 / Published online: 1 September 2016
© Springer-Verlag Berlin Heidelberg 2016

Abstract Ionizing radiation (IR) is considered ubiquitous in nature. The immediate early genes are considered the earliest nuclear targets of IR and are induced in the absence of de novo protein synthesis. Many of these genes encode transcription factors that constitute the first step in signal transduction to couple cytoplasmic effects with long-term cellular response. In this paper, coordinated transcript response of fos and jun family members which constitute activator protein 1 transcription factor was studied in response to IR in human peripheral blood lymphocytes at the G₀ stage. Gene expression was monitored 5 min, 1 h and 4 h post-irradiation with Co⁶⁰ γ -rays (dose rate of 0.417 Gy/min) and compared with sham-irradiated controls. When gene expression was analyzed at the early time point of 5 min post-irradiation with 0.3 Gy, the studied samples showed two distinct trends. Six out of ten individuals (called ‘Group I responders’) showed transient, but significant up-regulation for fosB, fosL1, fosL2 and c-jun with an average fold change (FC) ≥ 1.5 as compared to sham-irradiated controls. The Students’s *t* test *p* value for all four genes was ≤ 0.001 , indicating strong up-regulation. The remaining four individuals (called Group II responders) showed down-regulation for these same four genes. The average FC with 0.3 Gy in Group II individuals was 0.53 ± 0.22 ($p = 0.006$) for fosB,

0.60 ± 0.14 ($p = 0.001$) for fosL1, 0.52 ± 0.16 ($p = 0.001$) for fosL2 and 0.59 ± 0.28 ($p = 0.03$) for c-jun. The two groups could be clearly distinguished at this dose/time point using principal component analysis. Both Group I and Group II responders did not show any change in expression for three genes (c-fos, junB and junD) as compared to sham-irradiated controls. Though a similar trend was seen 5 min post-irradiation with a relatively high dose of 1 Gy, the average FC was lower and change in gene expression was not statistically significant (at $p < 0.05$), except for the down-regulation at fosL2 for Group II individuals (mean FC = 0.70 ± 0.15 , $p = 0.008$). Both groups of individuals did not show any differential change in expression (FC ~ 1.0) for most loci at the late time points of 1 and 4 h, neither with 0.3 Gy nor with 1 Gy.

Keywords Ionizing radiation · Immediate early genes · Activator protein 1 · Human peripheral blood lymphocytes

Introduction

Ionizing radiation (IR) is known to produce diverse types of DNA damage in mammalian cells including double-strand breaks, single-strand breaks and base damages. This sets off a cascade of events which involve recruitment and modifications of various proteins that can sense the damage, transduce the signal and activate specific transcription factors like AP-1, p53 and NF- κ B. These activated transcription factors can, in turn, influence various cellular responses like the ability to undertake DNA repair or enforce cell cycle arrest, cell proliferation, inflammatory responses and, in extreme cases, apoptosis. Most transcription factors modulate common set of genes that share the characteristics of rapid, but transient induction (Kruijer et al. 1984; Lau and Nathans 1987; Prasad et al. 1995).

Electronic supplementary material The online version of this article (doi:10.1007/s00411-016-0662-5) contains supplementary material, which is available to authorized users.

✉ Anu Ghosh
anugh@barc.gov.in

- ¹ Radiation Signaling Group, Radiation Biology and Health Sciences Division, Bio-Science Group, Bhabha Atomic Research Centre, Mumbai 400 085, India
- ² Homi Bhabha National Institute, Training School Complex, Anushakti Nagar, Mumbai 400 094, India

This set of genes, collectively referred to as ‘immediate early genes’ (IEGs) or ‘primary response genes’ (PRGs) (Fowler et al. 2011), are expressed at low or undetectable levels in many cell types, but are rapidly and transiently activated without the need for ‘*de novo*’ protein synthesis in response to various stimulations, including IR.

The activator protein 1 (AP-1) transcription factor is formed by dimers of protein complexes composed of Fos (c-Fos, FosB, FosL1 and FosL2), Jun (c-Jun, JunB, JunD) and ATF/CREB (ATF1-4, ATF-6, b-ATF, ATF α) subfamilies, which belong to the IEG family. Homodimers of Jun proteins or heterodimers of proteins from different subfamilies can recognize specific DNA sequences known as AP-1 sites (tetradecanoylphorbol acetate-responsive elements). The AP-1-binding sites have been identified in large number of cellular genes, including AP-1 genes themselves. AP-1 proteins are often the final targets in the canonical signal transduction pathways, activated as protein kinase cascades. The AP-1-driven promoters are involved in various cellular processes including cell growth and differentiation, DNA repair, cell proliferation, cell cycle and apoptosis. AP-1 has been shown to be activated by various types of radiation including IR, X-rays, electron beam and α -radiation (Chae et al. 1999; Lee et al. 1998; Morales et al. 1998; Turtoi and Schneeweiss 2009). Most such studies reported an increase in DNA-binding activity of AP-1 or alterations in gene expression of single (or few) members of AP-1 family.

In this study, we have analyzed the coordinated changes in transcript levels of constituent IEGs of fos and jun family with IR exposures with two doses (0.3 and 1 Gy). AP-1 has been shown to be activated by reactive oxygen species (ROS) and has been implicated in irradiation-induced oxidative stress (Hellweg et al. 2016). These cellular processes are crucial in this dose range. However, most published studies on IEGs have been performed on immortalized cell lines. Extrapolation of data from human cell lines to normal human cells is highly debatable. Several recent studies indicate that expression of many genes identified in normal tissues may be either down-regulated or absent in the corresponding cell lines (Uhlen et al. 2015). We thus, focused on time- and dose-dependent expressions of fos and jun family genes in non-dividing human peripheral blood mononuclear cells (PBMCs). Moreover, blood is easily accessible through semi-invasive means. The PBMCs at G₀ phase can, therefore, be used as sensitive indicators to capture early molecular events following IR.

Materials and methods

Sample selection

The study was conducted using blood samples from ten unrelated healthy volunteers. All individuals (age group:

25–30 years) were male, non-smokers, had no history of any chronic disease, toxic chemical exposure or radiation exposure, were not on medication (for the past 3 months) and non-fasted. Approximately 10 ml venous blood was collected in sterile EDTA tubes (BDTM Vacutainers, NJ, USA) from each individual during the same time of the day to minimize variations. The study was approved by the institutional medical ethics committee.

PBMC Isolation and irradiation

The blood samples were processed within 30 min of blood withdrawal to maintain consistency of processing. PBMCs were collected using density gradient media Histopaque-1077 according to manufacturer’s instructions and washed twice with phosphate buffer saline before further processing. Cells were counted and their viability assessed by trypan blue exclusion. The isolated PBMCs were irradiated in 500 μ l of PBS at room temperature using a Co⁶⁰ γ -ray source (Blood irradiator, 2000, BRIT, India) at a dose rate of 0.417 Gy/min. Two irradiation doses (0.3 Gy and 1 Gy) were used and sham-irradiated cells served as control. The irradiated cells were divided into three sets: One set was taken for RNA extraction within 5 min of extraction (henceforth, referred to as 0h time point), while the cells for other two sets were incubated in RPMI-1640 media at 37 °C in a humidified 5 % CO₂ atmosphere for the required time (1 h or 4 h) before RNA extraction. The RPMI media was supplemented with 10 % heat-inactivated fetal calf serum, 100 U/ml penicillin and 100 mg/ml streptomycin. All chemicals were procured from Sigma-Aldrich Corp MO, USA.

RNA extraction and gene expression

RNA was extracted from PBMCs of each set using HiPurATM Total RNA Miniprep Purification Kit (HiMedia Laboratory Pvt. Ltd., Mumbai, India) using manufacturer’s instructions. The concentration and the purity of RNA were determined by measuring the ratio of UV absorbance at 260 and 280 nm using Picodrop microliter spectrophotometer (Pico 100, Picodrop Ltd, UK). An aliquot of each RNA preparation was run on 1 % agarose gel and visualized with ethidium bromide to check the integrity. Only intact total RNA (500 ng) which showed sharp, clear 28S and 18S rRNA bands with \sim 2:1 ratio of 28S:18S was reverse-transcribed to cDNA using Transcriptor High Fidelity cDNA Synthesis Kit (Roche Diagnostics Pvt Ltd, GmbH, Germany). Real-Time quantitative Polymerase Chain Reaction (RT-qPCR) was performed on LC480 Real-time PCR machine (Roche Diagnostics, GmbH, Germany) in a 12.5- μ l reaction volume using 1X SYBR green master mix (Roche Diagnostics Pvt. Ltd., GmbH,

Table 1 List of primer sequences

Gene	Sequence 5' → 3'
c-fos (F)	CCCTCAGTGGAACCTGTCAAG
c-fos (R)	CATCAAAGGGCTCGGTCTTC
fosB (F)	CCAAAACCCACTCCCTTCCT
fosB (R)	CAGGCATACAGCAGGGAAGCT
fosL1 (F)	CTGGGAGAGAACAGGAACAAGAG
fosL1 (R)	ATGAGACAGGGAACTGAGACTGA
fosL2 (F)	AGGCGTGCCTCATACAATCTG
fosL2 (R)	TTCTCTCCCTCCCTCTCAAAAA
c-jun (F)	GGCCGGGAGCGAACTT
c-jun (R)	GTCTCGGTGGCAGCCTTAAG
junD (F)	TCAAGACCCTCAAAAGCCAGAA
junD (R)	TTGACGTGGCTGAGGACTTTC
junB (F)	GCCTGTGTCCCCATCAA
junB (R)	GTTCGCGAGCCGCTTTC
β -actin (F)	ATA CCC CTC GTA GAT GGG CAC
β -actin (R)	GAG AAA ATC TGG CACCAC ACC

Germany). All the reactions were done in duplicate. No-template controls were included on each plate for each primer pair. Gene-specific primer sequences used for the quantification are given in Table 1. The PCR profile consisted of an initial denaturation of 2 min at 95 °C followed by 40 cycles of denaturation 30 s at 94 °C, annealing 30 s at 60 °C and extension 30 s at 72 °C. Change in expression of the target gene was normalized to β -actin as reference gene. The stable expression of β -actin was validated in three studied samples at all the dose and time points used in this study. Melting curve analysis was performed for each primer set to confirm product-specific amplification.

Data analysis and statistics

The $2^{-\Delta\Delta C_t}$ method was used to analyze the relative changes in gene expression from real-time PCR experiments using the method by Livak and Schmittgen (2001). The C_t (cycle threshold) of the target gene was normalized to that of the reference gene (β -actin) for both the test sample and the calibrator sample. All the statistical analysis was performed with SPSS version 11.5 (IBM). Genes which showed p values ≤ 0.05 using Student's t test were considered to be differentially regulated. Statistical significance levels were further assessed with Bonferroni corrected p value ($p \leq 0.005$) for 10 subjects. A multivariate analysis on the gene expression data set, principal component analysis (PCA), was performed on the basis of differentially expressed genes to convert multiple correlated variables into a set of important linearly uncorrelated variables.

Results

In this study, transcripts of four members of fos family (c-fos, fosB, fosL1 and fosL2) and three members of jun family (c-jun, junB and junD) were analyzed in resting G_0 PBMCs after γ -irradiation. Two doses (0.3 Gy and 1 Gy) were used to compare and contrast relatively low and moderately high dose effects. To understand the early and late responses, analysis was done at three time points, viz. 5 min (termed 0 h), 1 h and 4 h post-irradiation. The viability of the cells at the dose points used was assessed using trypan blue exclusion, which showed that $>90\%$ of PBMC were viable. In an earlier study using propidium iodide (PI) and measurement of DNA content using flow cytometry, human PBMCs showed only a negligible decrease in cell viability at same irradiation dose and time points as used in the present study (Nishad and Ghosh 2016).

For quantitative analysis, β -actin was used to normalize the expression of target genes. Many reports in the literature recommend validation of reference genes for a given tissue and set of conditions used for the study. We, thus, analyzed the threshold cycle values (C_t) for β -actin in human PBMCs from three randomly selected individuals among the samples used in this study. The gene expression of β -actin was compared at all the three time points, as stated above, after irradiation of cells with two dose points (0.3 Gy and 1 Gy). β -actin was found to be highly expressed in PBMCs with the mean C_t values between 17 and 19 cycles. As evident from Fig. 1, β -actin

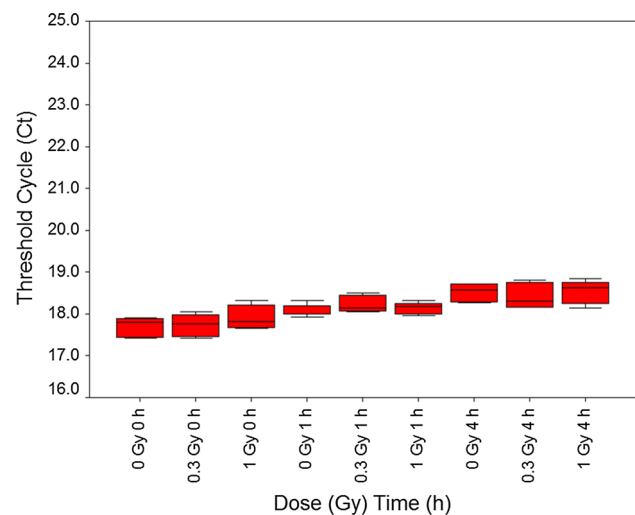


Fig. 1 Threshold cycle (C_t) values for beta-actin endogenous control gene following radiation exposure in human PBMCs. Each box represents C_t values for three individuals, at the respective dose (0, 0.3 and 1 Gy) and time points (0, 1 and 4 h), analyzed in duplicate. For each individual icon, the middle horizontal line is the median, the top and bottom of the boxes are the 25th and 75th percentiles, and the upper and lower horizontal lines (whiskers) indicate the ranges

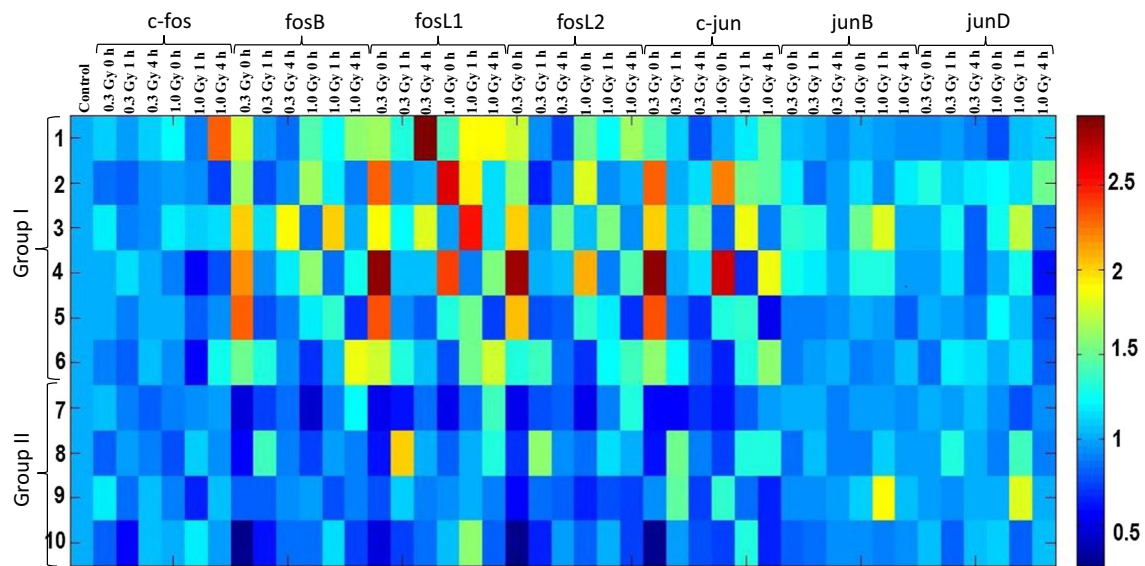


Fig. 2 Heat map showing alterations in gene expression in human PBMCs for seven early response genes, expressed as fold change in irradiated (0.3 and 1 Gy) cells *vis-à-vis* sham-irradiated cells at the indicated time points (0, 1 and 4 h). Each row represents an

individual. Numbers on the left represent sample codes. Samples 1–6 grouped as ‘Group I responders’; Samples 7–10 grouped as ‘Group II responders’

showed good stability and minimal variation with the irradiation doses used in the study, indicating its suitability for studying quantitative gene expression in non-proliferating human PBMCs with γ -irradiation. On the other hand, the average Ct values in the sham-irradiated controls (representing baseline expression) of the studied genes varied from 20.07 ± 0.01 (for junB) to 26.60 ± 0.06 (for c-jun).

The complete gene expression profile for all studied individuals is shown in Fig. 2. When the expression of IEG genes was analyzed within 5 min of irradiation (termed 0 h) with low dose of 0.3 Gy, two clear trends in expression could be observed. Six out of ten individuals studied showed significant increase in expression compared to the sham-irradiated controls at three out of four fos family genes (fosB, fosL1 and fosL2) and one out of three jun family (c-jun) genes (Fig. 3a). The average fold change (FC) for six individuals for fosB, fosL1, fosL2 and c-jun was 1.90 ± 0.32 , 2.14 ± 0.45 , 1.92 ± 0.51 and 2.09 ± 0.51 , respectively, as compared to sham-irradiated controls. The Students’s t test p value for all four genes was ≤ 0.001 , indicating strong up-regulation (Table 2a). The FC for c-fos, junB and junD was 1.01 ± 0.12 ($p = 0.79$), 1.12 ± 0.19 ($p = 0.16$) and 1.06 ± 0.13 ($p = 0.32$), respectively, indicating insignificant change as compared to sham-irradiated controls (Fig. 3b). The remaining four out of ten studied individuals showed

down-regulation for the same four genes (fosB, fosL1, fosL2 and c-jun) for which the above six individuals showed up-regulations when analyzed 0 h post-irradiation with 0.3 Gy. The average FC for these four individuals for fosB, fosL1, fosL2 and c-jun were 0.53 ± 0.22 ($p = 0.006$), 0.60 ± 0.14 ($p = 0.001$), 0.52 ± 0.16 ($p = 0.001$) and 0.59 ± 0.28 ($p = 0.03$), respectively (Fig. 3a), as compared to sham-irradiated controls. The FC for c-fos, junB and junD for these individuals was 0.98 ± 0.19 ($p = 0.82$), 0.91 ± 0.09 ($p = 0.08$) and 1.01 ± 0.04 ($p = 0.58$), again indicating insignificant alterations as compared to sham-irradiated controls (Fig. 3b).

Thus, an opposing expression pattern was observed for these four individuals as compared to the six individuals described earlier. Based on this expression pattern 0 h post-irradiation with 0.3 Gy, two groups can be defined: ‘Group I responders’ (Samples coded 1–6) which show up-regulation for fosB, fosL1, fosL2 and c-jun genes and ‘Group II responders’ (Samples coded 7–10) which show down-regulation for the same four genes (Fig. 2).

When the mRNA was analyzed 1 h and 4 h post-irradiation with 0.3 Gy, the mean FC in expression of most genes for both Group I as well as Group II responders was ~ 1.0 , indicating that there was no differential expression when compared to sham-irradiated

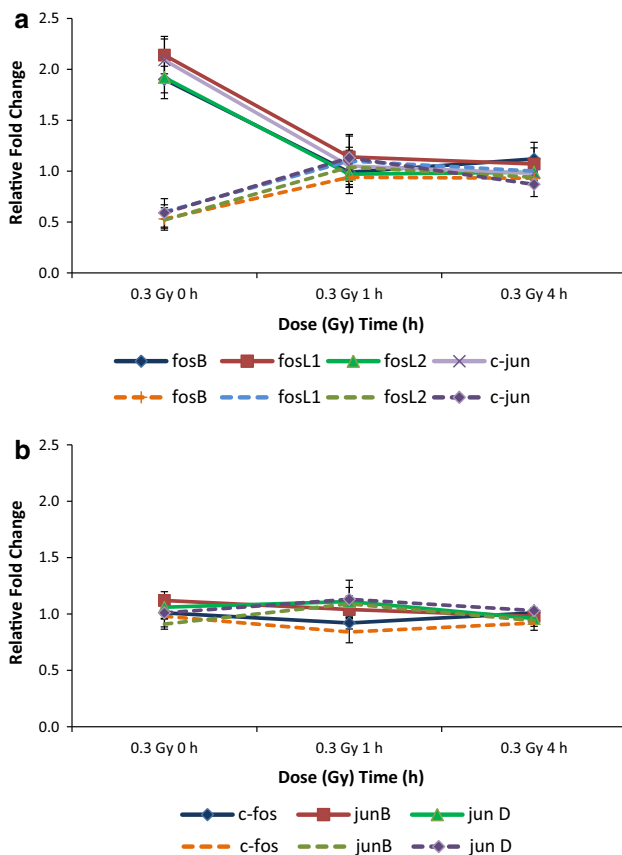


Fig. 3 Time kinetics of genes for individuals after irradiation with 0.3 Gy at the respective time points (0, 1, 4 h). **a** Profile of genes which showed significant change in expression (fosB, fosL1, fosL2 and c-jun) and **b** profile of genes which did not show significant change in expression (c-fos, junB and junD), when compared with sham-irradiated controls. For each gene at the respective dose/time point, each point on the *thick lines* represents average gene expression for six individuals grouped as ‘Group I Responders’ and on the *dashed lines* represents average gene expression for four individuals grouped as ‘Group II Responders’. *Error bars* represent standard error of the mean calculated from the average values obtained from respective individuals in each group

controls at the late time points (Table 2a, Supplementary Fig. 1a and 1b). Among the Group I responders, individual 1 at fosL1 and individual 3 at fosB and fos L1 showed an exception to the rule with a biphasic up-regulation at 4 h. Among the Group II responders, Sample 8 showed a deviation with an up-regulation at 0.3 Gy, 1 h post-irradiation, and returned to the baseline at 4 h (Supplementary Fig. 1a).

The expression pattern of the samples was then analyzed after irradiation of cells with a relatively high dose of 1 Gy and compared with sham-irradiated controls. At 0 h post-irradiation with 1 Gy, similar to the

trend seen with low dose of 0.3 Gy, Group I individuals showed an up-regulation and Group II individuals showed a down-regulation at fosB, fosL1, fosL2 and c-jun, respectively. However, the changes were not statistically significant (at $p < 0.05$) (Fig. 4a), except for significant down-regulation observed at fosL2 (mean FC = 0.70 ± 0.15 , $p = 0.008$) for Group II individuals. Most fold changes with 1Gy irradiation were lower than that observed with 0.3 Gy (Table 2b). For c-fos, junB and junD again, no significant change in gene expression was observed as compared to sham-irradiated controls (FC ≤ 1.1) (Fig. 4b). Likewise, when the transcripts were analyzed at late time points of 1 h and 4 h post-irradiation with 1 Gy, the expression levels were similar to the baseline of sham-irradiated controls (average FC ~ 1.0) for both Group I as well as Group II responders, again indicating no differential expression (Table 2b, Supplementary Fig. 2a and 2b). Notable exceptions were up-regulation at fosL1 (mean FC = 1.71 ± 0.53 , $p = 0.01$) and junD (mean FC 1.23 ± 0.24 , $p = 0.04$) at 1 h (Fig. 4a, b).

For both groups, individual-level differences in fold expression were seen after irradiation both with 0.3 Gy (Fig. 5a) and 1 Gy (Fig. 5b). A multivariate analysis of the gene expression data using PCA was performed to visually assess similarities and differences between samples and validate the two groups identified on the basis of gene expression. As shown in Fig. 6a, the first two principal components, explaining 98.75 % of the variance at 0.3 Gy, was well able to distinguish between Group I and Group II individuals. However, the division between the two groups was not very distinct (score, 97.59 %) at 1 Gy (Fig. 6b).

Discussion

The stress-inducible transcription factor AP-1 is considered a key player in radiation response, especially by modulating cellular defense against oxidative stress (Hellweg et al. 2016). Thus, it becomes pertinent to study IEGs that constitute AP-1 at low to moderately high doses of IR where limited information exists. Further, most published studies have been conducted on human cancer lines or cycling cells from lymphoblastoid cell lines, which may show varied response as compared to the primary cells. Therefore, we chose to focus on G_0 PBMCs which are known to be highly radiosensitive and effectively mimic the in vivo conditions.

Table 2 Mean fold change of gene expression in human PBMCs with acute IR at 0 h, 1 h and 4 h post-irradiation with (a): 0.3 Gy and (b): 1 Gy

Gene name	Group I responders			Group II responders						
	0 h		1 h	0 h		1 h				
	FC	<i>p</i> value	FC	FC	<i>p</i> value	FC				
(a)										
c-fos	1.01 ± 0.12	0.79	0.92 ± 0.13	1.01 ± 0.07	0.64	0.98 ± 0.19	0.84 ± 0.19	0.14	0.92 ± 0.13	0.26
fosB	1.90 ± 0.32	4.84283E-05	0.99 ± 0.22	1.12 ± 0.40	0.49	0.53 ± 0.22	0.006	0.71	0.93 ± 0.11	0.21
fosL1	2.14 ± 0.45	0.0001	1.14 ± 0.16	1.07 ± 0.39	0.66	0.60 ± 0.14	0.001	0.72	1.00 ± 0.25	1.00
fosL2	1.92 ± 0.51	0.001	0.97 ± 0.25	0.99 ± 0.29	0.93	0.52 ± 0.16	0.001	0.83	0.94 ± 0.12	0.34
c-jun	2.09 ± 0.51	0.0004	1.05 ± 0.13	0.98 ± 0.25	0.83	0.59 ± 0.28	0.03	0.57	0.87 ± 0.24	0.32
junB	1.12 ± 0.19	0.16	1.04 ± 0.17	0.98 ± 0.03	0.12	0.91 ± 0.09	0.08	0.57	0.94 ± 0.03	0.01
jun D	1.06 ± 0.13	0.32	1.11 ± 0.12	0.96 ± 0.17	0.58	1.01 ± 0.04	0.58	0.48	1.03 ± 0.05	0.32
(b)										
c-fos	1.04 ± 0.14	0.48	0.81 ± 0.22	1.19 ± 0.58	0.43	0.89 ± 0.10	0.07	0.76	0.99 ± 0.05	0.60
fosB	1.24 ± 0.40	0.17	1.29 ± 0.39	1.23 ± 0.44	0.24	0.75 ± 0.22	0.07	0.53	0.93 ± 0.21	0.56
fosL1	1.58 ± 0.77	0.10	1.71 ± 0.53	1.37 ± 0.44	0.07	0.83 ± 0.25	0.22	0.45	1.11 ± 0.30	0.50
fosL2	1.42 ± 0.51	0.07	1.18 ± 0.23	1.19 ± 0.36	0.22	0.70 ± 0.15	0.008	0.63	0.94 ± 0.27	0.70
c-jun	1.45 ± 0.83	0.21	1.32 ± 0.38	1.31 ± 0.49	0.16	0.85 ± 0.33	0.41	0.65	0.89 ± 0.32	0.53
junB	1.14 ± 0.23	0.18	1.16 ± 0.35	1.00 ± 0.13	0.99	0.99 ± 0.09	0.77	0.36	0.98 ± 0.06	0.47
jun D	1.08 ± 0.19	0.33	1.23 ± 0.24	0.94 ± 0.32	0.64	1.00 ± 0.08	0.98	0.46	0.99 ± 0.07	0.75

The FC ± SD represents mean fold change ± standard deviation for six individuals (termed as 'Group I responders') and four individuals (termed as 'Group II responders') relative to respective sham-irradiated control. '*p*' values were calculated using Student's *t* test. The significant *p* values (*p* ≤ 0.05) are represented in bold

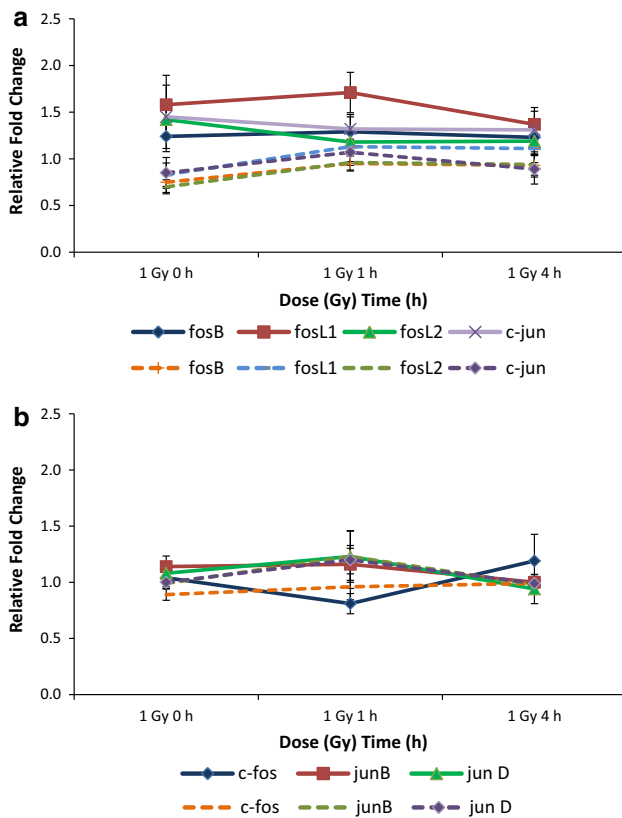


Fig. 4 Time kinetics of genes for individuals after irradiation with 1.0 Gy at the respective time points (0, 1, 4 h). **a** Profile of genes which showed significant change in expression (fosB, fosL1, fosL2 and c-jun) and **b** profile of genes which did not show significant change in expression (c-fos, junB and junD), when compared with sham-irradiated controls. For each gene at the respective dose/time point, each point on the *thick lines* represents average gene expression for six individuals grouped as ‘Group I Responders’ and on the *dash lines* represents average gene expression for four individuals grouped as ‘Group II Responders’. *Error bars* represent standard error of the mean calculated from the mean values obtained from the individuals in respective groups

In mammalian systems, unlike bacteria, most biologically relevant changes in response to a genotoxic stress like IR are manifested at low FC and cannot be ignored (St Laurent et al. 2013). For example, in normal cells, even a slight modulation of c-fos/AP-1 after UV treatment has been shown to elicit *xpf* and *xpg* resynthesis and trigger nucleotide excision repair (NER), in what is called homeostatic or maintenance regulation (Christmann and Kaina 2013). Difference in fold expression in response to IR using qPCR has also been found between actively dividing mitogen-stimulated lymphocytes and non-dividing G_0 cells similar to the PBMCs which have been used for the present study (Kabacik et al. 2011).

Our study showed time- and dose-specific co-ordinated transcript profiles of fos and jun family IEGs that constitute AP-1. Most changes were modest and immediate. When PCA was used to visualize this early gene expression with a relatively low-dose irradiation of 0.3 Gy, two distinct groups of responders could be delineated (Fig. 6a). This indicates individual differences in cellular radiosensitivity at the studied doses. This inter-individual variation among healthy subjects may result from polymorphisms in several gene loci or may be due to differences in normal gene expression. This is in line with many other studies which showed inter-individual differences in gene expression (Smirnov et al. 2009). However, this grouping of individuals based on early transcript levels was not so rigid at the relatively high dose of 1 Gy. This indicates that differences in radiation sensitivities may be more subtle at low doses of radiation, especially during early response to IR, as compared to inter-individual differences at high doses. Human PBMCs showed a similar trend at the proteome level for the same dose and time point (Nishad and Ghosh 2016). Low-dose IR-induced changes in IEGs have been thought to be associated with cellular survival response. Products of these IEGs may regulate several critical downstream genes like cytokines, growth factor and DNA repair genes as well as pro-survival signal transduction pathways (Lopez-Bergami et al. 2010).

Though a direct comparison of human lymphocytes with other cell types is not possible due to lack of data, conflicting results have been seen for gene expression of single IEGs in various cell lines. In a study on Epstein–Barr virus-transformed human lymphoblastoid 244B cells using 0.25–2 Gy IR, up-regulation of c-fos was observed upon irradiation with 250 mGy and c-jun with 0.5 Gy, with a peak at one hour post-irradiation (Prasad et al. 1995). In another study, irradiation of Syrian hamster embryo cells with either 900 mGy of γ -rays or 750 Gy of X-rays resulted in an up-regulation of c-fos mRNA within 3 h (Woloschak and Chang-Liu 1990). However, irradiation with high LET fission spectrum neutrons did not show any induction for c-fos. Studies done in human HL-60 human promyelocytic leukemia cells failed to elicit any transcriptional response for c-jun, c-fos and junB for doses below 5 Gy (Sherman et al. 1990). Another study on HL-60 cells showed up-regulation of fosB and junD with 5 Gy of IR (Datta et al. 1992). Our data thus assert that activation of AP-1 components occurs in a cell type-specific manner and there might be distinct mechanisms operating for low versus high doses of radiation. Many authors have shown a similar pattern for several other genes (Manning et al. 2013).

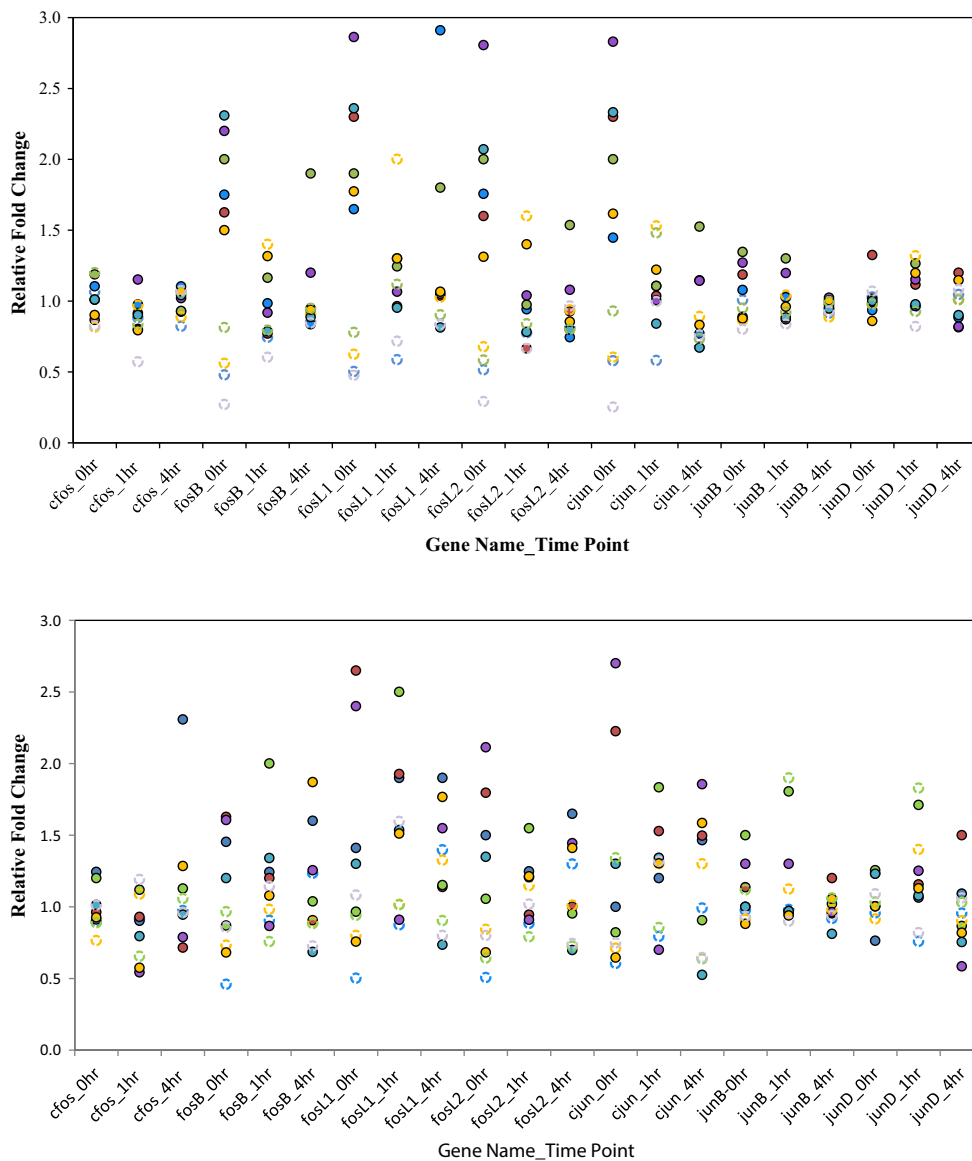


Fig. 5 Individual variation in gene expression response to ionizing radiation, expressed as relative fold change in seven early response genes with time (0, 1, 4 h), **a** after 0.3 Gy irradiation **b** after 1.0 Gy

irradiation. Data for each individual are shown as a *circle*; *filled circle* for ‘Group I responders’ and *open circle* for ‘Group II responders’

The present study further suggests that low to moderately high doses of radiation may elicit a defined transcriptional response of specific members of AP-1 leading to discrete dimerization in a cell type-specific manner. Different AP-1 dimers differ not only in their efficacy of binding to DNA but also in stability of binding and transcriptional activation of target gene. This difference may be dependent both on the type and dose of radiation. Jun, Fos and FosB are considered to be strong transactivators, while JunB, JunD, Fra1 and Fra2 are regarded as weak transactivators (Abate et al. 1991; Halazonetis et al.

1988). Though the present transcript data need to be validated with a more comprehensive analysis with large sample set and with protein expression levels, it might be possible that in primary human PBMCs which are at the G₀ stage, at least at the doses and dose rate used, seemingly minor members of the fos family might play a major role rather than the more ubiquitous c-fos. Among the jun family members, c-jun seems to be the more global player that is transcriptionally activated. This will put a constraint on the dimers that form with low doses of radiation and their genes targets. Transcriptional

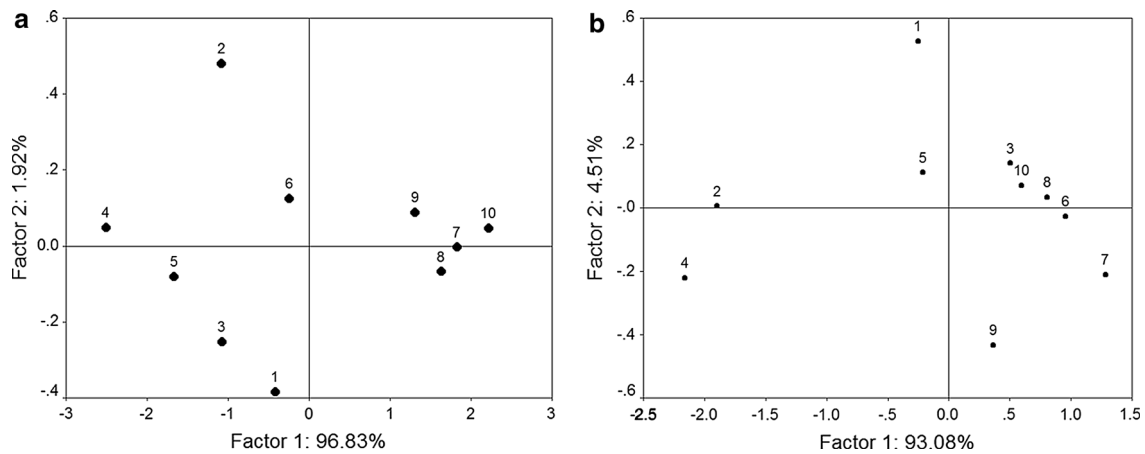


Fig. 6 Principal component analysis (PCA) of the gene expression data set. Principal components (PC) 1 and 2, explaining variance at 0 h post-irradiation with **a** 0.3 Gy, score 98.75 % and **b** 1 Gy, score 97.59 %, are plotted. *Each dot* represents an individual

modulation of genes that encode AP-1 subunits may, thus, provide a fine-tuning mechanism to the cells to regulate net activity after IR.

Acknowledgments The authors put on record their thanks to all the volunteers who donated blood for the study. Thanks are also due to Ms. Parbhu J.A. and Mr. Sangram Kamble, Trombay Dispensary, Bhabha Atomic Research Centre (BARC) for their help during withdrawal of blood from individuals. We also wish to extend our thanks to Mr. P. K. M. Koya for his valuable help during statistical analysis of the data. We also thank Dr Birajalaxmi Das and all laboratory members of Low Level Radiation Studies Section, BARC, for their support during this work.

Funding This work was supported by funding from Bhabha Atomic Research Centre, Department of Atomic Energy, Government of India.

Compliance with ethical standards

Conflict of interest The authors declare that they have no conflict of interest.

Ethics statement The study was conducted with the approval of Medical Ethics Committee, Bhabha Atomic Research Centre, Mumbai, India, and blood samples were drawn only after informed written consent from each subject.

References

- Abate C, Luk D, Curran T (1991) Transcriptional regulation by Fos and Jun in vitro: interaction among multiple activator and regulatory domains. *Mol Cell Biol* 11:3624–3632
- Chae HJ et al (1999) Effect of ionizing radiation on the differentiation of ROS 17/2.8 osteoblasts through free radicals. *J Radiat Res* 40:323–335
- Christmann M, Kaina B (2013) Transcriptional regulation of human DNA repair genes following genotoxic stress: trigger mechanisms, inducible responses and genotoxic adaptation. *Nucleic Acids Res* 41:8403–8420. doi:10.1093/nar/gkt635
- Datta R et al (1992) Involvement of reactive oxygen intermediates in the induction of c-jun gene transcription by ionizing radiation. *Biochemistry* 31:8300–8306
- Fowler T, Sen R, Roy AL (2011) Regulation of primary response genes. *Mol Cell* 44:348–360. doi:10.1016/j.molcel.2011.09.014
- Halazonetis TD, Georgopoulos K, Greenberg ME, Leder P (1988) c-Jun dimerizes with itself and with c-Fos, forming complexes of different DNA binding affinities. *Cell* 55:917–924
- Hellweg CE, Spitta LF, Henschenmacher B, Diegeler S, Baumstark-Khan C (2016) Transcription factors in the cellular response to charged particle exposure. *Front Oncol* 6:61. doi:10.3389/fonc.2016.00061
- Kabacik S et al (2011) Gene expression following ionising radiation: identification of biomarkers for dose estimation and prediction of individual response. *Int J Radiat Biol* 87:115–129. doi:10.3109/09553002.2010.519424
- Kruijer W, Cooper JA, Hunter T, Verma IM (1984) Platelet-derived growth factor induces rapid but transient expression of the c-fos gene and protein. *Nature* 312:711–716
- Lau LF, Nathans D (1987) Expression of a set of growth-related immediate early genes in BALB/c 3T3 cells: coordinate regulation with c-fos or c-myc. *Proc Natl Acad Sci USA* 84:1182–1186
- Lee SA, Dritschilo A, Jung M (1998) Impaired ionizing radiation-induced activation of a nuclear signal essential for phosphorylation of c-Jun by dually phosphorylated c-Jun amino-terminal kinases in ataxia telangiectasia fibroblasts. *J Biol Chem* 273:32889–32894
- Livak KJ, Schmittgen TD (2001) Analysis of relative gene expression data using real-time quantitative PCR and the 2^{-ΔΔC_T} method. *Methods* 25:402–408. doi:10.1006/meth.2001.1262
- Lopez-Bergami P, Lau E, Ronai Z (2010) Emerging roles of ATF2 and the dynamic AP1 network in cancer. *Nat Rev Cancer* 10:65–76. doi:10.1038/nrc2681
- Manning G, Kabacik S, Finnon P, Bouffler S, Badie C (2013) High and low dose responses of transcriptional biomarkers in ex vivo X-irradiated human blood. *Int J Radiat Biol* 89:512–522. doi:10.3109/09553002.2013.769694
- Morales A, Miranda M, Sanchez-Reyes A, Colell A, Biete A, Fernandez-Checa JC (1998) Transcriptional regulation of the heavy subunit chain of gamma-glutamylcysteine synthetase by ionizing radiation. *FEBS Lett* 427:15–20
- Nishad S, Ghosh A (2016) Dynamic changes in the proteome of human peripheral blood mononuclear cells with low dose

- ionizing radiation. *Mutat Res, Genet Toxicol Environ Mutagen* 797:9–20. doi:[10.1016/j.mrgentox.2016.01.001](https://doi.org/10.1016/j.mrgentox.2016.01.001)
- Prasad AV, Mohan N, Chandrasekar B, Meltz ML (1995) Induction of transcription of “immediate early genes” by low-dose ionizing radiation. *Radiat Res* 143:263–272
- Sherman ML, Stone RM, Datta R, Bernstein SH, Kufe DW (1990) Transcriptional and post-transcriptional regulation of c-jun expression during monocytic differentiation of human myeloid leukemic cells. *J Biol Chem* 265:3320–3323
- Smirnov DA, Morley M, Shin E, Spielman RS, Cheung VG (2009) Genetic analysis of radiation-induced changes in human gene expression. *Nature* 459:587–591. doi:[10.1038/nature07940](https://doi.org/10.1038/nature07940)
- St Laurent G et al (2013) On the importance of small changes in RNA expression. *Methods* 63:18–24. doi:[10.1016/j.ymeth.2013.03.027](https://doi.org/10.1016/j.ymeth.2013.03.027)
- Turtoi A, Schnee Weiss FH (2009) Effect of ²¹¹At alpha-particle irradiation on expression of selected radiation responsive genes in human lymphocytes. *Int J Radiat Biol* 85:403–412. doi:[10.1080/09553000902838541](https://doi.org/10.1080/09553000902838541)
- Uhlen M et al (2015) Proteomics. Tissue-based map of the human proteome. *Science* 347:1260419. doi:[10.1126/science.1260419](https://doi.org/10.1126/science.1260419)
- Woloschak GE, Chang-Liu CM (1990) Differential modulation of specific gene expression following high- and low-LET radiations. *Radiat Res* 124:183–187

Original Manuscript

Comparative proteomic analysis of human peripheral blood mononuclear cells indicates adaptive response to low-dose radiation in individuals from high background radiation areas of Kerala

Srambikkal Nishad and Anu Ghosh*

Radiation Signaling Group, Radiation Biology & Health Sciences Division, Bhabha Atomic Research Centre, Mumbai 400 085, India and Homi Bhabha National Institute, Mumbai 400 094, India

*To whom correspondence should be addressed. Dr Anu Ghosh, Radiation Signaling Group, Radiation Biology & Health Sciences Division, Bio-Science Group, Bhabha Atomic Research Centre, Mumbai 400085, India. Tel: +91-022-25592373; Email: anugh@barc.gov.in

Received 22 June 2018; Revised 9 October 2018; Editorial decision 17 October 2018; Accepted 25 October 2018.

Abstract

There remain significant uncertainties in estimation of risks with low doses of radiation. The small coastal belt in the southwestern state of Kerala, India, extending from Neendakara in the south to Purakkad in the north is one of the most extensively studied high-level natural background radiation areas (HLNRAs) of the world to address these concerns. The natural radioactivity here is due to occurrence of monazite sand bearing placer deposits along the coastline. In this study, proteomic approach was employed to study the response of human peripheral blood mononuclear cells (PBMCs) from individuals residing in HLNRA ($N = 10$; mean radiation dose: 15.60 ± 3.04 mGy/y) *vis-à-vis* responses in individuals from adjoining normal-level natural background radiation areas (NLNRA; $N = 10$; mean radiation dose: ≤ 1.50 mGy/y) using two-dimensional gel electrophoresis coupled with mass spectrometry. A total of 15 proteins were found to be statistically altered in individuals from HLNRA when compared to individuals from NLNRA ($P \leq 0.05$). Most of the changes in expression were small. The mean coefficient of variation for the differentially altered proteins was found to be ~34%. Pathway enrichment analysis with Database for Annotation, Visualization and Integrated Discovery distinguished 44 biological processes significantly ($P \leq 0.05$) modulated in HLNRA samples. More importantly, when challenged with an *ex vivo* dose of 2 Gy, HLNRA PBMCs responded with an up-regulation of many protective pro-survival proteins such as protein disulfide-isomerase A1 (PDIA1), peroxiredoxin 6 (PRDX6) and glucose-regulated protein 78 kDa (GRP78). PDIA1 and PRDX6 are known to play an important role in redox homeostasis. GRP78 is considered the master regulator of unfolded protein response that aims to restore endoplasmic reticulum homeostasis and thus, regulate cell survival. Principal component analysis identified clear clusters based on radiation dose. The expression changes of key proteins were validated by western blotting using additional samples from HLNRA and NLNRA. This indicates that the human cells respond to low dose of ionising radiation through dynamic changes in the proteome to maintain adaptive homeostasis. These findings emphasise that the dose–response relationship at low doses of radiation may not be linear and, thus, provide mechanistic challenge to the linear-no-threshold hypothesis.

Introduction

Natural background radiation is considered a major source of exposure to ionising radiation (IR) in humans. The global average annual effective dose from natural radiation is ~2.4 mSv. However, there are some high-level natural background radiation areas (HLNRAs) in the world where the background radiation is very high due to local geology and geochemistry (1). The sources of naturally occurring radionuclides and their decay products vary across these HLNRAs (2). In India, the 55-km long and 0.5-km wide coastal belt with major deposits of monazite-rich mineral sands, in the southwest state of Kerala, is one of the widely studied HLNRA in the world. The annual background radiation levels in this densely populated area vary from ≤ 1 to ≥ 45 mGy and are mainly due to thorium and its decay products.

The population residing in HLNRA of Kerala extends distinct potential to provide mechanistic understanding of effects of low-dose radiation directly on humans. Many studies conducted over the years have shown no significant differences between individuals from HLNRA as compared to those in normal-level natural radiation areas (NLNRAs) for major biological parameters such as cancer incidence, congenital malformations, chromosomal aberrations, spontaneous level of DNA double-strand breaks etc. (3–8). This indicates that biological effects of low-dose radiation may be markedly more uncertain than that predicted by the linear-no-threshold hypothesis. There is also some evidence to suggest radiation-induced adaptive response (RI-AR) in populations residing in HLNRA of Kerala (9–11). RI-AR postulates that a prior exposure to low doses of radiation, typically ≤ 100 mGy, decreases the biological effectiveness of a subsequent high dose of radiation. However, the mechanism of action of RI-AR is not fully elucidated, leading to ambiguities. A recent report from our lab showed that low levels of reactive oxygen species, high mitochondrial membrane potential and increased activity of many antioxidant enzymes characterise RI-AR in human G_0 peripheral blood mononuclear cells (PBMCs) (12).

Proteins are considered building blocks of life and are the key functional molecules of the cell. Proteomic analysis, thus, offers great promise to understand not only ‘real-time’ dynamic changes in the cell due to radiation but also to study the adaptive response (AR) that may be mounted to maintain homeostasis in the cellular system. Earlier work from our lab showed differential expression and moderate up-regulation of several proteins in G_0 PBMCs from healthy individuals 1 and 4 h after ‘*ex vivo*’ exposure with two acute radiation doses (300 mGy and 1 Gy) (13). In this report, we used radiation proteomics to analyse differential protein expression changes in G_0 PBMCs due to chronic low-dose natural background radiation. The basal protein expression in PBMCs was then compared and contrasted with proteomic changes in PBMCs challenged with a high dose of 2 Gy to provide evidence of protective AR in HLNRA subjects through critical cellular proteins.

Materials and Methods

Human subjects

Ethics approval for the study involving human subjects was obtained from the Medical Ethics Committee, Bhabha Atomic Research Centre, Mumbai, India. Venous blood samples were collected from 40 random healthy males in sterile EDTA tubes (BD™ Vacutainers, NJ, USA) with informed written consent. Of these, 20 subjects were from HLNRA (average age: 40.5 ± 7.18 y) and 20 subjects from NLNRA (average age: 34 ± 4.71 y). The first set of 10 samples each from HLNRA and NLNRA was used for proteomic analysis using

two-dimensional gel electrophoresis (2DE). An additional set of 10 samples each from both the areas was used for western blot analysis.

Dosimetry

A Geiger Muller tube-based survey meter (Type ER-709, Nucleonix Systems, India) was used to measure the external gamma radiation levels (inside/outside) in each subject’s house at a height of 1 m above the ground level in $\mu\text{R/h}$. The readings were converted into mGy/y by using a conversion factor of 0.0767 ($= 0.8763 \times 24 \text{ h} \times 365 \text{ days} \times 10^{-5}$) and an occupancy factor of 0.5 (14).

Irradiation and proteomic sample preparation

PBMCs were isolated using density-gradient centrifugation using Histopaque-1077 media (Sigma Aldrich, St Louis, USA) at room temperature. The isolated PBMCs of each donor from both the groups (NLNRA or HLNRA) were divided into two parts. One aliquot was processed to study the baseline proteomic profile of HLNRA and NLNRA. The second aliquot from both the groups was challenged with an *ex vivo* radiation dose of 2 Gy (dose rate 0.466 Gy/min) using a ^{60}Co gamma ray source (Blood irradiator, 2000, BRIT, India), henceforth, referred to as ‘challenged PBMCs’ [NLNRA (2 Gy) and HLNRA (2 Gy)]. Both the aliquots were incubated at 37°C for 1 h before homogenising in ice cold lysis buffer (10-mM Tris-Cl, pH 7.0, 1X Protease inhibitor cocktail) to make the protein extract as described earlier (13). The protein concentration was estimated by bicinchoninic acid method.

Two-dimensional gel electrophoresis

Protein extracts were prepared and separated using 2DE proteomic approach according to Nishad and Ghosh (13). The mean annual dose received by HLNRA ($N = 10$) and NLNRA ($N = 10$) individuals used for 2DE was 15.60 ± 3.04 mGy (range: 10.74–20.25 mGy/y) and 1.35 ± 0.08 mGy (range: 1.27–1.50 mGy/y), respectively. Briefly, the first dimensional separation was performed using ready-made 17-cm immobilized pH gradient strips of pH 4.0–7.0 (Bio-Rad, CA, USA). The sodium dodecyl sulphate–polyacrylamide gel electrophoresis electrophoresis was performed on 10% polyacrylamide gels using Protean II XL cells (Bio-Rad, CA, USA). The gels were stained with coomassie blue R-250 and digitally imaged using Image Scanner III (GE Healthcare, IL, USA). Spot detection and matching were performed using PDQuest software (ver 8, Bio-Rad, CA, USA).

Protein identification by matrix-assisted laser desorption ionisation-time of flight mass spectrometry

The differentially expressed ($P \leq 0.05$) protein spots were excised manually from the gels and prepared for identification as given in Nishad and Ghosh (13). Destaining was performed by repeated washings with 50-mM NH_4HCO_3 /acetonitrile (ACN) followed by in-gel proteolytic digestion with sequencing-grade modified trypsin (Sigma-Aldrich Corp., MO, USA; 25 ng/ μl) overnight at 37°C. The tryptic peptides were eluted with serial extractions with 0.1% trifluoroacetic acid (TFA), 0.1% TFA in 50% ACN and 100% ACN. The reconstituted peptide fragments (0.1% TFA in 50% ACN) were then mixed (v/v) with matrix-assisted laser desorption ionisation-time (MALDI) matrix (α -cyano-4-hydroxycinnamic acid or alpha-matrix) and analysed with MALDI-time of flight mass spectrometry (TOF-MS) (UltraFlexII or Autoflex, Bruker Daltonics, Germany) in positive ion reflector mode. The mass range (m/z 800–4500) was externally calibrated using the peptide calibration standard (Bruker Daltonics) with

nine standard peptides. The peak list was processed using Flexanalysis 3.0 software (Bruker Daltonics) and searched against SWISS-PROT database, specified for *Homo sapiens* taxonomy using Mascot search engine (<http://www.matrixscience.com>). The peptide mass fingerprinting search parameters were set as peptide error tolerance of ± 100 ppm, one missed cleavage, fixed modifications as 'carbamidomethyl on cysteine', and variable modification of 'oxidation on methionine'. Protein matches were computed using a probability-based MOlecular WEight SEarch (MOWSE) score, and MOWSE scores greater than 56 were considered as significant ($P \leq 0.05$).

Statistical analysis

For differences in baseline expression, mean values for 10 individuals for HLNRA were compared with mean values of 10 individuals from NLNRA (as given in column 1, Table 1). Similarly, differential expression was calculated for challenged PBMCs [NLNRA (2 Gy) vs HLNRA (2 Gy)] (as given in column 2, Table 1). For comparisons among the groups, fold changes in expression (\pm standard error of the mean) were calculated for 10 individuals from NLNRA vs NLNRA (2 Gy) (as given in column 3, Table 1) and HLNRA vs HLNRA (2 Gy) (as given in column 4, Table 1). The box plot visualisations of the protein expression data were prepared by using Statistics Program for Social Sciences (SPSS 11.5; IBM, NY, USA). Normalised spot intensities for differential analysis were compared using independent sample *t* test. A significance level of 0.05 was used and no adjustments for multiple tests were carried out. Coefficient of variation (CV) of normalised spot intensity, the ratio of standard deviation to mean expressed as %, was used to assess the variation in differential expression. A sample size of 10 was arrived by assuming an overall CV of 34%, as observed in previous work from our lab (13) and to detect a fold-change of 1.5 with 80% power at 5% level of significance by using the formula $n = \frac{2(Z_{\alpha/2} + Z_{\beta})^2 \times \log(CV^2 + 1)}{[(\log_e R)]^2}$,

where n is a sample size, $Z_{\alpha/2}$ is value from the standard normal distribution (two sided) corresponding to significance level (α), Z_{β} is value from the standard normal distribution corresponding to power ($1 - \beta$), R is the fold change and CV is the coefficient of variation (15). Correlation analysis was performed for all the differentially modulated proteins to evaluate the relationship between protein expression and annual dose received by HLNRA individuals (range: 10.74–20.25 mGy/y) using SPSS 11.5 (IBM, NY, USA) software.

The functional pathway analysis was performed using the open-source software DAVID (Database for Annotation, Visualization and Integrated Discovery) version 6.8 (<https://david.ncifcrf.gov>) to assess enriched biological process in HLNRA. The UniProt identification numbers of the modulated proteins were used for the enrichment analysis of functional annotation terms by searching against the human proteome database as previously described (16, 17). This analysis identified over-representation of certain group of proteins common to biological process, molecular function and cellular component. The Gene Ontology Term Enrichment (GOTERM) biological process was considered significant with a modified Fisher's exact *P*-value by DAVID with $P \leq 0.05$.

Factor analysis on raw spot densities of all quantified proteins was employed to identify underlying factors using principal component analysis (PCA). Analysis was also carried out to assess the power of detecting different fold changes from 1.25 to 3 and sample sizes from 1 to 20, assuming an overall CV of 34% (as observed in this work), using the formula given earlier for estimation of sample size.

Western blot analysis

The average background dose of samples used for western blot analysis varied from 13.30 ± 3.15 mGy/y (range: 7.29–17.79 mGy/y) in HLNRA and 1.33 ± 0.09 mGy/y (range: 1.23–1.46 mGy/y) in NLNRA. Pooled protein lysates (50 μ g) from the four experimental groups [NLNRA, HLNRA, NLNRA (2 Gy) and HLNRA (2 Gy)] were immunoblotted as described earlier (13) using primary antibodies against GRP78 (rabbit polyclonal, sc-13968), PRDX6 (mouse monoclonal, sc-101522) and PDI (goat polyclonal, sc-2005). The protein bands were quantified using Image J software normalised to GAPDH (rabbit monoclonal, 14C10) expression. GAPDH antibody was procured from Cell Signaling Technology (MA, USA) whereas all other antibodies were obtained from Santa Cruz Biotechnology, Inc. (TX, USA).

Results

To investigate the chronic low-dose-radiation-induced modulations in human PBMCs, comparative analysis using two-dimensional gel-based proteomics and MALDI-TOF MS or the 2DE-MS proteomic approach was used. Because, the sample pooling strategies nullifies the calculation of biological variations, 2D proteomic maps were prepared at an individual level [10 biological replicates per group for all the four groups, *viz* NLNRA (baseline), HLNRA (baseline), NLNRA (2 Gy) and HLNRA (2 Gy)]. Here, a biological replicate is an independently prepared protein lysate from a human subject. Then all 40 gels were normalised together to generate a master gel. This normalisation was essential to minimise the variability due to slight variations in protein load per gel, staining efficiency or image capture. All analyses were performed on normalised quantities as described earlier (13). For the identification of differentially expressed proteins, both inter-group comparisons for NLNRA vs HLNRA and NLNRA (2 Gy) vs HLNRA (2 Gy) as well as intra-group comparisons for NLNRA vs NLNRA + 2 Gy and HLNRA vs HLNRA + 2 Gy were made. Differentially expressed spots were analysed by MALDI-TOF/TOF tandem MS. The SWISS PROT accession number, MASCOT score, sequence coverage and peptide match for the identified proteins are given in Table 2 and marked on Figure 1.

Effect of chronic high-level natural background radiation on the proteome of HLNRA subjects

A total of 15 proteins were found to be statistically modulated in individuals from HLNRA when compared to individuals from NLNRA (Table 1, Figure 2). Six proteins were over-expressed (FIBB, FIBG, ACT-isoform 3, GRP78, LDHB and PDIA1) whereas nine proteins were under-expressed (RAP1B, RhoGD1 β , two isoforms of TPM2, VIME, ATPB, HSP90, PRDX6, TPM4) (Table 1, Figure 3A). When the samples were challenged with a 2-Gy gamma radiation, 24 proteins were significantly modulated in HLNRA (2 Gy) as compared to NLNRA (2 Gy) samples (Table 1, Figure 2). Out of these, 11 proteins were up-regulated (two isoforms of ACT, MV, PLS2, PSME1, ATPB, GRP78, LDHB, PDI1A, PRDX6 and TPM4), whereas 13 proteins (two isoforms of ACT, two isoforms of ALBU, CALR, CLIC, F13A, HSP70, LE1, PD1A3, TUBB, 2801, HSP90) were down-regulated (Table 1, Figure 3B). One protein (spot no. 31) could not be identified due to insufficient amount of peptide signals in the mass spectra.

Early antioxidant responses were earlier shown to play a significant role in the development of acute RI-AR in G_0 PBMCs (12). Extending the same supposition for chronic radiation, some of the major proteins involved in maintaining dynamic redox equilibrium were taken for validation using western blot analysis (Figure 4A).

Table 1. Differentially expressed proteins in human PBMCs with chronic exposure to high background natural radiation

Sl. No.	Protein name	Mean fold change in HLNRA vs NLNRA (1)		P value	Mean fold change in HLNRA (2 Gy) vs NLNRA (2 Gy) (2)		P value	Mean fold change (\pm SEM) in NLNRA vs NLNRA (2 Gy) (3)		P value	Mean fold change (\pm SEM) in HLNRA vs HLNRA (2 Gy) (4)		P value
		HLNRA	NLNRA		HLNRA	NLNRA		HLNRA	NLNRA		HLNRA	NLNRA	
1	Fibrinogen beta chain (FIBB)	1.39	1.01	P = 0.03	1.01	1.01	P = 0.97	1.35 \pm 0.16	1.10 \pm 0.23	P = 0.05	1.10 \pm 0.23	P = 0.97	
2	Fibrinogen gamma chain (FIBG)	1.43	1.04	P = 0.04	1.04	1.04	P = 0.82	1.29 \pm 0.18	0.88 \pm 0.11	P = 0.44	0.88 \pm 0.11	P = 0.20	
3	Ras-related protein Rap-1b (RAP1B)	0.71	0.76	P = 0.04	0.76	0.76	P = 0.12	1.50 \pm 0.15	1.61 \pm 0.16	P = 0.04	1.61 \pm 0.16	P = 0.03	
4	Rho GDP-dissociation inhibitor 2 (RhoGDI2)	0.78	1.08	P = 0.04	1.08	1.08	P = 0.59	0.97 \pm 0.12	1.40 \pm 0.15	P = 0.67	1.40 \pm 0.15	P = 0.03	
5	Tropomyosin beta chain (1) [TPM2 (1)]	0.67	1.05	P = 0.05	1.05	1.05	P = 0.86	0.74 \pm 0.14	1.01 \pm 0.21	P = 0.05	1.01 \pm 0.21	P = 0.98	
6	Tropomyosin beta chain (2) [TPM2 (2)]	0.82	0.99	P = 0.05	0.99	0.99	P = 0.97	0.88 \pm 0.12	1.09 \pm 0.14	P = 0.26	1.09 \pm 0.14	P = 0.79	
7	Vimentin (VIME)	0.76	0.88	P = 0.02	0.88	0.88	P = 0.43	0.87 \pm 0.13	0.92 \pm 0.09	P = 0.11	0.92 \pm 0.09	P = 0.56	
8	Actin gamma/Actin beta (3) [ACT (3)]	1.33	0.80	P = 0.05	0.80	0.80	P = 0.05	1.48 \pm 0.14	0.81 \pm 0.09	P = 0.05	0.81 \pm 0.09	P = 0.05	
9	ATP synthase subunit beta (ATPB)	0.69	1.38	P = 0.05	1.38	1.38	P = 0.04	0.79 \pm 0.10	1.50 \pm 0.18	P = 0.05	1.50 \pm 0.18	P = 0.05	
10	Glucose-regulated protein 78 kDa (GRP78)	1.48	1.52	P = 0.01	1.52	1.52	P = 0.01	1.40 \pm 0.12	1.45 \pm 0.09	P = 0.05	1.45 \pm 0.09	P = 0.01	
11	Heat shock protein 90-alpha/beta (HSP90)	0.59	0.55	P = 0.05	0.55	0.55	P = 0.04	0.66 \pm 0.11	0.70 \pm 0.18	P = 0.04	0.70 \pm 0.18	P = 0.06	
12	l-lactate dehydrogenase B chain (LDHB)	1.34	1.21	P = 0.05	1.21	1.21	P = 0.05	1.41 \pm 0.07	1.28 \pm 0.09	P = 0.05	1.28 \pm 0.09	P = 0.03	
13	Protein disulfide-isomerase A1 (PDIA1)	1.32	1.39	P < 0.001	1.39	1.39	P < 0.001	1.14 \pm 0.06	1.21 \pm 0.10	P = 0.04	1.21 \pm 0.10	P = 0.02	
14	Peroxiredoxin 6 (PRDX6)	0.91	1.31	P = 0.05	1.31	1.31	P = 0.05	0.86 \pm 0.10	1.29 \pm 0.13	P = 0.15	1.29 \pm 0.13	P = 0.05	
15	Tropomyosin alpha-4 chain (TMP4)	0.76	1.38	P < 0.001	1.38	1.38	P < 0.001	0.73 \pm 0.11	1.19 \pm 0.08	P = 0.01	1.19 \pm 0.08	P = 0.04	
16	Actin gamma/Actin beta (1) [ACT (1)]	0.91	1.74	P = 0.36	1.74	1.74	P = 0.02	0.81 \pm 0.05	1.46 \pm 0.18	P = 0.03	1.46 \pm 0.18	P = 0.05	
17	Actin gamma/Actin beta (2) [ACT (2)]	0.96	1.36	P = 0.82	1.36	1.36	P = 0.05	1.25 \pm 0.17	1.49 \pm 0.11	P = 0.88	1.49 \pm 0.11	P = 0.04	
18	Actin gamma/Actin beta (4) [ACT (4)]	0.92	0.66	P = 0.76	0.66	0.66	P = 0.05	1.79 \pm 0.32	1.98 \pm 0.74	P = 0.04	1.98 \pm 0.74	P = 0.74	
19	Serum Albumin [ALBU (1)]	1.08	0.59	P = 0.72	0.59	0.59	P = 0.04	1.58 \pm 0.22	0.84 \pm 0.16	P = 0.05	0.84 \pm 0.16	P = 0.48	
20	Serum Albumin [ALBU (2)]	0.68	0.47	P = 0.06	0.47	0.47	P = 0.01	1.14 \pm 0.25	0.74 \pm 0.14	P = 0.81	0.74 \pm 0.14	P = 0.06	
21	Calreticulin (CALR)	0.72	0.63	P = 0.23	0.63	0.63	P < 0.001	0.86 \pm 0.27	0.67 \pm 0.16	P = 0.05	0.67 \pm 0.16	P = 0.04	
22	Chloride intracellular channel protein 1 (CLIC)	0.96	0.66	P = 0.77	0.66	0.66	P = 0.04	1.48 \pm 0.17	1.20 \pm 0.21	P = 0.05	1.20 \pm 0.21	P = 0.98	
23	Coagulation factor XIII A chain (F13A)	1.07	0.53	P = 0.70	0.53	0.53	P = 0.01	1.17 \pm 0.12	0.62 \pm 0.14	P = 0.35	0.62 \pm 0.14	P = 0.04	
24	Heat shock cognate 71 kDa protein (HSP70)	0.87	0.72	P = 0.54	0.72	0.72	P = 0.05	1.08 \pm 0.09	1.02 \pm 0.09	P = 0.69	1.02 \pm 0.09	P = 0.61	
25	Leukocyte elastase inhibitor (LEI)	1.06	0.67	P = 0.69	0.67	0.67	P = 0.05	1.49 \pm 0.21	1.09 \pm 0.17	P = 0.05	1.09 \pm 0.17	P = 0.70	
26	Plastin-2 (PLS2)	0.90	1.21	P = 0.63	1.21	1.21	P = 0.05	1.26 \pm 0.19	1.31 \pm 0.10	P = 0.80	1.31 \pm 0.10	P = 0.02	
27	Protein disulfide-isomerase A3 (PDIA3)	0.94	0.66	P = 0.57	0.66	0.66	P = 0.03	1.04 \pm 0.11	0.70 \pm 0.12	P = 0.92	0.70 \pm 0.12	P = 0.04	
28	Proteasome activator complex subunit1 (PSME1)	1.08	1.24	P = 0.62	1.24	1.24	P = 0.05	0.91 \pm 0.43	1.00 \pm 0.08	P = 0.10	1.00 \pm 0.08	P = 0.61	
29	Tubulin beta chain (TUBB)	0.56	0.80	P = 0.10	0.80	0.80	P = 0.04	1.23 \pm 0.17	1.29 \pm 0.11	P = 0.69	1.29 \pm 0.11	P = 0.05	
30	Vinculin (MV)	0.90	1.39	P = 0.47	1.39	1.39	P = 0.05	0.79 \pm 0.07	1.19 \pm 0.15	P = 0.05	1.19 \pm 0.15	P = 0.43	
31	Ssp2801 (Not identified)	1.05	0.89	P = 0.81	0.89	0.89	P = 0.05	1.15 \pm 0.16	0.91 \pm 0.11	P = 0.75	0.91 \pm 0.11	P = 0.11	
32	Tubulin alpha-1B chain (TUBA)	1.30	0.80	P = 0.24	0.80	0.80	P = 0.16	1.25 \pm 0.12	1.37 \pm 0.54	P = 0.04	1.37 \pm 0.54	P = 0.25	
33	Actin gamma/Actin beta (5) [ACT (5)]	0.86	1.24	P = 0.36	1.24	1.24	P = 0.23	1.07 \pm 0.09	1.55 \pm 0.12	P = 0.84	1.55 \pm 0.12	P = 0.04	

The mean change in spot intensity in HLNRA subjects (baseline or 2-Gy challenged) relative to NLNRA subjects is represented as fold change. Abbreviations of names of proteins are given in brackets. The P values in 'bold' represent significant ($P \leq 0.05$) changes in the expression determined using Student's *t* test. The proteins are listed 1–33 as labelled on Figure 1. The abbreviations of names of proteins are given in brackets.

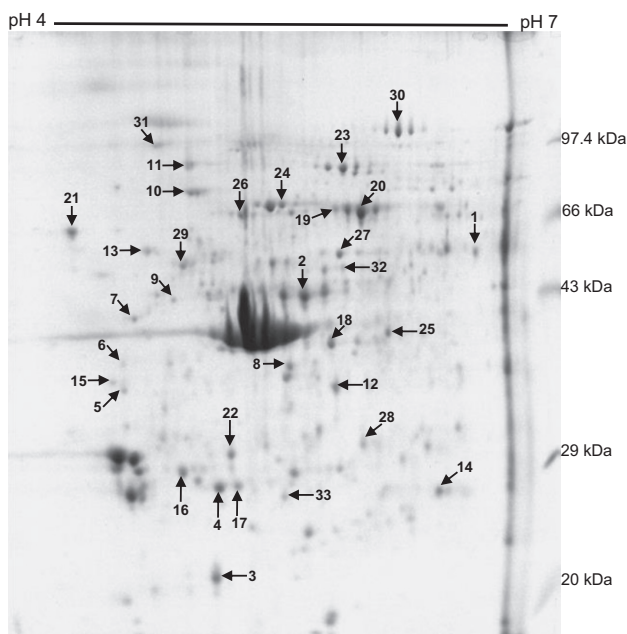


Figure 1. A representative 2DE image of human PBMCs exposed to chronic low-dose radiation from the HLNRA region of Kerala, India. The radiation responsive proteins, marked with arrows, were identified by mass spectrometry and are numbered as listed in Table 2.

The observed expression pattern at baseline level in HLNRA when compared with NLNRA samples for GRP78 (3.21 fold), PDIA1 (1.28 fold) and PRDX6 (1.34 fold) were consistent with the 2DE proteomic data (Figure 4B). The same was true for the challenged dose conditions: GRP78 (1.65 fold), PDIA1 (1.3 fold) and PRDX6 (1.21 fold) (Figure 4C).

The proteomic maps of human subjects from NLNRA or HLNRA were also compared with their respective 2-Gy irradiated cells (NLNRA vs NLNRA + 2 Gy and HLNRA vs HLNRA + 2 Gy). When the comparison was made among the two groups from the control areas, i.e. for NLNRA vs NLNRA + 2 Gy, 18 proteins showed differential modulation (11 over-expressed and 7 under-expressed) (Table 1, Figure 5). In contrast, 17 proteins (13 over-expressed and 4 under-expressed) showed differential modulation when comparisons for made among the two groups of HLNRA subjects *viz.* HLNRA vs HLNRA + 2 Gy (Table 1, Figure 5). Nine of these modulated proteins were common between the two sets of subjects (Figure 5).

The Pearson correlation coefficients (r) were calculated between the annual dose (range: 10.74–20.25 mGy/y) received by HLNRA individuals ($N = 10$) and the corresponding log₂ normalised spot intensity values of a specific protein individually for all the differentially expressed proteins. Out of the 31 differentially modulated proteins analysed, only four (TMP4, ACT3, PSME1 and ALBU1) showed significant correlation ($P \leq 0.05$) with radiation dose (Figure 6A). Proteins ACT3 ($r = 0.78$, $P = 0.01$) and ALBU1 ($r = 0.84$, $P = 0.002$) showed positive correlation with radiation dose, whereas TMP4 ($r = -0.74$, $P = 0.01$) and PSME1 ($r = -0.82$, $P = 0.003$) showed negative correlation. The expression pattern of many proteins involved in cell redox or stress homeostasis such as PDIA1 ($r = 0.17$, $P = 0.64$), PDIA3 ($r = 0.02$, $P = 0.95$), GRP78 ($r = 0.08$, $P = 0.82$), PRDX6 ($r = -0.30$, $P = 0.40$), LDHB ($r = -0.28$, $P = 0.44$) and ATPB ($r = -0.23$, $P = 0.52$) did not show any significant correlation with radiation dose (Figure 6B).

Functional pathway analysis

The enrichment analysis with DAVID identified 44 biological processes significantly ($P \leq 0.05$) activated in HLNRA samples (Supplementary Table 1, available at *Mutagenesis* Online.). This included important processes such as protein folding (HSP70, HSP90, PDIA3, CALR), cell redox homeostasis (PRDX6, PDIA1, PDIA3), cell-matrix adhesion (VINC, FIBB, FIBG), protein refolding (HSP70, HSP90), regulation of protein ubiquitination (HSP90A/B), regulation of ERK cascade (RAP1B, FIBB, FIBG), negative regulation of extrinsic apoptotic signalling pathway (FIBB, FIBG) and response to reactive oxygen species (PRDX6, PDIA1).

Assessment of variability in protein expression

CV was calculated for each protein spot that showed differential expression among all individuals of NLNRA and HLNRA. At the basal level, protein spots from NLNRA samples showed a mean CV of 35.6% (range: 11.5–80.4%) whereas protein spots from HLNRA gave a CV of 33.3% (range: 7.7–67.2%). The 2 Gy challenge dose did not alter the CV of protein spots significantly with average values of 32.3% (range: 6.7–62.5%) and 38.8% (range: 12.7–77.6%) in NLNRA (2 Gy) and HLNRA (2 Gy), respectively. When combined for all the samples from all four groups, a grand CV of ~34% was achieved. This was used to assess the statistical power (with 5% significance level) of the study at different fold changes of protein expression (Figure 7).

Principal component analysis

PCA was performed using the raw spot intensity data of all the quantified proteins. Although the first two components of the PCA explained only ~26.8% of the data variance, it clearly clustered proteins according to residential areas of the subjects and the radiation dose (Figure 8).

Discussion

In this study, a 2DE-MS approach was used to compare and contrast the proteome of human subjects from HLNRA and NLNRA and the differences in response when these samples were challenged with a high dose of 2 Gy. A moderate but distinct baseline differences were seen in the proteome of subjects from HLNRA *vis-à-vis* NLNRA. Most of the differences in expression were small. However, there are many studies that indicate that enrichment of biologically relevant functions occur even with subtle changes in expression. Almost 15 proteins were found to be differentially altered in PBMCs from HLNRA as compared to PBMCs from NLNRA, indicating radiation-specific response. However, only four proteins (ACT3, ALBU1, TMP4 and PSME1) showed significant correlation with the annual dose received by individuals (Figure 6). Use of 2DE-MS allowed separation of proteins according to their charge, isoelectric point and molecular weight, hence allowing resolution of multiple isoforms and variants of proteins such as actin (five isoforms) and tropomyosin beta chain (two isoforms).

When PBMCs from both groups were irradiated *ex vivo* with 2-Gy gamma radiations, as many as 24 proteins showed distinct changes in expression, indicating adaptive ability of cells from HLNRA subjects to mount a protective stress response when challenged with high doses. A comparative analysis of subjects from NLNRA or HLNRA with their respective 2 Gy irradiated cells (NLNRA vs NLNRA + 2 Gy and HLNRA vs HLNRA + 2 Gy) identified significant modulation of 26 proteins ($P \leq 0.05$). Using the

Table 2. List of differentially expressed proteins identified by MALDI-TOF/TOF tandem mass spectrometry.

Sl. No.	Protein name	SWISS PROT Accession No.	Mascot Score	Sequence coverage (%)	Peptide matches
1	Fibrinogen beta chain (FIBB)	P02675	139	42.0	23
2	Fibrinogen gamma chain (FIBG)	P02679	105	38.2	12
3	Ras-related protein Rap-1b (RAP1B)	P61224	186	67.4	14
4	Rho GDP-dissociation inhibitor 2 (RhoGDI β)	P52566	52	40.8	7
5	Tropomyosin beta chain (1) [TPM2 (1)]	P07951	62	24.3	9
6	Tropomyosin beta chain (2) [TPM2 (2)]	P07951	62	23.9	9
7	Vimentin (VIME)	P08670	266	62.2	38
8	Actin gamma/Actin beta (3) [ACT (3)]	P63261/P60709	85	40.3	10
9	ATP synthase subunit beta (ATPB)	P06576	273	71.8	30
10	Glucose-regulated protein 78 kDa (GRP78)	P11021	197	44.2	28
11	Heat shock protein 90-alpha/beta (HSP90)	P07900/P08238	93	26.1	17
12	L-lactate dehydrogenase B chain (LDHB)	P07195	105	38.3	12
13	Protein disulfide-isomerase A1 (PDIA1)	P07237	161	38.0	20
14	Peroxiredoxin 6 (PRDX6)	P30041	200	65.2	14
15	Tropomyosin alpha-4 chain (TMP4)	P67936	80	34.7	11
16	Actin gamma/Actin beta (1) [ACT (1)]	P63261/P60709	65	36.3	9
17	Actin gamma/Actin beta (2) [ACT (2)]	P63261/P60709	85	41.3	11
18	Actin gamma/Actin beta (4) [ACT (4)]	P63261/P60709	100	34.9	9
19	Albumin Serum [ALBU (1)]	Q56G89	98	17.0	11
20	Albumin Serum [ALBU (2)]	Q56G89	75	27.0	10
21	Calreticulin (CALR)	P27797	71	25.9	8
22	Chloride intracellular channel protein1 (CLIC)	O00299	193	78.4	15
23	Coagulation factor XIII A chain (F13A)	P00488	142	32.0	15
24	Heat shock cognate 71 kDa protein (HSP70)	P11142	70	21.7	13
25	Leukocyte elastase inhibitor (LEI)	P30740	102	33.0	10
26	Plastin-2 [PLS2]	P13796	201	44.2	27
27	Protein disulfide-isomerase A3 (PDIA3)	P30101	162	40.4	17
28	Proteasome activator complex subunit1 (PSME1)	Q06323	137	66.3	17
29	Tubulin beta chain (TUBB)	P07437	69	29.5	9
30	Vinculin (MV)	P18206	116	24.3	22
31	Ssp2801 (Not identified)	–	–	–	–
32	Tubulin alpha-8/4A/1C/1B chain (TUBA)	Q9NY65/ P68366/ Q9BQE3/ P68363	68	25	8
33	Actin gamma/Actin beta (5) [ACT (5)]	P63261/P60709	114	40	12

The SWISS PROT accession number, MASCOT score, sequence coverage and peptide matches are listed for the identified proteins. The proteins are listed 1–33 as labelled on [Figure 1](#) and the abbreviations of names of proteins are given in brackets.

UniProt/SwissProt protein database, these proteins could be broadly classified into processes such as cytoskeleton-associated proteins, molecular chaperones, cellular redox homeostasis, signalling, cellular metabolic process, and protein and peptide processing. The major biological processes modulated with 2 Gy in samples from Kerala region were similar to that observed in an earlier work from our laboratory on human PBMCs from random healthy adults, irradiated *ex vivo* with 1 Gy (13). The cytoskeleton and associated proteins formed the largest enriched group in both the studies.

Although, changes in the protein expression between various groups were modest, PCA analysis of the raw data clearly differentiated groups based on the radiation dose and residential area status. Interestingly, the clustering was tighter for the *ex vivo* 2 Gy irradiated samples. This clearly indicates a radiation-induced effect and evidence of AR.

The functional pathway analysis performed with DAVID grouped these modulated proteins into 44 biological processes. The major protein group altered by chronic low-dose radiation was structural proteins. Many of these structural proteins play an important role in cell movement, cell–cell adhesion, cell-matrix adhesion and cell junction assembly. A decrease in the baseline expression of three actin isoforms [ACT (1): -1.10 fold, $P = 0.36$; ACT (2): -1.04

fold, $P = 0.82$; ACT (4): -1.09 fold, $P = 0.76$], RhoGDI β (-1.28 fold, $P = 0.04$), tropomyosin beta isoforms [TPM2 (1): -1.49 fold, $P = 0.05$; TPM2 (2): -1.22 $P = 0.05$], VIME (-1.32 fold, $P = 0.02$), TMP4 (-1.32 fold, $P < 0.001$), PLS2 (-1.11 fold, $P = 0.63$), TUBB (-1.79 fold, $P = 0.10$) and MV (-1.11 fold, $P = 0.47$) was seen in HLNRA subjects in comparison to NLNRA. On the other hand, structural proteins such as ACT (3) [1.33 fold, $P = 0.05$], FIBB (1.39 , $P = 0.03$) and FIBG (1.43 fold, $P = 0.04$) showed significant up-regulation in HLNRA individuals compared to NLNRA individuals. With *ex vivo* irradiation, while expression of nine structural proteins [RhoGDI β , TPM2 (1), TMP4, actin isoforms—ACT (1) and ACT (2), PLS2, MV, FIBB and FIBG] showed over-expression in challenged HLNRA samples, four proteins [TPM2 (2), VIME, TUBB, and actin isoforms—ACT (3) and ACT (4)] showed down-regulation in challenged HLNRA samples.

Many proteins involved in cell redox homeostasis and response to reactive oxygen species were differentially altered in HLNRA samples. Some proteins such as PDIA1 presented higher expression in HLNRA samples (1.32 fold; $P < 0.001$) and remained high even when challenged with 2 Gy (1.39 fold; $P < 0.001$). On the other hand, PDIA3 remained consistently down-regulated. Other proteins such as PRDX6, though down-regulated under basal conditions in

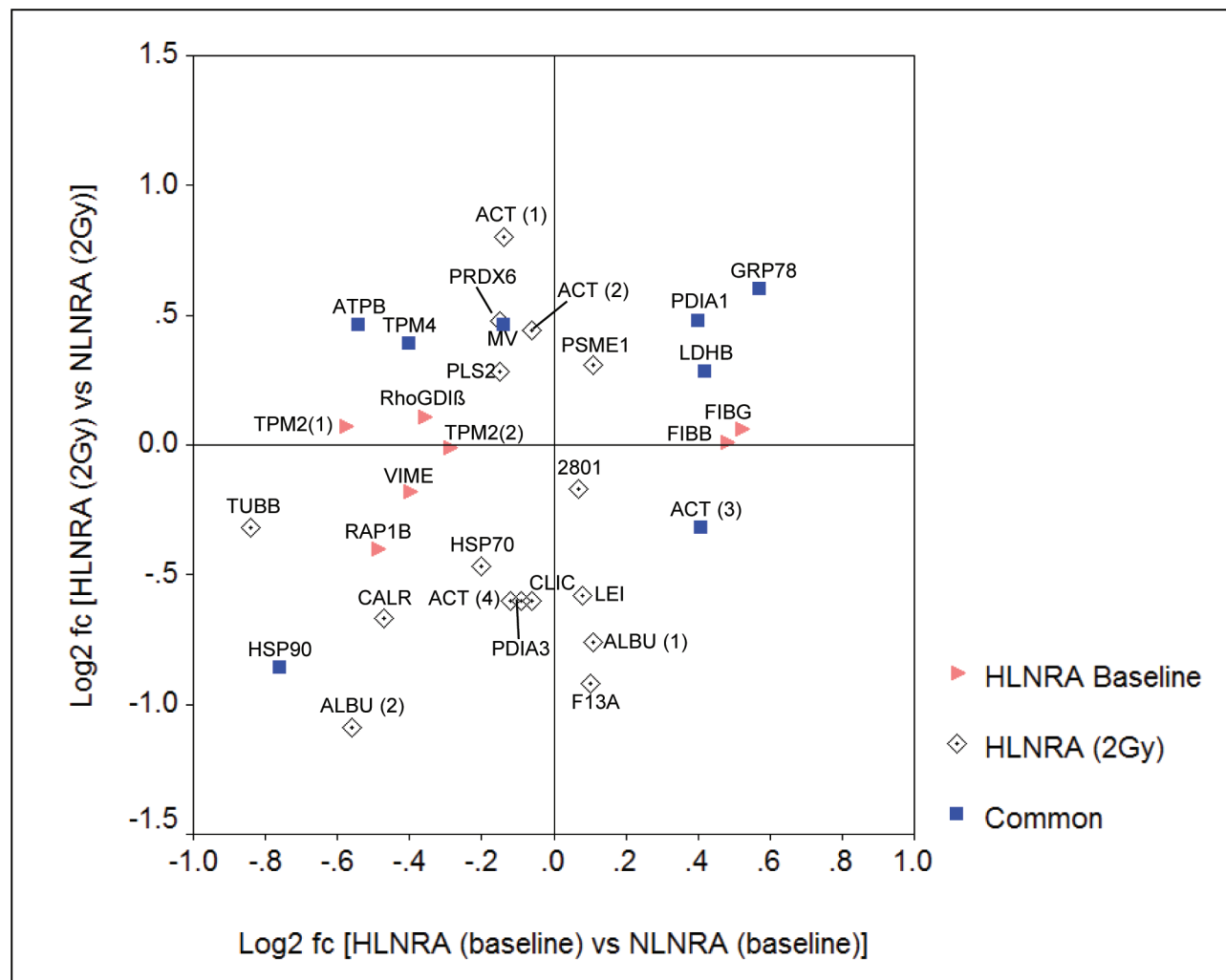


Figure 2. Scatter plot showing inter-group variations in protein expression between baseline and 2-Gy challenged human PBMCs from HLNRA and NLNRA. Each point corresponds to the log₂ transformed fold change of a single protein. The orange polygons represent significant variation in HLNRA as compared to NLNRA. The clear polygons represent significant variation in HLNRA (2 Gy) as compared to NLNRA (2 Gy). The blue polygons represent proteins common between HLNRA and HLNRA (2 Gy). The proteins were identified by mass spectrometry and are abbreviated as listed in Table 2.

HLNRA samples (-1.10 fold; $P = 0.05$), was significantly up-regulated (1.38 fold; $P = 0.05$) in HLNRA (2 Gy) samples when presented with *ex vivo* radiation stress.

There were two other proteins, ATPB and TPM4, which showed similar trend as PRDX6. ATPB has been shown to be a reversible 'molecular switch' with dual functions of ATP synthesis/hydrolysis. Its ATP hydrolysis function can contribute to maintain mitochondrial membrane potential ($\Delta\Psi_m$) after IR and thereby ensure cell survival. Our group had earlier shown that $\Delta\Psi_m$ is restored in human PBMCs during RI-AR (12). Here, though ATPB was down-regulated in HLNRA samples under basal conditions (-1.45 fold, $P = 0.05$), it is significantly up-regulated when HLNRA samples were challenged with 2 Gy (1.38 fold, $P = 0.04$). TPM4, which is basically a cytoskeletal protein that binds to actin filaments was recently shown to mediate ER-to-Golgi trafficking (18).

Among the other modulated proteins was the GRP78 protein that is considered a key adaptive, pro-survival stress-inducible molecular chaperone involved in maintenance of cellular homeostasis (19). GRP78 was consistently over-expressed both under basal conditions in HLNRA samples (1.48 fold, $P = 0.01$) as well as in

challenged PBMCs from HLNRA (1.52 fold, $P = 0.01$), indicating a protective survival advantage to these cells against radiation stress. Another pro-survival protein that showed consistent high abundance was LDHB (1.34-fold change, $P = 0.05$ as baseline expression in HLNRA and 1.21-fold change, $P = 0.05$ in HLNRA samples challenged with 2 Gy). LDHB, which catalyses production of pyruvate from lactate, has been shown to inhibit stress-mediated cell death and protect against multiple stresses in yeast (20).

Assessment of inter-individual variation in proteomic response to radiation stress was calculated by using CV as a tool. The CV values of the differentially modulated proteins ranged from 6.7 to 80.4%, with an overall mean CV of ~34%. Majority of the protein spots had a CV of <50%, with only a few proteins exhibiting >50% CV at the basal level (19.4% in NLNRA and 16.1% in HLNRA) and challenged dose [6.4% in NLNRA (2 Gy) and 29.0% in HLNRA (2 Gy)] conditions. The proteins with broader CV value ranges (>50%) were mainly from cytoskeletal [CALR, TUBB, ACT (2), ACT (4), ACT (1), TPM2 (1), PLS2] and extracellular [ALBU (2), F13A, FGB] protein families. The protein spots with minimum CV variation in the samples indicate that the corresponding protein expressions

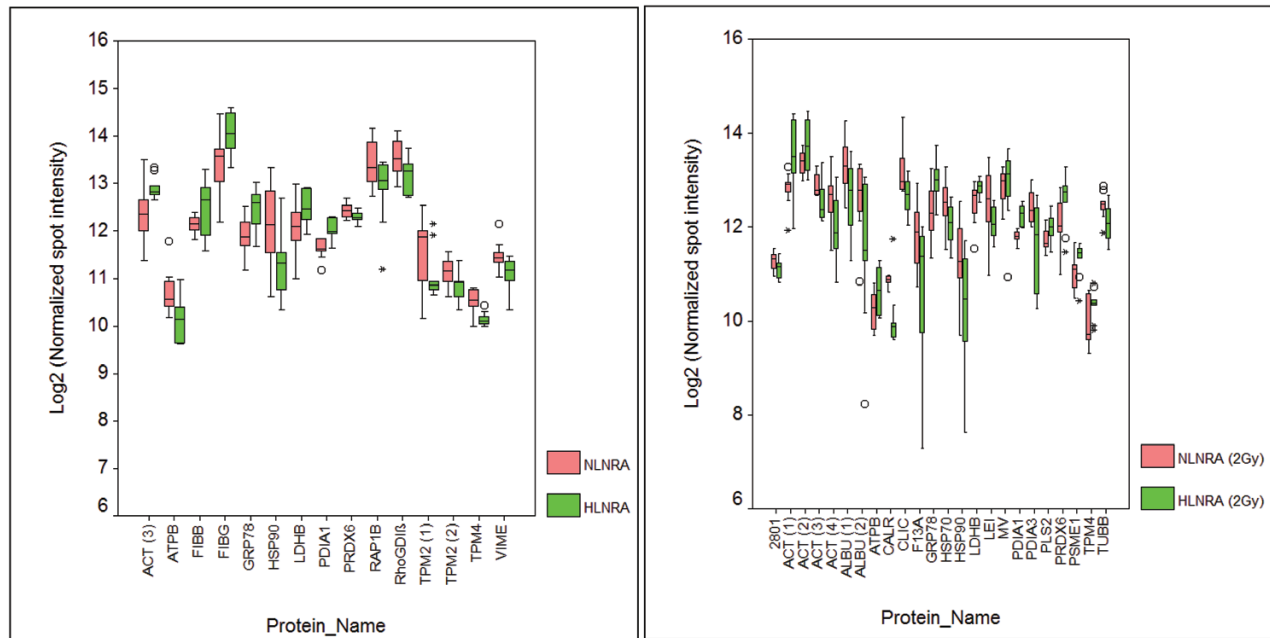


Fig. 3. Box-plot distribution of expression for differentially expressed proteins of PBMCs, expressed as log₂ transformed normalised spot intensities, in individuals from NLNRA and HLNRA. **(A)** Variations in baseline expression. **(B)** Variations after a challenge dose of 2 Gy. Each distribution contains protein expression values from 10 individuals. The top and bottom of the box represents the 25th and 75th percentiles and the whiskers shows the maximum and minimum values. The black 'bold line' is the median value. The open 'circles' indicates outliers and 'stars' indicates extreme values.

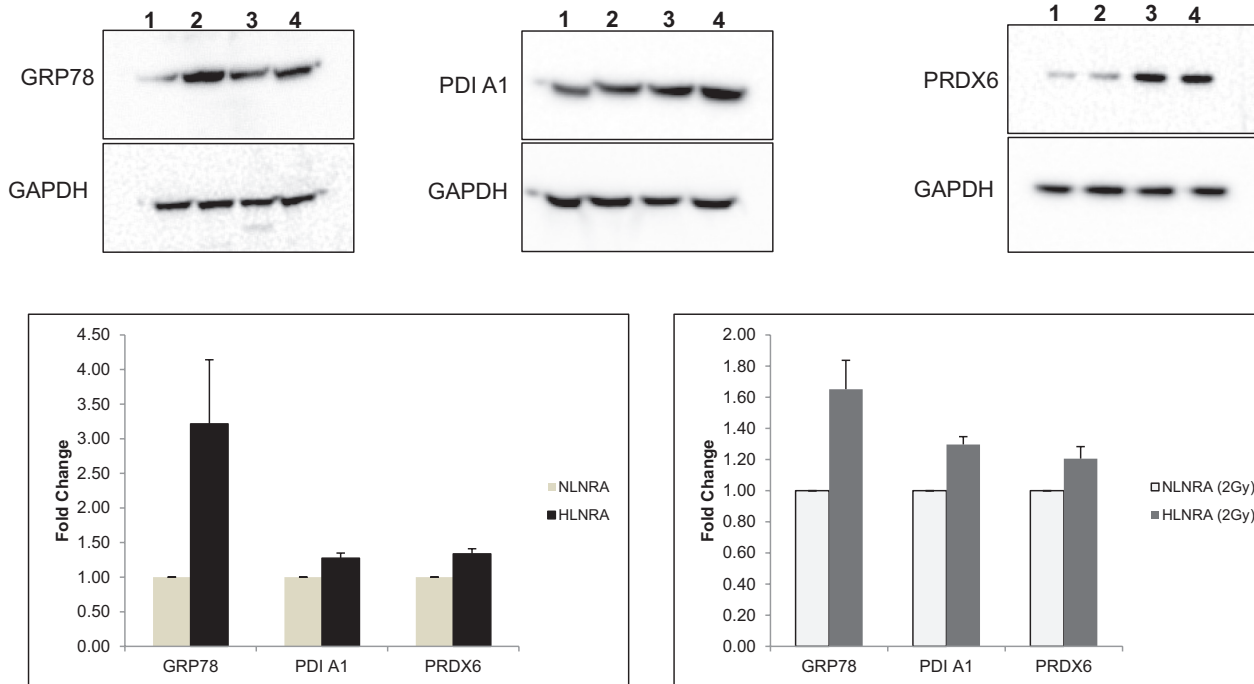


Figure 4. **(A)** Immunoblot validation of selected proteins (GRP78, PDI A1 and PRDX6). Pooled protein lysates from 10 subjects each for four experimental groups NLNRA (lane 1), HLNRA (lane 2), NLNRA (2 Gy) (lane 3) and HLNRA (2 Gy) (lane 4) were separated on 4–12% Bis-Tris gels, transferred to a PVDF membrane, probed with specific antibodies and quantified using Image J software relative to GAPDH. Histograms presenting mean \pm SD of fold change in relative protein expression for **(B)** (NLNRA vs HLNRA), and **(C)** NLNRA (2 Gy) vs HLNRA (2 Gy).

were relatively constant across individuals. The individual variation data was further used to understand the relationship between sample number and statistical power of the study. At the CV of 34%, the sample size used in this study was sufficient to detect a 1.5-fold change in mean protein expression with 80% statistical power at

5% level of significance. The study was able to detect even smaller changes in protein expression, albeit with low statistical power.

When a correlation analysis was performed between expressions of proteins to the annual dose received by an individual, only two proteins showed significant positive correlation; actin (ACT)

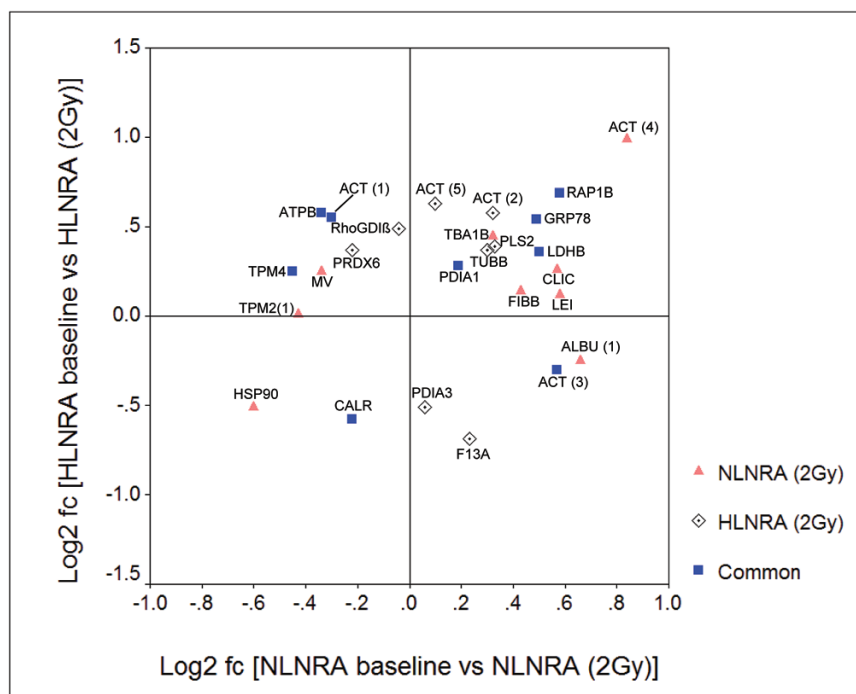


Figure 5. Scatter plot showing intra-group variations in protein expression between baseline and 2-Gy challenged human PBMCs from HLNRA and NLNRA. Each point corresponds to the log₂ transformed fold change of a single protein. The orange polygons represent significant variation in NLNRA (2 Gy) as compared to NLNRA. The clear polygons represent significant variation in HLNRA (2 Gy) as compared to HLNRA. The blue polygons represent proteins common between NLNRA (2 Gy) and HLNRA (2 Gy). The proteins were identified by mass spectrometry and are abbreviated as listed in Table 2.

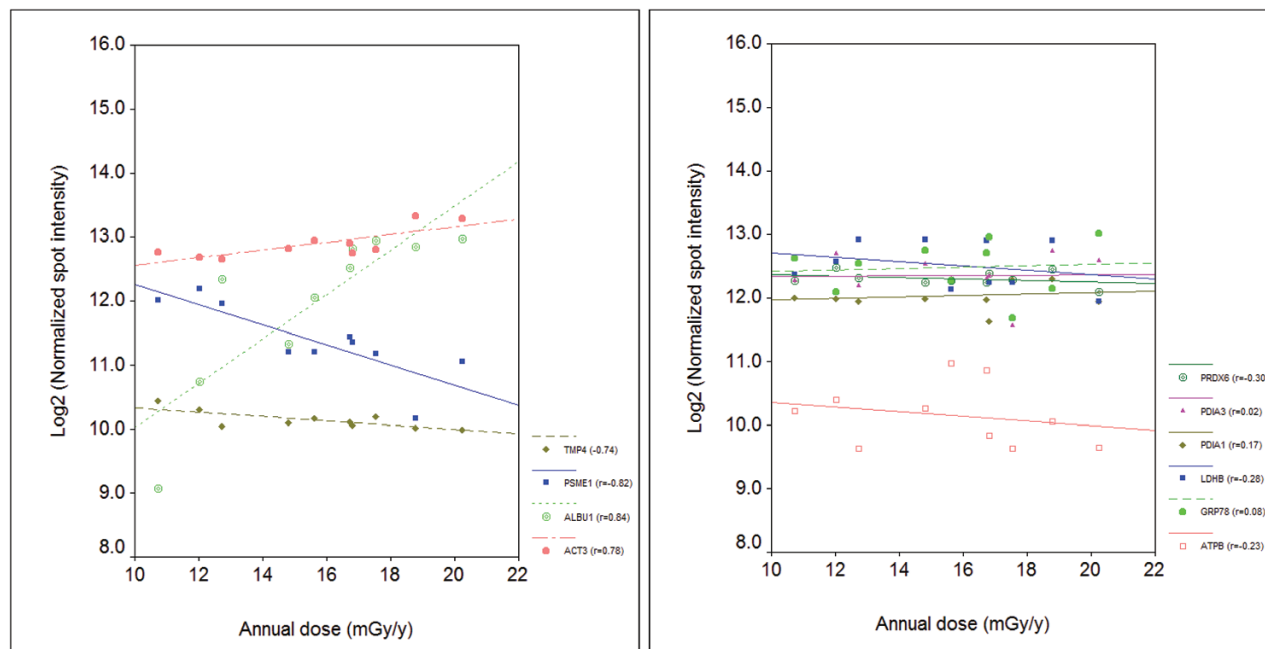


Figure 6. Scatter plot showing the Pearson correlation analysis of protein expression to annual dose (range: 10.74–20.25 mGy/y) received by HLNRA individuals ($N = 10$). (A) Four proteins showed statistically significant correlation. (B) Proteins involved in cell redox/stress homeostasis. Each point corresponds to the log₂ transformed normalised spot intensity data of a single protein for an individual. The best-fit line for each protein is shown with the Pearson correlation coefficient (r) values in legend.

and albumin (ALBU1). Positive correlation of ACT3 protein with radiation dose reaffirms the recognition of actin cytoskeleton as a highly dynamic network that plays a key role in response and adaptation of the cell to its microenvironment or internal signals. This is essential for many important processes of the cell including signal

transduction, cell division, cell adhesion, cell migration, chromatin remodelling, apoptosis, gene expression and contractility in muscle and non-muscle cells (21). The multifunctional protein albumin, which is the most abundant circulating protein in plasma, shows key antioxidant activities (22). Human lymphocytes are known to

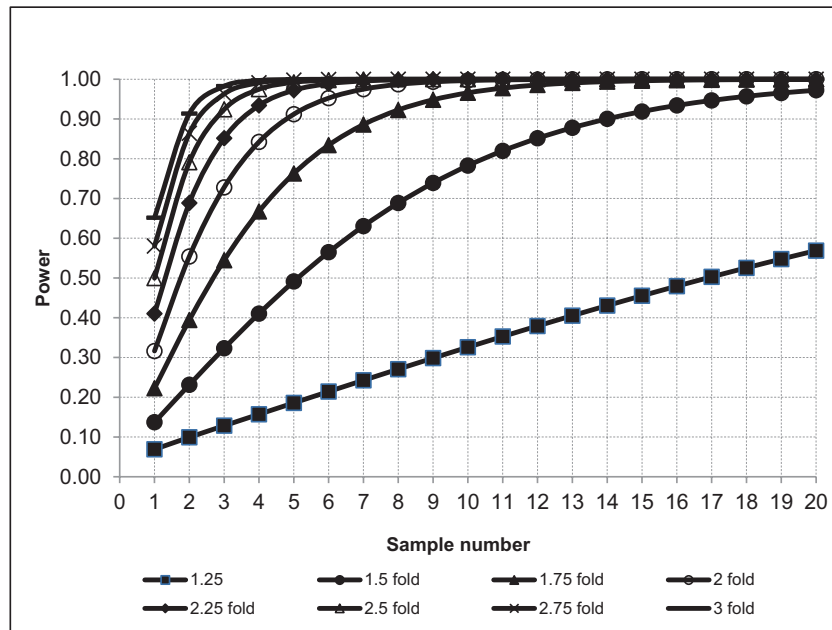


Figure 7. Relationship between statistical power and sample size. Results are plotted for various fold changes at 5% significance level and assuming CV of 34% observed in this study. Results show that a sample size of $N = 10$ in an experimental design detects a 1.5-fold change close to 80% power.

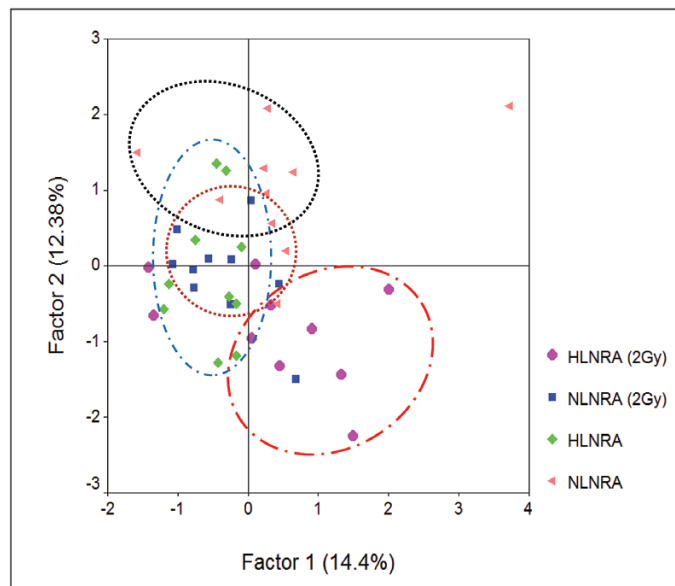


Figure 8. Principal component analysis (PCA) for the protein expression data set. PCA identified four clusters using the raw spot intensity data of all the quantified proteins. Biological replicates belonging to each group (10 subjects/group) were colour coded.

have membrane-bound albumin. Several reports have suggested that PBMC albumin may also contribute to the regulation of oxidative stress. Indirect evidence of this has come from association of decreased albumin content with decreased antioxidant activity in the PBMC of type 1 diabetic rats (23). Because this study is with primary lymphocytes, the albumin detected is not an artifact from plasma or from tissue-culture media. However, the functional role of PBMC albumin in radiation response needs to be further investigated.

There were two proteins, tropomyosin alpha-4 chain (TMP4) and proteasome activator complex subunit1 (PSME1), which showed negative correlation with the annual radiation dose received by studied individuals. TMP4 protein is known to be involved in

stabilisation of actin filaments in non-muscle cells (24). An inverse relationship of this protein with increasing radiation received by individuals indicates altered stability and rearrangement of cytoskeleton. The other protein shows inverse relationship with radiation, PSME1 protein, encodes a subunit of multicatalytic endoproteinase complex required for efficient presentation of tumour antigens by MHC class I molecule. Increased expression of PSME1 has been associated with diagnosis and prognosis of various tumour types such as prostate, breast and ovarian cancer, and poor survival in soft tissue sarcomas (25). However, the change in expression of PSME1 with radiation dose and its functional significance needs to be analysed further.

This work is in agreement with the earlier studies on RI-AR with chronic low dose. Human PBMCs from individuals residing in HLNRA of Kerala, India, when challenged with a high dose showed lower DNA strand breaks and better repair (measured using comet assay and γ H2AX) as compared to individuals from NLNRA (10,11). In a report by Ramachandran *et al.* (9), peripheral blood samples taken from individuals from HLNRA, Kerala, India, when challenged with a high dose, showed lower frequency of micronuclei but only in individuals older than 40 y of age. Similar results with micronuclei frequency after a high challenge dose were also observed in peripheral blood samples from individuals residing in high natural background radiation areas of Ramsar, Iran, as compared to subjects from control (26). However, the initial levels of DNA damage after a challenge dose was higher in these subjects (27). Gourabi and Mozdarani (28) provided evidence of AR in occupational workers in their study on micronuclei frequency in human lymphocytes from radiology and radiotherapy workers.

In conclusion, results from this study indicated that the human proteome is a dynamic system that responds to external low-dose radiation stress through changes in abundance of many pro-survival proteins. The changes in expression were modest, yet sufficient to assist cells attain adaptive homeostasis. Recent work from our lab described various mechanisms through which PBMCs induce AR in response to acute radiation doses (12). Whether the chronic radiation utilises similar mechanisms to evoke AR need to be probed further.

Despite the advent of newer technologies, 2DE still remains a mature, widely accepted and successfully implemented top-down method for providing simultaneous information on abundance, charge and various isoforms of thousands of proteins in a single run (29). Additional in-depth proteomic analysis using high-resolution gel-free techniques is currently underway in our lab. Integration of these two techniques will help provide more robust and comprehensive view of the networks of cellular responses to natural high background radiation.

Supplementary data

Supplementary Table 1 is available at *Mutagenesis* Online.

Funding

This work was supported by funding from Bhabha Atomic Research Centre, Department of Atomic Energy, Government of India.

Acknowledgements

We thank the volunteers who donated blood samples for this study and lab members of Low Level Radiation Research Laboratory (LLRRL), Kollam, Kerala, for their assistance during sample collection and dosimetry. We are thankful to Mr P. K. M. Koya, LLRRL, Kollam, Kerala, for his help with statistical analysis of the data. We also acknowledge the technical assistance provided by Paresh P. Khadilkar and Pritam N. Bhoir. MALDI-TOF MS was performed at ACTREC, Navi Mumbai and IIT Bombay, Mumbai. Conflict of interest statement: None declared.

References

- United Nations Scientific Committee on the Effects of Atomic Radiations (UNSCEAR). (2000) *Sources and Effects of Ionising Radiation Annex B Exposures from Natural Radiation Sources*. New York: United Nations.
- Hendry, J. H., Simon, S. L., Wojcik, A., Sohrabi, M., Burkart, W., Cardis, E., Laurier, D., Tirmarche, M. and Hayata, I. (2009) Human exposure to high natural background radiation: what can it teach us about radiation risks? *J. Radiol. Prot.*, 29, A29–A42.
- Nair, R. R., Rajan, B., Akiba, S., *et al.* (2009) Background radiation and cancer incidence in Kerala, India-Karanagappally cohort study. *Health Phys.*, 96, 55–66.
- Jaikrishan, G., Sudheer, K. R., Andrews, V. J., Koya, P. K., Madhusoodhanan, M., Jagadeesan, C. K. and Seshadri, M. (2013) Study of stillbirth and major congenital anomaly among newborns in the high-level natural radiation areas of Kerala, India. *J. Community Genet.*, 4, 21–31.
- Ramachandran, E. N., Karuppasamy, C. V., Cheriyan, V. D., Soren, D. C., Das, B., Anilkumar, V., Koya, P. K. and Seshadri, M. (2013) Cytogenetic studies on newborns from high and normal level natural radiation areas of Kerala in southwest coast of India. *Int. J. Radiat. Biol.*, 89, 259–267.
- Karuppasamy, C. V., Ramachandran, E. N., Anil Kumar, V., Vivek Kumar, P. R., Koya, P. K. M., Jaikrishan, G. and Das, B. (2018) Frequency of chromosome aberrations among adult male individuals from high and normal level natural radiation areas of Kerala in the southwest coast of India. *Mutat. Res.*, 828, 23–29.
- Jain, V., Kumar, P. R., Koya, P. K., Jaikrishan, G. and Das, B. (2016) Lack of increased DNA double-strand breaks in peripheral blood mononuclear cells of individuals from high level natural radiation areas of Kerala coast in India. *Mutat. Res.*, 788, 50–57.
- Kumar, P. R., Cheriyan, V. D. and Seshadri, M. (2012) Evaluation of spontaneous DNA damage in lymphocytes of healthy adult individuals from high-level natural radiation areas of Kerala in India. *Radiat. Res.*, 177, 643–650.
- Ramachandran, E. N., Karuppasamy, C. V., Kumar, V. A., Soren, D. C., Kumar, P. R., Koya, P. K., Jaikrishan, G. and Das, B. (2017) Radio-adaptive response in peripheral blood lymphocytes of individuals residing in high-level natural radiation areas of Kerala in the southwest coast of India. *Mutagenesis*, 32, 267–273.
- Jain, V., Saini, D., Vivek Kumar, P. R., Jaikrishan, G. and Das, B. (2017) Efficient repair of DNA double strand breaks in individuals from high level natural radiation areas of Kerala coast, south-west India. *Mutat Res Fund Mol Mech Mutagen.* 806, 39–50.
- Kumar, P. R., Seshadri, M., Jaikrishan, G. and Das, B. (2015) Effect of chronic low dose natural radiation in human peripheral blood mononuclear cells: evaluation of DNA damage and repair using the alkaline comet assay. *Mutat. Res.*, 775, 59–65.
- Paraswani, N., Thoh, M., Bhilwade, H. N. and Ghosh, A. (2018) Early antioxidant responses through concerted activation of NF- κ B and Nrf2 characterize gamma radiation induced-adaptive response in quiescent human peripheral blood mononuclear cells. *Mutat Res Genet Toxicol Environ Mutagen.* 831, 50–61.
- Nishad, S. and Ghosh, A. (2016) Dynamic changes in the proteome of human peripheral blood mononuclear cells with low dose ionizing radiation. *Mutat. Res. Genet. Toxicol. Environ. Mutagen.*, 797, 9–20.
- Nair, R. R., Akiba, S., Binu, V. S., Jayalekshmi, P., Gangadharan, P., Nair, M. K. and Rajan, B. (2005) Individual dose estimation—our experience with the Karunagapally study in Kerala, India. *Int Congress Ser.*, 1276, 41–45.
- Van Belle, G. and Martin, D. C. (1993) Sample size as a function of coefficient of variation and ratio of means. *The American Statistician*, 47, 165–167.
- Huang, da. W., Sherman, B. T. and Lempicki, R. A. (2009) Systematic and integrative analysis of large gene lists using DAVID bioinformatics resources. *Nat. Protoc.*, 4, 44–57.
- Huang, da. W., Sherman, B. T. and Lempicki, R. A. (2009) Bioinformatics enrichment tools: paths toward the comprehensive functional analysis of large gene lists. *Nucleic Acids Res.*, 37, 1–13.
- Kee, A. J., Bryce, N. S., Yang, L., Polishchuk, E., Schevzov, G., Weigert, R., Polishchuk, R., Gunning, P. W. and Hardeman, E. C. (2017) ER/Golgi trafficking is facilitated by unbranched actin filaments containing Tpm4.2. *Cytoskeleton (Hoboken)*, 74, 379–389.
- Lee, A. S. (2014) Glucose-regulated proteins in cancer: molecular mechanisms and therapeutic potential. *Nat. Rev. Cancer*, 14, 263–276.
- Sheibani, S., Jones, N. K., Eid, R., Gharib, N., Arab, N. T., Titorenko, V., Vali, H., Young, P. A. and Greenwood, M. T. (2015) Inhibition of stress

- mediated cell death by human lactate dehydrogenase B in yeast. *FEMS Yeast Res.*, 15, fov032.
21. Vedula, P. and Kashina, A. (2018) The makings of the 'actin code': regulation of actin's biological function at the amino acid and nucleotide level. *J Cell Sci*, 131, 1–11.
 22. Roche, M., Rondeau, P., Singh, N. R., Tarnus, E. and Bourdon, E. (2008) The antioxidant properties of serum albumin. *FEBS Lett.*, 582, 1783–1787.
 23. Park, K. T., Yun, C. H., Bae, C. S. and Ahn, T. (2014) Decreased level of albumin in peripheral blood mononuclear cells of streptozotocin-induced diabetic rats. *J. Vet. Med. Sci.*, 76, 1087–1092.
 24. Lin, J. J.-C., Eppinga, R. D., Warren, K. S. and McCrae, K. R. (2008) Human tropomyosin isoforms in the regulation of cytoskeleton functions. In Gunning, P. (ed.), *Tropomyosin*. Springer New York, New York, NY, pp. 201–222.
 25. Lou, S., Cleven, A. H., Balluff, B., de Graaff, M., Kostine, M., Briaire-de Bruijn, I., McDonnell, L. A. and Bovée, J. V. (2016) High nuclear expression of proteasome activator complex subunit 1 predicts poor survival in soft tissue leiomyosarcomas. *Clin. Sarcoma Res.*, 6, 17.
 26. Mohammadi, S., Taghavi-Dehaghani, M., Gharaati, M. R., Masoomi, R. and Ghiassi-Nejad, M. (2006) Adaptive response of blood lymphocytes of inhabitants residing in high background radiation areas of Ramsar- micronuclei, apoptosis and comet assays. *J. Radiat. Res.*, 47, 279–285.
 27. Masoomi, J. R., Mohammadi, S. H., Amini, M. and Ghiassi-Nejad, M. (2006) High background radiation areas of Ramsar in Iran: evaluation of DNA damage by alkaline single cell gel electrophoresis (SCGE). *J. Environ. Radioact.*, 86, 176–186.
 28. Gourabi, H. and Mozdarani, H. (1998) A cytokinesis-blocked micronucleus study of the radioadaptive response of lymphocytes of individuals occupationally exposed to chronic doses of radiation. *Mutagenesis*, 13, 475–480.
 29. Oliveira, B. M., Coorssen, J. R. and Martins-de-Souza, D. (2014) 2DE: the phoenix of proteomics. *J. Proteomics*, 104, 140–150.